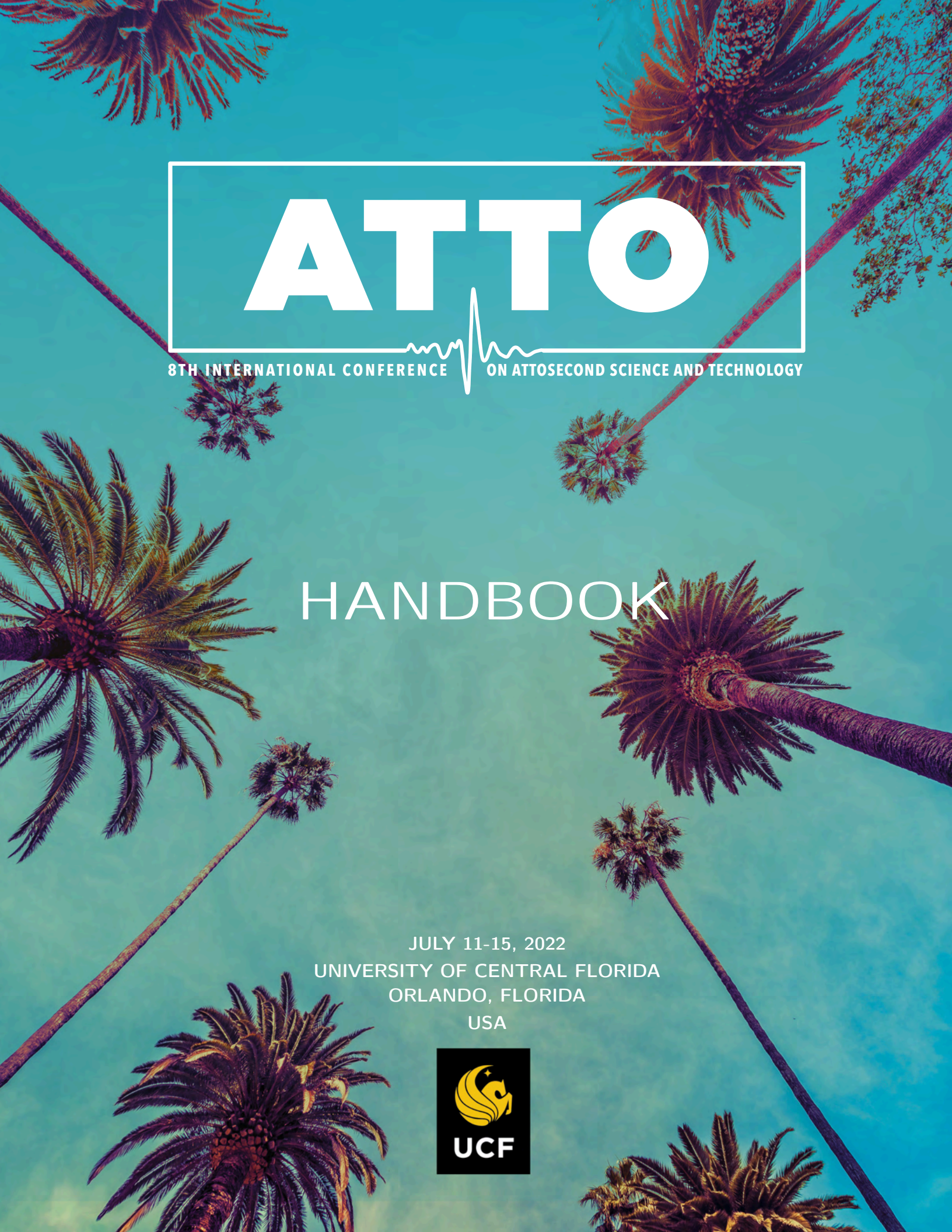

ATTO
8TH INTERNATIONAL CONFERENCE ON ATTOSECOND SCIENCE AND TECHNOLOGY
HANDBOOK
JULY 11-15, 2022
UNIVERSITY OF CENTRAL FLORIDA
ORLANDO, FLORIDA
USA
UCF

AMPHOS

Member of the TRUMPF Group

Amphos8000
Up to 200W, 5mJ

Amphos3000
Up to 600W, 20mJ



ATTO

8th International Conference On Attosecond Science And Technology

Visit us!

Booth 1

ATTO

8th International Conference On Attosecond Science And Technology

TRUMPF

Find us at

Poster Session III - Thursday, July 14

Poster R06

TRUMPF Scientific Lasers



Ultrashort pulses

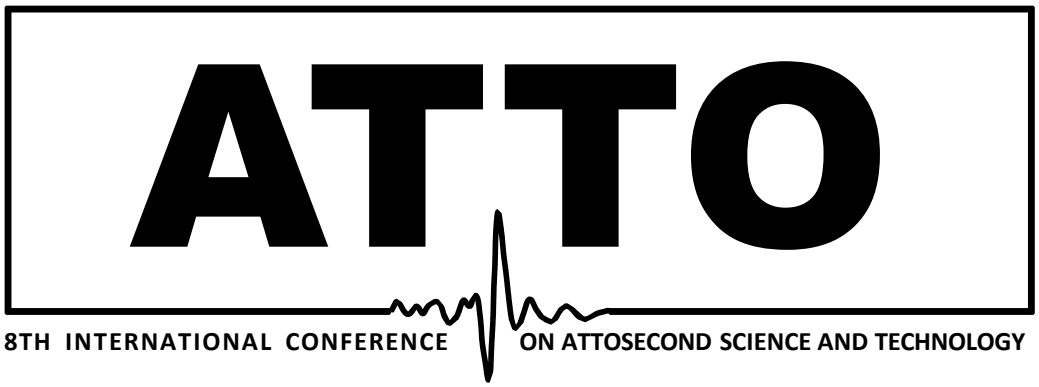
Pulse duration < 50 fs

High average power

Up to 1 kW at high repetition rate

High efficiency

More than 95 % optical transmission



Conference Handbook

July 11 - July 15 2022, Orlando, Florida, USA

Edited by L. Argenti, S. Chattopadhyay, M. Chini, N. Douguet, C. Marante

Index

Conference Venue v
Introduction vii
Acknowledgments ix

Governance

Local Organizing Committee xi
International Program Committee xi

Advisory Boards

International Advisory Board xii
National Advisory Board xii

Policies

Free-Circulation of Scientists xiii
Harassment Policy xiii
Accessibility xiii

Invited Speakers xiv
Contributed Abstracts xv
Conference Proceedings xvi
Social Program xvi
Attosecond Science at UCF xvii
Useful Information xviii
Program Summary xix

Oral Sessions

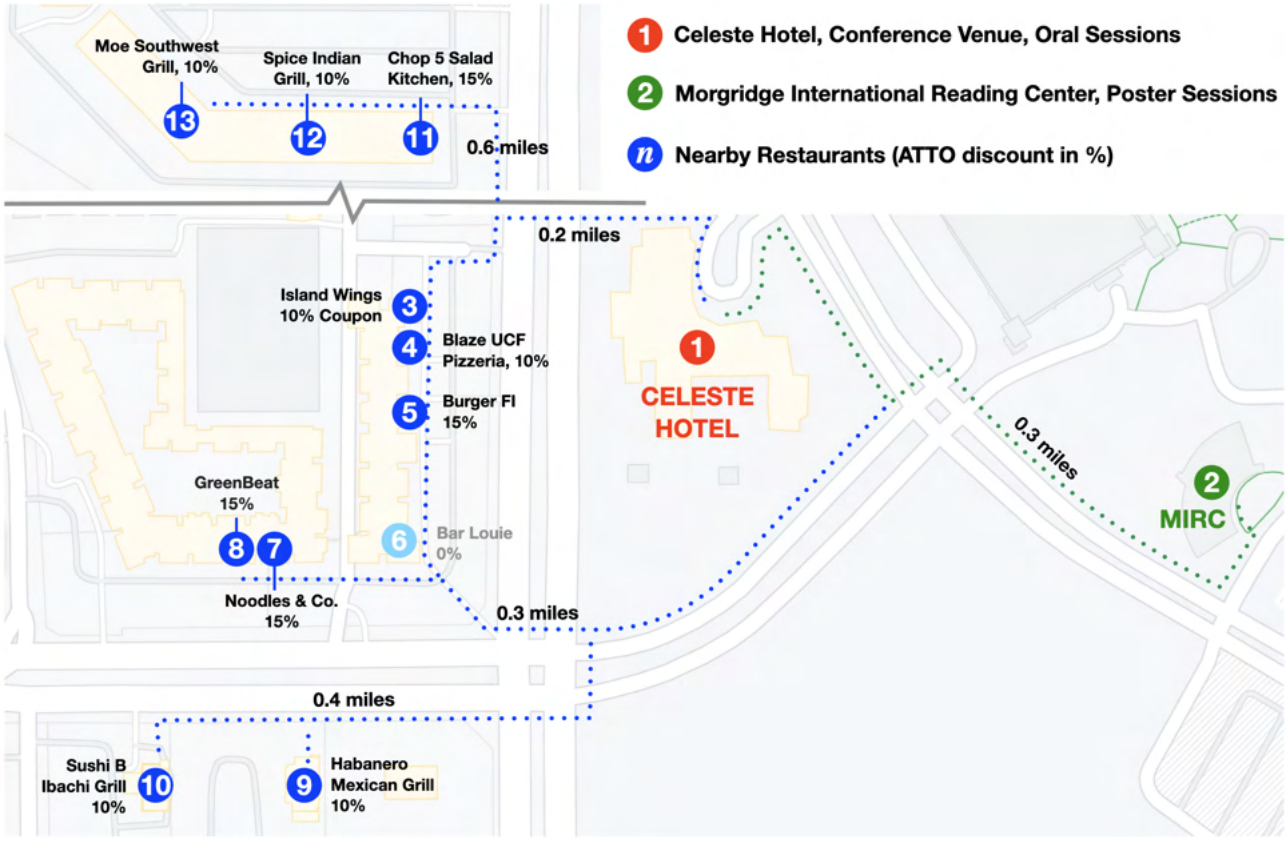
M1 Wolf-Prize Session 2
M2 Chiral Effects in Attosecond Science 6
M3 Imaging & Control of Molecular Structure 11
M4 Strong-Field Nonlinear Optics in Solids 16
ME US Funding Opportunities in Attosecond Science 23
T1 Attosecond Photoionization Dynamics 24
T2 Attosecond Dynamics in Low-D Materials 32
T3 High Order Harmonic Spectroscopy and Control 39
TE Overview of ATTOCHEM Network 46
W1 Attosecond Spectroscopy in Condensed Matter 48
W2 XFELs for Ultrashort XUV/X-ray Science 56
WE Panel: The Future of Attosecond Science 62
R1 Time-Resolved Charge Migration 63
R2 Table-Top Attosecond Sources 71
R3 Attosecond Transient Absorption and Four-Wave Mixing 78
F1 Entanglement in Attosecond Processes 85
F2 Laser Driven Dynamics in Molecules 93

Sponsors 100

Poster Sessions

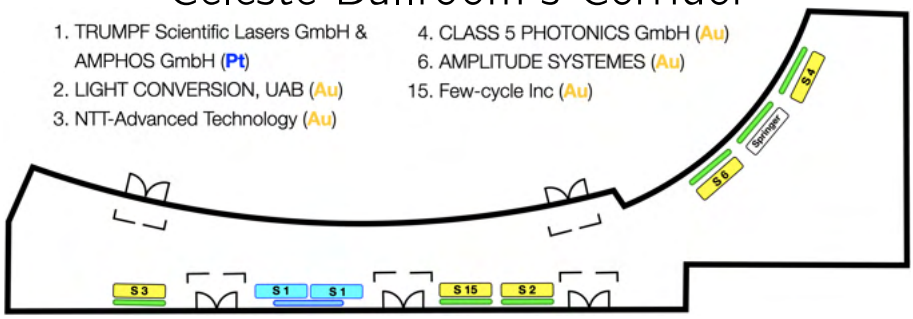
Highlighted Posters I A 102
Highlighted Posters I B 112
Highlighted Posters I C 122
Highlighted Posters II A 132
Highlighted Posters II B 142
Highlighted Posters II C 152
Highlighted Posters III A 162
Highlighted Posters III B 172
Highlighted Posters III C 182
Poster Abstracts I 192
Poster Abstracts II 255
Poster Abstracts III 326
Authors Index 389

Relevant Locations: The map below shows relevant conference locations as well as several restaurants within walking distance from the Celeste hotel, where you can consume a rapid dinner. On MTW (July 11-13), dinner recess is 6:30pm-8:00pm. Most of these restaurants have agreed to grant a discount to the ATTO participants who will exhibit their conference badge or, in the case of Island Wing, present the discount coupon that they will find in their attendee backpack.

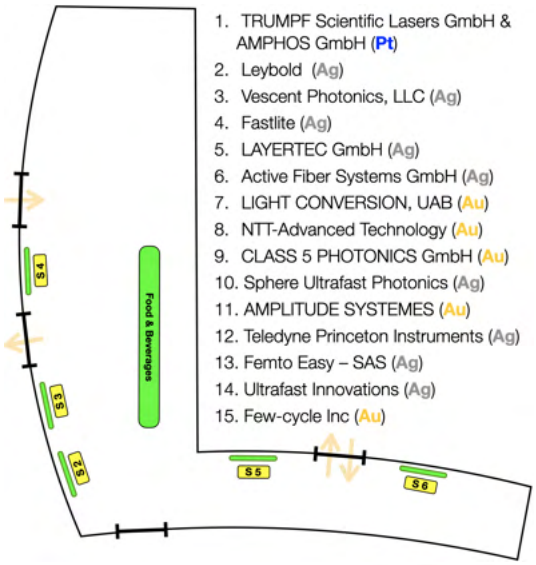


Celeste Ballroom's Corridor

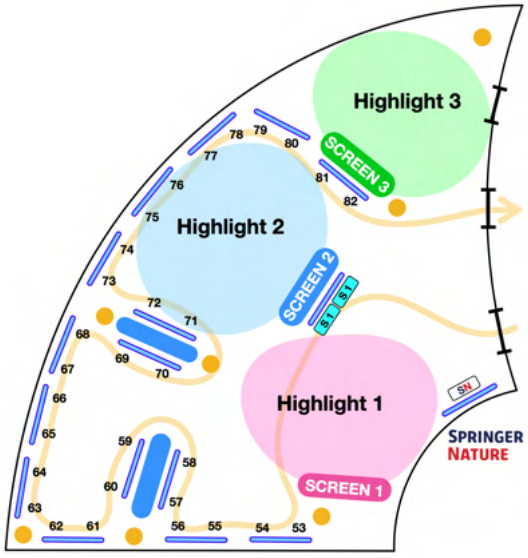
1. TRUMPF Scientific Lasers GmbH & AMPHOS GmbH (Pt)
2. LIGHT CONVERSION, UAB (Au)
3. NTT-Advanced Technology (Au)
4. CLASS 5 PHOTONICS GmbH (Au)
6. AMPLITUDE SYSTEMES (Au)
15. Few-cycle Inc (Au)

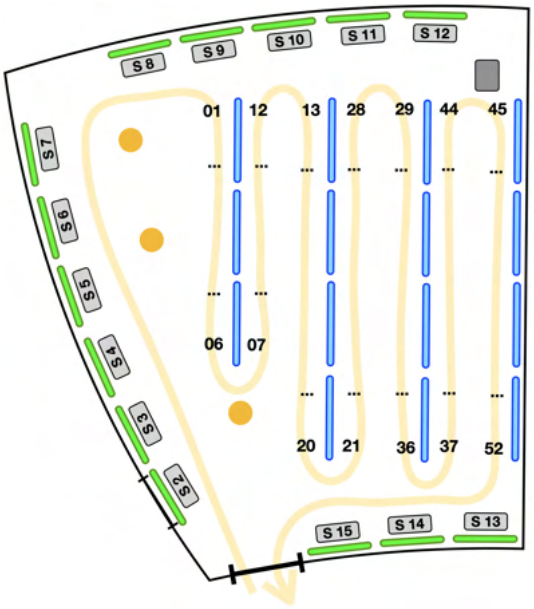


Poster Sessions MTR 16:00-18:30, MTW



1. TRUMPF Scientific Lasers GmbH & AMPHOS GmbH (Pt)
2. Leybold (Ag)
3. Vescent Photonics, LLC (Ag)
4. Fastlite (Ag)
5. LAYERTEC GmbH (Ag)
6. Active Fiber Systems GmbH (Ag)
7. LIGHT CONVERSION, UAB (Au)
8. NTT-Advanced Technology (Au)
9. CLASS 5 PHOTONICS GmbH (Au)
10. Sphere Ultrafast Photonics (Ag)
11. AMPLITUDE SYSTEMES (Au)
12. Teledyne Princeton Instruments (Ag)
13. Femto Easy – SAS (Ag)
14. Ultrafast Innovations (Ag)
15. Few-cycle Inc (Au)





Introduction to the conference

ATTO is the largest and most prestigious world conference in the field of attosecond science, covering topics such as attosecond pulse generation and characterization, time-resolved spectroscopies of ultrafast phenomena taking place on the attosecond and femtosecond timescales, and attosecond science with free-electron lasers.

The ATTO conference series started August 1-5, 2007 under the name of "Attosecond Physics", with the scientific coordination of Paul Corkum (National Research Council of Canada, Ottawa, Canada), Ferenc Krausz (MPI für Quantenoptik, Garching, Germany), and Jan-Michael Rost (MPI für Physik komplexer Systeme, Dresden, Germany). The original announcement read

> The interaction between intense ultra-short laser pulses and matter constitutes a new field of research. It challenges the experiment and also theory, since a non-perturbative description with regard to high non-linear multi-photon processes is required. So far, the biggest breakthrough which has emerged from the experimental and theoretical attosecond research in this highly non-linear non-perturbative regime of laser-matter-interaction, was the creation and measurement of attosecond pulses. Having them at our disposal we are at the beginning of a new scientific era, the age of attosecond science. It will give researchers a completely new microscopic insight into electron processes, taking place in atoms, molecules, biosystems, clusters, semiconductor nanostructures or plasmas. They can be observed in real-time and even controlled to an increasing extent on their natural (attosecond) time scale.
>
> The main purpose of the workshop will be to discuss the current status of attosecond research and the obstacles for further development of attosecond measurements towards shorter time intervals and higher intensities, as well as methods to resolve them. A second important aim is to discuss,understand and propose new applications of attosecond technique in biology, chemistry, physics and plasma physics.

The subsequent editions were held: July 29 - August 1, 2009, at Kansas State University (Manhattan, Kansas, USA) co-chaired by Chii-Dong Lin and Zenghu Chang; July 6-8, 2011, at Hokkaido University (Sapporo, Japan), co-chaired by Katsumi Midorikawa and Kaoru Yamanouchi; July 8-12, 2013, at the Institut Pasteur (Paris, France), co-chaired by Pascal Salières and Eric Constant; July 5-10, 2015, at Manoir Saint-Sauveur (Saint-Sauveur, Quebec, Canada), co-chaired by François Légaré and Paul Corkum; July 2-7, 2017, at Shaanxi Zhangbagou Guesthouse (Xi'an, China), co-chaired by Zhiyi Wei and Zenghu Chang; July 1-5, 2019, at the University of Szeged Congress Centre (Szeged, Hungary, EU), co-chaired by Katalin Varjú and Dimitris Charalambidis.

This year, therefore, it is the first time since 2009 that the ATTO conference will take place in the USA. The main conference sessions will be held at Celeste, a new hotel on the main campus of the University of Central Florida, whereas the poster sessions will be held at the Morgridge International Reading Center, a dynamic space designed to facilitate the exchange of information.

The conference format encourages extensive and open discussion. Conference sessions begin on the morning of Monday, July 11, 2022, and continue until Friday afternoon, July 15, when the meeting ends. There are no parallel sessions, with most sessions consisting of two invited talks (30 minutes each, 28 in total) and four or five contributed talks (15 minutes each, 52 in total). About 50% of the time, therefore, is devoted to contributed talks, many of which will be delivered by early career researchers. There are three 2.5-hour poster sessions. A fraction of the posters have been selected for a highlighted short oral presentation. Invited speakers are housed in the same complex as the main meeting activities, and lunch meals are provided on-site.

Four special scientific and business events are held at the conference: (1) The conference will be opened by a Wolf-Prize session dedicated to three invited talks by the three 2022 Physics Wolf-Prize laureates, Dr. Anne L'Huillier, Dr. Ferenc Krausz, and Dr. Paul Corkum, who received the award as the founders of the field of attosecond science. (2) There will be an evening round table on

"The Future of Attosecond Science" composed of established and emerging female leaders in the field, with the goals of highlighting the important contributions of women in attosecond science and inspiring the next generation of attosecond scientists. (3) There will be an evening session giving an overview of US funding in attosecond science, with the goal of introducing junior scientists to the world of research grants. (4) There will be an evening session devoted to AttoChem, a network funded by the European Cooperation in Science and Technology (COST) to coordinate experimental and theoretical efforts in attosecond chemistry, with the goal of stimulating a discussion on the need for similar coordination efforts in the US.

The main objectives of the conference are: i) to outline the state of the art of attosecond research; ii) to jump-start national and international collaborations that have been hindered by the pandemic; iii) to promote recruiting and training of postdocs and tenure-track candidates; iv) to consolidate the global and diverse identity of the attosecond science community.

Acknowledgments

This conference would not have been possible without the endorsement and material support of countless colleagues, administrators, federal agencies, and private sponsors, to whom we are deeply grateful. Even counting only the material contribution to the conference, American institutions and sponsors have contributed almost 40% of the overall conference budget, allowing us to offer many prime services to the ATTO community, and financial support to many of its junior members, while keeping the registration fee affordable.

We are grateful to Dr. Eduardo Mucciolo, chair of the Physics department in 2019, who allowed the formation of an *ad hoc* ATTO committee as a part of our departmental service assignment, and for directing the department's administrative staff to aid us in organizing the conference. This decision directed departmental resources to the organization of ATTO and allowed the members of the local organizing committee to dedicate sufficient time for this demanding task.

From the beginning, Dr. Michael Johnson, who in 2019 was Dean of the College of Sciences (COS), has granted the strongest support to the conference. He generously offered to cover the expenses associated with accounts at Continuing Education, the unit responsible for management of all conferences held at UCF. Dr. Johnson's support has continued in his subsequent role as Provost. In this capacity, he agreed to sign the contract with the Conference Hotel, thus relieving us from the liability associated to a possible cancellation of the event. Seresa Cruz, COS HR and Budget director, has assisted us with the stipulation of the contract with Continuing Education and with the Conference Hotel. She has also provided provided valuable guidance, and has been instrumental in helping us to cut through a large amount of "red tape".

UCF President, Dr. Alexander N. Cartwright, has endorsed the conference and, in collaboration with Provost Johnson, he has initiated a process to prepare a master contract between the University and the Celeste hotel to facilitate the organization of future conferences and events on campus.

We thank Bahaa Saleh, who in 2019 was Dean of CREOL, the College of Optics, and supported the conference by assigning to us the assistance of Denise Whiteside, Assistant to the Dean, and other administrative staff at CREOL to guide us in contracting with the conference hotel. Denise, who has professional experience in the hotel industry, was instrumental in helping us frame the initial conversations with the hotel, and following up with them in the negotiation for the hotel spaces. Mark Wagenhauser, the Budget Director of CREOL, directed us to the appropriate resources at UCF for Risk Management and for Contract administration.

Since 2019, both the College of Sciences and the College of Optics have new Deans, and the Department of Physics has a new Chair. The two new Deans, Dr. Maggy Tomova, at COS, and Dr. David Hagan, at CREOL, have been tremendously supportive of the conference and have provided assistance with completing the hotel contract, providing contacts with industrial sponsors, and other essential activities. Dr. Joshua Colwell, the current Physics Chair has continued the support from the department and offered guidance on how to overcome the occasional hiccup.

Dr. Eric Van Stryland, Emeritus Dean of CREOL, and past president of the Optical Society of America (now OPTICA), has helped us establish contact with the right people at OPTICA and has manifested his endorsement to the conference throughout the last three years.

The AMOS program at the Department of Energy, managed by Dr. Thomas Settersten, the Modern Optics Program at the Army Research Office, managed by Dr. James Joseph, and the Ultrashort Pulse Laser-Matter Interactions Program at the Air Force Office for Scientific Research, managed

by Dr. Andrew Stickrath, have each committed grant funding to the conference, which has promoted the participation of colleagues and junior scientists who wouldn't otherwise have been able to participate. IUPAP Commission *C15. Atomic, Molecular and Optical Physics* has also provided financial support, which has contributed making the conference proceedings open access.

We thank the Industrial Sponsors of the conference, whose generous support has enabled many of the conference functions, and whose participation will help foster future advances in the field.

We wish to thank the team at Continuing Education, Kevin Parker and Jana Breburdova, for their work in setting up the registration page and for managing the conference account. We are very grateful to the staff at the Department of Physics: Jessica Brooks, Nikitta Campbell, Sierra Cliburn, and Leida Vera Nater, for assisting us in the many administrative transactions of the conference, managing the spending from federal grants, and providing practical guidance in event organization.

We are grateful to the members of the *ad hoc* National and International Advisory Boards, who have helped us and the International Program Committee to put together a large pool of outstanding scientists from which the International Program Committee selected the invited speakers.

The International Program Committee has done a tremendous job in vetting not only the invited speakers but also the 300+ contributed abstracts we received. They have also been supportive of the local organization, consenting to postpone the conference by one year and thus giving us the opportunity to meet in-person.

We are thankful to our colleagues in the Local Organizing Committee, Nicolas Douguet, Li Fang, Madhab Neupane, and Mihai Vaida, who each took on important tasks.

We are grateful for the support of Dr. Samuel Harrison, the Editor of Springer Nature, who has guided us through the stipulation of the contract for the publication of the Conference Proceedings and the setup of the OCS webpage for abstract submission, and who has generously offered to donate relevant books to be used as awards to poster-prize winners.

ATTO VIII comprises fourteen technical oral sessions, nine highlight sessions, and three evening sessions, for a total of twenty six different functions. We wouldn't be able to manage this complex program without the expert and generous assistance of many colleagues who agreed to serve as chairs: Cord Arnold, Cosmin Blaga, Nicolas Douguet, Zenghu Chang, Jan Marcus Dahlström, Per Eng-Johnsson, Li Fang, Mette B Gaarde, Mathieu Gisselbrecht, Wendell T. Hill, Jiro Itatani, Kyung-Taec Kim, François Légaré, C. William McCurdy, Madhab Neupane, Mauro Nisoli, Thomas Pfeifer, Thierry Ruchon, Pascal Salières, Richard Taïeb, Uwe Thumm, Mihai Vaida, Katalin Varjú, Marc Vrakking, and Linda Young.

We thank the many undergraduate students who, even if they do not attend ATTO as presenters, have agreed to serve as Conference Staff to welcome its participants and to facilitate their access and contribution to the Conference.

Finally, we thank all the conference participants, who have enthusiastically contributed to the conference with their best science and decided to attend it in person.

Luca Argenti & Michael Chini
Co-Chairs of ATTO VIII

ATTO VIII Governance

Local Organizing Committee

The Local Organizing Committee is responsible for all the activities necessary for the successful conduction of the conference, as well as for facilitating and coordinating the activities of the International Program Committee.

Luca Argenti, chair (UCF)	Nicolas Douguet (Kennesaw U.)	Madhab Neupane (UCF)
Michael Chini, chair (UCF)	Li Fang (UCF)	Mihai Vaida (UCF)

International Program Committee

The International Program Committee is responsible for the governance and the scientific program of the ATTO conference. Its members oversee the conduction of ATTO, decide the conference program sessions and the list of invited speakers, vet the abstracts submitted to the conference, select the contributed speakers, and appoint the organizers of future ATTO conferences.

• Andrius Baltuška	Technical University of Vienna	Austria	EU
• Cosmin Blaga	Kansas State University	Kansas,	USA
• Thomas Brabec	University of Ottawa	Canada	
• Dimitris Charalambidis	University of Crete	Greece	EU
• Oren Cohen	Technion	Israel	
• Eleftherios Goulielmakis	University of Rostock	Germany	EU
• Jiro Itatani	University of Tokyo	Japan	
• Kyung Taec Kim	Institute for Basic Science	Korea	
• Matthias Kling	Ludwig-Maximilians-Universität	Germany	EU
• François Légaré	INRS	Canada	
• Eva Lindroth	Stockholm University	Sweden	EU
• Johan Mauritsson	Lund University	Sweden	EU
• Daniel M Neumark	UC Berkeley	California	USA
• José Antonio Pérez-Hernández	Pulsed Laser Center (CLPU)	Spain	EU
• Thierry Ruchon	CEA Saclay	France	EU
• Kenneth J Schafer	Louisiana State University	Louisiana	USA
• Olga Smirnova	Max Born Institute	Germany	EU
• Vasily Strelkov	Russian Academy of Sciences	Russia	
• Richard Taieb	Sorbonne Université	France	EU
• John Tisch	Imperial College London	UK	
• Katalin Varjú	ELI ALPS, Szeged	Hungary	EU
• Caterina Vozzi	CNR, Milano	Italy	EU
• Hans Jakob Wörner	ETH Zurich	Switzerland	
• Kun Zhao	Institute of Physics, CAS	China	

Advisory boards

The Local Organizing Committee relies on the expertise and advice of all colleagues working in attosecond science to prepare an event that meets the needs of the international attosecond community at large. To pursue this conversation in a systematic, transparent, and manageable fashion, the Local Organizing Committee has identified a selected group of researchers, representative of the various geographic regions and scientific interests of the attosecond community, who have agreed to serve in a National and an International Advisory Board on the occasion of ATTO VIII. The members of the advisory board received periodic updates on the progress of the conference organization, and hence they had the chance of offering feedback and suggestions on its practical aspects. Furthermore, the advisory board members were asked to bring to the attention of the Local Organizing Committee, as well as, ultimately, of the International Program Committee, any new and relevant research trend in their region and field of interest.

International Advisory Board

• Jens Biegert	ICFO - The Institute of Photonic Sciences	Spain	EU
• Paul Corkum	National Research Council	Canada	
• Nirit Dudovich	Weizmann Institute of Science	Israel	
• Feng He	Shanghai Jiaotong University	China	
• Ursula Keller	ETH Zurich	Switzerland	
• Ferenc Krausz	Max Planck Institute for Quantum Optics	Germany	EU
• Igor Litvinyuk	Griffith University	Australia	
• Jon Marangos	Imperial College London	UK	
• Fernando Martín	Universidad Autónoma de Madrid	Spain	EU
• Chang Hee Nam	Institute for Basic Science	Korea	
• Thomas Pfeifer	Max Planck Institute for Nuclear Physics	Germany	EU
• Françoise Remacle	University of Liège	Belgium	EU
• Pascal Salières	Paris-Saclay University	France	EU
• Kiyoshi Ueda	Tohoku University	Japan	

National Advisory Board

• Andreas Becker	UC Boulder	Colorado	USA
• Nora Berrah	University of Connecticut	Connecticut	USA
• Zenghu Chang	University of Central Florida	Florida	USA
• Lou DiMauro	The Ohio State University	Ohio	USA
• Mette B Gaarde	Louisiana State University	Louisiana	USA
• Wendell Hill	University of Maryland	Maryland	USA
• Stephen R Leone	UC Berkeley	California	USA
• C. William McCurdy	UC Davis	California	USA
• David Reis	Stanford University	California	USA
• Uwe Thumm	Kansas State University	Kansas	USA
• Linda Young	Argonne National Laboratory and U. Chicago	Illinois	USA

Statement on Free Circulation of Scientists

The principle of the Universality of Science is fundamental to scientific progress. This principle embodies freedom of movement, association, expression and communication for scientists, as well as equitable access to data, information and research materials.

In pursuing its objectives with respect to the rights and responsibilities of scientists, the International Union of Pure and Applied Physics (IUPAP) actively upholds this principle, and, in so doing, opposes any discrimination on the basis of such factors as ethnic origin, religion, citizenship, language, political stance, gender, or age. IUPAP should only sponsor conferences and events at institutions and in countries that uphold this principle. If scientists are excluded from attending IUPAP-sponsored international conferences by a host institution or country on the basis of any of these factors, IUPAP should register its concern at the highest level of that institution or country, and should not sponsor any future events in that country until such exclusions have been eliminated.

Statement on Harassment at Conferences

It is the policy of the International Union of Pure and Applied Physics (IUPAP) that all participants in Union activities will enjoy an environment which encourages the free expression and exchange of scientific ideas, and is free from all forms of discrimination, harassment, and retaliation. The conference organisers will name an advisor who will consult with those who have suffered from harassment and who will suggest ways of redressing their problems, and an advisor who will counsel those accused of harassment. The conference organisers may, after due consideration, take such action they deem appropriate.

Inclusivity and Accessibility

We aim for ATTO to be an inclusive and accessible conference for all members of the attosecond community. Gender-neutral bathrooms are located next to the Celeste Hotel's lobby. Attendees who benefit from captioning will be able to follow instant captioning from the zoom stream of the oral sessions from their own device.

Invited speakers

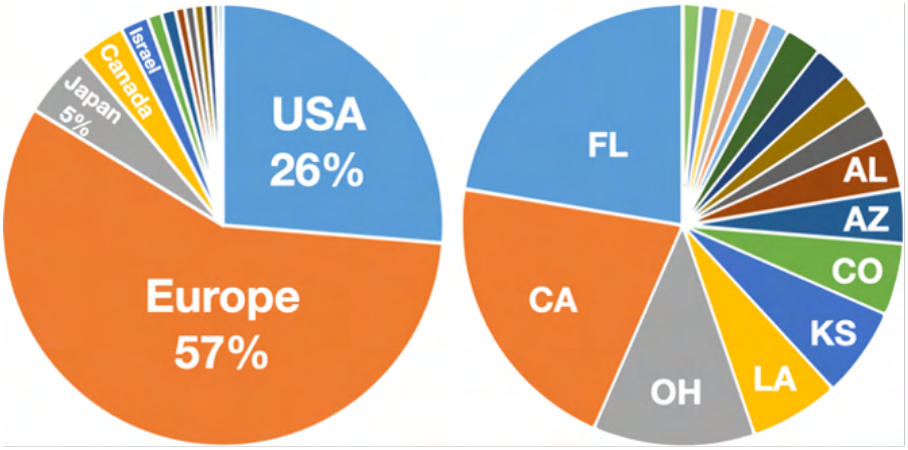
The conference comprises 27 invited speakers from 12 different countries.

• Lou Barreau	Universite Paris-Saclay	France	EU
• Jens Biegert	ICFO	Spain	EU
• Francesca Calegari	CFEL and University of Hamburg	Germany	EU
• Paul Corkum	National Research Council	Canada	
• Nirit Dudovich	Weizmann Institute of Science	Israel	
• Heide Ibrahim	INRS	Canada	
• Mikhail Yu. Ivanov	Max Born Institute	Germany	EU
• Ursula Keller	ETH Zurich	Switzerland	
• Matthias Kling	Stanford University and SLAC	California	US
• Ferenc Krausz	MPI Quantum Optics, Garching	Germany	EU
• Alexandra S Landsman	Ohio State University	Ohio	US
• Stephen R Leone	UC Berkeley	California	US
• Maciej Lewenstein	ICFO and ICREA	Spain	EU
• Anne L'Huillier	Lund University	Sweden	EU
• Eva Lindroth	Stockholm University	Sweden	EU
• Matteo Lucchini	Politecnico di Milano	Italy	EU
• Jon Marangos	Imperial College	UK	
• Agostino Marinelli	SLAC	California	US
• Katsumi Midorikawa	RIKEN Center for Advanced Photonics	Japan	
• Olga Smirnova	Max Born Institute	Germany	EU
• Nina Rohringer	DESY	Germany	EU
• Arvinder Sandhu	University of Arizona	Arizona	US
• Paraskevas Tzallas	IESL, FORTH-Hellas	Greece	EU
• Giulio Vampa	National Research Council of Canada	Canada	
• Caterina Vozzi	Consiglio Nazionale delle Ricerche, Milano	Italy	EU
• Hans Jakob Wörner	ETH Zurich	Switzerland	
• Michael Zuerch	UC Berkeley	California	US

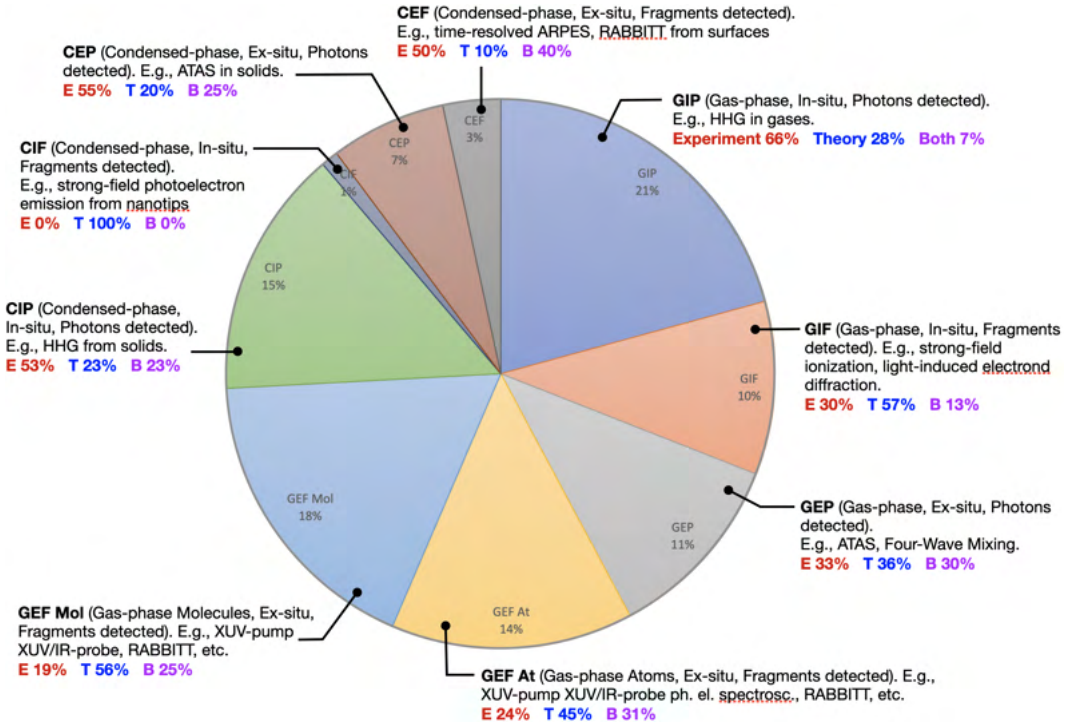
The invited speakers were selected in a process that involved nominations from the IPC, the LOC, and the NAB and IAB, followed by IPC's votes. IPC, NAB and IAB members have not been excluded from being considered as invited speakers. The four members of the IPC who are also invited speakers were considered based on the many nominations from all committees and boards scientists, and were selected through an anonymous vote by all the other IPC members. Once selected, these four speakers were excluded from any further IPC business concerning the conference invited program.

Contributed Abstracts

We have received more than 300 contributed abstracts by the deadline of February 18, 2022. The geographic distribution of the contributed abstracts is exceptionally diverse: 26% come from 18 different states within the United States, and the others 74% come from 30 different countries from all over the world. The abstracts, which have been reviewed by the IPC and the LOC, are all pertinent to the conference and of exceptional quality. None has been rejected.



The contributed abstracts cover the whole set of attosecond topics. We classified them according to four criteria: 1) Gas vs. Condensed Phase; 2) In-situ vs. Ex-situ; 3) Photon vs. Fragment (electrons, ions) detection; 4) Experimental vs. Theoretical vs. Both. Gas-phase ex-situ photoelectron spectroscopies are a third of all the abstracts, so we divided them in atomic and molecular targets.



Conference Proceedings

The conference proceedings will be published as an Open Access book, through an agreement with Springer Nature. Full papers for all invited and contributed talks, the report on the AttoChem post-dinner session, and the transcript of the post-dinner round table session on the future of attosecond science will be included in the proceedings.

Social Program

The social program will include an excursion to the Kennedy Space Center and informal social events on Friday evening and Saturday after the conference. The Saturday excursion will be a visit with BBQ to the Blue Spring State Park. The spring generates a flow of 102 million gallons (390,000 m^3) of mineral water at 73 °F (23 °C), which gives rise to a crystal-clear natural lazy river that winds through lush tropical forest for 0.4 miles ($\sim$600 m) before flowing into St. Johns River.

The interested visitor can book a cruise departing from nearby Port Canaveral or another of Florida's many ports, plan excursions to the gorgeous Florida Keys, historic St. Augustine, Everglades National Park, and the stunning gulf coast beaches, or spend a day at any of the myriad entertainment parks in and around Orlando: Disney's Magic Kingdom, Epcot, Hollywood Studios, and Animal Kingdom parks, Universal Orlando's Universal Studios, Islands of Adventure, and Volcano Bay, Legoland Florida, as well as SeaWorld, Aquatica, and Discovery Cove.

The University of Central Florida

Founded in 1963 as Florida Technological University, the University of Central Florida (UCF) has grown to become the second largest public university in the United States, with more than 70,000 students. UCF offers 106 bachelor's degrees, 95 master's degrees, 31 research doctoral programs, 3 professional doctorates and 3 specialist degree programs. UCF's $\sim$2000 faculty members (the smallest number in the US, compared to the number of students enrolled) raised in 2021 $213M in research funds. STEM disciplines remain a core component of UCF impact. The competitive programming and cyber defense team has repeatedly placed in the top 10 in the Annual Collegiate Programming Contest, and the cyber defense team has won four national championships in the last five years. UCF has been the world's top supplier of graduates to the US aerospace and defence industries for four consecutive years, followed by the University of Florida, the University of Arizona, Penn State University, and the University of Washington. The College of Optics and Photonics, a.k.a. as the Center for Research and Education in Optics and Lasers (CREOL), is the jewel in UCF's crown: while it comprises barely a 2% of the total number of UCF faculty, it attracts almost 10% of the research funds of the whole university. Thanks to CREOL prominent role, to the strong attosecond program at both CREOL and at the Physics department, and the photonic studies at Engineering and the Nanotechnology center, in 2022 US News has ranked UCF Optics program seventh in the Nation, third among public universities, immediately after Berkeley's and UCLA's, and its Atomic, Molecular, and Optical sciences program 12^{th} in the Nation, 5^{th} among public universities, tie with Duke, Princeton, and the University of Chicago.

Attosecond Science at UCF

The attosecond science group at the UCF Physics Department comprises five experimentalists, Dr. Zenghu Chang (Pegasus and BOT Professor), Dr. Michael Chini (Associate Professor), Dr. Li Fang (Assistant Professor), Dr. Madhab Neupane (Associate Professor), Dr. Mihai Vaida (Assistant Professor), and one theoretician, Dr. Luca Argenti (Associate Professor). The group has been highly successful in producing science in high-profile journals, and securing multiple grants, including three DOE career awards and two NSF Career awards. The experimentalists cover virtually all the important areas in attosecond science.

UCF has recently joined LaserNetUS, a consortium of high-power laser facilities in the US and Canada that have been funded by the DOE Office of Fusion Energy Sciences to dedicate a fraction of their operational time to supporting user experiments awarded by the network. Beginning in 2023, UCF will offer user time on multiple high-energy, long-wavelength femtosecond laser facilities, and aims to contribute to the network by developing high-intensity laser sources in new parameter spaces – specifically mid-infrared wavelengths and few-cycle pulse durations.

Useful Information

PARKING

If you are travelling by car, you can either purchase a parking permit at the Conference Hotel. A more economical option is to park the car in the UCF Parking Garage A, which is right in front of the Conference Hotel, across Gemini Boulevard. The daily cost for parking in Garage A is of $5, no permit is required for Saturdays or Sundays, and permits may be purchased for one day or up to 5 consecutive days from the day of purchase.

FOOD & BEVERAGES

Coffee breaks and boxed lunches (Mon, Tue, Thu) are included in the registration. Dinners are not included, nor are lunches on Wednesday 13 (visit to the KSC) and Friday 15 (end of conference). Tickets to the conference banquet must be paid separately. For the other days, there are several restaurants across the street, where participants can have dinner and drinks. Many of those business have granted variable discounts to the attendees of the ATTO VIII Conference. If you want to take advantage of those discounts, therefore, remember to bring your badge or discount coupon.

DIETARY RESTRICTIONS

We will try to accommodate dietary requests, following the data we collected in the registration survey. Participants with severe allergies must alert the conference chairs well in advance of the conference, and bring any allergy medication their doctors may prescribe. Participants must take primary responsibility for their own health.

MOBILE PHONES

As a courtesy to the other participants, please make sure your mobile is in silent mode during all the sessions and social functions.

INTERNET ACCESS

Internet will be available at the hotel. At MIRC you can connect either through eduroam or UCF_Guest.

HEALTH INSURANCE

We urge participants from outside the US to make sure they have health-care coverage in the US, either through their employer or by purchasing a private insurance. Even if it may come to you as a surprise, the United States do not have universal health coverage, let alone one for foreign visitors.

WEATHER

July climate in Central Florida tends to be highly predictable. The average day starts with a balmy temperature of 25-26 °C, it may grow to 28 / 32 °C, depending on whether the sky is overcast or not. Towards the evening, dark clouds from the sea come inland for a Summer shower that lowers the temperature somewhat. Historically, the average temperature in July is 28 degrees. July in 2021 has been particularly mild. The humidity is high, but not extreme. Central Florida has one of the best air quality in the Western world.

Monday, July 11, 2022

08:15 - 08:30 **ATTO VIII OPENING Session in Celeste Ballroom**
Chair: **Luca Argenti**, University of Central Florida, Florida, USA

Alexander N. Cartwright, UCF President

Michael D. Johnson, UCF Provost

Maggy Tomova, Dean of UCF College of Sciences

David J. Hagan, Dean of UCF College of Optics
Joshua Colwell, Chair of UCF Physics Dep.

08:30 - 10:00 **M1 Wolf-Prize Session** 2
Chair: **Michael Chini**, University of Central Florida, Florida, USA

08:30 **Anne L'Huillier**, Lund University, Sweden, EU
I: *An introduction to attosecond pulses and attosecond physics* 3

09:00 **Paul Corkum**, University of Ottawa, Canada
I: *Using nonlinear optics to measure attosecond dynamics* 4

09:30 **Ferenc Krausz**, Ludwig-Maximillian University, Germany, EU
I: *Attosecond Metrology 2.0: From Tracking Electronic Motion to Probing Human Health* 5

10:00 - 10:15 **Coffee Break**

10:15 - 11:30 **M2 Chiral Effects in Attosecond Science** 6
Chair: **François Légaré**, INRS, Québec, Canada

10:15 **Olga Smirnova**, Max Born Institute Berlin, Germany, EU
I: *Ultrafast Chirality: twisting light to twist electrons* 7

10:45 **Debobrata Rajak**, Université de Bordeaux, France, EU
C: *Asymmetric electron re-scattering in strong-field ionization of chiral molecules* 8

11:00 **Joshua Vogwell**, Imperial College London, United Kingdom
C: *Imaging molecular chirality on ultrafast timescales via enantio-sensitive sum-frequency generation* 9

11:15 **Andrés F. Ordóñez**, ICFO - Institut de Ciencies Fotoniques, Spain, EU
C: *Symmetry-protected chiral sensitivity in photoionization with bichromatic fields* 10

11:30 - 11:45 **Coffee Break**

Monday, July 11, 2022

11:45 - 13:00 **M3 Imaging and Control of Molecular Structure** 11
Chair: **Katalin Varjú**, ELI ALPS, Szeged, Hungary, EU

11:45 **Heide Ibrahim**, INRS, Canada
I: *Imaging ultrafast Dissociation Dynamics: Roaming in Formaldehyde* . . 12

12:15 **Francoise Remacle**, University of Liege, Belgium, EU
C: *Exploiting electronic coherences for steering selective bond formation in molecules pumped by ultrashort optical pulses* 13

12:30 **Pradrag Ranitovich**, LBNL, California, USA
C: *Control of Non-Equilibrium ICD Dynamics in Argon and Ethylene Dimers by Attosecond XUV and VUV Radiation* 14

12:45 **Katharina Chirvi**, ICFO - Institut de Ciencies Fotoniques, Spain, EU
C: *Retrieving a complex molecular structure from laser-induced electron diffraction using machine learning* 15

13:00 - 14:00 **Lunch Break**

14:00 - 16:00 **M4 Strong-Field Nonlinear Optics in Solids** 16
Chair: **Kyung Taec Kim**, IBS, Korea

14:00 **Matthias Kling**, Stanford University, California, USA
I: *Petahertz field sampling below the diffraction limit* 17

14:30 **Michael Zuerch**, UC Berkeley, California, USA
I: *Ultrafast Second-harmonic XUV Spectroscopy: A Novel Probe for Symmetry at Interfaces and in Quantum Materials* 18

15:00 **Tran-Chau Truong**, University of Central Florida, Florida, US
C: *Single-shot laser waveform measurement of short-wave infrared pulses* 19

15:00 **Natalie Nagl**, Max Planck Institute for Quantum Optics, Germany, EU
C: *Single-cycle infrared waveform generation and control* 20

15:15 **Mohammed Hassan**, University of Arizona, Arizona, USA
C: *Attosecond electron motion control* 21

15:30 **Markus Borsch**, University of Michigan, Michigan, US
C: *Ultrafast Momentum Combs for Electron-Band Tomography* 22

Monday, July 11, 2022

16:00 - 16:15 **Transfer to MIRC for Poster Session**

16:15 - 16:45 **Poster Highlights**

Highlights A 102
Chair: **Mathieu Gisselbrecht**, Department of Physics, Lund University, Sweden, EU

Highlights B 112
Chair: **Cord L. Arnold**, Lund University, Sweden, EU

Highlights C 122
Chair: **Thierry Ruchon**, LIDYL-CEA Saclay, France, EU

16:45 - 18:30 **Poster Session I** 192

18:30 - 20:00 **Dinner Recess**

20:00 - 21:00 **ME US Funding Opportunities in Attosecond Science** 23
Chair: **Uwe Thumm**, Kansas State University, Kansas, USA
AMOS Program

20:00 **Kevin Jones**, National Science Foundation
NSF programs of interest to the attosecond community

20:15 **James Joseph**, Army Research Office
Modern Optics Program

20:30 **Andrew Stickrath**, Air Force Office of Scientific Research

20:45 **Q&A**

Tuesday, July 12, 2022

08:30 - 11:00 **T1 Attosecond Photoionization Dynamics** 24
Chair: **Pascal Salières**, Paris-Saclay University, France, EU

08:30 **Eva Lindroth**, Stockholm University, Sweden, EU
I: *Photoionization delay in heavy atomic ions* 25

09:00 **Alexandra S Landsman**, Ohio State University, USA
I: *Tracking the ionization site in neutral molecules* 26

09:30 **Richard Taïeb**, Sorbonne Université, France, EU
C: *Real-time imaging of resonant photoemission dynamics* 27

09:45 **Miguel Alarcon**, Purdue University, USA
C: *Theoretical treatment of quantum beats in Argon.* 28

10:00 **Vicent Borràs**, Universidad Autónoma de Madrid, Spain, EU
C: *The effect of Feschbach resonances on the different vibrational states of N_2 in a RABBIT experiment.* 29

10:15 **Juan Martín Randazzo**, CONICET, Argentina
C: *ASTRA, a transition-density-matrix solution to the close-coupling problem in the molecular ionization continuum* 30

10:30 **Tomoya Mizuno**, University of Tokyo, Japan
C: *Experimental investigation of topological property of degenerate singularities in rescattering processes* 31

10:00 - 10:15 **Coffee Break**

11:00 - 13:00 **T2 Attosecond dynamics in low-D materials** 32
Chair: **Madhab Neupane**, University of Central Florida, Orlando, FL, USA

11:00 **Ursula Keller**, ETH Zürich, Switzerland
I: *Element Specific Screening Dynamics in $MoSe_2$* 33

11:30 **Mikhail Yu. Ivanov**, Max-Born-Institut, Germany, EU
I: *Lightwave electronics in trivial and strongly correlated solids* 34

12:00 **Alexis Chacon**, POSTECH, Republic of Korea
C: *Ultrafast spectroscopy of 3D-topological insulators by high-order harmonics* 35

12:15 **Amar Bharti**, Indian Institute of Technology Bombay, India
C: *High-Harmonic spectroscopy of nonlinear anisotropic anomalous Hall effect in topological materials* 36

12:30 **Sambit Mitra**, Max-Planck-Institute for Quantum Optics, Germany, EU
C: *Strong light-field controlled valleytronics* 37

12:45 **Jakub Schusser**, University of Würtzburg, Germany, EU
C: *Spin-, time- and angle-resolved photoemission spectroscopy (STARPES) on the transition metal dicalchogenide WTe_2* 38

13:00 - 14:00 Lunch Break

14:00 - 16:00 T3 High Order Harmonic Spectroscopy and Control 39
Chair: **Wendell T. Hill**, University of Maryland, Maryland, USA

14:00 **Nirit Dudovich**, Weizmann Institute of Science, Israel
I: *Attosecond Interferometry* 40

14:30 **Giulio Vampa**, National Research Council of Canada, Canada
I: *Nano-scale focusing of solid-state high harmonics* 41

15:00 **Toby Barnard**, Imperial College London, United Kingdom
C: *EUV high harmonic generation from a thin sheet of isopropanol* . . 42

15:15 **Christian Heide**, SLAC National Accelerator Laboratory, California, USA
C: *Controlling solid-state high-harmonics in monolayers via artificial stacking* 43

15:30 **Shima Gholam Mirzaeimoghadar**, JASL, Canada
C: *High Harmonic generation from metals* 44

15:45 **Igor Tyulnev**, ICFO - Institut de Ciencies Fotoniques, Spain, EU
C: *High harmonic spectroscopy of quantum phase transitions in a high-Tc superconductor* 45

16:00 - 16:15 Transfer to MIRC for Poster Session

16:15 - 16:45 Poster Highlights

Highlights A 102
Chair: **Mihai Vaida**, University of Central Florida, Florida, USA

Highlights B 112
Chair: **Richard Taïeb**, Sorbonne Université, France, EU

Highlights C 122
Chair: **Nicolas Douguet**, Kennesaw University, Georgia, USA

16:45 - 18:30 Poster Session II 255

Tuesday, July 12, 2022

18:30 - 20:00 **Dinner Recess**

20:00 - 21:00 **TE Overview of AttoChem Network** 46

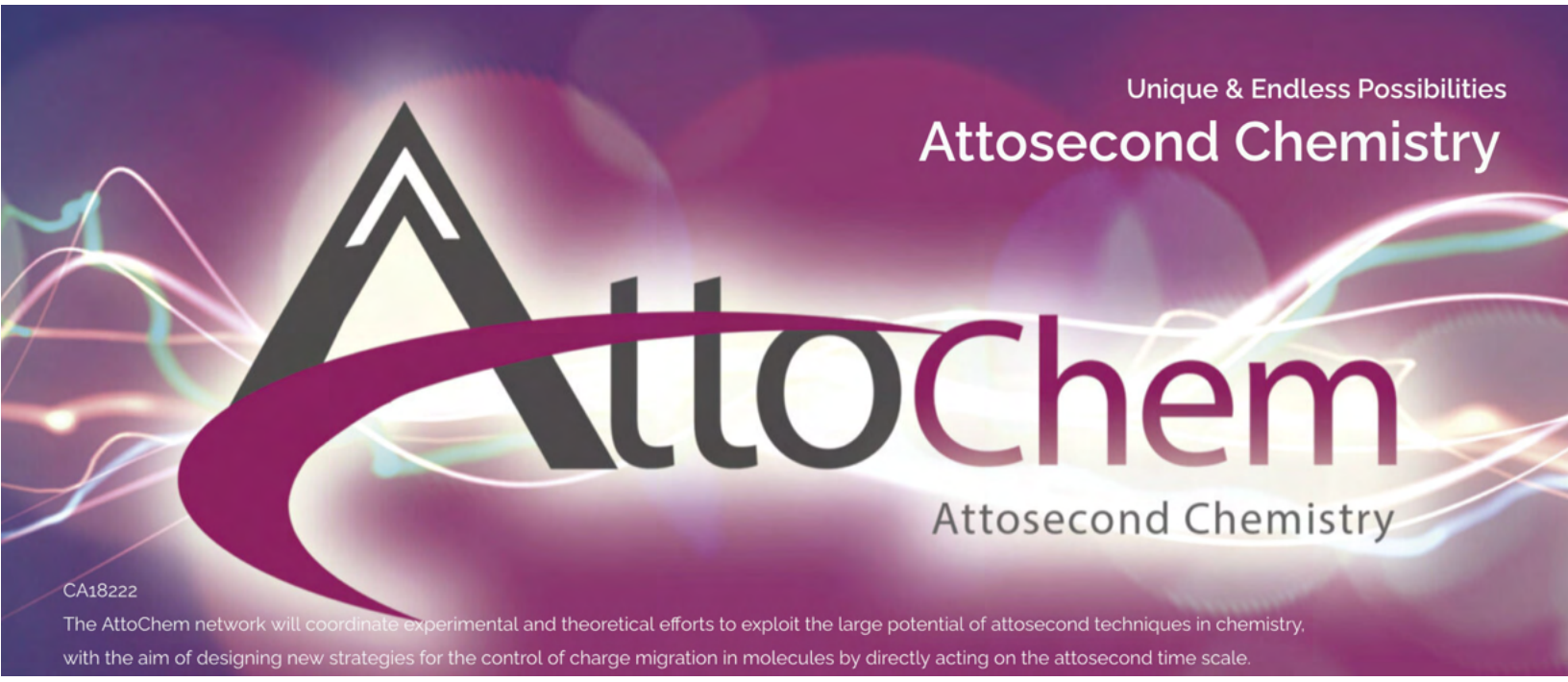
Chair: **Per Eng-Johnsson**, Lund University, Sweden, EU

20:00 **Fernando Martín**, Universidad Autónoma de Madrid, Spain, EU
The AttoChem Network

20:15 **Caterina Vozzi**, CNR, Milano, Italy, EU
WG1: New attosecond techniques for the control of electron dynamics in molecules

20:30 **Fernando Martín**, Universidad Autónoma de Madrid, Spain, EU
WG2: Computational tools for the description of attosecond electron and nuclear dynamics

20:45 **Francesca Calegari**, DESY, Germany, EU
WG3: Attosecond imaging and control of charge migration and chemical reactivity



Wednesday, July 13, 2022

07:45 - 08:00 **Boarding for Transfer to Kennedy Space Center**

08:00 - 09:00 **Transfer to Kennedy Space Center**

09:00 - 12:00 **Visit Kennedy Space Center**

12:00 - 12:45 **Lunch Break**

12:45 - 13:00 **Boarding for Transfer to Conference Hotel**

13:00 - 14:00 **Transfer from Kennedy Space Center to Conference Hotel**

14:00 - 14:15 **Coffee Break**

14:15 - 16:30 **W1 Attosecond Spectroscopy in Condensed Matter** 48
Chair: **Mette B Gaarde**, Louisiana State University, Louisiana, USA

14:15 **Jens Biegert**, ICFO - Institut de Ciencies Fotoniques, Spain, EU
I: *Attosecond soft X-rays revealing energy flow in materials* 49

14:45 **Matteo Lucchini**,Politecnico di Milano, Italy, EU
I: *Attosecond exciton dynamics in dielectrics* 50

15:15 **Fernando Martín**, Universidad Autónoma de Madrid, Spain, EU
C: *Real Space-Time sub femtosecond imaging of electron dynamics in molecules* 51

15:30 **Arthur Niedermayr**, ETH Zürich, Switzerland
C: *Few-femtosecond dynamics of free-free opacity in optically heated metals* 52

15:45 **Thierry Ruchon**, LIDYL - CEA Saclay, France, EU
C: *Magnetic helicoidal dichroism with XUV light carrying orbital angular momentum* 53

16:00 **Saijoscha Heck**, ETH Zürich, Switzerland
C: *Attosecond spectroscopy of water clusters* 54

16:15 **Katherine Légaré**, INRS, Canada
C: *Ultrafast magnetic scattering on rare-earth ferrimagnets enabled by a bright Yb-based soft X-ray source* 55

16:30 - 16:45 **Coffee Break**

Wednesday, July 13, 2022

16:45 - 18:30 **W2 XFELs for Ultrashort XUV/X-ray Science** 56
Chair: **Linda Young**, Argonne National Laboratory and U. Chicago, Illinois, USA

16:45 **Nina Rohringer**, CFEL - DESY - Universität Hamburg, Germany, EU
I: *Momentum resolved XUV polariton measurements by x-ray parametric down conversion* 57

17:15 **Agostino Marinelli**,SLAC National Accelerator Laboratory, USA
I: *Attosecond pulses from X-ray free-electron lasers* 58

17:45 **Claudio Emma**, SLAC National Accelerator Laboratory, USA
C: *A terawatt attosecond soft X-ray source based on a plasma accelerator-driven free electron laser* 59

18:00 **Francis Penent**, Sorbonne Université - CNRS, France, EU
C: *An atomic two-color XUV interferometer* 60

18:15 **Marcus Dahlström**, Lund University, Sweden, EU
C: *Rabi dynamics driven by a seeded FEL at XUV-wavelengths* 61

18:30 - 20:00 **Dinner Recess**

20:00 - 21:00 **WE The Future of Attosecond Science** 62
Chair: **Li Fang**, University of Central Florida, Florida, USA

Mina Bionta, MIT, Massachussets, USA

Mette B Gaarde, Louisiana State University, Louisiana, USA

Ursula Keller, ETH, Zürich, Switzerland

Alexandra S Landsman, Ohio State University, Ohio, USA

Maria Richter, Max Born Institute, Germany, EU

Nina Rohringer, Hamburg, Germany, EU

Linda Young, Argonne National Laboratory and U. Chicago, Illinois, USA

Nirit Dudovich, Weizmann Institute of Science, Rehovot, Israel

Thursday, July 14, 2022

08:30 - 10:45 **R1 Time-Resolved Charge Migration** 63
Chair: **Mauro Nisoli**, Politecnico di Milano, Italy, EU

08:30 **Francesca Calegari**, Deutsches Elektronen-Synchrotron, Germany, EU
I: *Realtime observation of el. processes in ionized and neutral molecules.* . . 64

09:00 **Jon Marangos**, Imperial College London, United Kingdom
I: *Ultrafast X-ray probing of electron and electron-nuclear coupling dynamics in molecules and organic semiconductors* 65

09:30 **Aderonke Folorunso**, Louisiana State University, USA
C: *Chemical Control Of Attosecond Charge Migration.* 66

09:45 **Taran Driver**, Stanford PULSE Institute/SLAC, USA
C: *Attosecond Science at the LCLS.* 67

10:00 **Patrick Rupprecht**, Max-Planck-Institut für Kernphysik, Germany, EU
C: *Control of el. exchange inside a molecule with ultrafast laser pulses.* . . 68

10:15 **Danylo Matselyukh**, ETH Zürich, Switzerland
C: *Direct measurement of few-femtosecond charge transfer mediated by a conical intersection.* 69

10:30 **Omer Kneller**, Weizmann Institute of Science, Israel
C: *A look under the tunneling barrier via attosecond-gated interferometry* 70

10:45 - 11:00 **Coffee Break**

11:00 - 13:00 **R2 Table-Top Attosecond Sources** 71
Chair: **Zenghu Chang**, University of Central Florida, Florida, USA

11:00 **Caterina Vozzi**, CNR, Milano, Italy, EU
I: *Bright coherent XUV generation in microfluidic glass devices for ultrafast x-ray spectroscopy.* 72

11:30 **Katsumi Midorikawa**, RIKEN, Japan
I: *Increase in photon flux of isolated attosecond pulses.* 73

12:00 **Ming-Chang Chen**, NTHU, Taiwan
C: *Generation of isolated-attosecond pulses driven by a post-compressed Yb laser* 74

12:15 **Roland E. Mainz**, Center for Free-Electron Laser Science, Germany, EU
C: *Tunable isolated attosecond pulse generation by sub-cycle optical pulses from a parametric waveform synthesizer.* 75

12:30 **Yi Wu**, University of Central Florida, USA
C: *100-GW 2.5-μm pulses generation by a double-stage Cr^{2+}:ZnSe amplifier* 76

12:30 **Stefan Haessler**, Laboratoire d'Optique Appliquée (LOA), France, EU
C: *Attosecond control of relativistic plasma mirror emission* 77

13:00 - 14:00 Lunch Break

14:00 - 16:00 R3 Attosecond transient absorption and four-wave mixing 78
Chair: **Thomas Pfeifer**, Max Planck Institute for Nuclear Physics, Heidelberg, Germany, EU

14:00 **Stephen R Leone**, University of California, Berkeley, USA
I: *Dynamics Via Attosecond Four Wave Mixing.* 79

14:30 **Arvinder Sandhu**, University of Arizona, USA
I: *Autoionizing polaritons and Raman interferometry: Advances in measurement and control of electron dynamics in the continuum.* 80

15:00 **Zhong Yin**, ETH Zürich, Switzerland
C: *Photoinduced Proton Transfer Dynamics in Aqueous Urea Solution Probed by Water-Window X-ray Absorption Spectroscopy.* 81

15:15 **Vyacheslav Leshchenko**, Ohio State University, USA
C: *Phase-resolved XUV transient absorption spectroscopy of argon.* 82

15:30 **Valentina Utrio Lanfaloni**, ETH Zürich, Switzerland
C: *Jahn–Teller dynamics in CH_4^+ probed at the carbon K-edge.* 83

15:45 **Nikolay Golubev**, EPFL, Switzerland
C: *Core-Valence Attosecond Transient Absorption Spectroscopy of Polyatomic Molecules.* 84

16:00 - 16:15 Transfer to MIRC for Poster Session

16:15 - 16:45 Poster Highlights

Highlights A 102
Chair: **Cosmin Blaga**, Kansas State University, Kansas, USA

Highlights B 112
Chair: **Jan Marcus Dahlström**, Lund University, Sweden, EU

Highlights C 122
Chair: **Jiro Itatani**, Tokyo University, Japan

16:45 - 18:30 Poster Session III 326

18:30 - 20:00 Conference Dinner

Friday, July 15, 2022

08:30 - 10:45 **F1 Entanglement in attosecond processes** 85
Chair: **C. William McCurdy**, University of California Davis & LBNL, California, USA

08:30 **Paraskevas Tzallas**, FORTH-IESL, Greece, EU
I: *Generation of optical Schrödinger "cat" states using "conditioning" approaches in intense laser-atom interactions.* 86

09:00 **Maciej Lewenstein**, ICFO and ICREA, Spain, EU
I: *Attosecond Physics and Quantum Information Science.* 87

09:30 **Matan Even Tzur**, Technion - Israel Institute of Technology, Israel
C: *High Harmonic Generation Driven by Quantum Light.* 88

09:45 **Charles Bourassin-Bouchet**, Institut d'Optique, France, EU
C: *Quantifying the decoherence of attosecond electron wavepackets.* . . . 89

10:00 **Lisa-Marie Koll**, MBI, Germany, EU
C: *Experimental control of quantum-mechanical entanglement in an attosecond pump-probe experiment.* 90

10:15 **Farshad Shobeiry**, Max-Planck-Institut für Kernphysik, Germany, EU
C: *Sub-femtosecond optical control of entangled states.* 91

10:30 **Sebastian Eckart**, Goethe University Frankfurt, Germany, EU
C: *Ultrafast preparation and detection of entangled atoms.* 92

10:45 - 11:00 **Coffee Break**

11:00 - 13:00 **F2 Laser Driven Dynamics in Molecules** 93
Chair: **Marc Vrakking**, Max-Born Institute, Berlin, Germany, EU

11:00 **Hans Jakob Wörner**, ETH Zürich, Switzerland
I: *Advances in attochemistry.* 94

11:30 **Lou Barreau**, CEA LIDYL, France, EU
I: *Multimode molecular vibrations observed with few-femtosecond X-ray transient absorption at the S L-edge and C K-edge.* 95

12:00 **Andrea Trabattoni**, Deutsches Elektronen-Synchrotron, Germany, EU
C: *An ultrafast photoelectron clock in molecular strong-field rescattering.* . 96

12:15 **Jiro Itatani**, University of Tokyo, Japan
C: *Attosecond electronic dynamics of core-excited states of N_2O probed by transient soft X-ray spectroscopy.* 97

Friday, July 15, 2022

12:30 **Rui E. Ferreira da Silva**, Universidad Autónoma de Madrid, Spain, EU
C: *Polaritonic molecular clock for all-optical ultrafast imaging of wavepacket dynamics without probe pulses.* 98

12:45 **Victor Despré**, Universität Heidelberg, Germany, EU
C: *Ab-initio simulations of ultrafast electron-nuclear dynamics: Paving the way to attochemistry.* 99

13:00 - 14:00 Lunch Recess

14:00 - 16:00 Visit to UCF Attosecond Labs

Saturday, July 16, 2022

6:30 - 22:30 Informal Social Excursion

6:30-6:45 **Pick up Folks**, Celeste Hotel

6:45-7:45 **Travel to Blue Springs**

7:45-8:15 **Enter Blue Springs**

8:15-8:45 **Take possession of a BBQ**

8:45-11:00 **Kayak / Swimm / Walk**

11:00-13:00 **BBQ**,

13:00-13:30 **Gathering to leave**

13:30-14:30 **Traveling Back to Hotel**

14:30-15:00 **Travel to Fort Christmas**

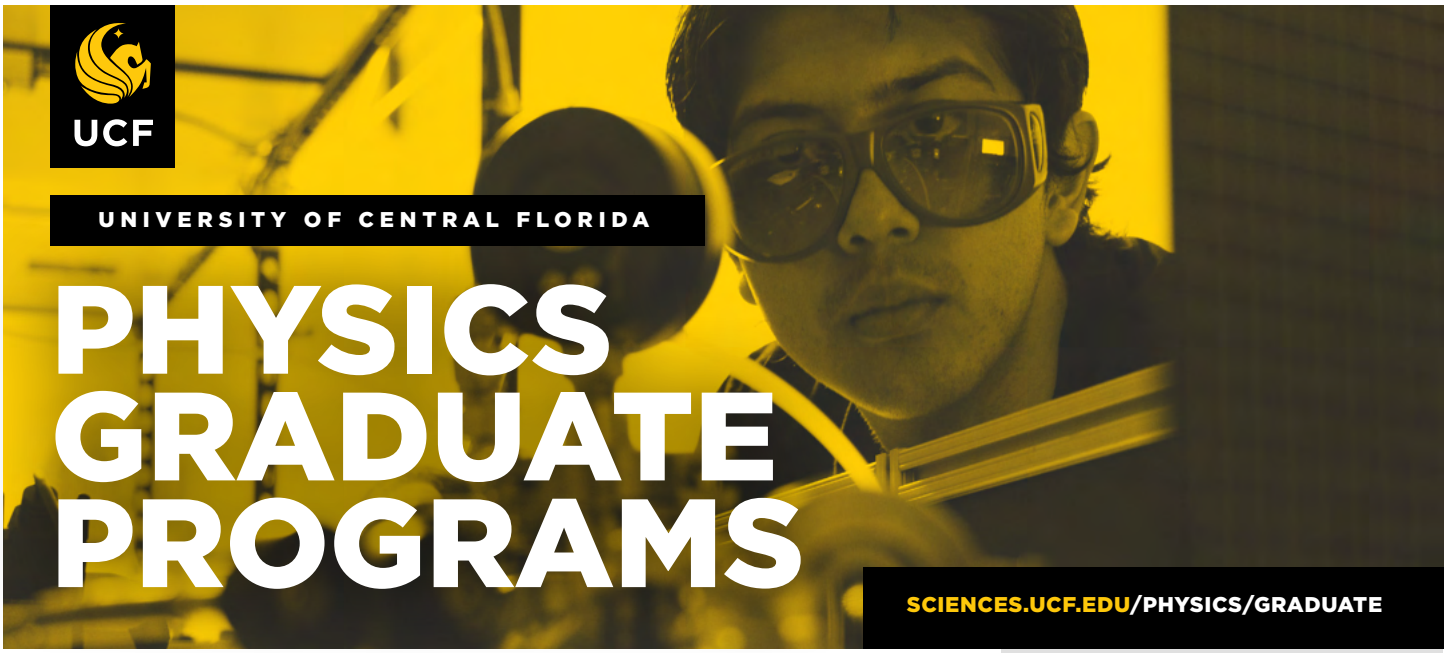
15:00-16:30 **Visit Fort Christmas**

16:30-17:00 **Return to Hotel**

18:00-18:30 **Travel Downtown / Universal**

18:30-21:30 **Tour and Dine**

21:30-22:00 **Return to Hotel**

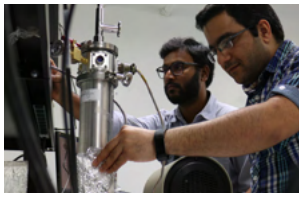


UCF

UNIVERSITY OF CENTRAL FLORIDA

PHYSICS GRADUATE PROGRAMS

SCIENCES.UCF.EDU/PHYSICS/GRADUATE



ATOMIC, MOLECULAR & OPTICAL

- Attosecond Physics
- Nonlinear Optics
- Ultra-Cold Collisions
- Light-Matter Interactions, Nanophotonics, and Optoelectronics



SOFT MATTER AND BIOLOGICAL PHYSICS

- Dynamics and micro-spectorscopy of soft matter systems
- Structure and function of proteins and biological assemblies
- Theoretical and computational soft matter and biological physics
- Molecular mechanisms of human diseases



CONDENSED MATTER

- Quantum Computation
- Topological Materials
- Nanomagnetism
- Surface Science



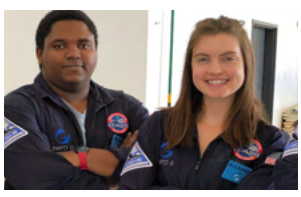
NANOSCIENCE

- 2D Materials
- Nanodevices
- Nanocatalysis and Fuel Cells
- Single-Molecule Magnets



PHYSICS EDUCATION RESEARCH

- Variation across physics learners
- Evaluating the efficiency of lessons
- Inclusive teaching techniques
- Tactics for online teaching



PLANETARY SCIENCES

- Remote Sensing
- Exoplanets
- Regolith and In-Situ Resource Utilization
- Microgravity and Cubesats

12 **BEST AMO PROGRAMS**
U.S. News and World Report

61 **BEST PHYSICS SCHOOLS**
U.S. News and World Report

100+ Graduate Students

- 30% Female
- 28% Under-represented minority

57 Current Faculty

- 20-25 person class size

Graduate Teaching Assistantship

- Guaranteed in the first year
- Tuition waiver
- Free health insurance

All Ph.D. students are supported by teaching or research assistantships, fellowships, scholarships, or other funding.

Deadline

- Apply by January 15 for full consideration

UCF Department of Physics

@UCFPhysics
@UCFPhysics

UCF Women in Physics Society

@ucf.wips
@ucfwips

M1 Wolf-Prize Session ▲

M1



Anne L'Huillier



Paul Corkum



Ferenc Krausz

"Anne L'Huillier, Paul Corkum, and Ferenc Krausz share the 2022 Wolf Prize in Physics for pioneering and novel work in the fields of ultrafast laser science and attosecond physics and for demonstrating time-resolved imaging of electron motion in atoms, molecules, and solids. Each of them made crucial contributions, both to the technical development of attosecond physics and to its application to fundamental physics studies."

[Wolf Foundation]

08:30 - 10:00 **M1 Wolf-Prize Session**
Chair: **Michael Chini**, University of Central Florida, Florida, USA

08:30 **Anne L'Huillier**, Lund University, Sweden, EU
I: *An introduction to attosecond pulses and attosecond physics* 3

09:00 **Paul Corkum**, University of Ottawa, Canada
I: *Using nonlinear optics to measure attosecond dynamics* 4

09:30 **Ferenc Krausz**, Ludwig-Maximillian University, Germany, EU
I: *Attosecond Metrology 2.0: From Tracking Electronic Motion to Probing Human Health* 5

An introduction to attosecond pulses and attosecond physics

A L'Huillier[1] *

[1]Department of Physics, Lund University, Lund, SE-22 100, Sweden

Synopsis After a brief historical perspective on the field of harmonic generation in gases, an introduction to the physics of the process will be given covering the single atom response and phase matching. The presentation will also discuss laser-assisted photoionization, used both for measurement and application of attosecond pulses.

Extreme Ultraviolet light sources based on high-order harmonic generation (HHG) in gases are now used in many areas of science. The radiation consists of a train of extremely short light bursts, in the attosecond range, allowing for outstanding temporal resolution. HHG has opened the field of attosecond science, capturing ultrafast electron dynamics in matter [1]. This presentation will give a short historical perspective on this field of research.

The HHG efficiency depends both on the response of a single atom to a strong laser field and, as in any coherent nonlinear optical process, on the phase matching between the waves emitted by individual atoms in a macroscopic medium. An introduction to the physics of HHG will be given, covering both aspects of the process. The importance of phase matching is illustrated in Figure 1, showing the conversion efficiency of the 23rd harmonic in argon. A good conversion efficiency can be obtained both with a long medium, low pressure and a short medium, high pressure, allowing for versatile setups. The implications of geometrical scaling [2] and wavelength scaling [3] will be discussed.

Attosecond sources undergo a rapid development today due to progress in laser technology, offering driving lasers covering a large range of central wavelengths, repetition rates and average/peak powers. An orientation about the evolution of the parameters and properties of attosecond sources will be given.

The short pulse duration and broad bandwidth of attosecond pulses allow the measurement of the phase and amplitude of an ionizing electronic wave packet using interferometric techniques. We will describe in particular the RABBIT (reconstruction of attosecond beating by two-photon transition) method [5], which has been used first for the measurement and characterization of attosecond pulses, then for measuring ultrafast dynamics of photoionization processes [6].

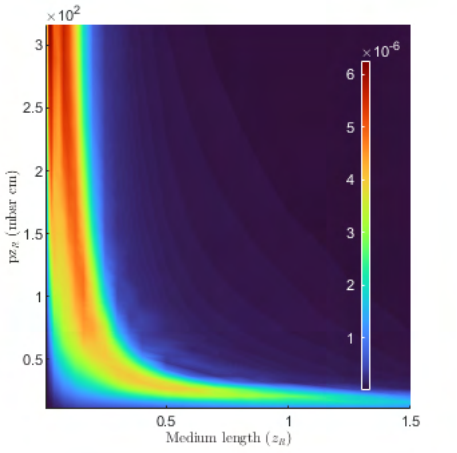


Figure 1. Conversion efficiency of the 23rd harmonic of 800 nm radiation generated in argon at an intensity of 2.5 x10^{14} W/cm^2. z_R denotes the Rayleigh length. Adapted from [1].

References

[1] F. Krausz and M. Ivanov, Rev. Mod. Phys. 81, 163 (2009)
[2] R. Weissenbilder R et al arXiv:2202.08202 (2022)
[3] B. Sheehy et al., Phys. Rev. Lett. 83, 5270 (1999); T. Popmintchev et al., Science 336, 1287 (2012)
[4] C. M. Heyl et al., J. Phys. B, 50, 013001 (2017)
[5] P.-M. Paul et al., Science 292, 1689 (2001)
[6] K. Klünder et al., Phys. Rev. Lett. 106, 143002 (2011)

* E-mail: anne.lhuillier@fysik.lth.se

Connecting attosecond time delay to recollision trajectories

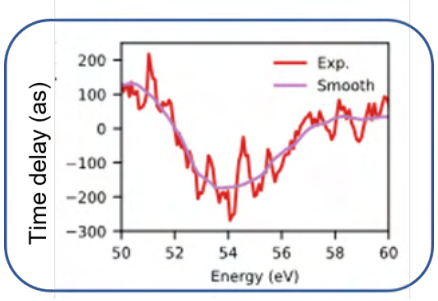
P B Corkum [*], G G Brown, D H Ko, and C Zhang

Joint Attosecond Science Lab, University of Ottawa and the National Research Council, Ottawa, K1N 6N5, Canada

Synopsis We describe how all-optical recollision electron trajectory measurements allow us to determine attosecond photoionization/photorecombination time delays.

Any short pulse is composed of many frequencies that are synchronized in phase to construct the pulse. Thus, a short pulse is an interference in time. Attosecond time delays are closely related. An electron pulse leaves an atom (molecule or its associated hole in the case of a solid) with a spectral phase that it gains from the optical pulse that created it and an additional complex phase of the transition moment. It is the latter that we aim to measure with attosecond time delay.

Argon is a good example. Near the Cooper minimum, argon has a two-lobed radial wavefunction that describes the 3p state of the valence electron. The phase of the transition moment in this region describes the change in the relative importance of different lobes of the transition moment as we move through the Cooper minimum. That is, we change the weighted average of where a photoelectron is formed or where a recollision electron recombines. If we change the endpoint, we change the recollision trajectory. Of course, the light-imposed trajectory also has an atto-chirp. Therefore, attosecond time delay will show up as a change in the atto-chirp. The figure shows the time delay that we measure.



We discuss argon because it provides a very physical means to see the link between trajectories and the transition moment phase. The strong field approximation provides a more mathematical justification. In the strong field approximation, classical trajectories arise from the saddle point approximation to the rapidly varying imaginary terms. In the equations, there is no distinction between the components of the imaginary contributions. The transition moment phase is as important as the kinetic phase of the driven electron. Thus, the trajectory is sensitive to the transition moment phase [1].

The phase of the transition moment encodes other phenomena than the Cooper minimum. In a many-electron atom, it encodes the interaction between the active electron and the others. For example, phase changes in xenon due to the giant plasmon resonance should modify recollision trajectories, as should the Fano resonances in helium.

Of course, the time of birth can also play a role and can, in principle, also be measured. In the case of H_2^+ with widely separated atoms, the relative change in position of birth and recollision cancel with each other, making both unresolvable.

There will be an ultimate time response of electronic matter. As a typical molecule gets larger, the number of electrons will increase in proportion to their volume. The fastest possible response of this "plasma" will be the plasma response (about 30 as). To measure such a fast response will require high frequency radiation, a method of accurately determining the atto-chirp and a means of using all available photons. The latter is now solved with single image measurement [2].

References

[1] G G Brown, D H Ko, C Zhang, P B Corkum, Phys. Rev. A **105,** 023520 (2022).

[2] D H Ko, G G Brown, C Zhang, P B Corkum, Optica **8,** 1632 (2021).

[*] E-mail: pcorkum@uOttawa.ca

ATTOSECOND METROLOGY 2.0
From Tracking Electronic Motions to Probing Human Health

F Krausz[1,2] *

[1]Max Planck Institute of Quantum Optics, Garching, 85748, Germany
[2]Ludwig-Maximilians-Universität München, Munich, 80539, Germany

Next-generation attosecond metrology (2.0) relies on sub-fs charge carrier injection into wide-gap materials. The injected carriers can be used to directly probe fundamental processes of ultrafast optoelectronics and sample optical fields up to PHz frequencies. Light fields from the infrared to the ultraviolet, with accurately measured temporal evolution, serve as a unique probe for the polarization response of matter. Field-resolved spectroscopy will access valence electronic as well as nuclear motions in all forms of matter and constitutes a generalization of pump-probe approaches. The multi-MHz-rate synthesis and measurement of infrared waveforms with 1-attosecond-scale precision opens the door for real-world applications. They include probing of human health by measuring miniscule changes of the molecular composition of blood (liquid biopsy) via field-resolved vibrational molecular fingerprinting.

* E-mail: ferenc.krausz@mpq.mpg.de, krausz@lmu.de
* Website: www.attoworld.de

M2 Chiral Effects in Attosecond Science ▲

M2

10:15 - 11:30 **M2 Chiral Effects in Attosecond Science**
Chair: **François Légaré**, INRS, Québec, Canada

10:15 **Olga Smirnova**, Max Born Institute Berlin, Germany, EU
I: *Ultrafast Chirality: twisting light to twist electrons* 7

10:45 **Debobrata Rajak**, Université de Bordeaux, France, EU
C: *Asymmetric electron re-scattering in strong-field ionization of chiral molecules* 8

11:00 **Joshua Vogwell**, Imperial College London, United Kingdom
C: *Imaging molecular chirality on ultrafast timescales via enantio-sensitive sum-frequency generation* 9

11:15 **Andrés F. Ordóñez**, ICFO - Institut de Ciencies Fotoniques, Spain, EU
C: *Symmetry-protected chiral sensitivity in photoionization with bichromatic fields* 10



Ultrafast chirality: twisting light to twist electrons

O Smirnova*

Max-Born-Institut, Max-Born-Str. 2A, 12489 Berlin, Germany
Technische Universität Berlin, Straße des 17. Juni 135, 10623 Berlin, Germany

I will describe several new, extremely efficient approaches to chiral discrimination and enantio-sensitive molecular manipulation, which take advantage of ultrafast electronic response [1,2]. One of them is based on the new concept of synthetic chiral light [3,4], which can be used to trigger bright nonlinear optical response in the molecule of a desired handedness while keeping its mirror twin dark in the same frequency range. The other is based on the new concept of geometric magnetism in photoionization of chiral molecules and leads to a new class of enantiosensitive observables in photoionization [5]. Crucially, the emergence of these new observables is associated with ultrafast excitation of chiral electronic or vibronic currents prior to ionization and can be viewed as their unique signature.

* E-mail: smirnova@mbi-berlin.de

References

[1] S Beaulieu *et al.*, Nature Physics **14**, 484 (2018).
[2] A F Ordonez and O Smirnova, Physical Review A **98**, 063428 (2018).
[3] D Ayuso *et al.*, Nature Photonics **13**, 866 (2019).
[4] D Ayuso et al., Nat Commun **12**, 3951 (2021).
[5] A F Ordonez, D Ayuso, P. Decleva, and O Smirnova, arXiv:2106.14264 [physics.chem-ph]

M2

Asymmetric electron re-scattering in strong-field ionization of chiral molecules

D Rajak[1]* , S Beauvarlet[1], O Kneller[2], B Pons[1], S Rozen[2], A Comby[1], D Descamps[1], S Petit[1], V Blanchet[1], N Dudovich[2] and Y Mairesse[1]

[1]CELIA-Universite de Bordeaux-CNRS-CEA, Talence, 33405, France
[2]Weizmann Institute of Science, Rehovot, 76100, Israel

Synopsis In this work, we photoionize chiral molecules by an intense elliptically polarized laser field. The angular distribution of the high energy photo-electrons shows a strong forward-backward asymmetry, resulting from their re-scattering on the chiral ionic potential. The interference between direct and indirect electrons opens the way to chiral photo-electron holography.

Strong-field ionization is a versatile tool for investigating the structure and dynamics of molecules. When a molecule is ionized in the strong-field regime, an electron is born into the continuum by tunneling out of the lowered potential barrier formed by the electromagnetic field and the molecular potential. Depending on the time, within the optical cycle, at which the electron tunnels out they may directly escape the molecular potential (direct) or be driven back and re-scatter from the ionic core. Some of these indirect electrons experience backscattering, and gain kinetic energies up to $10U_p$[1]. Photo-electron Angular Distribution is a coherent superposition of these two type of trajectories, thus encoding information about the molecular potential through photo-electron holography and laser-induced electron diffraction. Retrieving structural information for poly-atomic molecules is challenging due to the complexity of molecular potential and random distribution of the molecular orientation. In this work, we propose a novel approach to retrieve these structural and temporal information using a symmetric property that survives random alignment of molecules: Photo-Electron Circular Dichroism (PECD).

When a chiral molecule is ionized with a circularly polarized light, there is an asymmetric emission of electrons relative to the laser propagation axis, depending on the handedness of molecule and the impinged light. This chiroptical process is called PECD[2]. In strong-field approximation the influence of molecular potential on the electron wavepacket is expected to vanish. On contrary the indirect electrons recollide deep into the ionic core and thus are expected to be extremely sensitive to the chiral molecular potential. PECD measurements require circular polarized light, which suppresses drastically the re-collision probability of indirect electrons. As a compromise, we use elliptically polarized light. 2-D PAD is recorded using a velocity map imaging spectrometer. The 3-D PAD distribution is retrieved through tomographic reconstruction. In elliptical polarization we observe re-scattered electrons in PAD (Fig. 1b) with kinetic energies between $2U_p$ - $10U_p$. These re-scattered electrons show a strong forward-backward asymmetry, which is highly sensitive to the molecular structure. These results opens up the pathway to observe chiral re-scattering and chiral holographic imaging.

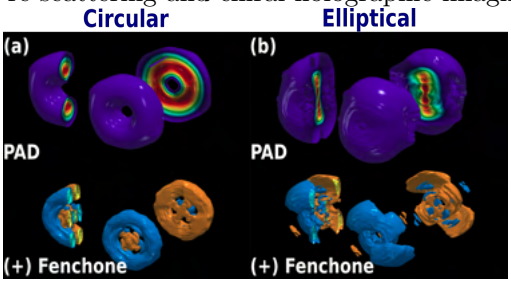


Figure 1. Cuts of the 3-D PAD (up) and its forward-backward asymmetric component (down) is obtained by ionizing (+) Fenchone molecules with a circularly (kinetic energy up to $2U_p$) (a) and an elliptically (b) polarized laser field of 2×10^{13} W/cm^2 (kinetic energy up to $10U_p$).

References

[1] B Walker, et. al. Phys. Rev. Lett. **77**, 5031 (1996); G G Paulus, et.al. Phys. Rev. Lett. **72**, 2851 (1994).

[2] B Ritchie, Phys. Rev. A **12**, 567 (1975); I Powis, J. Chem. Phys. **112**, 301 (2000); G A Garcia, et. al., J. Chem. Phys. **119**, 8781 (2003)

*E-mail: debobrata.rajak@u-bordeaux.fr

Imaging molecular chirality on ultrafast timescales via enantio-sensitive sum-frequency generation

J Vogwell[1*], O Smirnova[2,3] and D Ayuso[1,2†]

[1]Department of Physics, Imperial College London, SW7 2BW London, United Kingdom
[2]Max-Born-Institut, 12489 Berlin, Germany
[3]Technische Universität Berlin, 10623 Berlin, Germany

Synopsis We introduce an ultrafast and all-optical method for efficient chiral recognition based on chiral sum-frequency generation (SFG) spectroscopy. In chiral SFG, two non-collinear incident beams with frequencies $\omega_1 \neq \omega_2$ drive an optical response in a chiral medium at the sum-frequency $\omega_1+\omega_2$. In contrast to traditional SFG implementations, we can encode the medium's handedness in the *intensity* of the SFG signal, rather than in its *phase*, without the need of adding a local oscillator, and enabling full control over the enantio-sensitive response.

Oppositely "handed" versions of the same chiral molecule, or enantiomers, have identical properties, except when interacting with another chiral entity. Since nearly all biological molecules are chiral, different enantiomers can behave very differently in biochemical and pharmaceutical contexts, and so methods for quickly distinguishing enantiomers are of great interest.

Sum-frequency generation (SFG) is a well established chiroptical method [1]. It uses two incident beams that propagate in different directions with different frequencies ω_1 and ω_2 and polarization vectors $\hat{\mathbf{e}}_1$ and $\hat{\mathbf{e}}_2$, which drive a nonlinear response in the medium at frequency $\omega_3=\omega_1+\omega_2$, with polarization $\hat{\mathbf{e}}_3=\hat{\mathbf{e}}_1\times\hat{\mathbf{e}}_2$. SFG is strictly forbidden in isotropic media, such as randomly oriented molecules, unless they are chiral. It is driven by purely electric-dipole interactions, and thus the induced signals can be strong if ω_3 is close to an electronic resonance [2]. However, the *intensity* of SFG is not enantio-sensitive, it only depends on whether they are chiral or not. Their handedness remains hidden in the *phase* of the signal, which can be retrieved via heterodyne detection measurements.

To measure the medium's handedness, one can add an (achiral) reference signal to the setup using a local oscillator [3], i.e. a third beam with frequency ω_3 and polarization $\hat{\mathbf{e}}_3$ that interferes with the SFG signal. Another option is to generate the achiral reference signal from the chiral sample, making the near-field response already enantio-sensitive, although so far this strategy has offered limited enantio-sensitivity and poor opportunities for control [4].

Here we introduce an ultrafast and all-optical method for efficient chiral discrimination that enables full control over the intensity of SFG in a medium of randomly oriented chiral molecules. The achiral reference signal is generated from the chiral sample with full control over its intensity and phase, but without the need of adding a third beam to the setup, making the near-field response highly enantio-sensitive. By tuning the relative frequencies of the incident laser beams, we can maximize SFG in one enantiomer while fully quenching it in the other, Fig. 1. Which enantiomer emits SFG light remains under our complete control.

In contrast to our previous works [5-7], the proposed optical method relies on low-order multiphoton processes, and thus creates new opportunities for imaging molecular chirality and ultrafast chiral dynamics using laser beams with more gentle intensities.

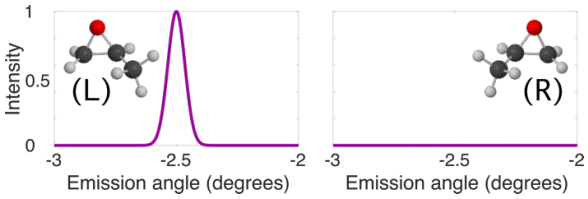


Figure 1. Intensity of SFG in the far field emitted from left- and right-handed randomly oriented propylene oxide driven by two incident laser beams with wavelengths 360 and 180nm, opening angle 10º, intensities 10^{13}Wcm^{-2} and pulse durations 7fs; preliminary TDDFT results.

References

[1] Fischer et al, *Chirality* **17**, 421–437 (2005)
[2] Belkin et al, *Phys Rev Lett* **87**, 113001 (2001)
[3] Okuno et al, *Phys Chem Lett* **5** 2874 (2014)
[4] Belkin et al, *Phys Rev Lett* **85**, 4474 (2000)
[5] Ayuso et al, *Nat Photon* **13**, 866–871 (2019)
[6] Ayuso et al, *Nat Commun* **12**, 3951 (2021)
[7] Ayuso et al, *Optica* **8**, 10, 1243-1246 (2021)

* E-mail: j.vogwell21@imperial.ac.uk
† E-mail: d.ayuso@imperial.ac.uk

M2

Symmetry-protected chiral sensitivity in photoionization with bichromatic fields

A F Ordóñez[1,2]*, D Ayuso[2,3], P Decleva[4] and O Smirnova[2,5]†

[1]ICFO, Barcelona, 08860, Spain.
[2]Max-Born-Institut, Berlin, 12049, Germany.
[3]Imperial College London, SW7 2AZ London, United Kingdom
[4]Università degli Studi di Trieste, 134127 Trieste, Italy
[5]Technische Universität Berlin, Berlin, 10623, Germany.

Synopsis We consider photoionization of randomly oriented chiral molecules with bichromatic fields of frequencies ω and 2ω linearly polarized perpendicular to each other. Our symmetry analysis reveals a new type of enantio-sensitive signal in the photoelectron angular distribution which does not change its sign upon reversal of the two-color relative phase, i.e. upon reversal of the instantaneous ellipticity of the field. We derive analytical expressions for this signal and propose an experimental setup for its measurement.

The fact that molecular chirality can be very efficiently recorded using table-top femtosecond lasers has spurred a flurry of activity in the ultrafast science community, partly driven by the immense potential of ultrafast chiral techniques for industrial applications. A property common to all ultrafast chiral techniques is that reversing the ellipticity of the driving field results in a reversal of the enantio-sensitive signal. Indeed, recent simulations and experiments [1, 2] have shown that even in bichromatic fields of the form $\vec{E} = E_x \cos(\omega t)\hat{x} + E_y \cos(2\omega t + \phi)\hat{y}$ tracing 8-like Lissajous figures, the enantio-sensitive part of the (photoelectron angular distribution) PAD is reversed upon reversal of their instantaneous ellipticity, i.e. upon a change of π in the relative phase ϕ between the x and y components.

Here we have found that, contrary to intuition, bichromatic fields also lead to an enantio-sensitive contribution to the PAD which does not change sign upon reversal of the instantaneous ellipticity. Moreover, this Enantio-sensitive and Non-Elliptically-Dichroic (ENED) signal can be entirely independent of the relative phase ϕ and thus provides an enantio-sensitive signal robust with respect to variations of ϕ, a very desirable feature for industrial applications.

This robustness stems from the symmetry properties of the Hamiltonian of the interacting system. Our analysis [3] reveals that these symmetries, constraining which tensors contribute to the PAD, allow for the emergence of a subset of ENED tensors, in particular for direct ionization pathways. The simplest scenario to obtain an ENED signal requires consecutive absorption of one photon of each color and the measurement geometry shown in Fig. 1 (previous works have used a different geometry for which the ENED signal is averaged out). We derived analytical expressions for this case [3] and performed numerical computations in methyloxirane that reveal an ENED signal corresponding to 1% of the total cross section.

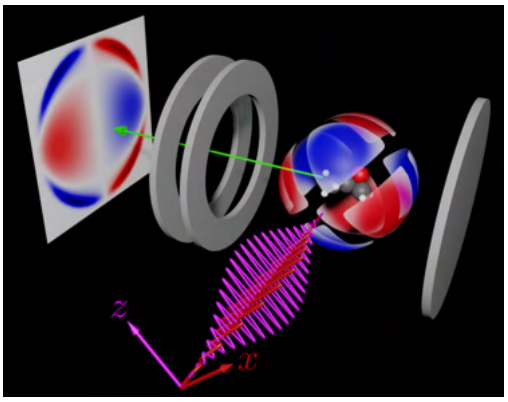


Figure 1. The contribution from the spherical harmonic $\tilde{Y}_3^{-2}(\mathbf{p}) \sim p_x p_y p_z$ to the PAD has opposite signs for opposite enantiomers but is independent of the relative phase between the ω and 2ω fields.

References

[1] Demekhin et al., Phys. Rev. Lett. **121**, 253201 (2018).
[2] Rozen et al., Phys. Rev. X **9**, 031004 (2019).
[3] Ordonez and Smirnova, Phys. Chem. Chem. Phys. **24**, 7264 (2022).

*E-mail: andres.ordonez@icfo.eu
†E-mail: olga.smirnova@mbi-berlin.de

M3 Imaging I& Control of Molecular Structure ▲

11:45 - 13:00 **M3 Imaging and Control of Molecular Structure**
Chair: **Katalin Varjú**, ELI ALPS, Szeged, Hungary, EU

11:45 **Heide Ibrahim**, INRS, Canada
I: *Imaging ultrafast Dissociation Dynamics: Roaming in Formaldehyde* . . 12

12:15 **Francoise Remacle**, University of Liege, Belgium, EU
C: *Exploiting electronic coherences for steering selective bond formation in molecules pumped by ultrashort optical pulses* 13

12:30 **Pradrag Ranitovich**, LBNL, California, USA
C: *Control of Non-Equilibrium ICD Dynamics in Argon and Ethylene Dimers by Attosecond XUV and VUV Radiation* 14

12:45 **Katharina Chirvi**, ICFO - Institut de Ciencies Fotoniques, Spain, EU
C: *Retrieving a complex molecular structure from laser-induced electron diffraction using machine learning* 15



Let's find your ultrafast solutions.



Find unique digits to solve the puzzle.
Claim your prize at our table.

M3

Imaging ultrafast Dissociation Dynamics: Roaming in Formaldehyde

T. Endo[1,2], S.P. Neville[3], P. Lassonde[1], C. Qu[4], H. Fujise[5], M. Fushitani[5], A. Hishikawa[5,6], P.L. Houston[7], J.M. Bowman[8], M.S. Schuurman[3,9], F. Légaré[1 *] and H. Ibrahim[1 †]

[1]Advanced Laser Light Source (ALLS) at Institut national de la recherche scientifique, Varennes, QC J3X 1S2, Canada
[2]Kansai Photon Science Institute, National Institutes for Quantum Science &Technology, Kyoto 619-0215, Japan.
[3]National Research Council Canada, Ottawa, ON K1A 0R6, Canada
[4]Dept. of Chemistry & Biochemistry, University of Maryland, Maryland 20742, USA
[5]Chemistry Dept., Graduate School of Science, Nagoya University, Nagoya, Aichi 464-8602, Japan
[6]Research Center for Materials Science, Nagoya University, Nagoya, Aichi 464-8602, Japan
[7]Cornell University, Ithaca, NY 14852, USA and Georgia Institute of Technology, Atlanta, Georgia 30332, USA
[8]Chemistry Dept. & Cherry L. Emerson Center for Scientific Computation, Emory University, Atlanta, GA 30322, USA
[9]Department of Chemistry and Biomolecular Sciences, University of Ottawa, Ottawa, ON K1N 6N5, Canada

Synopsis As a photoexcited molecule breaks apart, we can see fragments following the direct dissociation path, as well as fragments deviating from this minimum energy path. So-called roaming fragments explore the potential energy landscape in a statistical manner and are directly captured using Coulomb explosion imaging (CEI). Individual pathways are distinguished based on state-of-the-art theory analysis.

How to image statistical dynamics of individual reaction pathways hidden in an overwhelming background? We made use of the capability of CEI to detect the ion-breakup of single-molecules in real time. We investigated the uni-molecular dissociation reactions in the deuterated formaldehyde molecule (D_2CO). In addition to the conventional dissociation channels – molecular and radical dissociation – a third channel termed roaming has been discovered in 2004 [1], which bypasses the transition state. Identified through spectroscopic footprints using high-resolution spectroscopy and found in a variety of molecules, roaming fragments had however never been observed directly and in a time-resolved way. We succeeded in doing so by using the highly sensitive CEI method in combination with high-level first-principles simulations of all critical experimental steps [2,3]. Distinctive roaming signatures were identified in the experimental data (see Fig. 1). These were rendered observable by extracting rare stochastic events out of an overwhelming background. Additionally, this first identification of transient roaming features allowed to generalize the definition of roaming. While it was previously assumed that roaming results in molecular dissociation only, we observed that roaming might also be followed by radical dissociation. We further investigated how the overall dissociation depends on the employed UV pump wavelength [4].

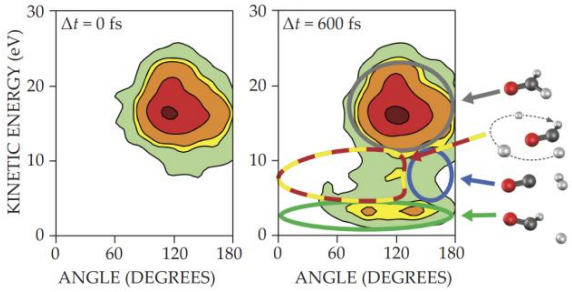


Figure 1. Snapshots of dissociating D_2CO molecules, with the total kinetic energy released in the Coulomb explosion plotted against the angle between the two deuteron momentum vectors. Geometries that correspond to different molecular roads are marked by the colored curves: gray, equilibrium; red–yellow dash, roaming; blue, molecular dissociation; green, radical dissociation. Figure taken from ref. [3].

References

[1] D. Townsend et al. *Science* **306**, 1158 (2004).
[2] T. Endo et al. *Science* **370**, 1072 (2020).
[3] T. Endo et al. *Physics Today* **74**, 62 (2021).
[4] T. Endo et al. *PCCP*, **24**, 1779 (2022).

* E-mail: francois.legare@inrs.ca
† E-mail: heide.ibrahim@inrs.ca

Exploiting electronic coherences for steering selective bond formation in molecules pumped by ultrashort optical pulses

F Remacle[1]*

[1]Theoretical Physical Chemistry, University of Liège, Liège, 4000, Belgium

Synopsis

Atto pulses allow tailoring the electronic coherences in the pumped initial state. These electronic coherences can be exploited for steering the nuclear dynamics to specific products. Two recent examples for which we demonstrate such a control by fully quantum dynamical computations are discussed: LiH excited by a 3 fs deep UV pulse and the ultrafast structural Jahn-Teller rearrangement in CH_4^+. Insights on the coherence control mechanism is provided by analyzing the time evolution of the entanglement resulting from the optical excitation and the non adiabatic coupling due to nuclear motion.

Photoexcitation or photoionization by short as or few fs pulses build a superposition of electronic states whose features can be tailored by tuning the pulse parameters. The engineered electronic coherences can be exploited for steering the nuclear motion through the network of conical intersections to specific products.

Two recent examples are discused for which we demonstrate control by fully quantum dynamical computations. For each of these examples, we analyze the time evolution of the entanglement between nuclear and electronic degrees of freedom using singular valued decomposition (SVD) of the wave function. At each time step, the wave function is matricized and written as a superposition of singular states weighted by their corresponding singular values ordered by decreasing order. The singular states are direct products of a component that depends only on the nuclear degrees of freedom and a component depending on the electronic coordinates.[1] When more than one singular state is necessary for describing the wave function, the latter is entangled. This analysis gives valuable insights on the role of the entanglement of the initial state, that can be tuned by the parameters of the pulse, and its subsequent modulation by the nuclear motion on coupled electronic states.

We begin with the case of the control of the fragmentation of the neutral diatomic molecule LiH photoexcited by short few fs deep UV pulses. For this system with a single nuclear degree of freedom, the quantum dynamics is described on a grid in the nuclear coordinate for 8 coupled electronic states. By tuning the carrier frequency of the UV pulse, it is possible to control the yield in fragments. Our results show that a few singular states are necessary for accurately describing the time evolving wave function and that their number is modulated in time bythe interpaly between the gradients of the potential energy curves of the excited states and the non adiabatic coupling between them driven by the nuclear motion.

The second example is that of the ultrafast Jahn-Teller rearrangement of the methane cation upon sudden ionization. The cation dynamics is described on a grid of 2 nuclear coordinates that sample the rearrangement from the Td to the D_2d and C_{2v} geometries for the three lowest excited states of the cation, D_0, D_1 and D_2. We showed in recent work that both sudden strong field ionization[2] and photoionization by a short XUV pulse[3] create a superposition of the three lowest states of the cation that are degenerate at the T_d geometry. Furthermore, our computations point to a crucial role of electronic coherences that involve the D_2 state in leading to a strong isotope effect. For strong field ionization of CH_4, we computed a ratio of ≈2.5 for the ratio autocorrelation functions of the two isotopomers, CH_4^+ and CD_4^+,[2] in good agreement with the reported yield in high harmonics.[4] We will discuss the time evolution of the entanglement between the three electronic states and the two nuclear degrees of freedom during the structural rearrangement and how it is affected by the isotopic substitution.

References

(1) Blavier, M.; Levine, R. D.; Remacle, F. **2022,** To be submitted.

(2) Blavier, M., et al. *J. Phys. Chem. A* **2021,** 125, 9495-9507.

(3) Gonçalves, C. E. M.; Levine, R. D.; Remacle, F. *Phys. Chem. Chem. Phys.* **2021,** 23, 12051-12059.

(4) Baker, S., et al. *Science* **2006,** 312, 424.

* E-mail:fremacle@uliege.be

M3

Control of Non-Equilibrium ICD Dynamics in Argon and Ethylene Dimers by Attosecond XUV and VUV Radiation

C Hogle[1], L Martin[1], XM Tong[2], K Ueda[3], T Miteva[4], L Cederbaum[5], H Kapteyn[1], M Murnane[1], and P Ranitovic[1,6,*]

[1]JILA and Department of Physics, University of Colorado and NIST, Boulder, CO 80309, USA
[2] Center for Computational Sciences, University of Tsukuba, Ibaraki 305-8573, Japan
[3]Institute of Multidisciplinary Research for Advanced Materials, Tohoku University, Sendai 980-8577, Japan
[4]Sorbonne Université, CNRS, Laboratoire de Chimie Physique—Matière et Rayonnement, F-75005 Paris, France
[5]Theoretical Chemistry, PCI, Universität Heidelberg, 69120 Heidelberg, Germany
[6]University of Belgrade, Faculty of Physics, Belgrade, 11000, Serbia

Synopsis In the process of X-ray interaction with matter, from atomic dimers to biological system, Interatomic-Coulomb-Decay (ICD) processes play a role of an important ultrafast relaxation mechanism. We show how tunable VUV and XUV radiation can be used to initiate and finely control non-equilibrium ICD dynamics in gas-phase dimers. Here, we have used tunable VUV attosecond pulse trains to initiate ultrafast dynamics in a C_2D_4 dimer in a gas phase. Furthermore, we show how non-equilibrium ICD dynamics in Ar dimer can be controlled by means of COLTRIMS and time-resolved XUV/IR radiation.

Since the experimental work first identifying the ICD process, extensive studies have unraveled its complex character [1,2]. Following X-ray ionization, an ultrafast interaction of the irradiated site with its environment produces a low-energy ICD electron that follows the initial direct-ionized electron. In contrast to the better-known Auger relaxation process, where the electron that fills the X-ray ionization hole originates from the same atom and the decay rate is essentially independent of environment, the ICD process is intrinsically complex in nature. Thus, a low energy ICD electron exhibits a broad energy spectrum due to the coupling of the ICD rate with the motion of the molecular nuclear wave-packet (NWP). Here, we demonstrate a laser-enabled ICD (LE-ICD) process -- a sophisticated control mechanism involving a valence, Rydberg, and an inner-valence electron transition -- allowing us to control bond breaking in the Ar dimer, after initiating a non-equilibrium dynamics by XUV radiation. The other example of non-equilibrium dimer dynamics would be discussed, where we combine broadband VUV pulses to excite an ethylene dimer, with IR pulses that ionize it.

Figure 1 shows the potentials energy surfaces in the vicinity of the double-ionization region. The NWP pathways, the XUV pulse initiate, were chosen to avoid triggering of the ICD process with the pump XUV pulse. The controlling IR pulse pathways are then used to precisely enable the internuclear distance where the LE-ICD starts. We also show how a shrinking dimer can be trapped at small Rs, creating thus a metastable dimer, half the original dimer size.

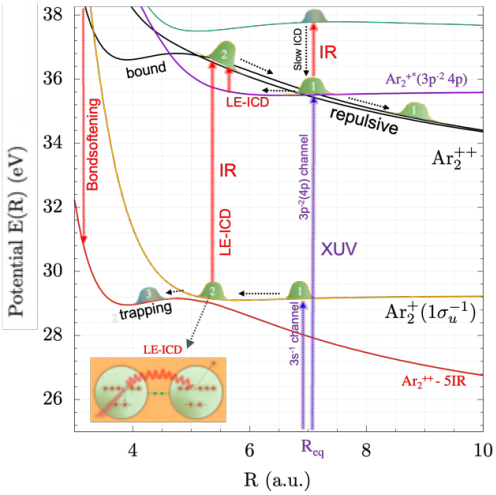


Figure 1. XUV-initiated, and IR-controlled ICD dynamics in a highly excited argon dimer. The inset shows a more intuitive, atomic-level model of the LE-ICD process.

The analysis of our experimental and theoretical non-equilibrium ICD data shows a surprising complexity, revealing the potential for further experimental and theoretical work in gas and liquid phase of matter interacting with light.

References

[1] Cederbaum L *et al* (1997) *Phys. Rev. Lett.* **79** 4778
[2] Jahnke T *et al* (2004) *Phys. Rev. Lett.* **93** 163401

* E-mail: p.ranitovic@ff.bg.ac.rs

Retrieving a complex molecular structure from laser-induced electron diffraction using machine learning

X Liu[1], K Amini[1], A Sanchez[1], B Belsa[1], T Steinle[1], K Chirvi[1] and Jens Biegert[1,2†]

[1]ICFO - Institut de Ciencies Fotoniques, The Barcelona Institute of Science and Technology, Castelldefels, Spain.
[2]ICREA, Pg. Lluís Companys 23, Barcelona, 08010, Spain

Synopsis We image the structure of the complex chiral molecule Fenchone ($C_{10}H_{16}O$) from laser-induced electron diffraction data by applying a machine learning algorithm with a convolutional neural network.

Imaging a molecular structure with electron or X-ray diffraction is based on finding a global extremum in a multidimensional solution space [1]. Laser-induced electron diffraction (LIED) [2] is a powerful laser-based method that can image the three-dimensional (3D) geometry of a single gas-phase molecule with a spatial resolution of atomic Ångstrom and a temporal resolution of tens of femtoseconds [3]. In LIED, the structural information of the molecule is extracted from the coherently scattered electron wave packet driven by an intense laser field after photoionization. However, identifying the molecular geometry from a diffraction pattern becomes increasingly challenging as the structural complexity of the object increases, which is a general issue for any diffraction-based imaging technique. A machine learning-based approach is well suited to overcome this limitation, as it can match patterns in a multidimensional solution space with high accuracy. We implemented LIED in combination with a machine learning algorithm with a convolutional neural network (CNN) to extract the structure of a complex molecule Fenchone ($C_{10}H_{16}O$) [4]. We generated a database for training and validation of the ML algorithm calculating molecular structures and their corresponding two-dimensional differential cross-section (2D-DCS) maps using the independent atomic model. An CNN interpolates between patterns in the precomputed database. Thus, we can significantly reduce the degrees of freedom of the precalculated structure by considering the change of only four groups of atoms of the molecule (see inset of Fig. 1a) and a molecule-wide global change in structure. After successfully training and validation with such a reduced database (see Fig.1a), the ML model predicts the 3D position of seven (+)-Fenchone atoms (see Fig 1b, green circles) based on the LIED measured 2D-DCS map.

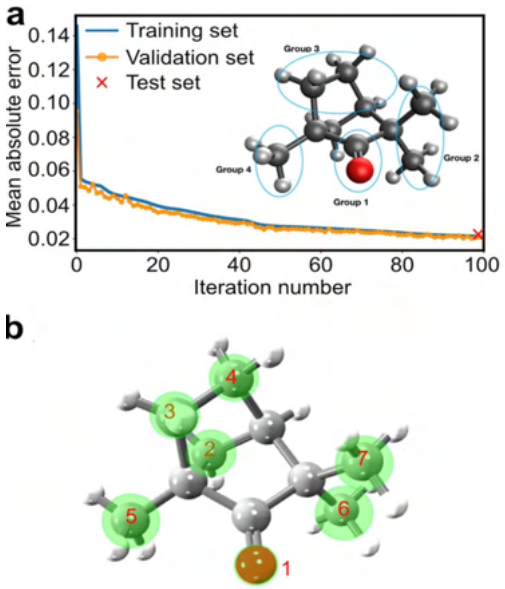


Figure 1 (a): Comparison between training and validation set of molecular structures. The inset shows the four groups of the (+)-Fenchone molecule which the ML algorithm has been trained on. (**b):** Schematic representation of the predicted 3D molecular structure of Fenchone, where the green circles indicate the area of uncertainty.

In summary, we implement ML-LIED to retrieve the position of atoms of a complex 3D molecule with combined picometre and attosecond resolution. Our results demonstrate that ML- LIED provides new opportunities for determining the structure of large and complex molecules from diffraction data.

References

[1] A. Sanchez-Gonzalez et al 2017 *Nat. Commun.* **8**, 15461
[2] A. Sanchez et al 2021 *Nat. Commun*. **12,** 1520
[3] T. Zuo et al 1996, *Chem. Phys. Lett.* **259**, 313
[4] X. Liu et al 2021., *Comm. Chem.* **4**, 154

† E-mail: jens.biegert@icfo.eu

M4 Strong-Field Nonlinear Optics in Solids ▲

M4

14:00 - 16:00 M4 Strong-Field Nonlinear Optics in Solids
Chair: **Kyung Taec Kim**, IBS, Korea

14:00 **Matthias Kling**, Stanford University, California, USA
I: *Petahertz field sampling below the diffraction limit* 17

14:30 **Michael Zuerch**, UC Berkeley, California, USA
I: *Ultrafast Second-harmonic XUV Spectroscopy: A Novel Probe for Symmetry at Interfaces and in Quantum Materials* 18

15:00 **Tran-Chau Truong**, University of Central Florida, Florida, US
C: *Single-shot laser waveform measurement of short-wave infrared pulses* 19

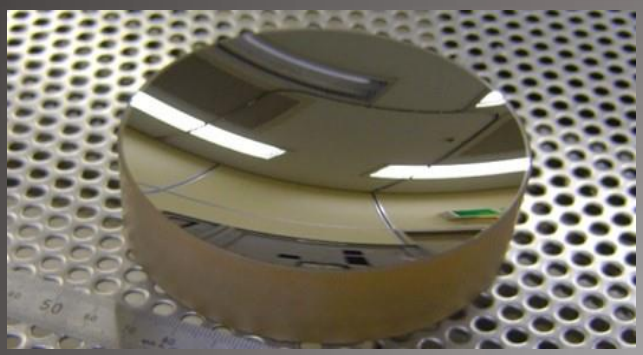
15:00 **Natalie Nagl**, Max Planck Institute for Quantum Optics, Germany, EU
C: *Single-cycle infrared waveform generation and control* 20

15:15 **Mohammed Hassan**, University of Arizona, Arizona, USA
C: *Attosecond electron motion control* 21

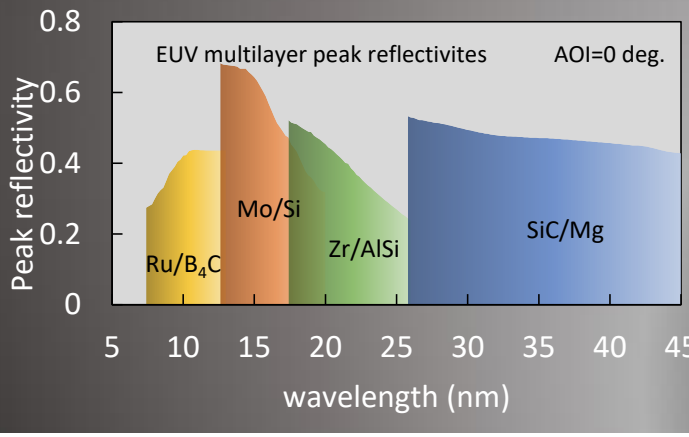
15:30 **Markus Borsch**, University of Michigan, Michigan, US
C: *Ultrafast Momentum Combs for Electron-Band Tomography* 22

NTT AT

EUV optics for Attosecond applications



Product lineup
- Multilayer mirror
- Multilayer polarizer
- Dichroic mirror
- Half mirror
- Beam separator
- Thin film sample
- Resolution test chart



Please visit our website for more details.
https://www.ntt-at.com/product/list_xuv_euv_x-ray_optics.html

Spatiotemporal sampling of near-petahertz vortex fields

Johannes Blöchl[1,2], Johannes Schötz[1,2], Boris Bergues[1,2], Matthias F Kling[1,2,3,4,*]

[1]Physics Department, Ludwig-Maximilians-Universität Munich, 85748 Garching, Germany
[2]Max Planck Institute of Quantum Optics, 85748 Garching, Germany
[3]SLAC National Laboratory, Menlo Park, CA 94025, USA
[4]Applied Physics Department, Stanford University, Stanford, CA 94305, USA

Synopsis The sampling of petahertz light fields opens up a new regime for field-resolved spectroscopy of ultrafast light-matter interactions. We derived a theoretical model tested against systematic experimental studies on the emergence of macroscopic currents in photoconductive field sampling. The model overcomes previous heuristic interpretations and can aid in the design of more sensitive and more efficient photoconductive devices. Furthermore, we implemented a near-field method for the spatio-temporal sampling of near-petahertz fields, enabling full vectorial field characterization of light beams with orbital angular momentum.

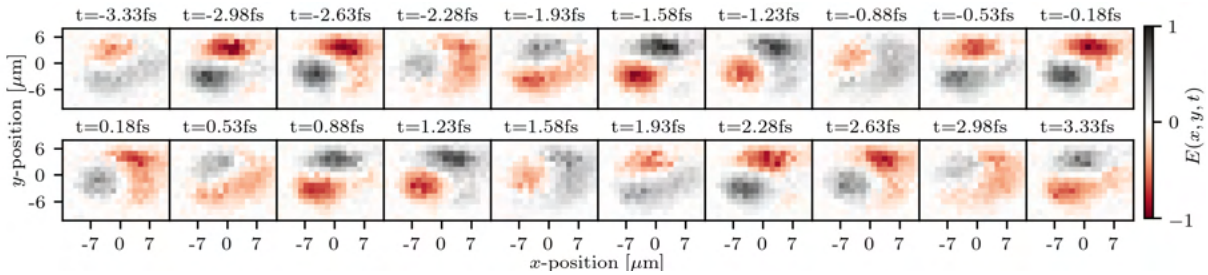


Figure 1. Spatially-resolved measurements of near-petahertz orbital angular momentum (OAM) beams employing nanoTIPTOE. The normalized field amplitudes are shown as a function of space and time.

Intense few-cycle laser pulses can induce conductivity within a fraction of an optical cycle, enabling the ultrafast manipulation of electric currents. Such optical-field driven currents have been measured in various materials. Using sub-cycle current injection as a temporal gate, in a generalization of the concept of THz photoconductive field-sampling, the field-resolved measurement of optical waveforms up to petaherz frequencies has been demonstrated [1]. The investigation and control of these field-driven currents does not only promise to revolutionize the field of attosecond physics, but also paves the way towards petahertz electronics.

Despite the growing importance of ultrafast photoconductive measurements, a rigorous model for connecting the microscopic electron dynamics to the macroscopic external signal was lacking. We have developed a theoretical framework tested against systematic experimental studies on the signal formation in gas-phase photoconductive sampling [2]. The quantitative model overcomes previous heuristic interpretations and can aid in the design of more sensitive and more efficient photoconductive devices.

Moreover, we implemented a new technique to probe petahertz light fields at arbitrary points in space. It relies on the tunneling ionization with a perturbation for the time-domain observation of an electric field (TIPTOE) [3] locally sampled with a single metallic nanometric needle tip. Not only do we demonstrate that this approach, termed nanoTIPTOE [4], is equally reliable as TIPTOE, but we also show that it enables the measurement of the time-dependent field evolution in the entire focal plane. By directly recording electric currents from the needle tip, we avoid the use of complex high-vacuum equipment and time-of-flight spectroscopy. The resolved bandwidth covers a range from 0.3−0.5 PHz. Importantly, nanoTIPTOE is polarization sensitive, which makes it applicable to vectorial field reconstruction of fields with orbital angular momentum (see Fig. 1).

References

[1] A Schiffrin *et al.,* Nature **493** 70–74 (2013)
[2] J Schötz *et al.,* Nat. Com. **13** 962 (2022)
[3] S B Park *et al.,* Optica **5** 402-408 (2018)
[4] J Blöchl *et al.* (in preparation)

* E-mail: kling@stanford.edu

Ultrafast Second-harmonic XUV Spectroscopy: A Novel Probe for Symmetry

M Zuerch[1,2] *

[1]University of California at Berkeley, Department of Chemistry, 237 Hildebrand Hall, CA-94720 Berkeley, USA
[2]Lawrence Berkeley National Laboratory, Materials Sciences Division, 1 Cyclotron Road, CA-94720 Berkeley, USA

Synopsis XUV-SHG, which requires intense ultrafast XUV pulses, enables probing element-selective symmetry-broken states on surfaces, at interfaces, and within bulk materials with broken inversion symmetry. XUV-SHG was successfully applied to study the Li displacement causing symmetry breaking and the emergence of polarity in the polar metal $LiOsO_3$.

Extreme ultraviolet second harmonic generation spectroscopy (XUV-SHG) is an emerging method probing inversion symmetry breaking with core-state specificity. Compared to hard X-ray SHG that due to its short wavelength becomes bulk sensitive [1], XUV-SHG offers element selectivity with access to buried interfaces and symmetry-broken states. Following the first demonstration of surface sensitivity on a carbon film [2], recently we demonstrated the quantification of the interfacial bond geometry of an organic-inorganic interface [3] and the measurement of a surface spectrum of titanium [4]. Notably the titanium measurement was achieved using a high harmonic seeded soft X-ray laser. Measuring the angular polarization of SXR-SHG has enabled additional sensitivities such as to the nature of the symmetry state [5].

The experiments in concert with advancements of numerical simulation using TD-DFT methods have provided deeper insights into how the XUV-SHG spectrum encodes information about the dielectric environment of a single atomic species in its symmetry-broken state. That has been utilized to study the polar metal phase of $LiOsO_3$ (Fig. 1) [6]. In polar metals the coexistence of polarity and metallicity is unexpected as screening should prohibit long-range order. XUV-SHG spectra were measured around the Li K-edge (56 to 66 eV) by focusing an intense free-electron laser beam onto the material with photon energies in the range of 28 to 33 eV. We find excellent agreement between experimental spectra and numerical simulations and find spectrally-resolved SHG varies with Li-displacement. The directional dependence of the $\chi^{(2)}$ tensor enables disentangling directional information of the anisotropies. These findings provide direct evidence pertaining to the origin of the polar property of the material and provides insights into the amount of Li displacement.

As the first demonstration of XUV-SHG spectroscopy around a phase transition, these results pave the way for investigating broken symmetry from an element-specific perspective in a dynamical manner taking advantage of the inherent ultrafast nature of the probe pulses. Recent advancements in achieving attosecond FEL pulses and the emergence of high-energy attosecond sources provide interesting new opportunities in materials sciences using XUV-SHG spectroscopy.

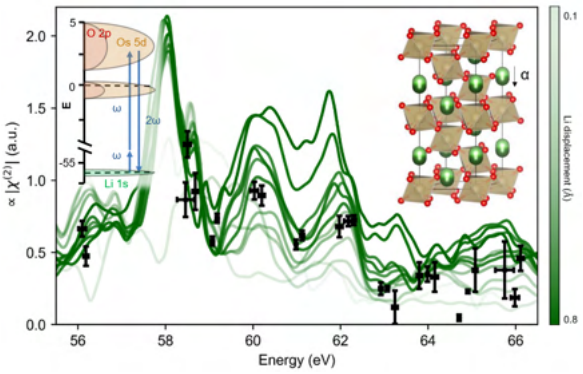


Figure 1. XUV-SHG spectra and simulation depending on Li displacement in $LiOsO_3$ at 60 K.

References

[1] S Shwartz, Phys. Rev. Lett. **112**, 163901 (2014).
[2] R K Lam, Phys. Rev. Lett. **120**, 023901 (2018).
[3] C P Schwartz, Phys. Rev. Lett. **127**, 096801 (2021).
[4] T Helk, Sci. Adv. **7**, eabe2265 (2021).
[5] C Uzundal, Phys. Rev. Lett. **127**, 237402 (2021).
[6] E Berger, Nano Letters **21**, 6095 (2021).

* E-mail: mwz@berkeley.edu

Single-shot laser waveform measurement of short-wave infrared pulses

T C Truong[1], Y Liu[1], D Khatri[1], and M Chini[1,2 *]

[1]Department of Physics, University of Central Florida, Orlando, FL, 32816, USA
[2] CREOL, the College of Optics and Photonics, University of Central Florida, Orlando, FL, 32816, USA

Synopsis Characterizing the electric field waveform of few-cycle pulses requires a sub-cycle temporal gate, which can be obtained from tunneling and multiphoton excitation processes. Previously, we have shown that spontaneous band fluorescence emission, following multiphoton absorption in a ZnO crystal, can be used as the sub-cycle gate. Here, by projecting the time delays onto a transverse axis of the crystals and imaging the band fluorescence, we demonstrate single-shot waveform measurements extending into the short-wave infrared.

Obtaining the phase information of oscillating few-cycle pulses is quite challenging due to the need for a sub-cycle temporal gate, which was first implemented by "streaking" photoelectrons generated by isolated attosecond pulses in a complex vacuum setup. Recently, a method called TIPTOE (tunnel ionization with a perturbation for the time-domain observation of electric fields) showed that tunneling and multiphoton excitation can be used as the sub-cycle gate [1]. Lacking any phase matching requirement, TIPTOE has been widely applied to characterizing arbitrary few-cycle waveforms first using tunnel ionization in air, and then expanded to multiphoton excitation in crystalline solids [2] and most recently single-shot measurements in the mid-IR using multiphoton excitation in a Si-based image sensor [3]. Here, we demonstrate that the single-shot adaptation of TIPTOE can be extended to the short-wave infrared by projecting the time delays onto the transverse axis of a ZnO crystal using a cylindrical mirror, and by spatially resolving the band fluorescence.

Few-cycle short-wave infrared pulses are obtained from a Yb:KGW laser amplifier, spectrally broadened in an N_2O gas-filled hollow core fiber. This spectrum has a strong red shift resulting from the nonlinear rotational response of the linear molecule [4], and a negative chirp which is then compensated by normal dispersion of materials. The beam is split into the fundamental and perturbing beam with 85% and 0.1% of the input pulse energy, using uncoated CaF_2 wedges, and focused with by a cylindrical mirror onto the ZnO crystal. As a result, the band fluorescence emission from ZnO, initiated by the multiphoton excitation of the fundamental, is perturbed by the weak perturbing beam. Due to a small angle between the fundamental and perturbing beams, the time delay varies linearly along a transverse dimension of the crystal. The spatially-resolved modulation, shown in Fig.1a, is spectrally filtered and imaged onto a CMOS camera, and converted to a time-domain electric field waveform, shown in Fig.1b, as in Ref. [3]. The spectrum and spectral phase calculated from the measured waveform are in good agreement with a measurement using frequency-resolved optical gating (FROG), as shown in Fig.1c.

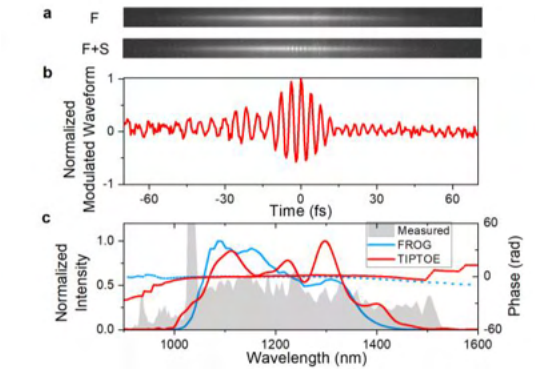


Figure 1. a, Band fluorescence images with and without perturbating beam; **b,** Time-dependent modulated signal; **c,** Retrieved, measured spectrum and spectral phase.

In conclusion, we demonstrated single-shot waveform characterization in the short-wave infrared. This technique can potentially be extended further to shorter wavelengths by using materials with a suitable band gap.

References

[1] Park S B *et al* 2018 *Optica* **5** 402
[2] Liu Y *et al* 2021 *Photon. Res.* **9** 929
[3] Liu Y *et al* 2022 *Nat. Photonics* **16** 109
[4] Beetar J E *et al* 2020 *Sci. Adv.* **6** eabb5375

* E-mail: michael.chini@ucf.edu

Single-cycle infrared waveform generation and control

N Nagl[1,2 *], P Steinleitner[1], M Kowalczyk[1,2,3], J Zhang[4], V Pervak[2], C Hofer[1,2,3], A Głuszek[5], J Sotor[5], A Weigel[1,2,3 †], K F Mak[1], and F Krausz[1,2,3]

[1]Max Planck Institute of Quantum Optics, Garching, 85748, Germany
[2]Ludwig Maximilian University Munich, Garching, 85748, Germany
[3]Center for Molecular Fingerprinting Research Nonprofit LLC., Budapest, 1093, Hungary
[4]School of Optical & Electronic Information, Huazhong University of Science & Technology, Wuhan, 430074, China
[5]Wrocław University of Science and Technology, Wrocław, 50-370, Poland

Synopsis Tailoring the electric-field waveform of ultrashort light pulses lays the foundation for controlling nonlinear optical phenomena on their genuine, attosecond, time scale. We present a novel approach for shaping few-cycle waveforms, and thereby achieved the first multi-octave synthesis of single-cycle transients in the mid-infrared spectral range, with a continuously adjustable and highly-reproducible electric-field evolution. The concept is generalizable towards the synthesis of a broader variety of infrared waveforms and will offer a diversity of hitherto unavailable technical capabilities.

The temporal confinement of laser light to a few periods of its oscillating electromagnetic field gave rise to extreme nonlinear interactions — the control and exploitation of which requires precise control of the fields' temporal evolution [1]. Extending waveform control from the near-infrared and THz spectral range — where it has been previously demonstrated — to the mid-infrared (mid-IR) region opens up new prospects, such as the realization of light-wave-driven electronic devices based on low-bandgap highly-doped semiconductors [2], and the advancement of electric-field-resolved molecular fingerprinting of biological systems [3].

In this work, we present a new approach for coherent multi-octave mid-IR generation with intrinsic capability of changing the relative phase and amplitude of different spectral regions and thereby shaping the emerging waveform. The fidelity and reproducibility of the reported waveforms benefits from the unprecedented carrier-envelope-phase (CEP) and amplitude stability of our diode-pumped laser.

Active CEP stabilization to an exceptional level of 8.6 mrad (Fig. 1a) allows to generate highly reproducible single-cycle pulses (Fig. 1b) from a Kerr-lens mode-locked Cr:ZnS laser system [4]. They are used to drive cascaded intrapulse difference-frequency generation (IPDFG) and control the electric-field evolution of the resulting coherent emission with the spectrum extending from 0.9 to 12 µm (Fig. 1c).

Specifically, we create mid-IR waveforms in several spectral bands by cascaded IPDFG and manipulate their spectral phases by exploiting their different dependence on the CEP of the driving pulse. This allows to tailor the electric field of the waveforms in time domain (Fig. 1d).

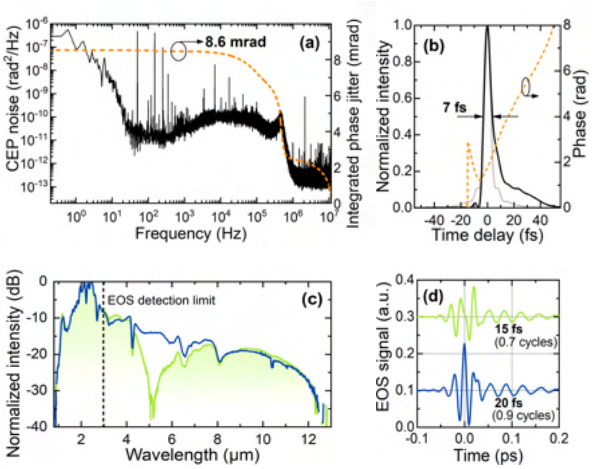


Figure 1. (a) *Out-of-loop* CEP noise and integrated phase jitter. (b) Single-cycle driving pulse (black) captured with SHG-FROG, and Fourier-transform limit (grey). (c) Supercontinuum from cascaded IPDFG for the extreme cases of constructive (blue) and destructive (green) interference. (d) Electric-field evolution of the mid-IR continuum pulses in c, captured by electro-optic sampling (EOS), and extracted pulse durations.

References

[1] T Brabec & F Krausz, Rev. Mod. Phys. **72**, 545 (2000).
[2] M Fischer *et al.*, Optica **8**, 898 (2021).
[3] I Pupeza *et al.*, Nature **577**, 52 (2020).
[4] N Nagl, Springer Theses, 978-3-030-89753-6 (2021).

* E-mail: Nathalie.Nagl@mpq.mpg.de
† E-mail: Alexander.Weigel@mpq.mpg.de

Attosecond electron motion control

D Hui[1], H Alqattan[1], S Yamada[2], V Pervak[3], K Yabana[2], and M Th Hassan[1]
1Department of Physics, University of Arizona, Tucson, AZ 85721, USA
[2]Center for Computational Sciences, University of Tsukuba, Tsukuba 305-8577, Japan
[3]Ludwig-Maximilians-[3]Universität München, Am Coulombwall 1, 85748, Garching, Germany

Synopsis In this work, we demonstrate the electron motion control in the SiO_2 dielectric system using synthesized light waveforms. This on-demand electron motion control paves the way for establishing the long-anticipated ultrafast switches and attosecond electronics.

The light field-induced electron motion in the dielectric can be controlled on-demand by tailoring the driver field's shape with attosecond resolution. In this work, we utilized the light field synthesizer (LFS) demonstrated elsewhere (1) to synthesize a few complex waveforms by changing the four channels' relative phases and intensities in the LFS to control the electron motion in SiO_2. These waveforms were characterized by the attosecond all-optical reflectivity modulation (Atto-ARM) methodology (2). These measured waveforms are shown in Fig 1 (a-e). Accordingly, these waveforms' corresponding instantaneous intensity profiles are shown in the solid red lines in Fig. 1 (f-j). The induced number of electrons and its direction in the SiO_2 system depends on the shape of the waveform—the calculated density of the excited carriers using the measured waveforms as the input triggering field. The number of triggered electrons by the waveform, shown in Fig. 1a, is maximized at the highest field crests for a time window of 400 as, as illustrated in Fig. 1f. The maximum electron triggering signal occurs at two-time instants separated by 0.9 fs (Fig. 1g) using the waveform presented in Fig. 1b. The separation interval can be controlled to be 2.7fs (Fig. 1h) using the waveform shown in Fig. 1c. For demonstrating a fine control of the electron motion, the synthesized waveform in Fig. 1d was used to excite the carriers of the SiO_2 system. The electron's maximum triggering occurs at three-time instants with equal time intervals of 0.9 fs (Fig. 1i). Moreover, the waveform, shown in Fig. 1e, maximizes the electrons' triggering at four events (Fig. 1j).

The four signals are separated in time. The first and second signals are separated from each other by 0.9 fs. The second and third signals are separated by 3.6 fs. Lastly, the third and fourth signals are separated by 0.9 fs.

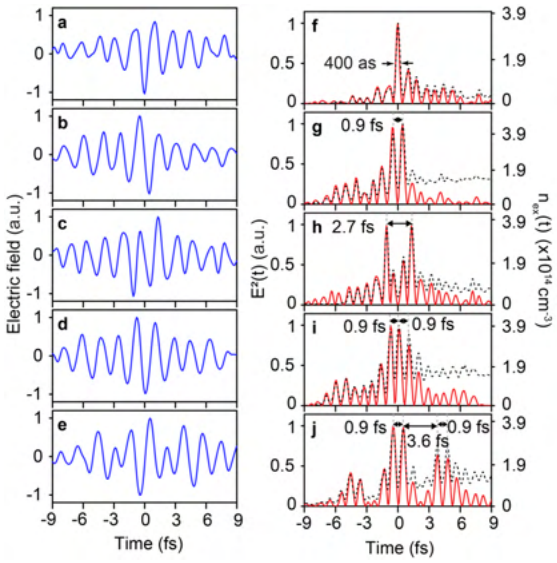


Figure 1. Attosecond electron motion control in SiO_2. (a-e) the measured synthesized waveforms. (f-j) the corresponding field intensity and calculated carrier density triggered by these synthesized waveforms.

In conclusion, we demonstrated a full control of electron motion in the dielectric system. This electron control would be used to develop quantum electronics, paving the way to extend the frontiers of modern electronics and data information processing technologies into the petahertz realm.

References

[1] Alqattan et al 2021 *arXiv:2112.10700*.
[2] Hui D et al 2022 Nat. Photon. 16, 33–37.

* E-mail: mohammedhassan@arizona.edu

M4

Ultrafast Momentum Combs for Electron-Band Tomography

M Borsch[1]*, C P Schmid[2], R Huber[2], and M Kira[1]

[1]Dept. of Electrical Engineering and Computer Science, University of Michigan, Ann Arbor, MI 48109, USA.
[2]Department of Physics, University of Regensburg, 93040 Regensburg, Germany.

Synopsis Ultrafast harmonic sideband generation in solids is discovered to exhibit prominent crystal-momentum combs formed by extreme nonlinear, femtosecond dynamics and interferences among coherent excitons. The presented meticulous theory–experiment comparison is demonstrated to tomographically map electronic bands of quantum materials with super-resolution, based on high-precision crystal-momentum localization of harmonic sideband emission by the crystal-momentum combs.

The electronic band structure of quantum materials is the foundation of quantum functionalities ranging from dynamic electronic and optical aspects to quantum-information and phase-transition properties. We demonstrate [1] how harmonic-sideband (HSB) generation [2, 3] can be devised to deliver all-optical, super-resolution mapping of diverse band structures. The approach is ideally suited for exploring buried, nanoscale quantum structures, in ambient and under operational conditions.

In our HSB approach, an ultrafast optical field resonantly excites an excitonic wave packet $P_{\mathbf{k}}$ at a precise crystal momentum $\hbar\mathbf{k}$ by promoting an electron (e) from a specific valence band into a single conduction band, leaving a hole (h) behind. Another nonresonant field is applied to displace $P_{\mathbf{k}}$ in momentum space, allowing it to probe the energy difference $E^{\mathrm{eh}}_{\mathbf{k}}$ of conduction and valence band. We use strong multi-terahertz (THz) fields that drive $P_{\mathbf{k}}$ on a roughly sinusoidal path, creating distinct interference patterns – crystal-momentum combs ($\mathbf{k}$ combs) – that pinpoint the emission of each HSB to discrete regions in $\mathbf{k}$ space. This assignment can directly map the nontrivial band structure of quantum materials from a series of HSB measurements performed in ambient, as we demonstrated for monolayer tungsten diselenide [1].

The emission of harmonic sidebands is intimately connected with the femtosecond, extremely nonperturbative, dynamics of $P_{\mathbf{k}}$ which we exactly solve using the dynamic cluster expansion approach [4], including all relevant correlations. We find that correlation effects on the $P_{\mathbf{k}}$ dynamics can be directly connected to changes in HSBs, which we observe in time resolved measurements with attosecond resolution.

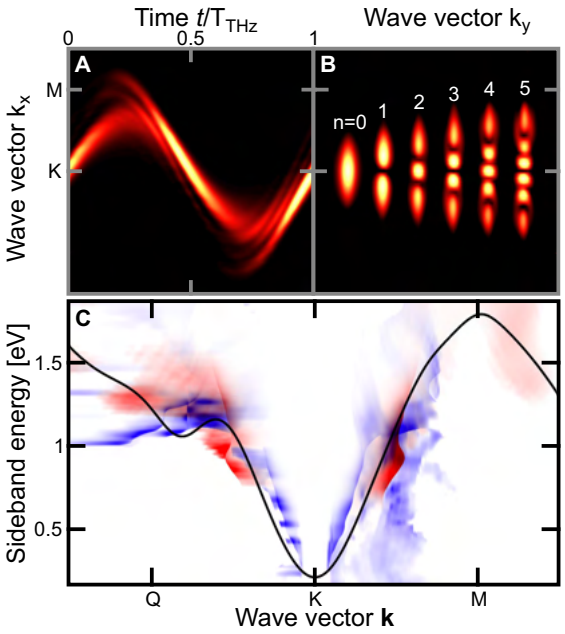


Figure 1. **A**, Computed $|P_{\mathbf{k}}(t)|$ dynamics as function of time over one full THz cycle (cycle length T_{THz}). **B**, Corresponding $\mathbf{k}$ combs for orders $n = 0$ to 5. **C**, Result of $\mathbf{k}$-comb tomography for monolayer WSe_2 from even (blue) and odd (red) HSB orders, respectively. The black line shows the target e–h band energy $E^{\mathrm{eh}}_{\mathbf{k}}$.

References

[1] M Borsch *et al.*, Science **370**, 1204 (2020).
[2] J Kono *et al.*, Phys. Rev. Lett. **79**, 1758 (1997).
[3] B Zaks *et al.*, Nature **483**, 580 (2012).
[4] M Kira and S W Koch, *Semiconductor Quantum Optics* (Cambridge University Press, Cambridge, 2012).

*E-mail: markbor@umich.edu

20:00 - 21:00 **ME US Funding Opportunities in Attosecond Science**
Chair: **Uwe Thumm**, Kansas State University, Kansas, USA
AMOS Program

20:00 **Kevin Jones**, National Science Foundation
NSF programs of interest to the attosecond community

20:15 **James Joseph**, Army Research Office
Modern Optics Program

20:30 **Andrew Stickrath**, Air Force Office of Scientific Research
Ultrashort Pulse Laser-Matter Interactions Program

20:45 **Q&A**

T1 Attosecond Photoionization Dynamics ▲

08:30 - 11:00 **T1 Attosecond Photoionization Dynamics** 24
Chair: **Pascal Salières**, Paris-Saclay University, France, EU

08:30 **Eva Lindroth**, Stockholm University, Sweden, EU
I: *Photoionization delay in heavy atomic ions* 25

09:00 **Alexandra S Landsman**, Ohio State University, USA
I: *Tracking the ionization site in neutral molecules* 26

09:30 **Richard Taïeb**, Sorbonne Université, France, EU
C: *Real-time imaging of resonant photoemission dynamics* 27

09:45 **Miguel Alarcon**, Purdue University, USA
C: *Theoretical treatment of quantum beats in Argon.* 28

10:00 **Vicent Borràs**, Universidad Autónoma de Madrid, Spain, EU
C: *The effect of Feschbach resonances on the different vibrational states of N_2 in a RABBIT experiment.* 29

10:15 **Juan Martín Randazzo**, CONICET, Argentina
C: *ASTRA, a transition-density-matrix solution to the close-coupling problem in the molecular ionization continuum* 30

10:30 **Tomoya Mizuno**, University of Tokyo, Japan
C: *Experimental investigation of topological property of degenerate singularities in rescattering processes* 31

Photoionization delay in heavy elements - spin dynamics and relativistic effects

E Lindroth[1]*

[1]Department of Physics, Stockholm University, SE-106 91 Stockholm, Sweden

Synopsis Relativistic effects become increasingly more important in heavy elements. The spin-orbit interaction splits thresholds and allows for transitions that involve spin-flips, leading to the opening of additional decay channels and an altered angular dependence of photoelectrons. Attsecond techniques adds temporal information to traditional spectral studies and offers a new path to an increased understanding of the complex electron dynamics involved.

Attosecond techniques have provided a new tool to study the photoionization processes. The phase information, and the insight into the temporal dynamics it gives, complements nicely cross-section measurements. With increasing capabilities to combine high temporal *and* spectral resolution [1, 2], a range of many-body effects such as resonances and shake-up processes can be revisited to gain a deeper understanding.

I will discuss attosecond delays in laser-assisted photoionization with an emphasis on heavy elements and how relativistic effects affect the angular dependence of the photoionization delay [3], how resonances can promote spin-dynamics [4] and how measurements of the atomic delay can be used to differentiate between different decay processes.

The focus will be on the theoretical treatment, but with examples from RABBIT-experiments. It is well established, see e.g. Ref. [5], that the measured *atomic delays* do not correspond directly to the delay associated with single-photon ionization. Instead, a significant part of the observed delays can be understood only if the full two-photon amplitudes, i.e. the quantity directly connected to the data available from experiments, are used in the analysis. Although it can be shown that the delay induced by the "second" photon to a large extent is *universal* [6] it has to be considered in detail in order to understand the angular dependence.

The quantum many-body problem remains a challenge, but the possibilities to study how it influences the phase of an electron wave packet is nevertheless a new path to gain understanding of electron correlation.

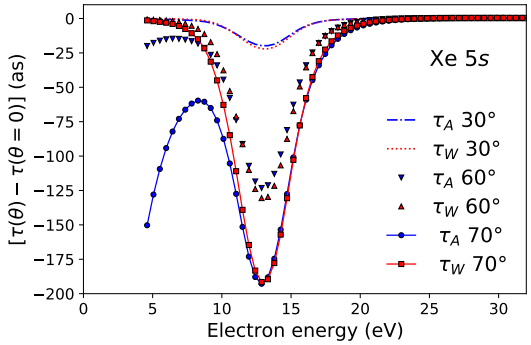


Figure 1. Atomic and Wigner photoionization delays for ionization in the Xe(5*s*) - channel. The curves show the delay in specific angles relative to the laser polarization (0°). The one-photon contribution (Wigner delay) is angular dependent solely through relativistic effects, while the two-photon contribution (atomic delay) is angular dependent even in the non-relativistic limit.

References

[1] M Isinger,*et al*, Science, **358** 893 (2017).
[2] C Alexandridi *et al*, Phys. Rev. Research, **3** L012012 (2021)
[3] Soumyajit Saha *et al*, Phys. Rev. A, **104**, 033108, (2021).
[4] Shiyang Zhong *et al*, Nat. Comm., **11** 5042, (2020).
[5] J M Dahlström *et al*, Chemical Physics **414**, 53 (2013)
[6] J M Dahlström and E Lindroth, J. Phys. B. **47**, 124012 (2014).

*E-mail: Eva.Lindroth@fysik.su.se

Tracking the Ionization Site in Neutral Molecules

L Ortmann[1 *], A AlShafey[1], A Staudte[2] and A Landsman[1†]

[1]Department of Physics, The Ohio State University, Columbus, 43210, USA
[2]Joint Attosecond Science Lab of the National Research Council/University of Ottawa, Ottawa, K1A 0R6, Canada

T1

Synopsis: We introduce a method to quantify the relative contribution of upfield versus downfield ionization when a diatomic molecule is exposed to intense infrared light. Applying this to previously measured electron momenta distributions following strong field ionization of N2, we find approximately a 2:1 ratio of electrons ionized from a downfield atom, relative to upfield. This suggests that the bound state wave function largely adapts adiabatically to the changing laser field, although the nonadiabatic process of ionization enhancement still contributes significantly even in neutral molecules.

When a diatomic molecule is exposed to intense light, the valence electron may tunnel from a higher potential (corresponding to an upfield atom) due to the suppressed internuclear barrier. This process is known as ionization enhancement and is a key mechanism in strong field ionization of molecules. Alternatively, the bound electron wave function can evolve adiabatically in the laser field, resulting in ionization from the downfield atom (see Figure 1).

We introduce a method for quantitatively retrieving the ratio of ionization events at the upfield and downfield atomic site in a diatomic molecule by comparing experimental data with quantum trajectory Monte Carlo simulations (QTMC). Our technique is based on the electron's deflection in the asymmetric Coulomb potential of the molecule that is tilted against the laser polarization direction. This introduces an asymmetry in the final photoelectron momentum distribution, which depends on the ratio of electrons born at the upfield or downfield atom [1].

We apply this method to available experimental data from strong field ionization of a neutral N_2 molecule with infrared laser light [2]. We find that although adiabatic evolution of the bound electron wave function (leading to increased downfield ionization) dominates for neutral molecules, nonadiabatic enhanced ionization still makes a significant contribution under typical experimental conditions, corresponding to the intermediate value $\gamma \approx 1$, where γ is the Keldysh parameter.

To describe the asymmetry observed in the experiment and in the QTMC simulations quantitatively, we define the average offset momentum, which we show depends on the fraction of electrons ionized upfield relative to downfield.

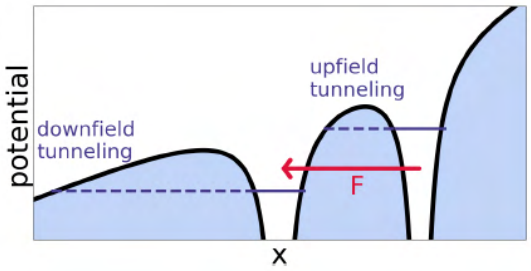


Figure 1. Diatomic potential for alignment of the internuclear axis along the polarization axis. The ionization barrier for the upper well is considerably lowered by the influence of the lower well, which can lead to upfield tunneling, corresponding to ionization enhancement. Alternatively, the electron position can adapt adiabatically to the laser field, resulting in downfield ionization.

By comparing the QTMC simulations to experimental data for different values of this offset momentum, which can be varied in the simulation, we extract approximately a 2:1 ratio of downfield vs. upfield atoms from the experimental data in [2].

References

[1] L Ortmann, A AlShafey, A Staudte, A Landsman, Phys. Rev. Lett. **127**, 213201, (2021).
[2] M Meckel, et al, Nature Phys. 10, 594, (2014).

* E-mail: ortmann.1@osu.edu
† E-mail: landsman.7@osu.edu

Real-time imaging of resonant photoemission dynamics

A. Autuori[1], D. Platzer[1], M. Lejman,[1] G. Gallician[1], L. Maëder[1]*, A. Covolo[1], L. Bosse[1], M. Dalui[1], D. Bresteau[1], J.-F. Hergott[1], O. Tcherbakoff[1], H.J.B. Marroux[1], V. Loriot[2], F. Lépine[2], L. Poisson[1,3], R. Taïeb[4], J. Caillat[4], P. Salières[1]

[1]Université Paris-Saclay, CEA, CNRS, LIDYL, 91191 Gif-sur-Yvette, France
[2]Université de Lyon, Université Claude Bernard Lyon 1, CNRS, Institut Lumière Matière, 69622 Villeurbanne, France
[3]Université Paris-Saclay, CNRS, Institut des Sciences Moléculaires d'Orsay,91405 Orsay, France
[4]Sorbonne Université, CNRS, Laboratoire de Chimie Physique-Matière et Rayonnement, 75005 Paris, France
†These authors contributed equally to this work.

Synopsis We study helium two-photon XUV+IR ionization through intermediate bound states. Using spectrally- and angularly-resolved attosecond electron interferometry, we characterize the complex-valued probability amplitude towards the photoelectron quantum state. This allows reconstructing in space, time and energy the complete formation of the photoionized wavepacket.

Imaging in real time the complete dynamics of a process as fundamental as photoemission has long been out of reach due to the difficulty of combining attosecond temporal resolution with fine spectral and angular resolutions. To achieve this, a key ingredient is the relative phase between the spectral components of the photoionized wavepacket, that can be measured using interferometric schemes such as the RABBIT technique [1], and its spectrally-resolved variant, the Rainbow RABBIT [2].

In the present study, we combine Rainbow RABBIT attosecond spectral interferometry with VMI momentum spectroscopy to record the modulus and phase variations of the photoelectron quantum state with high spectral resolution and angular sensitivity. This is performed in the test case of two-photon XUV+IR photoionization of helium through the intermediate resonant states $1s3p$ and $1s4p$. The resulting structured photoelectron wavepacket is fully characterized by measuring quasi-continuously (over a 800-meV range) the spectral and spatial variations of the two-photon transition amplitude $M(E,\theta)$. The latter display many structures such as sudden phase jumps of up to π rad *in both dimensions* [3].

These measurements give direct access to the complete, angularly-resolved, dynamics of the two-photon transition leading to photoemission. A Gabor analysis of the experimental $M(E,\theta)$ using a sliding 210-meV Gaussian gate is shown in Fig. 1 for two illustrative angles. *At resonances*, i.e. around $E_{1s3p}+\hbar\omega_0 \approx 0.06$ eV and $E_{1s4p}+\hbar\omega_0 \approx 0.66$ eV (indicated by blue and red dashed lines resp.), the dynamics are globally delayed due to the transient trapping of the electron in the intermediate bound states before completing the transition. *Between resonances*, the dynamics are strongly shaped by destructive interferences in the temporal profiles, appearing as 'holes' in the Gabor transform. The 'holes' shift towards higher energies when θ increases, e.g., from 0.33 eV at 0° to 0.59 eV at 65°. The spectro-temporal structuring of the dynamics therefore highly depends on the photoemission angle.

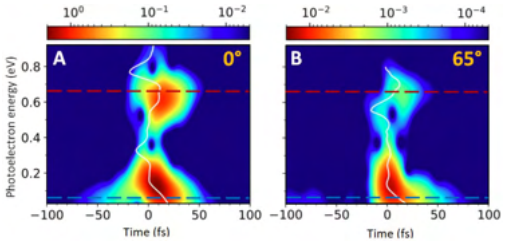


Figure 1. Spectro-temporal build-up of the photoemission process revealed by a Gabor analysis of the two-photon transition amplitude $M(E,\theta)$ at θ=0°(A) and θ=65°(B). The transition delay defined as the *local* spectral derivative of $M(E,\theta)$ is shown as white lines on each Gabor representation.

References

[1] Paul P M *et al* 2001 *Science* **292** 2001
[2] Gruson V *et al* 2016 *Science* **354** 2016
[3] Autuori A *et al* 2022 *Science Advances* in print

*E-mail: lucie.maeder@cea.fr

Theoretical treatment of quantum beats in Argon.

M A Alarcón[1]*, C H Greene[1]†, A Plunkett[2], J Wood[2] and A Sandhu[2]

[1]Department of Physics and Astronomy, Purdue University, West Lafayette, Indiana, 47907, USA.
[2]Department of Physics, University of Arizona, Tucson, Arizona, 85721, USA

T1

Synopsis An accompanying experimental study observed quantum beats in the photionization spetrum of argon. The beats are observed in the electron yield as a function of time delay when ionizing two types of wave packets: one formed of bound states and one formed of auto ionizing states. We successfully model the phenomena by implementing multichannel quantum defect theory and time-dependent perturbation theory. We find that the beats are caused by interference of two photon ionization pathways and that the value of these beats is the energy difference between the states forming the initial wave packet.

Argon atoms are excited to the bound excited states in the 3d'-5s' manifold through an ultra-fast extreme ultraviolet (EUV) laser. A simultaneous pulse is used to excite the autoionizing nf' states in a Rydberg autoionizing wave packet. This process creates two electronic wave packets that are photoionized utilizing a time-delayed femtosecond laser. The total yield of electrons is observed to oscillate in time delay.

Theoretically, we determine the electronic wavefunction of both wave packets by using multichannel quantum defect theory [1, 2] and model the time-delayed pulse as a Gaussian perturbation. Given the central frequency, we need to implement time-dependent perturbation theory to second-order [3] to describe the formation of the beats.

The purely bound wave packet will photoionize following two-photon absorption. Different intermediate state pathways will interfere, thus forming the beats. The autoionizing states can ionize with a single photon absorption, but the laser is long and intense enough to allow for Raman interference. The electron in the wave packet can absorb a photon, transition briefly into the continuum, then radiate and be recaptured. Provoking interference between autoionizing states and changing the total yield.

The finite bandwidth of the delayed laser is crucial since it is what permits the interference. This bandwidth allows different intermediate states to ionize to the same kinetic energy. In the Raman interference, it is what allows for photoelectrons to be recaptured at different energies, allowing for population redistribution.

As is seen in the figure, the resemblance between theoretical and experimental spectra is remarkable. Currently, results for the autoionizing wave packet are submitted and accepted for publication [4]. We are currently studying both the energy and angular distribution of the photoionized electrons.

This research is based upon work supported by the U.S. Department of Energy, Office os Science, Basic Energy Sciences, under Award No. DE-SC0010545.

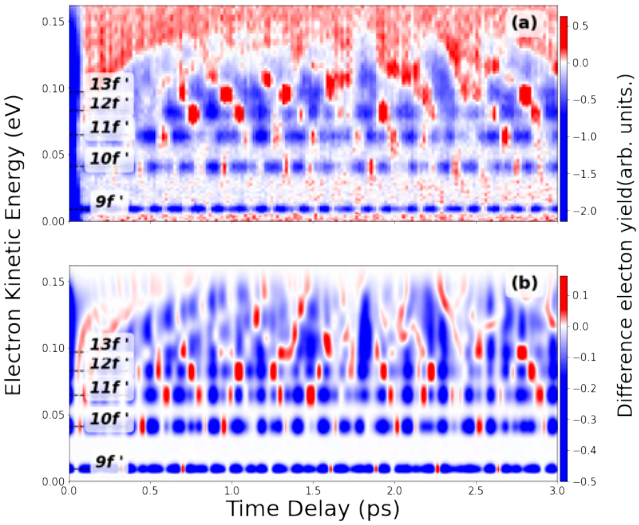


Figure 1. Comparison between experimental (a) and theoretical (b) difference between yield with and without a delayed laser. The energy axis is the kinetic energy of the autoionized electrons.

References

[1] Pellarin M *et al* 1998 *J. Phys. B: At. Mol. Opt. Phys.*, 21 **3833**
[2] C. M. Lee and K. T. Lu, 1973 *Phys. Rev. A*, vol. 8, no. 3, pp. **1241–1257**
[3] Faisal, Farhad H. Theory of Multiphoton Processes. Springer Science+Business Media, 1987.
[4] A. Plunkett, M. A. Alarcon, J. K. Wood, C. H. Greene, and A. Sandhu, [in press, PRL]. Available: **arXiv:2111.03975**

*E-mail: malarco@purdue.edu
†E-mail: chgreene@purdue.edu

The effect of Feschbach resonances on the different vibrational states of N_2 in a RABBIT experiment.

V J Borràs, [1]*, J González-Vázquez[1] and F Martín[1,2,3]†

[1]Departamento de Química, Módulo 13, Universidad Autónoma de Madrid, 28049 Madrid, Spain
[2]Instituto Madrileño de Estudios Avanzados en Nanociencia (IMDEA-Nano), Campus de Cantoblanco, 28049 Madrid, Spain
[3]Condensed Matter Physics Center (IFIMAC), Universidad Autónoma de Madrid, 28049 Madrid, Spain

Synopsis The inclusion of the nuclear motion in the TD-XCHEM code allows to describe the behaviour of the different vibrational states, while considering the presence of Feschbach resonances. This new method has been used to simulate a RABITT experiment of N_2, producing extraordinary results that have an excellent agreement with experimental data and allow to understand different unexplored features.

Due to the high photon energy of attosecond light sources, the theoretical description of attosecond experiments requires a proper representation of the ionization continuum. For polyelectronic molecules, the description of the ionization process requires the use of electronically correlated wave functions for the molecular bound states as well as the system's ionization continuum. Despite the huge success of state-of-the-art Quantum Chemistry Packages (QCP) for describing molecular bound sates, the combination with their ionization continuum at the same level of theory is still challenging. The XCHEM code, recently developed in our group, overcomes these difficulties by using a hybrid Gaussian-B-Spline (GABS) basis interfaced with existing QCPs via close-coupling scattering methods [1, 2]. The XCHEM approach has produced excellent results in different atomic and molecular systems [2, 3, 4, 5, 6, 7, 8].

By solving the time-dependent Schrödinger equation one can simulate attosecond experiments in which combinations of several pulses lead to complex interferometric patterns in the ionization continuum. We have extendeded the TD-XCHEM code to include both electronic and nuclear degrees of freedom.

We have employed this new method to simulate a Reconstruction of Attosecond Beating By Interference of Two photon Transitions (RABBIT) experiment of N_2 in a energy region that contains Feshbach resonances converging to $A^2\Pi_u$ and $B^2\Sigma_u^+$ states. Due to the inclusion of the nuclear movement and to the capability of the XCHEM code to describe the electronic correlation, this simulation is able to consider the population of Feshbach resonances by different vibrational states.

In this work, we present the results obtained, which have an excellent agreement with experimental data [9] and allow to understand different unexplored features.

References

[1] C. Marante et al., Phys. Rev. A 90, 012506 (2014).
[2] C. Marante et al., J. Chem. Theory Comp. 13, 499 (2017).
[3] L. Barreau et al., Phys. Rev. Lett. 122, 253203 (2019).
[4] M. Klinkeret al., Phys. Rev. A,98, 033413 (2018).
[5] S. Poullain et al., Phys. Chem. Chem. Phys.,21, 16497 (2019).
[6] M. Klinker et al., J. Phys. Chem. Lett. 9, 756 (2018).
[7] C. Marante et al., Phys. Rev. A, 96, 022507 (2017).
[8] V. J. Borràs. et al., J. Chem. Theory Comp. 7, 10, 6330 (2021).
[9] S. Haessler et al., Phys, Rev. A, 7, 80, 011404 (2009).

*E-mail: josep.borras@uam.es
†E-mail: fernando.martin@uam.es

ASTRA, a transition-density-matrix solution to the close-coupling problem in the molecular ionization continuum

J M Randazzo[1,2], C Marante[1], H Gharibnejad[3], B I Schneider[3], J Olsen[4], L Argenti[1]*

[1]Department of Physics and CREOL, University of Central Florida, Orlando, FL 32816, USA
[2]CONICET, San Carlos de Bariloche, Río Negro 8400, Argentina
[3]NIST, Gaithersburg, MD 20899, USA
[4]Department of Chemistry, Aarhus University, Aarhus 8000, Denmark, EU

Synopsis We present ASTRA, a new molecular photoionization code that leverages the formalism of transition density matrices to efficiently compute the many-body inter-channel-coupling interactions needed to simulate the highly correlated electron dynamics triggered in atoms and molecules by attosecond and dressing pulses.

Advances in laser technology have led to production of attosecond extreme-ultraviolet and x-ray pulses with ever increasing intensity and repetition rates [1, 2]. As a result, statistically significant attosecond-pump attosecond-probe experiments for molecular systems of chemical relevance are now within reach. These capabilities have opened the way to the detailed time-resolved study of photoelectron emission from core orbitals, of vibronic coupling in photoemission, and of Auger cascades. Since these experiments entail the formation of entangled photofragments, close-coupling (CC) is the ideal approach to simulate and interpret them. CC single-ionization codes suited for small molecules in interaction with XUV pulses, such as XCHEM [6] and UKRmol+ [4], already exist. The need of a theoretical framework extensible to multiple ionization, that can represent both slow (∼1 eV) and fast (∼1 keV) photoelectrons, and that scales favorably with molecular size and with the size of the ionic configuration-interaction space, however, is still needed. Here, we present ASTRA (AttoSecond TRAnsitions), a code that implements a new approach to the CC scheme, based on the use of High-Order Transition density matrices (HOTdms) between large-scale-CI ionic states with arbitrary symmetry and multiplicity. The HOTdms, which are not available in standard quantum-chemistry codes, are computed with an extension of the LUCIA code [3] and allow us to evaluate inter-channel matrix elements of arbitrary many-body operators with remarkable speed. Currently, ASTRA contemplates single-ionization states but it admits a natural extension to double-escape channel, whose implementation is under way. ASTRA also relies on the use of hybrid Gaussian B-spline functions, whose basic integrals are computed numerically using methods from the literature [4, 5]. We illustrate ASTRA results for a set of benchmark observables, such as N_2 photoionization cross section, for which theoretical and experimental results exist.

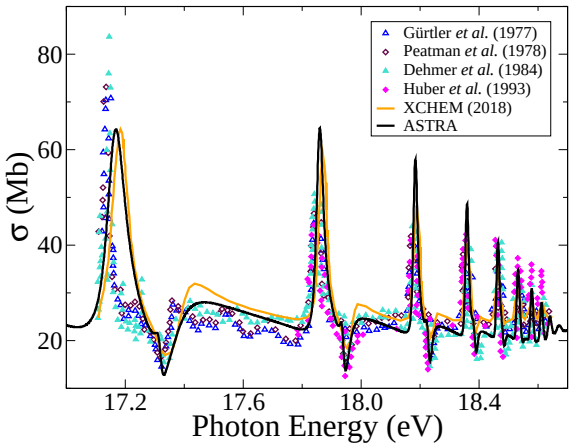


Figure 1. Comparison between experimental N_2 photoionization cross sections and the theoretical predictions with XCHEM and ASTRA.

This work is supported by the DOE CAREER grant No. DE-SC0020311.

References

[1] Duris J et al, Nat. Phot. **14**, 30 (2020).
[2] Saito N et al, Optica **6**, 1542 (2019).
[3] Olsen J et al, J. Chem. Phys. **104**, 8007 (1996).
[4] Mašín Z et al., CPC **249**, 107092 (2020).
[5] Gharibnejad H et al, CPC **263**, 107889 (2021).
[6] Klinker M et al., J. Phys. Chem. Lett. **9**, 756 (2018).

*E-mail: Luca.Argenti@ucf.edu

Experimental investigation of topological property of degenerate singularities in rescattering processes

T Mizuno[1]*, T Yang[1], T Kurihara[1] N Ishii[1], T Kanai[1], O I Tolstikhin[2], T Morishita[3] and J Itatani[1]

[1]The Institute for Solid State Physics, The University of Tokyo, Kashiwa, Chiba 277-8581, Japan
[2]Moscow Institute of Physics and Technology, Dolgoprudny 141700, Russia
[3]Institute for Advanced Science, The University of Electro-communications, Chofu-shi, Tokyo 182-8585, Japan

Synopsis We measure rescattering photoelectron momentum distribution (PEMD) of Kr atoms and CO_2 molecules by using a carrier-envelope phase (CEP)-stable few-cycle field. A cutoff structure of measured PEMDs agrees quantitatively with the Airy function-like universal distribution calculated by the adiabatic theory. This behavior is guaranteed by the singularity theory, and is attributed to topological property of a caustic. We experimentally reveal the topological properties underlying the caustic in the rescattering processes.

Photoionization of an atom and molecule in intense field is the most fundamental process in strong field physics [1, 2]. Recent works reveal that the cutoff structures of high order harmonic generation (HHG) [3] and rescattering photoelectron momentum distribution (PEMD)[1, 2] show the universal Airy function-like behavior. This is attributed to the caustic, which is the singularity of the action described by the Hamiltonian formulation.

In this work, we investigate PEMDs for Kr atom and CO_2 molecules near the rescattering caustic by a carrier-envelope phase (CEP)-stable few-cycle field. We use linearly-polarized intense IR fields at 1600 nm with a pulse duration of 14 fs from an OPCPA system. The PEMD in the parallel direction to the polarization is measured by a time-of-flight photoelectron spectrometer as a function of the CEP, as shown in Fig. 1.

In the scattering theory [4], a scattering amplitude $f(k)$ is approximately given in the oscillatory integral as following

$$f(k) = \int_{-\infty}^{\infty} g(t) \exp\left[iS(t;k)\right] dt. \qquad (1)$$

where $g(t)$ represents the amplitude, and $S(t;k)$ is action as a function of time t and photoelectron momentum that is parallel to the polarization k. The universality is originated from topological property of the singularity of the action S. The singular point t_0 and the caustic k_0 of an action are defined as

$$\partial S(t_0;k_0)/\partial t = \partial^2 S(t_0;k_0)/\partial t^2 = 0. \qquad (2)$$

The asymptotic evaluation of Eq. (1) exhibits the universal distribution around the caustic, which is characterized by the equivalence class of the caustic [4]. We experimentally confirmed the universality of the PEMDs around the caustic, where long and short backward rescattering trajectories coalesce, by comparing with calculated PEMDs by the adiabatic theory [1].

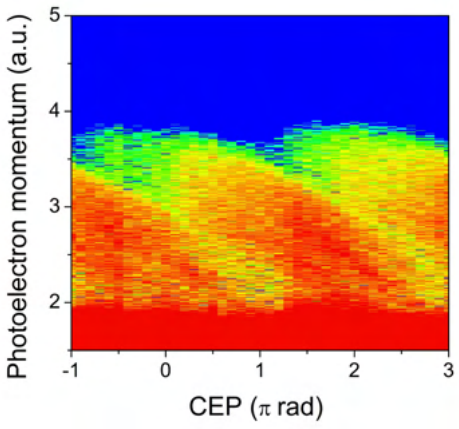


Figure 1. Measured PEMDs of CO_2 at an intensity of 7.4×10^{13} W/cm^2.

References

[1] T. Morishita and O. I. Tolstikhin, *Phys. Rev. A* **96**, 053416 (2017)
[2] T. Mizuno *et al. Phys. Rev. A* **103**, 043121 (2021)
[3] M. V. Frolov *et al. J. Phys. B* **42**, 035601 (2009)
[4] J. Connor, *Molecular Physics* **31**, 33 (1976)

*E-mail: mizuno.tomoya@issp.u-tokyo.ac.jp

T2 Attosecond Dynamics in Low-D Materials ▲

11:00 - 13:00 **T2 Attosecond dynamics in low-D materials** 32
Chair: **Madhab Neupane**, University of Central Florida, Orlando, FL, USA

11:00 **Ursula Keller**, ETH Zürich, Switzerland
I: *Element Specific Screening Dynamics in $MoSe_2$* 33

11:30 **Mikhail Yu. Ivanov**, Max-Born-Institut (MBI), Germany, EU
I: *Lightwave electronics in trivial and strongly correlated solids* 34

12:00 **Alexis Chacon**, POSTECH, Republic of Korea
C: *Ultrafast spectroscopy of 3D-topological insulators by high-order harmonics* 35

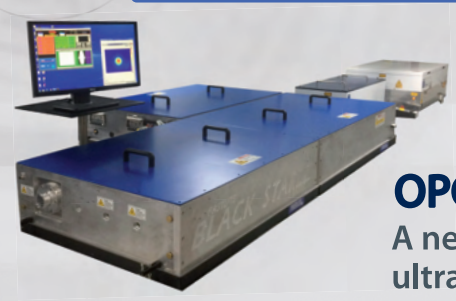
12:15 **Amar Bharti**, Indian Institute of Technology Bombay, India
C: *High-Harmonic spectroscopy of nonlinear anisotropic anomalous Hall effect in topological materials* 36

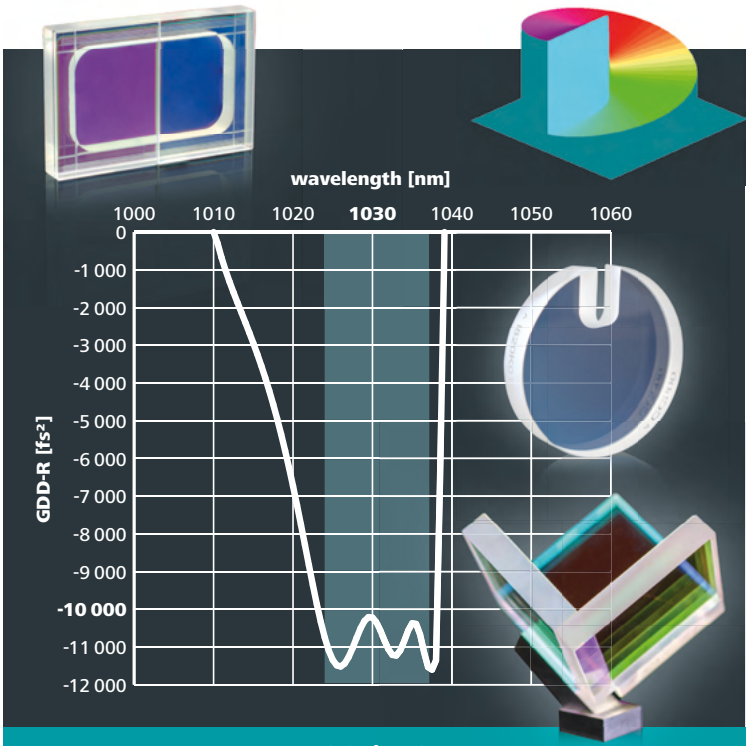
12:30 **Sambit Mitra**, Max-Planck-Institute for Quantum Optics, Germany, EU
C: *Strong light-field controlled valleytronics* 37

12:45 **Jakub Schusser**, University of Würtzburg, Germany, EU
C: *Spin-, time- and angle-resolved photoemission spectroscopy (STARPES) on the transition metal dicalchogenide WTe_2* 38

T2

FASTLITE
www.fastlite.com
Landmark technologies
for
the ultrafast laser users community
Dazzler
The reference of
ultrafast pulse shaping



OPCPA systems
A new generation of
ultrafast sources

LAYERTEC
OPTICAL COATINGS · OPTICS
Tailormade Ultrafast Optics
LAYERTEC – Your supplier for enhanced laser optics


LAYERTEC GmbH, GERMANY
www.layertec.de | info@layertec.de | Phone: +49 36453 744 0

Element Specific Screening Dynamics in $MoSe_2$

Z Schumacher[1,*], S A Sato[2,3], S Neb[1], A Niedermayr[1], A Rubio[3,4], L Gallmann[1] and U Keller[1]

[1]Department of Physics, ETH Zürich, 8093 Zürich, Switzerland
[2]Center for Computational Sciences, University of Tsukuba, Tsukuba, Ibaraki 305-8577, Japan
[3]Max Planck Institute for the Structure and Dynamics of Matter and Center for Free Electron Laser Science, 22761 Hamburg, Germany
[4]Center for Computational Quantum Physics (CCQ), Flatiron Institute, New York 10010, USA

Synopsis Attosecond transient absorption spectroscopy (ATAS) allows for the element-specific characterization of the ultrafast electronic response of nanometer thick solid state samples. We use a wide XUV spectrum (30-60 eV) to probe the response of two different core hole transitions into excited states around the Fermi level after strong NIR excitation in few-layer $MoSe_2$. Different spectral responses are observed for the Mo and Se transitions, which we attribute to localized screening around Mo 4d-states. We demonstrate how ATAS can be used for element-specific measurements of screening in 2D-materials.

ATAS allows for the element-specific characterization of population dynamics in the few fs to ps time scale, while more complex phenomena are observed during pump-probe overlap due to the strong NIR pump pulse [1-4]. One of our recent studies in transition metals has revealed screening effects due to pump-induced electron localization in titanium [4]. Here, we extend the application of ATAS to few-layer transition metal dichalcogenides (TMDs) for element-specific investigation of ultrafast screening dynamics.

The wide probe spectrum of our setup (30-60 eV) allows us to cover multiple transitions in $MoSe_2$. We simultaneously probe the vicinity of the valence and conduction bands (VB/CB) from two different core levels of the two involved elements. We find the transitions initiated from the molybdenum core level to be strongly affected by electron screening dynamics, whereas the selenium-based probe transition is dominated by state-blocking as well as broadening and red-shift of the absorption edge. Due to the different energies of the two core levels involved in the probe process, their respective VB/CB response is well separated in photon energy, fig. 1. The different orbital contributions to the VB/CB result in spectrally different responses of the XUV probe transition dominated by different physical processes, even though the carriers in the CB are excited by the same NIR excitation. We use time-dependent density-functional theory as well as independent particle calculations to identify the contribution of many-body screening effects to the spectral response of the two core-hole transitions. Our findings are a first experimental observation of how localized electron screening influences the spectral response on an element-specific level.

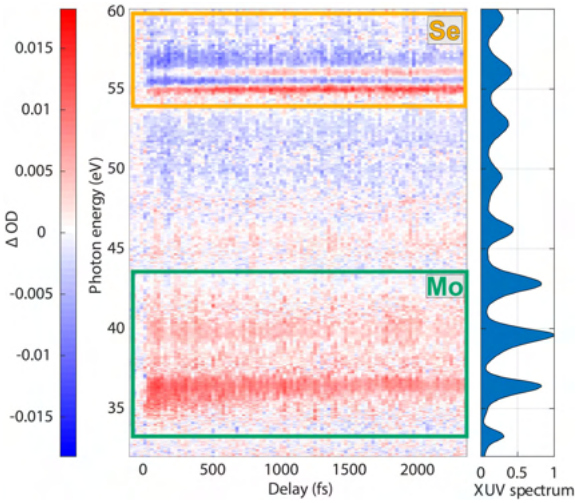


Figure 1. ATAS trace of few-layer $MoSe_2$ with the molybdenum transition visible above 35 eV as a wide positive feature (green box) and the selenium transition appearing around 55 eV with positive and negative response (yellow box) for the VB/CB transition, respectively.

References

[1] Schlaepfer F *et al* 2018 *Nat. Phys.* **14** 560-564
[2] Zürch M *et al* 2017 *Nat. Commun.* **8** 15734
[3] Zürch M *et al* 2017 *Struct. Dyn.* **4** 044029
[4] Volkov M *et al* 2019 *Nat. Phys.* **15** 1145-1149

* E-mail: zenos@phys.ethz.ch

Lightwave electronics in trivial and strongly correlated solids

Misha Ivanov[1,2,3]

[1]Max-Born-Institut, Berlin, Germany
[2] Humboldt Universität zu Berlin, Germany
[3] Department of Physics, Imperial College London, UK

Synopsis: Light pulses shaped on the time-scale of individual oscillations of the electric field open unique opportunities in controlling the electron motion in solids at the single-femtosecond time scale. I will review our recent results on sub-cycle control of electron dynamics in various solids, from trivial to strongly correlated.

Modern light generation technology has evolved to the point where a theorist may reasonably expect an experimentalist to generate light pulses where individual oscillations of the electric field are shaped almost at will. Control of the carrier-envelope phase of few-cycle pulses is now almost routine. One can also reliably generate complex polarization states in two and three dimensions, sculpting the Lissajous figures drawn by the electric field vector during a single optical cycle. As these fields can be made strong enough to compete with the internal electric fields in a medium, coherent electronic motion can be excited and shaped almost at will, at the time-scale of a single light oscillation.

How can we use such opportunities? What happens to a crystal exposed to such light? Do we change its effective band structure and density of states? Can these changes be controlled?

To address these question, I will consider several examples where our ability to control light on the sub-cycle time-scale leads to interesting results.

The first example is PHz valleytronics, which aims to use light to generate coherent electronic excitations in a desired valley of a Brillouin zone. In gapped graphene-type materials, the selection of a desired valley is typically achieved using circularly polarized pulses. I will present our new results [1] which show how a sequence of linearly, not circularly, polarized few-cycle pulses can be used to excite a desired valley in a two-dimensional gapped graphene material such as hexagonal Boron Nitride, then de-excite it, then switch the excitation to another valley, and finally read-out the results in an all-optical manner, all within about 10-20 fs. I will also show that even a single linearly polarized few-cycle pulse can generate selective valley excitation [2], and that PHz valleytronics is possible even in pristine graphene [3], a medium where selective valley excitation was thought to be impossible.

I will then present our new results on lightwave control of electronic excitations and metal-insulator phase transition in two canonical models of correlated materials: an Ising chain of spins (or pseudo-spins) and a two-dimensional Hubbard system. In the Ising spin chain, control over the carrier-envelope phase of a few-cycle (effective) magnetic field allows us to control the final spin state of the system, starting with equal population of the spin-up and spin-down states [4].

In the 2D Hubbard model with strong on-site interaction, a few-cycle laser pulse converts an initially metallic state into a Mott-insulating or a bad metallic state. At high field strength, the density of correlated states is strongly modified by the field. Importantly, this newly "minted" density of states survives after the end of the laser pulse: it appears that the re-shaped charge distribution generates a new self-consistent potential supporting new density of states [5].

[1] Á. Jiménez-Galán, R. E. F. Silva, et al, in preparation
[2] Á. Jiménez-Galán, R. E. F. Silva, O. Smirnova, and M. Ivanov, Optica 8, 277-280 (2021)
[3] M. S. Mrudul, A. Jiménez-Galán, M. Ivanov, G. Dixit, Optica 8, 422-427 (2021)
[4] N. Klimkin, A. Rubtsov, and M. Ivanov, in preparation
[5] V. Valmispild, E. Gorelov, M. Eckstein, A. Lichtenstein, H. Aoki, M. I. Katsnelson, M. Ivanov, and O. Smirnova, in preparation

* E-mail: mivanov@mbi-berlin.de

Ultrafast Spectroscopy of 3D-Topological Insulators by High-Order Harmonics

D. Baykusheva[1], A. Chacon[2,3*], J. Lu[1,4], T. P. Bailey[5], J. A. Sobota[6], H. Soifer[6], P. S. Kirchmann[6], C. Rotundu[6], C. Uher[5], T. F. Heinz[1], D. A. Reis[1], and S. Ghimire[1†]

[1]Stanford PULSE Institute, SLAC National Accelerator Laboratory, Menlo Park, California 94025, USA
[2]Department of Physics and Center for Attosecond Science and Technology, POSTECH, Pohang 37673, South Korea
[3]Max Planck POSTECH/KOREA Research Initiative, Pohang 37673, South Korea
[4]Department of Physics and Astronomy, University of Pennsylvania, Philadelphia, PA 19104-6396, USA
[5]Department of Physics, University of Michigan, Ann Arbor, Michigan 48109, USA
[6]Stanford Institute for Materials and Energy Sciences, SLAC National Accelerator Laboratory, Menlo Park, California 94025, USA

T2

Synopsis
We observe an anomalous strong-field optical response of the prototypical 3D topological insulator Bi_2Se_3, revealed through the process of high-harmonic generation driven by ultrashort mid-infrared fields. We find that the harmonic yield increases as the polarization of laser field is changed from linear to elliptical and it becomes maximum for a fully circular polarization. With the aid of a microscopic quantum-mechanical theory, we reveal that the observed anomalous enhancement arises from the unique band structure of the gapless topological surface states (TSSs). Our results bear implications for the ultrafast probing of topological phase transitions.

In the last decades, high-order harmonic generation (HHG) in gases established itself as a powerful tool for investigating electron structure and dynamics [1-2]. Ghimire *et al.* [3] expanded the HHG process from gases to condensed matter systems [3]. Surprisingly, one of the main features of HHG, the high-energy *cut-off* exhibits a linear scaling with respect to the laser-field strength in solids, while in gases, this scaling is quadratic. Microscopically, HHG in solids entails a plethora of interesting dynamical phenomena occurring at the attosecond time scale, such as inter-band electron tunneling, Bloch oscillations, and electron-hole (*e-h*) quasiparticle dynamics.

In this work, we extend the scope of HHG to a distinctly different class of matter, namely, topological materials. Our measurements on the prototypical topological insulator Bi_2Se_3 reveal an anomalous laser-ellipticity dependence of the high-harmonic generation process, manifested in a substantial enhancement of selected high-harmonic (H) orders for circularly polarized laser fields (see Fig. 1 a). We attribute the latter results to the nontrivial topology of the surface Bloch bands and states, in particular the dipole couplings and Berry connections close to the Γ-point of the Brillouin zone and the influence of the high-order "warping" terms at higher momenta [4]. Our interpretation is supported by a fully quantum-mechanical treatment of the HHG process in the framework of the semiconductor Bloch equations formalism (cp. Fig. 1 b).

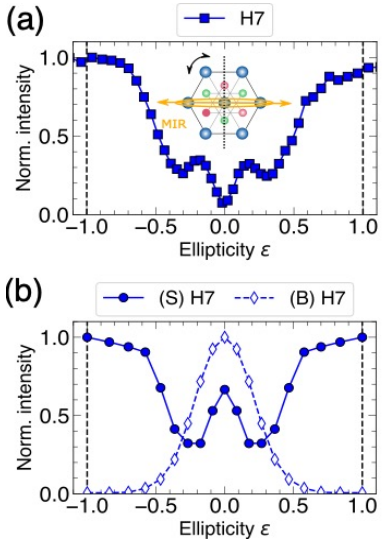


***Fig. 1**. Observation of anomalous ellipticity behavior. Upper panel: Experimental yield of H7 as a function of ellipticity. Bottom panel: Theoretical calculation of the surface and bulk contributions to the HHG yield. Reproduced from Ref. [4].*

References

[1] Li, X. F. *et. al*, *Phys. Rev. A*. **39** 5751–5761, (1989).
[2] P. B. Corkum and F. Krausz. *Nature Phys*. **3** no. SN, pp. 381–387 (2007).
[3] S. Ghimire et al. *Nature Phys*. **7**, 138 (2010)
[4]. D. Baykusheva, et al. *Phys. Rev. A* **103**, 023101 (2021). D. Baykusheva, *et. al*, **21**, 8970–8978, *Nano Lett.* (2021).

* E-mail: achacon@postech.ac.kr; † Email: shambhu@slac.stanford.edu

High-Harmonic Spectroscopy of Nonlinear Anisotropic Anomalous Hall Effect in Topological Materials

A Bharti[1]*, M S Mrudul[1] and G Dixit[1]†

[1]Department of Physics, Indian Institute of Technology Bombay, Powai, Mumbai 400076, India

T2

Synopsis Present work focuses on probing non-trivial aspects of the laser-driven electron dynamics in topological materials. For this purpose, high-harmonic spectroscopy of Weyl semimetal with broken time-reversal symmetry is investigated. It is found that Berry curvature due to non-trivial topology leads to the generation of odd anomalous harmonics, which are anisotropic in nature. We show that the non-trivial topology of the Berry curvature in topological materials can be probed by measuring the polarisation of emitted anomalous harmonics.

Discoveries of topological materials, such as topological insulators, Dirac and Weyl semimetals, have revolutionised contemporary physics. Moreover, these materials hold promises for upcoming technologies based on quantum science and electronics. The transition from Dirac to Weyl semimetal requires the breaking of either inversion or time-reversal symmetry. The present work shows that the laser-driven electron dynamics in a Weyl semimetal with broken time-reversal symmetry has intriguing features in its high-harmonic spectrum [1].

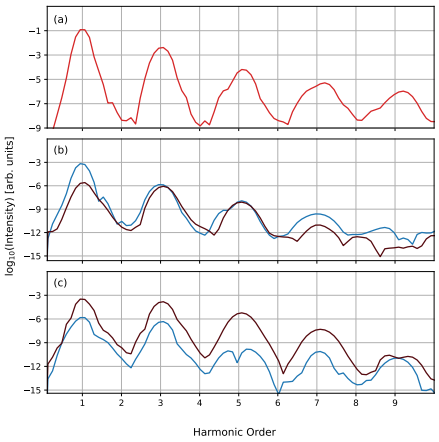


Figure 1. High-harmonic spectra corresponding to a linearly polarised pulse. The pulse is polarised along (a) x, (b) y, and (c) z directions. Driving pulse is 100 fs long with intensity 10^{11} W/cm^2, and wavelength 3.2 μm.

It is found that the parity and magnitude of the non-zero Berry curvatures components control the direction and strength of the anomalous current, which leads to the generation of the anomalous odd harmonics. We show that the non-trivial topology of the Berry curvature in time-reversal symmetry broken quantum materials can be probed by measuring the polarisation of the emitted anomalous odd harmonics. Density matrix based approach is used to investigate laser-driven electron dynamics in Weyl semimetal [2] [3].

Our findings unequivocally illustrate that the laser-driven electron dynamics leads to the generation of nonlinear anisotropic anomalous Hall effect in time-reversal symmetry broken quantum materials on ultrafast timescale. Present work opens a new avenue for studying strong-field driven electron dynamics and high-harmonic generation in systems with broken TRS, such as exotic magnetic and topological materials, and tailoring the polarization of the emitted harmonics.

References

[1] Amar Bharti, M. S. Mrudul, and Gopal Dixit, arXiv **2112**.01745 (2021)

[2] Mrudul MS and Gopal Dixit, Phy. Rev. B **103**, 094308 (2021).

[3] M. S. Mrudul, Ivaro Jimnez-Galn, Misha Ivanov, and Gopal Dixit, Optica **8**, 422-427 (2021).

*E-mail: a_bharti@iitb.ac.in
†E-mail: gdixit@iitb.ac.in

Strong light-field controlled valleytronics

S Mitra[1,2], Á Jiménez-Galán[3,4†], M Neuhaus[1,2], O Smirnova[3,5], M Ivanov[3,6,7], M F Kling[1,2,8,9] and S Biswas[1,2 *]

[1] Physics Department, Ludwig-Maximilians-Universität Munich, Garching, Germany
[2] Max Planck Institute of Quantum Optics, Garching, Germany
[3] Max-Born-Institute, Berlin, Germany
[4] National Research Council of Canada, K1N 5A2, Ottawa, Canada
[5] Technische Universität Berlin, Berlin, Germany
[6] Department of Physics, Humboldt University, Berlin, Germany.
[7] Blackett Laboratory, Imperial College London, London, UK
[8] SLAC National Accelerator Laboratory, Menlo Park, CA, USA.
[9] Department of Applied Physics, Stanford University, Stanford, CA, USA

Synopsis Inversion-symmetry broken 2d-quantum systems possess valley degree of freedom, which can be potentially utilized for efficient information processing by coupling with ultrafast light. Here, we demonstrate the sub-cycle manipulation and control of valley excitation in the strong field regime. This is achieved by tailored strong laser field that breaks the time reversal symmetry of the system resulting in selective valley tunneling excitation.

The fusion between modern quantum material science with the ability to control sub-cycle light fields promises ultrafast light-field-electronics, which can potentially operate million times faster than state-of-the-art electronics. Inversion-symmetry broken 2d-quantum materials, e.g., monolayer hexagonal boron nitride (hBN) or transition metal dichalcogenides (TMDs), possess valley degrees of freedom associated with the local minima in the band structure [1]. Their A) selective excitation, B) controlled inter-valley switching, and C) readout of the excited quantum states are the prerequisites for their use in information processing. Attempts to control valley polarization so far relied on resonant excitation [2, 3], along with valley switching with strong terahertz fields [4].

Here, following the recent theoretical prediction [5], we demonstrate all-optical non-resonant strong field control of all the three major steps (A-C). We used two-color bi-circular ultrashort laser fields to control the selective valley excitation in hBN and then probe the quantum valley states via third harmonic generation ellipsometry. The non-resonant pump field modifies the topological properties of the band structure by inducing Halden-type [6] next nearest neighbor hopping, which manifests the breaking of time-reversal symmetry. This hopping interaction controls the valley asymmetry and can be manipulated by varying the phase delay between the two colors of the bi-circular field. In agreement with the theoretical predictions, the experimental data shows selective enhancement of valley population as a function of the two-color phase delay. These results demonstrate a new regime of valleytronics and light-induced topology in quantum materials.

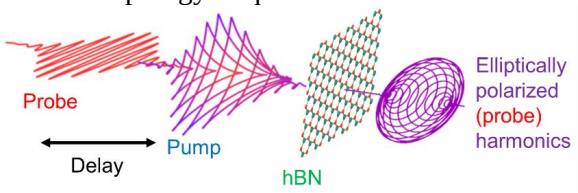


Figure 1. Strong light-field induced selective valley excitation in monolayer hBN by interferometrically merged 1 and 2 μm counter rotating laser fields. The delayed linearly polarized 2 μm probe generates intra-band harmonics whose ellipticity encodes the signature of the valley excitation state.

References

[1] Schaibley J R *et al* 2016 *Nat. Rev. Mater.* **1** 16055
[2] Mak K F *et al* 2012 *Nat. Nanotech.* **7** 494-498
[3] Zeng H *et al* 2012 *Nat. Nanotech.* **7** 490–493
[4] Langer F *et al* 2018 *Nature* **557** 76–80
[5] Jiménez-Galán Á *et al* 2020 *Nat. Photon.* **14** 728
[6] Haldane F D M 1988 *Phys. Rev. Lett.* **61** 2015

* E-mail: shubhadeep.biswas@mpq.mpg.de
† E-mail: alvaro.jimenez@mbi-berlin.de

Spin-, time- and angle-resolved photoemission spectroscopy (STARPES) on the transition metal dicalchogenide WTe2

M. Fanciulli [1,2*], J. Schusser [1,2,3], M. Lee[1,2], Z. El Youbia[2,4], O. Heckmanna[2], M. C. Richter[2], C. Cacho[4], C. Spezzani[5], D. Bresteau[2], J. F. Hergott[2], P. D'Oliveira[2], O. Tcherbakoff[2], T. Ruchon[2†], J. Minár[3] and K. Hricovini[2]

[1] LPMS, CY Cergy Paris Université, 95031 Cergy-Pontoise, France
[2] Université Paris-Saclay, CEA, CNRS, LIDYL, 91191 Gif-sur-Yvette, France
[3] New Technologies-Research Center, University of West Bohemia, 30614 Pilsen, Czech Republic
[4] Diamond Light Source, Harwell Campus, OX110DE Didcot, United Kingdom
[5] Elettra-Sincrotrone Trieste, 34149 Basovizza, Italy

Synopsis We combined a spin-resolved photoemission spectrometer with a high-harmonic generation (HHG) laser source, which allows to perform spin-, time- and angle-resolved photoemission spectroscopy (STARPES) experiments. Measurements of the spin polarization on bulk WTe_2 at different femtosecond pump-probe delays reveal a spin accumulation above the Weyl points region, shedding light on the electron dynamics in this transition metal dichalcogenide naturally close to a topological transition.

Weyl points (WPs) are topologically protected conical crossings of electron and hole states, which come in pairs of opposite chirality, and are connected by topological surface states dubbed as Fermi arcs. Bulk WTe2, a well-known transition metal dichalcogenide [1,2], is the first proposed topological type-II Weyl semimetal, characterized by tilted cones [3]. However, its topological classification has been controvertial, since WPs are extremely close to each other in reciprocal space and energy. It is now considered to lie very close to a trivial to topological phase transition depending on its purity [4]. Whether the electronic structure is gapless and thus is hosting topological low energy excitations dubbed as Weyl fermions, or the structure is just a gapped precondition for a topological phase, it is irrelevant for the overall electron spin dynamics. Instead, it is the peculiar spin-polarized, cone-like electronic structure of WTe_2 that is useful to explain its anomalous transport properties. Thus, we performed spin-, time- and angle-resolved photoemission spectroscopy (STARPES) with a high-harmonic generation (HHG) laser source in order to study the spin dynamics in WTe_2 [5]. Measurements at different femtosecond pump-probe delays and comparison with spin-resolved one-step photoemission calculations provide insight into the spin polarization of the electrons above the Fermi level in the region where Weyl points are expected [Figure 1]. We find a nonzero spin polarization abouve the Fermi level with two zero crossings, and we observe a spin accumulation above the Weyl points region, that is consistent with a spin-selective bottleneck effect due to the presence of spin polarized cone-like electronic structure. More in general, our results support the feasibility of STARPES with HHG, which despite being experimentally challenging provides a unique way to study spin dynamics in photoemission.

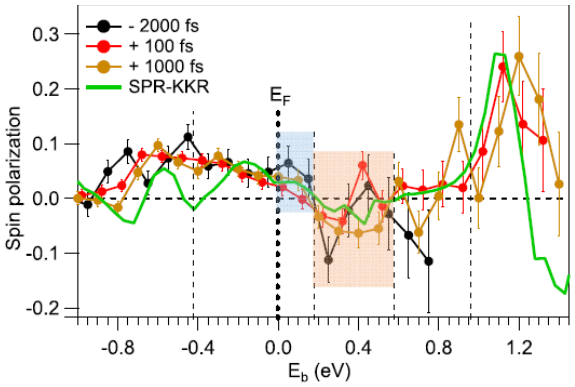


Figure 1.Spin polarization around the Fermi level along a selected quantization axis and in a selected reciprocal space region corresponding to the Weyl points, as a function of pump-probe time-delay. Comparison with one-step photoemission calculations (SPR-KKR) is also shown.

References

[1] M. Fanciulli *et al.*, Phys. Rev. Res. 2, 013261 (2020)
[2] A. A. Soluyanov *et al.*, Nature 527, 495 (2015)
[3] M. N. Ali *et al.*, Nature (London) 514, 205 (2014)
[4] X.-C. Pan *et al.*, Nat. Comm. 6, 7805 (2015)

* E-mail: mauro.fanciulli@u-cergy.fr
† E-mail: thierry.ruchon@cea.fr

T3 High Order Harmonic Spectroscopy & Control ▲

14:00 - 16:00 **T3 High Order Harmonic Spectroscopy and Control** 39
Chair: **Wendell T. Hill**, University of Maryland, Maryland, USA

14:00 **Nirit Dudovich**, Weizmann Institute of Science, Israel
I: *Attosecond Interferometry* 40

14:30 **Giulio Vampa**, National Research Council of Canada, Canada
I: *Nano-scale focusing of solid-state high harmonics* 41

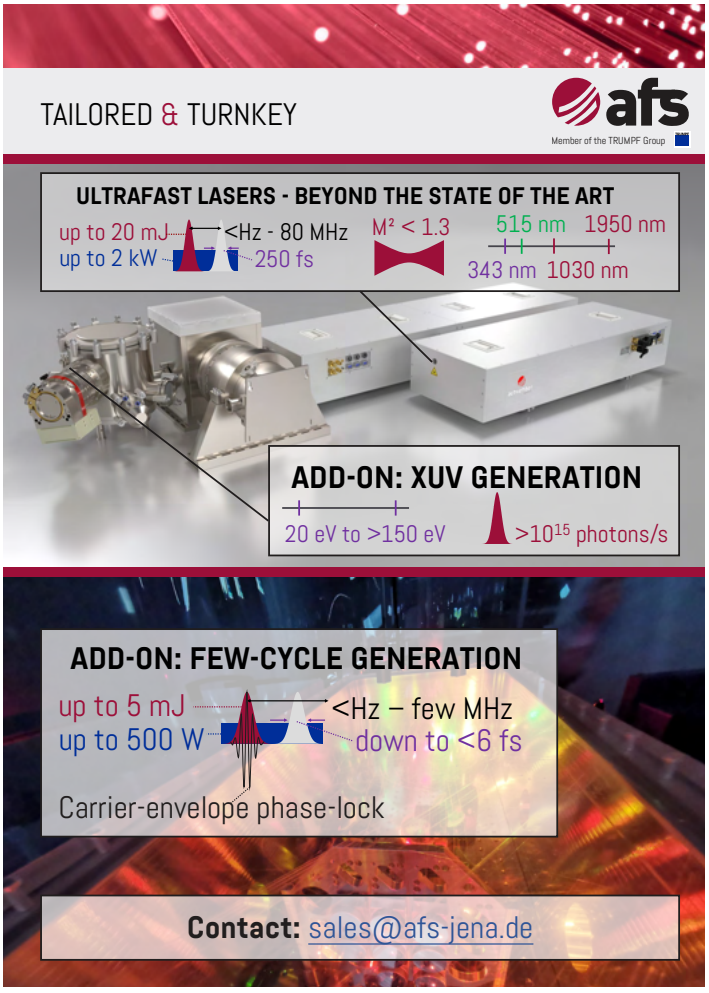
15:00 **Toby Barnard**, Imperial College London, United Kingdom
C: *EUV high harmonic generation from a thin sheet of isopropanol* . . 42

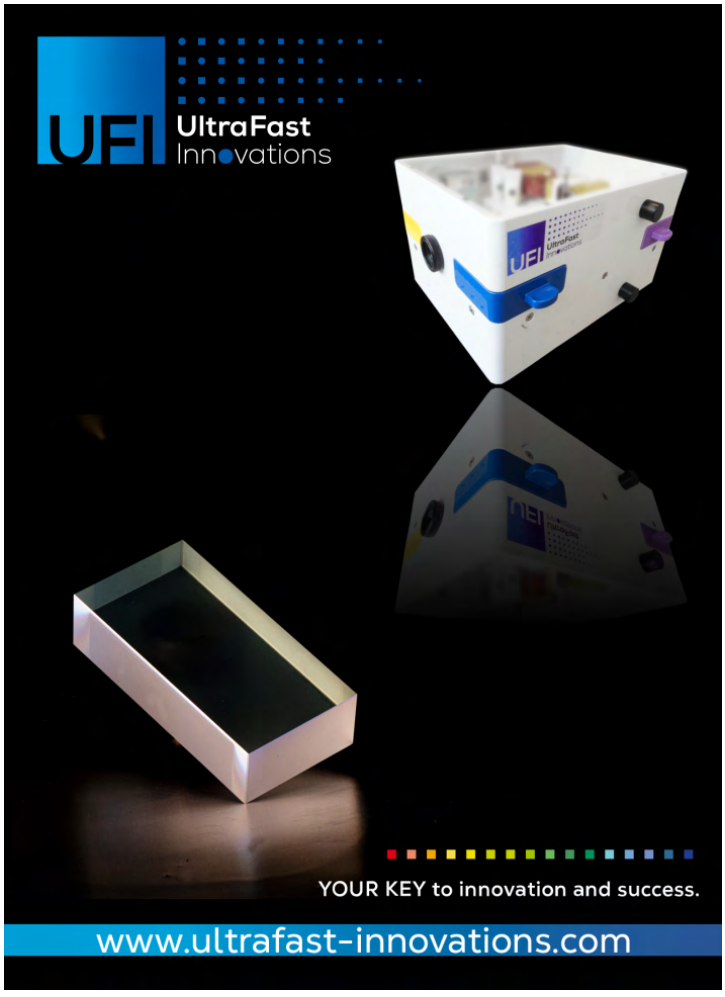
15:15 **Christian Heide**, SLAC National Accelerator Laboratory, California, USA
C: *Controlling solid-state high-harmonics in monolayers via artificial stacking* 43

15:30 **Shima Gholam Mirzaei**, JASL, Canada
C: *High Harmonic generation from metals* 44

15:45 **Igor Tyulnev**, ICFO - Institut de Ciencies Fotoniques, Spain, EU
C: *High harmonic spectroscopy of quantum phase transitions in a high-Tc superconductor* 45

T3





Attosecond Interferometry

N Dudovich*

Department of Physics, Weizmann Institute of Science, Rehovot 76100, Israel

Synopsis: Interferometry has been at the heart of wave optics since its early stages. Transferring this concept to the attosecond time domain shed new light on fundamental ultrafast electron phenomena. In my talk, I will describe several schemes for attosecond interferometry. Applying these schemes revealed a range of fundamental phenomena in atomic, molecular and condense matter systems.

Attosecond science is a young field of research that has rapidly evolved over the past decade. One of the most important aspect of attosecond spectroscopy lies in its coherent nature. Resolving the internal coherence is a primary **challenge** in this field, serving as a key step in our ability to reconstruct the internal dynamics. As in many other branches in physics, coherence is resolved via interferometry. In this talk, I will describe advanced schemes for attosecond interferometry. The application of these schemes provides direct insights into a range of fundamental phenomena in nature, from tunneling and photoionization in atomic systems to ultrafast chiral phenomena and attosecond scale currents in solids.

The first part of my talk will be dedicated to the study of one of the most fundamental strong field phenomena – field induced tunnel ionization. Applying an all optical interferometry [1] resolved, with attosecond accuracy, the barrier's modifications during the tunneling mechanism as well as the excitation of the electron as it propagates under the tunneling barrier [2,3]. Interferometry can be induced in the spatial domain as well. By shaping of 2D electron trajectories, we have induced a microscopic spatial interferometer, and probed the spatial properties of molecular systems [4]. Finally, Attosecond interferometry has been applied to explore subcycle dynamics in condense matter systems, resolving field induced band gap dynamics [5,6].

* E-mail: nirit.dudovich@weizmann.ac.il

References

[1] D Azoury *et al.*, Nature Photonics **13**, 54 (2019).

[2] O Pedatzur et al., *Nature Physics* **11,** 815 (2015).

[3] O Kneller *et al.*, Nature Photonics (2022).

[4] A J Uzan *et al.*, Nature Photonics 14, 188 (2020).

[5] A J Uzan *et al.*, Nature Photonics 14, 183 (2020).

[6] A J Uzan *et al.*, Nature Photonics (2022)

In situ nanoscale focusing of extreme ultraviolet solid-state high harmonics

A Korobenko[1], S Rashid[2], C Heide[3], A Yu Naumov[1], D A Reis[3], P Berini[2,4,5], P Corkum[1] and G Vampa[1*].

[1]Joint Attosecond Science Laboratory, National Research Council of Canada and University of Ottawa, Ottawa, Canada
[2]Center for Research in Photonics, University of Ottawa, Ottawa, Canada
[3]Stanford PULSE Institute, SLAC National Accelerator Laboratory, Menlo Park, California, CA 94025, USA
[4]School of Electrical Engineering and Computer Science, University of Ottawa, Ottawa, Canada
[5]Department of Physics, University of Ottawa, Ottawa, Canada

Synopsis We demonstrated tight focusing of an extreme-ultraviolet beam with an *in-situ* approach that integrates the generation of coherent short-wavelength high-order harmonics from an MgO crystal with a high numerical aperture, nano-structured, focusing element etched onto the surface of the crystal itself. We focus extreme ultraviolet light, 7th harmonic of an 800 nm laser, with a zone plate of numerical aperture 0.35, down to a waist radius of 150 nm, with 18% focusing efficiency. The estimated intensity approaches 10^7 W/cm^2. Future developments may demonstrate nanoscale laser ablation, and reach intensities sufficient to trigger nonlinear optical phenomena.

Focused photon beams have been utilized for decades to write micron-scale features on surfaces, either by direct laser machining or by lithographic methods. Reaching nanometer resolution, however, is still a frontier. Extreme ultraviolet light (XUV) allows focusing to nanoscale volumes, but suitable optical elements with high numerical aperture as difficult to produce due to the tight tolerance on the quality of the optics' surface.

He we adopt an *in-situ* approach to focusing, whereby XUV radiation is focused as it is generated from a dielectric surface. Using a newly-developed procedure, we etch a set of Fresnel zone plates, 60 nm deep, 30 x 30 μm-wide, on the surface of a 100 μm-thick, (100)-cut magnesium oxide (MgO) single crystal. The plates have numerical apertures of 0.18 and 0.35 for 114 nm wavelength radiation, the 7th harmonic of an 800 nm Ti-Sapphire laser.

Figure 1 shows the XUV power as a function of the position of a knife edge, when the latter is scanned across the zone plate's focus. We measure a waist radius (1/e^2) of 150 nm, the smallest XUV focus reported to date. Based on the detected power in the first order focus (18% of the total XUV flux), we estimate that the intensity in the nanofocus is ~ 4 x 10^6 W/cm^2. Irradiating MgO with shorter, few-cycle, pulses is expected to boost the intensity beyond 10 GW/cm^2.

The current fluence is particularly suited for two-color ablation, where the XUV beam creates a nanoscopic volume of free electrons that a moderately-intense infrared field avalanches to the critical density for ablation [2]. We expect the unique combination of short wavelength, small focus and high intensity to enable many applications, such as direct laser nanostructuring, nonlinear imaging with chemical specificity, and photoelectron spectro-nanoscopy.

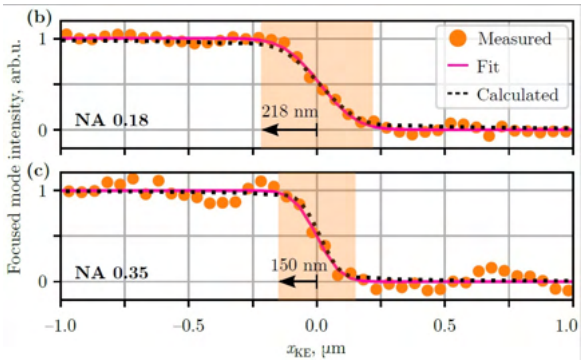


Figure 1. Scan of the knife edge across the XUV focus, for the 0.18 NA (b) and 0.35 NA (c) zone plates. The solid purple line is a fit of a cumulative Gaussian distribution function to the data, with waist radius (1/e^2) as the only fit parameter.

References

[2] X. Yu, Z. Chang, P. Corkum, and S. Lei, Opt. Lett. **39**, 5638 (2014).

* E-mail: gvampa@uottawa.ca

EUV High Harmonic Generation from a thin sheet of isopropanol

J C T Barnard[1] *, O Alexander[1], E W Larsen[1], T Avni[1], S Jarosch[1], C Ferchaud[1], A Gregory[1], S Parker[1], G Galinis[1], A Toffol[1], D Garratt[1], M R Matthews[1], J P Marangos[1]

[1]Quantum Optics and Laser Science Group, Blackett Laboratory, Imperial College London, London, SW7 2BW, UK

T3

Synopsis We have measured EUV radiation resulting from high harmonic generation in a thin sheet of isopropanol with energies up to around 50 eV. The harmonic cutoff has been shown to exhibit CEP and intensity dependence consistent with an electron recombination mechanism, with no obvious plateau-like structure in the harmonic spectra. We model our liquid phase harmonics using a recombination model, modified to account for electron scattering, and find agreement with our experimental results. We have also investigated the plasma breakdown of the sheet during this process, finding breakdown at 50 TW/cm2.

Coherent EUV radiation was generated in micrometer thick sheets of isopropanol running in vacuum [1] using a 1750 nm, 13 fs laser, and measured using a flat field grating spectrometer. We observed harmonics up to 50 eV, around twice the highest reported value [2], which we achieved by carefully controlling the intensity of the generating field. Above a critical intensity of around 50 TW/cm^2 the amount of plasma generated by the driving field becomes significant enough to both inhibit the phase-matching of HHG and distort the EUV radiation produced.

In order to verify that the harmonics were generated from the liquid and not from the vapour we attempted to generate harmonics from just the vapour surrounding the sheet. However we were unable to do so, observing a sudden loss of harmonic generation when the liquid sheet was moved out of the path of the laser. In addition, our harmonic signal gets stronger when there is less vapour in the focal volume, further indicating the harmonics are generated from the sheet itself.

We have investigated the CEP dependance of the harmonics produced. The CEP dependence follows the pattern expected of gas-like harmonics produced by a few cycle pulse [3], and the intensity dependance similarly follows the electric field squared as would be expected from the classical cutoff law. As a result of this we have concluded that an electron recombination model is an appropriate way of modelling the process of HHG in liquids.

In order to support this assertion, we performed some SFA calculations (using the model outlined in [4]). Modelling the liquid as a dense gas and using a simple scattering model to account for interactions between the free electrons and the surrounding environment we found substantive agreement between the calculations and measured results.

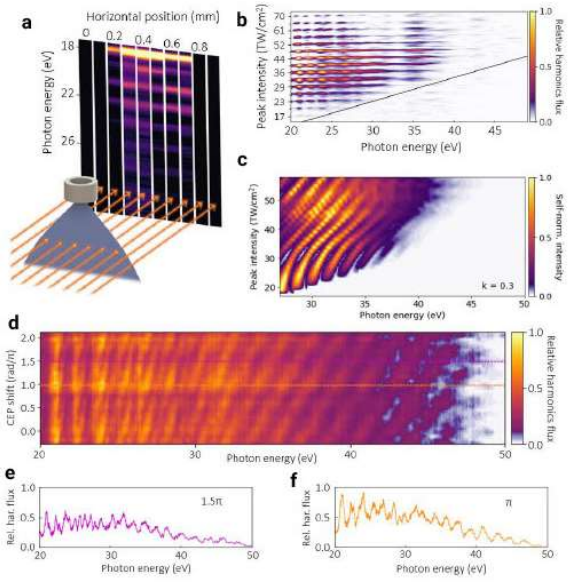


Figure 1. a showing the harmonics with and without the sheet, **b** measured and **c** simulated harmonic cutoff with intensity, **d** variation of harmonic cutoff with CEP, with **e** and **f** showing the harmonic spectra at 1.5π and π radians respectively

References

[1] Galinis G *et al* 2017 Rev. Sci. Inst. 88, 083117
[2] Luu T T *et al* 2018 Nat. Comms. 9:3723
[3] Rudawski P *et al* 2013 Eur. Phys. J. D 69: 70
[4] Johnson A S *et al* 2019 Phil. Trans. R. Soc. A 377:2145

* E-mail: j.barnard16@imperial.ac.uk

Controlling solid-state high-harmonics in monolayers via artificial stacking

C Heide[1,*], Y Kobayashi[1], A Johnson[2], A S McKeown-Green[1], S Wittigschlager[1], F Liu[1], T F Heinz[1], D. A Reis[1], S Ghimire[1]

[1]Stanford PULSE Institute, SLAC National Accelerator Laboratory, Menlo Park, CA 94025, USA

We report a coherent build-up of high-harmonic generation from artificially stacked multi-layers of tungsten disulfide. The natural stacking configuration is AB type, without the generation of even-order harmonics due to symmetry. We stack multi-layers in various configurations including an AAAA-type. In this configuration, both even and odd-order harmonics are produced and the harmonic yield scales quadratically with the number of layers.

The lattice of TMDC monolayers exhibits significant nonlinear optical susceptibility, which can be used for efficient nonlinear light conversions, such as frequency up- and down-conversion. A particular advantage of atomically thin 2D materials is negligible absorption and relaxed phase-matching condition, which makes it particularly useful for light pulses with short time duration and/or short wavelengths. Recently it has been demonstrated that two-dimensional materials are an ideal platform to study coherently driven electron dynamics, which can range from light-field driven electronics [1] to high-harmonic generation down to UV wavelengths [2, 3]. Compared to HHG in gas-phase systems, solid-state HHG is desirable for more compact extreme ultraviolet sources, on-chip ultrafast photonics and electronics, and all-optical processors. One particular benefit of access to isolated monolayers is that they can be artificially stacked to tailor their electrical and optical properties. For example, it has been shown that artificially stacked monolayers exhibit efficient and tunable second harmonic generation. We extend these concepts to high-harmonic generation down to UV wavelengths by assembling multilayer WS_2 with a symmetry differing from that of the natural bulk crystal.

Here, we present the results on high-harmonic generation in monolayer tungsten disulfide (WS_2) driven by mid-IR 5 µm fields from artificially stacked monolayers [4]. The monolayers are prepared using a gold-assisted exfoliation technique, which enables the creation of mm-sized single-crystalline flakes. In natural bulk TMDCs, successive layers are typically rotated by 180° with respect to one another, resulting in the presence of inversion symmetry, as shown in Figure 1a. As a result in such AB stacked samples, no even order harmonics are generated under normal incidence. In contrast, we can reassemble the layers to create an artificial structure by stacking the sample in AA configuration, as shown in Figure 1b, in which the broken inversion symmetry remains.

When exciting the sample with mid-IR (5 µm, 0.25 eV, ~100 fs, ~1 V/nm) laser fields, high harmonics of the fundamental driving frequency are observed up to the 15th harmonic. The presence of even-order harmonics for AA stacking is a clear indication of broken inversion symmetry.

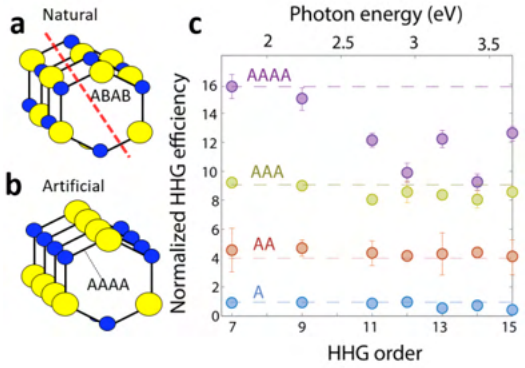


Figure 1 a shows the natural AB configuration, **b** shows the artificial AA configuration. **c** shows the measured harmonic yield as a function of number of layers, where A represents an isolated monolayer, AA represents two layers, AAA represents three layers, and so on.

Figure 1c shows the HHG-yield normalized to a single layer for AA stackings up to 4 layers. As previously observed for SHG, we see that the HHG intensity scales quadratically with the number of layers. For 4 layers and high photon energies, we note a deviation from quadratic scaling, which we attribute to phase-mismatch and reabsorption effects.

Our results represent an important step towards designing efficient and functional high-harmonic sources by artificially tailoring solid-state materials.

References

[1] Boolakee T, Heide C *et al* 2022 Nature in press.
[2] Liu H, *et al* 2017 Nature Physics 13 **262**
[3] Heide C *et al* 2021 arXiv:2109.04508
[4] Heide C *et al* 2021 in preparation.

* E-mail: cheide@stanford.edu

High Harmonic Generation from Metals

S. Gholam-Mirzaei [1,*], A. Korobenko[1], S. Saha[2], G. Vampa[1], A. Y. Naumov[1], A. Staudte[1], A. Boltasseva[2], V. M. Shalaev[2] and P. B. Corkum[1]

[1]Joint Attosecond Science Laboratory (JASLab), National Research Council of Canada and University of Ottawa, Ottawa, ON, Canada
[2]Purdue University, School of Electrical & Computer Engineering and Birck Nanotechnology Center, West Lafayette, IN, USA

T3

Synopsis We observe extreme-ultraviolet (XUV) high harmonics from both epitaxial thin film and bulk crystalline silver when exposed to the intense few-cycle near-infrared light pulses. Silver has a higher damage threshold than metallic titanium nitride, enabling high-harmonics generation up to photon energies of about 19 eV. As well, circularly polarized harmonics are efficiently generated by using circularly polarized incident light. High harmonic emission from metals can be a route to compact XUV frequency combs.

Since the first observation of high-order harmonics from bulk ZnO [1], solid-state high-harmonic generation (HHG) has been studied in a variety of materials and has been recognized as a signature of strong field physics in solids [2]. Recent observation of high harmonics from metallic phase of titanium nitride (TiN) [3] opened the path to high harmonics in metallic crystals. Here, we generate high harmonics from both epitaxial thin film and bulk single crystal silver (Ag) with the harmonic cut-off extending to the XUV. We also show that high harmonics can be emitted from a conventional metal.

In the experiment, few-cycle near-infrared (NIR) pulses (λ_{center}=780 nm), obtained by compressing 30 fs, 1 mJ pulses of a commercial Ti:Sapph laser with a neon filled hollow-core fiber, are focused onto the 200 nm thick epitaxial Ag on a silicon substrate in reflection geometry (the incident angle is close to normal). The emitted harmonics are detected in the far-field using a grating spectrometer. As shown in Fig. 1.a) bright high harmonics up to the 11th order (19 eV) are generated while the target withstands the threshold intensity of several tens of TW/cm^2, exceeding the experimentally measured damage threshold in TiN [3]. Additionally, when both TiN and Ag are illuminated with the same pulse energy and focusing condition, a higher harmonics yield is obtained from silver than TiN. We relate these effects to the higher reflectivity and possibly lower electron scattering in Ag.

We further study the ellipticity dependence of harmonics from Ag by changing the polarization state of incident NIR beam from linear to circular polarization. We find that the yield of 5th and 7th harmonics does not drop by more than 30%. More importantly, circularly polarized harmonics are generated due to space-time symmetry imposed selection rules. Moreover, as seen in the orientation dependence of the harmonics, the maxima in the spectral yield of 5th and 7th harmonics exhibit six-fold symmetry imprinted by (111) plane of the crystal (Fig. 1. b). Our measurements highlight the role of crystalline structure in high harmonics from thin film Ag.

In conclusion, we report the first observation of high harmonic emission from a classic metal. We expect high-harmonic emission to be a universal characteristic of metals when illuminated by light fields close to their damage threshold. The emission of high energy photons is a spectroscopic tool that will help unlock the role of electronic states on metal surfaces. At higher field strength, we predict that solid-state intraband harmonics will merge into plasma harmonics due to the loss of crystaline structure.

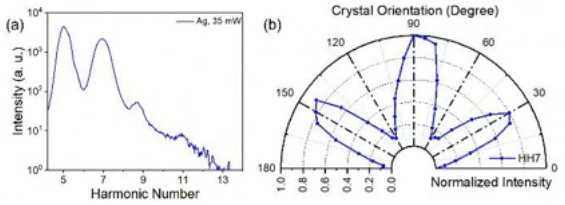


Figure 1. a) High harmonics spectrum from Ag reaching 19 eV. **b)** Orientation dependence of 7th harmonic.

References

[1] S. Ghimire et. al., Nat. Phys. 7 138–141 (2011).
[2] G. Vampa, et. al., Nat. 522, 462–464 (2015).
[3] A. Korobenko et. al., Nat. Commun. 12 (2021).
*E-mail: sgholamm@uottawa.ca

High harmonic spectroscopy of quantum phase transitions in a high-Tc superconductor

Jordi Alcalà[1], Utso Bhattacharya[2], Marcelo Ciappina[3,4], Ugaitz Elu[2], Tobias Graß[2], Piotr T. Grochowski[2,5,6,7], Maciej Lewenstein[2,8], Anna Palau[1], Themistoklis P. H. Sidiropoulos[2], Tobias Steinle[2], Igor Tyulnev[2], Jens Biegert[2,8,*]

[1]ICMAB-CSIC - Institut de Ciència de Materials de Barcelona, Campus UAB, Bellaterra, Spain
[2]ICFO - Institut de Ciencies Fotoniques, The Barcelona Institute of Science and Technology, Castelldefels, Spain
[3]Guangdong Technion - Israel Institute of Technology, Shantou, Guangdong, China
[4]Technion - Israel Institute of Technology, Haifa, Israel
[5]Center for Theoretical Physics, Polish Academy of Sciences, Aleja Lotników 32/46, Warsaw, Poland
[6]Institute for Quantum Optics and Quantum Information, Austrian Academy of Sciences, Innsbruck, Austria
[7]Institute for Theoretical Physics, University of Innsbruck, Innsbruck, Austria
[8]ICREA, Pg. Lluís Companys 23, Barcelona, Spain

Synopsis We report on the new non–linear optical signatures of quantum phase transitions in the high-temperature superconductor YBCO, observed through high harmonic generation.

The sensitivity of HHG to the intricate microscopic details of carriers and lattice predestines high-harmonic spectroscopy (HHS) [1,2] to investigate strong interactions and quantum correlations which lead to fascinating new states of matter such as superconductivity. HHS is a novel sensitive probe of the dynamic evolution of the superconducting phase transition since the formation of composite bosons by pairing two fermionic spin-1/2 particles (Cooper pairs) changes the distribution of charge carriers and this sensitively registers in the high harmonic amplitudes and spectral distribution. We use HHS to identify all additional phase transitions between quantum phases of the unconventional high-Tc superconductor $YBa_2Cu_3O_{7-d}$ (YBCO) [3]. For our investigation, we induce non-perturbative high harmonic generation with sub-bandgap, ultrashort mid-infrared (mid-IR) pulses at 3200 nm (0.4 eV) from a mid-IR OPCPA [4]. Figure 1 shows that the fundamental (red dots) does not vary significantly with temperature, all the harmonic orders exhibit varying and strong trends with temperature. Most strikingly, HH7 increases in amplitude by over one order of magnitude over the measured temperature range while HH3 and HH5 amplitudes initially decrease with temperature. The first critical point marks the transition between strange metal into the pseudogap phase, at $T^* = 173$ K, and the amplitude of all harmonics varies very little. Further cooling to $T_c = 88$ K, a dramatic exponential increase is measured for all harmonic orders. This marks the quantum phase transition into the superconducting state. A novel two-band quasi-Hubbard model with BCS d-wave pairing is used to describe the experiment and we find excellent match with the data.

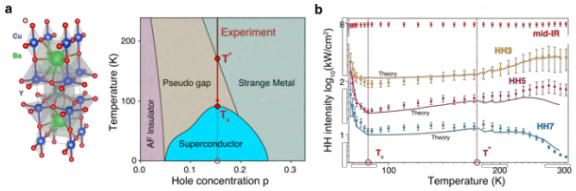


Fig. 1. (a) Unit cell of YBCO and the phase diagram. (b) HH3, HH5 and HH7 as a function of temperature. Results from the strong-field quasi-Hubbard model are overlaid as solid lines. All harmonic orders show a clear turning point at the critical temperature Tc and T* marking the transition from strange metal to the pseudogap phase.

Our investigation [5] provides the first strong-field investigation of a high Tc su- perconductor and measurement of its quantum phase transitions.

References

[1] S. Ghimire et al., Nature Physics 7, 138 (2011).
[2] M. Hohenleutner et al., Nature 523, 572 (2015).
[3] V. J. Emery, Phys. Rev. Lett. 58, 2794 (1987).
[4] U. Elu et. al. Nature Photonics 15, 277 (2020).
[5] J. Alcala et al., arXiv:2201.09515

* E-mail: jens.biegert@icfo.eu

TE Overview of ATTOCHEM Network ▲

TE

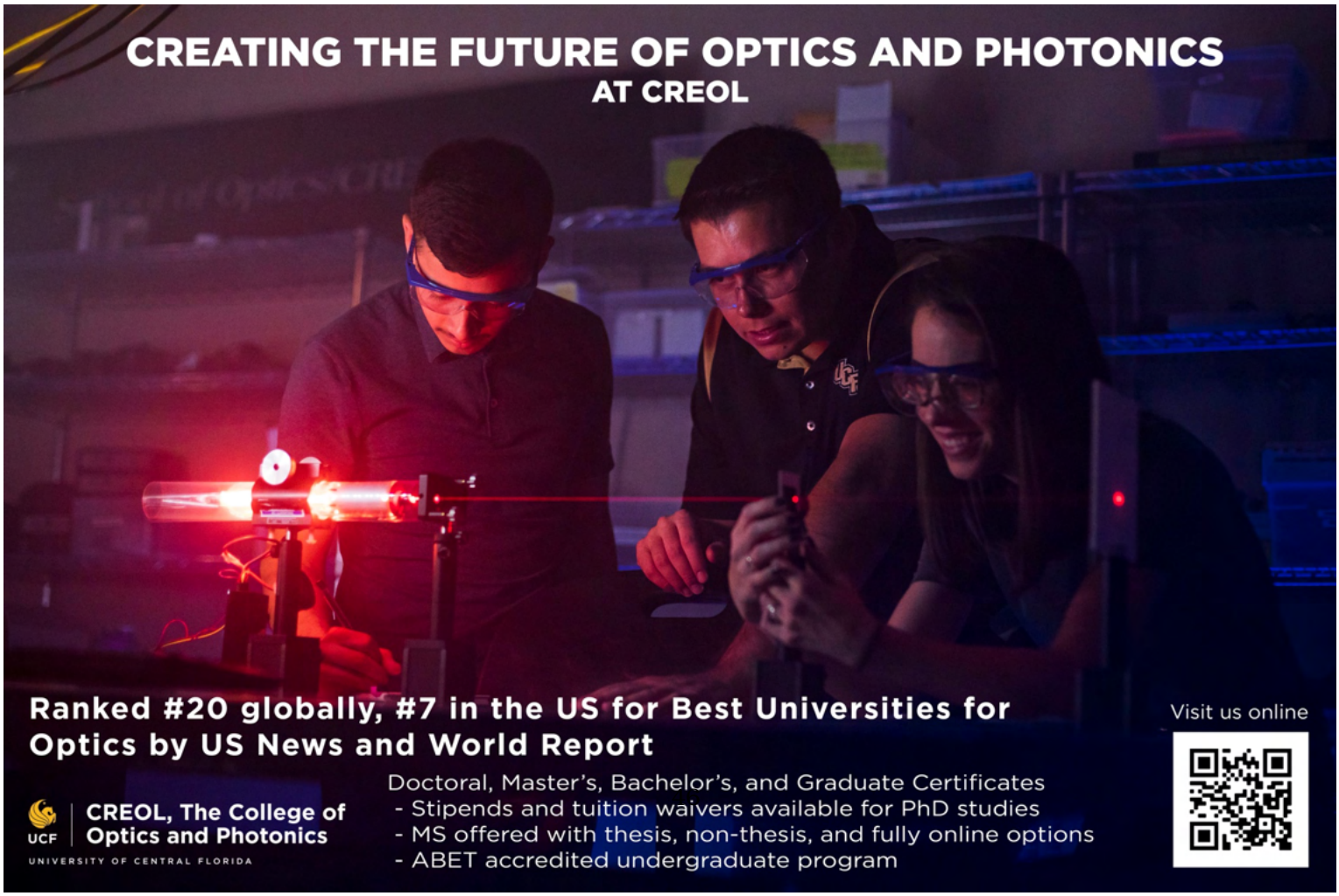
20:00 - 21:00 **TE Overview of AttoChem Network**
Chair: **Per Eng-Johnsson**, Lund University, Sweden, EU

20:00 **Fernando Martín**, Universidad Autónoma de Madrid, Spain, EU
The AttoChem Network

20:15 **Caterina Vozzi**, CNR, Milano, Italy, EU
WG1: New attosecond techniques for the control of electron dynamics in molecules

20:30 **Fernando Martín**, Universidad Autónoma de Madrid, Spain, EU
WG2: Computational tools for the description of attosecond electron and nuclear dynamics

20:45 **Francesca Calegari**, DESY, Germany, EU
WG3: Attosecond imaging and control of charge migration and chemical reactivity



A European effort towards Attosecond Chemistry: the AttoChem network

Caterina Vozzi[1], Ladislau Nagy[2], Franck Lépine[3], Francesca Calegari[4 *] and Fernando Martín[5 †]

[1]CNR, piazza Leonardo da Vinci 32, 20133 Milano, Italy
[2]Babes-Bolyai University, str. Kogalniceanu nr. 1, 400084 Cluj-Napoca, Romania
[33]Univ Lyon, Univ Claude Bernard Lyon 1, CNRS, Institut Lumière Matière, F-69622, Villeurbanne, France
[4] Center for Free-Electron Laser Science, DESY, Notkestrasse 85, 22607 Hamburg, Germany
[5]Departamento de Química, Universidad Autónoma de Madrid and IMDEA Nanoscience, 28049 Madrid, Spain

Synopsis The European AttoChem network coordinates experimental and theoretical efforts to exploit the large potential of attosecond techniques in chemistry, with the aim of designing new strategies for the control of charge migration in molecules by directly acting on the attosecond time scale. The network gathers researchers from all Europe, neighboring countries, Japan and USA working in attosecond science. In the conference, we will describe the networking possibilities offered by this network as well as some of the most important scientific and technological achievements made since its inception in 2019.

Recent developments of ultrashort intense light sources operating in the XUV and X-ray spectral regions are starting to revolutionize chemistry, as they give access to dynamical processes occurring in the attosecond time scale, the natural time scale for electronic motion in atoms and molecules. Thus, such light sources allow one to address new fundamental questions about the role and possible control of electron dynamics in chemical reactivity, to investigate photoinduced charge migration in relevant molecular systems, and to image, with attosecond resolution, fast structural changes in molecules during proton transfer, isomerization, or motion through conical intersections. Medium-size and large-scale facilities are currently being developed all over the world, accompanied by an increasing demand of accurate theoretical support for an optimal use of these resources.

The European AttoChem COST Action [1,2] coordinates experimental and theoretical efforts to exploit the large potential of attosecond techniques in chemistry, with the aim of designing new strategies for the control of charge migration in molecules, from simple ones to complex systems and aggregates in an aqueous environment, by directly acting on the attosecond time scale. This ability will be used to selectively break and form chemical bonds, thus opening new avenues for the control of chemical reactions. The results of the Action are expected to have a significant impact in several areas of chemistry, such as photovoltaics, radiation damage, catalysis, photochemistry, or structural determination. AttoChem is also acting as a liaison with the relevant stakeholders to bridge the gap to industrial applications.



The AttoChem network

In the special section devoted to the AttoChem network, we will briefly describe the activities organized under its umbrella since its launch in November 2019, as well as the networking possibilities it will offer, at both the European and international levels, until its conclusion in October 2023, and beyond. We will also present some of the most important scientific and technological achievements made during the last two years.

References

[1] https://attochem.qui.uam.es/
[2] https://www.cost.eu/actions/CA18222/

* E-mail: francesca.calegari@desy.de
† E-mail: fernando.martin@uam.es

W1 Attosecond Spectroscopy in Condensed Matter ▲

14:15 - 16:30 **W1 Attosecond Spectroscopy in Condensed Matter** 48
Chair: **Mette B Gaarde**, Louisiana State University

14:15 **Jens Biegert**, ICFO - Institut de Ciencies Fotoniques, Spain, EU
I: *Attosecond soft X-rays revealing energy flow in materials* 49

14:45 **Matteo Lucchini**,Politecnico di Milano, Italy, EU
I: *Attosecond exciton dynamics in dielectrics* 50

15:15 **Fernando Martín**, Universidad Autónoma de Madrid, Spain, EU
C: *Real Space-Time sub femtosecond imaging of electron dynamics in molecules* 51

15:30 **Arthur Niedermayr**, ETH Zürich, Switzerland
C: *Few-femtosecond dynamics of free-free opacity in optically heated metals* 52

15:45 **Thierry Ruchon**, LIDYL - CEA Saclay, France, EU
C: *Magnetic helicoidal dichroism with XUV light carrying orbital angular momentum* 53

16:00 **Saijoscha Heck**, ETH Zürich, Switzerland
C: *Attosecond spectroscopy of water clusters* 54

16:15 **Katherine Légaré**, INRS, Canada
C: *Ultrafast magnetic scattering on rare-earth ferrimagnets enabled by a bright Yb-based soft X-ray source* 55

Attosecond soft X-rays revealing energy flow in materials

T.P.H. Sidiropoulos[1,†], N. Di Palo[1], D.E. Rivas[1,2], S. Severino[1], M. Reduzzi[1], B. Nandy[1], B. Bauerhenne[3], S. Krylow[3], T. Vasileiadis[4], T. Danz[5], P. Elliott[6,7], S. Sharma[6], K. Dewhurst[7], C. Ropers[5], Y. Joly[8], M. E. Garcia[3], M. Wolf[4], R. Ernstorfer[4], J. Biegert[1,9]

1 ICFO - Institut de Ciencies Fotoniques, The Barcelona Institute of Science and Technology, Castelldefels, Spain
2 European XFEL GmbH, Holzkoppel 4, Schenefeld, Germany
3 Theoretische Physik, FB-10, Universität Kassel, Kassel, Germany
4 Fritz Haber Institute of the Max Planck Society, Berlin, Germany
5 4th Physical Institute - Solids and Nanostructures, University of Göttingen, Germany
6 Max-Born-Institut für Nichtlineare Optik und Kurzzeitspektroskopie, Berlin, Germany
7 Max-Planck-Institut für Mikrostrukturphysik, Weinberg 2, Halle, Germany
8 Université Grenoble Alpes, CNRS, Grenoble INP, Institut Néel, Grenoble, France
9 ICREA - Institució Catalana de Recerca i Estudis Avançats, Barcelona, Spain

Synopsis Attosecond core-level soft X-ray spectroscopy identifies the energy conversion pathways between photons, charge carriers and lattice in real time in graphite.

We show that core-level x-ray absorption near edge structure (XANES) spectroscopy with attosecond soft x-ray (SXR) pulses [1] can image the flow of energy inside a material in real time [2]. We photoexcite graphite with a 11 ± 1 fs pump pulse at 1850 nm, or with a 15 ± 1 fs pulse at 800 nm, for various pump fluences between 2.8 ± 0.2 mJ/cm^2 and 81 ± 5 mJ/cm^2. Figure 1(a) shows the measured differential x-ray absorption ΔA(E) (pumped minus unpumped) from which striking changes of up to 15% are immediately apparent. We identify these features as π bonding state and as π* and σ* antibonding states. Attosecond-resolved measurement with a pump-probe delay step size of 0.6 fs show the buildup of coherent charge oscillations, i.e., polarization of the material. These oscillations occur at occupied states below and unoccupied states above the Fermi level predominantly at the pump carrier frequency. We identify the incoherent background due to the dephasing of coherent charge oscillation. This background rises within a few oscillations of the light field, signifying the ultrafast transfer of energy from the light field into the electron and hole excitation of the material. We find that ultrafast dephasing of the coherent carrier dynamics is governed by impact excitation (IE) for electrons, while holes exhibit a switchover from impact excitation to Auger heating (AH) already during the 11-fs duration of the infrared light field. We further analyze the coherent phonon signal by analyzing the oscillatory pattern exhibited by the σ* data with a short-time Fourier transform (STFT) analysis This analysis shows that already during and shortly after the laser excitation, coherent motion emerges over a broad range of frequencies. A comparison with the phonon dispersion from two-temperature-model molecular dynamics (TTM MD) simulations [4] [Fig. 1(e)] identifies them as the Raman-active Γ − E_{2g} and the non-Raman-active K – A'$_1$ SCOPs at 46.4 ± 2.7 and 42.7 ± 1.1 THz, respectively. The surprising early contribution from the (non-Raman-active) A'$_1$ mode originate from the very strong electron-SCOPs coupling, thus acting almost impulsively.

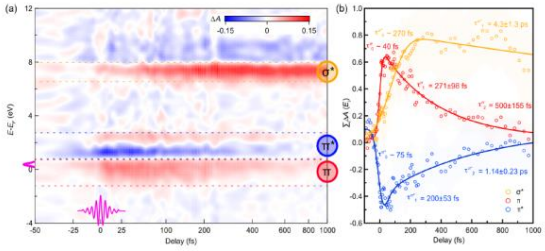


Fig. 1. (a) Differential absorption ΔA(E) with and without pump pulse. The pump pulse bandwidth and duration are indicated in pink.

We demonstrate a new experimental methodology with a single technique to track energy flow upon light absorption between electrons, holes, and phonons in real time.

References

[1] S. M. Teichmann et al. Nat. Com. **7,** 11493 (2016).
[2] T. P. H. Sidiropoulos et al. 11, 041060 (2021).
[3] B. Buades et al. Optica **5**, 502 (2018).
[4] S. Krylow et al. Phys. Rev. B **101**, 205428 (2020).

Attosecond core-exciton dynamics in wide-gap insulators

M. Lucchini[1,2] *

[1] Department of Physics, Politecnico di Milano, 20133 Milano, Italy
[2]Institute for Photonics and Nanotechnologies, IFN-CNR, 20133 Milano, Italy

Synopsis We studied the ultrafast dynamics of core excitons in MgF_2 with attosecond transient reflection spectroscopy. By comparing the few-fs and attosecond optical response of the system with numerical simulations, we found that the quasi-particles manifest its atomic or solid nature on different ultrafast time scales.

The comprehension of the ultrafast dynamics which unfold in solids immediately after interaction with light opens the possibility of manipulating the electrical properties of matter beyond the speed limits of the current electronics [1]. Among all the interesting and relevant phenomena to be investigated, exciton formation, (quasi-particles formed by an electron and a hole coupled by Coulomb interaction) determines the electro-optical properties of several materials [2]. As a consequence, a deeper understanding of ultrafast exciton dynamics in dielectrics and semiconductors can have far reaching implications in many relevant technological fields. For example, the ultrafast processes unfolding at the femto- and attosecond domain are of primary relevance in view of the desired extension towards the petahertz regime.

By combining a unique beamline for attosecond transient reflection spectroscopy with precise, on-the-fly, time-delay calibration [3], here we report the first observation of sub-femtosecond exciton dynamics in a dielectric (MgF_2) driven by few-femtosecond, intense (I_{IR} ~10^{12}-10^{13} W/cm^2) infrared (IR) pulses [4]. The experimental data are compared to 1D numerical simulations, allowing us to disentangle the dual atomic and bulk nature of the exciton. In particular, we used a few-fs IR pulses to drive the exciton dynamics in crystalline MgF_2 and probed them with isolated attosecond pulses (~250 as) around the Mg $2p^{2+} \rightarrow \Gamma_1$ core exciton transitions (Fig. 1(a)) [5]. The resulting differential reflectivity trace is reported in Fig. 1(b) as a function of the pump-probe delay and photon energy. We observe a rich dynamics composed by fast oscillations superimposed to a slower, few-fs signal.

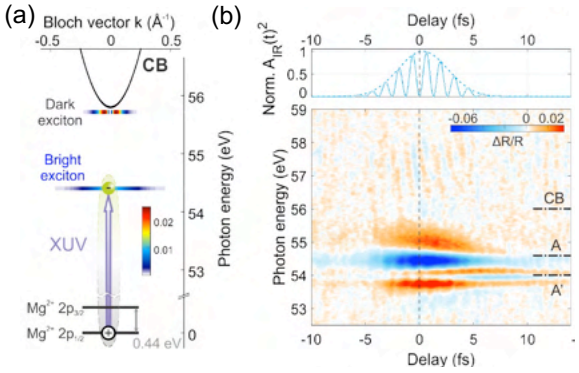


Figure 1. (a) MgF_2 conduction band and the excitonic states. **(b)** Experimental differential reflectivity, ΔR/R. The upper panel shows the square of the simultaneously measured IR vector potential.

We found that while the few-fs component in ΔR originates from ac Stark shift of the excitonic transitions and can be described within an atomic model, the faster sub-fs component originates from the dispersive nature of the conduction band states, thus requiring a solid-like description. Exploiting the theoretical simulations, we found that the system optical response can be controlled by tuning the exciton binding energy, providing the community with a possible new lever to develop innovative devices.

References

[1] H.J. Caulfield, S. Dolev, Nat. Phot. **4**, 261 (2010).
[2] L.V. Butov, Superlattices Microstruct. **108**, 2–26 (2017).
[3] G. D. Lucarelli, et al., Rev. Sci. Instrum. **91**, 053002 (2020).
[4] M. Lucchini, et al., Nat. Commun. **12**, 1021 (2021).
[5] W. F. Hanson, et al., J. Appl. Phys. **43**, 1661 (1972).

* E-mail: matteo.lucchini@polimi.it

Real Space-Time sub femtosecond imaging of electron dynamics in molecules

M Garg[1], A Martin-Jimenez[1], M Pisarra[2,3] †, Y Luo[1], F Martín[2] *, and K Kern[1,4]

[1]Max Planck Institute for Solid State Research, Stuttgard, 70569, Germany
[2]Departamento de Química, Universidad Autónoma de Madrid, and Imdea Nano, Madrid, 28049, Spain
[3]INFN-LNF Gruppo Collegato di Cosenza, Rende (CS), 87036, Italy
[4]Institut de Physique, Ecole Polytechnique Fédérale de Lausanne, Lausanne, CH-1015, Switzerland

Synopsis Using a cutting-edge experimental set-up, which combines scanning tunneling microscopy with ultra-short laser pules, and advanced computational modelling, based on a combination of density functional theory with a two-state solution of the time-dependent Schrödinger equation, we show that it is possible to generate and follow electron dynamics in real time and real space with attosecond and picometer resolutions, respectively.

'Seeing' electron motion at both its natural length and time scales is a long-awaited dream of natural sciences. Reaching such spatial or temporal resolutions is nowadays possible, but not simultaneously. Current attosecond science techniques allows generating and tracking electronic motion in real time with incredible time resolution (200 attoseconds to few femtoseconds) in ever larger systems, but not in real space. Scanning tunneling microscopy (STM), on the other hand, can locally probe the electron density in molecules and solids with the necessary (picometer) resolution, but cannot provide by itself the dynamical information at the ultrafast time scale that is inherent to electronic motion.

In this work [1], we break this space-time limitation by combining STM and attosecond technologies (Fig1a). We show that the coherent electronic motion generated by two temporally delayed CEP-stable near-infrared pulses of < 6 fs duration can be locally and non-invasively probed with both picometer and 300 attosecond resolution, thus allowing for a direct visualization of electron dynamics without the need for any additional reconstruction. We apply our technique to self-assemblies of PCTDA molecules deposited on a Au(111) surface. Thanks to state of the art DFT calculations we are able to correctly identify the specific electronic states that participate in the coherent oscillations and the corresponding dipole transition matrix elements. By combining this information with a two-state solution of the time-dependent Schrödinger equation, we are able to correctly predict the population of each state (Fig.1c) and the STM images (Fig.1c) recorded in the experiment as a function of the delay between the two pulses.

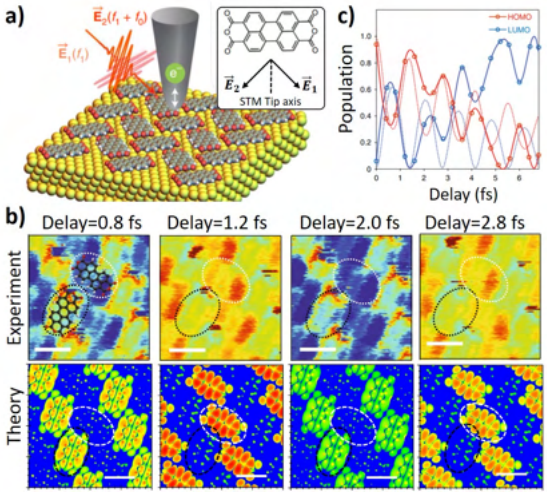


Figure 1. a) Sketch of the experiment: Two ultrashort laser pulses impinge on a self-assembly of PTCDA molecules deposited on a gold surface, in tunnel contact with an STM. **b)** Comparison between the experimental and calculated STM images for different laser pulse delays for a 4-Layer PCTDA self assembly on Au(111): depending on the delay between the laser pulses either the HOMO or the LUMO in different molecules are visualized [1]. **c)** Experimental (solid lines and dots) and computed (dashed lines) populations for the HOMO and LUMO as function of the laser pulse delay.

References

[1] Garg, M., Martin-Jimenez, A., Pisarra, M., Luo, Y., Martín, F. and Kern, K. 2021 *Nature Photonics* DOI: 10.1038/s41566-021-00929-1

* E-mail: fernando.martin@uam.es
† E-mail: michele.pisarra@lnf.infn.it

Few-femtosecond dynamics of free-free opacity in optically heated metals

A Niedermayr[1]*, M Volkov[1,2], S A Sato[3,4], N Hartmann[1], Z Schumacher[1], S Neb[1], A Rubio[4,5], L Gallmann[1] and U Keller[1]

[1]Department of Physics, ETH Zürich, 8093 Zürich, Switzerland
[2]University of Konstanz, 78457 Konstanz, Germany
[3]Center for Computational Sciences, University of Tsukuba, Tsukuba, Ibaraki 305-8577, Japan
[4]Max Planck Institute for the Structure and Dynamics of Matter and Center for Free Electron Laser Science, 22761 Hamburg, Germany
[5]Center for Computational Quantum Physics (CCQ), Flatiron Institute, New York 10010, USA

W1

Synopsis We investigate non-equilibrium electron dynamics in the free-free opacity window of the simple metal aluminum by using attosecond transient absorption spectroscopy. The free electrons are excited by a strong, few-femtosecond near-infrared (NIR) pulse and subsequently, the change in optical density is probed by an XUV pulse. We get a good quantitative and qualitative agreement between the experimental results and ab-initio calculations. In addition, we are able to explain the experimental findings with a simple interband model for a free electron gas.

In a recent study, we investigated the time-dependent photoabsorption process using attosecond transient absorption spectroscopy for the first time in metals [1]. This prior work showed a strong response close to the giant dipole resonance of titanium due to an induced change in electron localization. Here, in contrast, we investigate the interaction of light with the simple metal aluminum which approximates the behavior of an ideal free-electron gas between its plasma frequency (15 eV) and the $L_{2,3}$ absorption edge (72-74 eV) very well [2]. Few-femtosecond time resolution allows us to track the purely electronic contribution to non-equilibrium absorption and unambiguously separate it from the slower lattice contribution.

The transient absorption data at a fixed pump-probe delay of 20 fs, i.e., when the sample is in a hot-electron, cold-lattice state, are shown in Fig. 1(a). The NIR pump pulse smears out the Fermi-Dirac distribution which causes a global increase of absorption at all photon energies in the free-free absorption window of aluminum. Additionally, the pump-induced temperature increase leads to a reduction of the chemical potential to fulfill particle conservation. This manifests itself as a decrease in absorption around the Fermi level (Fig. 1(b)), which is, however, outside of the experimentally accessible range of photon energies.

We find that the simplest independent-particle model with a fixed band structure is sufficient to explain the experimental findings qualitatively and quantitatively in the experimentally accessible energy window between 30 and 50 eV. This shows that collective effects do not play a significant role in the observed response. An interband model (Fig. 1(b)) for a free electron gas confirms our findings by considering only the chemical potential as a material-specific parameter.

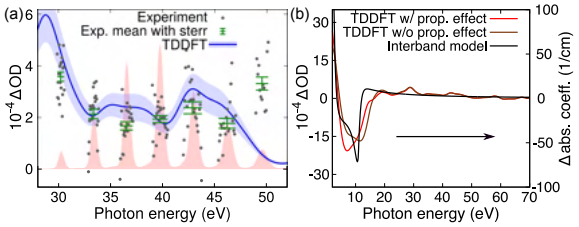


Figure 1. (a) Comparison of experiment with theory of the spectrally resolved change in optical density. (b) Comparison of TDDFT calculations with a simple interband model which mimics a free electron gas.

The mechanisms that lead to the observed absorption change in aluminum are universal in the sense that they are present in all materials with a finite number of free carriers. However, in materials with a more complex electronic structure like titanium [1] they may be masked by other, stronger contributions. Due to the similarities of free-electron-like metals with dense plasmas, our work may also provide a benchmark for improving the understanding of dense non-equilibrium plasma at higher electron temperature.

References

[1] Volkov M *et al* 2019 Nat. Phys. **15** 1145-1149
[2] Ichimaru S *et al* 1982 Rev. Mod. Phys. **54** 1017
[3] Locher R *et al* 2014 Rev. Sci. Instrum. **85** 13113

* E-mail: niedermayr@phys.ethz.ch

Magnetic Helicoidal Dichroism with XUV Light Carrying Orbital Angular Momentum

M. Fanciulli[1, 2], M. Pancaldi[3], E. Pedersoli[3], M. Vimal[1], D. Bresteau[1], M. Luttmann[1], D. De Angelis[3], P. R. Ribic[3], B. Rösner[4], C. David[4], C. Spezzani[3], M. Manfredda[3], R. Sousa[5], I.-L. Prejbeanu[5], L. Vila[5], B. Dieny[5], G. De Ninno[3,6], F. Capotondi[3], M. Sacchi[7,8], and T. Ruchon[1†]

[1]LIDYL, Université Paris-Saclay, CEA, CNRS, 91191 Gif-sur-Yvette, France
[2]Laboratoire de Physique des Matériaux et Surfaces, CY Cergy Paris Université, 95031 Cergy-Pontoise, France
[3]Elettra-Sincrotrone Trieste S.C.p.A., 34149 Basovizza, Trieste, Italy
[4]Paul Scherrer Institut, 5232 Villigen, Switzerland
[5]IRIG-SPINTEC, Université Grenoble Alpes, CNRS, CEA, Grenoble INP, 38000 Grenoble, France
[6]Laboratory of Quantum Optics, University of Nova Gorica, 5001 Nova Gorica, Slovenia
[7]Institut des NanoSciences de Paris, CNRS, Sorbonne Université, 75005 Paris, France
[8]Synchrotron SOLEIL, L'Orme des Merisiers, Saint-Aubin, B.P.48, 91192 Gif-sur-Yvette, France

Synopsis We report magnetic helicoidal dichroism (MHD) in the interaction between XUV beams carrying orbital angular momentum (OAM) and magnetic vortices. It appears as a differential intensity profile of beams with OAM, reflected off magnetic structures with opposite curling sense The results match theoretical predictions and confirm the potential of MHD for studying laser-triggered ultrafast dynamics in complex magnetic materials.

The interaction of polarized light beams with magnetic materials defines the rich set of analytical tools used in magneto-optics and is widely employed for studying magnetization dynamics. Light polarization is associated with a spin angular momentum, whose projection on the propagation axis, takes values $\sigma=\pm\hbar$ for circular polarization, imparting a well-defined handedness to the photon beam. It is less common to exploit the orbital angular momentum (OAM) carried by light beams characterized by an helicoidal wavefront. The quantified projection of the OAM ($\ell\hbar$) can take any integer multiple of $\hbar$, with a sign determined by the spiraling sense of the phase. After finding many applications in the visible range, OAM beams with ultra-short pulse duration and XUV wavelengths became available recently at high-harmonic generation (HHG) and free-electron laser (FEL) sources [1,2], widening considerably their application range.

We analyzed theoretically the interaction of OAM beams with magnetic structures featuring non-uniform magnetization, in particular of XUV beams with magnetic vortices. We predicted that the far field intensity profile encodes the vortex symmetry in a way that depends on the sign and value of ℓ. We named this effect Magnetic Helicoidal Dichroism (MHD) [3]. As for magnetic circular dichroism, MHD can be observed by inverting the sign of either the orbital momentum or of the magnetization. We observed the first experimental evidence of MHD (see, e.g., Fig. 1) at the DiProI station of the FERMI free-electron laser source. It further allowed to follow the evolution of the magnetization topology at the sub-ps timescale after an optical excitation. The obtained experimental results [4] match very well our theoretical predictions [3], confirming the potential of the new toolset provided by MHD for studying complex magnetic structures dynamics.

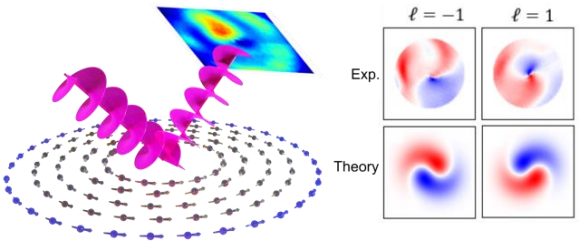


Figure 1. (Left) Experimental sketch for the observation of magnetic helicoidal dichroism. (Right panel) Differences between the images acquired for two opposite curling senses of the magnetic vortex, showing a typical 2D chiral structure, which depends on the incoming orbital angular momentum (top). Theoretical result (bottom).

References

[1] R. Géneaux, et al., Nat. Comm., 7, 12583 (2016).
[2] P. R. Ribič, et al, Phys. Rev. X 7, 031036 (2017).
[3] M. Fanciulli et al., Phys. Rev. A, 103, 013501 (2021)
[4] M. Fanciulli et al.,accepted in Phys. Rev. Lett.

† E-mail: thierry.ruchon@cea.fr

Attosecond spectroscopy of size-resolved water clusters

X Gong[1,2,*], S Heck[1], D Jelovina[1], R R Lucchese[3], H J Wörner [1,*]

[1] Laboratory of Physical Chemistry, ETH Zürich, Vladimir-Prelog-Weg 2, CH-8093 Zürich, Switzerland
[2]State Key Laboratory of Precision Spectroscopy, East China Normal University, Shanghai, 200241, China
[3]Chemical Sciences Division, Lawrence Berkeley National Laboratory, Berkeley, California 94720, USA

Synposis We introduce a novel attosecond size-resolved cluster spectroscopy and build up a molecular-level understanding of the electron dynamics in water. We measure the photoionization time delays in water clusters and how it is affected by the addition of single water molecules. We find a continuous increase of the delay for clusters containing up to 4-5 molecules and little change towards larger clusters. A detailed analysis of the dependence of the time delays on the spatial extension of the ionized orbitals suggests that the observed increase in photoionization time delay is correlated with the increasing spatial extension of the electron-hole created upon ionization, which first increases with cluster size and then partially localizes through the onset of structural disorder that is characteristic of large clusters and bulk liquid water. These results suggest a previously unknown sensitivity of photoionization delays to electron-hole delocalization and indicate a direct link between electronic structure and attosecond photoionization dynamics.

Bridging the ultrafast electron dynamics between gas and condensed phases has been a long-standing challenge both in experiment and theory. Previous works using RABBITT and attosecond streaking have successfully revealed the photoionization time delay of atoms, molecules, and solids in the time and frequency domain. Recently, these techniques have been extended to the liquid phase [1] by combing the high-vacuum-compatible liquid microjet technique and attosecond interferometer, which is of particular interest in bridging the fundamental and applied sciences. The role of electron delocalization, photoelectron elastic/inelastic scattering, and the mean-free path of low-energy electrons in liquid water is of fundamental importance in elucidating the photoionization dynamics and radiation damage. Clusters serve as a useful bridge between the well-known gas phase and the complex condensed phase. However, attosecond time-resolved measurements on clusters have not been reported yet.

Here, we report the first experimental observation and theoretical interpretation of the photoionization dynamics in size-resolved water clusters by using a new developed attosecond coincidence metrology [2]. Experimentally, we obtain a unique RABBIT trace for each measured water-cluster size. We have extracted the photoionization time delay of the SB12 and SB14 of the HOMO and HOMO-1 photoelectron bands in the RABBIT trace corresponding to each cluster size. As shown in Fig.1, the photoionization time delay increases as a function of the cluster size and saturates for pentamer and hexamer.

We compare these experimental results to ab-initio calculations of photoionization time delays using a recently developed scattering calculation method to extract photoionization time delays. Our experimental results agree with the theoretical prediction qualitatively as well as quantitatively within the error bars. This study has revealed an unexpectedly clear relationship between orbital localization and time delays, suggesting an experimental pathway to probing electron-hole localization in complex matter.

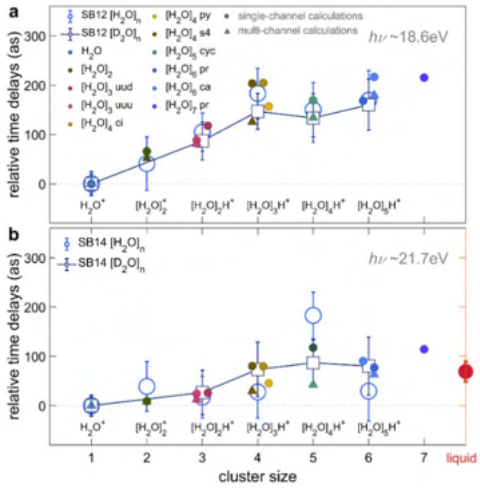


Figure 1. a, Calculated time delays for photoionization out of the 1b1 band of water clusters relative to H2O for SB12. **b**, Same as a, but calculated/measured for SB14.

References

[1] Jordan I *et al* 2020 Science 369 974.
[2] Gong X *et al* 2021 *arXiv:*2106.09459

* E-mail: xcgong@lps.ecnu.edu.cn

Ultrafast Magnetic Scattering on Rare-Earth Ferrimagnets Enabled by a Bright Yb-based Soft X-ray Source

K. Légaré[2], G. Fan[1,2,3], V. Cardin[2], X. Xie[1,10], R. Safaei[2], E. Kaksis[1], G. Andriukaitis[1], A. Pugžlys[1], B. E. Schmidt[4], J.P. Wolf[5], M. Hehn[6], G. Malinowski[6], B. Vodungbo[7], E. Jal[7], J. Lüning[7], N. Jaouen[8], G. Giovannetti[11], F. Calegari[3,11], Z. Tao[9*], A. Baltuška[1], F. Légaré[2*] and T. Balčiūnas[1,5]

1 Institute of Photonics, TU Wien, Gusshausstrasse 27/387, Vienna, Austria.
2 Institut National de la Recherche Scientifique, Varennes, Quebec J3X1S2, Canada.
3 The Hamburg Centre for Ultrafast Imaging CUI, Universität Hamburg, 149 Luruper Chaussee, 22761 Hamburg, Germany
4 few-cycle, Inc., 2890 Rue de Beaurivage, Montreal, Quebec H1L 5W5, Canada.
5 GAP-Biophotonics, Université de Genève, 1205 Geneva, Switzerland.
6 Institut Jean Lamour, CNRS UMR 7198, Université de Lorraine, 54000 Nancy, France.
7 Sorbonne Université, CNRS, Laboratoire de Chimie Physique - Matière et Rayonnement, LCPMR, 75005 Paris, France.
8 Synchrotron SOLEIL, L'Orme des Merisiers, 91192 Gif-sur-Yvette, France.
9 State Key Laboratory of Surface Physics, Department of Physics, Fudan University, Shanghai 200433, People's Republic of China.
10 SwissFEL, Paul Scherrer Institute, 5232 Villigen PSI, Switzerland.
11 Center for Free-Electron Laser Science CFEL, Deutsches Elektronen-Synchrotron DESY, Hamburg, Germany

Synopsis In this work, we present, for the first time, time-resolved resonant magnetic scattering measurements that probe inner-shell electrons of a rare-earth composite ferrimagnet using a bright soft X-ray (>200 eV) high harmonic generation source. We confirm that, far from the cross-contamination of low energy absorption edges in multi-element systems, the highly localized states of 4d electrons associated with the $N_{4,5}$ edges can provide high-quality core-level magnetic information on par with what can be obtained at the M edges, which are so far only accessible at large-scale X-ray facilities.

Development of ultrafast table-top X-ray sources that can map various spin, orbital, and electronic configurations and reordering processes on their natural time and length scales is an essential topic for modern condensed matter physics as well as ultrafast science. Recently, X-ray sources based on high harmonic generation (HHG) have received significant attention for time- and space-resolved spin dynamics measurements utilizing the magnetic dichroism sensitivity.

Here, we present a bright HHG source of photons that reaches above 200 eV with a record photon flux of $>2\times10^9$ photons/s/1% bandwidth and which completely covers the resonant energy range of RE's $N_{4,5}$ edges (Fig. 1a). This source, driven by power-scalable, high-energy Yb laser technology, is then used to probe the magnetic properties of a CoTb alloy through X-ray resonant magnetic scattering (XRMS) [1]. Ultrafast demagnetization excited by a synchronised infrared pulse is recorded (Fig. 1b). A fast demagnetization time of 500±126 fs is resolved, in agreement with previous results probing the M edge of Tb [2]. Simultaneously, an expansion of the magnetic domain periodicity corresponding a velocity for the domain walls of ~750 m/s is observed.

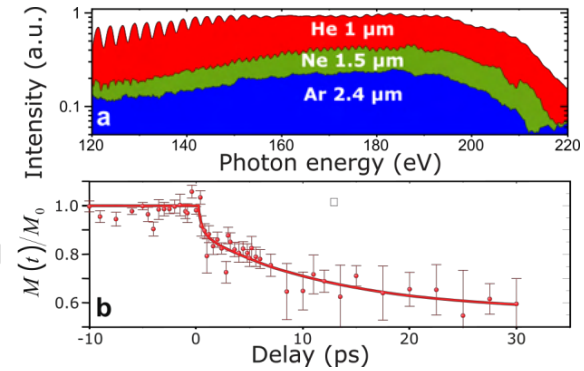


Figure 1. (a) HHG spectrum driven by the Yb laser pulses in helium. Compared with red-shifted drivers in gases with a lower ionization potential, the HHG yield is greatly improved. (b) Ultrafast demagnetization of the CoTb alloy.

Considering the rapidly emerging high power Yb lasers and nonlinear compression methods, this work represents important technologic potential of the next-generation high-performance soft X-ray HHG sources for many future extreme photon hungry applications on the table-top scale.

References

[1] Kortright J B *et al* 2013 *Phys. Rev. B* **64** 1-4
[2] López-Flores V *et al* 2013 *Phys. Rev. B* **87** 214412

* E-mail: Zhenshengtao@fudan.edu.cn
† E-mail: Francois.Legare@inrs.ca

W2 XFELs for Ultrashort XUV/X-ray Science ▲

16:45 - 18:30 **W2 XFELs for Ultrashort XUV/X-ray Science** 56
Chair: **Linda Young**, Argonne National Laboratory and U. Chicago, Illinois, USA

16:45 **Nina Rohringer**, CFEL - DESY - Universität Hamburg, Germany, EU
I: *Momentum resolved XUV polariton measurements by x-ray parametric down conversion* 57

17:15 **Agostino Marinelli**,SLAC National Accelerator Laboratory, USA
I: *Attosecond pulses from X-ray free-electron lasers* 58

17:45 **Claudio Emma**, SLAC National Accelerator Laboratory, USA
C: *A terawatt attosecond soft X-ray source based on a plasma accelerator-driven free electron laser* 59

18:00 **Francis Penent**, Sorbonne Université - CNRS, France, EU
C: *An atomic two-color XUV interferometer* 60

18:15 **Marcus Dahlström**, Lund University, Sweden, EU
C: *Rabi dynamics driven by a seeded FEL at XUV-wavelengths* 61

W2

Pioneering Laser Technology, Empowering Science.

CLASS 5 Photonics

Discover our OPCPAs:

- Extreme power
- Extreme wavelengths
- Ultra short
- CEP stable
- Excellent temporal contrast
- Including Yb-based pump lasers







More details at: www.class5photonics.com Let's connect

Revealing extreme-ultraviolet interband excitonic polaritons by momentum resolved x-ray parametric down conversion

C Boemer[1], D Krebs[2], F Kerker[2], S Huotari[3], B Detlefs[4] , C Sahle[4] and N Rohringer[1,2,*]

[1]Center for Free-Electron Laser Science (CFEL), Deutsches Elektronen-Synchrotron (DESY), Hamburg, Germany
[2]II. Institute for Theoretical Physics, Universität Hamburg, Hamburg, Germany
[3]Department of Physics, University of Helsinki, Helsinki, Finland
[4]European Synchrotron Radiation Facility, Grenoble, France

Synopsis Despite their small cross sections, nonlinear x-ray parametric frequency conversion processes are accessible at storage-ring based x-ray sources. X-ray parameric down conversion of an incoming x-ray photon in a pair of x-ray and long-wavelength photons is linked to microscopic nonlinear optical response functions of the underlying material. Here we present momentum resolved nonlinear x-ray scattering patterns of 10 keV photons in diamond that reveal microscopic polaritonic properties of the nonlinear optical response connected to light propagation on valence- to conduction-band transitions.

X-ray optical wave mixing (XOWM) effects have been proposed in the early 1970ies [1], recognizing that x-ray scattering from an optically modulated charge density will give access to the microscopic electronic structure that determines macroscopic optical properties such as the complex dielectric constant or the index of refraction. For radiation of frequencies far from any electronic transitions, we identified that the underlying material property probed in XOWM processes is an electronic current-density density correlation function [2]. For propagating electromagnetic fields involving frequencies of interband transitions – radiation inducing an excitonic valence to conduction band transition in insulating crystals – it was theoretically predicted in 1959, that the microscopic description of the complex dielectric function of the material involves hybridized states of electronic polarization and light – polaritons [2]. In a recent experiment on x-ray parametric down conversion (XPDC), we, for the first time, revealed microscopic signatures of these polariton states.

At beamline ID 20 of the ESRF, we measured XPDC of 9.79 keV x-ray photons into photon pairs of x-ray photons and photons of extreme ultraviolet light (100 eV) in diamond. The energy- and momentum conservation of this parametric process results into a characterisc cone emission [3] of the nonlinearly scattered, down converted x-ray photon (see Fig. 1), a feature that allows for an unequivocal identifcition of the weak XPDC signal versus Compton background. The scattering cone clearly shows the contribution of two distinct branches, manifested by a positive and negative signal versus background. We interpret this finding as inelastic x-ray scattering from an XUV polariton state in diamond. A simple nonlinear scattering model, involving a polariton of two coupled electronically and photonically excited states corroborates our interpretation. Momentum-resolved nonlinear x-ray scattering thus provides a pathway to characterize the microscopic structure of polaritons on the length scale of the x-ray wavelength.

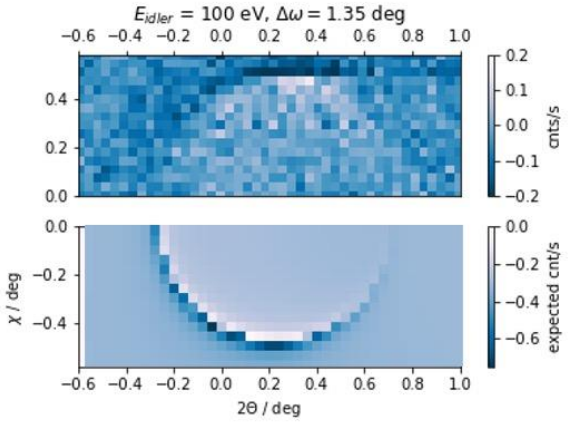


Figure 1. Mesured (upper panel) versus calculated (lower panel) XPDC scattering patteron of Diamond at G= (100) and a rocking angle of 1.35 deg for incoming photon energy of 9.79 keV and an idler energy of 100 eV.

References

[1] Freund I Levine B F 1970 *Phys. Rev. Lett.* **25**, 1241.
[2] Krebs D, Rohringer N *2021 submitted, arXiv:*2104.05838
[3] Hopfield J J 1958 *Phys. Rev.* **112**, 1555.
[4] Boemer C *et al* 2021 *Faraday Discuss*. **228** 451

* E-mail: nina.rohringer@desy.de

Attosecond Science at the Linac Coherent Light Source

A. Marinelli on behalf of the XLEAP and LCLS Attosecond Campaign Collaborations

[1]SLAC National Accelerator Laboratory, Menlo Park, 94025 USA

Synopsis The recent demonstration of attosecond X-ray pulses at the Linac Coherent Light Source (LCLS) and other facilities has opened new avenues for attosecond science, increasing the available peak brightness of sub-fs X-ray pulses by more than six orders of magnitude. In my talk I will discuss the development of attosecond X-ray capabilities at LCLS, including recent advances in terawatt-scale pulses and attosecond pump/probe methods. Finally I will present the application of attosecond XFEL pulses to the time-resolved measurement of coherent electron dynamics in gas-phase molecules.

Attosecond X-ray free-electron lasers can deliver isolated sub-fs pulses with a peak power that surpasses conventional table-top sources by more than six orders of magnitude in the soft X-ray region [1] (see Fig. 1). The intensity at the focus is sufficient for non-linear X-ray spectroscopy methods, and two-color configurations enable applications such as attosecond pump/attosecond probe experiments.

In my talk I will discuss the development of attosecond XFELs at the Linac Coherent Light Source: from the demonstration of isolated soft X-ray pulses with the XLEAP project, to the recent development of terawatt-scale pulses and attosecond pump/probe capabilities. I will also present our plans for attosecond science with the LCLS-II linac, which will enhance the available repetition rate by up to four orders of magnitude (up to 1 MHz [2]).

Finally, I will present the observation of coherent electron dynamics with angular streaking of Auger electrons [3], as well as the recent demonstration of pump/probe experiments with sub-femtosecond resolution.

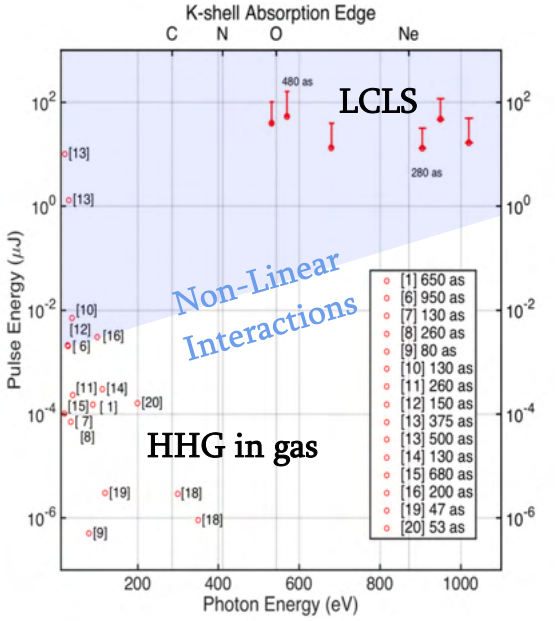


Figure 1. Survey of isolated attosecond pulse sources from [1]. LCLS is capable of deliverying up more than six orders if magnitude higher pulse energy than other available soft X-ray sources, with enough pulse energy for non-linear spectroscopy applications.

References

[1] J. Duris et al. *Nat. Photonics* 14.1 (2020): 30-36.
[2] Abbamonte, P., et al. SLAC-R-1053. 2015.
[3]Li et al., Science375, 285–290 (2022)

* E-mail: marinelli@slac.stanford.edu

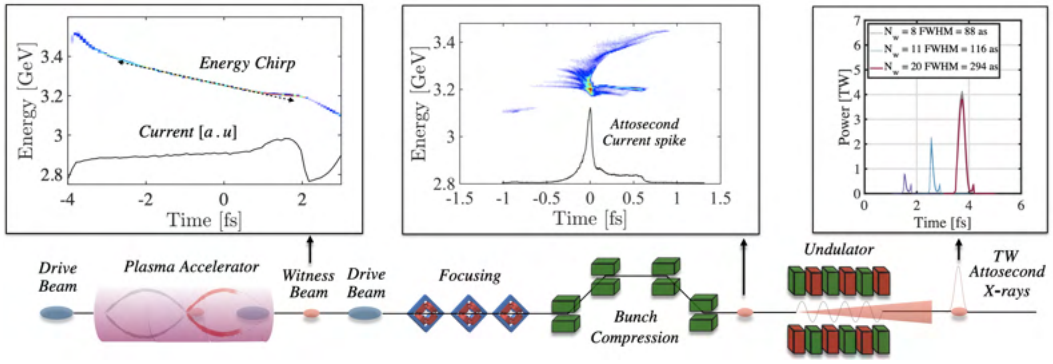


Figure 1: Schematic of a terawatt-attosecond X-ray source driven by a plasma accelerator. Adapted from Ref. [1]

A terawatt attosecond soft X-ray source based on a plasma accelerator-driven free electron laser

C Emma[1]*, X Xu[1], R Hessami[1], M J Hogan[1], K Larsen[1], R Robles[1], and A Marinelli[1]

[1]SLAC National Accelerator Laboratory, Menlo Park, CA 94025, USA

Synopsis We present a novel light source capable of generating few-cycle coherent tunable soft X-ray pulses with TW peak power and a duration of tens of attoseconds, an order of magnitude more powerful, shorter, and with better stability than state-of-the-art X-ray Free Electron Lasers [1]. A light source based on our approach would rival HHG sources in the shortest possible pulse durations while increasing the power and maintaining the flexibility of X-ray FELs, opening up new science in the study of electron motion in atomic and molecular systems.

The recent attosecond science revolution has been driven by two types of attosecond light sources: ones based on High-Harmonic Generation (HHG) in gas and, more recently, X-ray Free Electron Lasers (XFELs). These light sources have complementary properties desirable for ultrafast science. HHG sources can generate ultrashort pulses down to 43 as duration, but with limited pulse energy in the pJ-range for soft X-rays while XFELs have the benefits of much larger pulse energy (approximately 6 orders of magnitude) and wavelength tunability compared with HHG, albeit with a longer pulse duration down to 280 as.

In this work, we demonstrate that electron beams from a plasma wakefield accelerator can be used to generate few-cycle coherent soft X-ray pulses in the 0.1-1 mJ energy range with tens of attosecond pulse duration, thus combining the benefits of HHG and XFEL sources. These unique light source features enable experiments that map the evolution of valence electronic excitations occurring on the 100 as timescale. The X-ray emission in this source is driven by coherent radiation from a pre-bunched, ultra-high current electron beam of attosecond duration, compressed following the exit of a plasma accelerator and injected into a m-length undulator (Fig. 1). This approach presents a new paradigm for plasma accelerator-driven light sources as it relaxes the tight beam energy spread, emittance, and pointing stability constraints, which have hindered progress toward achieving XFEL gain thus far. This contribution will discuss the method, expected source properties and progress towards experimental realization of this concept at the FACET-II accelerator facility at SLAC.

References

[1] C. Emma et al., APL Photonics **6**, 076107 (2021).

*E-mail: cemma@slac.stanford.edu

An atomic two-color XUV interferometer

M Žitnik[1]*, A Mihelič[1], K Bučar[1], Š Krušič[1], R Squibb[2], R Feifel[2], I Ismail[3], P Lablanquie[3], J Palaudoux[3], O Plekan[4], M Di Fraia[4], M Coreno[4,5], M Manfredda[4], A Simoncig[4], P Rebernik Ribič[4,6], F Sottocorona[4], E Allaria[4], K C Prince[4], C Callegari[4] and F Penent[3]

[1] Jožef Stefan Institute, Jamova cesta 39, SI-1000 Ljubljana, Slovenia
[2] University of Gothenburg, Department of Physics, SE-412 96 Gothenburg, Sweden
[3] LCP-MR (UMR 7614), Sorbonne Université and CNRS, 4 Place Jussieu, F-75005 Paris, France
[4] Elettra-Sincrotrone Trieste, Strada Statale 14 - km 163.5, I-34149 Basovizza, Trieste, Italy
[5] Consiglio Nazionale delle Ricerche –Istituto di Struttura della Materia, LD2 unit, 34149 Trieste, Italy
[6] Laboratory of Quantum Optics, University of Nova Gorica, Nova Gorica 5001, Slovenia

W2

Synopsis The relative phase of first (ω) and third harmonics (3ω) extreme ultraviolet light pulses was varied to control the population of the $2s^2$ state in helium through the interference of $\omega+\omega$ and $3\omega-\omega$ two-photon excitation paths. Maximum photoelectron yield occurs when the relative phase of the two harmonics matches the phase difference of complex atomic amplitudes governing the two excitation paths. These results open the way to access phase differences of two-photon ionization paths involving energetically distant intermediate states and to perform interferometry in the extreme ultraviolet range by monitoring final state populations.

Quantum mechanics offers a unique possibility to control transition probability by setting up relative amplitudes of two or more paths leading from one initial to one final state. The last decade has seen rapid development of intense free-electron laser (FEL) sources and the question arises whether the coherent control can be executed entirely by using the extreme ultraviolet (XUV) light. We report here the results of an experiment at the free electron laser facility FERMI where the novel $\omega+\omega$ and $3\omega-\omega$ two-photon interference scheme (Fig. 1) is employed to manipulate the population of $2s^2$ doubly excited state in He. Recently, the 2ω and $\omega+\omega$ absorption paths were combined to measure angle-resolved phases in atomic photoemission [1]. The presented approach is a development of previous all-optical coherent-control experiments [2] and RABBITT experiments [3], entering the XUV wavelength range, and demonstrates the possibility to measure phase difference of multi-photon excitation paths connecting energetically distant intermediate states by observing the final state populations. The two-path experimental configuration thus forms an atomic XUV interferometer, where an ensemble of atoms delivers a maximum response in terms of the emitted electron yield when the phase difference of the ω and 3ω XUV harmonic components at the target equals an atom-specific value for the selected pair of light frequencies.

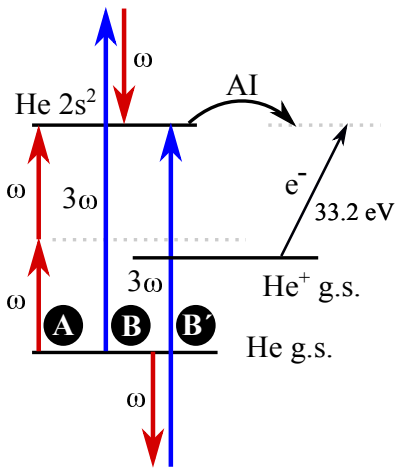


Figure 1. Two-photon excitation of the $2s^2$ autoionizing state in helium with the fundamental (ω, short red vertical arrow) and the third harmonic (3ω, long blue vertical arrow). Path A: two-photon $\omega+\omega$ excitation; path B: two-photon $3\omega-\omega$ excitation; path B' (time-reversed path B): two-photon $-\omega+3\omega$ excitation; AI: autoionization decay.

References

[1] D You *et al*, *Phys. Rev. X* **10**, 031070 (2020).
[2] C K Chan, P Brumer and M Shapiro, *J. Chem. Phys.* **94**, 2688 (1991).
[3] M Isinger *et al*, *Phil. Trans. R. Soc. A* **377**, 20170475 (2019).

*E-mail: matjaz.zitnik@ijs.si

Rabi dynamics driven by a seeded FEL at XUV-wavelengths

S Nandi[1], E Olofsson[2], M Bertolino[2], S Carlström[2], F Zapata[2], D Busto[2], C Callegari[3], M Di Fraia[3], R Feifel[4], G Gallician[5], M Gisselbrecht[2], P Johnsson[2], S Maclot[2], L Neoričić[2], J Peschel[2], O Plekan[3], K C Prince[3], R J Squibb[4], S Zhong[2], P V Demekhin[6], M Meyer[7], C Miron[5], L Badano[3], M B Danailov[3], L Giannessi[3], M Manfredda[3], F Sottocorona[3], M Zangrando[3] and J M Dahlström[2]*

[1]Universite Lyon, Universite Claude Bernard Lyon 1, CNRS, Institut Lumière Matière, F-69622, Villeurbanne, France
[2]Department of Physics, Lund University, SE-22100 Lund, Sweden
[3]Elettra-Sincrotrone Trieste, Basovizza, 34149 Basovizza, Trieste, Italy
[4]Department of Physics, University of Gothenburg, 41258 Gothenburg, Sweden
[5]Université Paris-Saclay, CEA, CNRS, LIDYL, 91191 Gif-sur-Yvette, France
[6]Institute of Physics and CINSaT, University of Kassel, 34132 Kassel, Germany
[7] European XFEL, 22869 Schenefeld, Germany

Synopsis Short-wavelength Rabi oscillations are observed in helium atoms using intense pulses from a seeded free-electron laser. Single-cycle Rabi dynamics take place on the ultra-fast timescale in the extreme-ultraviolet regime. An analytical model, based on a Dyson series of the Rabi oscillating two states, is developed to quantitatively explain interference effects of ejected photoelectrons and non-linear decay mechanisms of the short-wavelength Rabi oscillations.

Sinusoidal population transfers in two level quantum systems, due to resonant external fields, are known as Rabi oscillations. While long-wavelength Rabi oscillations are frequently used in quantum computing and cavity quantum electrodynamics, short-wavelength Rabi oscillations have so far not been observed experimentally. In this work [1], we demonstrate that it is possible to drive Rabi oscillations at extreme-ultraviolet (XUV) wavelengths using intense pulses from a seeded free-electron laser (FEL) [2]. Our experiments are performed on helium atoms between two states: $|a\rangle = 1s^2(^1S_0)$ and $|b\rangle = 1s4p(^1P_1)$ with an atomic resonance at $\hbar\omega_{ba} = 23.742$ eV. Ultra-short FEL pulses of 56 ± 13 fs duration are shown to trigger Rabi oscillations with a period of $2\pi/\Omega \approx 52$ fs, which implies ultra-fast Rabi dynamics in the *single-cycle* regime.

Measurements are performed *in-situ* by recording electrons from two-photon ionization processes of the helium atoms. The photoelectron signal splits up into a doublet structure, identified as an Autler-Townes (AT) doublet [3], when the FEL frequency is blue detuned relative to the atomic resonance by $\Delta \approx 11$ meV. While the AT splitting was expected [4], we find that it exhibits a strong asymmetry with detuning of the FEL frequency that can not be explained as a break-down of the rotating wave approximation, due to the weak-coupling condition: $\omega \approx \omega_{ba}$ and $\Omega/\omega_{ba} = 0.34\%$ [3]. Instead, the recorded asymmetry shows that the high intensities of the FEL pulses balance photoionization rates of one-photon ionization from the excited state: $|b\rangle$, with *non-resonant* two-photon ionization from the ground state: $|a\rangle$. This results in a complex interference phenomenon that explains the blue shift of the observed AT doublet.

Our experimental observations are supported by *ab initio* simulations based on the time-dependent configuration-interaction singles (TDCIS) method [5]. Furthermore, we have developed an analytical model, based on a Dyson series of the Rabi oscillating two states, that quantitatively explains the interference and decay mechanisms of Rabi oscillations at short-wavelengths [1].

*E-mail: marcus.dahlstrom@matfys.lth.se

References

[1] S Nandi et al. arXiv:2201.10950v1 [quant-ph] (2022)
[2] E Allaria et al. Nat. Photon. **6**, 699 (2012).
[3] S H Autler & C H Townes Phys. Rev. **100**, 703 (1955).
[4] K J LaGattuta, Phys. Rev. A **47**, 1560 (1993).
[5] L Greenman et al. Phys. Rev. A **82**, 023406 (2010).

WE Panel: The future of Attosecond Science ▲

WE

20:00 - 21:00 **WE The Future of Attosecond Science**

Chair: **Li Fang**, University of Central Florida, Florida, USA

Mina Bionta, MIT, Massachussets, USA

Mette B Gaarde, Louisiana State University, Louisiana, USA

Ursula Keller, ETH, Zürich, Switzerland

Alexandra S Landsman, Ohio State University, Ohio, USA

Maria Richter, Max Born Institute, Germany, EU

Nina Rohringer, Hamburg, Germany, EU

Linda Young, Argonne National Laboratory and U. Chicago, Illinois, USA

Nirit Dudovich, Weizmann Institute of Science, Rehovot, Israel

Vescent FFC Frequency Combs

The FFC-100 is a fully stabilizable octave-spanning frequency comb with precise control over f_{rep}, f_{opt}, and f_{CEO}. The Er-doped fiber MOPA architecture is simple and robust, and yet high-performance. A highly non-linear fiber broadens the spectrum and our unique fCEO lock detection reduces the size, weight, and power of the system. The FFC frequency combs are designed and built to ensure stable, low-phase noise operation with Allan Deviations supporting the next generation of optical atomic clocks, gravimeters, quantum computers, optical sensors, and more.



FFC-100 turnkey frequency combs

The FFC-100 was designed for low SWaP and turn-key, stable operation: A single 2U 19" rack mount chassis contains the oscillator, amplifier, pump lasers, supercontinuum generation module, and f_{CEO} detection and lock as well as the control electronics. The simple oscillator mode locks at start up every time and the innovative passive SESAM mode-locker is specially designed for a robust, long life. Our unique oscillator design also makes it easy to precisely factory match the repetition rate of two (or more) FFC-100 combs for multi-comb spectroscopy experiments.

Features:

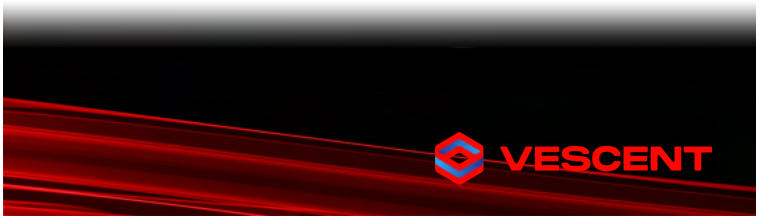
- Turn-key operation
- 1560 nm center wavelength
- Low phase & amplitude noise
- 2U 19" rack-mounted enclosure or modular
- f_{rep} monitoring, control, and matching
- Input port for f_{opt}
- Repetition rates from 80 to 250 MHz
- Optional visible extensions
- Optional super continuum flattening
- Made in America

Applications:

- Time & frequency readout & transfer
- Frequency ruler
- Dual- and multi-comb spectroscopy
- Quantum sensing, computing, & cryptography
- Low-phase noise rf generation



Also available in compact modular form for OEM integration.



R1 Time-Resolved Charge Migration ▲

08:30 - 10:45 **R1 Time-Resolved Charge Migration** 63
Chair: **Mauro Nisoli**, Politecnico di Milano, Italy

08:30 **Francesca Calegari**, Deutsches Elektronen-Synchrotron, Germany, EU
I: *Realtime observation of electronic processes in ionized and neutral molecules.* 64

09:00 **Jon Marangos**, Imperial College London, United Kingdom
I: *Ultrafast X-ray probing of electron and electron-nuclear coupling dynamics in molecules and organic semiconductors* 65

09:30 **Aderonke Folorunso**, Louisiana State University, USA
C: *Chemical Control Of Attosecond Charge Migration.* 66

09:45 **Taran Driver**, Stanford PULSE Institute/SLAC, USA
C: *Attosecond Science at the LCLS.* 67

10:00 **Patrick Rupprecht**, Max-Planck-Institut für Kernphysik, Germany, EU
C: *Control of electronic exchange inside a molecule with ultrafast laser pulses.* 68

10:15 **Danylo Matselyukh**, ETH Zürich, Switzerland
C: *Direct measurement of few-femtosecond charge transfer mediated by a conical intersection.* 69

10:30 **Omer Kneller**, Weizmann Institute of Science, Israel
C: *A look under the tunneling barrier via attosecond-gated interferometry* 70

Realtime observation of electronic processes in ionized and neutral molecules

F Calegari[1] *

[1] Center for Free-Electron Laser Science, DESY and Hamburg Universität, Notkestr. 85, 22607 Hamburg, Germany

Synopsis Here I present the first attosecond beamline combining sub-2fs UV pulses with few-fs IR and/or attosecond XUV pulses. This technology enables us not only to oserve correlation-driven charge migration in a ionized DNA building block, but also to control the chiral response of a UV-excited molecule via the creation of electronic coherences in the neutral molecule. These results pave the way to new schemes, based on purely electronic mechanisms, to stabilizing molecules against dissociation or to achieve ultrafast chiro-optical switching.

Attosecond technology offers formidable tools for the realtime investigation of electronic processes [1]. In this context, we have demonstrated that attosecond pulses can initiate charge migration in aromatic amino-acids [2]. Still, there is a long path towards attochemistry and the full control of the molecule via electronic coherences.

Here, I will give a few examples on how attosecond/few-femtosecond technology can be used to create electronic coherences in ionized or neutral molecles and how this excitation can be used to control the molecular response.

At first, I will present a time-resolved study of the correlation-driven charge migration process occurring in the DNA nucleobase adenine after ionisation by a 15-35 eV attosecond pulse. Our most intriguing observation is that a stable dication of the parent molecule can be produced if the probing NIR pulse is delayed of 2.3 fs from the XUV pulse. The delayed creation of the dication is the signature of a many-body effect resulting in a charge migration mechanism occurring on a sub-3 fs time scale. I will show that by properly synchronizing a sequence of XUV and IR pulses one can take advantage of this purely electronic mechanism to stabilize the molecule against dissociation.

I will then present the first attosecond beamline combining sub-2fs UV pulses [4] with few-fs IR and/or attosecond XUV pulses. UV-induced processes are fundamental in chemistry and biology, however, until now the technological challenge of producing few-cycle UV pulses have hampered their investigation on the few-fs time scale. We recently have combined our sub-2fs linearly polarized UV pulses with circularly polarized NIR pulses to perform time-resolved Photo Electron Circular Dichroism (PECD) in Methyl-lactate and Ethyl-lactate with sub-5 fs resolution. We demonstrate that the broadband UV pulse can excite a coherent superposition of Rydberg states. The resulting coherent electron dynamics can be used to modulate the chiral response of the molecule on a sub-15 fs time scale (Fig 1).

Finally, I will also present a time resolved study of the UV-induced dynamics in iodomethane (CH_3I) and acetone (C_3H_6O) with few-fs time resolution. By simultaneously acquiring both the electron angular momentum distribution and the ion mass spectrum, we have been able to perform covariance analysis of the data.

In iodomethane, the few-fs time resolution allows us to observe an ultrafast decay of the parent ion signal of 5.5 fs. We assigned this decay to the short time window available to produce a stabile and intact molecule before the ultrafast relaxation thorugh a conical intersection inevitably leads to molecular dissociation.

In acetone, the sub 2-fs UV pulses are used to excite a coherent superposition of Rydberg states, and the resulting evolution of the electronic wavepacket is probed by ionization by a single NIR photon. In the energy region between 0.5-1.2 eV of the photoelectron spectrum we can observe clear modulations with a resulting periodicity of 3.2 fs, which we assigned to the populated electronic coherences in the neutral molecules.

References

[1] F. Calegari et al. 49, J. Phys. B 062001 (2016)
[2] F. Calegari et al 336, Science 346 (2014)
[3] E. Månnson et al, (Nature) Commun. Chem. 4, 73 (2021)
[4] M. Galli et al, Optics Letters, 44, 1308 (2019)

* E-mail: francesca.calegari@desy.de

Ultrafast X-ray probing of electron and electron-nuclear coupling dynamics in molecules and organic semiconductors

LR25 collaboration, LCLS Attosecond Campaign, DESY collaboration at FLASH, J Marangos[1 *]

[1] Blackett Laboratory, Imperial College London, South Kensington, London SW7 2AZ U.K.

Synopsis Using HHG and XFEL few-femtosecond to attoseccond x-ray pulses we study electronic and electron-nuclear coupling dynamics in molecular cations and organic semiconductors uncovering the ultrafast electronic and electron-nuclear couplings that characterize the initial events in photoexcitation.

Time-resolved x-ray spectroscopy provides sensitivity to both the localized electronic excitation and electron-nuclear couplings in matter. We have used ultrafast x-ray pulses from both HHG sources and XFELs to study these dynamics in molecular cations and organic semiconductors. This provides not only an incisive probe of electron dynamics on the timescale of electron coherences (<10 fs) but also the unfolding electron-nuclear coupling to vibrational modes over longer timescales.

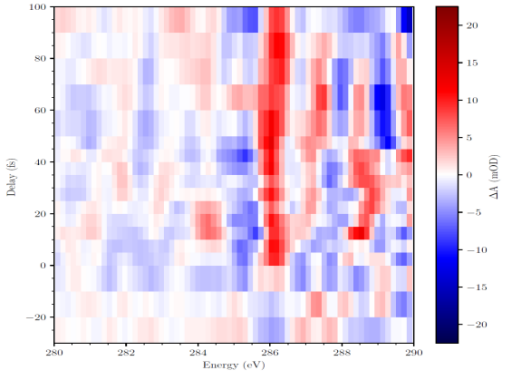


Figure 1. Exciton dynamics in P3HT probed at the C K edge using time-resolved x-ray absorption.

Using a HHG source to generate water window sub-femtosecond pulses [1] we have probed the exciton dynamics in the organic semiconductor polythiophene (P3HT). A ~16 fs pulse centred at 550 nm is used to pump the exciton and this is probed over the first 100 fs of its evolution at the C K edge (Figure 1). We observe the signature of atomically resolved electron density changes following exciton formation, and also a transient pre-edge feature that correlates to the initial delocalization of the exciton across neighbouring polythiophene chains as predicted by TDDFT [2].

Electronic dynamics in inner valence states of molecular cations of isopropanol and glycine are probed using an x-ray pump-probe methodology using few-fs pulses. In isopropanol we capture breathing mode charge migration dynamics of the excitation formed in a superposition of single hole and 2 hole- 1 particle states [3] which is a signature of frustrated Auger-Meitner decay (Figure 2). In glycine we observe oscillatory signatures of charge migration at early times (to 20 fs) that apparently couple to vibrational motion over longer timescales.

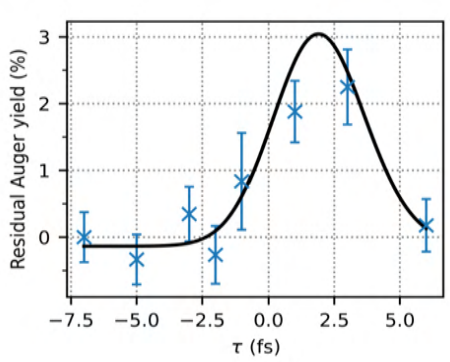


Figure 2. Highly transient hole signature of frustrated Auger-Meitner decay in isopropanol

We are now exploring the use of XLEAP (attosecond) pulses at LCLS to capture cation dynamics due to formation of superpositions of distinct single hole states. Early results are showing sub-femtosecond temporal evolution in such a cases opening the door to widespread application of XFELs to attosecond science.

References

[1] A.Johnson et al,Science Advances **4,** 3761 (2018)
[2] doi.org/10.33774/chemrxiv-2021-bm7nj
[3] T.Barillot et al, PRX **11**, 031048 (2021)

* E-mail: j.marangos@imperial.ac.uk

Chemical Control of Attosecond Charge Migration

A Folorunso[1]*, F Mauger[2], K A Hamer[2], D Jayasinghe[1], R R Jones[3], L F DiMauro[4], M B Gaarde[2], K J Schafer[2], and K Lopata[1,5]†

[1]Department of Chemistry, Louisiana State University, Baton Rouge, LA 70803, USA.
[2]Department of Physics and Astronomy, Louisiana State University, Baton Rouge, LA 70803, USA.
[3]Department of Physics, University of Virginia, Charlottesville, VA 22904, USA.
[4]Department of Physics, The Ohio State University, Columbus, OH 43210, USA.
[5]Center for Computation and Technology, Louisiana State University, Baton Rouge, LA 70803, USA.

Synopsis Charge migration (CM) is a coherent, attosecond-scale, process in which localized holes move across a molecule. CM has been the focus of a lot of experimental and theoretical efforts, but the relationship between molecular structure and the dynamics remains poorly understood. In this work, we use time-dependent density-functional theory to simulate CM in linear and ring-shaped halogenated molecules, following a sudden ionization at the halogen. We show that conjugation is essential for CM, and that higher atomic-number halogens and stronger electron donating groups result larger CM contrast.

CM is an attosecond process that involves the rapid movement of holes across a molecule following either ionization or excitation. CM, which can occur faster than nuclear motion, is expected to be important for understanding and controlling electronic dynamics in a wide range of systems. CM has been studied in some molecules, however, there are still many questions to be answered such as: Which type of molecules support CM? Does it manifest in such a way that its periodicity and visibility can be predicted using simple rules? What is the relationship between molecular structure and these dynamics? To address these questions,we systematically study groups of molecules with similar structures but different chemical functionalization.

In this work, we study CM in halogenated linear and functionalized bromobenzene molecules using first-principles calculations. In particular, we define a number of CM metrics and investigate how they can be influenced by chemically accessible features such as the length of the molecule, bond order, and different functional groups. We initially created a localized on the halogen, emulating a strong-field ionization and then propagate the density using time-dependent density functional theory (TDDFT).

In linear molecules, we find that the CM speed is independent of the molecular length, but slower in the triple- than for the double-bonded chains. We also show that double- and triple-bonded molecules and higher atomic number halogen atoms all support robust CM that progresses via hopping from π bond to π bond [1]. In the ring molecules, we identify the mechanisms of CM as well as the relationship between chemical functional groups in charge dynamics. We find that the stronger the electron donating strength of an "acceptor" group, the greater its ability to accept a hole, and thus the CM has a higher hole contrast (*i.e.*, more sensitive to local probes of the electron density). Our trends are qualitatively consistent with those predicted by the Hammett sigma value, a metric for the susceptibility of a chemical reaction to the influence of the substituent group.

In conclusion,we predict these investigations will form a set of guiding principles for identifying molecules that exhibit charge migration and help interpreting attosecond experiments.

References

[1] A S Folorunso *et al.*, Phys. Rev. Lett. **126**, 133002 (2021).

*E-mail: afolor1@lsu.edu
†E-mail: klopata@lsu.edu

Attosecond Science at the LCLS

Taran Driver[1] * on behalf of the X300, LU00 and LCLS Attosecond Campaign Collaborations

[1]Stanford PULSE Institute, Menlo Park, CA 94025, USA
[2]Linac Coherent Light Source, SLAC National Accelerator Laboratory, Menlo Park, CA 94025, USA

Synopsis We present measurements of attosecond coherent electron motion and electron correlation effects performed at the Linac Coherent Light Source (LCLS) X-ray free-electron laser.

The Linac Coherent Light Source (LCLS) produces attosecond x-ray pulses and pulse pairs with wavelength tunability across the soft x-ray region and peak power the approaching terawatt regime [1]. These attosecond x-ray pulses are close to the Fourier limit, with a coherent spectral bandwidth of ~5-10 eV. We present an array of recent measurements performed with this source, leveraging the unique properties of x-ray/matter interactions to initiate and probe coherent electron dynamics and correlated electron motion on its natural attosecond timescale.

Time-resolved measurements with a single attosecond pulse were performed by attosecond angular streaking with a circularly polarized infrared laser field [2]. This technique was used to perform a direct temporal characterization of the x-ray pulses [1]. We also used angular streaking to time-resolve resonant Auger-Meitner decay in the nitric oxide molecule following x-ray excitation at the oxygen 1s→2pπ resonance. With the attosecond x-ray pulse we prepared a coherent superposition of core-excited states. We observed a quantum beat in the time-dependent electron current from the subsequent Auger-Meitner decay. We tuned the amplitude of this beat by changing the central photon energy of the x-ray pulse [3].

With the same experimental setup, we measured the wavelength-dependent x-ray photoemission delay of O 1s photoelectrons. We tuned the x-ray central photon energy above the oxygen 1s ionization potential and recorded the angular difference in the momentum shift experienced by the O 1s and N 1s photoelectrons in the streaking interaction. This angle maps to the photoemission delay between the two photoionization channels. We observed an increase in O 1s photoemission delay at the position of a known shape resonance, ~7 eV above the O *K*-edge.

With the split-undulator method [4] we produced attosecond x-ray pulse pairs separated by a controllable delay and with independent wavelength tunability. With a pulse pair tuned to ~260 eV (pump) and ~520 eV (probe), we performed an attosecond x-ray pump/attosecond x-ray probe measurement of coherent valence electron dynamics in the para-aminophenol molecule. With the pump pulse we prepared a coherent superposition of valence-ionized electronic states *via* impulsive ionization. By scanning the delay between the x-ray pulses we time-resolved the attosecond motion of this coherent wave packet with atomic-site spatial localization, by measuring the transient absorption of the probe pulse just below the oxygen *K*-edge. We have also produced single-color attosecond x-ray pulse pairs separated by a controllable phase-stable delay.

Beyond impulsive ionization, stimulated electronic Raman scattering offers a path to the site-specific creation, control and probing of valence excited wavepackets in molecular systems. In nitric oxide, we tuned the x-ray photon energy of a single attosecond pulse to the oxygen 1s→2pπ resonance and drove coherent population transfer to valence-excited states *via* stimulated impulsive electronic Raman scattering [5]. The demonstration of stimulated electronic Raman scattering is an important step to the realization of other nonlinear x-ray spectroscopies.

References

[1] Duris J, Li S *et al* 2020 *Nat. Phot.* **14** 30
[2] Eckle P *et al* 2008 *Nat. Phys.* **4** 565
[3] Li S, Driver T *et al* 2022 *Science* **375** 285
[4] Lutman A A *et al* 2013 *Phys. Rev. Lett.* **110** 134801
[5] O'Neal J T *et al* 2020 *Phys. Rev. Lett.* **125** 073203

* E-mail: tdriver@stanford.edu

Control of electronic exchange inside a molecule with ultrafast laser pulses

Patrick Rupprecht[1]*, Lennart Aufleger[1], Simon Heinze[2], Alexander Magunia[1], Thomas Ding[1], Marc Rebholz[1], Stefano Amberg[1], Nikola Mollov[1], Felix Henrich[1], Maurits Haverkort[2], Christian Ott[1], and Thomas Pfeifer[1]

[1]Max-Planck-Institut für Kernphysik, Heidelberg, 69117, Germany.
[2]Universität Heidelberg, Institut für theoretische Physik, Heidelberg, 69120, Germany.

Synopsis We present the transient control of the electronic exchange interaction in sulfur hexafluoride (SF_6) molecules. The sulfur $L_{2,3}$ absorption edge around 173 eV was probed and spectrally resolved while the SF_6 molecules were under the influence of an intense infrared (IR) laser field. The spin-orbit-split $6a_{1g}$ doublet resonance shows IR-intensity-dependent relative transition strengths of the $j_\pm=\{3/2, 1/2\}$ peaks. This branching-ratio change is attributed to a change of the effective core-hole—excited-electron exchange energy. An *ab-initio* quantum many-body simulation confirms our finding.

R1

While electron–electron interactions play a fundamental role in any atom beyond hydrogen, they also govern molecular structure and reactivity. We introduce and experimentally demonstrate a general concept to control the purely quantum mechanical electron–electron exchange interaction by intense, ultrashort laser fields [1]. In particular, strong coupling to excited states allows to modify the effective electronic exchange energy by valence-orbital mixing. For a proof-of-principle, we focus on the sulfur hexafluoride molecule SF_6, considering the coupling of a sulfur 2p core hole with a valence excited electron on the few-femtosecond timescale, using a combination of soft x-ray and few-cycle infrared (IR) laser pulses in a table-top x-ray transient absorption measurement. The experiment investigates the relative oscillator strengths within the spin-orbit-split $6a_{1g}$ [2] absorbance doublet around 173 eV. This branching ratio of the $j_\pm = \{3/2, 1/2\}$ peak areas acts as an experimental observable for the exchange energy [3, 4]. In the presented experiment, the branching ratio is altered by IR laser pulses of tunable intensity as shown in figure 1. Applying a minimal toy-model Hamiltonian enables to correctly emulate the $6a_{1g}$ branching ratio and peak splitting and thus extract an effective exchange energy increase of up to 50 %. Furthermore, an *ab-initio* restricted active space quantum many-body simulation was conducted and confirmed our experimental results and interpretation. Such direct control of effective electronic interactions is a significant step towards laser-directed chemistry on the fundamental electronic level with single-atomic site selectivity.

*E-mail: patrick.rupprecht@mpi-hd.mpg.de

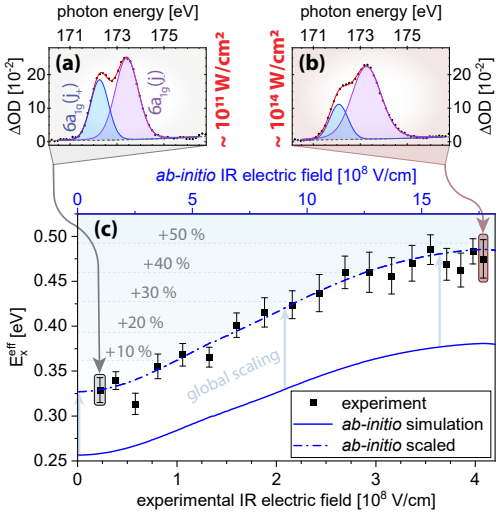


Figure 1. Electronic exchange control. Absorbance of the spin-orbit-split $6a_{1g}$ doublet resonance in SF_6 under the influence of a (a) weak and (b) strong IR field. (c) Effective electronic exchange energy E_x^{eff} over field strength. The experimental data as well as the *ab-initio* simulation results are shown.

References

[1] P. Rupprecht *et al.*, Phys. Rev. Lett. accepted manuscript (2022).
[2] E. Hudson *et al.*, Phys. Rev. A **47**, 361 (1993).
[3] Y. Onodera and Y. Toyozawa, J. Phys. Soc. Jpn. **22**, 883 (1967).
[4] B. T. Thole and G. van der Laan, Phys. Rev. B **38**, 3158 (1988).

Direct measurement of few-femtosecond charge transfer mediated by a conical intersection

D T Matselyukh[1]*, F Rott[2]†, P Zhang[1], T Schnappinger[3], Z Li[4], R de Vivie-Riedle[2], HJ Wörner[1]

[1]Laboratorium für Physikalische Chemie, ETH Zürich, 8093 Zürich, Switzerland
[2]Department of Chemistry, LMU Munich, 81377 Munich, Germany
[3]Department of Physics, Stockholm University, 114 21 Stockholm, Sweden
[4]School of Physics, Peking University, 100871 Beijing, People's Republic of China

Synopsis Thanks to the simultaneous sub-femtosecond temporal and atomic spatial resolution offered by core-valence attosecond transient-absorption spectroscopy, we directly observe the few-femtosecond transfer of an electron hole from fluorine to iodine in CF_3I^+ only 9 fs after its creation through strong-field ionization (SFI). This assignment is confirmed through RASPT2 simulations of the iodine $N_{4,5}$ absorption spectrum, as well as the detection of charged fragments. This is the fastest charge-transfer process observed to date.

A molecule known to offer the characteristic prerequisites for charge transfer (CT) [1] is the trifluoroiodomethane cation (CF_3I^+), which we probe with a novel experimental scheme that combines attosecond transient absorption spectroscopy (ATAS) on the $N_{4,5}$ edge of iodine, with SFI mass spectrometry. In such a way, we take advantage of the sub-femtosecond time resolution of ATAS as well as its site specificity. Our electronic-state assignment is supported with theory [2] and the comparison of measured fragmentation patterns with previous velocity-map-imaging studies [1].

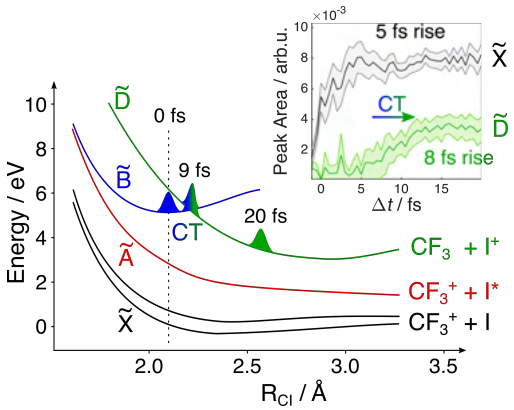


Figure 1. Potential energy surfaces of CF_3I^+ showing the conical-intersection-mediated CT between the $\tilde{B}$ and $\tilde{D}$ states. Inset: Time-resolved experimental XUV absorption of the $\tilde{X}$ and $\tilde{D}$ states showing the 9 fs delay between the two signals.

Our multi-state CASPT2 calculations show that CF_3I^+ features a conical intersection (CI) between two electronic states close to the Franck-Condon region that can mediate ultrafast CT (shown in Fig. 1). The $\tilde{B}$ $^2A_2$ state, accessible through SFI from the neutral CF_3I molecule, is described by a valence hole located on the fluorine atoms while the $\tilde{D}$ diabat it crosses with at the conical intersection corresponds to a valence hole on the iodine atom.

Our site-specific ATAS measurements reveal that this CT takes place only 9 fs after SFI, manifesting as the delayed appearance of the characteristic I^+ $N_{4,5}$-edge absorption feature at 47.3 eV [3] (shown in the inset of Fig. 1). By analysing the rise time, we find that the non-adiabatic CT takes 8 fs to occur, whereas the ground state signal of CF_3I^+ experiencing adiabatic dynamics appears in 5 fs (atomic systems exhibit a 2 fs rise time). All assignments are supported by the high-quality description of the valence and core-excited states and the transitions between them, offered by multiconfigurational second-order perturbation theory restricted active space (RASPT2) calculations [2].

References

[1] P Downie, I Powis, Faraday Discuss. **115** 103-117 (2000).
[2] F Rott et al., Struct. Dyn. **8**, 034104 (2021).
[3] G O'Sullivan et al., Phys. Rev. A **53**, 3211 (1996).

*E-mail: mdanylo@ethz.ch
†DTM and FR have contributed to this work equally

A look under the tunneling barrier via attosecond-gated interferometry

O Kneller[1*], D Azoury[1], Y Federman[1], M Krüger[1], A J Uzan[1], G Orenstein[1], B D Bruner[1], O Smirnova[2], S Patchkovski[2], M Ivanov[2] and N Dudovich[1]

[1]Department of Physics of Complex Systems, Weizmann Institute of Science, 7610001 Rehovot, Israel
[2] Max-Born-Institute, 12489 Berlin, Germany

Synopsis Interferometry resolves the coherence of light, enabling a direct reconstruction of the complex information it encodes. Here, we demonstrate attosecond-gated interferometry, increasing the dimensionality of the interferometric measurement by adding the time domain – following the interferogram's evolution within a fraction of an optical cycle. This scheme perturbs the dynamics of field induced tunneling, probing the electronic wavefunction under the tunneling barrier, and records the phase acquired by an electron as it propagates in a classically forbidden region.

R1

Tunnelling is a fundamental quantum process which governs a large range of phenomena and applications. In the strong-field regime, optical tunneling plays an important role, serving as a starting point of many attosecond scale phenomena. In this regime, the rapid oscillations of the laser field may excite the electronic wavefunction as it propagates under the modulated tunneling barrier [1,2]. Such an excitation is encoded in the phase the electron accumulates under the tunneling barrier [3].

The ability to resolve the coherence of the electron's wavefunction and then project back its evolution under the barrier requires the integration of an attosecond-scale control scheme with state-of-the-art metrology. In my talk I will present *attosecond-gated interferometry* [3], as a novel spectroscopic scheme. This scheme combines two fundamental concepts in attosecond spectroscopy, sub-cycle temporal gating and extreme-ultraviolet (XUV) interferometry, as presented in Figure 1a.

Synchronizing the fundamental field with its second harmonic (SH) field serves as a sub-cycle gate that perturbs the tunneling dynamics, modifying the electron's tunneling amplitude and phase. These complex properties are mapped onto a coherent XUV field via high-harmonic generation (HHG). Interfering it with a reference HHG source, we resolve its phase.

By Integrating this measurement with quantum path analysis and ab-initio numerical simulations, we are able to isolate the electron's tunneling phase-shift and follow its evolution with attosecond precision (see Figure 1b).

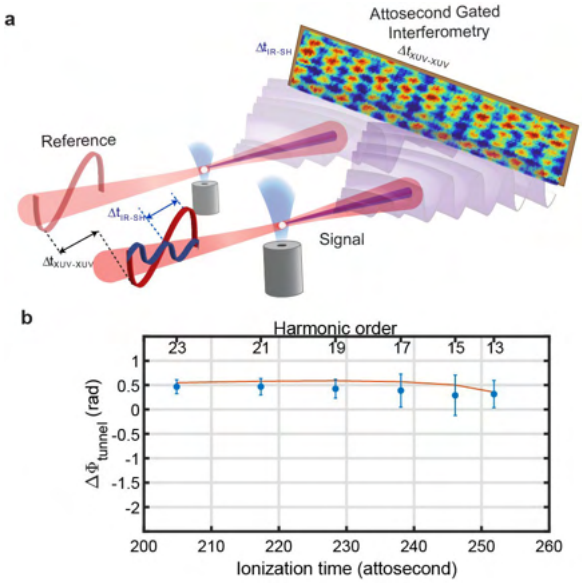


Figure 1. a, HHG is temporally gated with attosecond precision by an SH field, via the two-color delay, influencing the harmonic's amplitude and phase. This phase is resolved by an interferometric measurement, interfering the generated harmonics with a reference field by controlling their relative delay. **b**, Reconstructed tunneling phase shifts (blue) as a function of the ionization time and harmonic order, compared with quantum path analysis results (red).

References

[1] Eckle P *et al* 2008 *Science*: 322.5907 1525-1529.
[2] Eckart S *et al* 2018 *Physical review letters*: 121.16 163202.
[3] Han M *et al* 2021 *Nature Photonics*: 15.10 765-771.
[4] Kneller O *et al* 2022 *Nature photonics* : accepted

* E-mail: omer.kneller@weizmann.ac.il

R2 Table-Top Attosecond Sources ▲

11:00 - 13:00 **R2 Table-Top Attosecond Sources** 71
Chair: **Zenghu Chang**, University of Central Florida, Florida, USA

11:00 **Caterina Vozzi**, CNR, Milano, Italy, EU
I: *Bright coherent XUV generation in microfluidic glass devices for ultrafast x-ray spectroscopy.* 72

11:30 **Katsumi Midorikawa**, RIKEN, Japan
I: *Increase in photon flux of isolated attosecond pulses.* 73

12:00 **Ming-Chang Chen**, NTHU, Taiwan
C: *Generation of isolated-attosecond pulses driven by a post-compressed Yb laser* 74

12:15 **Roland E. Mainz**, Center for Free-Electron Laser Science, Germany, EU
C: *Tunable isolated attosecond pulse generation by sub-cycle optical pulses from a parametric waveform synthesizer.* 75

12:30 **Yi Wu**, University of Central Florida, USA
C: *100-GW 2.5-μm pulses generation by a double-stage Cr^{2+}:ZnSe amplifier* 76

12:30 **Stefan Haessler**, Laboratoire d'Optique Appliquée (LOA), France, EU
C: *Attosecond control of relativistic plasma mirror emission* 77

R2





Bright coherent XUV generation in microfluidic glass devices for ultrafast x-ray spectroscopy

A G Ciriolo[1], R Martìnez Vàzquez[1], G Crippa[1,2], M Devetta[1], D Facciàlà[1], E. Cinquanta[1], F Frassetto[3], L Poletto[3], R Osellame[1], S Stagira[1,2], and C Vozzi[1*]

[1]Istituto di Fotonica e Nanotecnologie CNR-IFN, Milano, 20133, Italy
[2]Dipartimento di Fisica, Politecnico di Milano, Milano, 20133, Italy
[3]Istituto di Fotonica e Nanotecnologie CN-IFN, Padova, 35131, Italy

Ultrafast X-ray spectroscopy allows studying light-matter interaction with an unprecedented temporal and spatial resolution, with the further advantage of being element-selective and oxidation- and spin-state specific. I will discuss the recent developments we implemented toward attosecond X-ray spectroscopy based on tabletop sources, namely a bright XUV source based on high-order harmonic generation in microchannels and a new beamline for XUV transient absorption spectroscopy experiments up to a few hundred eV.

R2

High Harmonic Generation (HHG), arising from the interaction of intense femtosecond laser pulses with noble gases, led to the realization of table-top sources of coherent Extreme UltraViolet (EUV) and Soft-X Ray radiation. As a result, ultrafast spectroscopy can nowadays be performed with extreme temporal resolutions, down to the attosecond regime, and site and chemical selectivity. These peculiar features grant access to purely electronic dynamics in molecules and solids, initiated by ultrafast laser pulses and to fundamental processes of light-matter interaction.

One of the most promising all-optical techniques to perform these experiments is transient absorption in the XUV. However, the full exploitation of ultrafast spectroscopy in this spectral range is somehow hindered, even today, by the technological complexity of the required setups and the low generation efficiency of the HHG sources, particularly when moving towards higher photon energies.

Here, we report the efficient XUV generation inside a microfluidic device fabricated by femtosecond laser irradiation followed by chemical etching [1]. This microfluidic approach allows controlling and manipulating the harmonic generation conditions in gas on the micro-meter scale with unprecedented flexibility, enabling a high photon-flux and phasematching on broadband harmonics up to 200 eV.

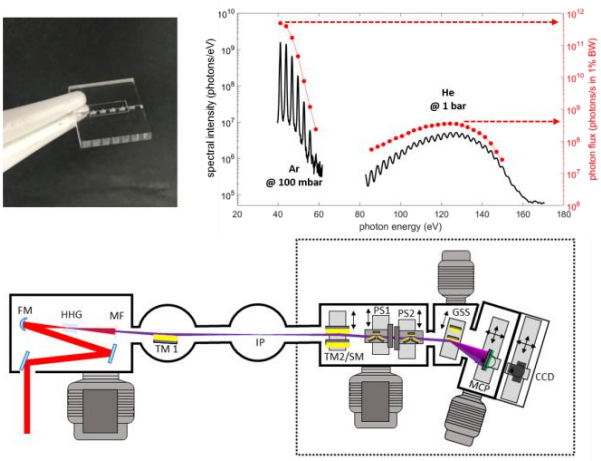


Figure 1. Upper panel: the device for HHG and harmonic spectra generated in argon and helium. Lower panel: scheme of the beamline for ultrafast soft-X spectroscopy.

We also report on the design and commissioning of a new beamline for transient absorption/reflectivity measurements in molecules and solids recently developed at CNR-IFN and equipped with a flexible XUV spectrometer for high-resolution and high dynamic range measurement, with a polarimeter for the characterization of the HHG polarization.

References

[1] A. G. Ciriolo et al., J. Phys. Photonics 2, 024005 (2020)

* E-mail: caterina.vozzi@cnr.it

Increase in photon flux of isolated attosecond pulses

K Midorikawa*

RIKEN Center for Advanced Photonics, RIKEN, Wako, Saitama 351-0198, Japan

Synopsis We demonstrate the remarkable increase in photon flux of isolated attosecond pulses with a novel high-energy Mid-IR driving source and multi-color waveform synthesizer. A peak power of 1.1 GW with a pulse duration of 226 as was obtained around 60 eV.

Research on isolated attosecond pulses (IAPs) changed substantially around 2010. Before then, the Ti:sapphire laser was the de facto standard as the driving light source, so the cutoff energy was limited to ~100 eV and the repetition rate was of the order of 1 kHz. After 2010, Mid-IR OPA, which brings the advantages of extending the cutoff and increasing the repetition rate, became the mainstream driving source. Owing to the quadratic dependence of the cutoff energy on the driving wavelength, the harmonic photon energy was extended to over 300 eV by using an OPA, reaching the water-window spectral region. However, the increase in driving wavelength results in a substantial decrease in conversion efficiency. To compensate for the low photon flux associated with the low conversion efficiency, attempts to optimize the waveform of the driving laser pulse and to increase the driving laser energy and repetition rate have been pursued vigorously [1].

To increase the photon flux of IAPs, it is essential to increase the driving laser pulse energy as well as improve the conversion efficiency. In this talk, I show our novel results on the remarkable increase of photon flux of IAPs with a high-energy Mid-IR driving source and multi-color waveform synthesizer. For the former, based on the dual-chirped optical parametric amplification with type-I BiBO crystals, we generated 105 mJ, 10.4 fs, 10 Hz, carrier-to-envelope phase (CEP) stable laser pulses centered at 1.7 μm, resulting in a peak power of 10 TW. The CEP-dependent high harmonic generation is implemented to confirm the sub-two-cycle pulse duration and CEP stabilization of the infrared laser pulses. For the latter, a fully stabilized multi-TW three-color synthesizer was developed [2]. With full active stabilization of all relative time delays, relative phases, and the carrier-envelope phase, a shot-to-shot stable IAP was obtained around 60 eV with pulse energy above 0.24 μJ. The peak power was evaluated to be beyond 1 GW with a pulse duration of 226 as, which was confirmed by streaking measurement at 10 Hz [3].

* E-mail: kmidori@riken.jp

References

[1] K Midorikawa, Nat. Photo. March (2022).
[2] B Xue et al., Sci. Adv. 6, eaay2802 (2020).
[3] B Xue et al., Optica 9, (2022) in press.

Generation of isolated-attosecond pulses driven by a post-compressed Yb laser

An-Yuan Liang[1], Ming-Shian Tsai[1], Yu-Zhi Fu[1], Yu-En Chien[1], Ming-Chang Chen[1,2,*]

[1]Institute of Photonics Technologies, National Tsing Hua University, Hsinchu 300044, Taiwan
[2]Department of Physics, National Tsing Hua University, Hsinchu 300044, Taiwan

We introduce a new post-compression, cascaded focus and compression, to achieve 50-fold compression of millijoule-level pulses at 1030 nm from 157 fs to 3.1 fs, with an output pulse energy of 0.98 mJ and an overall efficiency of 73%. When driving high-harmonic generation, these single-cycle pulses enable the creation of a carrier-envelope-phase-dependent extreme ultraviolet continuum with energies extending up to 180 eV, providing isolated ≈ 290-attosecond pulses at the output.

The advancement of contemporary ultrafast science requires reliable sources to provide high-energy few-cycle light pulses. Nonlinear pulse compression is one of the most common methods to generate intense few- (or single-) cycle pulses [1].

We recently demonstrated a new post-compression technique that can efficiently compress the pulse to the single-cycle regime [2]. We refer to this as CAScaded foCus AnD comprEssion (CASCADE). One CASCADE unit comprises a focus in matter to carry out nonlinear broadening, together with one compressor that shortens the pulse duration. When using only four-unit CASCADE in Ar, we realized the compression of millijoule-level 1030 nm pulses from 157 fs to 3.1 fs (single-cycle) with a good overall efficiency of 73 %, as presented in Fig. 1(a).

In high harmonic generation using such single-cycle pulses, we observed a broad and highly CEP-dependent EUV continuum. The resulting HH EUV supercontinua in He covers photon energies up to 180 eV. Fig. 1(b) shows the effect of the CEP on EUV continua (photonelectron spectrum from Ne). The high contrast of the fringes demonstrates the single-cycle nature and an excellent CEP stability of our driving pulses. The streaked photoelectron spectrum as a function of delay between the EUV pulse and the streaking IR pulse is measured and depicted in Fig. 1(c). The PROOF reconstructs single attosecond pulses [3], providing a pulse duration of ≈ 290, as presented in Fig. 1(d).

In summary, our new post-compression method paves the way for the direct use of cost-effective, compact, and efficient Yb laser technologies in strong-field laser-driven experiments and attosecond science.

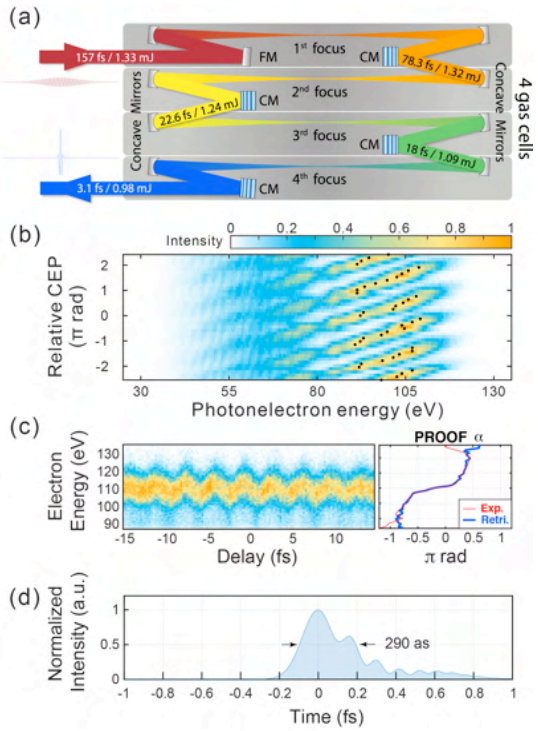


Figure 1. (a) Schematic of a four-unit CASCADE. (b) CEP dependence of EUV supercontinua. (c) Photoelectron streaking spectrogram was obtained by ionizing neon with an attosecond pulse generated in He by varying the delay between the EUV and mid-IR pulses. The right column compares the PROOF phase angle α (see Ref. [3]) extracted from the experiment to that from the best retrieval. (d) The retrieval suggests the EUV pulse duration is ≈ 290 as.

[1] T. Nagy, P. Simon, and L. Veisz, Adv. Phys.: X 6, 1845795 (2021).
[2] Tsai et al.," Nonlinear compression towards high-energy single-cycle pulses by cascaded focus and compression", submitted (2022)
[2] M. Chini et al., Opt. Express. 18, 13006–13016 (2010).

* E-mail: mingchang@mx.nthu.edu.tw

Tunable isolated attosecond pulse generation by sub-cycle optical pulses from a parametric waveform synthesizer

R E Mainz[1,2] *, Y Yang[1,2], G M Rossi[1,2], F Scheiba[1,2], M A Silva-Toledo[1,2], G Cirmi[1,2], and F X Kärtner[1,2]

[1]Center for Free-Electron Laser Science, Deutsches Elektronen-Synchrotron DESY, Notkestrasse 85, 22607 Hamburg, Germany

[2]Physics Department and The Hamburg Centre for Ultrafast Imaging, University of Hamburg, Luruper Chaussee 149, 22761 Hamburg, Germany

Synopsis We present direct isolated attosecond pulse (IAP) generation with waveform controlled non-sinusoidal pulses generated by parametric waveform synthesis. Pulses as short as 0.6 optical cycle are generated by the synthesis of two broadband OPA channels and span the range from 650 nm to 2.2 µm with milijoule-level energy. Driving HHG with such a source directly generates IAPs without the need of additional gating methods. The synthesis parameters (CEP, relative phase) allow for intricate tuning of the IAP spectrum and pulse duration confirmed with attosecond streaking.

With the recently demonstrated parallel parametric waveform synthesis (PWS), it is possible to synthesize multi-octave spanning laser pulses with Fourier-limits below one optical cycle [1]. The PWS is a bandwidth and energy scalable approach to generate sub-cycle optical electric field transients and can deliver currently millijoule level pulses. In such a scheme, separate broad-band and CEP-stable pulses from different OPA-channels are coherently combined [2]. Here, we synthesize the output of an NOPA in the NIR (650-1100 nm) and a DOPA emitting between 1.2-2.2 µm. A multi-phase meter allows to stabilize the CEP and relative phase (RP) between the pulses to better than 220 mrad (RP: 100 mrad) to generate a consistent and reproducible waveform. The pulses can be synthesized to be as short as 0.6 optical cycles at a center wavelength of 1.4 µm. Such pulses are highly interesting for strong-field applications such as high harmonic generation (HHG) [3] due to their capability to generate isolated attosecond pulses directly without the use of gating techniques. The center wavelength aims to generate efficient IAPs covering the whole water-window spectral range for novel pump-probe experiments. The synthesis parameters (CEP, RP) directly allow to shape and influence the electric field transient and thus the IAP characteristics. We present tunable HHG-emission and characterize the corresponding attosecond pulses by means of attosecond streaking (Fig. 1a-b). In Argon a vast tunability between 30-110 eV is observed with IAP-pulse durations between 82-241 as. In Neon tunable HH-continua are observed up to 200 eV (Fig 1.c-e). HHG in Helium is currently explored.

References

[1] G M Rossi, Nat. Phot. **14**, 629-635 (2020).
[2] C Manzoni, LPR **9**, 2 (2015).
[3] Y Yang, Nat. Comm. **12**, 6641 (2021).

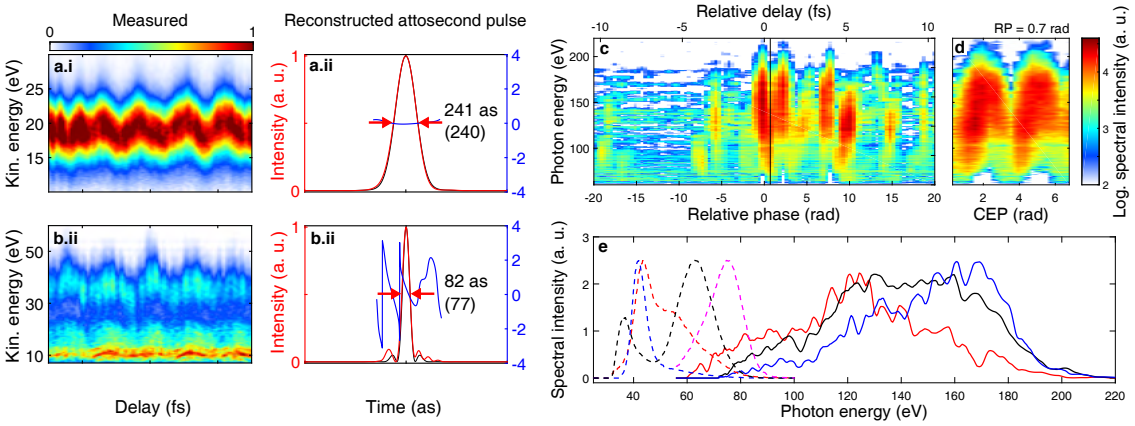


Figure 1: (a, b) Two streaking traces of IAPs generated in Argon by synthesized pulses ranging between 82-241 as of pulse duration. (c, d) Relative phase scan showing tunable HH-generation in Neon up to 200 eV. (e) various generated HH-spectra in Ar (dotted) and Ne (solid).

*E-mail: roland.mainz@desy.de

100-GW 2.5-μm pulses generation by a double-stage Cr^{2+}:ZnSe amplifier

Yi. Wu, Fangjie Zhou, and Zenghu Chang *

CREOL and Department of Physics, University of Central Florida, Orlando, Florida 32816, USA.

Synopsis An OPA seeded two-stage chirped-pulse amplifier centered at 2.5 μm was developed to produce 6.5 mJ, 65 fs pulses at 1 kHz with superior pulse stability. The 100-GW peak power allows further advance to attosecond X-ray pulses generation in the water window.

To extend attosecond capabilities into and beyond the soft X-ray (SXR) "water window," CPA based on the four-level gain medium Cr^{2+}:ZnSe is a promising choice[1]. Previously a one-stage Intrapulse Difference Frequency Generation (IDFG) seeded Cr^{2+}:ZnSe chirped-pulse amplifier (CPA) was demonstrated to deliver 3.5-mJ pulse energy[2]. Since optical parametric amplification (OPA) allows few-cycle pulse delivery at both high peak and average power, by adopting a commercial OPA as the front-end, further improvement on pulse energy and stability was permitted on such a CPA system.

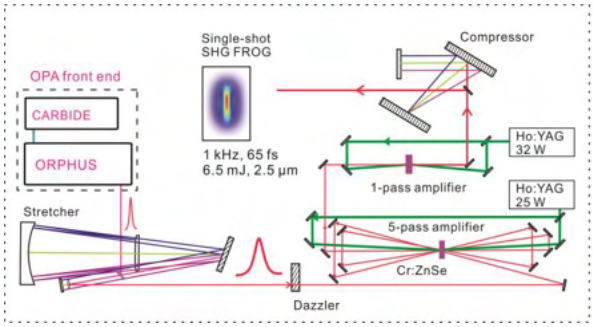


Figure 1. The layout of Cr^{2+}:ZnSe CPA system.

The layout of the Cr^{2+}:ZnSe laser system is shown in Figure 1. The 2-μJ seed pulse was provided by a commercially available OPA (Light conversion, ORPHEUS) covering the 2.1 μm to 2.8 μm spectrum range. The seed pulse is then sent to an aberration-free Öffner-triplet stretcher containing a reflective grating with a groove density of 300 l/mm. A mid-infrared Acousto-Optic Programmable Dispersive Filter, DAZZLER, is deployed after the stretcher to pre-compensate the high-order phase in the amplifier. The first stage amplifier has five passes with a gain medium of a 40-mm long rectangular poly-crystalline Cr^{2+}:ZnSe water-cooled to 18 °C. The second stage is a single pass configuration. Both stages are pumped by 50-ns, 2.09-μm pump lasers (IPG Photonics) from both ends, with pump pulse energies at 25 mJ and 32 mJ, respectively. The first stage output is 5.2 mJ while the second stage boosts pulse energy to 10 mJ. After the amplifier, the pulses are compressed in a double-pass grating compressor with the same groove density as the stretcher with an output pulse energy of 6.5 mJ. The temporal profile of the output was characterized by a home-built single-shot second harmonic Frequency Resolved Optical Gating (FROG). The entire system is built inside a sealed box and is purged with nitrogen during operation. The purging is needed, due to strong absorption in water vapor for wavelengths ≥ 2.5 μm.

In summary, we have demonstrated a two-stage Cr^{2+}:ZnSe CPA capable of producing 6.5-mJ, 65-fs laser centered at 2.5 μm with the peak power at 100 GW. Such pulse energy level and stability provide the foundation for further pulse duration compression, also attosecond X-rays HHG in the SXR water window.

References

[1] Slobodchikov, E. & Moulton, P. F. 1-GW-peak-power, Cr:ZnSe laser. In CLEO:2011 - Laser Applications to Photonic Applications, PDPA10.

[2] Wu, Y., Zhou, F., Larsen, E.W. et al. Generation of few-cycle multi-millijoule 2.5 μm pulses from a single-stage Cr2+:ZnSe amplifier. Sci Rep 10, 7775 (**2020**).

* *E-mail: Zenghu.Chang@ucf.edu*

Attosecond control of relativistic plasma mirror emission

J Kaur[1], M Ouillé[1,2], I Andriyash[1], Z Cheng[1], S Haessler[1]*, R Lopez-Martens[1]

[1] Laboratoire d'Optique Appliquée, Institut Polytechnique de Paris, ENSTA-Paris, Ecole Polytechnique, CNRS, 91120 Palaiseau, France

[2] Ardop Engineering, Cité de la Photonique, 11 Avenue de la Canteranne, Bât. Pléione, 33600 Pessac, France

Synopsis We report on the attosecond control of relativistic collective electron dynamics on plasma mirrors by CEP-stable near-single-cycle laser waveforms at 1 kHz repetition rate. The simultaneously measured XUV high harmonic and MeV electron emission both shown clear imprints of the driving light waveform.

High-harmonic generation at the surface of plasma mirrors (SHHG) driven at relativistic light intensities is a promising candidate for generating intense attosecond pulses [1, 2, 3]. SHHG can be time-gated by using few-cycle driving pulses to the emission of either an isolated attosecond pulse (IAP) or a short train of 2-3 attosecond pulses, depending on the driver's carrier-envelope phase (CEP). Thus far, CEP effects on SHHG have been observed *ex post*, i.e. after binning acquisitions according to the simultaneously measured CEP drift [3, 4, 5].

Here, we now make the decisive step from mere observation to actual control by driving a relativistic plasma mirror with the long-term CEP-locked (< 400 mrad rms shot-to-shot) 'Salle Noire' laser system [6], delivering high-temporal-contrast, terawatt peak-power, 1.5-cycle (< 4 fs at 720 nm) transients at 1 kHz repetition rate. The p-polarised laser is focused down to a 1.7µm-spot onto a rotating optically polished fused silica target at a 55° incidence, reaching intensities $\sim 10^{19}$ W/cm^2. A weaker time-delayed prepulse prepares a surface plasma density gradient of ≈ 40 nm scale length, maximizing the SHHG efficiency and spectral extent in the specular direction. We simultaneously measure the spatio-spectral properties of the correlated relativistic electron emission between specular and target normal directions.

Figure 1 shows a measurement made with a 3.6-fs driver whose locked CEP was scanned randomly to eliminate any experimental bias. We finely resolve the transition between a continuous and a modulated SHHG spectrum, with the clear time-domain interpretation of an IAP or double-pulse, respectively, as well as an intriguing CEP-dependent double-hump structure in the electron spectra, which may be associated with two driving field cycles. 2D PIC simulations are underway to unravel the encoded interaction dynamics, involving the formation and acceleration of electron nano-bunches and the resulting attosecond XUV emission at the critical plasma surface [5].

Our demonstrated reproducible and stable generation of IAP and synchronized relativistic electron bunches opens exciting prospects for plasma mirrors as a potential source for applications in attosecond science.

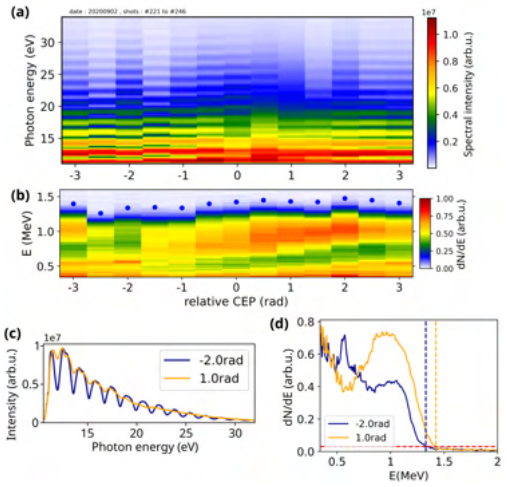


Figure 1. Measured XUV (a) and electron spectra (b) as a function of the locked relative CEP of a 3.6-fs driver pulse. Panels (c) and (d) show line-outs at relative CEPs of -2.0 and 1.0 rad.

References

[1] C Thaury *et al.*, J. Phys. B **43**, 21 (2010)
[2] G D Tsakiris *et al.*, New J. Phys. **8**, 19 (2006)
[3] O Jahn *et al.*, Optica **6**, 280–287 (2019)
[4] D Kormin *et al.*, Nature Comms. **9**, 4992 (2018).
[5] F Böhle *et al.*, J. Phys. Photonics **2**, 034010 (2020)
[6] M Ouillé *et al.*, Light Sci. Appl. **9**, 47 (2020)

*E-mail: stefan.haessler@cnrs.fr

R3 Attosecond transient absorption and four-wave mixing ▲

14:00 - 16:00 **R3 Attosecond transient absorption and four-wave mixing** 78
Chair: **Thomas Pfeifer**, Max-Planck Institute for Nuclear Physics, Heidelberg, Germany, EU

14:00 **Stephen R Leone**, University of California, Berkeley, USA
I: *Dynamics Via Attosecond Four Wave Mixing.* 79

14:30 **Arvinder Sandhu**, University of Arizona, USA
I: *Autoionizing polaritons and Raman interferometry: Advances in measurement and control of electron dynamics in the continuum.* 80

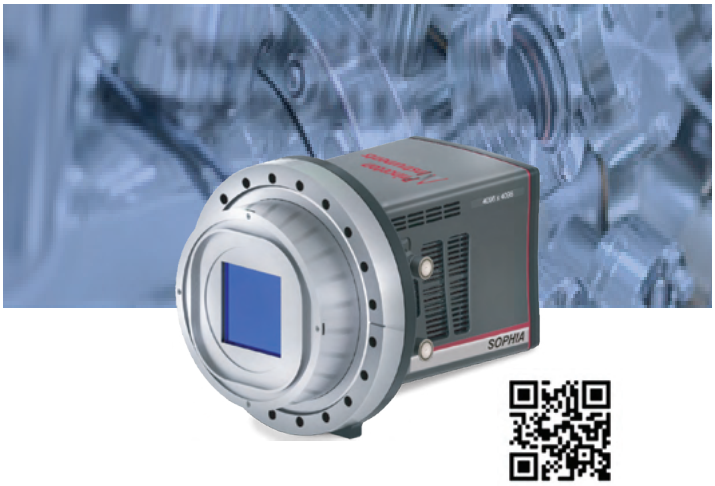
15:00 **Zhong Yin**, ETH Zürich, Switzerland
C: *Photoinduced Proton Transfer Dynamics in Aqueous Urea Solution Probed by Water-Window X-ray Absorption Spectroscopy.* 81

15:15 **Vyacheslav Leshchenko**, Ohio State University, USA
C: *Phase-resolved XUV transient absorption spectroscopy of argon.* 82

15:30 **Valentina Utrio Lanfaloni**, ETH Zürich, Switzerland
C: *Jahn–Teller dynamics in CH_4^+ probed at the carbon K-edge.* 83

15:45 **Nikolay Golubev**, EPFL, Switzerland
C: *Core-Valence Attosecond Transient Absorption Spectroscopy of Polyatomic Molecules.* 84

R3



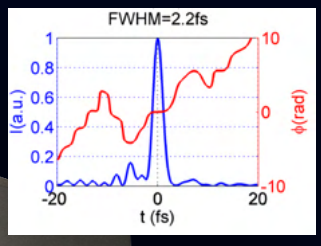
SOPHIA-XO

Deep cooled, highly sensitive, large format CCD cameras, providing a wide range of energy, flux, and spatial distribution.

TELEDYNE PRINCETON INSTRUMENTS
www.princetoninstruments.com

sphere
ULTRAFAST PHOTONICS

Sphere's d-scan is the technology of choice for handling ultrashort laser pulses - down to true **single-cycle durations** - for cutting edge attoscience in gases and in solids. Get a d-scan now and **boost your attosecond experiments and applications.**





www.sphere-photonics.com

Dynamics Via Attosecond Four Wave Mixing

S. R. Leone[1,2,*]

[1]Departments of Chemistry and Physics, University of California, Berkeley, CA 94720 USA
[2]Lawrence Berkeley National Laboratory, Berkeley, CA 94720 USA

Synopsis A background-free method of attosecond four wave mixing provides a new, multidimensional level of analysis for time dynamics. In this method, two few-cycle optical pulses are mixed noncollinearly with one attosecond extreme ultraviolet (XUV) pulse, and angularly resolved 4WM emissions are detected as a function of time delays between all three pulses. New measurements are presented on atoms, molecules and solids, and future multidimensional techniques with near infrared pulse shaping are described that can isolate individual state detail.

Attosecond pulses produced by high harmonic generation can generate coherent superpositions of electronic and vibrational states in atoms and small molecules. The resultant coherent superpositions are probed by a time-delayed optical pulse, which modifies the polarization of the medium by coupling to neighboring states. The time dependent spectral interferences in this method, called attosecond transient absorption, in the collinear configuration, are recorded with outstanding temporal and spectral resolution to reveal electronic and vibrational structure and dynamics.

A recent method of attosecond four wave mixing combines two optical/near infrared pulses with one attosecond extreme ultraviolet pulse [1]. Noncollinear geometries (Fig. 1) generate new, directed emission beams that are wave-vector phase-matched to provide background-free measurements of wave packets and used to investigate short time dynamics.

In atoms (Fig. 1) and molecules, the decays of autoionizing states are observed in the four wave mixing emission signals, and lifetimes are obtained. The dynamics of a vibrational wave packet on the inner and outer turning points of an electronic state are directly accessed [2]. In a solid, attosecond four wave mixing is used to disentangle features underlying the line broadening of core level excitons, to identify lifetimes and spectral features of localized core level exciton states of the cations in the solid lattice [3].

Using a spatial light modulator to remove frequencies or alter the phase of specific frequencies in one of the optical pulses, a new coherent multidimensional attosecond spectroscopy in the extreme ultraviolet is obtained [4]. Self-heterodyned signal amplification is also achieved, resulting in many orders of magnitude improvement in sensitivity [5].

The speaker gratefully acknowledges the Department of Energy, collaborator D Neumark, and co-workers W Cao, E Warrick, A Fidler, H Marroux, E Bloch, J Gaynor, N Puskar, Y-C Lin, and M Schuchter.

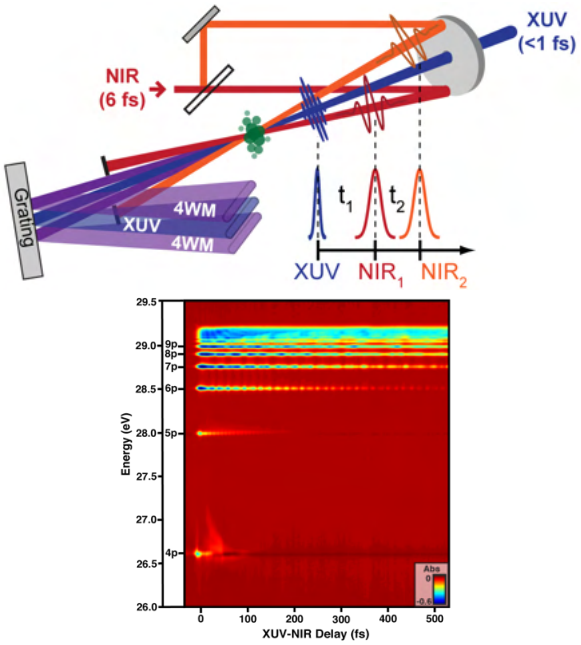


Figure 1. Attosecond 4WM arrangement and background free quantum beats in Ar.

References

[1] Cao W *et al* Phys. Rev. A 94, 053846 (2016).
[2] Warrick E *et al* Faraday Disc. **212**, 157 (2018).
[3] Gaynor J D *et al* Phys. Rev. B **103**, 245140 (2021).
[4] Marroux, H J B *et al* Sci. Adv. **4**, 1 (2018).
[5] Fidler, A P *et al* J. Phys. Photonics **2**, 034003 (2020).

* E-mail: srl@berkeley.edu

Autoionizing polaritons and Raman interferometry: Advances in measurement and control of electron dynamics in the continuum

A Sandhu[1*]

[1]Department of Physics and College of Optical Sciences, University of Arizona, Tucson AZ 85721 USA

Synopsis We present new approaches for the coherent manipulation of continuum electron dynamics in argon. The ability to modify the lifetime of entangled light-matter states, i.e. the autoionizing polaritons, is demonstrated. Using tunable attosecond transient absorption, we control the interferences between radiative and Auger paths to stabilize the autoionizing state. We also devised a Raman interferometry scheme to measure the electron wavepacket dynamics with high temporal and spectral resolution. These studies opens the path for optical control of metastable states in complex systems.

Attosecond spectroscopy has opened new avenues for the real-time control of fast reactions in atoms and molecules. Autoionizing states are natural stepping-stones to achieve this goal thanks to their correlated character, reasonably long lifetimes, and high polarizability.

Here, we report the study of radiatively coupled autoionizing states in argon, and present evidence of their stabilization [1]. We used an extreme ultraviolet pulse to excite $3s^{-1}4p$ state in Argon (Fig. 1). An IR field couples it the dark autoioizing state (e.g. $3s^{-1}3d$). We systematically varied the IR probe wavelength to control the detuning between bright and dark autoionizing resonances, which leads to splitting of the resonance pair into polaritonic branches.

Using laser control parameters, we arranged destructive interference between coherently interefering auger and radiative ionization paths, leading to stabilization of the polaritonic branch against autoionization, which we observe through narrowing of the linewidth in time dependent XUV absorption spectra. As a function of laser detuning, we also investigated the avoided crossings between the bright states and several light induced autoionizing states. This work breaks new ground in manipulation of autoionizing states, opening the doors for implementation of quantum control protocols in the electronic continuum.

In another work [2], we advanced photoelectron interferometry to show that one can simultaneously obtain both high temporal and spectral resolution by stimulating Raman interferences with a light pulse and monitoring the modification of the electron yield in a separate step. Applying this approach to the autoionizing *nf*' wavepacket between the spin-orbit split ionization thresholds in argon, we resolved its electronic composition and time evolution in exquisite detail, demostrating highly sensitive probing and control of electron dynamics.

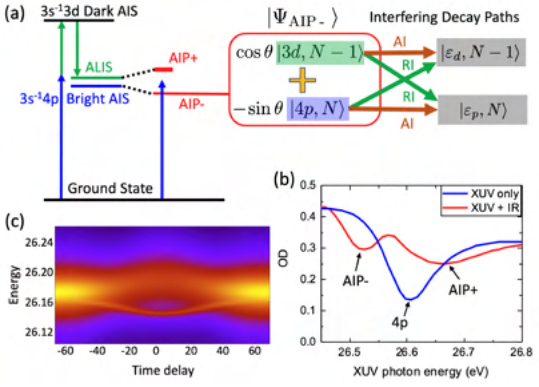


Figure 1. (a) Formation of autoionizing polaritons (AIP) from mixing between bright autoionizing state and autoionizing light-induced state. The IR laser controls the interference between Auger (AI) and radiative (RI) paths leading to stabilization. This manifests as the narrow width of the lower polariton branch in experimental spectra in (b) and the simulated profile in (c).

Work at the University of Arizona was supported by the grant DE-SC0018251 funded by the U.S. Department of Energy, Office of Science and by the NSF awards PHY 1912455 and PHY 1919486.

References

[1] N. Harkema, C. Cariker, E. Lindroth, L. Argenti, A. Sandhu, Phys. Rev. Lett. **127**, 023202 (2021).
[2] A. Plunkett, M. Alarcón, J. Wood, C. H. Greene, A. Sandhu, Phys. Rev. Lett. **128**, 083001 (2022).

* E-mail: asandhu@arizona.edu

Photoinduced Proton Transfer Dynamics in Aqueous Urea Solution Probed by Water-Window X-ray Absorption Spectroscopy

Zhon Yin[1 *], Yi-Ping Chang[2], Tadas Balciunas[2], Yashoj Shakya[3,4], Giuseppe Fazio[1], Ludger Inhester[3], Robin Santra[3,4,5], Jean-Pierre Wolf[2], and Hans Jakob Wörner[1†]

[1]*Laboratorium für Physikalische Chemie, ETH Zürich, 8093 Zürich, Switzerland*
[2]*GAP-Biophotonics, Université de Genève, 1205 Geneva, Switzerland*
[3]*Center for Free-Electron Laser Science, DESY, Notkestrasse 85, 22607 Hamburg, Germany*
[4]*Department of Physics, Universität Hamburg, Jungiusstrasse 9, 20355 Hamburg, Germany*
[5]*Hamburg Centre for Ultrafast Imaging, Luruper Chaussee 149, 22761 Hamburg, Germany*
**yinz@ethz.ch*

Synopsis We present the observation of light-induced femtosecond proton transfer in urea solutions using flat-jet table-top X-ray absorption spectroscopy in the water window. The experimental results are supported by QM/MM simulations coupled to X-ray absorption calculations.

Photoionization-induced dynamics are essential for a broad range of scientific fields ranging from biology to chemistry [1]. Most light-induced ultrafast dynamics involve an intimate coupling of electronic and nuclear degrees of freedom. However, decoupling electronic and nuclear dynamical processes remains a great experimental challenge.

In this work, we present femtosecond time-resolved X-ray absorption spectroscopy (trXAS) of aqueous urea (CH_4N_2O) solutions utilizing a high-harmonic-generation (HHG) source covering the essential carbon and nitrogen K-edges. We use this technique to investigate solvated urea in liquid water after multiphoton ionization, as illustrated in Fig. 1. The inherently broadband HHG spectrum allows us to probe both K-edges simultaneously and therefore offers atomic site resolution [2,3]. Here, we demonstrate the remarkable properties of trXAS as an element and site-specific method in revealing coupled electronic and nuclear dynamics of matter including intermolecular dynamics in a liquid environment.

Another great advantage of the experimental setup compared to free-electron lasers is that the pump and probe pulse are derived from the same source and are therefore, in principle, timing-jitter free. Furthermore, we utilized a sub-µm-thin flat jet to record artefact free XAS in transmission mode [4]. Our experimental results indicate spectral features appearing after ~200 fs and increasing in absorbance up to around 700 fs before they saturate, which are assigned to ionization-induced ultrafast proton transfer in urea dimers.

The experimental findings are supported by nonadiabatic dynamics calculations of several urea-dimer and urea-water geometries and can reproduce the main spectral features. Quantum mechanical and molecular-dynamics calculations (QM/MM) enable us to elucidate the origin of the spectral features. They show that the shift of the absorption band highlighted by a black line in panel C) and E) traces the transfer of the charged proton, whereas the gradually increasing intensity traces the increasing amplitude of the valence hole at the carbon atom with site selectivity. Our results reveal a proton transfer between urea molecules caused by valence ionization elucidating the ultrafast electronic and nuclear dynamics driving proton transfer in a solvated biomolecule.

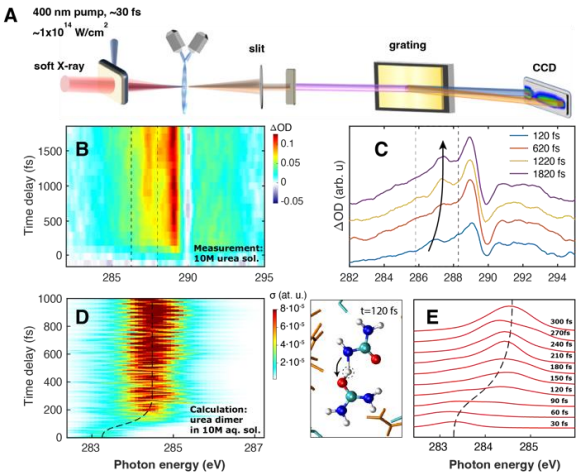


Figure 1. A) Schematic overview of the experimental setup. B) Transient XAS at the carbon K-edge of a concentrated urea solution with femtosecond time resolution. C) XAS spectra for various time delays. The spectral feature emphasized by the black line originates from proton transfer in urea dimers. This is supported by theoretical QM/MM results shown in D) and E).

References

[1] T. Kumpulainen et. al. Chem. Rev. 117 10826 (2017)
[2] J. Smith et al Chem. Rev. 117, 13909 (2017)
[3] A. Smith et al., J. Phys. Chem. Lett. 11, 1981 (2020)
[4] Z. Yin et al, J. Phys. Photonics 2, 044007 (2020)

Phase-resolved XUV transient absorption spectroscopy of argon

V Leshchenko[1]*, S Hageman[1], C Cariker[2], G Smith[1], P Agostini[1], L Argenti[2], L DiMauro[1]

[1]Department of Physics, The Ohio State University, Columbus, Ohio 43210, USA
[2]Department of Physics and CREOL, University of Central Florida, Orlando, FL 32816, USA

Synopsis
The presented phase-resolved transient absorption spectroscopy technique enables reconstruction of the full dipole response of a sample and can be applied to a broad range of XUV spectroscopy experiments in both transmission and reflection.

Experimental access to the characterization of full dipole response is a key to optical control of electrons in atoms and molecules. In standard transient absorption spectroscopy (TAS) experiments [1] only the imaginary part of the dipole (corresponding to absorption) is measured, which is not always enough to reconstruct the full dipole response. We present a modified extreme ultraviolet (XUV) TAS experimental setup that enables simultaneous detection of both real and imaginary parts of the dipole response. The presented setup works in transmission but with minimum modifications it can be adapted to experiments in reflection.

The detection of the real part of the XUV induced dipole is enabled by the measurement of the interference between two nearly identical XUV beams generated by a two-foci infrared (IR) driving pulse, with only one of the XUV beams being dressed with an optical pulse. The two-foci IR beam is generated using a binary 0–π phase grating [2]. The transmitted signal is measured with a flat-field spectrometer, which provides spectral resolution in the dispersion plane and phase information in the orthogonal dimension.

The proof-of-principle experiment is performed using the argon Fano resonance as a case study. The sample is dressed with 1350 nm pulses that resonantly couples the $3s^{-1}4p$ bright state to $3s^{-1}3d$ and $3s^{-1}5s$ dark states. The measured light-induced dipole phase is in a good agreement with TDSE (time-dependent Schrödinger equation) simulations [3]. We also study the validity of the Kramers–Kronig (KK) relation, which is commonly used to reconstruct the real part of the dipole from its imaginary part. In this study, the standard form of the KK relation is proven to be valid both experimentally and theoretically, although the assumptions, which the relation is based on, are not satisfied in pump-probe experiments especially at the temporal overlap between the pump and the probe.

The proposed technique can be applied to a broad range of HHG-based spectroscopy applications with almost any sample in both transmission and reflection, and so it can advance these applications.

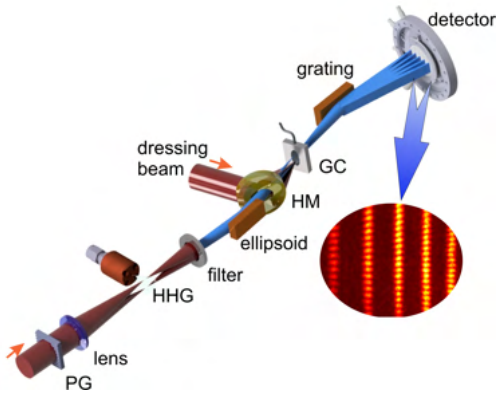


Figure 1. Scheme of the experimental setup. PG: phase grating; HM: holey mirror; GC: gas cell; HHG: high harmonic generation.

References

[1] A.R. Beck, D.M. Neumark, and S.R. Leone, Chem. Phys. Lett. **624**, 119 (2015).
[2] A. Camper et al. Opt. Lett. **44**, 5465 (2019).
[3] N. Harkema et al. Phys. Rev. Lett. **127**, 023202 (2021).

*E-mail: leshchenko.1@osu.edu

Jahn–Teller dynamics in CH_4^+ probed at the carbon K-edge

V. Utrio Lanfaloni[1]*, K. S. Zinchenko[1], F. Ardana-Lamas[2], N. Monahan[1], I. Seidu[3], S. P. Neville[3], M. S. Schuurman[3], and H. J. Wörner[1]

[1]Laboratory of Physical Chemistry, ETH Zürich, 8093 Zürich, Switzerland
[2]European XFEL GmbH, 22869 Schenefeld, Germany
[3]National Research Council of Canada, Ottawa, ON, Canada

Synopsis We demonstrate attosecond transient-absorption spectroscopy (ATAS) at the carbon K-edge as a powerful technique to detect few-femtosecond strongly coupled non-adiabatic dynamics driven by Jahn-Teller effect in methane cation.

Time-resolved X-ray absorption spectroscopy, by probing element-specific dynamics, is nowadays a decisive key technique for addressing fundamental open questions in photochemistry and photophysics [1, 2]. In this work, a passively carrier-envelope-phase–stable sub-two-cycle pulse at 1.8 μm is used to prepare multiple electronic states of molecular methane cation through strong-field ionization and an attosecond super-continuum soft-X-ray (SXR) pulse with a cutoff at 450 eV is used to detect their electronic and nuclear dynamics. Strong-field ionization of methane enforces an ultrafast non-adiabatic relaxation driven by the Jahn-Teller effect [3]. Following removal of an electron from the triply degenerate HOMO, CH_4^+ is rapidly evolving to the trigonal C_{3v}, to tetragonal D_{2d} or the C_{2v} symmetry towards the equilibrium structure [4]. Here we want to observe and investigate the timescale of this coupled electronic and structural relaxation. Figure 1A shows the experimental attosecond transient-absorption spectroscopy (ATAS) trace of CH_4. The structural dynamics driven by the Jahn-Teller can be identified through the large-amplitude modulation of the absorption line centered at around 281 eV. The Fourier transformation of its center-of-mass reveals the following periods: 39 ± 20 fs, 27 ± 7 fs, 17 ± 3 fs, 12 ± 1 fs (Figure 1C). Additionally, this absorption band at 281 eV shows a red shift around time zero. Multiconfigurational time-dependent Hartee (MCTDH) calculations performed on the methane cation confirm our interpretation (Figure 1B). By Fourier transformation of the center-of-mass of the band at 281 eV (Figure 1C), the presence of two frequencies has been confirmed: one with a period of 11 fs assigned to symmetric CH stretching and a second one with a period of 18 fs that could correspond to a bending mode. The red shift of the absorption band from 278 eV to 282 eV within a few fs is also reproduced and assigned to the steep potential-energy gradient of the core-excited surface. We also observed a 3-fs quantum beat in the band centered at 285 eV, which can only correspond to an electronic wave packet.
In conclusion, we have demonstrated ATAS at the carbon K-edge to reveal coupled electronic and nuclear dynamics, enabling studies of charge-migration and charge-transfer in organic molecules.

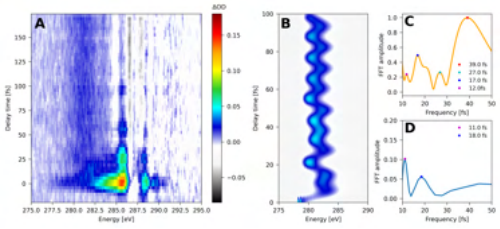


Figure 1. (**A**) Methane experimental ATAS trace. (**B**) Theoretical ΔOD at the band centered at around 281 eV. Fourier transform of the center-of-mass of the absorption band at 281 eV for the measured data (**C**) and theoretical calculations (**D**).

References

[1] Y. Pertot *et al.*, Science. **335**, 264 (2017).
[2] K. S. Zinchenko *et al.*, Science. **161**, 220 (1937).
[3] H. J. Wörner and F. Merkt, Angewandte Chemie International Edition. **48**, 6404 (2009).
[4] H. J. Wörner *et al.*, The journal of chemical physics. **126** , 144305 (2007).

*E-mail: valentina.lanfaloni@phys.chem.ethz.ch

Core-valence attosecond transient absorption spectroscopy of polyatomic molecules

N V Golubev[1 *], J Vaníček[1] and A I Kuleff[2]

[1]Laboratory of Theoretical Physical Chemistry, Institut des Sciences et Ingénierie Chimiques, Ecole Polytechnique Fédérale de Lausanne (EPFL), CH-1015 Lausanne, Switzerland
[2]Theoretische Chemie, Universität Heidelberg, Im Neuenheimer Feld 229, D-69120 Heidelberg, Germany and ELI-ALPS, Wolfgang Sandner utca 3, H-6728 Szeged, Hungary

Synopsis In this work, we report an extension of the theory underlying the attosecond transient absorption spectroscopy (ATAS) for the case of molecules, including a full account for the coupled electron-nuclear dynamics in the initially created wave packet, and apply it to probe the oscillations of the positive charge created after ionization of the propiolic acid molecule. By taking advantage of element-specific core-to-valence transitions induced by x-ray radiation, we show that the resolution of ATAS makes it possible to trace the dynamics of electron density with atomic spatial resolution.

R3

With the advent of ultrashort laser pulses, the scientific community obtained a unique tool to study such phenomena as charge transport in molecules and the elementary steps of chemical reactions. Being able to observe fundamental processes with attosecond temporal resolution, it also becomes possible to steer and probe electron dynamics on its natural timescale.

One of the most powerful experimental techniques to trace the ultrafast electron dynamics which combines high spectral and high temporal resolution is the attosecond transient absorption spectroscopy (ATAS) [1]. Measuring the transmission of a broadband laser pulse through a sample, one can gain intuitive and highly detailed insights about dynamics of the system.

So far, the theory underlying ATAS has only been developed for atoms [2], or for molecules either in absence of nuclear motion or in absence of electronic coherence. In this work [3], we extend the theory of ATAS to the case of polyatomic molecules, fully accounting for the coupled electron-nuclear dynamics in the initially created wave packet. We demonstrate on the example of propiolic acid that the resolution of ATAS is sufficient to clearly observe the ultrafast oscillations of the electron density, as well as the follow-up decoherence caused by the nuclear rearrangement. We perform high-level *ab initio* simulations of x-ray ATAS, showing the possibility to trace the dynamics of the created hole through the molecular chain, and thus demonstrate that x-ray ATAS can be a very useful technique to study ultrafast electron motion in molecules.

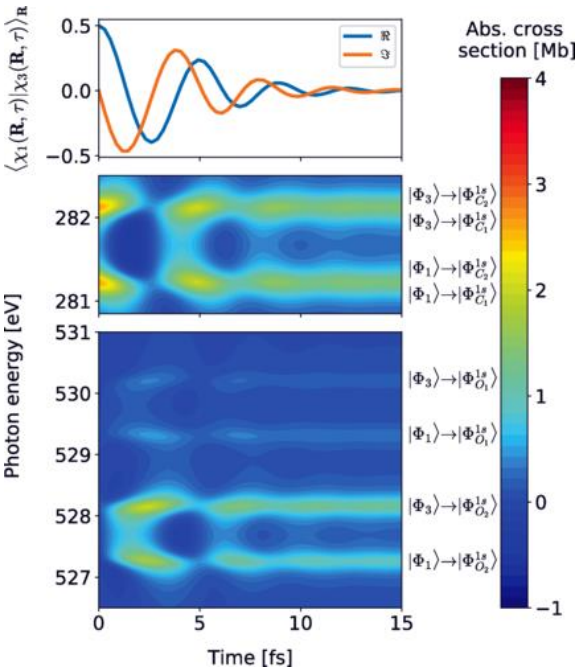


Figure 1. Electronic coherence (top panel) and ATAS spectrum of the propiolic acid computed for energy windows corresponding to transitions between initially populated valence ionic states and 1s core states of carbon (middle panel) and oxygen (bottom panel) atoms.

References

[1] Goulielmakis E *et al* 2010 *Nature* **466** 739
[2] Santra R *et al* 2011 *Phys. Rev. A* **83** 033405
[3] Golubev NV *et al* 2021 *Phys. Rev. Lett.* **127** 123001

* E-mail: nik.v.golubev@gmail.com

F1 Entanglement in attosecond processes

08:30 - 10:45 **F1 Entanglement in attosecond processes** 85
Chair: **C. William McCurdy**, University of California Davis & LBNL, California, USA

08:30 **Paraskevas Tzallas**, FORTH-IESL, Greece, EU
I: *Generation of optical Schrödinger "cat" states using "conditioning" approaches in intense laser-atom interactions.* 86

09:00 **Maciej Lewenstein**, ICFO and ICREA, Spain, EU
I: *Attosecond Physics and Quantum Information Science.* 87

09:30 **Matan Even Tzur**, Technion - Israel Institute of Technology, Israel
C: *High Harmonic Generation Driven by Quantum Light.* 88

09:45 **Charles Bourassin-Bouchet**, Institut d'Optique, France, EU
C: *Quantifying the decoherence of attosecond electron wavepackets.* . . . 89

10:00 **Lisa-Marie Koll**, MBI, Germany, EU
C: *Experimental control of quantum-mechanical entanglement in an attosecond pump-probe experiment.* 90

10:15 **Farshad Shobeiry**, Max-Planck-Institut für Kernphysik, Germany, EU
C: *Sub-femtosecond optical control of entangled states.* 91

10:30 **Sebastian Eckart**, Goethe University Frankfurt, Germany, EU
C: *Ultrafast preparation and detection of entangled atoms.* 92

Generation of optical Schrödinger "cat" states using "conditioning" approaches in intense laser-atom interactions

P Tzallas[1*], Th Lamprou[1], J Rivera-Dean[2], P Stammer[2], A S Maxwell[2,3], A F Ordóñez[2], E Pisanty[4], M F Ciappina[5,6], M Lewenstein[2,7†]

[1]Foundation for Research and Technology-Hellas, Institute of Electronic Structure & Laser, GR- 70013 Heraklion (Crete), Greece.
[2]ICFO-Institut de Ciencies Fotoniques, The Barcelona Institute of Science and Technology, Castelldefels (Barcelona) 08860, Spain.
[3]Department of Physics and Astronomy, Aarhus University, DK-8000 Aarhus C, Denmark.
[4]Department of Physics, King's College London, Strand, London, UK
[5]Physics Program, Guangdong Technion - Israel Institute of Technology, 241 Daxue Road, Shantou, Guangdong, China, 515063
[6]Technion-Israel Institute of Technology, Haifa, 32000, Israel
[7]ICREA, Pg. Lluís Companys 23, 08010 Barcelona, Spain

Synopsis After a brief overview on the generation, characterization and applications of optical Schrödinger cat states, I will present you our recently developed method, with which, optical Schrödinger "cat" states have been produced by implementing "conditioning" approaches in the high harmonic generation process induced by intense laser-atom interactions.

F1

Quantum optics is a research direction that played a major role to the development of quantum technologies [1], advancing investigations ranging from fundamental tests of quantum theory to quantum information processing. Central to these investigations are the optical Schrödinger cat states created by the superposition of two distinct coherent states. Despite the progress achieved so far, the development of schemes for the generation of high photon-number-shifted and large optical cat states with controllable quantum features is considered a challenging task and "hot" topic. Here, after a brief overview on the generation, characterization and applications of optical cat states, I will present our recent findings concerning the development of a new method with which a coherent light state superposition (optical Schrödinger cat states) (Fig. 1) has been produced [2]. The method relies on the implementation of "conditioning" approaches in the high harmonic generation process induced by intense laser-atom interactions, and can be used for the creation of high photon-number-shifted and large optical cat states with controllable quantum features [3,4].

The findings is the beginning of a very long and exciting "story" targeting, I) on the development of a new and novel class of non-classical light states (ranging from XUV to the mid-IR [5]) produced by implementing "conditioning" approaches in a large variety of intense laser-matter interactions, and II) on novel applications in quantum technologies.

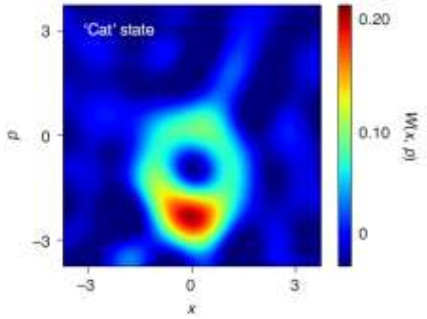


Figure 1. Measurement of the Wigner function of the optical Schrödinger "cat" state. *x* and *p* are the values of the quadrature field operators. Fig. from ref. [2].

References

[1] A. Acín, *et al* 2018 *New J. Phys.* **20**, 080201
[2] M. Lewenstein, *et al* 2021 *Nat. Phys.* **17**, 1104
[3] J. Rivera-Dean, *et al* 2021 *arXiv:*2110.01032v2
[4] J. Rivera-Dean, *et al* 2021 *JCE* **20**, 2111
[5] P. Stammer *et al* 2021 *arXiv*:2107.12887v2

* E-mail: ptzallas@iesl.forth.gr
† E-mail: maciej.lewenstein@icfo.eu

Attoscience and Quantum Information

M. Lewenstein[1,2]*

[1]ICFO-Institut de Ciencies Fotoniques, The Barcelona Institute of Science and Technology, Castelldefels (Barcelona) 08860, Spain
[2]ICREA, Pg. Lluís Companys 23, 08010 Barcelona, Spain

Synopsis In my lecture I will focus on the new project of ICFO, FORTH, Technion, CEA, and IOTA toward a symbiosis for attoscience and quantum information.

In my lecture I will focus on ATTOQUIS, the new joint project of ICFO, FORTH, Technion, CEA, and IOTA toward a symbiosis of attoscience (AS) and quantum information (QI). This is in particular aimed at studying the generation of entangled/quantum correlated states using conditioning methods. I will describe our joint efforts to generate Schrödinger cat states (SCS) of photons conditioned on high harmonic generation (HHG) [1] (see Fig. 1) and/or above threshold ionization. I will also talk about generation of topological order using laser pulses with orbital angular momentum (OAM). I will also discuss HHG as a tool to detect phase transitions and topological in strongly correlated systems. If time permits, I will speculate about measurement of entanglement of OAM of electrons in double ionization, and violation of Bell inequalities by SCS states.

Contemporary Quantum Technologies face major difficulties in fault tolerant quantum computing with error correction, and focus instead on various shades of analogue and digital Quantum Simulators and quantum annealers. There is a clear need and quest for such systems that, without necessarily simulating quantum dynamics of some physical systems, can generate massive, controllable, robust, entanglement and superpositions states. In the ATTOQUIS project, we propose an answer to these needs, by opening new avenues for QI science in symbiosis with Atto-science (AS) and Quantum Optics (QO). To date, there are no existing platforms that can bring processes at such short time-scales to Quantum Information systems.

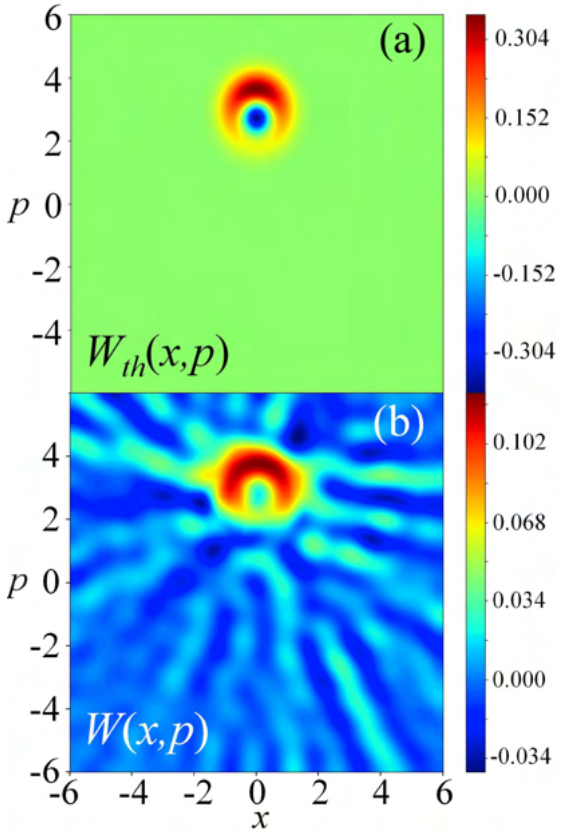


Figure 1. High-photon number optical cat state created by conditioning on HHG. (a) Theoretical prediction for the Wigner function. (b) Experimental reconstruction of the Wigner function, which shows an optical Schrödinger cat state.

References

[1] M. Lewenstein, M.F. Ciappina, E. Pisanty, *et al.*, "Generation of optical Schrödinger cat states in intense laser–matter interactions", Nature Phys. **17**, 1104–1108 (2021).

*E-mail: maciej.lewenstein@icfo.eu

High Harmonic Generation Driven by Quantum Light

M Even Tzur*†[1], A Gorlach†[2], M Birk[1,2], N Rivera[3], M Krüger[1], I Kaminer[2], and Oren Cohen[1]**

1. Department of Physics and Solid State Institute, Technion – Israel Institute of Technology, 32000 Haifa, Israel
2. Department of Electrical and Computer Engineering and Solid State Institute, Technion – Israel Institute of Technology, 32000 Haifa, Israel
3. Massachusetts Institute of Technology, Cambridge MA 02139, USA

† - Equally contributing authors

Synopsis We present recent theoretical and experimental advances towards high harmonic generation (HHG) driven by quantum states of light such as bright squeezed vacuum. Specifically, we present a quantum-optical theory of HHG driven by quantized light, predicting that the photon statistics of the driving field can significantly extend the HHG cutoff, and modify electronic trajectories in the continuum. We will describe our experimental progress towards HHG driven by bright squeezed vacuum, and quantum-optical attosecond science.

High harmonic generation (HHG) [1] is an extremely nonlinear process in which a system driven by an intense laser emits coherent ultraviolet and X-ray radiation. Until now, all experiments in the field employed classical (i.e., coherent state) light to drive the HHG process. However, advances in the generation of intense ultrashort pulses of thermal and squeezed light [2] suggest driving extremely nonlinear processes using non-classical light is becoming experimentally feasible – paving the way toward a new era of extremely nonlinear quantum optics, and quantum-optical attosecond science. Notably, HHG driven by quantum light has never been explored before, neither theoretically nor experimentally.

Here we present recent theoretical and experimental advances towards HHG driven by quantum light. Firstly, we present a general quantum optical theory of HHG driven by non-classical light, showing that squeezed states of light such as bright squeezed vacuum can dramatically extend the cutoff energy of HHG, relative to classical light of the same intensity. Then, we employ the strong-field approximation (SFA), formulating a theory that directly extends the semi-classical SFA theory [3] to account for the interaction of an atom (or another emitting system) with non-classical states of intense light.

Our quantum-optical SFA theory directly relates the driver's photon statistics (which may be arbitrary) to the emitted harmonics, the underlying electronic trajectories, and the resulting attosecond pulses. We show that squeezing of the driver's photonic state modifies the temporal profile of the emitted attosecond pulses. Finally, we will discuss the ongoing experimental efforts in this direction, towards the observation of HHG driven by fs pulses of bright squeezed vacuum, and observation of attosecond time delays in HHG, induced by photon statistics.

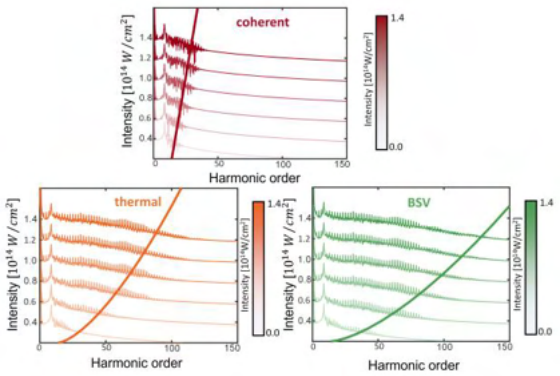


Fig 1. Numerical simulations of the HHG spectrum for different intensities, driven by a coherent state (red), thermal light (orange), and bright squeezed vacuum (greed).

References

[1] Pherson, A. et al., *JOSA B* **4**, 595 (1987).
[2] Qu, Y. & Singh, S, *Opt. Commun.* **90**, 111 (1992); Jechow, A et al, *Nat. Photon.* **7**, 973 (2013);
[3] Lewenstein, M et al, *Phys. Rev. A* **49**, 2117 (1994).

* E-mail: matanev@campus.technion.ac.il
** E-mail: alexey.gorlach@gmail.com

Quantifying the decoherence of attosecond electron wavepackets

C. Bourassin-Bouchet[1]*, L. Barreau[2], V. Gruson[2], J. Im[1,2], G. Granveau[1], J.-F. Hergott[2], F. Quéré[2], P. Salières[2] and T. Ruchon[2]

[1]Université Paris-Saclay, Institut d'Optique Graduate School, CNRS, Laboratoire Charles Fabry, 91127 Palaiseau, France

[2]Université Paris-Saclay, CEA, CNRS, LIDYL, 91191 Gif-Sur-Yvette, France

Synopsis We report the experimental measurement of the full quantum state of an attosecond electron wavepacket using laser-dressed photoionization. This proof-of-concept experiment opens new prospects for the study of fundamental decoherence, for instance due to ion-electron entanglement following photoionization.

Laser-dressed photoionization spectroscopy has been the cornerstone of attosecond metrology since 2001 [1, 2]. In the photoionization of a gas jet by an XUV attosecond pulse combined with a femtosecond infrared pulse, the spectrogram (photoelectron kinetic energy distribution as a function of the laser-XUV delay) gives access to intimate information on the ionization process.

Here we show that this historical approach strictly corresponds to a quantum state tomography of the released photoelectron (PE) [3]. Accessing this full quantum state makes it possible to decipher the quantum phenomena that unavoidably affect the PE, such as state superpositions and decoherence. In practice, being based on the sole observation of the kinetic energy of the PE, the technique builds a reduced electron density matrix (EDM), where all the unresolved degrees of freedom have been traced over. The latter can arise due to classical ensemble averaging (e.g. shot-to-shot XUV pulse fluctuations) or due to fundamental quantum mechanical reasons. Indeed although rapidly separated in space, the ion and the PE still form a single quantum system, a pure wavepacket described by a total wavefunction that encompasses all the degrees of freedom of both subsystems. If the kinetic energy of the PE turns out to be entangled with an unresolved degree of freedom, then the reconstructed EDM will exhibit decoherence [4].

We have implemented this approach experimentally on an attosecond beamline at CEA-Saclay. The reconstructed EDM is shown in Fig.1 and exhibits a purity of 0.11 (1 for full coherence) due to the progressive disappearance of its off-diagonal elements (see ρ_{15} and ρ_{17}). This reconstruction, performed in standard photoionization conditions, allowed one to quantify the technical sources of decoherence in the experiment, such as mechanical instabilities in the beamline inducing arrival time fluctuations of the attosecond pulses and the resolution of the electron spectrometer. This work deepens our understanding of laser-dressed photoionization, opening new prospects for the study of decoherence on an attosecond timescale [4, 5].

*E-mail: charles.bourassin-bouchet@institutoptique.fr

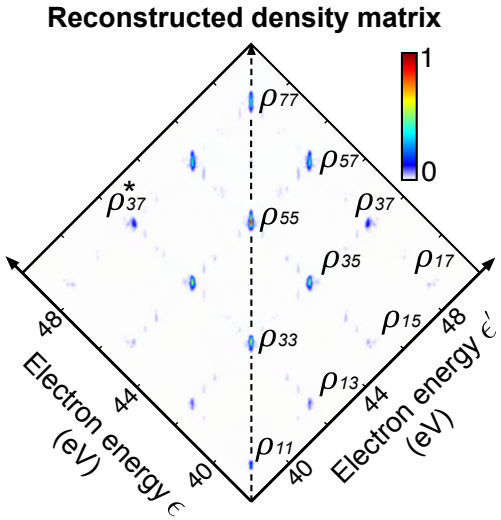


Figure 1. Reconstructed electron density matrix (only modulus shown).

References

[1] P. Paul *et al.* Science **292**, 1689-1692 (2001).
[2] M. Hentschel *et al.* Nature **414**, 509-513 (2001).
[3] C Bourassin-Bouchet *et al.* Phys. Rev. X **10**, 031048 (2020).
[4] S. Pabst *et al.* Phys. Rev. Lett. **106**, 053003 (2011).
[5] S. Carlström *et al.* J. Phys. B: At. Mol. Opt. Phys. **51**, 015201 (2018).

Experimental control of quantum-mechanical entanglement in an attosecond pump-probe experiment

L M Koll[1]*, L Maikowski[1], L Drescher[1,2], T Witting[1], and M J J Vrakking[1]

[1]Max Born Institute, Berlin, 12489, Germany
[2]Department of Chemistry, University of California, Berkeley, California 94720, USA

Synopsis The quantum-mechanical entanglement between an ion and photoelectron has been controlled by changing the time delay between two phase-locked extreme ultra-violet pulses that ionize hydrogen molecules.

The bipartite quantum-system (ion and photoelectron) generated in a molecular photoionization process is typically entangled, since the wavefunction describing the electronic and rovibratonal states of the ion and the energy and angular momenta of the photoelectron cannot be expressed as a single product state. In many pump-probe experiments the observability of the physical quantity of interest relies on the coherence between different parts of the ionic or electronic wave function. However, entanglement between the ion and photoelectron can limit this coherence and the observability of time-dependent observables that rely on this coherence [1]. We show control of the degree of entanglement by tuning the delay between two phase-locked extreme ultra-violet (XUV) pulses [2] in the photoionization of H_2 [3]. The two ionizing XUV pulses create a photoelectron and a coherent superposition of vibrational states in the $1s\sigma_g$ state of the H_2^+ ion. The vibrational wave packet is probed by a near-infrared (NIR) pulse and the momenta of the H^+ ions are measured by velocity map imaging spectrocopy. Fig. 1(a) and (b) show the motion of the vibrational wave packet for two different XUV-XUV time delays. In Fig. 1(c) and (d) the corresponding Fourier transform power spectrum is shown. At an XUV-XUV time delay of 29 fs, the ion and photoelectron area only weakly entangled. Consequently, the vibrational states of the H_2^+ are in a coherent superposition leading to strong quantum beats in the frequency domain (cf. Fig. 1(c)). However, at a time delay of 45 fs, the ion and photoelectron are strongly entangled limiting the vibrational coherence and the strength of the corresponding quantum beats (cf. Fig. 1(d)). By changing the XUV-XUV time delay over a range of 100 fs the strength of the different quantum beats, i.e. the degree of vibrational coherence, oscillates with a period given by the inverse of the energy difference of the two contributing vibrational states ($\pi/\Delta E(v,v')$) (cf. Fig. 1(e)-(h)).

The ability to control entanglement is relevant for current research in the field of ultrafast charge migration and charge-directed reactivity. It also provides new possibilities to link ultrafast laser spectroscopy with the field of quantum information.

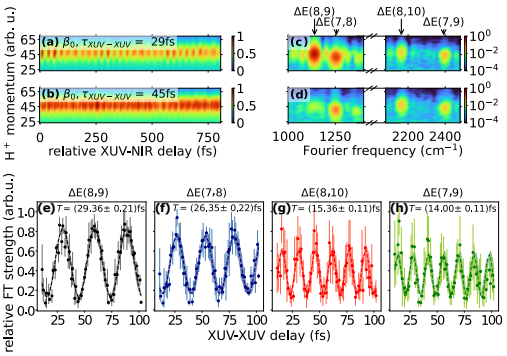


Figure 1. (a)-(b) H^+ momentum in arbitrary units as a function of the XUV-NIR delay for two different XUV-XUV delays. (c)-(d) Fourier transform of the data shown in the left column. Pronounced quantum beats $\Delta E(v,v')$ are visible, due to the intefering dissociative ionization pathways involving the two vibrational states v and v'. (e)-(h) strength of the different quantum beats as a function of the XUV-XUV delay, which oscillate with a period given by the inset.

References

[1] M J J Vrakking, Phys. Rev. Lett. **126**, 113203 (2021).
[2] L M Koll, et al., Opt. Express in press (2022)
[3] L M Koll, et al., Phys. Rev. Lett. **128**, 043201 (2022).

*E-mail: lisa.koll@mbi-berlin.de

Sub-femtosecond optical control of entangled states

F Shobeiry*, E Brunner, P Fross, H Srinivas, A Buchleitner, T Pfeifer, A Harth and R Moshammer

Max Planck Institute for Nuclear Physics, Heidelberg, 69117, Germany

Synopsis We present kinematically complete experiments on the photodissociation of H_2 using a combination of XUV and IR pulses and demonstrate sub-fs control of electronic entangled states by applying few-photon interactions with adjustable relative delays in a single H_2 molecule. This molecular entanglement manifests itself in the asymmetric emission direction of the photoelectron with respect to the ejected proton, where both entangled particles are measured specially separated in coincidence. Our experimental results are supported by a semiclassical simulation based on the WKB approximation.

Molecules are unique systems to study entanglement since it can be encoded in various molecular degrees of freedom [1]. Entanglement exists naturally in photoionization of molecules and has been showcased in many experiments [2,3]. Nonetheless, control of these processes after spatially separating entangled particles is an experimental challenge due to the fast molecular dynamics governed by electrons which move on an attosecond time scale. These challenges can, however, be overcome using a combination of a single-event two-particle measurement scheme and ultra-short laser pulses.

Going beyond earlier work on attosecond delays [4], we perform XUV-IR pump-probe measurements using a 50-kHz laser amplifier (1030 nm). 80% of the beam is used to produce XUV photons using high-harmonic generation (XUV pump), and the remaining portion (IR probe) is delayed in time using a translation stage. Both beams are focused into a reaction microscope (COLTRIMS) to interact with a gas target of randomly oriented H_2 molecules where we retrieve vector momenta of the ejected electron and H^+, detected in coincidence as a result of molecular photodissociation.

We define molecular-frame asymmetry as A$=\frac{N_{\alpha<90}-N_{\alpha>90}}{N_{\alpha<90}+N_{\alpha>90}}$, where $N_{\alpha<90}$ and $N_{\alpha>90}$ are the number of events where the electron and proton are emitted in the same and the opposite hemisphere, respectively. Fig. 1 shows the time-dependent asymmetry parameter A in a region of the coherent superposition of ground-state dissociation (1) and bond-softening (2) pathways which results in a final Bell-like state

$$|\psi\rangle = \alpha \overbrace{|+,-\rangle}^{\text{pathway 1}} + \beta e^{i2\phi(\tau)} \overbrace{|-,+\rangle}^{\text{pathway 2}},$$

where $|+\rangle$ and $|-\rangle$ are the electronic states with positive and negative parities, respectively. We use the notation |parity of the bound, parity of the free electron⟩. The phase ϕ is a delay-dependent controllable quantity.

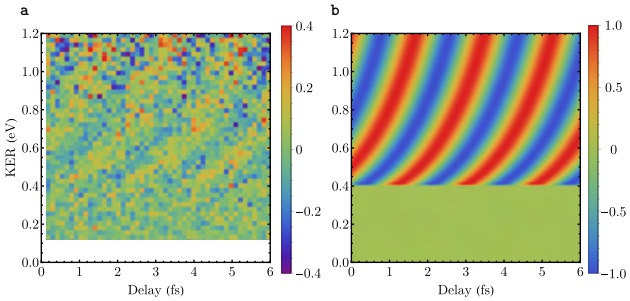


Figure 1. Asymmetry parameter A as a function of the delay between XUV and IR pulses for the experiment (a) and semi-classical simulation (b).

This effect should not be confused with the light-driven localization of the bound electron on one of the nuclei reported in [5,6]. In those experiments only the proton/deuteron is detected and an asymmetric time-dependent proton/deuteron emission with respect to the laser polarization is presented irrespective of the direction of the photoelectron. However, we demonstrate the signature of the entanglement in the bipartite system of photoelectron/ion by detecting the photoelectron and proton in coincidence and their phase-dependent entangled ejection direction, and control it on a sub-fs time scale.

References

[1] Koll L M *et al* 2022 *Phys. Rev. Lett.* **128** 043201
[2] Martín F *et al* 2007 *Science* **315** 5812
[3] Schöffler M S *et al* 2008 *Science* **320** 5878
[4] Cattaneo L *et al* 2018 *Nat. Phy.* **14** 733738
[5] Kling M *et al* 2006 *Science* **312** 5771
[6] Sansone S *et al* 2010 *Nature* **465** 763766

*E-mail: shobeiry@mpi-hd.mpg.de

Ultrafast preparation and detection of entangled atoms

S Eckart[1]*, D Trabert[1], J Rist[1], A Geyer[1], L Ph H Schmidt[1], K Fehre[1], and M Kunitksi[1]

[1] Institut für Kernphysik, Goethe-Universität Frankfurt, Frankfurt am Main, 60438, Germany

Synopsis We break the molecular bond of an oxygen molecule by strong field excitation and obtain two atoms in their ground state which are spatially separated and still entangled in the magnetic quantum number of the valence electrons. Detection is achieved by non-adiabatic tunnel ionization, which is a magnetic quantum number-sensitive mechanism. Both, preparation and detection of the entangled atoms occur on ultrafast time scales. Our experimental results reveal a fingerprint of entanglement and thereby establish a platform to study spatially separated, entangled atoms on femtosecond time scales.

F1

Atoms can form a molecule by sharing electrons in binding orbitals. These electrons are entangled [1]. We experimentally demonstrate that it is possible to break the molecular bond of O_2 using a femtosecond laser pulse at a central wavelength of 390 nm and show that the emerging spatially separated atoms are entangled and form a Bell-like state [2, 3]. 1.5 picoseconds after preparation, in a time-delayed probe step, we trigger non-adiabatic tunnel ionization [4], which is a magnetic quantum number-sensitive mechanism, by applying a femtosecond laser pulse at a central wavelength of 780 nm [3].

The three-dimensional electron and ion momenta upon strong field ionization of O_2 are measured in coincidence using cold-target recoil-ion momentum spectroscopy (COLTRIMS) [8]. The molecular orientation prior to dissociation is inferred using the axial recoil approximation [3, 9].

The measured probability to liberate one electron from *one* of the two atoms is shown as a function of α in Fig. 1(a) [3]. α is the angle between the molecular axis [9] and the light-propagation direction. The results from Fig. 1(a) are used to adjust all free parameters of two models: one model which includes entanglement and a classical model that uses separable states (see Fig. 1(b)). The measured probability to liberate one electron from *each* of the two atoms (two electrons in total) is shown in full analogy in Fig. 1(c).

The simulation for Fig. 1(d) is done using the same free parameters that were found for Fig. 1(b). The experimental results show that properties of spatially separated, entangled atoms are accessible on femtosecond time scales using highly intense laser fields. [3]

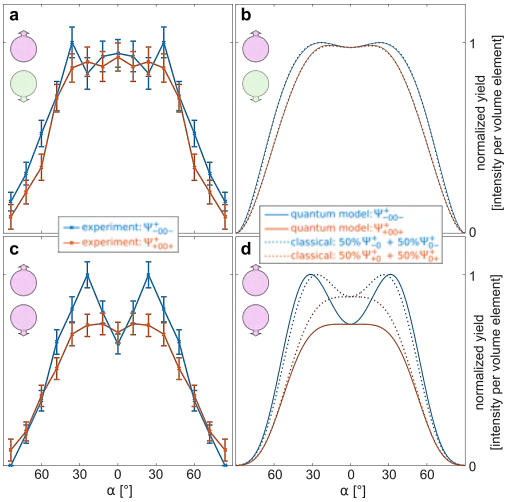


Figure 1. Results for the strong-field ionization of two different Bell-like states. (a) and (c) show experimental data. (b) and (d) show simulations for entangled states ("quantum", solid lines) and separable states ("classical", dashed lines). [3]

References

[1] A Einstein, B Podolsky, N Rosen, Phys. Rev. **47**, 777 (1935).
[2] J S Bell, Phys. Phys. Fiz. **1**, 195 (1964).
[3] S Eckart *et al*, arXiv:2108.10426.
[4] M Ivanov, M Spanner, O Smirnova, J. Mod. Opt. **52**, 165 (2005).
[5] I Barth, O Smirnova, Phys. Rev. A **84**, 063415 (2011).
[6] T Herath *et al*, Phys. Rev. Lett. **109**, 043004 (2012).
[7] S Eckart *et al*, Nat. Phys. **14**, 701 (2018).
[8] O Jagutzki *et al*, IEEE Transactions on Nuclear Science **49** 2477 (2002).
[9] R M Wood *et al*, Rev. Sci. Instrum. **68** 1382 (1997).

*E-mail: eckart@atom.uni-frankfurt.de

F2 Laser Driven Dynamics in Molecules ▲

11:00 - 13:00 **F2 Laser Driven Dynamics in Molecules** 93
Chair: **Marc Vrakking**, Max-Born Institute, Berlin, Germany, EU

11:00 **Hans Jakob Wörner**, ETH Zürich, Switzerland
I: *Advances in attochemistry.* 94

11:30 **Lou Barreau**, CEA LIDYL, France, EU
I: *Multimode molecular vibrations observed with few-femtosecond X-ray transient absorption at the S L-edge and C K-edge.* 95

12:00 **Andrea Trabattoni**, Deutsches Elektronen-Synchrotron, Germany, EU
C: *An ultrafast photoelectron clock in molecular strong-field rescattering.* . 96

12:15 **Jiro Itatani**, University of Tokyo, Japan
C: *Attosecond electronic dynamics of core-excited states of N_2O probed by transient soft X-ray spectroscopy.* 97

12:30 **Rui Ferreira da Silva**, Universidad Autónoma de Madrid, Spain, EU
C: *Polaritonic molecular clock for all-optical ultrafast imaging of wavepacket dynamics without probe pulses.* 98

12:30 **Victor Despré**, Universität Heidelberg, Germany, EU
C: *Ab-initio simulations of ultrafast electron-nuclear dynamics: Paving the way to attochemistry.* 99



Advances in attochemistry

H J Wörner*
Laboratorium für Physikalische Chemie, ETH Zürich, Zürich, 8093, Switzerland

Synopsis Recent advances of our group will be reviewed with a focus on attosecond chronoscopy, charge migration and charge transfer. We have extended attosecond chronoscopy to molecules, clusters and liquids, providing a fundamental understanding of electron dynamics in chemically relevant environments. We have also observed charge migration in ionic and neutral molecules, its decoherence and revivals caused by nuclear motion and the transfer of electronic coherence through conical intersections. I will conclude with the observation of electronic and nuclear dynamics through soft-X-ray spectroscopy of solutions.

The development of attochemistry faces two major challenges. First, the techniques of attosecond science need to be extended to the liquid phase, in which most chemical and biochemical processes take place. Second, more versatile techniques for attosecond spectroscopy need to be developed, such that molecules embedded in a complex environment can be studied and the results can be interpreted without the limitations imposed by the theoretical state of the art.

With these goals in mind, our group has recently focused its efforts on advancing attosecond spectroscopy from atoms to molecules [1], clusters [2] and the liquid phase [3]. In the first part of this lecture, I will discuss these studies of photoionization delays and the overarching picture that emerges from this work regarding attosecond electron dynamics in liquids and solutions. The first measurement of photoionization delays in molecules revealed their sensitivity to the molecular potential and the delayed photoelectron emission caused by molecular shape resonances [1]. Extending the system from one to several water molecules revealed a systematic increase of the ionization delays up to a cluster size of 4-5 molecules, followed by a saturation of the time delays [2]. This effect was traced back to the spatial extension of the electron hole created by ionization which extends, at most, over 4-5 molecules, even in large clusters. The extension to bulk liquid water [3] further confirms this picture through a quantitative agreement between the time delays observed in clusters of 4-6 molecules [2] and liquid water [3]. These results suggest that attosecond chronoscopy might be used to probe electron-hole delocalization and its attosecond dynamics in condensed-phase systems.

In the second part of this lecture, I will discuss recent progress in probing charge migration and charge transfer with attosecond soft-X-ray spectroscopy (SXRS), exploiting its element specificity and site selectivity to simplify the interpretation of attosecond dynamics in complex systems. Following the first measurement of charge migration on the attosecond time scale [4], we have focused on the development of SXRS [5] as a more versatile approach to this goal. Recently, we have achieved the obseration of attosecond charge migration in a neutral molecule [6]. Importantly, the decoherence of charge migration and its revival caused by coupling to the nuclear dynamics could be observed for the first time [6]. This shows that electronic coherences in molecules can indeed be very long lived, suggesting that their control might indeed result in control over chemical dynamics. Another key result is the observation of the transfer of electronic coherence through a conical intersection in [6]. This opens new perspectives in electronic coherent control of chemical reactivity. Using attosecond SXRS at the carbon K-edge, we have observed the fastest conical-intersection dynamics to date, mediating internal conversion in less than 7 fs [7]. Finally, the extension of SXRS to the liquid phase will be presented [8], with its recent application to electronic and nuclear dynamics in ionization-induced proton transfer in aqueous urea solutions [9].

References

[1] M Huppert, I Jordan et al., Phys. Rev. Lett. 117, 093001 (2016).
[2] X Gong, S Heck et al., arxiv:2106.09459 (2021).
[3] I Jordan et al., Science 369, 974 (2020).
[4] P Kraus et al., Science 350, 790 (2015)
[5] Y Pertot et al., Science 355, 264 (2017)
[6] D Matselyukh et al., arxiv:2110.00357 (2021)
[7] K Zinchenko et al., Science 371, 489 (2021)
[8] A Smith et al., J. Phys. Chem. Lett. 11, 1981 (2020)
[9] Z Yin et al., submitted (2021)

* E-mail: hwoerner@ethz.ch

Multimode molecular vibrations observed with few-femtosecond X-ray transient absorption at the S L-edge and C K-edge

L Barreau[1,2,3 *], A D Ross[2,3], S Blinov[4], P Kranov[4], T Noblet[1], A Texier[1], V Kimberg[4,5], F Gatti[1], J F Stanton[6], D M Neumark[2,3], S R Leone[2,3]

[1]Institut des Sciences Moléculaires d'Orsay (ISMO), UMR 8214, CNRS, Université Paris-Saclay, Orsay, France
[2]Department of Chemistry, University of California, Berkeley, CA, 94720, USA
[3]Chemical Sciences Division, Lawrence Berkeley National Laboratory, Berkeley, CA, 94720, USA
[4]International Research Center of Spectroscopy and Quantum Chemistry IRC SQC, Siberian Federal University, Krasnoyarsk, Russia 660041
[5]Department of Theoretical Chemistry and Biology, KTH Royal Institute of Technology, 10691 Stockholm, Sweden
[6]The Quantum Theory Project, Department of Chemistry, The University of Florida, Gainesville, Florida 32611, USA

Synopsis Vibrational wavepackets in SF_6 and CO_2 molecules are excited with a few-cycle infrared laser and probed with soft X-ray transient absorption spectroscopy at the few-femtosecond timescale. The information gathered on the S and C core-excited states are discussed and compared to quantum chemistry calculations.

Owing to the chemical and site-sensitivity of X-ray absorption, time-resolved absorption spectroscopy at the sulfur L-edge and carbon K-edge holds promise of revealing local structural and electronic information about ultrafast dynamics in organic molecules. To that end, recent experimental effort has focused on the development of table-top high-order harmonic generation sources producing few-femtosecond to attosecond pulses extending into the soft X-ray domain [1]. Here, we demonstrate the use of such a source [2] to observe ultrafast multimode coherent vibrational dynamics in sulfur hexafluoride and carbon dioxide.

In SF_6, the intensity of the few-cycle infrared pulse is used to control the shape of the vibrational wavepacket produced in the ground electronic state by impulsive stimulated Raman excitation [3-4]. After vibrational exciation, X-ray absorption to three different sulfur core-excited states ($2p^{-1}$ a_{1g}, $2p^{-1}$ t_{2g} and $2p^{-1}$ e_g) probes regions of the potential energy surfaces (PES) that are unreachable by standard X-ray absorption spectroscopy. This allows to retrieve the PES gradients, in good agreement with TDDFT calculations.

In CO_2, coherent excitation of the Fermi resonance in the electronic ground state is probed with time-resolved soft X-ray absorption to C core-excited states and shows a characteristic ~25 fs oscillation period. *Ab initio* calculations of the core-excited states reveal the strong pseudo-Jahn Teller coupling between the $1s^{-1}$ $2\pi_u$ and $1s^{-1}$ 3s states. The experimental results are in very good agreement with MCTDH calculations of the vibrational wavepacket dynamics and of the corresponding X-ray transient absorption.

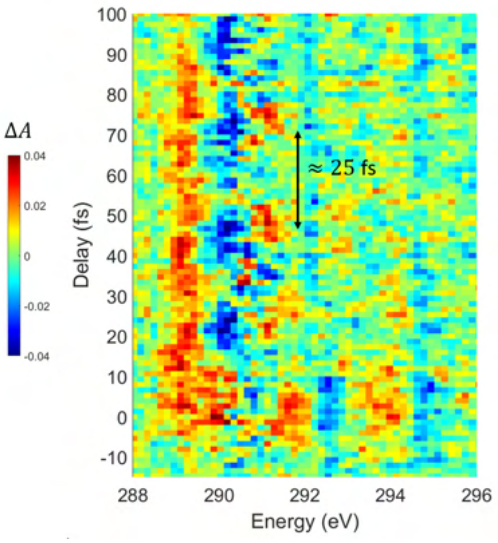


Figure 1. Measured X-ray transient absorption spectrogram of vibrationally excited CO_2 at the carbon K-edge.

References

[1] Ren, X. *et al.*, . J. Opt. **20**, 023001 (2018).
[2] Barreau, L. *et al.*, Sci. Rep. **10**, 5773 (2020).
[3] Wagner, N. L. *et al.*, PNAS **103**, 13279 (2006).
[4] Ferré, A. *et al.*, Nat. Commun. **6**, 1 (2015).

* E-mail: lou.barreau@universite-paris-saclay.fr

An ultrafast photoelectron clock in molecular strong-field rescattering

Andrea Trabattoni*,[1] Joss Wiese,[1, 2] Umberto De Giovannini,[3, 4] Jean-François Olivieri,[1] Terry Mullins,[1] Jolijn Onvlee,[1] Sang-Kil Son,[1, 5] Biagio Frusteri,[4] Angel Rubio,[3, 6, 7] Sebastian Trippel,[1, 5] and Jochen Küpper[1, 2, 5,7]

[1]Center for Free-Electron Laser Science, Deutsches Elektronen-Synchrotron DESY, Hamburg, Germany
[2]Department of Chemistry, Universität Hamburg, Martin-Luther-King-Platz 6, 20146 Hamburg, Germany
[3]Max Planck Institute for the Structure and Dynamics of Matter and Center for Free-Electron Laser Science, 22761 Hamburg, Germany
[4]Dipartimento di Fisica e Chimica, Universitá degli Studi di Palermo, Via Archirafi 36, I-90123, Palermo, Italy
[5]The Hamburg Center for Ultrafast Imaging, Universität Hamburg, Luruper Chaussee 149, 22761 Hamburg, Germany
[6]Center for Computational Quantum Physics (CCQ), The Flatiron Institute, 162 Fifth Avenue, New York NY 10010
[7]Department of Physics, Universität Hamburg, Luruper Chaussee 149, 22761 Hamburg, Germany

Synopsis Strong-field-based imaging is a powerful tool to interrogate transient dynamics with an extremely high spatiotemporal resolution. Here, we study strong-field ionisation of laser-aligned molecules and show that the molecular potential sets the clock for the emission of electrons with a given rescattering kinetic energy. This result has an important impact for the development of advanced self-diffraction experiments. Furthermore, the resulting encoding of the time-energy relation in the photoelectron momentum distributions enables probing the molecular potential in real-time.

F2

In the landscape of ultrafast molecular imaging, laser-induced electron diffraction (LIED) is emerging as a highly competitive method to probe transient molecular structures with attosecond and picometer spatiotemporal resolution [1]. Such a self-imaging method relies on the coherent diffraction pattern imprinted in the rescattered photoelectrons after revisiting the parent ion in a strong-field-driven photointeraction. However, the relevance of the ionised molecular orbital for the rescattered photoelectrons is still under discussion and intense research in this direction is ongoing. Here, we experimentally and computationally study molecular-frame photoelectron spectroscopy from strongly aligned molecules in order to investigate the relation between the molecular frame and the strong-field-induced ultrafast electron dynamics. In addition, we demonstrated how the molecular frame governs the rescattering time for the photoelectron and, consequently, its final kinetic energy [2].

In the experiment, carbonyl sulfide (OCS) molecules were adiabatically aligned in the laboratory frame ($\langle\cos^2\theta_{2D}\rangle=0.9$) and strong-field photoionized. The molecular-frame angle-resolved photoelectron spectra (MF-ARPES) were recorded for parallel and perpendicular alignment (see Fig. 1a). The energy distributions are shown in units of the ponderomotive energy U_p, in Fig. 1b for parallel (blue) and perpendicular (red) alignment. They show a reduced cutoff for the parallel case (Fig. 1c).

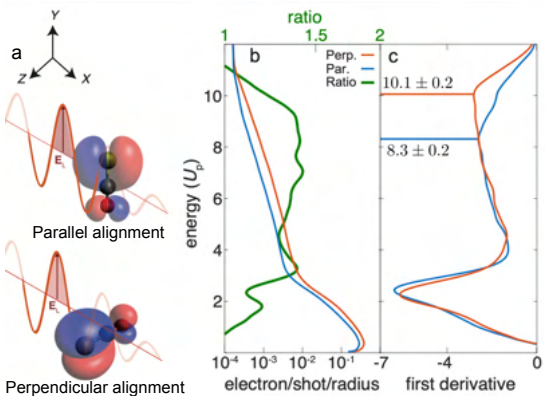


Figure 1. Parallel and perpedicular alignments of OCS and corresponding energy distributions.

TDDFT simulations, together with semiclassical single-active-electron calculations [3], assigned the reduced cutoff to the dominant contribution of later revisits of the photoelectron at the parent ion for parallel alignment. It demonstrates that the molecular potential sets a clock in the photoelectron rescattering and determines its kinetic energy, with a large impact on the interpretation of time-resolved LIED.

References

[1]Blaga C. et al., *Nature* **483**, 194 (2012).
[2]Trabattoni A. et al., *Nat. Commun.* **11,** 2546 (2020).
[3] Wiese J. et al., *Phys. Rev. Research* **3**, 013089 (2021).

* E-mail : andrea.trabattoni@desy.de

Attosecond electronic dynamics of core-excited states of N_2O probed by transient soft X-ray spectroscopy

N. Saito[1], N. Douguet[2], N. Ishii[3], T. Kanai[1], Y. Wu[4], A. Chew[4], S. Han[4,5], B. I. Schneider[6], J. Olsen[7], L. Argenti[4], Z. Chang[4], and J. Itatani[1*]

[1] The Institute for Solid State Physics, The University of Tokyo, 5-1-5 Kashiwanoha, Kashiwa, Chiba 277-8581, Japan
[2] Kennesaw State University, Marietta, Georgia 30060, USA
[3] Kansai Photon Science Institute, National Institutes for Quantum and Radiological Science and Technology, 8-1-7 Umemidai, Kizugawa, Kyoto 619-0215, Japan
[4] CREOL and Department of Physics, University of Central Florida, 4111 Libra Drive, PS430, Orlando, Florida 32816, USA
[5] School of Mechanical Engineering, Chonnam National University, 77 Yongbong-ro, Buk-gu, Gwangju 61186, South Korea
[6] National Institute of Standards and Technology, Gaithersburg, Maryland 20899, USA
[7] Department of Chemistry, qLEAP Center for Theoretical Chemistry, Aarhus University, Langelandsgade 140, DK-8000 Aarhus C, Denmark

Synopsis Half-cycle oscillation is observed in transient absorption spectra of N_2O molecules at Nitrogen *K* edge (400 eV) when irradiated by intense IR pulses. The origin of this oscillation is attributed to tunneling ionization of core-excited neutral molecules by a TDSE-based simulation.

Recent advances of intense ultrashort-pulse IR and MIR sources have extended the cutoff energy of high harmonics into the soft X-ray (SX) region. With SX high harmonics, femtosecond pump-probe spectroscopy, or transient absorption spectroscopy (TAS), has been demonstrated to trace chemical dynamics [1,2]. SX TAS also offers new opportunities to probe intramolecular electron dynamics on the attosecond time scale.

We measure the transient absorption spectra of N_2O molecules irradiated by intense IR pulses. A BiB_3O_6-based optical parametric chirped-pulse amplifier (1.5 mJ, 10 fs at 1.6 μm with a stable CEP) [3] is used to produce isolated attosecond pulses that cover the Nitrogen *K* edge around 400 eV for SX TAS and to pump the N_2O molecules.

Figure 1 shows the measured transient abosoption spectra, showing two striking features: (i) modulation of the absorption spectra with a period that corresponds to one half-cycle of the IR field, and (ii) rapid increase of N_2O^+ N 1s-3π (~403 eV) absorption and decrease of N_2O N_t 1s-3π (~401 eV) and N_2O N_c 1s-3π (~405 eV) absorption due to tunnel ionization of N_2O moleclues in the ground state. A TDSE-based theoretical model is developed to include three processes of core excitation and tunnel ionization. The simulation successfully reproduced these features, and the half cycle oscillation is attributed to the tunnel ionization of the core-excited states [4].

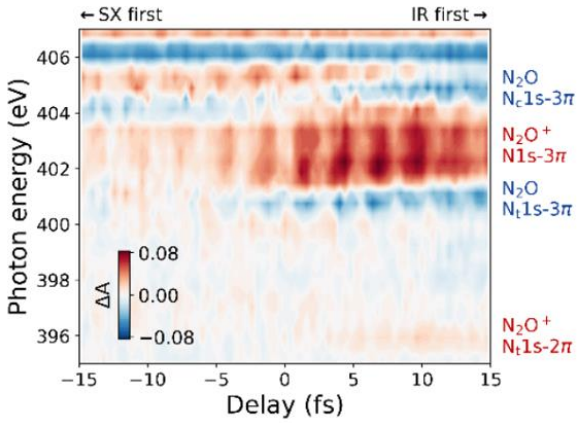


Figure 1. Measured transient absorption spectra.

References

[1] Pertot Y *et al* 2017 *Science* **355** 264.
[2] Attar A R *et al* 2017 *Science* **356** 54.
[3] Ishii N *et al* 2017 *J. Opt.* **20** 014003 (2017).
[4] Saito N *et al* 2021 *Phys. Rev. Research* **3**, 043222.

* E-mail: jitatani@issp.u-tokyo.ac.jp

Polaritonic molecular clock for all-optical ultrafast imaging of wavepacket dynamics without probe pulses

Rui E. F. Silva[1,2]*, **Javier del Pino**[4], **Francisco José García-Vidal**[3], **and Johannes Feist**[3]

[1]Instituto de Ciencia de Materiales de Madrid (ICMM-CSIC), Madrid, Spain
[2]Max-Born-Institut, Max Born Strasse 2A, D-12489 Berlin, Germany
[3]Departamento de Física Teórica de la Materia Condensada and Condensed Matter Physics Center (IFIMAC), Universidad Autónoma de Madrid, E-28049 Madrid, Spain
[4]Institute for Theoretical Physics, ETH Zürich, 8093 Zürich, Switzerland

Synopsis In this work, we present a scheme combining ultrafast laser pulses and strong coupling in organic molecules allowing the imaging of molecular polaritonic dynamics in time domain. When a single molecule is coupled to a cavity mode that is excited using an ultrafast laser pulse, we observe the fingerprint of molecular dynamics in the time-dependent emission from the cavity mode opening a new way to observe ultrafast phenomena in molecules.

F2

Conventional approaches to probing ultrafast molecular dynamics rely on the use of synchronized laser pulses with a well-defined time delay. Typically, a pump pulse excites a wavepacket in the molecule. A subsequent probe pulse can then dissociate or ionize the molecule, and measurement of the molecular fragments provides information about where the wavepacket was for each time delay. In this work, we propose to exploit the ultrafast nuclear-position-dependent emission obtained due to large light-matter coupling in plasmonic nanocavities to image wavepacket dynamics using only a single pump pulse. We show that the time-resolved emission from the cavity provides information about when the wavepacket passes a given region in nuclear configuration space. This approach can image both cavity-modified dynamics on polaritonic (hybrid light-matter) potentials in the strong light-matter coupling regime as well as bare-molecule dynamics in the intermediate coupling regime of large Purcell enhancements, and provides a new route towards ultrafast molecular spectroscopy with plasmonic nanocavities [1].

We illustrate these ideas by using a simple displaced harmonic oscillator model, i.e. the Holstein Tavis-Cummings model, and we show that the time-resolved emission can directly give us information of the nuclear dynamics in the polaritonic potential energy surfaces. To confirm the robustness of the proposed method, we show that it can be applied to anharmonic potentials (Morse potential), and it can be observed not only in the single molecule regime but it also works in the few molecule regime case. By performing matrix product state calculations, in which we take into account several nuclear degrees of freedom, we show that this effect persists even in the presence of vibrational dephasing. Finally, we take advantage of Dicke superradiance to further enhance the emitted signal [2].

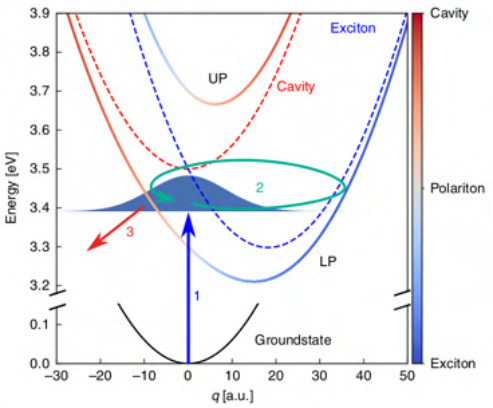


Figure 1. PoPES in the single-excitation subspace for a single molecule coupled to a confined light mode. The arrows represent the excitation by the laser pulse (1), oscillatory motion of the excited vibrational wavepacket (2) and radiative emission (3).

References

[1] R. E. F. Silva, J. del Pino, F. J. García-Vidal and J. Feist, Nature Communications **11**, 1423 (2020).
[2] R. E. F. Silva and J. Feist, in preparation

*E-mail: ruiefdasilva@gmail.com

Ab-initio simulations of ultrafast electron-nuclear dynamics: Paving the way to attochemistry

V Despré[1] *

[1]Theoretische Chemie, PCI, Universität Heidelberg, Im Neuenheimer Feld 229, D-69120 Heidelberg, Germany

Synopsis The possibility for achieving the dream of attochemistry, namely to control chemical reactions through the manipulation of the pure electron dynamics, will be discussed. It will be shown, through ab-initio calculations allowing to interpret experiments performed on silane and adenine, that two of the prerequisites for its realization, the existence of long-lasting coherence and the possibility for charge migration to impact molecular reactivity, can be fulfilled.

The advent of attosecond physics allowed the observation and manipulation of dynamic processes occurring within the intrinsic time scale of the charge motion in atoms and molecules. This has opened the door to the realization of the dream of attochemistry, namely to control chemical reactions through the manipulation of the pure electron dynamics taking place in the first instants after the excitation of the system.

Thereby, the existence of long-lasting electronic coherences in molecular systems is the first key prerequisite to its realization. Furthermore, understating the mechanism leading to or preventing the loss of coherence is necessary for its development.

The first measurement of decoherence and revival in attosecond charge migration will be presented [1]. This dynamics occurs after excitation of silane (SiH_4) by an IR pulse. Simulations treating quantum mechanically both the electronic and nuclear degrees of freedom permitting the interpretation of the experimental results will be discussed. Using these simulations, the behavior of the coherence and the possibility to conserve coherence trough conical intersection will be rationalized.

The second key prerequisite of the realization of attochemistry is the understanding of how charge migration can impact the reactivity of a molecular system. Recently, an XUV-pump IR-probe experiment performed on adenine has demonstrated a sub 3 fs delay in its dicationic signal [2]. It will be shown, using multielectron wave-packet propagation, that this delay is due to a correlation-driven charge migration occurring in the correlation band [3] region of the molecule that stabilizes the system. The stabilization is due to the delocalization of the created hole and its change from σ to π character (see Fig. 1) [4]. The generality of the observed dynamics makes correlation bands a promising playground for the exploration of the possibilities offered by attochemistry.

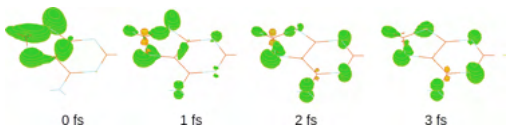


Figure 1. Snapshot of the hole density at 0, 1, 2, and 3 fs following the removal of an electron from HOMO−16. Lack of electron density (hole) is depicted in green, while areas with excess of electron density are depicted in orange.

References

[1] D T Matselyukh, V Despré, N V Golubev, A I Kuleff, H J Wörner, arXiv preprint arXiv:2110.00357.

[2] E P Månsson, S Latini, F Covito, V Wanie, M Galli, E Perfetto, G Stefanucci, H Hbener, U De Giovannini, M C Castrovilli, A Trabattoni, F Frassetto, L Poletto, J B Greenwood, F Légaré, M Nisoli, A Rubio, F Calegari, Commun. Chem. **4**, 1 (2021).

[3] M Hervé, V Despré, P Castellanos Nash, V Loriot, A Boyer, A Scognamiglio, G Karras, R Brdy, E Constant, A G G M Tielens, A I Kuleff, F Lépine, Nature Physics **17**, 327 (2021).

[4] V Despré, A I Kuleff, arXiv preprint arXiv:2111.00760.

*E-mail: victor.despre@pci.uni-heidelberg.de

Platinum





Gold











Silver

VESCENT

UFI UltraFast Innovations

Leybold

FASTLITE

activefiber systems

LAYERTEC OPTICAL COATINGS · OPTICS

TELEDYNE PRINCETON INSTRUMENTS Everywhereyoulook™

Femto Easy ultrafast instrumentation

sphere ULTRAFAST PHOTONICS

Bronze

FEMTOCHROME® Research, Inc.

THORLABS

Ultrafast Science A SCIENCE PARTNER JOURNAL

SCIΦ SINGLE CYCLE INSTRUMENTS

Other Sponsors

IUPAP

RoentDek Handels GmbH
Supersonic Gas Jets
Detection Techniques
Data Acquisition Systems
Multifragment Imaging Systems

Springer

MA

Poster Session I, Highlights A
Chair: **Mathieu Gisselbrecht**, Department of Physics, Lund University, Sweden, EU

M64 **Ultrafast laser-driven dynamics in metal-insulator interface model**
Abdallah AlShafey, Gerard McCaul, Xuyan Gia, Shoushu Gong, Denys Bondar, Yuan-Ming Lu, Mohit Randeria, Alexandra S Landsman 103

M65 **High-order harmonic generation in semiconductor quantum dots**
Harshitha Nandiga Gopalakrishna, Raktim Baruah, Christian Hünecke, Viacheslav Korolev, Alexander Croy, Martin Richter, Ingo Uschmann, Heike Marschner, Christian Reichardt, Andreas Undisz, Jan Dellith, Christian Spielmann, Ulf Peschel, Stefanie Gräfe, Maria Wächtler, Daniil Kartashov 104

M68 **Attosecond Optical Switching by Synthesized Light Field**
Dandan Hui, Husain Alqattan, Simin Zhang, Vladimir Pervak, Enam Chowdhury, Mohammed Hassan 105

M69 **Mechanisms for Attosecond Carrier Thermalization in Metals**
Bethany R. de Roulet, Lorenz Drescher, Stephen R Leone 106

M72 **Spatiotemporal characterization of few-cycle Bessel-Gaussian waveforms**
Yangyang Liu, Shima Gholam Mirzaeimoghadar, Tran-Chau Truong, Dipendra Khatri, Paul B Corkum, Michael Chini 107

M73 **Ultrafast electron-phonon relaxations in 2D carbide $Ti_3C_2T_x$ (MXene): A case study by attosecond transient absorption spectroscopy**
Sergej Neb, Dongbin Shin, Zeno Schumacher, Arthur Niedermayr, Denis A. Kuznetsov, Christoph R. Müller, Alexey Fedorov, Shunsuke Sato, Angel Rubio, Lukas Gallmann, Ursula Keller 108

M76 **Tracing sub-cycle electron dynamics in two-color nearfields of nanometric metal tips**
Philip Dienstbier, Lennart Seiffert, Timo Paschen, Thomas Fennel, Peter Hommelhoff 109

M77 **Ultrafast exciton dynamics reconstruction via a new ptychographic approach**
Gian Luca Dolso, Bruno Moio, Giacomo Inzani, Nicola Di Palo, Rocío Borrego-Varillas, Mauro Nisoli, Matteo Lucchini 110

M79 **Probing nanoplasma expansion dynamics from rare-gas clusters through NIR-wavelength Pump-Probe experiments**
Abraham Camacho Garibay, Bryan Smith, Vyacheslav Leshchenko, Li Fang, Pierre Agostini, Louis DiMauro 111

Ultrafast laser-driven dynamics in metal-insulator interface model

A AlShafey[1] *, G McCaul[2], X Jia[3], SS Gong[3], D Bondar[2], YM Lu[1], M Randeria[1] and AS Landsman[1]

[1]The Ohio State University, Columbus, 43210, USA
[2]Tulane University, New Orleans, 70118, USA
[3]Beihang University, Beijing, 100191, China

Synopsis We study the effect of coupling an insulating Hubbard chain to a free chain on its charge response to a strong laser pulse. We find that a small interchain coupling enhances the response compared to the uncoupled Hubbard chain by introducing large charge fluctuations in the Hubbard chain. We also find an interesting reversal of trend in the large interchain coupling regime, where the system only responds for large Hubbard U interactions. This effect is attributed to a charge gap which *decreases* with U, in stark contrast with the uncoupled Hubbard chain.

We consider the model illustrated in the top of Figure 1. The uncoupled Hubbard chain is known to undergo dielectric breakdown of its Mott insulating phase when a field larger than $F_{\text{th}} = \Delta/2e\xi$ is applied [1, 2], where Δ is the charge gap and ξ is the correlation length of the elementary charge excitations, doublon-hole pairs. As the Hubbard interaction U increases, Δ increases [3] and ξ decreases [4], meaning that for a given pulse, the pulse peak F_0 will eventually fail the threshold condition $F_0 \geq F_{\text{th}}$ for large U, and the insulating phase is preserved.

We find that, for small interchain coupling g, the maximum U value for which dielectric breakdown is observed increases. The coupling to a free chain opens up new mechanisms of creating doublon-hole pairs in the Hubbard chain, facilitating the process of dielectric breakdown. This is supported by a significant recorded increase in ξ as a finite coupling g is introduced to the system, leading to a decrease in F_{th} for any given U.

In the large interchain coupling regime, we find an interesting reversal of trend. A charge response is now only observed for large U, while no response is observed for small U values.

For $g \gg t_0$, the electrons become localized on dimers, and we can analytically solve for the spectrum of the resulting two-site Hubbard problem. Figure 1 depicts the two lowest energy states in this model. The many-body ground state is a product of singlets on the dimers, and the lowest energy excitation is *two* $S = 1/2$ which can disperse throughout the chain. The charge gap Δ between these states *decreases* with U (see bottom-right of Figure 1). The correlation length ξ is also shown to increase with U. The combined effect means that the threshold field F_{th} decreases with increasing U, in stark contrast to the uncoupled chain and the small g regime. Finally, we mention a close correspondence is observed between doublon production and HHG response in the Hubbard chain.

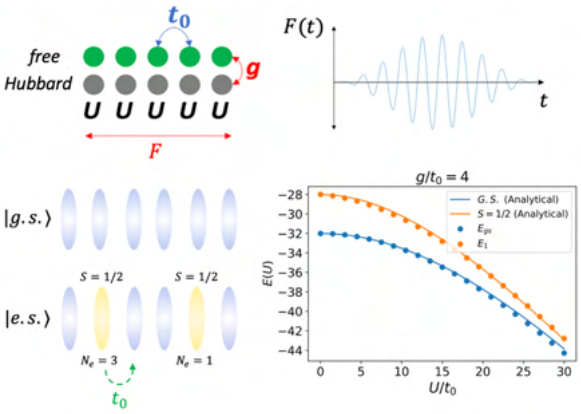


Figure 1. Top: Model system with hopping parameters t_0 and g, and Hubbard interaction U, along with the driving field of N=10 cycles. Bottom: ground state and first excited state in large interchain coupling regime $g \gg t_0$, along with their energy plots from the ED results and perturbative calculation, showing good agreement. Notice the gap between the two states decreases with increasing U.

References

[1] T. Oka 2012 Physical Review B 86.7 (2012): 075148
[2] R. Silva *et al* 2018 Nature Photonics12, 266
[3] Essler *et al* 2005 Cambridge University Press
[4] Stafford *et al* 1993 Physical Review B 48.3 (1993): 1409

* E-mail: alshafey.1@osu.edu

MA

High-order harmonic generation in semiconductor quantum dots

H N Gopalakrishna[1,2*], R Baruah[3,4], C Hünecke[1], V Korolev[1], A Croy[4], M Richter[4], I Uschmann[1,2], H Marschner[1,2], C Reichardt[3], A Undisz[5, 6], J Dellith[3], C Spielmann[1,2], U Peschel[7], S Gräfe[4], M Wächtler[3,4], D Kartashov[1†]

[1]Institute of Optics and Quantum Electronics, Friedrich-Schiller University Jena, Max-Wien-Platz 1, 07743 Jena, Germany

[2]Helmholtz-Institut Jena, Helmholtzweg 4, 07743 Jena, Germany

[3]Leibniz Institute of Photonic Technology, Albert-Einstein-Straße 9 07745 Jena, Germany

[4]Institute of Physical Chemistry, Friedrich Schiller University Jena, Helmholtzweg 4, 07743 Jena, Germany

[5]Institute of Materials Science and Engineering, Chemnitz University of Technology, Erfenschlager Str. 73, 09125 Chemnitz, Germany

[6]Otto Schott Institute of Materials Research, Friedrich Schiller University Jena, Löbdergraben 32, 07743 Jena, Germany

[7]Institute of Condensed Matter Theory and Solid State Optics, Friedrich Schiller University Jena, Fröbelstieg 1, 07743 Jena, Germany

Synopsis We report results on our experimental investigation of high-order harmonic generation (HHG) in thin layers of semiconductor quantum dots in dependence on dot diameter, laser wavelength and intensity. We show that HHG is able to detect the onset of spatial confinement effects in the electron dynamics at the nanoscale.

Recently, it has been demonstrated that high-order harmonic generation (HHG) in nanoscale solids might be substantially mediated by local field enhancement and various resonant effects [1-4]. Here, we investigate what happens to the extreme nonlinear response when the size is reduced further, leading to a strong spatial confinement of the electron and hole dynamics.

Experiments were conducted with 100 fs mid-IR laser pulses interacting with a few micron thick layers of CdSe quantum dots deposited on a sapphire substrate. As a bulk reference, we used a 140 nm thick polycrystalline CdSe film. We observe a strong suppression of the harmonic intensity for harmonics with photon energies larger than the bandgap when dot size is reduced below 3 nm (see Fig.1). This effect is more pronounced for longer wavelength driving laser field. We also confirmed that the suppression of the above bandgap harmonics in 2.2 nm dots is not very sensitive to variations of the laser intensity. Finally, the intensity dependence of HHG spectra show that the degree of nonlinearity of the interaction grows when reducing the dot size.

Our numerical simulations suggest that the observed suppression of interband harmonics is due to scattering of electron wavepacket off the dot's walls leading to an efficient dephasing between electrons and holes.

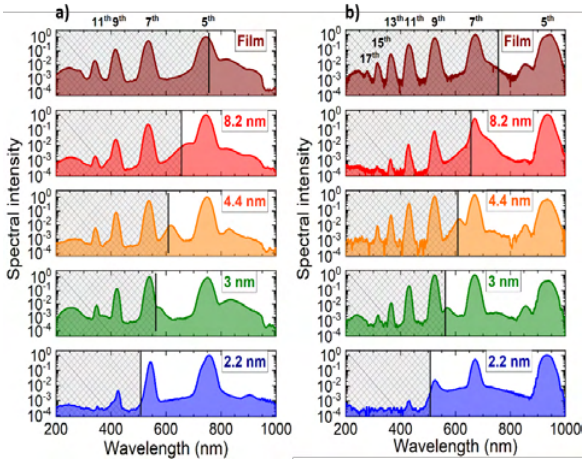


Figure 1. Dependence of HHG spectrum on dot diameter for a) 3.72 μm and b) 4.74 μm laser wavelength.

References

[1] Sivis M *et al* 2017 *Science* **357** 303
[2] Liu H *et al* 2018 *Nature Phys.* **14** 1006
[3] Franz D. *et al* 2019 *Sci. Rep.* DOI :**10.1038/s41598-019-41642-y**
[4] Zograf G. *et al* 2022 *ACS Phot.* **DOI :10.1021/acsphotonics.1c01511**

* E-mail: harshitha.nandiga.gopalakrishna@uni-jena.de
† E-mail: daniil.kartashov@uni-jena.de

Attosecond Optical Switching by Synthesized Light Field

D Hui[1], H Alqattan[1], S Zhang[2], V Pervak[3], E Chowdhury[2], and M Th Hassan[1]

[1]Department of Physics, University of Arizona, Tucson, AZ 85721, USA
[2]Department of Material Science and Engineering, The Ohio State University, Columbus, OH 43210, USA
[3]Ludwig-Maximilians-Universität München, Am Coulombwall 1, 85748, Garching, Germany

Synopsis Optical switching with light frequencies holds great promise for revolutionizing the speed of information processing, photonic processor technologies, and optical communications. Here we demonstrate the optical switching with attosecond speed in a dielectric system. We will present the capability of modulating the reflectivity of the fused silica in the strong field following the optical driver field with sub-femtosecond control resolution.

Modern electronics switch the electric signal on and off based on radio frequency(RF), which limits the signal processing speed to gigahertz. Yet, steering electrons with synthesized few-cycle optical field is expected to extend the ultimate speed in signal manipulation to optical frequencies, femtoseconds or even attoseconds timescale.

In the presence of a strong light field, the electrons in dielectric system will be injected from the valence band (VB) to conduction band(CB), inducing a phase transition due to the strong field interaction. The excited electrons acquire a time dependent momentum in reciprocal space following the vector potential of the driving pulse[1,2,3,4]. Accordingly, the dielectric system undergoes an instantaneous modulation in the electronic structure, leading to alternations of the dielectric constant and optical properties, thus the reflectivity modulation following the driver field waveforms. In this work, we demonstrated the attosecond optical switching in a fused silica using complex synthesized light fields[5,6]. The reflectivity of the dielectric sample oscillates from maximum to minimum in a half field-cycle time scale following the driver light field. Hence, the reflected light signal switches on and off with attosecond speed and the complex synthesized light waveforms even enable the on-demand electron motion control and data encoding.

In the experiment, a synthesized few-cycle light waveform generated by the attosecond light field synthesizer[5,6](pulse duration=2.7 fs) is used to modify the fused silica reflectivity, which is probed by another weak laser pulse. The reflected probe beam spectrum is recorded as a function of the time delay between the two pulses as shown in figure 1, in which the reflectivity switches between maximum to minimum alternatively in 900 attosecond scale.

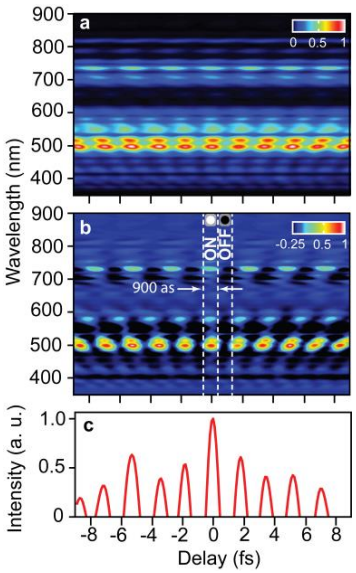


Figure 1. Attosecond optical switching control measurement. a, the measured spectrogram of the reflected probe beam. b, the obtained spectrogram after subtracting the spectrum with no pump field. c, the positive value of the probe spectra integration as a function of time.

The demonstrated all optical driven switching technologies open an avenue towards petahertz or even exahertz signal sampling, information processing technologies and data storage.

References

[1] Hui D et al 2022 Nat. Photon. 16, 33–37.
[2] Schultze M et al 2013 Nat. Photon. 493, 75–78.
[3] Schiffrin A et al 2013 Nature 493, 70-74.
[4] Liu Y et al 2022 Nat. Photon. 16, 109–112.
[5] Hassan M Th et al 2016 Nature 530, 66–70.
[6] Alqattan H et al 2021 arXiv preprint arXiv:2112.10700.

* E-mail: mohammedhassan@arizona.edu

MA

Mechanisms for Attosecond Carrier Thermalization in Metals

B. R. de Roulet[1]*, L. Drescher[1], S. R. Leone[1,2,3]

[1]Department of Chemistry, University of California, Berkeley, Berkeley, CA 94720, USA.
[2]Chemical Sciences Division, Lawrence Berkeley National Laboratory, Berkeley, CA 94720, USA.
[3]Department of Physics, University of California, Berkeley, Berkeley, CA 94720, USA.

Synopsis After optical excitation, excited carriers in metals thermalize from a non-equilibrium distribution to a hot Fermi-Dirac distribution. This thermalization occurs within a few femtoseconds for some metals and over ten femtoseconds for other metals. We have used attosecond, extreme ultraviolet light transient absorption spectroscopy to elucidate the underlying mechanisms by which optically excited carriers thermalize and present a method for predicting the timescale of initial carrier thermalization before measurement.

Following laser excitation, metals redistribute the energy of highly excited carriers from a non-equilibrium distribution to a hot Fermi-Dirac distribution via carrier-carrier scattering. Extreme ultraviolet light attosecond transient absorption spectroscopy is a suitable technique for probing the initial carrier thermalization in metals, as it is sensitive to carrier distribution and has the necessary time resolution to observe these fast dynamics. Previous studies observed a very fast response at the metal adsorption edge upon laser excitation due to a strong local field effect (LFE), which enhances carrier-carrier interactions thereby decreasing carrier thermalization time [1]. However, a much slower response to laser excitation has been observed in other metals [2]. To consider the underlying mechanisms responsible for thermalization in metals, we systematically studied two metals, Fe, which has predominantly d-orbitals above the Fermi level (FL) and is therefore expected to have a strong LFE and Pt, which has a more equal distribution of d and p orbitals above the FL and is therefore expected to have a weak LFE. We found the initial carrier thermalization time is 3.4±1.8 fs for Fe and 16±2.9 fs for Pt. Our results strengthen the hypothesis that the LFE leads to very fast carrier thermalization, while further exploring possible mechanisms for longer thermalization times. We propose that when the LFE is absent, collisional carrier-carrier scattering is the main mechanism of thermalization. Because the LFE is related to the orbital character above the FL, our results suggest that the timescale of initial metal response to laser excitation can be predicted from the structure of the density of states. These investigations were supported by the U.S. Air Force Office of Scientific Research Grant No. FA9550-19-1-0314.

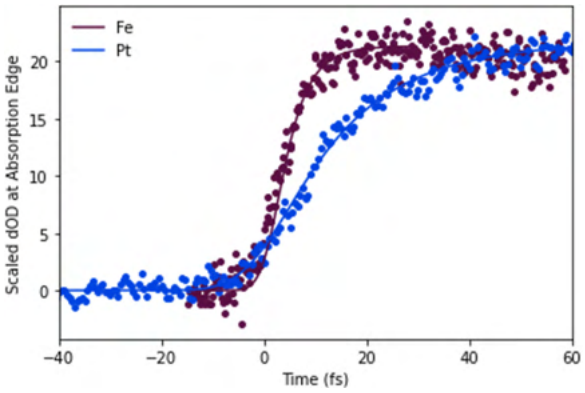


Figure 1. The transient absorption signal at the Fe $M_{2,3}$-edge (purple), which has a very fast response to optical excitation, and the Pt N_7-edge (blue), which has a slower response to optical excitation, shows the range of timescales observed in carrier thermalization of metals.

References

[1] M Volkov *et al.*, Nat. Phys. **15**, 1145 (2019).
[2] H T Chang, Phys. Rev. B **103**, 064305 (2021).

*E-mail: blamo@berkeley.edu

Spatiotemporal characterization of few-cycle Bessel-Gaussian waveforms

Y Liu[1] , S Gholam-Mirzaei [2] , T C Truong[1], D Khatri[1], P B Corkum[2] and M Chini[1,3] *

[1]Department of Physics, University of Central Florida, Orlando FL 32816
[2]Joint Attosecond Science Laboratory (JASLab), National Research Council of Canada and University of Ottawa, Ottawa, Ontario K1A 0R6, Canada
[3]CREOL, the College of Optics and Photonics, University of Central Florida, Orlando FL 32816

Synopsis We demonstrate a novel variant of TIPTOE (tunnel ionization with a perturbation for the time-domain observation of electric fields) capable of resolving three-dimensional (2D space + time) laser waveforms. By using nonlinear excitation in a silicon-based image sensor as the sub-cycle "gate", we characterize the spatio-temporal properties of few-cycle mid-infrared Bessel beams. The reversal of the electric field direction in adjacent Bessel rings is directly observed in the field-resolved measurement.

Knowledge of the space-time properties of ultrafast laser pulses is necessary both for characterizing spatiotemporal distortions and for applications using structured beams. In the past, such characterization has relied mainly upon measurements of linear interference between an 'unknown' pulse and a 'reference' pulse [1]. To measure the unknown pulse, the reference must be spatially homogeneous, and its amplitude and phase must be characterized independently. In addition, the linear interference measurement has been confined to the visible and near-infrared regions of the spectrum due to the wavelength range of CCD and CMOS detectors. Our recent work has shown that nonlinear excitation of photocarriers in a silicon-based image sensor can provide a sub-cycle temporal gate, which can be used to characterize optical waveforms in the mid-IR [2]. Here, we show that by using a scanning geometry, the two-dimensional sensor allows the space and time dimensions to be characterized simultaneously. We demonstrate the technique through the measurement of few-cycle Bessel-Gaussian waveforms.

The experiment is carried out using few-cycle mid-IR pulses centered near 3.4 μm, which are generated by nonlinear compression of multi-cycle pulses from an optical parametric amplifier [2]. After collimation, the few-cycle mid-IR pulses are split into an intense fundamental and weak perturbing pulse. The beam diameter of the fundamental pulse is maintained at approximately 3 mm, while the perturbing pulse is converted into a Bessel-Gaussian beam using a narrow annular aperture and a focusing lens. The collimated fundamental and Bessel-Gaussian perturbing pulses are then recombined and directed onto a silicon image sensor. After recombination, the intensity of the perturbing pulse is less than 1% that of the fundamental, and the time delay between the two fields is scanned using a piezo stage. When scanning the delay, nonlinear excitation of photocarriers by the fundamental allows us to map out the electric field of the perturbing pulse at each pixel of the image sensor, as shown in Fig. 1a. As expected, the electric field is inverted in adjacent Bessel rings. The reconstructed intensity profile of the Bessel beam (Fig.1b) compares well with that obtained using a thermal camera (Fig.1c).

In conclusion, we demonstrate a novel technique, which could characterize the spatial and temporal properties of ultrafast mid-IR beams simultaneously.

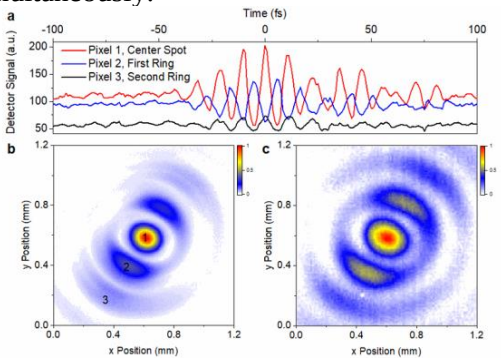


Figure 1. a Time-dependent fields and **b** reconstructed intensity profiles obtained from TIPTOE; **c** intensity profile obtained with a thermal camera.

References

[1] Miranda M *et al* 2014 *Opt. Lett.* **39** 5142
[2] Liu Y *et al* 2022 *Nat. Photonics* **16** 109

* E-mail: michael.chini@ucf.edu

MA

Ultrafast electron-phonon relaxations in 2D carbide $Ti_3C_2T_x$ (MXene): A case study by attosecond transient absorption spectroscopy

S Neb[1 *], D Shin[2], Z Schumacher[1], A Niedermayr[1], D A Kuznetsov[3], C R Müller[3], A Fedorov[3], S A Sato[2,4], A Rubio[2,5], L Gallmann[1] and U Keller[1]

[1]Department of Physics, ETH Zürich, 8093 Zürich, Switzerland
[2]Max Planck Institute for the Structure and Dynamics of Matter and Center for Free Electron Laser Science, 22761 Hamburg, Germany
[3]Department of Mechanical and Process Engineering, ETH Zürich, 8092 Zürich, Switzerland
[4]Center for Computational Sciences, University of Tsukuba, Tsukuba, Ibaraki 305-8577, Japan
[5]Center for Computational Quantum Physics (CCQ), Flatiron Institute, New York 10010, USA

Synopsis Attosecond transient absorption spectroscopy (ATAS) combined with displacive excitation of coherent phonons (DECP) in a two-dimensional functionalized transition metal carbide $Ti_3C_2T_x$ (MXene) reveals ultrafast element, site, and carrier-specific relaxations between hot excited carriers and out-of-plane A_{1g} phonons on the timescale of a few femtoseconds (fs). Quantitative agreement with time-dependent density functional theory (TDDFT) validates the experimental results and deciphers the driving forces behind the observations. Moreover, our case study provides guidance for how heat dissipation at the atomic scale can be controlled through materials engineering design.

Exceptionally fast electron-phonon relaxations on the order of 2 fs have been theoretically predicted around the conduction band minimum of TiO_2 [1]. In [2], phonon phase shifts with regards to the DECP model have been attributed to a relaxation time of 20 fs. However, direct evidence for the predicted faster dynamics is still pending.

In the present case study, the powerful ATAS technique is applied in combination with DECP [3] to achieve unprecedented sensitivity to ultrafast relaxations in $Ti_3C_2T_x$ (T: O, OH, F) MXene [4]. Intense 10 fs long near-infrared (NIR) pulses induce a change in the optical density ΔOD and excite predominantly 6 THz A_{1g} phonons (Fig. 1a). The excitation from two core-levels (Ti 3p / O 2s) to the valence- and conduction bands (VB, CB) by attosecond pulse trains allows to energetically separate different elements and even sites.

According to the DECP model, a substantial charge redistribution quasi-instantly forms a new equilibrium, so that only cosine oscillations can be generated [3]. However, careful phase analysis in Fig. 1b shows a significant deviation which mirrors the signature found in *ab initio* calculations of the electron-phonon coupling strength $\lambda_{e\text{-}ph}$. The phase shifts can be explained by additional perturbation of the DECP mechanism caused by ultrafast cooling processes on the timescale of only a few fs (Fig. 1c).

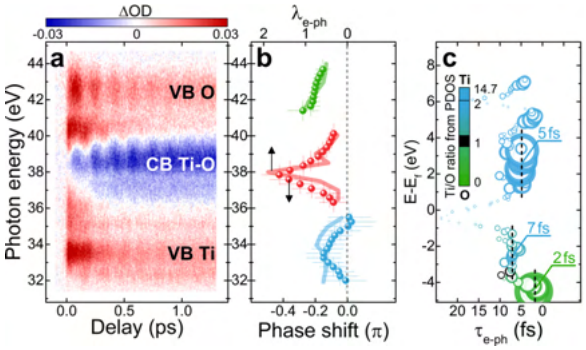


Figure 1. (a) ATAS ps-scan in $Ti_3C_2T_x$. (b) Phonon phase retrieval (spheres) in comparison with electron-phonon coupling strength in $Ti_3C_2O_2$ (lines) and corresponding electron-phonon relaxation times in (c).

TDDFT confirms the experimental results and allows to differentiate between both Ti sites (carbidic/oxocarbidic). Furthermore, it predicts surface functional-dependent NIR-induced charge transfer and allows us to develop strategies for controlling heat dissipation through materials engineering design.

References

[1] Zhukov V P and Chulkov E V 2010 *J. Phys.: Condens. Matter* **22** 435802
[2] Bothschafter E M *et al* 2013 *Phys Rev Lett* **110** 067402
[3] Zeiger H J *et al* 1992 *Phys Rev B* **45** 768
[4] Naguib M *et al* 2011 *Adv. Mater.* **23** 4248-4253

* E-mail: sneb@phys.ethz.ch

Tracing sub-cycle electron dynamics in two-color nearfields of nanometric metal tips

P Dienstbier[1 *], L Seiffert[2], T Paschen[1, 3], T Fennel[2] and P Hommelhoff[1]

[1]Chair for Laser Physics, Friedrich-Alexander-Universität (FAU), Erlangen, 91058, Germany
[2]Institute of Physics, Rostock University, Rostock, 18059, Germany
[3] now with Korrelative Mikroskopie und Materialdaten, Fraunhofer-Institut für Keramische Technologien und Systeme IKTS, Forchheim, 91301, Germany

Synopsis Metal nanostructures exposed to intense laser fields provide strongly localized fields, enabling well-controlled sub-cycle electron dynamics therein. Here we show that phase-resolved photoemission in two color-laser fields can disentangle the propagation from ionization dynamics of electrons at the surface of nanometer sharp needle tips. The relative phase-dependent rescattering spectra contain a characteristic cut-off energy modulation and optimal phase, which allow us to determine precise values for the optical nearfield strengths and to infer an emission duration of 710±30 as from the solid.

Metal nanostructures are readily used as high-brightness electron sources and initial building blocks for petahertz electronics, see, e.g., [1]. Despite broad initial success in these applications, the mapping of electron emission and propagation with attosecond precision has so far been restricted to gas phase atomic and molecular systems, see, e.g., [2].

Addressing this problem, we demonstrate a new method, which disentangles electron propagation from emission dynamics at the surface of a nanometric tungsten needle tip using a linearly polarized few-cycle, two-color laser field (Fig 1a). The emitted electrons either directly leave the tip or elastically rescatter with the surface forming the well-known plateau and high-energy cut-off in electron energy spectra. By controlling the relative phase between the strong fundamental and weak second harmonic field we modify the emitted yield and energy distribution imprinting an optimal phase depending on energy as well as a modulation of the high-energy cut-off (Fig 1b). Trajectory and quantum simulations allow us to identify the cut-off modulation with trajectory modifications during rescattering and relate the optimal phase to the width of the instantaneous rate. Matching these markers with theory provides the precise nearfield strengths directly from the cut-off modulation and allows us to infer an emission duration of 710±30 attoseconds from the shape of the optimal phase [3].

The disentanglement of the dynamics and the precise knowledge of the emission duration will have direct ramifications for electron sources, petahertz electronics and fundamental quantum degeneracy studies.

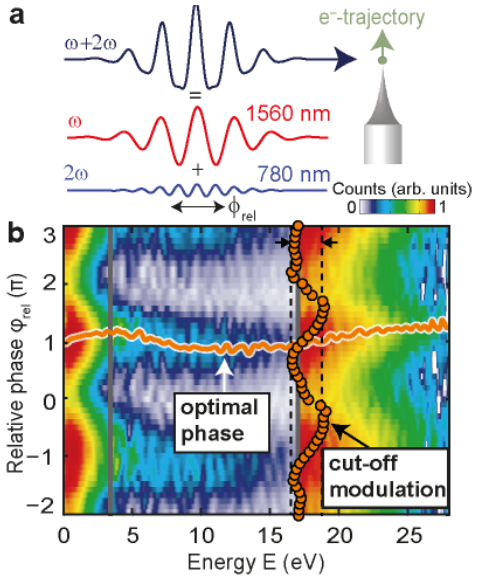


Figure 1. a, Experimental scheme. **b**, Relative-phase dependent spectra with optimal phase and cut-off modulation.

References

[1] Bionta M R *et al* 2021 *Nat. Phot.* **15** 456-60
[2] Shafir D *et al* 2012 *Nature* **485** 343-6
[3] Dienstbier P *et al* manuscript in preparation

* E-mail: philip.dienstbier@fau.de

MA

Ultrafast exciton dynamics reconstruction via a new ptychographic approach

G L Dolso[1]*, B Moio[1,2], G Inzani[1], N Di Palo[1,2], R Borrego-Varillas[2], M Nisoli[1,2] and M Lucchini[1,2]

[1]Department of Physics, Politecnico di Milano, 20133 Milano, Italy
[2]Institute for Photonics and Nanotechnologies, IFN-CNR, 20133 Milano, Italy

Synopsis Excitons play a major role in the ultrafast response of many materials of technological interest. While attosecond science has achieved a suitable time-resolution for the observation of such phenomena, the access to the underlying exciton properties remains a crucial, non-trivial step towards their active optical control. We propose a novel phase-retrieval approach to reveal the physical properties determining ultrafast exciton dynamics.

The complete understanding of exciton physical properties is fundamental for future promising applications in optoelectronics. In this context, attosecond transient absorption and reflection spectroscopies are useful tools in the study of ultrafast exciton dynamics in solids [1]. However, determining the relevant parameters governing the excitonic response, such as lifetime and phonon coupling strength, directly from the experimental results is a difficult task, and needs *a priori* assumptions. This work proposes a new approach to solve this issue: ePIX (the extended Ptychographic Iterative engine for eXcitons).

We adopt the model presented in Ref. [2] for atomic-like quasiparticles to describe exciton dynamics. The attosecond extreme-ultraviolet (XUV) pulse induces an exciton population, described by an electric dipole $O(t)$. The time-evolution of $O(t)$ is affected by the Auger lifetime and the coupling to phonon dynamics. The interaction with an intense infrared (IR) field determines the complex dynamic permittivity:

$$\epsilon(\omega,\tau) = \epsilon_0 + \int_{-\infty}^{+\infty} O(t)\, P(t,\tau)\, e^{-i\omega t}\, dt \qquad (1)$$

where τ is the IR - XUV delay, ϵ_0 is the crystal structure permittivity and $P(t,\tau)$ models the dynamical Stark interaction of the dipole $O(t)$ with the IR field $E(t)$. Our reconstruction method employs Eq. (1), in tandem with the Fresnel equations, to extract $O(t)$ and $E(t)$ from a transient reflection trace. The algorithm follows a ptychographic approach in the time domain [3], suitably adapted to the new physical context.

*E-mail: gianluca.dolso@polimi.it

To test its performances, we applied ePIX to a set of simulated transient reflectance traces, obtained with Eq. (1), such as the trace in Fig. 1a). All features are correctly retrieved by ePIX, as shown Fig. 1b). Furthermore, both the reconstructed IR field, in Fig. 1c), and dipole, in Fig. 1d), compare well to the simulated ones.

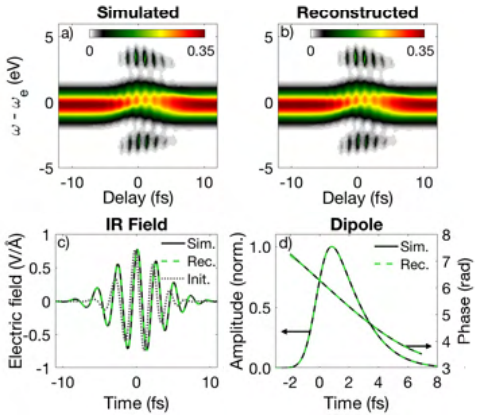


Figure 1. ePIX reconstruction. a) Simulated and b) reconstructed transient reflectivity trace. c) IR field: simulated (black solid), reconstructed (green dashed) and an initial guess example (gray dotted). d) Simulated (black solid) and reconstructed (green dashed) dipoles, representing exciton population.

In conclusion, ePIX allows investigating the physical properties underlying ultrafast exciton dynamics, even with no prior knowledge on the parameters dictating light-matter interaction.

References

[1] M Lucchini, Nat. Commun. **12**, 1021 (2021)
[2] A Moulet, Science **357**, 1134 (2017)
[3] M Lucchini, Opt. Express **23**, 29502 (2015)

Probing nanoplasma expansion dynamics from rare-gas clusters through NIR-wavelength Pump-Probe experiments

A Camacho Garibay[1] *, B Smith[1], V Leschenko[1], L Fang[2], P Agostini[1] and L F DiMauro[1]

[1]The Ohio State University, Columbus, 43210, United States
[2]University of Central Florida, Orlando, 32816, United States

Synopsis Through the use of a pump-probe experimental scheme with laser pulses of tunable wavelength, we are able to induce and map the expansion of rare-gas clusters. With complementing classical molecular dynamics (MD) simulations we are able to provide an while simultaneously provide a time resolved glimpse into the cluster disintegration dynamics.

Rare-gas atomic clusters are interesting systems due to their near-solid density and finite nanometric size, making them capable of efficiently absorbing large amounts of energy when exposed to intense femtosecond laser pulses, vastly larger compared to the case of isolated atoms or even solids. Such strong absorption leads to the disintegration of the cluster, emitting energetic electrons and ions.

Due to their heavy masses, ionic expansion takes place over timescales much larger than the exciting pulse, which can only weakly drive them. Instead, ions acquire their energies from the electrostatic forces at play, emerging as a combination of hydrodynamic expansion (due to electronic pressure) and Coulomb explosion (from a net positive charge) [1]. The charge imbalance between quasi-free electrons and charged ions leads to the formation of a nanoplasma [2] at the cluster core, while the exterior shells are left largely unscreened with a net positive charge. Additionally, other processes such as electron recombination and evaporation can also occur, rendering the expansion dynamics remarkably rich and complex.

Despite numerous theoretical and experimental efforts, many aspects of cluster expansion and relaxation still remain unknown. Nanoplasmas are known to posses a characteristic frequency associated with their charge density, which evolves in time as the system expands and their density decreases. If the system is exposed to a second laser pulse of appropriate frequency, it will be resonantly excited absorbing additional amounts of energy and producing even more energetic ions. It is therefore possible, at least in principle, to map and follow the electronic density of the system by using pulses of tunable wavelength in order to provide a glimpse into the temporal evolution of the nanoplasma.

Here, we explore this idea both from theory and experiment. Our experimental approach uses a pump-probe setup with a wavelength-scanning technique, while measuring kinetic energy distributions for the ions. A scan series was captured for a set of probe wavelengths ranging from 1.0 to 2.5 μm, providing a time resolved mapping of the cluster size and density. These results are complemented with molecular dynamics simulations (Figure 1), allowing us to better understand the more subtle aspects of cluster expansion.

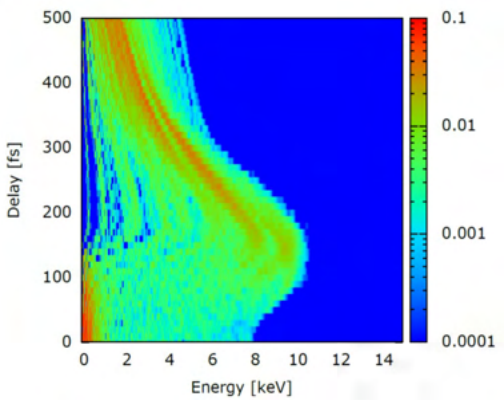


Figure 1. Kinetic Energy Distribution of Ions from an MD simulation of a 0.8 μm pump, 2.0 μm probe experiment for R = 2.4 nm Ar clusters.

References

[1] Ditmire T et al 1996 *Phys Rev A.* 1 53(5)
[2] Lezius M et al 1998 *Phys Rev Lett.* 12 80(2)

* E-mail: camachogaribay.1@osu.edu

MB

Poster Session I, Highlights B
Chair: **Cord L. Arnold**, Lund University, Lund, Sweden, EU

M16 **Continuous variable quantum state tomography of photoelectrons**
Hugo Laurell, Daniel Finkelstein-Shapiro, Christoph Dittel, Chen Guo, Ron Demjaha, Robin Weissenbilder, Mattias Ammitzböll, Lana Neoricic, Sizuo Luo, Mathieu Gisselbrecht, Cord L. Arnold, Andreas Buchleitner, Tönu Pullerits, Anne L'Huillier, David Busto 113

M05 **Attosecond control of XUV multiphoton ionization**
M. Kretschmar, A. Hadjipittas, B. Major, J. Tümmler, I. Will, T. Nagy, M. J J Vrakking, A. Emmanouilidou, B. Schütte 114

M06 **Phase retrieval from angular streaking of XUV atomic ionization**
Anatoli Kheifets, Igor Ivanov, Anna Wang, James Cryan 115

M11 **Probing electronic decoherence with attosecond photoelectron interferometry**
D. Busto, H. Laurell, D. Finkelstein-Shapiro, C. Alexandridi, M. Isinger, S. Nandi, R. Squibb, M. Turconi, S. Zhong, C. Arnold, R. Feifel, M. Gisselbrecht, P. Salières, T. Pullerits, F. Martín, L. Argenti, A. L'Huillier 116

M19 **Ultra-stable and high spectral resolution attosecond beamline for photoelectron interferometry**
Robin Weissenbilder, Sizuo Luo, Anton Ljungdahl, Hugo Laurell, David Busto, Lana Neoričić, Mattias Ammitzböll, Chen Guo, Richard Squibb, Mathieu Gisselbrecht, Cord L. Arnold, Raimund Feifel, Luca Argenti, Eva Lindroth, Anne L'Huillier 117

M20 **Ultrafast dynamics of multi-channel single photon ionization**
Jasper Peschel, David Busto, Marius Plach, Mattias Bertolino, Maria Hoflund, Sylvain Maclot, Jimmy Vinbladh, Hampus Wikmark, Felipe Zapata, Eva Lindroth, Mathieu Gisselbrecht, Jan Marcus Dahlström, Anne L'Huillier, Per Eng-Johnsson 118

M21 **Complete reconstruction of an electron wavepacket generated by absorption of an attosecond pulse**
John Vaughan, Saad Mehmood, Coleman Cariker, Trevor Olsson, Swapneal Jain, Spenser Burrows, Eva Lindroth, Luca Argenti, Guillaume Laurent 119

M26 **Nonadiabatic Strong Field Ionization of Atomic Hydrogen**
Daniel Trabert, Nils Anders, Simon Brennecke, Markus S. Schöffler, Till Jahnke, Lothar Ph. H. Schmidt, Maksim Kunitski, Manfred Lein, Reinhard Dörner, Sebastian Eckart 120

M27 **Angular anisotropy parameters for photoionization delays**
S. Saha, J. Vinbladh, J. Sörngård, A. Ljungdahl, E. Lindroth 121

Continuous variable quantum state tomography of photoelectrons

H Laurell[1]*, D Finkelstein-Shapiro[2], C Dittel[3,4], C Guo[1], R Demjaha[1], R Weissenbilder[1], M Ammitzböll[1], L Neoričić[1], S Luo[1], M Gisselbrecht[1], C L Arnold[1], A Buchleitner[3,4], T Pullerits[5], A L'Huillier[1] and D Busto[1,3]

[1]Department of Physics, Lund University, Box 118, 22100 Lund, Sweden
[2]Instituto de Quimica, Universidad Nacional Autonoma de Mexico, Circuito Exterior, Ciudad Universitaria, Alcalda Coyoacán C.P. 04510, Ciudad de Mexico
[3]Physikalisches Institut, Albert-Ludwigs-Universität Freiburg, Hermann-Herder-Straße 3, 79104 Freiburg, Germany
[4]EUCOR Centre for Quantum Science and Quantum Computing, Albert-Ludwigs-Universität Freiburg, Hermann-Herder-Straße 3, 79104 Freiburg, Germany
[5]Chemical Physics and NanoLund, Lund University, Box 124, 22100 Lund, Sweden

Synopsis We propose a continuous variable quantum state tomography protocol for photoelectrons that originate from the ionization of atoms or molecules by the absorption of extreme ultraviolet light pulses. We numerically demonstrate our results in helium and argon. In the case of argon, we further show that our protocol allows us to quantify ion-photoelectron entanglement due to the spin-orbit splitting.

The development of attosecond light sources has opened the possibility to study electron dynamics on their natural time scale. Attosecond photoelectron spectroscopy techniques such as the reconstruction of attosecond beating by interference of two-photon transitions (RABBIT) and attosecond streaking, initally developed for the characterisation of the attosecond pulses, rely on the assumption that photoelectrons are emitted in a pure quantum state. In general, these techniques fail at fully characterising the photoelectron quantum state, which must be described by a density operator instead of a wavefunction.

This requires the development of quantum state tomography (QST) methods recently proposed for characterization of trains of attosecond wavepackets [1, 2].

We propose and numerically demonstrate a continuous variable quantum state tomography protocol (KRAKEN) for the reconstruction of photolectron wavepackets ionized by using extreme ultraviolet light pulses. Our tomography protocol is demonstrated for electrons emitted via autoionizing resonances in helium and argon and benchmarked against direct calculations of the photoelectron quantum state. In the case of argon, we further show that our protocol allows us to quantify ion-photoelectron entanglement due to the spin-orbit splitting. This opens new routes for the investigation of quantum coherence and entanglement on the ultrafast timescale.

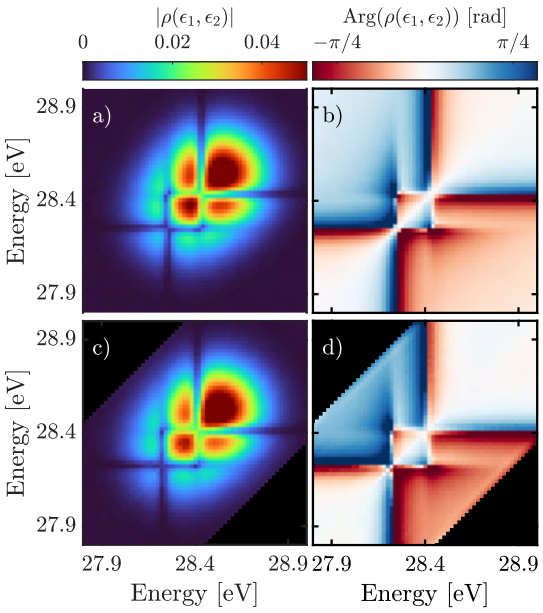


Figure 1. Amplitude (a,c) and phase (b,d) of the density matrix of photoelectrons emitted via the $3s^{-1}4p$ resonance in argon. (a,b) are direct calculations and (c,d) are retrieved with KRAKEN.

References

[1] K. E. Priebe et al., *Nat. Photon* **11**, 793-797, (2017)
[2] C. Bourassin-Bouchet et al., *Phys. Rev. X* **10**, 031048, (2020)

*E-mail: hugo.laurell@fysik.lth.se

MB

Attosecond control of XUV multiphoton ionization

M Kretschmar[1], A Hadjipittas[2], B Major[3], J Tümmler[1], I. Will[1], T Nagy[1], M J J Vrakking[1], A Emmanouilidou[2] and B Schütte[1]*

[1]Max-Born-Institut, 12489 Berlin, Germany
[2]University College London, London WC1E 6BT, United Kingdom
[3] ELI-ALPS, 6728 Szeged, Hungary

Synopsis We study the nonlinear multiple ionization of Ar using a pair of intense attosecond pulse trains (APTs). By controlling the delay between the two APTs with attosecond precision and the spatial overlap with nanometer precision, complex multiphoton ionization pathways can be identified. We show that the experimental results are in good agreement with the results of Monte Carlo calculations.

HHG is typically considered to be a weak source of XUV pulses. By optimizing the pulse energy or the generation geometry, it has recently become possible to obtain XUV intensities around 10^{15} W/cm^2, resulting in the observation of multiply charged ions up to Ar^{4+} [1] and Ar^{5+} [2]. Attosecond-pump attosecond-probe spectroscopy represents a promising tool to understand the underlying nonlinear ionization pathways. So far, experiments demonstrated direct two-photon ionization of atoms and molecules by intense XUV pulses with durations as short as 1.5 fs [3] and 500 as [4].

Here we demonstrate attosecond control over the XUV multiphoton ionization of Ar atoms using a pair of intense attosecond pulse trains (APTs) with a peak intensity of 1×10^{14} W/cm^2 each and a $16 - 34$ eV photon energy range. To study the simultaneous absorption of multiple XUV photons, the XUV peak intensity was varied in a first experiment by changing the delay between the two APTs. As shown in Fig. 1(a), the Ar^{2+} ion yield (red curve) is only weakly modulated as a function of the XUV-XUV time delay, whereas the Ar^{3+} ion yield (blue curve) clearly oscillates with a period of about 1.3 fs.

In a second experiment, sequential absorption of multiple XUV photons was studied by varying the XUV fluence. Using a delay of 20 fs between the two APTs, the focus of one of the APTs was spatially displaced with respect to the second APT. As shown in Fig. 1(b), the Ar^{2+} ion yield is enhanced by a factor of 1.6 (red curve) at spatial overlap between the two APTs, and the Ar^{3+} ion yield is enhanced by a factor of 3.2 (blue curve).

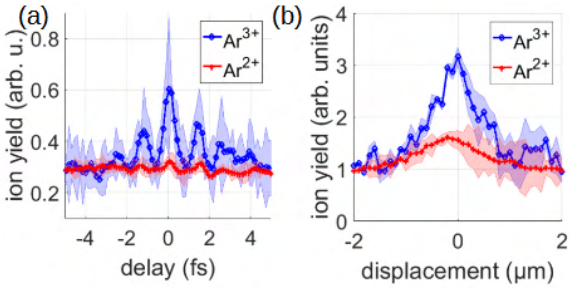


Figure 1. Ar^{2+} and Ar^{3+} ion yields as a function of (a) the time delay and (b) the spatial overlap between two APTs, when they were delayed by 20 fs with respect to each other.

Based on the temporal and spatial measurements, our analysis shows that Ar^{2+} is predominantly generated by a sequential two-photon process. It further suggests that Ar^{3+} is formed by a simultaneous two-photon absorption process from the Ar^{2+} ground state. These results are well reproduced by Monte Carlo calculations.

Our experiments demonstrate that it is feasible to study XUV multiphoton absorption using intense attosecond pulses. In the future, the experiments could be extended to higher photon energies to study the generation of inner-shell vacancies and their decay via complex Auger processes.

References

[1] A. Nayak *et al.*, Phys. Rev. A **98**, 023426 (2018).
[2] B. Senfftleben *et al.*, J. Phys. Photonics **2**, 034001 (2020).
[3] P. Tzallas *et al.*, Nat. Phys. **7**, 781 (2011).
[4] E. J. Takahashi *et al.*, Nat. Commun. **4**, 2691 (2013).

*E-mail: Bernd.Schuette@mbi-berlin.de

Phase retrieval from angular streaking of XUV atomic ionization

AS Kheifets[1]*, IA Ivanov[2], AL Wang[3] and JP Cryan[3]

[1]Research School of Physics, The Australian National University, Canberra ACT 2601, Australia
[2]Center for Relativistic Laser Science, Institute for Basic Science, Gwangju 61005, South Korea
[3] Stanford PULSE Institute, SLAC National Accelerator Laboratory, Menlo Park, California 94025, USA

Synopsis We achieve an accurate phase retrieval of XUV atomic ionization by streaking the photoelectron in a circularly polarized IR laser field. The streaking phase can then be converted to the atomic time delay which opens access to atomic and molecular photoionization on the attosecond time scale. This novel technique will find its use in XFEL facilities and will be instrumental for studying inner shell atomic and molecular ionization.

Angular streaking of XUV atomic ionization with a circularly polarized IR laser radiation has become a powerful tool for a shot-to-shot characterization of isolated attosecond pulses from free-electron laser sources [1, 2]. This technique is analogous to the attosecond streak camera [3] in that XUV pulses are the primary source of ionization while it is common to the attoclock [4] in that the ionized electrons interact with a circularly polarized laser field which alters the photoelectron momentum distribution. Both the streak camera and the attoclock are senitive to the ionization phase that can be converted to the atomic time delay and the tunneling time, respectively. Here [5] we demonstrate, for the first time, an accurate phase retrieval of XUV atomic ionization by angular streaking.

In our numerical simulations, we solve the time-dependent Schrödinger equation for an atom ionized by a short XUV pulse in the presence of circularly polarized laser radiation. Our qualitative analysis is based on the strong field approximation [6] and the lowest order perturbation theory [7]. The two alternative techniques suggest the phase retrieval methods that can be applied both to the simulated and experimental data. In simulations, the XUV/IR delay is systematically varied. In an experiment, a second ionization feature in the same target or a mixed target could be used as a reference.

We test the proposed technique by comparing the XUV ionization phase of the hydrogen atom delivered by angular streaking with the analogous set of data returned by a well established RABBITT (reconstruction of attosecond beating by interference of two-photon transitions) technique [8]. The two sets of data agree very well in a wide range of XUV photon energies.

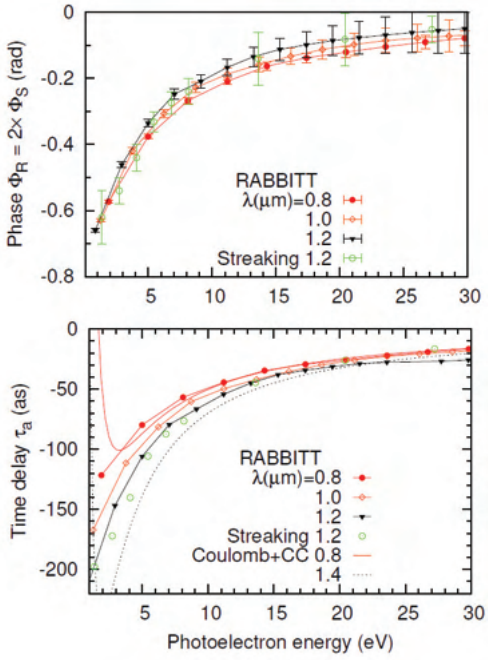


Figure 1. Top: RABBITT phase Φ_R is compared with the twice the streaking phase $2\Phi_s$ obtained from the isochrone ansatz of [6]. Bottom: the RABBITT time delay $\tau_a = \Phi_R/(2\omega)$ is compared with the Coulombic Wigner time delay augmented by the CC correction [7] at various wavelengths.

References

[1] N Hartmann *et al*, Nat. Photon. **12**, 215 (2018).
[2] J Duris *et al*, Nat. Photon. **14**, 30 (2020).
[3] J Itatani *et al*, Phys. Rev. Lett. **88**, 173903 (2002).
[4] P Eckle *et al*, Nat. Phys. **4**, 565 (2008).
[5] A S Kheifets *et al*, arXiv: 2202.06147 (2022).
[6] A K Kazansky *et al*, Phys. Rev. A **93**, 013407 (2016).
[7] J M Dahlström *et al*, Chem. Phys. **414**, 53 (2013).
[8] P M Paul *et al*, Science **292**, 1689 (2001).

*E-mail: A.Kheifets@anu.edu.au

MB

Probing electronic decoherence with attosecond photoelectron interferometry

D Busto[1,2 *], H Laurell[1], D Finkelstein-Shapiro[3], C. Alexandridi[4], M Isinger[1], S Nandi[1], R J Squibb[5], M Turconi[4], S Zhong[1], C L Arnold[1], R Feifel[5], M Gisselbrecht[1], P Salières[4], T Pullerits[6], F Martín[7,8,9] L Argenti[10,11] and A L'Huillier[1]

[1]Department of Physics, Lund University, 22100 Lund, Sweden
[2]Institute of Physics, Albert Ludwig University, 79104 Freiburg, Germany
[3]Institute of Chemistry, Universidad Nacional Autónoma de México, 04510 Ciudad de México, Mexico
[4]Université Paris-Saclay, CEA, CNRS, LIDYL, 91191 Gif-sur-Yvette, France
[5]Department of Physics, University of Gothenburg, 41296 Gothenburg, Sweden
[6]Department of Chemical Physics, Lund University, 22100 Lund, Sweden
[7]Department of Chemistry, Universidad Autónoma de Madrid, 28049 Madrid, Spain
[8]IMDEA-Nanoscience, 28049 Madrid, Spain
[9]Condensed Matter Physics Center, Universidad Autónoma de Madrid, 28049 Madrid, Spain
[10]Department of Physics, University of Central Florida, 32816 Orlando, USA
[11]CREOL, University of Central Florida, 32816 Orlando, USA

Synopsis Quantum coherence is at the heart of ultrafast dynamics in matter. In this study, we investigate the degree of coherence of photoelectrons emitted via the 2s2p Fano resonance using high-resolution photoelectron interferometry. We show that the strong dipole coupling of the 2s2p and $2p^2$ states by an infrared photon entangles the radial and angular degrees of freedom of the photoelectron, resulting in a dynamic loss of coherence in our measurements.

The photoionization of matter by attosecond pulses leads to the emission of photoelectrons corresponding to a broad superposition of continuum states. Techniques such as reconstruction of attosecond beating by interference of two-photon transitions (RABBIT) [1] can measure the photoelectron spectral amplitude and phase. This has been applied to the investigation of autoionization dynamics [2], assuming that the photoelectron quantum state is pure, *i.e.* it can be described by a wave function.

As demonstrated for microwave cavities, Fano resonances are sensitive probes of decoherence due to their interferometric nature [3]. Here, we investigate the photoionization via the 2s2p Fano resonance in helium using RABBIT measurements with unprecedented spectral resolution. We compare the amplitude and phase of the two sidebands adjacent to the resonant harmonic (SB38 and SB40) and show that, in the case where an infrared photon is absorbed (SB40), the strong dipole coupling of the 2s2p and $2p^2$ states, leads to a loss of interference contrast and a reduced phase variation (Fig. 1).

We show that the reduced interference contrast and phase variation can be attributed to the entanglement of the radial and angular degrees of freedom of the photoelectron, which, in our angle-integrated measurements, leads to a dynamic loss of coherence during autoionization [4]. These results pave the way towards a systematic study of entanglement and decoherence in photoionization dynamics.

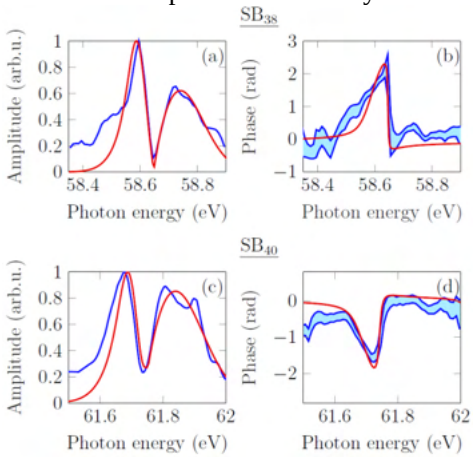


Figure 1. Amplitude (a,c) and phase (b,d) of the two sidebands adjacent to the resonant harmonic. Experimental data is in blue and theory in red.

References

[1] P M Paul *et al.* 2001 *Science* **292** 1689
[2] Gruson V *et al* 2016 *Science.* **875** 022021
[3] Bärnthaler A *et al.* 2010 *Phys. Rev Lett.* **105** 056801
[4] Busto D *et al.* 2021 arXiv:2111.12037

† E-mail: david.busto@physik.uni-freiburg.de

Ultra-stable and high spectral resolution attosecond beamline for photoelectron interferometry

R Weissenbilder[1,*], S Luo[1,†], A Ljungdahl[5], H Laurell[1], D Busto[1,2], L Neoričić[1], M Ammitzböll[1], C Guo[1], R J Squibb[3], M Gisselbrecht[1], C L Arnold[1], R Feifel[3], L Argenti[4], E Lindroth[5] and A L'Huillier[1]

[1]Department of Physics, Lund University, Box 118, 22100 Lund, Sweden
[2]Physikalisches Institut, Albert-Ludwigs-Universität Freiburg, Hermann-Herder-Straße 3, 79104 Freiburg, Germany
[3]Department of Physics, University of Gothenburg, Origovägen 6B, SE-412 96 Gothenburg, Sweden
[4]Department of Physics & CREOL, University of Central Florida, FL 32816, United States of America
[5]Department of Physics, Stockholm University, AlbaNova University Center, SE-106 91 Stockholm, Sweden

Synopsis We describe an ultra-stable and high spectral resolution attosecond pump-probe setup for photoelectron interferometry. The system is based on an actively stabilized Mach-Zehnder interferometer, stable to within 14 as root-mean-square (RMS) error over several hours. The photoelectron spectral phase is determined with high spectral resolution by using a narrowband probe pulse. This allows us to measure for the first time a 2π phase shift across the spin-orbit resolved $3s^1 3p^6 4p$ Fano resonance in argon.

Many actively stabilized interferometers for attosecond pump-probe experiments use a continuous wave (CW) laser and an active feedback system to keep the two arms the same length [1]. Here, we describe a stabilization system, based on a Mach-Zehnder interferometer, which stabilizes directly the phase relation of the pump and probe femtosecond laser pulses. Our interferometer design does not require an additional CW laser, making it both simple and versatile while also reducing heating and making it less sensitive to beam drifts. We measure a RMS error over 70 minutes of 14 as [see Figure 1(a) and (b)], and a RMS error within 20 as for over 9 hours. The pump-probe delay scan range is up to 400 fs.

With a 2 m long, high resolution (≈ 80 meV), magnetic-bottle spectrometer we can use the rainbow reconstruction of attosecond beating by two-photon transitions (RABBIT) technique to measure the spectral phase within the sidebands [2]. By using a 10 nm narrowband filter in the probe arm we further increase the spectral phase resolution of our measurements by reducing the effects of spectral phase variations in the probe pulse, and mixing of different frequencies of the photoelectron wavepacket. With this technique, we perform a RABBIT measurement of the $3s^1 3p^6 4p$ Fano resonance in argon [Figure 1(c)][3], and measure a phase shift of 2π across both the spin-orbit split components in sideband (SB) 16 [Figure 1(d)][4]. A theoretical interpretation is proposed.

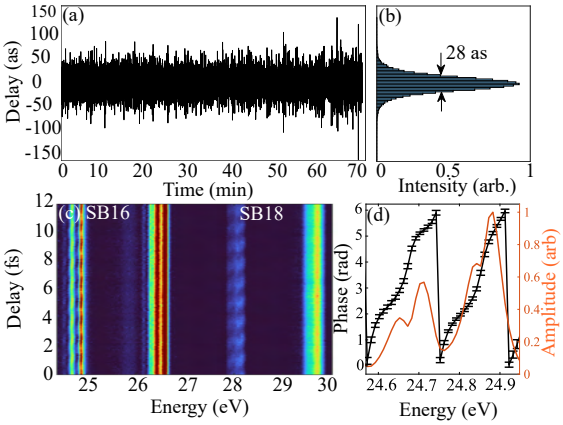


Figure 1. (a) Stability of interferometer over time. (b) RMS error of interferometer over one hour. (c) Resonant RABBIT spectrogram in argon. (d) Amplitude and phase of 2ω oscillation in SB16.

References

[1] M Sabbar et al., Rev. Sci. Instrum. **85**, 103113 (2014).
[2] V Gruson et al., Science **354**, 734 (2016).
[3] M Turconi et al., J. Phys. B: At. Mol. Opt. Phys. **53**, 184003 (2020).
[4] M Kotur et al., Nat. Commun. **7**, 10566 (2016).

*E-mail: robin.weissenbilder@fysik.lth.se
†E-mail: sizuo.luo@fysik.lth.se

MB

Ultrafast dynamics of multi-channel single photon ionization

J Peschel[1]*, D Busto[1,2], M Plach[1], M Bertolino[1], M Hoflund[1], S Maclot[1], J Vinbladh[3], H Wikmark[1], F Zapata[1], E Lindroth[3], M Gisselbrecht[1], J M Dahlström[1], A L'Huillier[1], and P Eng-Johnsson[1]

[1]Department of Physics, Lund University, P.O. Box 118, 22100 Lund, Sweden,
[2]Physikalisches Institut, Albert-Ludwigs-Universität, Stefan-Meier-Strasse 19, 79104 Freiburg, Germany,
[3]Department of Physics, Stockholm University, AlbaNova University Center, SE-106 91 Stockholm, Sweden

Synopsis Using angular-resolved attosecond interferometry, we measure the phase and amplitude of the individual angular momentum channels in the outer-shell photoionization of neon.

Photoionization of atoms and molecules is one of the fastest processes in nature. The understanding of the ultrafast temporal dynamics of this process often requires the characterization of different angular momentum channels over a broad energy range.

We characterize one-photon ionization from the $2p^6$-ground state of neon, obtaining the amplitude and phase of the electric dipole transition matrix elements towards ϵs- and ϵd-continuum states [1]. To extract channel-resolved one-photon ionization phases, we apply the reconstruction of attosecond beating by interference of two-photon transitions (RABBIT) technique [2] while detecting electrons with full angular resolution. We take advantage of the fact that continuum-continuum transitions, far enough from resonances, are largely insensitive to the short-range potential and depend only on the Coulomb potential, making them universal quantities [3]. This allows us to extract channel-resolved one-photon phases from the angle-resolved RABBIT data using a global fit procedure, shown in Fig. 1(a). We then determine the channel-resolved one-photon amplitudes by combining the one-photon phases with measurements with only the XUV field, shown in Fig. 1(b). The retrieved values for the phases and amplitudes are in excellent agreement with calculations using angular-channel-resolved many-body perturbation theory.

Since our method allows us to determine the energy variation of channel-resolved phases (in contrast to phase differences between channels), we are able to reconstruct the spatial and temporal dynamics of the photoionization process, including the coherent or incoherent contributions of the different channels. In addition, the results allow the study of the effects of the Coulomb, centrifugal, and in particular the short-range potential, which compares well with calculated values [4] as well as predictions from quantum defect theory.

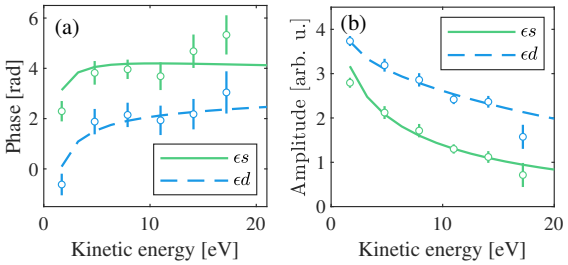


Figure 1. Extracted one-photon phases (a) and radial amplitudes (b) as a function of the kinetic energy for the ionization channel towards ϵs- (green) and ϵd-continua (blue) for experimental (dots) and simulated data (lines). Adapted from [1].

References

[1] J Peschel et al., arXiv:2109.01581 (2021).
[2] P M Paul et al., Science, 292:1689 (2001).
[3] D Busto et al., Phys. Rev. Lett., 123:133201 (2019).
[4] D J Kennedy and S T Manson, Phys. Rev. A, 5:227 (1972).

*E-mail: jasper.peschel@fysik.lth.se

Complete reconstruction of an electron wavepacket generated by absorption of an attosecond pulse

J Vaughan[1], S Mehmood[2], C Cariker[2], T Olsson[1], S Jain[1], S Burrows[1], E Lindroth[3], L Argenti[2,4] * and G M Laurent[1] †

[1] Department of Physics, Auburn University, 380 Duncan Drive, Auburn, AL 36849, USA
[2] Department of Physics, University of Central Florida, Orlando, Florida 32816, USA
[3]Department of Physics, Stockholm University, Stockholm SE-106 91, Sweden
[4] CREOL, University of Central Florida, Orlando, Florida 32816, USA

Synopsis In this work, we propose a novel interferometric scheme to measure time delays in photoionization. Our method is based on two angularly resolved RABBITT measurements performed sequentially with the same attosecond pulse train (APT) and two distinct probe field energies. We show that the time delays in the *bound-to-continuum* and *continuum-to-continuum* transitions can be retrieved from the experiment. Our method is supported by theoretical calculations demonstrating the feasibility of the retrieval procedure.

The recent development of XUV light sources with attosecond duration has opened up new avenues for experimentalists to probe electron dynamics in matter. So far, time-resolved measurements have been mostly achieved by using an attosecond pulse to trigger a given electronic process, and a phase-locked femtosecond field to probe its dynamics. The electron dynamics under scrutiny are thus unravelled by varying the time delay between the two pulses.

Several procedures have been proposed to extract the dynamics from such pump-probe measurements. The RABBITT technique [1] has proved to be particularly promising for accessing photoemission time delays. This measurement, however, probes three entangled unknowns, namely, the time delays in the *bound-to-continuum* and *continuum-to-continuum* transitions, as well as the spectral phase of the attosecond pulses. The retrieval of a given time delay, therefore, is impossible without some *a-priori* knowlegde of the other two unknowns. To circumvent this issue, most RABBITT studies measure only the relative measurement between two distinct transitions [2, 3].

In this work, we propose a novel interferometric scheme to retrieve the time delays in the *bound-to-continuum* and *continuum-to-continuum* transitions from the same experiment. As shown in Fig. 1, our method is based on two angularly resolved RABBITT measurements performed sequentially with the same APT made of odd harmonics and two distinct probe fields (the fundamental field and its second harmonics). Within some approximations, we show that the time delays can be retrieved from the photoelectron angular distributions. Our method is supported by theoretical calculations demonstrating the feasibility of the retrieval procedure.

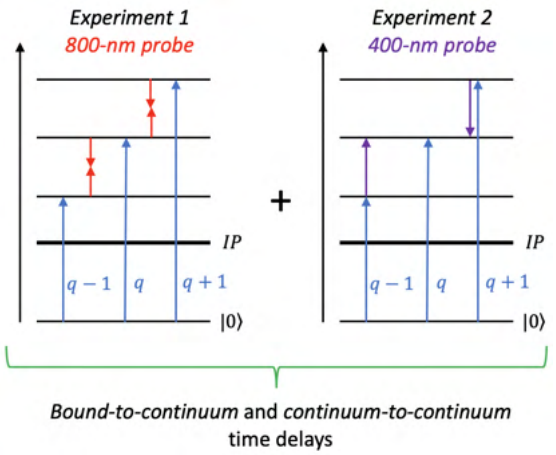


Figure 1. Schematic view of the experiment: two RABBITT traces taken sequentially with the same APT allows to reconstruct the *bound-to-continuum* and *continuum-to-continuum* time delays.

References

[1] Paul P M *et al* 2001 *Science* **292** 1689
[2] Klnder K *et al* 2011 *New Journal of Physics* **106** 143002
[3] Fuchs J *et al* 2020 *Optica* **7** 154

*E-mail: Luca.Argenti@ucf.edu
†E-mail: glaurent@auburn.edu

MB

Nonadiabatic Strong Field Ionization of Atomic Hydrogen

D Trabert[1] *, N Anders[1], S Brennecke[2], M S Schöffler[1], T Jahnke[1], L Ph H Schmidt[1], M Kunitski[1], M Lein[2], R Dörner[1] and S Eckart[1†]

[1]Institut für Kernphysik, Goethe-Universität, Frankfurt, 60438, Germany
[2] Institut für Theoretische Physik, Leibniz Universität, Hannover, 30167, Germany

Synopsis In a recent publication [1], we have presented experimental data on the nonadiabatic strong field ionization of atomic hydrogen using elliptically polarized femtosecond laser pulses at a central wavelength of 390 nm. Our measured results are in agreement with a numerical solution of the time-dependent Schrödinger equation (TDSE). Experiment and TDSE show four above-threshold ionization peaks in the electron's energy spectrum. The most probable emission angle (also known as "attoclock offset angle" or "streaking angle") is determined for each energy peak individually.

In a pioneering experiment, Sainadh *et al* have applied the technique of angular streaking [2,3] to adiabatic tunnel ionization of atomic hydrogen hydrogen using a driving laser field at a central wavelength of 770 nm [4].

Here, we present experimental data on a similar experiment but choose a driving field at a central wavelength of 390 nm and thus increased the nonadiabaticity of the ionization process significantly. Our results have been published in [1] recently. In short, we study the strong field ionization of atomic hydrogen using elliptically polarized femtosecond laser pulses at an ellipticity of ε=0.85, and a peak intensity of 1.4×10^{14} W/cm^2.

A COLTRIMS reaction microscope was used to measure the three-dimensional momenta of electron and ion in coincidence. Figure 1(a) shows the electron momentum distribution projected onto the laser's polarization plane (p_xp_y plane). Figure 1(b) shows the corresponding result that is obtained from a numerical solution of the time-dependent Schrödinger equation (TDSE). Experiment and TDSE result are in agreement. This is underlined by Figure 1(c), which shows the corresponding electron energy distributions.

The "angular offset" α_{off} (see Fig. 1(a),(b)) is found to increase with energy, a trend that is opposite to standard predictions based on Coulomb interaction with the ion. This increase of deflection angle can be explained by a nonadiabatic, classical two-step model (NACTS) that includes nonadiabatic corrections of the initial momentum distribution at the tunnel exit and nonadiabatic corrections of the tunnel exit position itself [5,6].

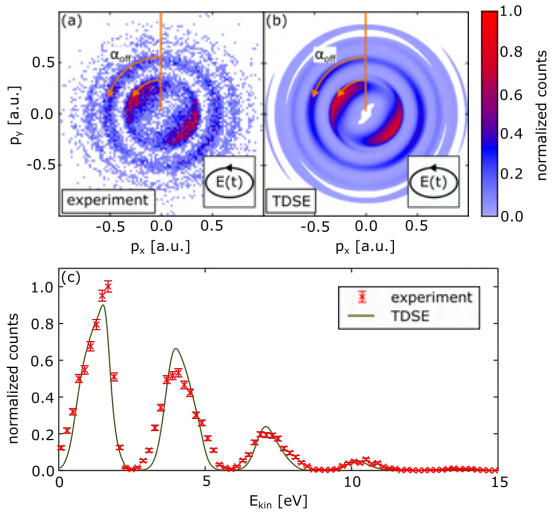


Figure 1. (a) Measured electron momentum distribution projected onto the laser's polarization plane for the ionization of atomic hydrogen by femtosecond laser pulses at a central wavelength of 390 nm, an ellipticity of ε = 0.85, and a peak intensity of 1.4×10^{14} W/cm^2. The light's helicity and the orientation of the polarization ellipse are indicated by the inset in the lower right corner. (b) Focal-averaged numerical solution of the TDSE for the parameters that were used in (a). α_{off} indicates the "angular offset" with respect to the minor axis of the ellipse of the laser electric field in (a) and (b). (c) shows a comparison of the electron energy distribution for the data shown in (a) and (b). The data is the same as in Ref. [1].

References

[1] Trabert D *et al* 2021 *Phys. Rev. Lett.* **127**, 273201
[2] Smolarski M *et al* 2010 *Opt. Express* **18**, 17640
[3] Eckle P *et al* 2008 *Science* **322**, 1525
[4] Sainadh U *et al* 2019 *Nature* **568**, 75
[5] Brennecke S *et al* 2020 *Phys. Rev. Lett.* **124**, 153202
[6] Brennecke S *et al* 2021 *J. Phys. B* **54**, 164001

* E-mail: trabert@atom.uni-frankfurt.de
† E-mail: eckart@atom.uni-frankfurt.de

Angular anisotropy parameters for photoionization delays

S Saha*, J Vinbladh, J Sörngård, A Ljungdahl and E Lindroth†

Department of Physics, Stockholm University, AlbaNova University Center, SE-106 91 Stockholm, Sweden

MB

Synopsis Anisotropy parameters describing the angular dependence of the photoionization delay are defined. The parametrization has a form very similar to that traditionally used for cross sections, but the new anisotropy parameters are complex. Results for the measurable *atomic delay* will be presented.

The photoelectron angular distribution is conveniently described with angular anisotropy parameters [1]. For linearly polarized light and within the dipole approximation:

$$\frac{d\sigma}{d\Omega} = \frac{\sigma_{int}}{4\pi}\left(1 + \sum_{n=1}^{N} \beta_{2n} P_{2n}\left(\cos\theta\right)\right) \qquad (1)$$

where P are Legendre polynomials and θ is the detection angle relative to the polarization axis. N is the number of exchanged photons and σ_{int} is the cross section integrated over all angles.

Attosecond techniques such as *Reconstruction of Attosecond Beating by Interference of Two-photon Transitions* are based on interference of electron wavepackets that are released by an XUV pulse train and then modified by absorption or emission of an IR photon. This creates spectral *sidebands* that oscillate with the delay between the light fields, and carry information on the phase of the electron wave packet. The spectral derivative of this phase can be interpreted as a delay. Rather recently angle-resolved experiments [2, 3] have highlighted that not only cross sections (amplitudes), but also delays (phases) depend on angle.

Here we define anisotropy parameters, describing the angular dependence of the measurable two-photon *atomic delay*, τ_A. The parametrization is similar to that in Eq. (1):

$$\tau_A\left(\theta\right) = \tau_A^{int} + \frac{1}{2\omega}\arg\left(1 + \sum_{n=1}^{2} \tilde{\beta}_{2n} P_{2n}\left(\cos\theta\right)\right)$$

where τ_A^{int} is the angular integrated atomic delay and ω is the laser frequency. The new $\tilde{\beta}$-parameters, are closely related to the ordinary parameters in Eq. (1), but they are complex. Also the the underlying one-photon *Wigner delay*, τ_W, can be similarly parametrized.

Angular dependent delays for ionization from the outermost s-shell and p-shell in rare gases will be presented. The s-shell Wigner delay is isotropic in a non-relativistic framework, but the presence of two channels, $s \rightarrow p_{1/2}, p_{3/2}$, relativistically allow for an angular dependence. The atomic delay, being due to a two-photon process will, on the other hand, always allow for an angular dependence. Some important results for krypton are shown in Fig. 1.

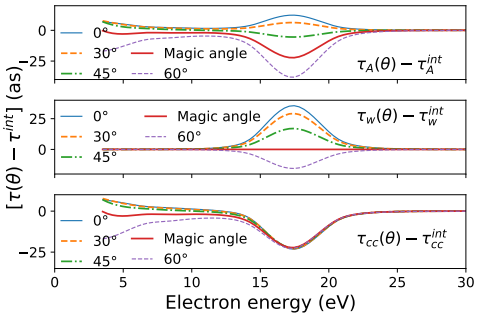


Figure 1. Ionization from Kr(4s). The upper panel shows $\tau\left(\theta\right) - \tau^{int}$ for the measurable *atomic delay*. The middle panel displays it for the underlying *Wigner delay*. Here the angular dependence around the so-called Cooper minimum is of purely relativistic origin. The bottom figure shows the *difference* between the *atomic delay* and the *Wigner delay* (labelled *cc-delay*). It is clear that for low electron energies the angular dependence is mainly a two-photon effect, while the Cooper minimum region is dominated by the one-photon contribution.

References

[1] J Cooper & RN Zare, J.Chem.Phys. **48** 942 (1968).
[2] S Heuser *et al*, Phys. Rev. A **94** 063409 (2016).
[3] C Cirelli *et al*, Nat. Commun. **9** 955 (2018).

*E-mail: soumyajit.saha@fysik.su.se
†E-mail: Eva.Lindroth@fysik.su.se

MC

Poster Session I, Highlights C
Chair: **Thierry Ruchon**, Université Paris-Saclay, CEA, CNRS, LIDYL

The SYLOS COMPACT beam line at ELI-ALPS for intense High-Order
M32 **Harmonic Generation**
Arjun Nayak, Mathieu Dumergue, Ioannis Orfanos, Emmanouil Skantzakis, Sergei Kühn, Paraskevas Tzallas, Dimitris Charalambidis, Subhendu Kahaly, Katalin Varju . 123

Resonant and Anti-Resonant Phases of Two- and Three-Photon Ionization
M33 **of Helium**
Lorenz Drescher, Tobias Witting, Oleg Kornilov, Marc J J Vrakking 124

M37 **NeXUS - first US attosecond user facility**
Vyacheslav Leshchenko, Timothy Scarborough, Theodore Ronningen, Louis DiMauro, Robert Baker 125

M38 **Sub-2-Cycle Carrier-Envelope-Phase–stabilized 110W, 1.1mJ Laser**
Steffen Hädrich, Maxim Tschernajew, Evgeny Shestaev, Fabian Stutzki, Nico Walther, Florian Just, Florian Karl, Sven Breitkopf, Christian Gaida, Oliver Herrfurth, Imre Seres, Zsolt Bengery, Barnabás Gilicze, Péter Jójárt, Zoltán Várallyay, Ádám Börzsönyi, Michael Müller, Christian Grebing, Dominik Hoff, Gerhard G. Paulus, Tino Eidam, Jens Limpert 126

M42 **Soft X-ray Generation with Ultrashort Pulses: The Krypton Surprise**
Pierre-Alexis Chevreuil, Fabian Brunner, Ursula Keller, Lukas Gallmann 127

Towards Field Sampling of Ultrabroadband Continuum Radiation from
M46 **deep-UV to NIR**
Amelie Schulte, Corinna Konrad, Matthew Weidman, Ferenc Krausz, Johannes Schötz 128

Control of high harmonic spectral characteristics in a non-collinear
M51 **generation geometry**
Lénárd Gulyás Oldal, Peng Ye, Zoltán Filus, Tamás Csizmadia, Tímea Grósz, Massimo De Marco, Zsolt Bengery, Imre Seres, Barnabás Gilicze, Péter Jójárt, Katalin Varjú, Subhendu Kahaly, Balazs Major 129

High repetition rate few-cycle short-wave infrared light source for
M55 **strong-field experiments**
Ivan Sytcevich, Anne-Lise Viotti, Chen Guo, Jan Vogelsang, Ann-Kathrin Raab, Fabian Langer, Anne L'Huillier, Cord L. Arnold 130

The ELI-ALPS MIR-HE ATTO - design and status of the 1 keV attosecond
M61 **beamline**
Filippo Campi, Torsten Golz, Jan Heye Buss, Sebastian Starosielec, Michael Schulz, Subhendu Kahaly, Eric Cormier, Sergei Kühn, Katalin Varjú, Robert Riedel 131

The SYLOS COMPACT beam line at ELI-ALPS for intense High-Order Harmonic Generation

A Nayak[1]*, M Dumergue[1], I Orfanos[2], E Skantzakis[2], S Kühn[1]†, P Tzallas[1,2], D Charalambidis[1,2,3], S Kahaly[1] and K Varju[1]

[1]ELI-ALPS, ELI-HU Non-Profit Ltd., Wolfgang Sandner utca 3, Szeged 6728, Hungary
[2]FORTH - IESL, P.O. Box 1527, GR71110 Crete, Greece
[3]Department of Physics, University of Crete, P.O. Box 2208, GR71003 Crete, Greece

Synopsis The SYLOS COMPACT beam line implemented at ELI-ALPS Research Institute targets nonlinear processes in the XUV domain at 1 kHz repetition rate. We present the capabilities of the beam line, as well as results on XUV nonlinear ionization of atoms obtained in a first user campaign.

The discovery of High-order Harmonic Generation in Gasses (GHHG) has led to a rapid spread of table-top ultrashort XUV pulse sources. For the investigation of dynamics on the femto- to attosecond time scale, this technology currently represents the only viable option. Although the research field of attosecond sciences is lively and growing rapidly, some limitations related to the low conversion efficiency of GHHG are still challenging to overcome. To date, there is only a limited number of laboratories worldwide that can reach XUV pulse energies suitable for the observation of non-linear interactions or XUV-XUV pump-probe experiments on the sub-femtosecond time scale. Pulse energy, repetition rate and photon energy are often subject to a trade off with current GHHG technology and thus restrict the range of possibilities available to the scientist.

In this communication we present the GHHG SYLOS COMPACT beam line [1] implemented at the ELI-ALPS Research Institute and User Facility, located in Szeged, Hungary. The beam line operates at 1 kHz and provides XUV pulse energies in the μJ range. The ultrashort pulse duration of the driving laser not only provides access to photon energies in the > 150 eV range but also easy access to isolated attosecond pulses.

At the heart of the beam line is the SYLOS laser (EKSPLA Ltd. [2]) delivering 4.5 TW in 7 fs CEP-stable pulses centered on 910 nm at 1 kHz. These parameters are achieved through modern OPCPA technology and we verify here how such a laser can be used for efficient GHHG. We discuss the design features of the COMPACT beam line that enable it to handle the high average power while still fitting into a modest size lab, to improve the XUV conversion efficiency through purposeful target design [3], and to perform comprehensive XUV pulse diagnostics. We also present the built-in opportunities for experimentation and the current performance characteristics. As a highlight, we demonstrate our first results on the two-photon double ionization of neon and argon which has been achieved in a first user campaign. These results demonstrate the capability of the beam line to observe nonlinear phenomena in the XUV spectral range.

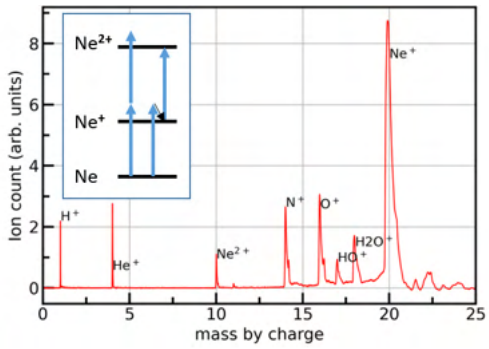


Figure 1. Ion mass spectrum showing a strong peak at Ne^{2+} as a result of XUV two-photon double ionisation according to the processes shown in the inset.

References

[1] S Kühn *et al.*, J. Phys. B **50**, 132002 (2017).
[2] S Toth *et al.*, J. Phys. Photonics **2**, 045003 (2020).
[3] A Nayak *et al.*, Phys. Rev. A **98**, 023426 (2018)

*E-mail: arjun.nayak@eli-alps.hu
†E-mail: sergei.kuhn@eli-alps.hu

MC

Resonant and Anti-Resonant Phases of Two- and Three-Photon Ionization of Helium

L Drescher[1,2 *], **T Witting**[1], **O Kornilov**[1] **and M J J Vrakking**[1]

[1]Max-Born-Institut für nichtlineare Optik und Kurzzeitspektroskopie, Max-Born-Strasse 2A, 12489 Berlin, Germany
[2]Department of Chemistry, University of California, Berkeley, California 94720, USA

Synopsis A high-resolution and broad spectral coverage High Harmonic Generation setup is presented, using tuneable bandpass filters. The scheme is applied to study the phase of resonance enhanced two-color XUV+NIR photoexcitation via the 1s*n*p $_1$P^1 (n=3,4,5) Rydberg series of helium, revealing characteristic phase evolution across the resonant and anti-resonant wavelengths.

Intermediate states play an important role in multiphoton excitation. Resonant excitation of an intermediate state can for example lead to enhancement of the final state amplitude. The final state phase depends on intermediate state resonances and can for example be leveraged to suppress the final state amplitude in an excitation scheme with multiple interfering pathways [1]. Swoboda *et al.* [2] demonstrated that RABBITT (Reconstruction of attosecond beating by interference of two-photon transitions) is well suited to study the two-photon ionization phase, however exploration of the full phase dynamic across the resonant excitation was hindered by limited spectral range.

Here we present a novel approach to probe RABBITT phases over a broad spectral range [3]. The HHG driving and probing NIR laser pulses are spectrally filtered by a narrowband transmission filter. With a combination of different filters and angle-tuning we cover a spectral range from 770 to 810 nm. We present results on studying the RABBITT phase in two-color (XUV+NIR) two-photon and three-photon ionization of He via the 1s*n*p $_1$P^1 (*n*=3,4,5) Rydberg series. Our results show the characteristic stepwise change of the RABBITT phase when the frequency of the XUV pulse is scanned across the resonance (see Figure 1). We observe a reverse phase behavior around the anti-resonant condition, i.e. when phases through two near-resonant pathways between two resonances cancel each other out. While the anti-resonant condition leads to an abrupt change of phase at the anti-resonant wavelength in the two-photon signal, the transition is less steep in the three-photon signal. Numerical results obtained by a perturbative model approach show, that this difference originates from the phase of the continuum-continuum transition. It adds a real valued contribution to the otherwise purely imaginary excitation amplitude near the anti-resonance, changing the phase behavior.

Similar results for the two-photon ionization of He have recently been reported using rainbow RABBITT [4]. Our scheme provides a new way to obtain RABBITT phases with high spectral resolution across the broad range without requiring a high spectral resolution of the photoelectron detector.

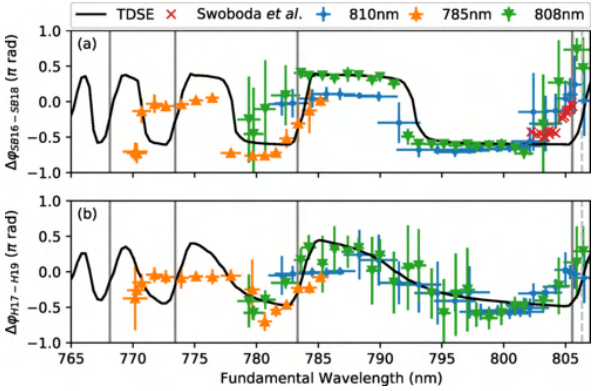


Figure 1. Measured and calculated wavelength dependence of the RABBITT phase of (a) two and (b) three photon ionization. Points correspond to experiments performed at different wavelengths. TDSE simulations are shown as black curve. Vertical grey bars indicate fundamental wavelengths for which the 15th harmonic is resonant with the members of the 1s*n*p $_1$P^1 series of He.

References

[1] Dudovich et al., Physical Review Letters 86, no. 1 (2001): 47–50.
[2] Swoboda et al., Physical Review Letters 104, no. 10 (2010): 103003.
[3] Drescher et al., Physical Review A 105, no. 1 (2022): L011101.
[4] Autori et al., arXiv:2107.13990 (2021)

* E-mail: lbdrescher@berkeley.edu

NeXUS - first US attosecond user facility

V Leshchenko[1] [*], T Scarborough[1], T Ronningen[1], L DiMauro[1] and R Baker[1] [†]

[1] The Ohio State University, Columbus, Ohio 43210, USA

Synopsis NeXUS is one of the NSF mid-scale facilities, which major mission is to make the cutting-edge attosecond technology available to the scientific community.

The National eXtreme Ultrafast Science (NeXUS) facility is an NSF funded mid-scale-research infrastructure project at The Ohio State University. Its mission is to provide users access to cutting-edge attosecond and femtosecond laser-driven extreme-ultraviolet (XUV) and soft-X-ray sources and state-of-the-art end-stations. The facility is based on a kW-class high-repetition-rate ultrashort laser driving three high-order harmonic generation (HHG) sources and other secondary sources, e.g. an optical parametric amplifier (OPA) providing tunable pump pulses.

The system is presently in the implementation and optimization phase, and it is expected to become available in 2024. In this paper, we will provide a snapshot of currently planned capabilities.

The facility includes the following end-stations:

- XAS/XRS/ATTO. Time-resolved XUV/soft-X-Ray absorption and reflection spectroscopy of solid, liquid and gas samples; and an attosecond end-station with double-time-of-flight detector. It has a number of add-ons, e.g. liquid sheet sample setup and circular polarized XUV pulses for magnetic circular dichroism studies.
- TR-ARPES. Time-resolved angular-resolved photo-electron spectroscopy end-station with a pulse-duration-preserving monochromator in the HHG beamline and a state-of-the-art commercial spectrometer.
- TR-STM. Time-resolved scanning tunneling microscopy (STM) end-station with a pulse-duration-preserving monochromator and state-of-the-art commercial STM. It should enable direct elemental imaging on the atomic scale.
- TR-LIED. Time-resolved laser induced electron diffraction end-station with a molecular beam add-on.

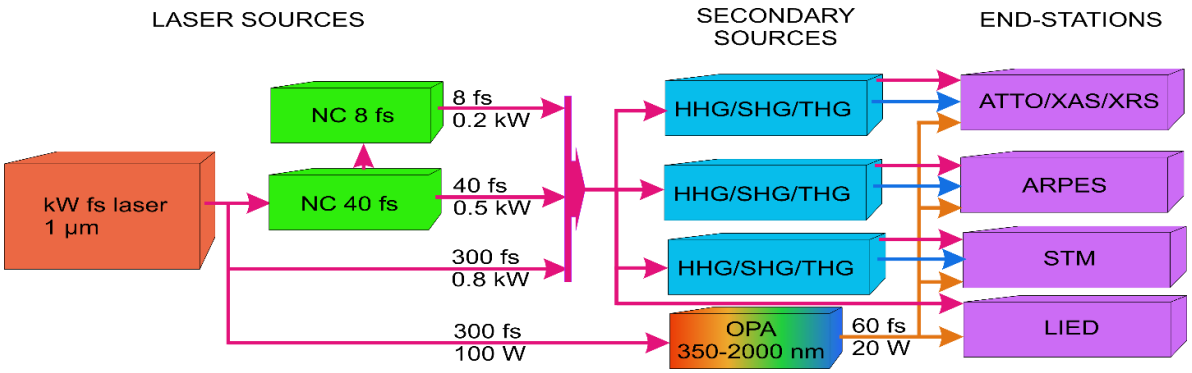


Figure 1. NeXUS scheme. (NC: nonlinear compression; SHG: second harmonic generation; THG: third harmonic generation).

[*] E-mail: leshchenko.1@osu.edu
[†] E-mail: baker.2364@osu.edu

MC

Sub-2-Cycle Carrier-Envelope-Phase–stabilized 110W, 1.1mJ Laser

S Hädrich[1], M Tschernajew[1], E Shestaev[1,2], F Stutzki[1], N Walther[1], F Just[1], F Karl[1], S Breitkopf[1], C Gaida[1], O Herrfurth[1], I Seres[3], Z Bengery[3], B Gilicze[3], P Jójárt[3], Z Várallyay[3], A Börzsönyi[3], M Müller[2], C Grebing[2,4], D Hoff[5,6], G G Paulus[6,7], T Eidam[1,*] and J Limpert[1,2,4,7]

[1]Active Fiber Systems GmbH, Ernst-Ruska-Ring 17, 07745 Jena, Germany.
[2]Institute of Applied Physics, Abbe Center of Photonics, Friedrich-Schiller-University Jena, 07743 Jena, Germany.
[3]ELI-ALPS, ELI-HU Non-Profit Ltd., H-6728 Szeged, Hungary
[4]Fraunhofer Institute for Applied Optics and Precision Engineering, 07743 Jena, Germany
[5]Single Cycle Instruments, 07743 Jena, Germany
[6]Institute of Optics and Quantum Electronics, Friedrich Schiller University Jena, 07743 Jena, Germany
[7]Helmholtz-Institute Jena, Fröbelstieg 3, 07743 Jena, Germany

Synopsis We present a sub-2-cycle laser system combining high average power, pulse energy and repetition rate with CEP-stable operation making this system an ideal driver for next-generation attosecond sources. The system is based on a fiber-chirped pulse amplification system emits 300fs pulses, which are post-compressed down to the few-cycle regime in a two-stage multi-pass cell (MPC) nonlinear pulse compression. The second MPC allows to achieve a pulse duration of 5.8fs at a pulse energy of 1.1mJ. The stabilization of the carrier-to-envelope phase is presented.

High-repetition-rate few-cycle laser systems with high average power and CEP-stable operation are requested by various scientific applications. We present a sub-2-cycle laser system combining high average power, pulse energy and repetition rate with CEP-stable operation. The system builds up on a fiber-based chirped-pulse-amplification system incorporating coherent combination of 8 main amplifier channels. The emitted 300 fs pulses with 1.8 mJ energy are nonlinearly post-compressed down to few optical cycles in a two-stage multipass cell (MPC). The first multipass cell is based on highly efficient dielectric mirrors. Due to the excellent efficiency of the MPC of 94% an intermediate output of 1.7 mJ pulse energy, 170 W average power and <35 fs pulse duration is achieved. The second MPC utilizes unique metal-based mirrors capable of high-average-power operation with broadest spectrum. This allows to achieve a pulse duration of 5.8 fs (less than two optical cycles) at a pulse energy of 1.1 mJ, which corresponds to the shortest pulses and highest compressed average power for few-cycle MPCs with 110 W at the used 100 kHz pulse repetition rate. The entire system provides an excellent power stability featuring only 0.1% standard deviation of the average power over 8h. The CEP stability measured with a Stereo-ATI phase meter is 300 mrad for Fourier frequencies above 2 kHz. This fact is depicted in the parametric-asymmetry plot shown in Figure 1: While the CEP varies from 0 to 2π for the freely running laser (grey), the CEP amounts to 300 mrad in the CEP-stabilized case (red).

This unique combination of high average power, pulse energy, pulse repetition rate and CEP stability makes this system an ideal driver for next-generation attosecond sources.

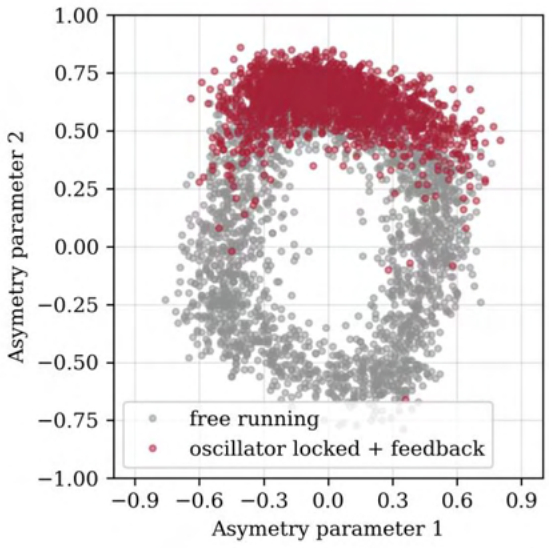


Figure 1. Parametric asymetry plot showing the CEP of the free-running (grey) and the CEP-stabilized system (red)

* E-mail: publications@afs-jena.de

Soft X-ray Generation with Ultrashort Pulses: The Krypton Surprise

Pierre-Alexis Chevreuil[1]*, Fabian Brunner[1], Ursula Keller[1], and Lukas Gallmann[1]

[1]Department of Physics, Institute for Quantum Electronics, ETH Zurich, Switzerland

Synopsis We study the generation of radiation with 150-1000 eV photon energy in He, Ne, Kr and Xe using intense 10-fs, 0.8-µm pulses, focused to an intensity of 3×10^{16} W·cm^{-2}. We find that in helium and neon, photons between 150 and 400 eV originate mostly from HHG, while in Kr and Xe, they originate from plasma radiation. Between 600 and 1000 eV, the photons may originate from a mix of high-harmonic and incoherent plasma radiation for He, Ne, Kr and Xe.

Conventional phase matching of high harmonic generation (HHG) can be achieved only up to ≈ 200 eV with a 0.8-µm driver. To generate higher photon energies, one approach consists in using high laser intensities in a nonadiabatically self-phase-matched (NSPM) regime [1]. All demonstrations of NSPM have so far been performed in He and Ne. However, heavier gases, such as Kr or Xe, generally lead to a higher HHG flux because of higher ionic screening effects at the moment of recollision and the lower ionization potential.

To study whether those gases can also lead to an increase in flux at higher photon energies, we use a 100 kHz repetition-rate OPCPA, which produces 340 µJ, 10-fs pulses at 0.8 µm that we focus to an intensity of 3×10^{16} W·cm^{-2}. We detect the soft x-rays (SXR) with the setup described in [2].

When using Kr or Xe, the SXR flux between 150 and 1000 eV is 1 to 2 orders of magnitude higher than in He and Ne. To verify whether those photons originate from HHG or from incoherent plasma radiation, we modify the laser ellipticity with a quarter wave plate (QWP) and record SXR spectra for several QWP angles. We summarize our experimental results in Fig. 1.

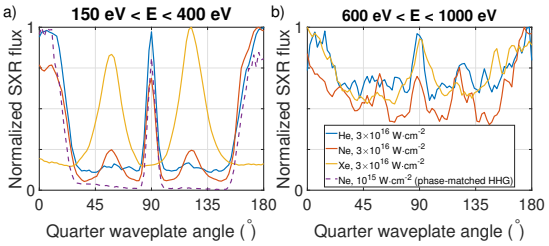


Figure 1. Normalized integrated SXR flux for different gases, different photon energy ranges and peak intensities as a function of the QWP angle.

Between 150 and 400 eV, the flux drops quickly when the polarization is changed from linear (QWP angles of 0, 90° and 180°) to circular (QWP angles of 45° and 135°) in He and Ne (blue and orange curves). The flux follows the same trend as phase-matched HHG performed in Ne (dotted purple curve), indicating that photons in this energy range originate from HHG. In Kr and Xe, the behaviour is very different: at low photon energies, the flux remains almost constant with increasing ellipticity, hinting at an incoherent origin.

Between 600 and 1000 eV, where NSPM is expected to be most pronounced, we observe a SXR flux decrease when the polarization is changed from linear to circular in He, Ne, Kr and Xe. However, when the polarization is fully circular, the flux does not vanish as between 150 and 400 eV, suggesting that the light may originate from a mix of coherent high-harmonics and incoherent plasma radiation.

We note that the flux obtained in Xe is more than 2 orders of magnitude higher than the one in He, making its flux comparable to that obtained with 2.2 µm-driven HHG using the same setup [2]. This finding may represent an alternative route towards high-flux SXR HHG.

References

1. M. Geissler, G. Tempea, and T. Brabec, "Phase-matched high-order harmonic generation in the nonadiabatic limit," Phys. Rev. A **62**, 033817 (2000).
2. P.-A. Chevreuil, F. Brunner, S. Hrisafov, J. Pupeikis, C. R. Philips, U. Keller, and L. Gallmann, "Water-window high harmonic generation with 0.8-µm and 2.2-µm OPCPAs at 100 kHz", Opt. Express **29**, 32996-33008 (2021).

*E-mail: chpierre@phys.ethz.ch

MC

Towards Field Sampling of Ultrabroadband Continuum Radiation from deep-UV to NIR

A Schulte[1,2]*, C Konrad[1,2], M Weidman[1,2], F Krausz[1,2], and J Schötz[1,2]†

[1]Max-Planck-Institute of Quantum Optics, Laboratory for Attosecond Physics, Hans-Kopfermann-Str. 1, 85748 Garching, Germany

[2]Ludwig-Maximilians-Universität München, Am Coulombwall 1, 85748 Garching, Germany

Synopsis We report the generation of ultrabroadband continuum radiation via nonlinear broadening in a gas-filled hollow-core fiber, extending the spectral bandwidth of ultrashort NIR laser pulses down to all across the deep-ultraviolet (DUV) reaching the vacuum-ultraviolet (VUV). We aim to measure the electric field oscillations with nonlinear photoconductive sampling (NPS), a compact attosecond field sampling technique. Hence we aim to extend the bandwidth of this technique towards the VUV, enabling the investigation of light-matter interaction on the attosecond timescale and with DUV photon energies.

The combination of ultrashort laser pulses and field-resolved detection enables the investigation of light-matter interaction on the timescale of the electric field oscillations. Recently, field-resolved detection has been demonstrated down to the UV spectral range, which was limited by the spectral width of the laser pulse [1, 2].

In this work, we present an ultrabroadband continuum ranging from the NIR down to all across the deep-ultraviolet (DUV) reaching the vacuum-ultraviolet (VUV) generated in a gas-filled hollow-core fiber. We aim to measure the electric field oscillations with nonlinear photoconductive sampling (NPS), thereby extending the bandwidth of this technique towards the VUV.

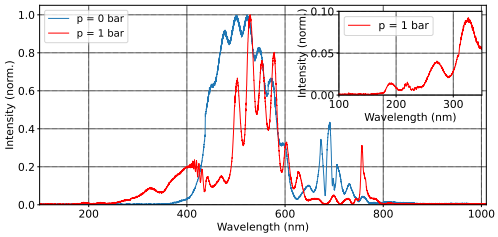


Figure 1. Measured spectrum after the fiber, filled with either 0 or 1 bar of Ar. The inset shows a magnification into the DUV/VUV region.

Here, the output of a 4 fs, CEP-stable, chirped pulse amplified and broadenend Ti:Sapph laser system gets broadened further by self-phase modulation in a gas-filled hollow-core fiber. The spectral bandwidth of the laser radiation is extended in the gas-filled fiber, reaching down to 170 nm. The measured spectrum with and without gas in the fiber is shown in Fig. 1.

We use nonlinear photoconductive sampling (NPS) to perform ultrafast optical field sampling. In this technique, two cross-polarized fields are collinearly focused onto a medium in a pump-probe configuration. The medium can be either a solid [2] or a gas [3, 4] and is surrounded by electrodes that measure the generated electronic current. Electrons are excited from the valence to the conduction band (or ionized in case of gas) via high-order nonlinear photon absorption. The high intensity of the main peak of the incident electric field drives this process and confines it to a duration of hundreds of attoseconds. The thereby created temporal gate allows waveform sampling of the probe pulse with attosecond temporal resolution.

Measurements of the electric field of the above presented broadened light (Fig. 1) will be performed with this NPS technique. We aim to extend the bandwidth of NPS into the DUV, up to 7 eV. This spectral range allows the direct excitation of a large number of different materials. Therefore, ultrafast electronic dynamics in low as well as in large bandgap materials can be studied in the future.

References

[1] A Schiffrin et al., Nature **493**, 70-74 (2013).
[2] S Sederberg et al., Nat. Commun. **11**, 430 (2020).
[3] A Korobenko et al., Optica **7**, 1372 (2020).
[4] D Zimin et al., Optica **8**, 586 (2021).

*E-mail: amelie.schulte@mpq.mpg.de
†E-mail: johannes.schoetz@mpq.mpg.de

Control of high harmonic spectral characteristics in a non-collinear generation geometry

L Gulyás Oldal[1*], P Ye[1,2], Z Filus[1], T Csizmadia[1], T Grósz[1], M De Marco[1], Zs Bengery[1], I Seres[1], B Gilicze[1], P Jójárt[1], K Varjú[1], S Kahaly[1], B Major[1]

[1]ELI ALPS, ELI-HU Non-Profit Ltd., Szeged, H-6728, Hungary
[2]Current address: LIDYL, CEA, CNRS, Université Paris-Saclay, CEA Saclay 91191, Gif-sur-Yvette, France

Synopsis We propose and demonstrate an all optical method to tune the central photon energy and the spectral bandwidth of the high-order harmonics. The technique relies on time domain interference of two replica ultrashort laser pulses and can be employed in any gas based high harmonic generation source, opening up new application possibilities.

It is well known that under appropriate conditions, there is a direct correspondence between the spectral characteristics of the driving laser and high-order harmonics generated in gas [1,2]. Here we introduce an all optical method that benefits from such correlation.

The proposed scheme utilizes the interference of two replica ultrashort pulses, having a pulse duration comparable with the delay between them [3]. This results in spectral interference in the frequency domain with a certain evolution of the electric field in the time domain. This effect was investigated theoretically, and then its impact on the high-order harmonic generation process was studied. We observed variations in the central photon energy and spectral bandwidth of the generated harmonics achieved by introducing controlled delay between the constituting pulses of the double-pulse structure [3].

For experimental validation of the theoretically observed effects, double pulses are produced by a custom-made Split-and-Delay Unit (SDU) [4], which contains two separately movable half mirrors [5]. The SDU splits the driving laser beam into two identical pulses having exactly the same characteristics, including CEP and spectral phase [6]. In the focal plane where the harmonics are generated, the two pulses are overlapped spatially. By using SDU, the delay between the two half beams can be varied and the required spectral interference can be achieved in the driving laser spectrum. Generated harmonic spectra as a function of the time delay between the two replica pulses is shown in Figure 1. The produced harmonics are presented by the colored map. The black dots represent the exact harmonic peaks and the black curves are an estimation of the central photon energy of high harmonics, according to the central angular frequency variation of the driving laser. By applying the proposed technique the central photon energy of the generated harmonics can be tuned within 1000 meV and their spectral bandwidth can be varied in the range of 200 meV [6].

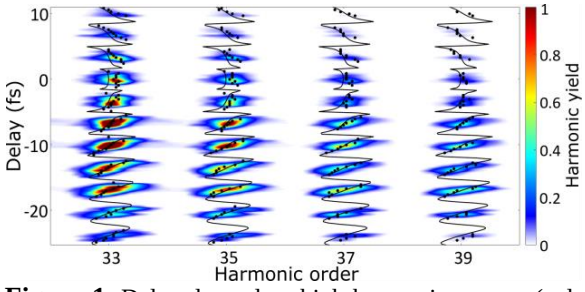


Figure 1. Delay-dependent high harmonic spectra (colored map), the exact spectral position of the harmonic peaks (black dots), and an estimation where the harmonics should appear according to the driving laser (black curves).

References

[1] Salières P *et al* 1995 *Phys. Rev. Lett.* **74** 3776
[2] Ciappina M F *et al* 2012 *Phys. Rev. A* **85** 033828
[3] Gulyás Oldal L *et al* 2020 *Phys. Rev. A* **102** 013504
[4] Campi F *et al* 2016 *Rev. Sci. Instrum.* **87** 023106
[5] Ye P *et al* 2020 *J. Phys. B* **53** 154004
[6] Gulyás Oldal L *et al* 2021 *Phys. Rev. Applied* **16** L011001

* E-mail: lenard.gulyas@eli-alps.hu

MC

High repetition rate few-cycle short-wave infrared light source for strong-field experiments

I Sytcevich[1], A-L Viotti[1,2], C Guo[1], J Vogelsang[1,3], A-K Raab[1], F Langer[1,4] A L'Huillier[1] and C L Arnold[1]*

[1]Department of Physics, Lund University, P.O. Box 118, SE-221 00 Lund, Sweden
[2]Deutsches Elektronen-Synchrotron DESY, Notkestraße 85, 22607 Hamburg, Germany
[3]Institut für Physik, Universität Oldenburg, 26111 Oldenburg, Germany
[4] Present address: Carl Zeiss SMT GmbH, Rudolf-Eber-Straße 2, 73447 Oberkochen, Germany

Synopsis We present a compact 200 kHz short-wave infrared optical parametric chirped pulse amplifier, capable of delivering sub-16 fs carrier-envelope-phase-stable pulses around 2 µm with 13 µJ pulse energy, sufficient to drive high-order harmonic generation in argon.

Recently, compact sources of soft-X-ray radiation driven via High-order Harmonic Generation (HHG) have become more common owing to advances in laser technology. High-power Ytterbium (Yb) lasers are now routinely used to drive Optical Parametric Chirped Pulse Amplifiers (OPCPAs) with central wavelengths in the short-wave infrared (SWIR) and mid-infrared (MIR) spectral regions [1, 2, 3]. On the other hand, direct nonlinear post-compression of Thulium-doped fiber lasers appears to be promising route as well [4].

In this work, we report on the development of a white-light seeded, 200 kHz OPCPA in the SWIR, pumped by the output of an Yb fiber-based Chirped Pulse Amplification (CPA) system. The output features carrier-envelope-phase (CEP) stable, 1600-2500-nm-broad pulses with 13 µJ pulse energy and 15.7 fs duration full width at half maximum.

The OPCPA system presented in this work is inspired by the work of Neuhaus *et al.* [1]. It is based on an Yb-fiber CPA laser, delivering pulses with 180 µJ of energy and duration of 300 fs at 200 kHz repetition rate. Passively CEP-stabilized SWIR pulses are generated via difference frequency generation between the output of a visible noncollinear OPA (NOPA) and the 1030 nm Yb pulses, and further amplified to the energy of 13 µJ in two consecutive NOPA stages. Dispersion management is performed by third-order-dispersion-compensating chirped mirrors and a pair of zinc sulfide wedges, achieving pulses very close to the transform limit. Third-harmonic generation (THG) dispersion-scan (d-scan) is applied for pulse characterisation (Figure 1(a)) and the retrieved pulse duration is 15.7 fs (Figure 1(b)), corresponding to 2.3 cycles at the 2 µm central wavelength.

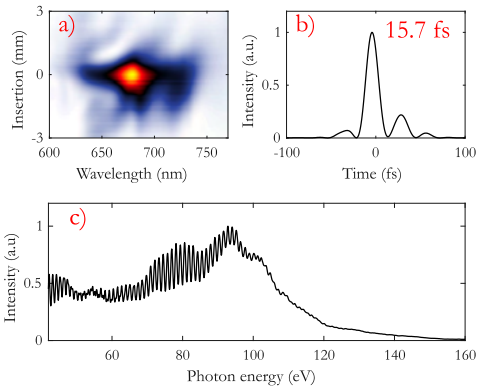


Figure 1. a) Measured THG d-scan trace; b) Retrieved pulse intensity profile; c) High-order harmonic spectrum generated in argon.

The system is capable of driving HHG in argon, obtaining photon energies exceeding 130 eV (Figure 1(c)) in a 40 µm long gas jet with a density corresponding to several bars. Further development and optimization is planned through an upgrade of the Yb pump laser.

References

[1] M. Neuhaus *et al.*, Opt. Express. **26**, 16074-16085 (2018)
[2] J. Pupeikis *et al.*, Optica **7**, 168-171 (2020)
[3] G.M. Archipovaite *et al.*, Opt. Lett **42**, 891-894 (2017)
[4] M.Gebhardt *et al.*, Opt. Lett **42**, 4179-4182 (2017)

*E-mail: cord.arnold@fysik.lth.se

The ELI-ALPS MIR-HE ATTO - design and status of the 1 keV attosecond beamline

F. Campi[1], Torsten Golz[1], J. H. Buss[1], S. Starosielec[1], M. Schulz[1], Subhendu Kahaly[2], Eric Cormier[2,3,4], Sergei Kühn[2], and Katalin Varjú[2] and R. Riedel[1]

[1]Class 5 Photonics GmbH, Luruper Hauptstraße 1, 22547 Hamburg, Germany

[2]ELI-ALPS, ELI-HU Non-Profit Ltd., Wolfgang Sandner utca 3., Szeged, H-6728, Hungary

[3]Laboratoire Photonique Numérique et Nanosciences, CNRS-IOGS-Université Bordeaux, 33400 Talence, France

[4]Institut Universitaire de France (IUF),1 rue Descartes, 75231 Paris, France

Abstract We report on the design and construction of a 1 kHz attosecond beam-line operating in the spectral range from 285 – 1250 eV. The high-pressure gas high harmonic generation (GHHG) source will be driven by a 20 mJ laser system at a central wavelength up to 3 µm, based on optical parametric chirped-pulse amplification (OPCPA).

For the generation of isolated attosecond pulses in the water-window and keV regime, mid-infrared drivers represent a promising road-map [1]. Several groups achieved scaling of the HHG cutoff energy to the water window spectral region [2–7] or even beyond, up to 1.6 keV [8] by exploiting mid-infrared optical parametric amplifiers (OPA). Though, HHG yield decreases dramatically with longer driving wavelengths. The goal of the MIR-HE project is to mark the next milestone in the quest for isolated keV attosecond pulses, and to provide users of the ELI-ALPS facility with XUV/SXR attosecond pulses for pump-probe experiments.

Table 1. Target Specifications of the MIR-HE ATTO Gas-High-Harmonic-Generation (GHHG).

Parameter	Specification
Maximum photon energy using 3 µm driver wavelength	1200 eV
Maximum photon energy using 1600 nm driver wavelength	500 eV
Photon flux at the interaction point using 1600 nm driver wavelength	10^9 ph/s/10% bandwidth at 300 eV

To accomplish this challenge, a robust and stable high-energy, few-cycle mid-infrared laser system producing CEP stabilized pulses is required within the scope of the MIR-HE laser system will be realized. The optical parametric chirped-pulse amplifier (OPCPA) will deliver pulse energies >20 mJ at 3 µm wavelength with few-cycle pulse durations and > 12 mJ at 1.6 µm wavelength with < 100 fs pulse durations. The laser system and beam-line will be operated at a pulse repetition rate of 1 kHz.

The general optical beam-line is divided into major functional modules, all guided in vacuum: (1) GHHG driver beam preparation section, (2) MIR pump optical path and delay unit, (3) High-pressure gas HHG target, (4) High-power MIR/SXR filtering section, (5) SXR focusing and MIR recombination, (6) Experimental chamber for streaking and x-ray near-edge absorption spectroscopy, (7) SXR diagnostics chamber with spectrometer.

The high-pressure GHHG target will cover different generation regimes from high-intensity (> 10^{15} W/cm2) overdriven regime [3] to lower-intensity (10^{14} W/cm2) loose focusing regime [7] by adapting the MIR driver focusing and gas target geometry.

References

[1] Bing Shan *et al.* 2001 *Phys. Rev. A,* **65:011804**.
[2] J. Pupeikis *et al.* 2018 *Optica,* **7(2):168–171**.
[3] Allan S. Johnson *et al.* 2018 *Science Advances,* **4(5)**.
[4] Cédric Schmidt *et al*. 2018 *Opt. Express*, **26(9):11834–11842**.
[5] V Cardin *et al.* 2018 *Phys. B: At. Mol.,* **51(17):174004**.
[6] S. L. Cousin *et al.* 2014 *Opt. Lett.*, **39(18):5383–5386, 2014.**
[7] Fu *et al.* 2020 *Comm. Phys..*, **3(92).**
[8] Popmintchev T *et al.* 2012 *Science*, **336:1287–1291.**

* E-mail: filippo.campi@class5photonics.com

Poster Session II, Highlights A
Chair: **Mihai Vaida**, University of Central Florida, Florida, USA

T58 **Petahertz optical valley switches**
Alvaro Jimenez Galan, Rui Silva, Giulio Vampa, Mikhail Yu. Ivanov 133

T59 **Observation of light driven band structure via multi-band high harmonic spectroscopy**
Ayelet Uzan, Alvaro Jimenez-Galan, Gal Orenstein, Rui Silva, Talya Arusi-Parpar, Sergei Shames, Barry D. Bruner, Binghai Yan, Olga Smirnova, Misha Ivanov, and Nirit Dudovich 134

T62 **Tracing dissociation dynamics and ultrafast cooling in liquid pyridine using time-resolved X-ray absorption spectroscopy**
Tadas Balciunas, Yi-Ping Chang, Zhong Yin, Cedric Schmidt, Vit Svoboda, Thomas Penfold, Jean-Pierre Wolf, Hans Jakob Wörner 135

T63 **Uncovering the mechanism of high-harmonic generation in liquids**
Angana Mondal, Ofer Neufeld, Zhong Yin, Zahra Nourbakhsh, Vit Svoboda, Angel Rubio, Nicolas Tancogne-Dejean, Hans Jakob Wörner 136

T66 **Photoexcited electron and hole dynamics in ZnTe and $ZnTe_xSe_{1-x}$ alloys**
Jonathan Michelsen, Hanzhe Liu, Isabel Klein, Sage Bauers, Andriy Zakutayev, Scott Cushing 137

T67 **Dynamical band imaging of simultaneous light-dressed Volkov state and pho-to-induced carrier state in WSe_2 using high-harmonic-based Tr-ARPES**
Ryo Yoshioka, Yasushi Shinohara, Takuya Okamoto, Yoji Kunihashi, Keiko Kato, Hiroki Mashiko, Yoshiaki Sekine, Hiroki Hibino, Ikufumi Katayama, Jun Takeda, Katsuya Oguri 138

T69 **Ultrafast XUV Magnetic Circular Dichroism: Observing Spin Transport at Interfaces**
Robert Baker, Martin Schutlze, Harshad Gajapathy, Savini Bandaranayake, Emily Hruska, Stephen Londo 139

T70 **Attosecond pulse and crystal band reconstruction with symmetry-aware deep neural networks**
Nikolai Klimkin, Álvaro Jiménez Galán, Rui Silva, Mikhail Yu. Ivanov 140

T71 **Wavelength dependence of high-order haronic generation in a single atomic layer and bulk semiconductors**
Viacheslav Korolev, Vipin Krishna, Mohammad Monfared, Thomas Lettau, Amin Sadeghifaraz, Elnaz Irani, Christian Hünecke, Giancarlo Soavi, Christian Spielmann, Ulf Peschel, Stefanie Gräfe, Daniil Kartashov 141

Petahertz optical valley switches

A Jimenez-Galan[1,2,3]*, R E F Silva[4], G Vampa[1,2] and M Ivanov[3,5,6]

[1]National Research Council of Canada, Ottawa, K1N 5A2, Canada
[2]University of Ottawa, Ottawa, K1N 6N5, Canada
[3]Max Born Institute, Berlin, 12489, Germany
[4]ICMM-CSIC, Madrid, 28050, Spain
[5]Humboldt University, Berlin, 12489, Germany
[6]Imperial College, London, SW7 2BX, United Kingdom

TA

Synopsis We demonstrate a new, ultrafast regime for light manipulation of the valley degree of freedom in 2D semiconductors with which we are able to induce, manipulate and read-out valley polarization on shorter timescales than valley lifetime and decoherence, opening the way to petahertz valley switches.

On-demand modification of quantum material properties is one of the holy grails of material science. Recently, the demonstrated feasibility to apply intense light fields, controlled at the level of individual oscillations [1], to 2D materials without optical damage [2, 3], opened the opportunity to induce and control quantum properties that can be manipulated on the timescales of coherent electron motion.

One of the most relevant quantum properties of 2D semiconductors is their ability to host two valleys in the band structure, at K and K' crystal momenta, that can be selected via circularly-polarized light fields resonant with the excitonic band gap [4]. Yet, to be of practical use, such valley initialization must be accompanied by ultrafast valley manipulation and reading. The one-photon resonant fields that are currently used in valleytronics preclude ultrafast valley switching on timescales shorter than valley lifetime and decoherence (around 100fs in the 10-50K temperature range [5, 6]), limiting their use for future technological applications.

Here, using concepts from attosecond physics, we propose a new regime for valleytronics, epitomized by three schemes that are able to induce, coherently-control and read-out the valley degree of freedom faster than valley decoherence times. In the first of them, a strong, non-resonant field tailored to the symmetry of the lattice is able to controllably lift the valley degeneracy on few-cycle timescales [7]. In the second, a few-cycle, non-resonant linearly-polarized field can drive carrier-envelope-phase-controlled valley population asymmetry [8]. In the third, a train of polarization- and time-controlled weak attosecond pulses is used to switch on and off the valley state in less than 100fs in transition metal dichalcogenides. The latter also allows measurement of excitonic decoherence timescales [9]. In all three schemes, the valley polarization can then be read-out all-optically through even-order high harmonic generation, which we demonstrate experimentally. Attosecond physics in solids holds the promise of petahertz electronics; here we give the necessary steps towards the practical implementation of ultrafast valley switches.

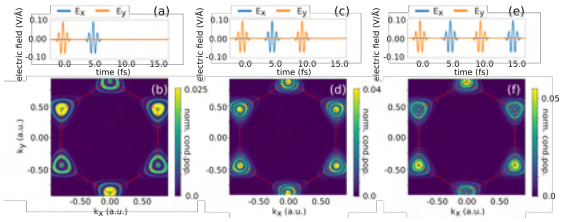


Figure 1. Femtosecond valley switching in hexagonal boron nitride with a train of polarization-controlled attosecond pulses, between (a,b) K-valley polarization, (c,d) no valley polarization, (e,f) K'-valley polarization.

References

[1] A Wirth et al., Science **334**, 6053 (2011).
[2] A Roberts et al., App. Phys. Lett. **99**, 051912 (2011).
[3] H Liu et al., Nat. Phys. **13**, 262 (2017).
[4] J Schaibley et al., Nat. Rev. Mat. **1**, 16055 (2016).
[5] K Hao et al., Nat. Phys. **12**, 677 (2016).
[6] G Moody et al., Nat. Comm. **6**, 8315 (2015).
[7] A Jimenez-Galan et al., Nat. Photonics **14**, 728 (2020).
[8] A Jimenez-Galan et al., Optica **8**, 3 (2021).
[9] A Jimenez-Galan et al., to be submitted (2022).

*E-mail: jimenez@mbi-berlin.de

Observation of light driven band structure via multi-band high harmonic spectroscopy

A Uzan-Narovlansky[1]*, A Jiménez-Galán[2], G Orenstein[3], R E F Silva[4], T Arusi-Parpar[3], S Shames[3], B D Bruner[3], B Yan[3], O Smirnova[2], M Ivanov[2], and N Dudovich[3]

[1]Princeton University, [2]Max-Born-Institute for Nonlinear Optics and Short Pulse Spectroscopy, [3]Weizmann Institute of Science, [4]Universidad Autónoma de Madrid

TA

Synopsis Our work reveals the link between highly nonlinear light-matter interaction in strongly driven crystals and sub-cycle modifications of their effective band structure, providing a general framework for resolving and interpreting light driven band structure.

Intense light-matter interactions have revolutionized our ability to probe and manipulate quantum systems at sub-femtosecond time scales, opening routes to all-optical control of electronic currents in solids at petahertz rates, the time-scale of a single optical cycle [1]. Such control typically requires electric field amplitudes of V/Å, when the voltage drop across a lattice site becomes comparable to the characteristic band gap energies. In this regime, intense light-matter interaction induces significant modifications of electronic and optical properties and is certain to dramatically modify the band structure of the light-dressed crystal [2]. Yet, identifying and characterizing such modifications remains an outstanding problem. As the oscillating electric field changes from V/Å to zero within a quarter-cycle of the driving field, does the band-structure follow, and how can it be defined? Here we address this fundamental question, proposing all-optical spectroscopy of strongly driven crystals, and probe laser-induced closing of the band-gap between adjacent conduction bands [3]. Our work reveals the link between extreme nonlinear light matter interactions in strongly driven crystals to the sub-cycle modifications in their effective band structure.

In our study we describe how the effective band structure can be introduced in such interaction regime within a time-domain perspective. Our theoretical study show that light-induced modifications of the bands are directly linked to the sub-cycle Landau-Dykhne-type transitions between them. Experimentally, we resolve these links using two-color HHG spectroscopy [4], revealing an anomalous spectral intensity response. We identify the dynamical transitions between several conduction bands as well as probe their structural dependence. Importantly, we resolve the clear signature of harmonics emission from an energy gap, between two conduction bands, probing its modification by the laser field. This study provides a general framework for resolving and interpreting attosecond electronic response phenomena in strongly driven solids.

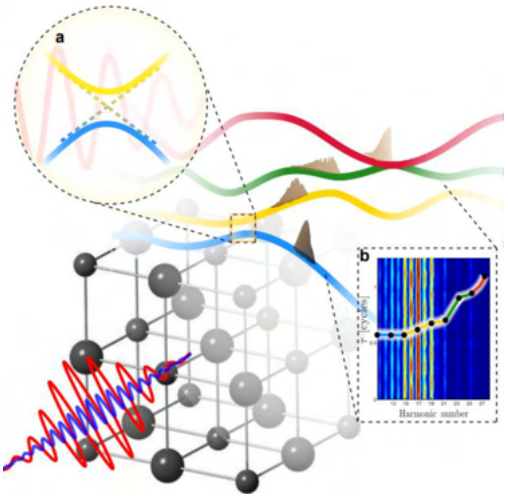


Figure 1. a, Non-adiabatic Landau-Dykhne transition between a pair of bands. b, Two color HHG spectroscopy probes the internal dynamics.

References

[1] M Garg *et al.*, Nature **538**, 359 (2016).
[2] A Schiffrin *et al.*, Nature **493**, 70 (2013).
[3] A Uzan-Narovlansky *et al.*, *Accepted at Nature Photonics*.
[4] G Vampa *et al.*, Nature **522**, 462 (2015).

*E-mail: auzan@princeton.edu

Tracing dissociation dynamics and ultrafast cooling in liquid pyridine using time-resolved X-ray absorption spectroscopy

T Balčiūnas[1], Y–P Chang[2], Z Yin[1], C Schmidt[2], V Svoboda[1], T Penfold[3], J-P Wolf[2] and H J Wörner[1]

[1] Laboratory for Physical Chemistry, ETH Zürich, 8093 Zürich, Switzerland
[2] GAP-Biophotonics, Université de Genéve, 1205 Geneva, Switzerland
[3] Newcaste University, NE1 7RU Newcastle upon Tyne, UK

TA

Synopsis In this work, by utilizing time-resolved soft X-ray transient absorption spectroscopy of liquid and gaseous pyridine at the carbon and nitrogen K-edges, we reveal the different reaction pathway dynamics initiated by multiphoton ionization. We show that photolytic cage effect and excited cationic state cooling via environment-coupled vibrational relaxation leads to long-lived cationic, ring-open and hydrogen-transfer isomerized species in the liquid phase, while in the gas phase the excess energy leads to fragmentation.

Ultrafast pump-probe investigations facilitate the direct probing of the highly non-equilibrium state created by the initial photoexcitation, which often leads to a number of dissipation channels, including radiative decay and non-radiative processes such as internal conversion (IC) and intramolecular vibrational redistribution (IVR). These are usually accompanied by structural modifications which can lead to isomerisations, such as ring-opening, and/or bond fission. The ultrafast dynamics of ionization-induced bond fission have been revealed by time-resolved X-ray transient absorption (TR-XAS) spectroscopy at the carbon and nitrogen K-edges [4], while photoinduced isomerization studied using X-ray and electrons for the model system 1,3-cyclohexadiene [3] and prototypical heterocyclic molecule, 2(5H)-thiophenone [5]. These studies have been performed in the gas-phase, providing exquisite information about the purely intramolecular relaxation pathways. However, changes occurring upon the transition from the gas to the condensed phase is crucial for understanding the role a surrounding medium (typically a solvent) has on the intermediates and product states formed during a transformation.

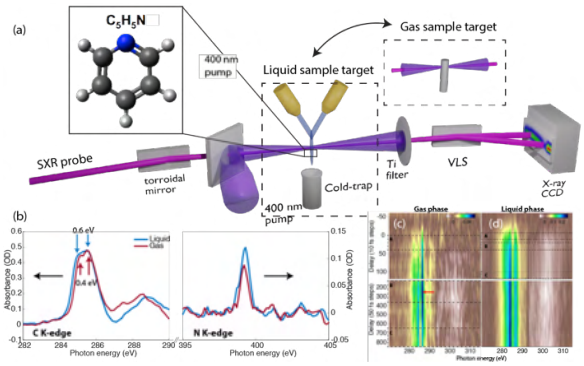


Figure 1. (a) experimental scheme; (b) measured transmission spectra of liquid ethanol and methanol at C-K and N-K absorption edges; (c, d) time-resolved X-ray differential absorption spectra of pyridine in the gas and liquid phases.

Here we demonstrate the key role played by intermolecular interactions in selecting the reactive pathways after strong-field ionization using TR-XAS in a liquid (pyridine, C_5H_5N). While the pyridine cation is stabilized in an isomerized structure via ring-opening and hydrogen-transfer in the liquid phase, it dissociates into fragments involving ring-open intermediates in the gas phase. The broadband soft-X-ray probe pulse covers the carbon and nitrogen absorption edges as outlined in Fig. 1 (b). The experimental setup allows directly comparing the dynamics in liquid and gas phase samples thus enabling the direct comparison of dynamics in the two phases. The transient absorption signal in liquid and gas samples (Fig. 1 (c-d)) exhibit features on different time scales in the 1 ps time range and were attributed to the differences of photoionized pyridine dissociation and isomerization in the gas phase and rapid cooling of excited cationic states in the liquid phase. The analysis has been performed using the static molecular structure XAS (hydrogen migration, ring-opening, fragmentation) based on DFT calculations of reactive pathways and fitting of the statistical weight via a least square optimization procedure. In order to verify the most probable fragmentation channels in the gas phase, we performed complementary experiments using mass spectrometry that indicate ≈ 30 % yield of the fragmentation channel.

References

[1] C. Schmidt, Y. Pertot, T. Balciunas, K. Zinchenko, M. Matthews, H. J. Wörner, and J.-P. Wolf, Opt. Express **26**, (2018).
[2] Y. Pertot, C. Schmidt, M. Matthews, A. Chauvet, M. Huppert, V. Svoboda, A. von Conta, A. Tehlar, D. Baykusheva, J.-P. Wolf, and H. J. Wörner, Science (80) (2017).
[3] A. R. Attar, A. Bhattacherjee, C. D. Pemmaraju, K. Schnorr, K. D. Closser, D. Prendergast, and S. R. Leone, Science 356, 54–59 (2017).
[4] A. D. Smith, T. Balciunas, Y.-P. Chang, C. Schmidt, K. Zinchenko, F. B. Nunes, E. Rossi, V. Svoboda, Z. Yin, J.-P. Wolf, and H. J. Wörner, J. Phys. Chem. Lett. 1981–1988 (2020).
[5] Pathak, S. et al. Nat. Chem. 12, 795–800 (2020).

TA

Uncovering the mechanism of high-harmonic generation in liquids

A Mondal[1], O Neufeld[2,3], Z Yin[1], Z Nourbakhsh[2,3], V Svoboda[1], A Rubio[2,3,4,5], N Tancogne-Dejean[2,3] *, and H J Wörner[1] †

[1]Laboratorium für Physikalische Chemie, ETH Zürich, Zurich, Switzerland
[2]Max Planck Institute for the Structure and Dynamics of Matter, Hamburg, Germany
[3]Center for Free-Electron Laser Science CFEL, DESY, Hamburg, Germany
[4]The Hamburg Centre for Ultrafast Imaging, Department of Physics, University of Hamburg, Germany
[5]Center for Computational Quantum Physics (CCQ), The Flatiron Institute, New York, USA

Synopsis High-harmonic generation (HHG) in gases is well-described by the three-step model (TSM) that explains the quadratic scaling of the cut-off energy (E_c) on the wavelength (λ) and field amplitude (E). However, in liquids, we show that E_c is wavelength-independent above a threshold intensity. An intuitive semi-classical model of electron trajectories limited by a liquid-dependent scattering length is proposed and validated by rigorous ab-initio calculations. Our results reveal the HHG process in liquids and allow for the extraction of the effective mean-free paths of slow electrons ($\leq$ 10 eV) in liquids.

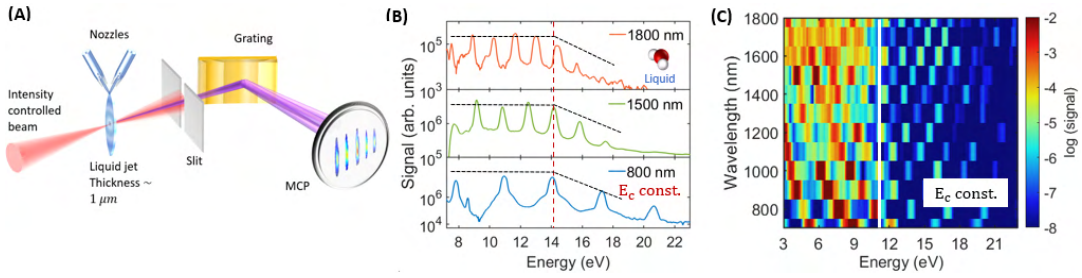


Figure 1. (A) Schematic of the HHG setup in liquids. (B) High-harmonic spectra of liquid water measured for different wavelengths at 4.3-4.4·10^{13}W/cm^2. The E_c is indicated by the red dashed line. (C) TDDFT simulations of HHG in water clusters show a constant E_c (white solid line) over a broad range of wavelengths.

The success of high-harmonic spectroscopy in unravelling attosecond electron dynamics in gases can be attributed to the robustness of the TSM, especially in predicting properties like the $(E\lambda)^2$ scaling of E_c [1]. This has made temporal mapping of molecular orbitals and charge-migration dynamics [2, 3] possible. In crystalline solids a linear $E\lambda$ scaling of E_c was proposed based on a trajectory model in momentum space [4]. Since the lack of single-particle approximation (like in gases) or long-range order (like in crystalline solids) make numerical simulations challenging for liquids, and experiments are scarce no such intuitive model exists thus far.

Here, we show that the E_c for liquid water and alcohols, measured over a broad spectrum of drivers, is wavelength independent and significantly lower than the TSM prediction. Using a combination of ab-initio simulations, we explain these observations and develop a scattering-limited trajectory model for HHG in liquids. Our model successfully reproduces the wavelength independence of E_c and identifies the effective mean-free path (λ_{MFP}) as the principal factor in defining E_c. We support this conclusion by showing that increasing λ_{MFP} (by decreasing the liquid density), in both experiments and simulations, increases E_c because longer trajectories with higher kinetic energies are able to recombine with the parent molecule. Our results provide the first intuitive picture of liquid-phase HHG and pave the way for attosecond spectroscopy of bio-chemical processes in their native liquid environment.

*E-mail: nicolas.tancogne-dejean@mpsd.mpg.de
†E-mail: hansjakob.woerner@phys.chem.ethz.ch

References

[1] P B Corkum, Phys. Rev. Lett. **71**, 1994 (1993).
[2] J. Itatani *et al.*, Nature **432**, 2004 (2004).
[3] P.M. Kraus *et al.*, Science **350**, 2015 (2015).
[4] S. Ghimire and D. A. Reis, Nature physics **15**, 2019 (2018).

Photoexcited electron and hole dynamics in ZnTe and $ZnTe_xSe_{1-x}$ alloys

J. M. Michelsen[1], H. Liu[1], I. M. Klein[1], S. R. Bauers[2], A. Zakutayev[2] and S. K. Cushing[1] *

[1]Division of Chemistry and Chemical Engineering, California Institute of Technology, Pasadena, CA 91125, USA.
[2]Materials Science Center, National Renewable Energy Laboratory, Golden, CO 80401, USA.

Synopsis Carrier-specific kinetics control reactivity in photoelectrochemistry, where photoexcited electrons or holes drive reduction or oxidation reactions. We report the measurement of photoexcited electron and hole dynamics, mid-gap defect states, and phonon oscillations in ZnTe and $ZnTe_xSe_{1-x}$ using transient reflectivity extreme ultraviolet (XUV) spectroscopy. This measurement enables the extraction of ultrafast electron and hole thermalization times. We robustly assign experimentally observed features with a theoretical approach based on density functional theory and the Bethe-Salpeter equation.

TA

Photoelectrochemical CO_2 reduction is an attractive strategy for converting captured CO_2 to useful chemical products such as liquid fuels. The development of efficient photoelectrodes is critical for enabling the CO_2 reduction reaction (CO2RR) and other PEC reactions. II-VI semiconductors, including ZnTe and ZnSe, are promising photocathodes for CO2RR due to their suitable band gap and negative conduction band minimum. Further, the bandgap and band alignment of these materials can be tuned through alloying.

We report the measurement of excited state carrier dynamics and phonon oscillations in ZnTe and $ZnTe_xSe_{1-x}$ using transient extreme ultraviolet (XUV) reflectivity spectroscopy. We track the carrier and structural dynamics by probing the Te 4d absorption edge around 40 eV after photoexcitation with a ~50 fs, 400 nm pump pulse. We observe increased absorption at the valence band corresponding to photogenerated holes, as well as decreased absorption at the conduction band from photoexcited electrons. These features at the valence and conduction band are confirmed to correspond to photoexcited electrons and holes using theoretical modeling based on density functional theory and the Bethe-Salpeter equation (BSE). Comparing the materials, we observe the dynamic population of midgap states in bulk ZnTe, attributed to surface defects.

We present the use of the BSE equation to model the effects of photoexcited carriers on transient XUV spectra. We developed a novel approach based on the OCEAN package, using excited state rather than ground state carrier occupations to calculate the core-hole transition matrix. To incorporate excited state effects, we input these modified valence and conduction band occupations and fit the corresponding XUV spectra to experimental data.

With this carrier-specific measurement, we can extract electron and hole thermalization kinetics. We report the thermalization of hot electrons to the conduction band minimum within the first 100 fs after photoexcitation, as well as the thermalization of hot holes to the valence band maximum within the first picosecond. Finally, we investigate the effect of atomic substitution in a thin film $ZnTe_xSe_{1-x}$ sample on carrier dynamics, including thermalizion.

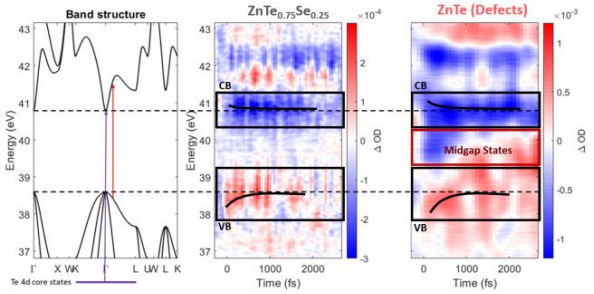


Figure 1. The photoexcited electron and hole occupations are probed with a core-level probe as illustrated ontop of the band structure for ZnTe (left panel). The resulting transient spectra are shown for thin film $ZnTe_{0.75}Se_{0.25}$ (center panel) and bulk ZnTe (right panel). In bulk ZnTe, we observe dynamic population of midgap states, attributed to surface defects.

References

[1] Biswas S *et al* 2018 *Chem. Commun.* **54** 4216-4230
[2] Zürch M *et al* 2017 *Nat. Commun.* **8** 15734

* E-mail: scushing@caltech.edu

TA

Dynamical band imaging of simultaneous light-dressed Volkov state and photo-induced carrier state in WSe_2 using high-harmonic-based Tr-ARPES

R. Yoshioka[1,2], Y. Shinohara[1], T. Okamoto[1], Y. Kunihashi[1], K. Kato[3], H. Mashiko[4], Y. Sekine[1], H. Hibino[5], I. Katayama[2], J. Takeda[2] and K. Oguri[1]*,

[1] NTT Basic Research Laboratories, NTT Corporation, Atsugi, Kanagawa 243-0198, Japan
[2] Department of Physics, Yokohama National University, Yokohama, Kanagawa 240-8501, Japan
[3]Department of Chemistry, Nagoya University, Nagoya, Aichi 464-8602, Japan
[4] Center for Ultrafast Intense Laser Science, The University of Tokyo, Tokyo 113-0033, Japan,
[5] School of Science and Technology, Kwansei Gakuin University, Sanda, Hyogo 669-1337, Japan

Synopsis Employing time- and angle-resolved photoemission spectroscopy (Tr-ARPES) based on sub-5-fs high harmonic source, we have demonstrated dynamical band imaging for coherent lightwave-matter interaction in a layered semiconductor WSe_2. Our data clearly shows the instantaneous replica band originated from the light-dressed Volkov state of the valence band accompanied with the incoherent carrier population simultaneously photoexcited in the conduction band. This observation is an important step towards realizing the coherent manipulation of Bloch electronic system with petahertz lightwave field.

The coherent manipulation of a quantum degree of freedom in solid state systems by an intense and well-controlled lightwave field with petahertz frequency has attracted much attention as one of the most promising future directions in attosecond technology [1]. Interaction between intense lightwave and Bloch electronic system generally induces remarkable modification of band structure, but it is still challenging to directly investigate instantaneous change of band structures. Here we show that Tr-ARPES technique is capable of dynamical band imaging for coherent lightwave-matter interaction throughout the Brillouin zone with a few femtosecond temporal resolution.

The experiment was performed by our developed Tr-ARPES system based on the 27th high-harmonic source at 42.1 eV with 5-fs temporal duration [2]. By irradiating 34-fs pump pulse, we measured a light-dressed response of the band structure for a cleaved single crystal of 2H-WSe_2 along the Γ - *K* direction at room temperature.

Figure 1 shows typical snapshots of ARPES spectra without (Fig. 1(a)) and with pump irradiation at the timing when the peaks of the pump and probe pulses just overlap. A linearly *p*-polarized pump pulse with an energy of 1.56 eV was introduced to the sample (Fig. 1(b)). A U-shape energy band transiently appeared approximately 1.5 eV above the valence band (V. B.) between the Γ and *K* points. When the *s*-polarized pump pulse was introduced, the U-shape band almost completely disappeared (Fig. 1(c)). The shape of the band and its pump polarization dependence support that the U-shape band corresponds to the

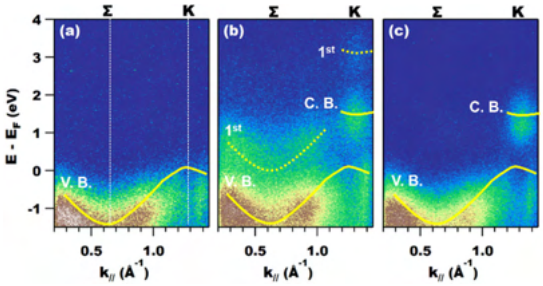


Figure 1. Snapshots of ARPES spectra at the zero time-delay (a) without and with the irradiation of (b) *p*- and (c) *s*- polarized pump pulse. The peak intensity was 8×10^{11} W/cm^2. Yellow solid and dashed curves are eye guides for V. B. and C. B., and Volkov state.

replica band characterized by the first-order Volkov state of the V. B., which has been known as laser-assisted photoelectric effect [3]. In addition, a resonantly photoexcited electronic population in the conduction band (C. B.) clearly appeared at the *K* point across the band gap. Interestingly, the replica of the photoexcited population was also observed at the *K* point 1.5 eV above the C. B. This Tr-ARPES observation has confirmed that an intense lightwave simultaneously induces coherent Volkov state of the V. B., incoherent photoexcited state of C. B., and the coupling of both states at the earliest stage of light-matter interaction.

This work was partially supported by JSPS KAKENHI #19H02637, 20H02703, and 20H05670.

References

[1] Langer F *et al*., *Nature* **557**, 76 (2018).
[2] Toume K *et al*., Jtu2A.153 *CLEO* (2018).
[3] Mahmood F *et al*., *Nat. Phys*. **12**, 306 (2016).

* E-mail: katsuya.oguri.hf@hco.ntt.co.jp

Ultrafast XUV Magnetic Circular Dichroism: Observing Spin Transport at Interfaces

L R Baker[1 *], M Schultze[2], H Gajapathy[1], S Bandaranayake[1], E Hruska[1], and S Londo[1]

[1]Department of Chemistry and Biochemistry, The Ohio State University, Columbus, Ohio, 43210, USA
[2]Institute of Experimental Physics, Graz University of Technology, Graz, Austria

TA

Synopsis XUV magnetic circular dichroism performed in reflection geometry provides direct observation of spin-dependent electron dynamics at material surfaces. A combination of linearly and circularly polarized XUV spectroscopy provides a detailed picture of site-dependent electron dynamics in yttrium iron garnet. This material consists of two sublattices with anti-aligned spins, which can be resolved using circularly polarized XUV light at the Fe $M_{2,3}$-edge. Findings show that site dependent hopping in the two spin sublattices give rise to a spin polarized current upon band gap excitation.

In this talk, we describe the recent ability to directly observe spin-polarized electron transport at semiconductor surfaces using XUV Magnetic Circular Dichroism (XUV-MCD) in a reflection geometry. The ability to produce spin polarized currents at interfaces underlies many promising applications ranging from spintronics to enantioselective photocatalysis, but designing materials capable of these applications requires an improved understanding of spin-dependent electron dynamics at interfaces.

Towards this goal, XUV reflection-absorption spectroscopy provides direct observation of electron dynamics with ultrafast time resolution and surface sensitivity.[1,2] In this recent work, we extend linearly polarized XUV-RA spectroscopy to perform time-resolved MCD measurements of the magnetic structure and spin transport at the surface of yttrium iron garnet ($Y_3Fe_5O_{12}$, YiG).

YiG is a ferrimagnetic semiconductor, consisting of two sub-lattices based on octahedrally and tetrahedrally coordinated Fe(III) centers. A combination of linearly and circularly polarized XUV measurements at the Fe $M_{2,3}$-edge of YiG provides a detailed picture of these lattice-dependent electron dynamics. Due to the anti-alignment of the two sub-lattices, site dependent electron hopping gives rise to spin polarized current upon band gap excitation. These findings have important applications towards the development of spin selective photocatalysts as well as new platforms for light-induced control of ultrafast spin polarization at material interfaces.

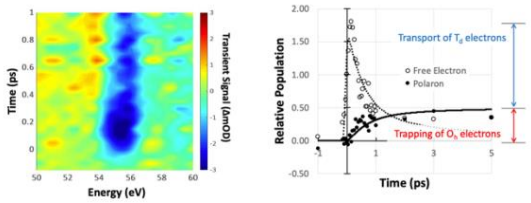


Figure 1. Transient linear XUV-RA spectrum of YiG measured at the Fe $M_{2,3}$-edge (left). Kinetic analysis of spectral data showing ultrafast transport of T_d electrons in comparison to polaronic trapping of O_h electrons (right).

References

[1] Biswas S *et al* 2018 *ChemComm.* **54** 4216.
[2] Bandaranayake, S *et al* 2020 *J. Phys. Chem. C* **124** 22853.

* E-mail: baker.2364@osu.edu

TA

Attosecond pulse and crystal band reconstruction with symmetry-aware deep neural networks

N Klimkin[1,2,3]*, Á Jiménez-Galán[1], R E F Silva[4] and M Ivanov[1,5,6]

[1] Max Born Institute, Max-Born Straße 2A, D-12489 Berlin, Germany
[2] Russian Quantum Center, Bolshoy Bulvar 30, bld. 1, Moscow, Russia 121205
[3] Faculty of Physics, Lomonosov Moscow State University, Leninskie Gory 1-2, Moscow 119991
[4] Dpto. Física Teórica de la Materia Condensada, Universidad Autónoma de Madrid, Madrid, Spain
[5] Department of Physics, Humboldt University, Newtonstraße 15, D-12489 Berlin, Germany
[6] Blackett Laboratory, Imperial College London, South Kensington Campus, SW7 2AZ London, United Kingdom

Synopsis High-order harmonics generation (HHG) spectra contain a multitude of information about the underlying attosecond electron dynamics of a system, but extracting such information proves to be a challenge even with advanced numerical methods. We compute theoretical HHG spectra for unknown crystals with various noise disturbances within and beyond the ranges expected in a typical HHG experiment. We then use symmetry-aware deep neural networks to demonstrate the reconstruction of various pulse parameters, including the carrier envelope phase (CEP), and the crystal band parameters.

The experimentally demonstrated capability to generate CEP-stable near- and mid-IR pulses spanning an octave necessitates advanced methods of measuring the phase properties of such pulses. The currently used methods (FROG, SPIDER, D-Scan) do not resolve the CEP, which becomes crucial when the pulse length is comparable to a single fundamental laser cycle. Additionally, a pioneering experiment [1] has recently been reported, demonstrating that a pulse waveform can be extracted using nonlinear response, subject to well-known and well-characterized nonlinearity, for relatively weak pulses. The nonlinearity of the response changes in the interaction region if intense light-matter interaction is desired, and we extend the findings to this high-intensity regime, looking at the pulse directly in the interaction region, and assuming no detailed *a priori* knowledge of the material.

We compute a large set of CEP-dependent solid-state HHG spectra from short pulses for various band parameters and pulse shapes. For each of the simulated experiments, the measurements are conducted while varying the CEP on a uniform grid between φ_0 and $\varphi_0 + 2\pi$, where the initial CEP φ_0 is chosen randomly. We apply strong amplitude noise to the spectra and phase noise to the pulses. We train a deep neural network (NN) to resolve the 2-dimensional spectra in the $\omega - \varphi$ coordinates by reproducing the CEP, band and spectral phase parameters correctly.

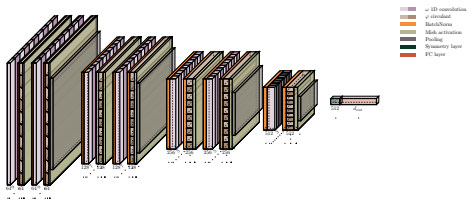


Figure 1. The architecture of the NN used in the work. For the CEP resolution, the final FC layer is complex-valued.

We introduce a custom symmetry-aware architecture of the NN. All transformations along the φ axis are defined by circulant matrices that preserve the invariance of the underlying data to circular shifts. This allows to either force the outputs to be strictly angle-invariant, such as for the band and the spectral phase parameters, or define a specific form of angle variance for the CEP angle.

We demonstrate accurate recovery of the underlying parameters even for highly nonlinear spectral phases and a wide range of band gaps.

References

[1] Liu Y, Beetar JE, Nesper J, Gholam-Mirzaei S, Chini M. Single-shot measurement of few-cycle optical waveforms on a chip. Nature Photonics. 2021 Dec 13:1-4.

*E-mail: Nikolai.Klimkin@mbi-berlin.de

Wavelength dependence of high-order haronic generation in a single atomic layer and bulk semiconductors

V Korolev[1*], V Krishna[2], M Monfared[3], T Lettau[3], A Sadeghifaraz[4], E Irani[4], C Hünecke[5], G Soavi[2], C Spielmann[1,6], U Peschel[3], S Gräfe[5], D Kartashov[1,†]

[1]Institute of Optics and Quantum Electronics, Friedrich-Schiller University Jena, Max-Wien-Platz 1, 07743 Jena, Germany
[2]Institute of Solid State Physics, Friedrich-Schiller University Jena, Helmholtzweg 3, 07743 Jena, Germany
[3]Institute of Condensed Matter Theory and Solid State Optics, Friedrich Schiller University Jena, Fröbelstieg 1, 07743 Jena, Germany
[4]Department of Physics, Faculty of Basic Sciences, Tarbiat Modares University, P.O. Box 14115-175, Tehran, Iran
[5]Institute of Physical Chemistry, Friedrich Schiller University Jena, Helmholtzweg 4, 07743 Jena, Germany
[6]Helmholtz-Institut Jena, Helmholtzweg 4, 07743 Jena, Germany

TA

Synopsis We report results of our experimental investigation of high-order harmonic generation in a single atomic layer WS_2 crystal and comparing it to the bulk as a function of the laser wavelength. We show that the harmonic emission yield drops exponentially when increasing the wavelength in both samples. Our results underline importance of the dephasing time and allow its precise determination.

The basic model of high-order harmonic generation (HHG) in solids, based on the density matrix equations, requires the introduction of a dephasing time to match experimentally measured spectra [1]. Although the concept of such a phenomenological dephasing time is still under debates [2], its value significantly determines the theoretically predicted wavelength dependence of the HHG yield [1,3].

Here, we present results in which we experimentally measured the dependence of the HHG yield in solids as a function of the laser wavelength. To avoid the contribution of propagation effects, the experiments are carried out within a single atomic layer WS_2 deposited on a sapphire substrate. For comparison, the same wavelength dependence of the HHG yield was also measured for multilayer (bulk) WS_2 crystal and a polycristaline 140 nm thick CdSe film.

The integrated yield of harmonics for a single layer and bulk WS_2 is shown in Fig.1. We observe an exponential drop in the yield of both, below and above bandgap harmonics when increasing the laser wavelength for both samples. A similar dependence is observed also for the CdSe film, confirming that such a dependence is a rather universal phenomenon not linked to particular material.

Our experimental results, supported by numerical simulations, solve the puzzle of the empirical dephasing time and allow a quite precise determination of its value.

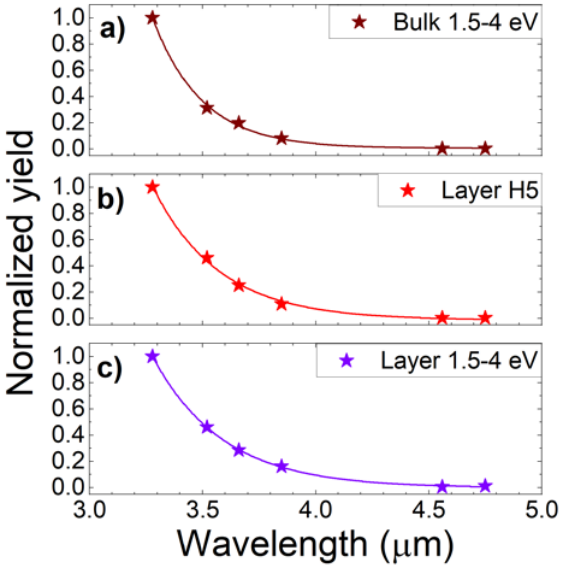


Figure 1. Wavelength dependence of the integrated harmonic yield for a) above bandgap harmonics in bulk WS_2, b) below bandgap 5th and c) above bandgap harmonics in a single layer WS_2.

References

[1] Vampa G *et al* 2014 *Phys.Rev.Lett.* **113** 073901
[2] Floss I. *et al* 2018 *Phys.Rev. A* **97** 011401
[3] Liu X. *et al* 2018 *Phys.Rev. A* **98** 063419

* E-mail: viacheslav.korolev@uni-jena.de
† E-mail: daniil.kartashov@uni-jena.de

Poster Session II, Highlights C
Chair: **Richard Taïeb**, Sorbonne Université, Paris, France, EU

T01 **Probing molecular dynamics using ultrafast XUV transient spectroscopy**
John E Beetar, Sonia Marggi Poullain, Kristina Chang, Yuki Kobayashi, Stephen R Leone 143

T02 **Imaging intramolecular hydrogen migration via polarization-averaged molecular-frame photoelectron angular distributions**
Keisuke Hatada, Shigeru Abe, Soki Goto, Yoshiaki Tamura, Fukiko Ota, Hao Xue, Manabu Kanno, Naoki Kishimoto, Kiyoshi Ueda, Sergio Díaz-Tendero, Fernando Martín 144

T07 **Attosecond coincidence spectroscopy of CH_4 and CD_4**
Dominik Ertel, David Busto, Hamed Ahmadi, Jakub Benda, Marvin Schmoll, Matteo Moioli, Ioannis Makos, Fabio Frassetto, Luca Poletto, Robert Moshammer, Claus Dieter Schröter, Thomas Pfeifer, Zdeněk Mašín, Serguei Patchkovskii, Giuseppe Sansone 145

T08 **State-resolved attosecond photoionization of molecular nitrogen**
Mikhail Osolodkov, Tobias Witting, Federico Furch, Claus Peter Schulz, Vicent Borràs, Jesús González-Vázquez, Fernando Martín, Marc Vrakking 146

T12 **Direct observation of dissociation dynamics of methyl iodide by two-color time resolved photo-electron spectroscopy**
Mariusz Lejman, Dominique Platzer, Alice Autuori, Basile Wurmser, David Bresteau, Thierry Ruchon, Jérôme Palaudoux, Francis Penent, Pascal Lablanquie, Gildas Goldsztejn, Loïc Journel, Renaud Guillemin, Oksana Travnikova, Tatiana Marchenko, Denis Cubaynes, Marc Simon, Basile Wurmser, Richard Taïeb, Jérémie Caillat, Pascal Salières 147

T13 **Rotating the rotationless: Laser-induced dynamics of the 4He dimer**
Jan Kruse, Maksim Kunitski, Qingze Guan, Dörte Blume, Reinhard Dörner 148

T20 **Probing autoionization and dissociation at conical intersections with photoelectron spectroscopy and interferometry**
Dipayan Biswas, James K. Wood, Alexander Plunkett, Arvinder Sandhu 149

T21 **Femtosecond-resolved chiroptical switching in methyl-lactate**
Vincent Wanie, Etienne Bloch, Erik P. Månsson, Lorenzo Colaizzi, Krishna Saraswathula, Sergey Ryabchuk, François Légaré, Andrea Trabattoni, Valérie Blanchet, Marie-Catherine Heitz, Nadia Ben Amor, Yann Mairesse, Bernard Pons, Francesca Calegari 150

T28 **Ion-Photoelectron Entanglement Controlled with Attosecond Pulse Pairs**
Jun Wang 151

Probing molecular dynamics using ultrafast XUV transient spectroscopy

J. Beetar[1], S. Marggi Poullain[2], K. F. Chang[1] Y. Kobayashi[1] and S. R. Leone[1,3,4]

[1]Department of Chemistry, University of California, Berkeley, CA 94720, USA.
[2]Departamento de Química Física, Universidad Complutense de Madrid, 28040, Madrid, Spain, EU
[1]Department of Chemistry, University of California, Berkeley, CA 94720, USA.
[3]Chemical Sciences Division, Lawrence Berkeley National Laboratory, Berkeley, CA 94720, USA.
[4]Department of Physics, University of California, Berkeley, CA 94720, USA

Synopsis Ultrafast extreme ultraviolet transient absorption spectroscopy is employed to investigate the electronic and nuclear dynamics on small polyatomic iodinated molecules. The motion of the wavepacket on the excited states is directly mapped allowing to visualize in real-time the photodynamics. The results presented include imaging coherent nuclear motion in molecular iodine and visualizing the wavepacket bifurcation at the conical intersection in the photodissociation of alkyl iodides.

Attosecond probing of core-to-valence electronic transitions is a powerful tool for real-time observation of chemical dynamics.[1] Here, ultrafast extreme ultraviolet (XUV) transient absorption spectroscopy is employed to investigate the electronic and nuclear dynamics on small polyatomic iodinated molecules. The dynamics induced by one- or two-photon absorption using either few-femtosecond visible pulses, ranging between 500 nm and 900 nm, or 20-fs UV pulses around 260-280 nm is probed by XUV attosecond isolated pulses through iodine-4d core-to-valence transitions.

This method allows us to directly map in real time the motion of the wavepacket on the excited states, due to the strong shift of the XUV core-to-valence transitions with internuclear separation and the high sensitivity of the wave packet to the electronic configuration. The result presented will involve the direct visualization of time-resolved photodynamics from a diatomic system (I_2) to polyatomic molecules.

First, coherent nuclear motion in the B excited state of molecular iodine is visualized with great detail [2] including the wave packet spreading and later recompression, at the outer and inner turning points, respectively. Second, the photodissociation dynamics of alkyl iodides such as CH_3I, C_2H_5I and C_3H_5I, following one-photon absorption into the A band, is imaged in real-time [3, 4]. In particular, the wave packet bifurcation at the conical intersection is mapped. Structural effects, with special attention to the presence of a double bond, on the dissociation dynamics will be considered.

* E-mail: smarggi@ucm.es

References

[1] Kobayashi Y *et al* 2019 *Science* **375** 79
[2] Marggi Poullain S *et al* 2021 *Phys. Rev. A* **104** 022817
[3] Chang K F *et al* 2020 *Nature Comm.* **11** 4042.
[4] Chang K F *et al* 2021 *J. Chem. Phys.* **154** 234301.

TB

Imaging intramolecular hydrogen migration via polarization-averaged molecular-frame photoelectron angular distributions

K Hatada[1]*, S Abe[1], S Goto[1], Y Tamura[1], F Ota[1], H Xue[2], M Kanno[2], N Kishimoto[2], K Ueda[2], S Díaz-Tendero[3,4,5], and F Martín[3,4,6]

[1]Department of Physics, University of Toyama, 3190 Gofuku, 930-8555 Toyama, Japan
[2]Department of Chemistry, Tohoku University, 6-3 Aramaki Aza-Aoba, Aoba-ku, 980-8578 Sendai, Japan
[3]Departamento de Química, Módulo 13, Universidad Autónoma de Madrid, 28049 Madrid, Spain, EU
[4]Condensed Matter Physics Center (IFIMAC), Universidad Autónoma de Madrid, 28049 Madrid, Spain, EU
[5]IAdChem, Universidad Autónoma de Madrid, 28049 Madrid, Spain, EU
[6]IMDEA-Nano, Campus de Cantoblanco, 28049 Madrid, Spain, EU

Synopsis We theoretically investigated the signature of ultrafast hydrogen dynamics in polarization-averaged molecular-frame photoelectron angular distributions and studied intramolecular hydrogen migrations by the spectra for CH_3OH^{2+}, $C_2H_5OH^{2+}$ and $C_3H_7OH^{2+}$.

Ultrafast hydrogen migration in a molecule is one of the most important processes in chemistry and biochemistry. To probe it is, however, a challenge because of the small X-ray scattering cross-section of the hydrogen atom and a requirement of a high temporal resolution of ~ 1 fs. One way to overcome these limitations is to measure photoelectron angular distributions emitted from a core level of the molecule by an attosecond X-ray pulse, in the molecular frame, averaged over the incident X-ray polarization, abbreviated as PA-MFPADs. In the present study, we have performed Global Reaction Route Mapping (GRRM) and Molecular Dynamics (MD) simulations to find the trajectories of hydrogen migration in CH_3OH^{2+}, $C_2H_5OH^{2+}$ and $C_3H_7OH^{2+}$, which are to be created via Auger decay after core-level photoionization, and then calculated PA-MFPADs along the trajectories corresponding to the hydrogen migration. Our results demonstrate that the intramolecular hydrogen migration accompanied with the photodissociation, which occurs within 20 fs, can be visualized by the time-resolved PA-MFPADs measurements.

The isomeric photo-dissociation trajectory of CH_3OH^{2+} was explored using the GRRM and MD simulations for both triplet and singlet states. For MD simulations, the initial velocities of individual atoms were randomly sampled assuming that the excess vibrational energy of 5 eV was obtained by instantaneous electronic relaxation and the temporal evolution of the nuclear coordinates after the initial time $t = 0$ was traced. 1000 classical trajectories were computed for both singlet and triplet states. For $C_2H_5OH^{2+}$ and $C_3H_7OH^{2+}$, only MD simulations were carried out for the singlet states [1, 2]. The PA-MFPADs calculations were performed for trajectories corresponding to hydrogen migrations, using the multiple scattering theory with the muffin-tin approximation, at photoelectron kinetic energies 100 eV and 2500 eV. To simulate the experiments that may be carried out in the future, we took the averages over tens of trajectories.

The results for C 1s and O 1s PA-MFPADs of CH_3OH^{2+} calculated from a single trajectory show a clear peak in the direction from the emitter to the migrating hydrogen atom for both energies 100 eV and 2500 eV, though the signals are clearer for 2500 eV. The peak moves from the C site to the O site, as a function of time. The peak appears also after the average over the tens of trajectories, illustrating that the hydrogen migration can be imaged by the time-resolved PA-MFPADs measurements. We obtained similar results for O 1s PA-MFPADs of $C_2H_5OH^{2+}$ [1]. Further investigations for O 1s PA-MFPADs of $C_3H_7OH^{2+}$ using structures from MD simulations [2] are in progress.

References

[1] F. Ota *et al.*, *Phys. Chem. Chem. Phys.*, **23**, 20174-20182 (2021).
[2] D. Mishra *et al.*, *Phys. Chem. Chem. Phys.*, **24**, 433-443 (2022).

*E-mail: hatada@sci.u-toyama.ac.jp

Attosecond coincidence spectroscopy of CH_4 and CD_4

D Ertel[1*], D Busto[1,2], H Ahmadi[1], J Benda[3], M Schmoll[1], M Moioli[1], I Makos[1], F Frassetto[4], L Poletto[4], R Moshammer[5], C D Schröter[5], T Pfeifer[5], Z Mašín[3], S Patchkovskii[6] and G Sansone[1†]

[1]Institute of Physics, University of Freiburg, Freiburg, 79104, Germany
[2]Department of Physics, Lund University, Lund, 22100 Sweden
[3]Institute of Theoretical Physics, Charles University, Prague, 180 00, Czech Republic
[4]CNR-Institute of Photonics and Nanotechnologies (CNR-IFN), Padova, 35131, Italy
[5]Max-Planck-Institute for Nuclear Physics, Heidelberg, 67119, Germany
[6]Max-Born-Institute for Nonlinear Optics and Short Pulse Spectroscopy, Berlin, 12489, Germany

TB

Synopsis The investigation of the photoionization process occurring in atoms and molecules gives insight into electronic and coupled electronic-nuclear correlation effects. Here, we present angle-resolved measurements of dissociative and non-dissociative photoionization of CH_4 and CD_4 combining attosecond photoelectron interferometry and electron-ion coincidence spectroscopy.

Attosecond photoionization of atomic or even molecular systems has been widely explored in attosecond science. The measurement of photoionization time delays over last decade has provided unprecedented insights into the role of electron correlations in atomic systems [1]. Time delay measurements in molecules is more challenging due to the lack of spherical symmetry and the high density of accessible ionic states resulting in spectrally congested photoelectron spectra. This problem can be partially circumvented by combining attosecond measurement techniques with angle-resolved electron-ion coincidence detection [2,3].

In this work we use the RABBIT (reconstruction of attosecond beating by interference of two-photon transitions) technique [4] to investigate photoionization dynamics in CH_4 and CD_4. Our experimental setup combines a 50 kHz attosecond pulse-train source with a reaction microscope and an ultra-stable collinear attosecond interferometer, consisting of two drilled fused silica plates [5]. This design offers attosecond passive stability and allows us to acquire experimental data over several days.

CH_4/CD_4 are of particular interest as one of the simplest hydrocarbons. Figure 1 shows experimental photoelectron spectra for the cation (CH_4^+, left) and the dissociated fragment (CH_3^+, right) as a function of XUV-IR delay integrated over all orientations of the CH_4 molecule and electron emission angle. We measure angle-integrated and angle-resolved amplitude and phase of the photoelectrons, which are in good agreement with theoretical calculations combining state of the art photoionization [6] and nuclear dynamics approaches [7]. The comparison of the results obtained in CH_4 and CD_4 allows us to get new insights into the role of nuclear motion in attosecond photoionization dynamics.

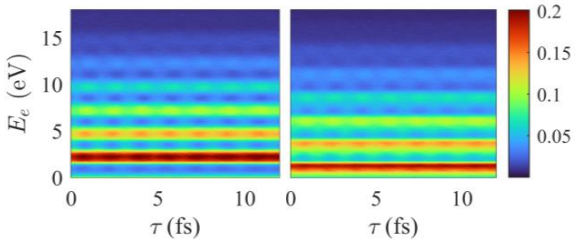


Figure 1. Recorded RABBIT traces (photoelectron energy E_e over XUV-IR delay τ) for the CH_4^+-ion (left) and the dissociated fragment CH_3^+-ion (right).

References

[1] Pazourek R *et al* 2015 *Rev. Mod. Phys.* **87** 765
[2] Vos J *et al* 2018 *Science* **360** 1326
[3] Cattaneo L *et al* 2018 *Nature Phys.* **14** 733
[4] Paul P M *et al* 2001 *Science* **292** 1689
[5] Ahmadi H *et al* 2020 *J. Phys. Photonics* **2** 024006
[6] Benda J *et al* 2021 *Sci. Rep.* **11** 11686
[7] Patchkovskii S *et al* 2017 *Phys. Rev. A* **96** 053405

* E-mail: dominik.ertel@physik.uni-freiburg.de
† E-mail: giuseppe.sansone@physik.uni-freiburg.de

State-resolved attosecond photoionization of molecular nitrogen

M Osolodkov[1]*, T Witting[1], F J Furch[1], C P Schulz[1], V J Borrás[2], J González-Vázquez[2], F Martin[2] and M J J Vrakking[1]

[1]Max Born Institute, Berlin, 12489, Germany; [2]Universidad Autónoma de Madrid, 28049, Spain

TB

Synopsis Attosecond photoionization dynamics ending in the predissociative C state of molecular nitrogen ion is studied with vibrational resolution using the RABBITT technique. The corresponding photoelectron signals are accessed by detecting electrons and ions in coincidence. The experimentally determined photoionization delays are compared with atomic references revealing a non-trivial energy dependence. This finding is attributed to the multi-electron nature of the XUV-induced ionization process.

Studying ultrafast photoionization dynamics in molecules is presently one of the hot topics in attosecond science. Here we report on a series of RABBITT (Reconstruction of Attosecond Beating By Interference of Two photon Transitions) experiments on the predissociating $C\,^2\Sigma_u^+$ state of N_2^+, performed at the attosecond beamline combining a table-top high-order harmonic generation (HHG) based extreme ultraviolet (XUV) laser pulse source with a reaction microscope (REMI). The HHG setup is driven by a 100 kHz noncollinear optical parametric chirped pulse amplification (NOPCPA) system operating at 800 nm central wavelength and delivering few-cycle laser pulses with approximately 7 fs duration [1]. Using these pulses for HHG relatively short attosecond pulse trains (APTs) containing approximately 7 pulses are obtained [2].

The measurements were performed in gas mixtures of N_2 with argon or helium, respectively. Due to the electron-ion coincidence capability of the REMI, the RABBITT spectrograms of nitrogen and the rare gases could simultaneously be measured. Photoelectrons accompanying the formation of different vibrational states ($v = 3, 4, 5$) of the C state were identified by the kinetic energy release of the N_2^+ ions determined from the momentum of the detected N^+ fragments. From the acquired RABBITT spectrograms the photoionization delays were extracted, which show a non-trivial energy dependence with respect to the atomic reference. This behaviour may be attributed to the multi-electron nature of the XUV-induced transition to the N_2^+ C state. For a deeper understanding of the observed effect theoretical calculations are required and are currently in progress.

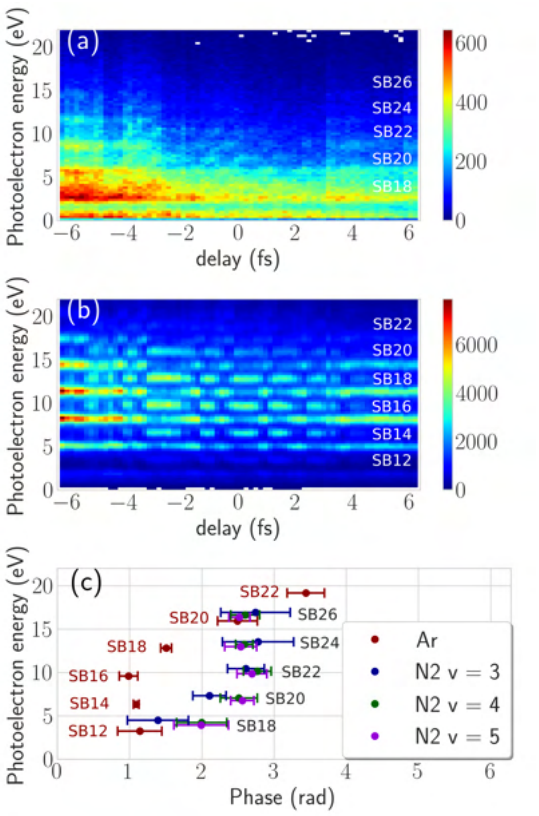


Figure 1. The RABBITT spectrograms measured simultaneously in the vibrational state $v = 4$ of the N_2^+ $C\,^2\Sigma_u^+$ state (a) and in Ar as reference (b). The extracted sideband phases are shown in (c).

References

[1] F J Furch *et al.*, Optics Letters **42**, 2017
[2] M Osolodkov *et al.*, J. Phys. B: At. Mol. Opt. Phys. **53**, 2020

*E-mail: Mikhail.Osolodkov@mbi-berlin.de

Direct observation of dissociation dynamics of methyl iodide by two-color time resolved photo-electron spectroscopy

M. Lejman[1], D. Platzer[1], A. Autuori[1], B. Wurmser[2], D. Bresteau[1], T. Ruchon[1], J. Palaudoux[2], F. Penent[2], P. Lablanquie[2], G. Goldsztejn[3], L. Journel[2], R. Guillemin[2], O. Travnikova[2], T. Marchenko[2], D. Cubaynes[3], M. Simon[2], R. Taïeb[2], J. Caillat[2,], P. Salières[1] *.

[1]Université Paris-Saclay, CEA, CNRS, LIDYL, 91191 Gif-sur-Yvette, France
[2] Sorbonne Université, CNRS, Laboratoire de Chimie Physique-Matière et Rayonnement, 75005 Paris, France
[3] Université Paris-Saclay, CNRS, Institut des Sciences Moléculaires dOrsay, 91405 Orsay, France

TB

Synopsis We present and analyse the direct detection of transient excitation and dissociation dynamics of methyl iodide probed by ATI spectra in a $\omega - 3\omega$ scheme.

Methyle iodide (CH_3I) is a workhorse of ultrafast dynamics experiments, extensively studied since the 1940's by means of different techniques, either using single or multiphoton ionization and detecting ionic fragments or photoelectrons, see *eg* [1]. These previous studies showed that the probed dynamcis can be influenced by many channels involved in the process.

Here, we study the dissociative dynamics of CH_3I probed through resonant multiphoton ATI detected in a Magnetic Bottle Electron Spectrometer, using a 267 nm (3ω) - 800 nm (ω) pump-probe scheme. The underlying mechanism could be identified using several models accounting for the observed electron spectra and the ionisation yields dependencies with respect to the pump-probe delay τ and to the field intensities.

In particular, when varying τ the ATI yields exhibits a long-lived exponential tail with a typical decay time of 75 ± 5 fs, see Figure below. This characteristic time cannot be assigned to the lower A-dissociative state and one has to invoke a path involving complex excitation scheme through bound states coupled to dissociative ones.

Furthermore, the obtained spectra exhibit ATI peaks corresponding to the $\tilde{X}(^2E_{3/2})$ and $\tilde{X}(^2E_{1/2})$ channels, see Figure below. In between, one clearly sees an additional peak, labelled R, indicating another ionization path. We assigned the latter to a transient excitation by the probe occuring at specific internuclear distances, in a process reminiscent of a Freeman resonance [2].

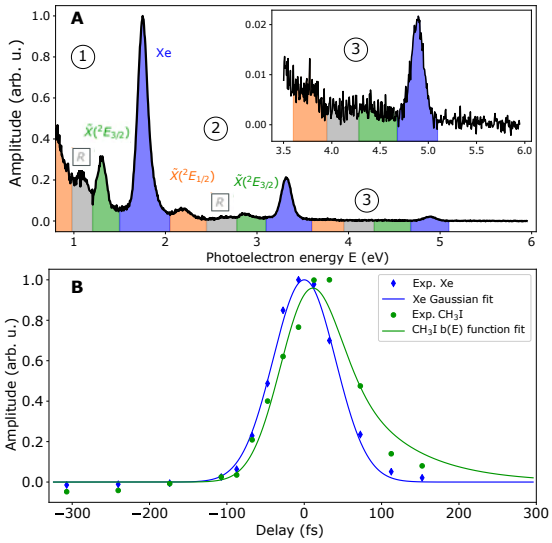


Figure 1. (A) Typical spectrum obtained in a Xe-CH_3I mixture. (B) evolution of the integrated Xe (blue) and CH_3I lowest ATI peaks as a function of the pump-probe delay τ.

References

[1] R. S. Mulliken, J. Chem. Phys., **8**, 382 (1940) ; J. Durá *et al*, J. Chem. Phys. **131**, 134311 (2009) ; A. Tehlar and H. J. Wörner, Molecular Physics **111** 2057 (2013) ; F. Brauße *et al*, Phys. Rev. A **97**, 043429 (2018).

[2] R. R. Freeman *et al*, Phys. Rev. Lett. **59**, 1092 (1987).

*E-mail: jeremie.caillat@sorbonne-universite.fr

Rotating the rotationless: Laser-induced dynamics of the ^{4}He dimer

J Kruse[1] *, M Kunitski[1] †, Q Guan[2], D Blume[2] and R Dörner[1]

[1]Institut für Kernphysik, Goethe-Universität, Frankfurt am Main, 60483, Germany
[2]Homer L. Dodge Department of Physics and Astronomy, The University of Oklahoma, Norman, 73019, US

TB

Synopsis The helium dimer $^4He_2$ is a fragile bound state of two helium atoms, being delocalized over a large region of space. It is said to be a quantum halo state, since the bulk of the dimer wave function resides in the classically forbidden tunnel region. We use a combination of the pump-probe technique and Coulomb explosion imaging in order to observe the time-resolved dynamics of the helium dimer, which is initiated by a femtosecond laser pulse. We report the laser-induced population of a quantum superposition, in which the $J = 0$ dimer ground state interferes with the dissociative $J = 2$ angular momentum state.

The weakness of the helium-helium interaction gives rise to exotic quantum effects in small helium clusters, such as the huge quantum halo state of the helium dimer $^4He_2$ and the Efimov state of the helium trimer $^4He_3$, which is a huge quantum halo as well [1]. Previous experiments demonstrated that the helium dimer has a size of 200 Å, while its binding energy is only 152 neV [2]. Because of the tiny binding energy, the helium dimer exists only in the rotational ground state. Higher angular momentum states, however, are unbound since the helium-helium potential is rendered repulsive by the centrifugal barrier. Here, we investigate the response of the helium dimer if acted on by a laser-induced torque [3]. In our experiment, dimers are produced in the supersonic expansion of helium gas by the collisions of single helium atoms. Subsequently, dimers are mass-selected from the gas jet by matter-wave diffraction at a grating [4]. Temporal information about the laser-induced response of the dimer is obtained by a pump-probe scheme, in which an ionizing probe pulse measures the dynamics initiated by a non-ionizing pump pulse. Changes in the spatial structure of the dimer wave function are observed by Coulomb explosion imaging: The probe pulse triggers the Coulomb explosion of dimers by singly ionizing each of the two atoms. Since the Coulomb repulsion depends on the separation of the ions, the internuclear distance, as well as the orientation of the dimer axis at the instant of ionization are imprinted onto the ion momenta gained in the Coulomb explosion. In this experiment, the ion momenta are measured in coincidence by a COLTRIMS reaction microscope.

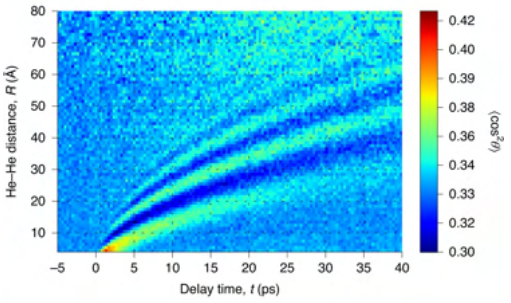


Figure 1. Observed spatial and temporal evolution of the anisotropy of the angular dimer wave function.

We observe the population of a quantum superposition of the $J = 0$ dimer ground state and the dissociative $J = 2$ angular momentum state due to the action of the pump pulse. The superposition evolves in space and time. For example, Figure 1 shows the evolution of the anisotropy of the angular dimer wave function. Here, the anisotropy is quantified by $\langle \cos^2 \theta \rangle$, where θ is the angle between the dimer axis and the field direction of the linearly polarized pump pulse. The observed response of the helium dimer is quite different from the field-induced dynamics of other noble gas clusters, like, e.g., the argon dimer [5], which evolve in time as bound rotational wave packets.

References

[1] M Kunitski et al., Science **348**, 551 (2015).
[2] S Zeller et al., PNAS **113**, 14651 (2016).
[3] M Kunitski et al., Nat. Phys. **17**, 174 (2020).
[4] W Schöllkopf et al., Science **266**, 1345 (1994).
[5] J Wu et al., Phys. Rev. A. **83**, 061403 (2011).

*E-mail: kruse@atom.uni-frankfurt.de
†E-mail: kunitski@atom.uni-frankfurt.de

Probing autoionization and dissociation at conical intersections with photoelectron spectroscopy and interferometry

D Biswas[1]*, J K Wood[1], A Plunkett[1] and A Sandhu[1]†

[1] Department of Physics, University of Arizona, Tucson, Arizona 85721, USA

Synopsis We probe the evolution of molecular Rydberg wavepacket near the ionic conical intersection in carbon dioxide using differential photoelectron spectroscopy. We employ a new approach of Raman photoelectron interferometry which simultaneously yields high spectral and temporal resolution. Our results provide insight into the interaction of Rydberg electron with the ion-core undergoing non-adiabatic dynamics and we report the competing predissociation and autoionization lifetimes. Our study paves the path for energy-resolved probing of complex electron hole dynamics near the conical intersection of polyatomic molecules.

TB

Attosecond XUV-IR pump-probe techniques have opened the doors to the study of electronic correlations and coupled electron-nuclear dynamics. In particular, the photoelectron spectroscopy is a powerful tool to investigate the electron dynamics in atoms and molecules. However, the time-resolved photoelectron interferometry is usually poor in energy resolution due to time-bandwidth constraints. In a new approach to photoelectron interferometry, we demonstrate that the probe-induced stimulated Raman transitions, followed by a delayed autoionization detection can be used to simultaneously obtain high spectral and temporal resolution[1]. This technique offers new opportunities to study the dynamics of autoionizing Rydberg states near the conical intersection [2] in carbon dioxide.

An attosecond XUV pulse excites the carbon dioxide molecule to its neutral autoionizing Rydberg states above the first ionization threshold. These states, termed Henning and Tanaka-Ogawa series, can either autoionize to the lowest continuum limit($X^2\Pi_g$) of CO2 or dissociate into neutral fragments with very different timescales for the two pathways. The IR probe further ionizes the neutral Rydberg states as well as their neutral dissociation fragments to corresponding continuum limits of $A^2\Pi_u$ and $B^2\Sigma_u^+$ ionic states.

In Fig. 1, we show the differential increase in the photoelectron signal (red features) in conjunction with the decrease in autoionization yield (blue features) due to the action of probe pulse. From these results, we obtained the previously unexplored lifetimes of Rydberg states, which highlight the competition between autoionization and predissociation. Furthermore, by using the quantum number selectivity in our energy resolved data, we are able to investigate how the interaction of the Rydberg electron with the ion-core impacts the conical intersection dynamics [2] between vibronically coupled ionic states.

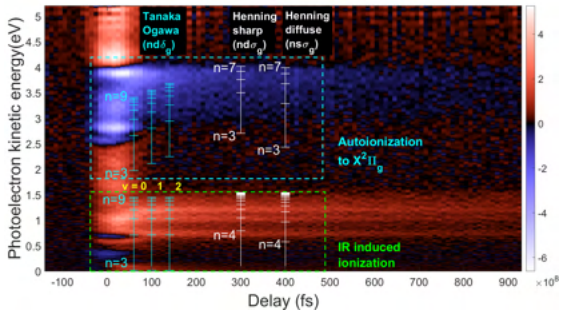


Figure 1. Differential photoelectron spectrogram in carbon dioxide molecule using an attosecond XUV pump and a delayed infrared probe.

This work was supported by the National Science Foundation grants 1912455 and 1919486 and the U.S. Department of Energy, Office of Science, Basic Energy Sciences, Award No. DE-SC0018251.

References

[1] A. Plunkett, M. A. Alarcon, J. K. Wood, C. H. Greene, and A. Sandhu, Raman interferometry between autoionizing states to probe ultrafast wavepacket dynamics with high spectral resolution, Phys. Rev. Lett. (in press) arXiv:2111.03975

[2] H. Timmers, Z. Li, N. Shivaram, R. Santra, O. Vendrell, and A. Sandhu, Coherent electron hole dynamics near a conical intersection, Phys. Rev. Lett. **113**, 11303 (2014)

*E-mail: dbiswas@email.arizona.edu
†E-mail: asandhu@email.arizona.edu

TB

Femtosecond-resolved chiroptical switching in methyl-lactate

Vincent Wanie[1*], Etienne Bloch[2], Erik P. Månsson[1], Lorenzo Colaizzi[1,3], Krishna Saraswathula[3], Sergey Ryabchuk[3,4], François Légaré[5], Andrea Trabattoni[1], Valérie Blanchet[2], Marie-Catherine Heitz[6], Nadia Ben Amor[6], Yann Mairesse[2], Bernard Pons[2], Francesca Calegari [1, 3, 4]

[1]Center for Free-Electron Laser Science, Deutsches Elektronen-Synchrotron DESY, Hamburg, 22607, Germany
[2]Université de Bordeaux - CNRS - CEA, CELIA, Talence, F-33405, France
[3]Physics Department, Universität Hamburg, Hamburg, 22761, Germany
[4]The Hamburg Centre for Ultrafast Imaging, Universität Hamburg, Hamburg, 22761, Germany
[5]Institut National de la Recherche Scientifique, Varennes, J3X 1P7, Canada
[6]CNRS, UPS, LCPQ (Laboratoire de Chimie et Physique Quantiques), FeRMI, Toulouse, F-31062, France

Synopsis Investigating UV-induced molecular dynamics at the few-femtosecond and attosecond timescales has long been impeded because of the difficulties to generate and manipulate ultrabroadband, few-femtosecond UV pulses. Here, we use a novel light source delivering such pulses to study the UV-induced Rydberg states dynamics of chiral methyl-lactate. Time-resolved photoelectron circular dichroism (TR-PECD) reveals a sub-10 fs periodic inversion of the photoelectron emission direction in the laboratory frame. The corresponding oscillation is barely visible in the angularly integrated electron yield, highlighting the capabilities of TR-PECD to study chiral systems.

The recent advances of few-femtosecond (fs) UV light sources open a route to the investigation of important UV-induced phenomena with unprecedented temporal resolution [1].

We present a pump-probe experiment combining linearly polarized few-fs UV pulses [2] and few-cycle circularly polarized near-infrared (NIR) pulses for time-resolved measurements in chiral molecules (Fig. 1a). Following UV-photoexcitation of methyl-lactate – a derivative of lactic acid, the relaxation dynamics of Rydberg states lying just below the ionization threshold is tracked through time-resolved photoelectron circular dichroism (TR-PECD), a method that was identified to be a sensitive probe of the transient properties of chiral molecules [3].

Photoelectron angular distributions are recorded as a function of the pump-probe time delay with a velocity map imaging spectrometer. For each time delay, an image is acquired for both left (LCP) and right circular polarization (RCP) of the probe pulse. The resulting differential image, defined as (LCP-RCP) and normalized to the average signal [0.5(LCP+RCP)], is shown in Figure 1b for two distinct time delays. The high temporal resolution of the experiment allows us to capture a periodic inversion of the photoelectron forward-backward asymmetry within a timescale as short as 6 fs. We will present an energy-resolved analysis of the PECD images, comparing both enantiomers of methyl-lactate. Noteworthy, the oscillations are not visible in the standard angularly integrated electron yield.

Ongoing theoretical modelling indicates that the UV-pump pulse induces Rydberg electronic beatings which may be responsible for the experimental observations. Our results show that TR-PECD is the suitable tool to investigate the few-femtosecond dynamics of a large variety of chiral bio-relevant molecules.

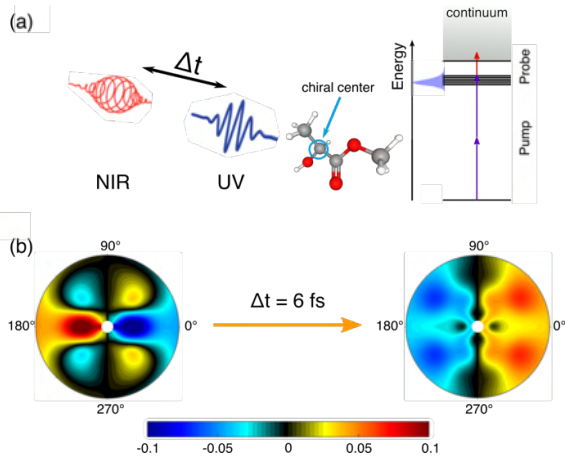


Figure 1. (a) Exciting and probing methyl-lactate molecules. (b) PECD at probe times t=5 fs and t=11 fs, illustrating an inversion of the forward-backward asymmetry along the light propagation axis, defined from left to right. The radial axis of the plots is associated to the photoelectron kinetic energy which ranges from 25 to 300 meV.

References

[1] Wanie V *et al* 2021 in *Emerging Laser Technologies for High-power and Ultrafast Science*. IOP publishing
[2] Galli M *et al* 2019 *Opt. Lett.* **44**, 1308-1311
[3] Comby A *et al* 2016 *JPCL* **7**, 4514-4519

* E-mail: vincent.wanie@desy.de

Ion-Photoelectron Entanglement Controlled with Attosecond Pulse Pairs

J Wang[1,2]* on behalf of the X400 Collaboration

[1]Stanford PULSE Institute, SLAC National Laboratory, Menlo Park, CA, USA, 94025
[2]Department of Applied Physics, Stanford University, Stanford, CA, USA, 94305

Synopsis With phase-stable pulse pairs generated in Linac Coherent Light Source (LCLS), we study the control of entanglement in photoionization of nitrous oxide (N_2O). The advent of attosecond x-ray pulses facilitates the study on coherence of core-hore wavepacket from the perspective of ion-photoelectron entanglement.

Coherent spectroscopies provide methods for probing dynamics with high precision, and extending these spectroscopies to the x-ray domain will provide new insights into electronic dynamics. A subfemtosecond pulse can create superpositions of hole states in molecules, producing an entangled ion-photoelectron system. The entanglement plays an important role in coherent properties of the ion or electron [1]. To this end, we use phase-stable x-ray pulse pairs produced by an x-ray free electron laser (FEL) source to create interesting hole states in N_2O.

The spectra of the $\sim$ 800 eV pulse pair produced by the split-undulator configuration of the Linac Coherent Light Source (LCLS) [2], is shown in Figure 1(a). The spectral fringes are shifted by controlling the phase shifter between adjacent undulator sections. The bandwidth of the pulses is sufficiently broad to cover the energy spacing between the core-hole cation states at the terminal and central nitrogen atoms (N_t^{-1} and N_c^{-1}), leading to an entangled ion-photoelectron system. By shifting of spectral fringes, it is possible to manipulate the overlap between photoelectron wave-packets and thus the entanglement [3]. We study the degree of entanglement with the correlation between photoelectron and Auger-Meitner (AM) electron, shown in the electron-electron partial covariance map plotted in Fig. 1(b). By varying the fringe spacing in the pulse pair, we are able to modify the entanglement.

*E-mail: junwang9@stanford.edu

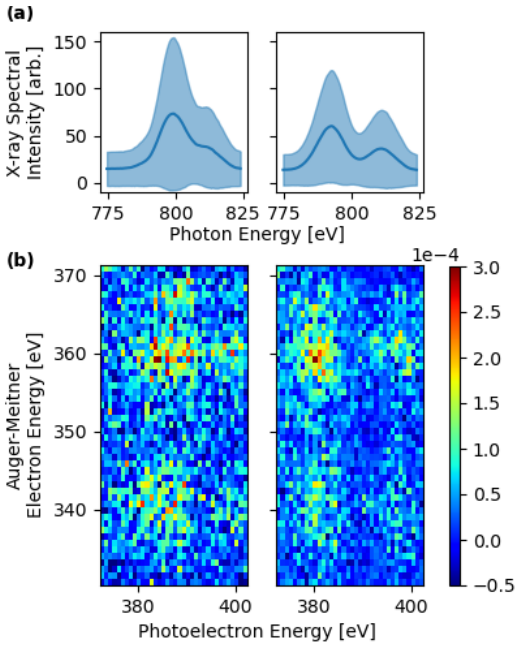


Figure 1. Comparison between two sets of phase shift. (a) Intensity spectra of the pulse pair, with the solid line (shaded region) indicating the mean (1σ region) over shots; (b) Partial covariance maps at the energy region corresponding to the correlation of photoelectron and AM electron.

This work was supported by the U.S. Department of Energy (DOE), Office of Science, Office of Basic Energy Sciences (BES), Chemical Sciences, Geosciences, and Biosciences Division (CSGB). Use of the (LCLS), SLAC National Accelerator Laboratory, is supported by the DOE, Office of Science, BES under Contract No. DE-AC02-76SF00515.

References

[1] E Goulielmakis, Nature **466**, 739–743 (2010).
[2] J Duris, Nat. Photonics. **14**, 30–36 (2020).
[3] M Vrakking, Phys. Rev. Lett. **126**, 113203 (2021).

Poster Session II, Highlights C
Chair: **Nicolas Douguet**, Kennesaw University, Georgia, USA

T36 **Characterization of light-induced potentials in the strong-field dissociation of O_2^+**
Uwe Thumm, Paul Abanador . . . 153

T37 **Attosecond dynamics in O_2 with ASTRA, a transition-density-matrix approach to molecular ionization**
Carlos Marante, Juan Martín Randazzo, Heman Gharibnejad, Barry I. Schneider, Jeppe Olsen, Luca Argenti . . . 154

T41 **Attosecond pump-probe spectroscopy of quantum electronic coherence**
Marco Ruberti . . . 155

T42 **Theory behind the real-time imaging of resonant photoemission dynamics**
Alice Autuori, Dominique Platzer, Mariusz Lejman, Guillaume Gallician, Lucie Maëder, Antoine Covolo, Lea Bosse, Malay Dalui, David Bresteau, Jean-François Hergott, Olivier Tcherbakoff, Hugo J B Marroux, Vincent Loriot, Franck Lepine, Lionel Poisson, Pascal Salières, Jérémie Caillat, Richard Taïeb . . . 156

T46 **Stationary molecular R-matrix approach for above-threshold multi-photon ionization and the coupling delay in RABITT processes**
Jakub Benda, Zdeněk Mašín, Jimena Gorfinkiel . . . 157

T47 **Three-Sideband RABBITT in Argon: Experiment and Theory**
Divya Bharti, Hemkumar Srinivas, Farshad Shobeiry, Robert Moshammer, Thomas Pfeifer, Kathryn Hamilton, Klaus Bartschat, Anne Harth . . . 158

T50 **Angle-resolved phases in photoemission: from atomic to molecular systems**
Roger Bello, Fernando Martín . . . 159

T51 **Attosecond electron dynamics near the ionization threshold in Ne**
Kathryn Hamilton, Klaus Bartschat, Matteo Moioli, Hamed Ahmadi, David Busto, Dominik Ertel, Ioannis Makos, Marvin Schmoll, Maria M. Popova, Elena V. Gryzlova, Alexei N. Grum-Grzhimailo, Maxim D. Kiselev, Sergey N. Yudin, Claus Dieter Schröter, Robert Moshammer, Thomas Pfeifer, Giuseppe Sansone . . . 160

T55 **Spectral Signature of Molecular Charge Migration**
Rubén Fernández Carbón, Luca Argenti . . . 161

Characterization of light-induced potentials in the strong-field dissociation of O_2^+

U Thumm[1]* **and P Abanador**

Department of Physics and J. R.Macdonald Lab., Kansas State University, Manhattan, KS 66506, USA

Synopsis We numerically examine the imprints of light-induced potentials (LIPs) on the dissociation dynamics of O_2^+ molecular ions, as observed in angle-resolved fragment kinetic-energy-release (KER) spectra, following the vibrational and rotational motion of O_2^+ molecular ions exposed to 800-nm, 40-fs laser pulses. For peak intensities between 10^{13} and 10^{14} W/cm^2, we calculate angle-resolved KER spectra, which reveal characteristic energy- and angle-dependent fringe structures associated with the LIPs.

Floquet theory elucidates underlying mechanisms behind fundamental molecular strong-field processes. Within this Floquet description, LIPs result from the dipole-coupling between molecular Born-Oppenheimer (BO) states in the presence of a laser field [1, 2]. Notably, the *bond hardening* mechanism refers to transient population trapping in light-induced vibrational potential wells [3]. We have recently theoretically demonstrated the role of bond hardening in a pulse-duration-dependent molecular stabilization effect during the dissociation of O_2^+ molecular ions [4].

We further explored how the bond hardening mechanism and associated LIPs might be revealed in experiments. By numerically solving the TDSE within the Born-Oppenheimer approximation, we analyzed the rovibrational dynamics of O_2^+ molecular ions interacting with infrared (IR) laser pulses and calculated observable, angle-resolved fragment kinetic-energy-release (KER) spectra.

Figure 1 compares our numerical results for the lowest IR-pulse peak intensity considered in [5] from calculations that include rotational excitations (2D) with simplified calculations in which the rotational motion is frozen (1D). For the given peak intensity, the angle-resolved KER spectra from 1D and 2D calculations are almost indistinguishable. This indicates that the rotational motion is of marginal relevance. The TDSE results reveal striking fringe structures that shift downward in energy for increasing alignment angles $0 \leq \theta \leq \pi/2$. To explain this downward trend, we compared our TDSE results with a Floquet model, based on the vibrational energies in the light-induced potential well [5].

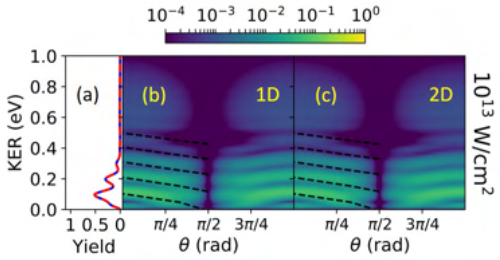


Figure 1. (a) Total, angle-integrated KER spectra for an 800-nm, 40-fs pulse with a peak intensity of 10^{13} W/cm^2. TDSE calculations without (1D) and including rotational excitations (2D) are represented by red dashed and blue solid curves, respectively. Corresponding angle-resolved KER spectra are shown for (b) 1D and (c) 2D TDSE calculations. Superimposed black dashed lines show the lowest five vibrational levels in the light-induced Floquet bond-hardening well (see Eq. (4) in Ref. [5]).

This work was supported by the Chemical Sciences, Geosciences, and Biosciences Division, Office of Basic Energy Sciences, Office of Science, U.S. Department of Energy under Award N° DEFG02-86ER13491.

References

[1] Aubanel E E *et al* 1993 *Phys. Rev. A* **48** R4011
[2] Chu S-I and Telnov D A 2004 *Phys. Rep.* **390** 1
[3] Ibrahim H *et al* 2018 *J. Phys. B* **51** 042002
[4] Abanador P M *et al* 2020 *Phys. Rev. A* **101** 043410
[5] Abanador P M and Thumm U 2020 *Phys. Rev. A* **102** 053114

*E-mail: thumm@phys.ksu.edu

TC

Attosecond dynamics in O_2 with ASTRA, a transition-density-matrix approach to molecular ionization

C Marante[1]*, J M Randazzo[2], H Gharibnejad[3], B I Schneider[3], J Olsen[4] and L Argenti[1,5]†

[1]Department of Physics, University of Central Florida, Orlando, FL 32816, USA
[2]CONICET, San Carlos de Bariloche, Río Negro 8400, Argentina
[3]NIST, Gaithersburg, MD 20899, USA
[4]Department of Chemistry, Aarhus University, Aarhus 8000, Denmark, EU
[5]CREOL, University of Central Florida, Orlando, Florida 32816, USA

Synopsis ASTRA, which employs a new fast algorithm to evaluate inter-channel coupling in the molecular electronic continuum, is used to study the photoionization dynamics and the optical response of the O_2 molecule, under the action of sequences of extreme-ultraviolet attosecond pulses and of IR/VIS femtosecond pulses.

Recent advances in XUV and soft-x-ray ultrafast technologies have made it possible to generate attosecond-pulses with shorter durations, larger intensities and higher central frequencies [1, 2]. These ultra-short pulses give electrons the chance to populate many excited states, across a broad range of energies that can encompass several ionization thresholds. A time-dependent wave-function approach, therefore, is needed to represent the coherent superposition of multiple photoelectron-photoion pairs as well as to describe the correlated and entangled character of the ionization states. To do so, we have developed ASTRA (AttoSecond TRAnsitions), a molecular code that implements a new algorithm to construct arbitrary operators in the close-coupling electronic continuum, based on high-order transition density matrices between correlated ionic states, which are obtained with an extension of the LUCIA general configuration-interaction code [3]. ASTRA is remarkably fast, and it scales favorably with the molecular size. Here, we apply ASTRA to study the ultrafast electron dynamics triggered in molecular oxygen by sequences of attosecond laser pulses. We focus in particular on the attosecond transient absorption spectrum of the laser-dressed molecule, and on the role of autoionizing states in the large energy interval between the ionization threshold and the $c^4\Sigma_u^-$ ionic channel. To compute the optical response of the dressed target, we propagate the wave function in a basis of essential Siegert states. This approach greatly accelerates the calculation without appreciably compromising its accuracy. The basic integrals between hybrid Gaussian-B-spline functions utilized in ASTRA are computed with the GBTOlib library [4]. Our computed photoionization and transient absorption spectra are compared with other theoretical and experimental results reported in the literature [5, 6]. This work is supported by the DOE CAREER grant No. DE-SC0020311.

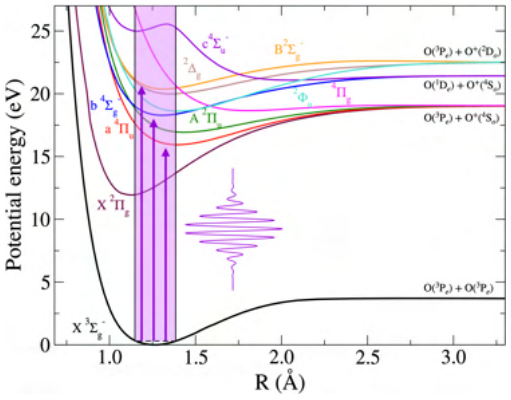


Figure 1. Sketch of the most relevant O_2^+ electronic states, included in our calculation, that participate in the dynamics triggered by attosecond pulses.

References

[1] J Duris *et al*, Nat. Phot. **14**, 30 (2020).
[2] N Saito *et al*, Optica **6**, 1542 (2019).
[3] J Olsen *et al*, J. Chem. Phys. **104**, 8007 (1996).
[4] Z Mašín *et al*, Comp. Phys. Comm. **249**, 107092 (2020).
[5] C T Liao *et al*, Phys. Rev. A **95**, 043427 (2017).
[6] S Marggi *et al*, Phys.Chem.Chem.Phys. **21**, 16497 (2019).

*E-mail: carlos.marante@ucf.edu
†E-mail: luca.argenti@ucf.edu

Attosecond pump-probe spectroscopy of quantum electronic coherence

M Ruberti*

Department of Physics, Imperial College London, Prince Consort Road, London SW7 2AZ, United Kingdom.

Synopsis I present advanced *ab initio* simulations of pump-probe experiments of ultrafast many-electron dynamics in molecular systems, based on X-ray attosecond transient absorption (ATAS) and attosecond time-resolved photoelectron spectroscopies. The interactions of the molecule with the pump and probe laser pulses are described with the state-of-the-art time-dependent (TD) B-spline Restricted Correlation Space- Algebraic Diagrammatic Construction (RCS-ADC) method for coherent many-body ionization dynamics. The results unveil the mapping of the observables onto the electronic coherences triggered upon ionization of the neutral molecule.

The advent of attosecond laser pulses generated by high-harmonic generation and X-ray free electron lasers has created unique opportunities for studying the very first few femtoseconds of the many-electron dynamics triggered by photoionization in atoms, molecules, and condensed matter. Two interrelated, fundamental quantum-mechanical concepts characterize these many-electron dynamics: quantum coherence and quantum entanglement. For example, quantum electronic coherence in photoionized molecules, arising at the attosecond and persisting at the femtosecond time scales, underpins the few-femtosecond charge dynamics (hole migration) and therefore also the ensuing photochemical transformation of matter. Here I will present advanced *ab initio* simulations of a series of complete pump-probe experiments of ultrafast many-electron dynamics in molecular systems, capable of capturing attosecond to few-femtosecond quantum electronic coherences. These include a fully *ab initio* time-resolved study of ATAS in a prototypical polyatomic molecule such as pyrazine, where I demonstrate the possibility of retrieving the many-electron quantum ionic coherences arising in attosecond molecular photoionization and pre-determining the subsequent charge-directed photochemical reactivity [1], as well as new results based on the simulation of attosecond time-resolved photoelectron spectra [2]. The simulations I will present explicitly describe the interaction of the molecular many-electron system with both the pump and probe laser pulses. I will examine three different pump probe setups, namely all XUV, all X-ray and a hybrid XUV/X-ray one. The calculations are carried out by means of the recently-developed *ab initio* method for many-electron dynamics in polyatomic molecules, the TD B-spline RCS-ADC [3], which extends the *ab initio* ADC approach, originally developed to describe bound state dynamics, to the realm of ultrafast ionization dynamics, combining the accurate description of electron correlation of quantum chemistry with the full account of the continuum dynamics of the photoelectron, and allowing one to accurately predict the mixed state of the ionized system prepared by attosecond ionization of a molecular system [4]. Complete theoretical characterization of the atto-ionized many-electron state and photo-induced attosecond charge dynamics is achieved by calculating the reduced ionic density matrix (R-IDM) of the bipartite ion–photoelectron system, with full inclusion of the correlated shakeup states. I will show how the Schmidt decomposition of the R-IDM unravels the many-electron dynamics triggered by the pump, allowing for the identification of the key pure-state channels involved in the quantum coherent many-electron dynamics. Finally, I will present the theoretical ATAS and time-resolved photoelectron spectra of the pump-ionized molecular cation and show how the results unveil the mapping of the pump-probe measurements onto the quantum electronic coherences, and related non-zero R-IDM matrix elements, produced upon ionization of the neutral by the pump laser pulse.

References

[1] M Ruberti, Faraday Discussions **228**, 286 (2021).
[2] M Ruberti, *in preparation* (2022).
[3] M Ruberti, J. Chem. Theory Comput. **15**, 3635 (2019).
[4] M Ruberti, Phys. Chem. Chem. Phys. **21**, 17584 (2019).

*E-mail: m.ruberti11@imperial.ac.uk

Theory behind the real-time imaging of resonant photoemission dynamics

A. Autuori[1,†], D. Platzer[1,†], M. Lejman[1], G. Gallician[1], L. Maëder[1], A. Covolo[1], L. Bosse[1], M. Dalui[1], D. Bresteau[1], J.-F. Hergott[1], O. Tcherbakoff[1], H.J.B. Marroux[1], V. Loriot[2], F. Lépine[2], L. Poisson[1,3], P. Salières[1], J. Caillat[4], R. Taïeb[4,*].

[1]Université Paris-Saclay, CEA, CNRS, LIDYL, 91191 Gif-sur-Yvette, France
[2] Université Claude Bernard Lyon 1, CNRS, Institut Lumière Matière, 69622 Villeurbanne, France
[3] Université Paris-Saclay, CNRS, Institut des Sciences Moléculaires dOrsay, 91405 Orsay, France
[4] Sorbonne Université, CNRS, Laboratoire de Chimie Physique-Matière et Rayonnement, 75005 Paris, France
[†]These authors contributed equally to this work.

TC

Synopsis We present theoretical developments in order to investigate two-photon XUV+IR ionization of helium through intermediate bound states. Using both the Time Dependent Schrödinger Equation (TDSE) and a perturbative approach, we could reproduce with high-fidelity and intepret the outcomes of experimental results, giving access to the complete formation of the photoionized wavepacket in time, space and energy.

Imaging in real time the *complete dynamics* of a process as fundamental as photoemission has long been out a reach due to the difficulty of combining attosecond temporal resolution with fine spectral and angular resolutions. A key ingredient to access the dynamics is the relative phase between the spectral components of the photoionized wavepacket – which can be measured nowadays using the most advanced tools of experimental attosecond science.

Here, we present numerical simulations based on the resolution of the TDSE in order to explain experimental results obtained with the Rainbow RABBIT [1] interferometry and VMI momentum spectroscopy, which when combined, provide both the spectral and angular resolutions. Using a single-active electron model potential, we focused on the two-photon XUV+IR photoionization of helium through the intermediate $1s3p$ and $1s4p$ states and obtained the theoretical spectral and spatial variations of the two-photon transition amplitude $M(E,\theta)$.

The latter is highly structured by several $\sim \pi$ rad phase jumps in both dimensions [2], which fully agree with experimental results. In the figure below, we compare the variations of the radial matrix elements for the two main angular momentum channels, i.e. s and d, either extracted from our simulations or from the experimental results. One can see that the variations are very similar and strongly depend on the final angular momentum, which result in the observed π jumps in the phase of $M(E,\theta)$ and explain its variations in both directions.

These numerical results support and validate the interpretation of the measured data and allow reconstructing the "movie" of the full photoemission process out of the modulus and phase variations of the photoelectron quantum state with respect to both its energy and ejection direction.

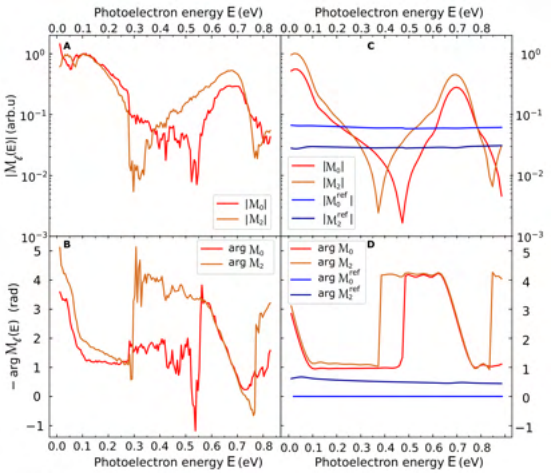


Figure 1. Modulus (up) and phase (down) of the experimental (left) and theoretical (right) transition amplitudes of the investigated process.

References

[1] V. Gruson *et al* Science **354**, 2016 (2016).
[2] A. Autuori *et al* Science Advances, *in print* (2022).

*E-mail: richard.taieb@upmc.fr

Stationary molecular R-matrix approach for above-threshold multi-photon ionization and the coupling delay in RABITT processes

J. Benda[1], Z. Mašín[1]*, and J. D. Gorfinkiel[2]

[1]Institute of Theoretical Physics, Faculty of Mathematics and Physics, Charles University, V Holešovičkách 2, Prague 8, 180 00, Czech Republic

[2]School of Physical Sciences, The Open University, Walton Hall, MK7 6AA, Milton Keynes, UK

TC

Synopsis We describe an R-matrix based stationary approach for efficient calculation of molecular multi-photon transition matrix elements of an arbitrary order. We use it to study in detail RABITT delays in H_2, N_2, CO_2, H_2O and N_2O. Our results are in excellent agreement with most of the available experimental data. We have studied conditions of validity of the standard approximations to RABITT delays and found that for CO_2 an important contribution in the B- and C-channels comes from a hitherto ignored laser-induced ionic coupling delay.

Many quantum mechanical processes involving photons can be described using multi-photon transition matrix elements. Nevertheless, in practice their calculation has been a difficult problem for multi-electron systems such as atoms and molecules. For molecules the problem is compounded by the absence of spherical symmetry. In this contribution we describe an efficient approach for the calculation of molecular matrix elements for below- and above-threshold multi-photon ionization of an arbitrary order [1].

The method is based on R-matrix division of space. The complicated close-range multi-electron contribution to the matrix element is evaluated with the help of quantities naturally provided by the R-matrix method while the infinite-range outer region part is evaluated combining numerical and asymptotic analytic techniques. As a result we obtain a highly efficient stationary method capable of routinely treating multi-channel problems, including hundreds of channels, on a dense grid of photon energies.

We have applied our methodology to angle-resolved and orientationally averaged RABITT delays in molecules (two-photon above-threshold ionization). The results are in excellent agreement with available experimental data for H_2, N_2 and CO_2. Surprisingly, we find disagreement with measurements for H_2O and N_2O.

Most importantly, the availability of full and accurate two-photon molecular matrix elements enables benchmarking of approximations currently used for the delays including the asymptotic approximation. We compare our R-matrix two-photon delays with the approximate ones and establish that the regions of validity of the approximations vary strongly depending on the molecule. We find that in some cases the asymptotic approximation remains severely inaccurate up to a few tens of eV above threshold.

The case of strongly dipole-coupled channels B and C of CO_2 near resonant with the commonly used laser frequencies demonstrates that the hitherto ignored laser-induced ionic coupling may generate a significant contribution to the RABITT delay. We derive an asymptotic approximation to this coupling delay based on the ionic transition dipole matrix element.

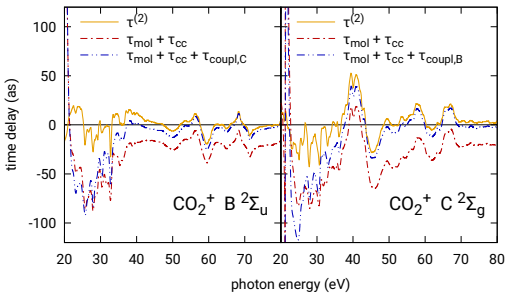


Figure 1. RABITT delays for B and C channels of CO_2: two-photon delays, approximate delays without and with inclusion of the coupling delay.

References

[1] J. Benda and Z. Mašín, Sci Rep **11**, 11686 (2021).
[2] M. Huppert et al, Phys. Rev. Lett. **117**, 093001 (2016).

*E-mail: zdenek.masin@utf.mff.cuni.cz

TC

Three-Sideband RABBITT in Argon: Experiment and Theory

D Bharti[1]*, H Srinivas[1], F Shobeiry[1], R Moshammer[1], T Pfeifer[1], K R Hamilton[2], K Bartschat[2], and A Harth[1,3]†

[1]Max-Planck-Institute for Nuclear Physics, D-69117 Heidelberg, Germany
[2]Department of Physics and Astronomy, Drake University, Des Moines, IA 50311, USA
[3]Faculty of Optics and Mechatronics, Aalen University, D-73430 Aalen, Germany

Synopsis Using a 3-sideband RABBITT technique, we explore continuum-continuum couplings by extracting the RABBITT phase and the corresponding time delays when several transitions occur in the continuum.

The reconstruction of attosecond beating by interference of two-photon transitions (RABBITT) is a technique to measure attosecond time delays in photoionization processes [1]. It is an interferometric technique in which an extreme ultraviolet (XUV) attosecond pulse train (APT) ionizes a target by single-photon absorption, thereby creating main peaks in the photoelectron kinetic energy spectrum. A temporally and spatially overlapped near-infrared (NIR) field creates one or more sidebands (SBs) [2] in between these main peaks, whose intensities oscillate sinusoidally as the delay between the XUV and the NIR beams is varied.

Recently, we extended the applicability of the "asymptotic approximation" [3] to multi-sideband RABBITT schemes and analyzed it in detail for atomic hydrogen [4]. The most important prediction of this extension is a similarity of the RABBITT phase, and hence the corresponding time delay extracted from it, in the lower (S_l), central (S_c), and higher (S_h) sidebands.

Here we present our first realization of a 3-SB RABBITT experiment using argon as the target gas (cf. Fig. 1). Argon is easier to handle experimentally but more challenging for theory, due to its multi-electron nature and the non-vanishing orbital angular momentum of the initial 3p electron. Consequently, we use the multi-electron R-matrix with time dependence (RMT) [5] method to generate theoretical predictions for comparison with our experimental data.

Figure 1 exhibits the basic scheme and an example of our latest experimental results. The similarity of the RABBITT phases within the first three sideband groups (π added to S_c [4]) supports the validity of the decomposition approximation, with some deviation for small ejected energies. The "missing" π for S_l in the highest group is due to the weak H_{15} harmonic.

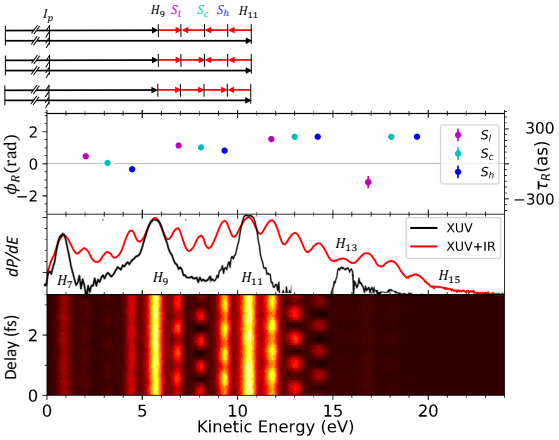


Figure 1. 3-SB RABBITT scheme [4], relative experimental photoelectron spectra (log scale), extracted phases, and corresponding time delays for argon. The IR wavelength is 1030 nm, and the XUV-harmonics are odd multiples of 515 nm.

Multi-sideband RABBITT, together with a reaction microscope, opens a new way to study continuum-continuum (cc) couplings by comparing the angle-dependent phase $\Delta\phi_{cc}$ within a particular sideband group.

References

[1] P M Paul *et al.*, Science **292** 1689 (2001).
[2] A Harth *et al.*, Phys. Rev. A **99** 023410 (2019).
[3] J M Dahlström *et al.*, J. Phys. B **45** 183001 (2012).
[4] D Bharti *et al.*, Phys. Rev. A **103** 022834 (2021).
[5] A C Brown *et al.*, Comp. Phys. Commun. **250** 107062 (2020).

This work was supported, in part, by the United States National Science Foundation, the DFG-QUTIF program, and IMPRS-QD.

*E-mail: bharti@mpi-hd.mpg.de
†E-mail: Anne.Harth@hs-aalen.de

Angle-resolved phases in photoemission: from atomic to molecular systems.

R. Y. Bello [1,2] * **and F. Martín** [1,2]

[1] Departamento de Química, Módulo 13, Universidad Autónoma de Madrid, 28049 Madrid, Spain.
[2] Instituto Madrileño de Estudios Avanzados en Nanociencia (IMDEA-Nanociencia), Cantoblanco, 28049 Madrid, Spain

Synopsis Phase differences between one- and two photon ionization channels, ω-2ω, are calculated. First, the effect of Rydberg autoionizing states and bound intermediate states will be studied in an atomic system over a whole range of frequencies. Second, results in a molecular system will be presented with special focus where the frequencies are in resonance with vibrationally bound intermediate states of the molecule.

Attosecond science has paved the way for studying electron dynamics in real time, from atomic to molecular systems. In particular, attosecond interferometrics techniques have been used to access not only the ionization amplitudes but also the phases associated with the scattering states describing the ejected photoelectron Ref. [1]. Thus, opening up the prospect of steering molecular dynamics, extracting photoionization time delays and more importantly reconstruct electronic wave-packets. Currently, two methods are mainly used to retrieve the phases and amplitudes, the streaking technique which combines a single attosecond pump pulse with an infrared probe pulse and the RABBITT technique which combines a train of attosecond pulses with the infrared pulse used to generate them. Recently an alternative method for measuring the phases in photoemission has been put forward Ref. [2, 3]. This method combine two-phase locked extreme ultraviolet pulses of frequency ω and 2ω, from a free electron laser. By varying the relative optical-phase between the two pulses the phase difference between the two ionization channels can be measured. In the present work, we apply this technique to theoretically obtain the phase difference, as a function of the electron emission angle, between the two ionization channels. First, we consider atomic systems such as Argon over a large range of frequencies, paying special attention where one or both of the two-colors (ω or 2ω) is in resonance with a bound electronic state or with an autoionizing Rydberg state. Second, in a molecular system, we investigate the role played by the nuclear degrees of freedom in such interferences. As in the atomic case, we consider the region where the frequencies are in resonance with a vibrationally bound intermediate state Ref. [4].

References

[1] L. Cattaneo Nat. Physics **14**, 733–738 (2018).
[2] Daehyun You, Phys. Rev. X **10**, 031070 (2020).
[3] K C Prince, Nat. Photonics **10**, 176–179 (2016).
[4] F Holzmeier, Phys. Rev. Lett. **121**, 103002 (2018).

*E-mail: roger.bello@uam.es

Attosecond electron dynamics near the ionization threshold in Ne

K R Hamilton[1]*, K Bartschat[1], M Moioli[2], H Ahmadi[2], D Busto[2], D Ertel[2], I Makos[2], M Schmoll[2], M M Popova[3], E V Gryzlova[3], A N Grum-Grzhimailo[3], M D Kiselev[3], S N Yudin[3], C D Schröter[4], R Moshammer[4], T Pfeifer[4], and G Sansone[2]

[1]Department of Physics and Astronomy, Drake University, Des Moines, IA 50311, USA
[2]Physikalisches Institut, Universität Freiburg, 79106 Freiburg, Germany
[3]Skobeltsyn Institute of Nuclear Physics, Lomonosov Moscow State University, 119991 Moscow, Russia
[4]Max-Planck-Institute for Nuclear Physics, 69117 Heidelberg, Germany

TC

Synopsis Using a combination of XUV and IR sources, with a controlled time delay between them, we report results for photoionization time delays in neon with emphasis on the dynamics near the ionization threshold.

The RABBITT (Reconstruction of Attosecond Beating By Interference of Two-photon Transitions) technique is commonly used to access photoionization time delays [1]. The idea is to employ synchronized extreme ultraviolet (XUV) and infrared (IR) pulses, which are delayed with respect to each other [2]. The absorption and emission of the IR photons leads to sidebands (SBs) in the ejected-electron spectra between the peaks generated by the absorption of an XUV photon.

In our setup, the XUV pulses are composed of a frequency comb of odd harmonics of the IR with photon energies chosen in such a way that one harmonic has an energy below the ionization potential of neon, thus leading to excitation of an intermediate bound state before the atom is ionized by absorbing an additional IR photon. The time delay between the XUV and the IR photons leads to clearly visible oscillations in the sideband intensity. The phase of this oscillation can be converted to a time delay, which is due to the group delay τ_{GD} of different harmonics and an atomic time delay τ_{A}.

Figure 1 shows that the delay τ_{A} determined from one harmonic below and one above the ionization threshold largely deviates from the value obtained from XUV photons all above threshold. The variation is attributed to excited states of neon (indicated by lines left of the ionization threshold in Fig. 1) that can be effectively populated by the lowest XUV harmonic. Comparison of the experimental data with theoretical predictions from the nonperturbative all-electron R-Matrix with Time Dependence (RMT) [3] approach and perturbation theory (PT) [4] shows very good agreement between theory and experiment, except for PT in the lowest sideband.

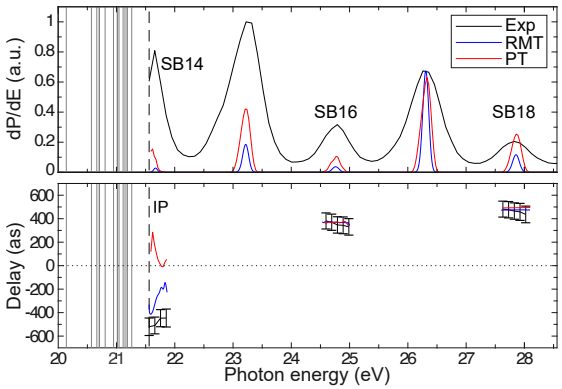


Figure 1. Relative emission spectrum (top, not normalized) and photoionization time delays (bottom) for SB-14 (one harmonic below threshold), SB-16, and SB-18 in neon for a RABBITT scheme with an IR wavelength of 800 nm, a peak intensity of 10^{12} W/cm^2, and a FWHM of 15 fs. The experimental data are compared with PT and RMT predictions. A meaningful delay can only be extracted in the energy region of the sidebands.

This work is supported by the NSF under PHY-1803844, PHY-2012078, OAC-1834740, and XSEDE PHY-090031, the Frontera Pathways allocation PHY20028, the European Union's Horizon 2020 project 641789 MEDEA, the DFG under IRTG CoCo (2079) and INST 39/1079, and the Russian Foundation for Basic Research under 20-52-12023.

References

[1] P M Paul *et al.*, Science **292** 1689 (2001).
[2] H Ahmadi *et al.*, J. Phys. Photonics **2** 02406 (2020).
[3] A C Brown *et al.*, Comp. Phys. Commun. **250** 107062 (2020).
[4] A Messiah, *Quantum Mechanics*, Dover (1961).

*E-mail: kathryn.hamilton@drake.edu

Spectral Signature of Molecular Charge Migration

R Fernández Carbón[1]* **and L Argenti**[1,2]†

[1]Department of Physics, University of Central Florida, Orlando, FL 32816, USA
[2]CREOL, University of Central Florida, Orlando, FL 32816, USA

Synopsis We present an *ab initio* method to simulate the evolution of the correlated electronic state of a molecule under the action of arbitrarily polarized non-ionizing light pulses in the presence of decoherence, using the time-dependent Lindblad master equation. We apply the method to identify the spectral signature of charge migration in organic molecules of biological relevance.

TC

Mounting experimental evidence suggests that the high efficiency of energy conversion in living beings, refined by natural selection over billions of years, relies on the quantum nature of charge transfer [1]. The recent development of attosecond laser technology allows us to study these ultrafast processes at the molecular level and natural time scale. To interpret the ultrafast electron dynamics of biomolecules, it is necessary to account for: i) correlation in excited electronic states, ii) the loss of electronic coherence caused by the progressive entanglement with the nuclear degrees of freedom and with electronic excited states in other molecules in the matrix, and iii) the non-perturbative character of the light matter interaction. Here we present a study on small organic molecules of biological relevance employing a new *ab initio* method to simulate the evolution of the correlated electronic state of a molecule under the action of arbitrarily polarized non-ionizing light pulses in the presence of decoherence. The electronic states are obtained from MCSCF calculations [2]. The effects of the driving pulses and decoherence are taken into account by numerically solving the time-dependent Lindblad equation [3] for the density matrix of the system. We reconstruct the susceptibility from the dipolar response of the light-dressed molecule, which is an experimental observable, and we use Becke's charge-partitioning algorithm [4] to theoretically predict the migration of charge associated to each spectroscopic signal. We demonstrate the potential of this method by mapping the profile of individual charge-migration modes in the molecule, and show how these modes are reproduced in the four-wave-mixing spectrum of the target.

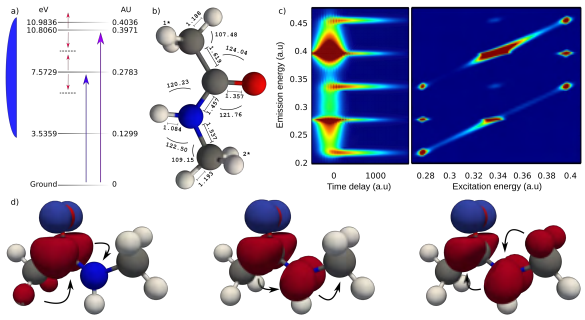


Figure 1. Simulation of the transient absorption spectrum and charge migration in N-Methylacetamide (NMA). a) Energy diagram of the relevant states in the molecule and of the main multiphoton paths responsible for the signals observed in c and d. b) Molecular structure of NMA. c) Spectrum of the Y dipole component, as a function of the pump-probe delay and the corresponding 2D spectrum obtained by taking the Fourier transform with respect to the time delay of the IR probe. d) Change of electronic density in N-Methylacetamide, with respect to the ground state, after a Y-polarized pump-probe pulse sequence; red and blue representing excess and depletion of electronic charge, respectively.

References

[1] Y Kim *et al* Quantum Rep. **3** 80 (2021).
[2] I Fernández Galván *et al* J. Chem. Th. Comput. **15** 5925 (2019).
[3] F Nathan and M Rudner *et al* Phys. Rev. B **102** 115109 (2020).
[4] H Gharibnejad *et al* Comput. Phys. Commun. **263** 107889 (2021).

*E-mail: rfernandez06@knights.ucf.edu
†E-mail: Luca.Argenti@ucf.edu

Poster Session III, Highlights A
Chair: **Cosmin Blaga**, Kansas State University, Kansas, USA

R62 **Signatures of multi-band effects in high-harmonic generation in monolayer MoS_2**
B R Nebgen, L Yue, R Hollinger, C B Uzundal, Z Gan, E Najafidehaghani, A George, C Spielmann, D Kartashov, A Turchanin, D Y Qiu, M B Gaarde, M Zuerch 306

R63 **A 4.1 μm Fe:ZnSe-based CPA for Driving High-Order Harmonics beyond the Water Window**
Alphonse Marra, Arnold Banner, Zenghu Chang 164

R66 **Time evolution of the high harmonics spectra from the liquid water driven by double MIR pulses**
Tianqi Yang, Takayuki Kurihara, Tomoya Mizuno, Teruto Kanai, Yoshihisa Harada, Jiro Itatani 165

R67 **Attosecond electron pulse trains from metal nanotips**
Avraham Eitan, Maor Eldar, Salma Abo-Toame, Adi Goldner, Michael Krüger . . . 166

R71 **Sub-cycle control of valley polarization in WSe_2 monolayer**
Arqum Hashmi, Shunsuke Yamada, Atsushi Yamada, Kazuhiro Yabana, Tomohito Otobe 167

R72 **Multi-dimensional HHG-spectroscopy of ultrafast phonon dynamics via CEP**
Ofer Neufeld, Jin Zhang, Umberto De Giovannini, Hannes Hübener, Angel Rubio . . 168

R75 **Enhanced high-harmonic generation (HHG) from Cr-doped MgO crystals**
Uwe Thumm, Viktoria Nefedova, Francisco Navarrete, Nicolas Tancogne-Dejean, Sven Fröhlich, Willem Boutu, Marcelo Fabian Ciappina, David Gauthier, Aimrane Hamdou, Shatha Kaassamani, Angel Rubio, Hamed Merdji 169

R77 **1.5mJ, 30W OPA at 2um via spectrally selective amplification**
Bruno E. Schmidt, Derrek Wilson, Maksym Ivanov, Pedram Abdolghader, Antoine Raffray, Tadas Balciunas, François Légaré, Hans Jakob Wörner 170

R78 **Polarization shaping of light for strong field valleytronics**
Igor Tyulnev, Lenard Vamos, Jens Biegert 171

Signatures of multi-band effects in high-harmonic generation in monolayer MoS_2

B R Nebgen[1,2 *], L Yue[3 †], R Hollinger[1,2], C B Uzundal[1,2], Z Gan[4], E Najafidehaghani[4], A George[4], C Spielmann[5,6,7], D Kartashov[5,6], A Turchanin[4,6], D Y Qiu[8], M B Gaarde[3], M Zuerch[1]

[1]Department of Chemistry, University of California, Berkeley, 94720, USA; [2]Lawrence Berkeley National Laboratory, Materials Science Division, Berkeley, 90720, USA; [3]Department of Physics and Astronomy, Louisiana State University, Baton Rouge, 70803, USA; [4]Institute of Physical Chemistry, Friedrich Schiller University, Jena, 07743, Germany; [5]Institute of Optics and Quantum Electronics, Friedrich Schiller University, Jena, 07743, Germany; [6]Abbe Center of Photonics, Friedrich Schiller University, Jena, 07743, Germany; [7]Helmholtz Institute, Jena, 07743, Germany; [8]Department of Mechanical Engineering and Materials Science, Yale University, New Haven, 06520, USA

Synopsis Experimental observation of high harmonic generation (HHG) in monolayer MoS_2 reveals high-harmonic yield dependence on crystal orientation due to spatial symmetry as well as recombination from multiple conduction bands. Observation of such specific material properties through HHG paves the way for using solid-state HHG spectroscopy to probe ultrafast dynamics and trace phase transitions in condensed matter.

High-harmonic generation (HHG) from intense laser pulses in solids is increasingly attracting attention as a probe of ultrafast electronic processes and crystalline symmetries in condensed matter systems [1]. HHG from atomically thin semiconductors provides an opportunity to investigate the microscopic origin of HHG due to the absence of laser propagation effects [2]. In addition, few-layer transition metal dichalcogenides (TMDs) offer a tunable material platform with unique properties to interrogate with solid-state HHG and diverse applications in optoelectronics and spintronics [3].

Here, we investigate the polarization properties of high-order harmonics generated in monolayer MoS_2 as a function of crystal orientation relative to the mid-IR laser field polarization [4]. We experimentally observe that crystal symmetries impose constraints on harmonic emissions, leading to pronounced nodes in the HHG spectra at certain angles (dots in Fig 1a). These symmetry constraints have been explored previously in MoS_2 [5]. Building on previous studies, we additionally find an angular shift such that for several mid-IR wavelengths, the parallel-polarized odd-order harmonics below (above) 3.5 eV are enhanced for driver polarization along the armchair (zigzag) direction (Fig 1a). By solving the time-dependent density matrix equations involving a valence band and two conduction bands, we trace these angular shifts to electron-hole recombinations from different conduction bands, mapping lower energy harmonics to recombinations involving the first conduction band and higher energy harmonics to recombinations involving the second conduction band (see theory results in Fig 1b). This measurement effectively probes the vectorial nature of recombination dipoles from different bands in MoS_2, building up from the single conduction band picture of solid-state HHG that has been considered previously. This material specific analysis paves the way for solid-state HHG as a detailed probe of ultrafast dynamics in condensed matter systems.

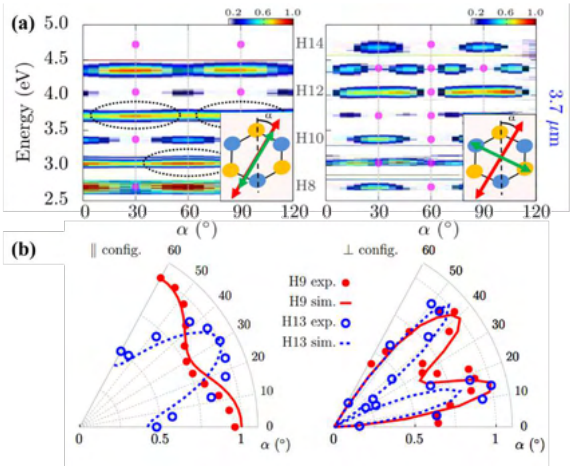


Figure 1. (a) Orientation dependent HHG spectra of MoS_2 with a 3.7 μm driver highlighting the angular shift in parallel-oriented odd harmonics at 3.5 eV (dotted ovals). (b) Comparison of experimental and simulated orientation-dependent HHG yields with a 3.7 μm driver.

References

[1] S Ghimire and D A Reis, Nat. Phys. 90, 10-16 (2019). [2] S Manzeli, et. al., Nat. Rev. Mater. 2, 17033 (2017). [3] I Kilen, et. al., Phys. Rev. Lett. 125, 083901 (2021). [4] L Yue, et. al., arXiv:2112.13032v2 [cond-mat.mtrl-sci] (2022). [5] H Liu, et. al., Nat. Phys. 13, 262-265 (2017).

* E-mail: bailey_nebgen@berkeley.edu
† E-mail: lyue3@lsu.edu

A 4.1 µm Fe:ZnSe-based CPA for Driving High-Order Harmonics beyond the Water Window

Z A Marra[1] [*], A Banner[1], and Z Chang[1]

[1]Institute for the Frontier of Attosecond Science and Technology (iFAST), CREOL and Department of Physics, University of Central Florida, 4111 Libra Drive, Orlando, FL 32816, USA

Synopsis Mid-wave infrared pulses with 350 nJ energy and 315 nm bandwidth were generated via difference frequency generation in $LiGaS_2$ at 60 kHz. These pulses were then stretched and are to be amplified in an Fe:ZnSe-based multi-pass amplifier. Work is ongoing, but recent progress suggests that the final, compressed output pulses will at the mJ-level, at 300 Hz, 80 fs in duration, and centered at 4.1 µm. These pulses will be used to generate keV-level high harmonics in noble gas spanning the water window (282–533 eV) and beyond.

RA

The near infrared (NIR) Ti:Sapphire laser has been the workhorse for intense-field science since the advent of chirped pulse amplification (CPA) in the 1980s. While the technology behind such systems is relatively mature allowing high pulse energies and short durations, the next generation of drivers of attosecond pulses will take advantage of wavelength scaling laws. By increasing driving laser center wavelength, the high-harmonic spectrum cutoff energy increases nearly quadratically [1]. With recent advances in longer wavelength driving sources, pulses extending into the water window and beyond have now been demonstrated, e.g. [2], but photon flux has never been high enough for time-resolved study the Oxygen K-edge (533 eV).

Thus, this research focuses on the design of a next-generation driver of attosecond pulses. The Fe:ZnSe-based CPA centered at 4.1 µm, at 300 Hz, and seeded by a carrier-envelope phase- (CEP) locked multi-stage optical parametric amplifier (OPA) will be capable of generating pulses extending into the keV region. Femtosecond, mJ-level CPA based on Fe:ZnSe at -7°C has been demonstrated at 4.4 µm; however, its repetition rate is low (10 Hz) [3].

The seed generation system relies on a turnkey, Yb:KGW pump laser at 60 kHz and 101 µJ per pulse. A 10 mm YAG crystal is used as a nonlinear crystal to generate a NIR supercontinuum which is parametrically amplified in the first stage in BBO. In the second stage difference frequency generation (DFG) in $LiGaS_2$ provides 4.1 µm, 350 nJ pulses which seed the CPA. The pulses have a bandwidth of 315 nm supporting a transform-limited duration of ~80 fs and are passively CEP stabilized. These pulses are then stretched to ~150 ps with an Öffner stretcher.

Fe:ZnSe is an attractive gain medium for its broad stimulated emission cross section spanning 3.5 to 5 µm and peaking at ~4.1 µm. By cooling Fe:ZnSe to cryogenic temperatures, commercially available, microsecond Er:YAG lasers which overlap with its absorption cross section may be used as pumps [4]. Two 10 mm-long, Fe:ZnSe single-crystals are pumped by two Er:YAG lasers, each delivering 100 µs, 33 mJ pulses to each crystal respectively.

Work is ongoing, but initial results are promising. A small-signal, single-pass gain of 29±2 was measured, as shown in Fig. 1. Femtosecond pulses with mJ-level energy are expect to be generated after six passes through the system.

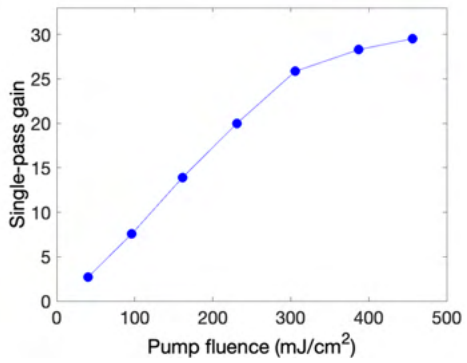


Figure 1. Single-pass gain vs fluence for an Fe:ZnSe system pumped by two Er:YAG lasers.

References

[1] Shan B *et al* 2001 *Phys. Rev. A* **65** 011804
[2] Ren X *et al* 2018 *J. Opt.* **20** 023001
[3] Migal E *et al* 2019 *Opt. Lett.* **44** 2550-2553
[4] Evans J W *et al* 2017 *Opt. Mater. Express Lett.* 7 4296-4303

[*] E-mail: alphonse.marra@ucf.edu

Time evolution of the high harmonics spectra from the liquid water driven by double MIR pulses

T Yang[1]*, T Kurihara[1], T Mizuno[1], T Kanai[1], Y Harada[1,2] and J Itatani[1]

[1]Institute for Solid State Physics, The University of Tokyo, Kashiwa, Chiba, 277-8581 JAPAN
[2]Graduate School of Frontier Science, The University of Tokyo, Kashiwa, Chiba, 277-8581 JAPAN

Synopsis Odd-order high harmonics up to 11th generated by 3.2 μm MIR pulses from liquid water are confirmed by using a flat water-jet. The time evolution of the spectra is recorded by introducing a double pulses excitation, configured by deploying a D-shaped mirror pairs to separate the beam. An oscillating modulation is found lasting over 400 fs, exceeding the pulse duration, which suggests the interaction between a vibrational oscillation excited by the first pulse and the second pulse.

RA

High harmonic generation (HHG) is one of the center topics among the fields of ultrafast optics and transient phenomena. The HHG from liquid phases has been a no-man's land until the first report in 2018 [1] based on the flat liquid-jet technique which was originally designed for the X-ray absorption spectroscopy [2]. The HHG beyond 20eV were reported with a 1.5 μm near-infrared (NIR) laser pump.

In this work, we deployed the flat liquid-jet system after a KTA-based optical parametric amplifier (OPA) which provides intense mid-infrared pulses (3.3 μm, 120 fs, 45 μJ)[3]. The homemade flat liquid-jet consists of two identical 50 μm nozzles, producing a stable 1-3 μm thick liquid sample. To realize a double-pulse excitation, the MIR beam is spatially split by a D-shape mirror pairs and is temporally separated by motorized stages. Two individual beams are then tightly focused by a parabolic mirror (f=25.4mm) onto the liquid-jet, and the HHG spectra are collected in a transmission geometry. The HHG signal from one of the beam is spatially blocked to study the laser-induced HHG performance. All experiments are performed using distilled liquid water.

Under this tight-focus configuration, even-order high harmonics up to 11$^{\text{th}}$ order (290nm) is successfully observed. To obtain the time evolution of the HHG spectra, the time delay between two pulses are scanned within a sufficiently long range. The intensities of high harmonics show a clear interference-like modulation (Figure. 1), which can be regards as an autocorrelation due to the fact that the oscillation period is very close to the optical cycle of the MIR field. However, we found this oscillation continued over 400 fs, exceeding the pulse duration of 120 fs. Considering the existence of the infrared-active broad absorption peak covering from 3000 cm^{-1} (3.3 μm) to 3600 cm^{-1} (2.7 μm), which corresponds to the OH vibration of H_2O molecules, we suppose that a resonant excited electronic dipole carries on with the first pulse's waveform and then coherently with the second pulse, causing an extension of the coherence range. This result enables the potential manipulation of the HHG in the view of the molecular dynamics, as well as a deeper understanding of the underlying complex liquid system.

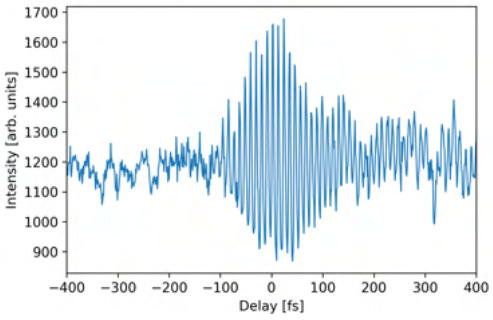


Figure 1. Integrated intensity of the time-dependent 5$^{\text{th}}$ harmonic spectrum (650nm).

References

[1] T T Lu and Z Yin et al., Nat. Commun. **9**, 1 (2018).
[2] M Ekimova et al., Struct. Dyn. **2**, 5 (2015).
[3] F Lu and P Xia et al., Opt. Lett. **43**, 2720 (2018).

*E-mail: tianqiyang@issp.u-tokyo.ac.jp

Attosecond electron pulse trains from metal nanotips

A Eitan[1], M Eldar[1], S Abo-Toame[1], A Goldner[1], and M Krüger[1*]

[1]Physics Department and Solid State Institute, Technion – Israel Institute of Technology, Haifa 32000, Israel

Synopsis The coherent modulation of swift electron beams with strong laser fields has enabled the generation of attosecond electron pulses, opening up new research avenues in ultrafast science. Here we study a simple alternative, the production of electron pulse trains directly at the source, a metal nanotip. In our experiment, we trigger tip photoemission by plasmonic nanofocusing and find signatures of attosecond tunneling emission. Our numerical simulations show that the electrons can retain the sub-cycle temporal fingerprint in a point-projection microscope setup due to low matter-wave dispersion.

RA

In recent years, studies of the interaction of free electron beams with intense light fields [1] and the generation of attosecond electron pulses [2] have opened up a new perspective for attosecond science. Attosecond electron pulse trains (AEPTs) open up real-time studies of electromagnetic waveforms [3] and nano-optical excitations [4], among other ultrafast applications. Photon-induced near-field electron microscopy produces AEPTs by modulating electron pulses near a nanophotonic structure [2]. In this work, we propose and implement a simple alternative for the production of AEPTs, sub-cycle tunneling emission right at the electron source, a metallic nanotip, for time-resolved probing of the dynamics of a nearby sample.

Laser-triggered nanotips are known to be highly coherent emitters of ultrashort electron pulses [5,6]. In the tunneling regime, AEPTs emerge from the tip. However, matter-wave dispersion leads to detrimental smearing of the temporal sub-cycle fingerprint upon long distances downstream from the nanotip. In contrast to scanning electron microscopy, point-projection microscopy [7] enables low dispersion because the electrons traverse only a distance of ~1µm to the sample (Fig. 1(a)). We numerically simulate electron emission and wavepacket propagation using the time-dependent Schrödinger equation (TDSE) and find that the sub-cycle temporal fingerprint is retained when two criteria are fulfilled: rapid acceleration to high kinetic energies by a static field and a sufficiently long optical cycle duration. Figure 1(b) shows the electron arrival probability at the sample plane for a 830nm pulse, with sub-cycle modulations clearly visible.

In our experimental realization, we trigger photoemission from a sharp gold tip using plasmonic nanofocusing [8]. A single groove at the tip shank ensures coupling of 6fs infrared light pulses to a surface plasmon which localizes at the nanotip apex, resulting in photoemission. We observe the characteristic kink [6] in the scaling of the electron current with laser power, indicating the transition from the multiphoton regime to the tunneling regime (see Fig. 1(c)). Experimental efforts for confirming the concomitant sub-cycle temporal modulation of the photoelectrons are currently underway.

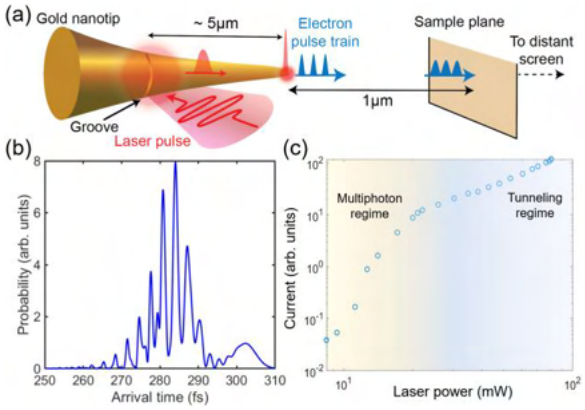


Figure 1. (a) Sketch of the ultrafast electron point-projection microscope setup (not to scale). The nanotip emitter is triggered by a surface plasmon. (b) Arrival probability of an AEPT in the sample plane calculated with the TDSE. (c) Experimental current-power scaling.

References

[1] Barwick B *et al* 2009 *Nature* **462** 902
[2] Feist A *et al* 2015 *Nature* **521** 200
[3] Morimoto Y *et al* 2018 *Nature Phys.* **14** 252
[4] Garcia de Abajo F J and Di Giulio V 2021 *ACS Photon.* **8** 945
[5] Krüger M *et al* 2011 *Nature* **462** 902
[6] Krüger M *et al* 2018 *J. Phys. B* **51** 172001
[7] Quinonez E *et al* 2013 *Rev. Sci. Instr.* **84** 103710
[8] Vogelsang J *et al* 2018 *ACS Photon.* **5** 3584

* E-mail: krueger@technion.ac.il

Sub-cycle control of valley polarization in WSe_2 monolayer

A Hashmi[1] *, S Yamada[2], A Yamada[2], K Yabana[2], and T Otobe[1†]

[1] Kansai Photon Science Institute, National Institutes for Quantum and Radiological Science and Technology (QST), Kyoto 619-0215, Japan
[2] Center for Computational Sciences, University of Tsukuba, Tsukuba 305-8577, Japan

Synopsis Very short valley lifetimes demand the ultrafast control of valley pseudospin. By using the time-dependent density functional theory (TDDFT), we demonstrate the control of valley pseudospin in WSe_2 monolayer by sub-cycle linearly polarized laser pulse. We use the asymmetric field controlled by the carrier-envelope phase (CEP) to make the valley polarization. Valley polarization remains zero within the linear optical limit while strong valley asyemmtery is experienced in the nonlinear regime. The valley polarization is robust against field strength but oscillates as a function of CEP.

The lack of inversion symmetry in transition metal dichalcogenides (TMDC) monolayer induces a novel Zeeman type spin splitting which results in two degenerate yet inequivalent valleys in the band structure [1]. Valleys are local minima that correspond to different crystal momentum in the reciprocal space. Manipulation of valley pseudospin thus becomes a central theme in the field of valleytronics. Very short valley lifetimes demand ultrafast control of valley selection on sub-femtosecond time scales [2]. In this regard, attosecond control of electron dynamics in the WSe_2 monolayer is investigated by using the linearly polarized single-cycle laser pulse. Time-dependent density functional theory (TDDFT) is used to study the various factors that are vital for valley polarization both in linear and non-linear optical limits.

In contrast to long pulses, ultrashort pulses containing few optical cycles where the $A(t)$ value at $E(t) = 0$ can be controlled by CEP (φ). φ is the relative phase of the pulse envelope and the oscillating electric field which plays a significant role in the pulse waveform for ultrashort laser pulses. To explore the φ dependence on valley pseudospin, we apply linearly polarized pulses parallel to armchair (Γ-M) and zigzag (Γ-K) directions. Valley polarization does not exist for the field polarized along Γ-M because of the lattice symmetry in that direction.

On the other hand, owing to trigonal wrapping, the polarization parallel to Γ-K experiences different band curvature with respect to K and K' point.

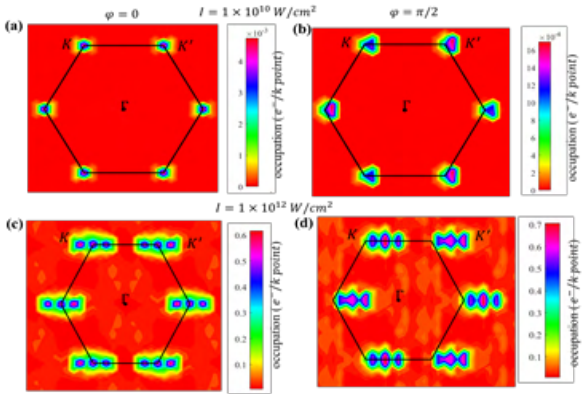


Figure 1. Distribution of k-resolved electron populations in the first Brillion zone of the conduction band at the end of a single optical cycle pulse.

The valley polarization for weak intensity is zero for all φ confirm the fact that the valley polarization is absent within the linear-optical limit. By increasing the intensity, we enter in the nonlinear regime and the substantial valley polarization is observed. The valley polarization increases gradually with φ and reaches its maximum value at $\varphi = \pi/2$, shows a typical sine wave curve. Valley polarization is robust against field strength but in all cases oscillate as a function of CEP.

References

[1] D. Xiao, G.-B. Liu, W. Feng, X. Xu, and W. Yao, Phys. Rev. Lett. **108**, 196802 (2012).
[2] S. A. Vitale, D. Nezich, J. O. Varghese, P. Kim, N. Gedik, P. Jarillo-Herrero, D. Xiao, and M. Rothschild, Small **14**, 1801483 (2018).

* E-mail: *hashmi.arqum@qst.go.jp*
† E-mail: *otobe.tomohito@qst.go.jp*

Multi-dimensional HHG-spectroscopy of ultrafast phonon dynamics via CEP

O Neufeld[1] *, J Zhang[1], U De Giovannini[1], H Hübener[1], and A Rubio[1]

[1]Max Planck Institute for the Structure and Dynamics of Matter and Center for Free-Electron Laser Science, Hamburg, 22761, Germany

Synopsis We theoretically explore high harmonic generation (HHG) in a pump-probe set-up as a tool for studying ultrafast structural dynamics. We show, with state-of-the-art calculations that include dynamical electron-phonon couplings, that the HHG yield is highly sensitive to the pump-probe delay (timing) and to the relative orientation (direction) of a THz-driven phonon. We develop a spectroscopy technique that characterizes the degree of carrier-envelope-phase sensitivity in the HHG yield *vs.* pump-probe delay, which can identify phonon-induced bond compression with ~2fs resolution.

RA

High harmonic spectroscopy has recently been pioneered as a promising method for probing ultrafast electron dynamics in solids[1]. However, its possible applications for tracking structural and phonon dynamics are not yet clear[2]. We theoretically explore pump-probe high harmonic generation (HHG) from monolayer hexagonal-Boron-Nitride (hBN), where active optical phonons are probed. Through state-of-the-art *ab-initio* calculations, we show that the structure of the HHG spectrum is attenuated by the presence of phonons, and comprises a continuous emission in the plateau region. The HHG yield strongly oscillates with the pump-probe delay, corresponding to femtosecond changes in the lattice such as bond compression or stretching. Remarkably, the HHG process can become sensitive to the carrier-envelope-phase (CEP) of the driving laser due to the phonon dynamics, even if the pulse duration is long. We find that the degree of CEP sensitivity *vs.* pump-probe delay is a highly selective measure for instantaneous structural changes in the lattice.

Figure 1(a) presents the simulated set-up: a THz pump excites phonons in hBN, which are subsequently probed by an intense IR pulse that generates harmonics. The electron dynamics are modeled with time-dependent density functional theory (TDDFT). Importantly, the electronic equations of motion are coupled to classical Ehrenfest dynamics of the nuclei, such that the simulation fully incorporates electron-phonon coupling in both directions. This allows us to correlate spectral features in the harmonic yield with the ultrafast structural changes due to phonon motion. For instance, the HHG yield oscillates with the phonon period (Fig. 1(b)). For enhanced phonon sensing, we developed a new observable that estimates the degree of CEP-sensitivity in the HHG yield for a given pump-probe delay (η, Fig. 1(c)). η provides unique nonlinear sensitivity for B-N bond compression, with a temporal resolution of ~2fs well below the total pulse dutration (made possible due to the CEP origin of the sensitivity).

Our work shows new routes for probing ultrafast structural changes, and provides a mechanism for controlling solid HHG emission.

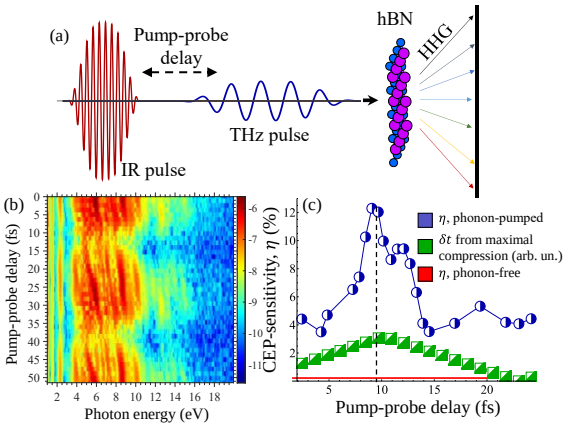


Figure 1. (a) Illustration of pump-probe set-up for observing phonon dynamics with multi-dimensional HHG spectroscopy. (b) Calculated HHG spectrum *vs.* pump-probe delay (1600nm, 10^{12} W/cm^2, driving). (c) Degree of CEP sensitivity *vs.* pump-probe delay, showing a peak that correlates with B-N bond stretching at ~10fs.

References

[1] Ghimire S *et al* 2019 *Nat. Phys.* **15**, 10-16
[2] Bionta M R *et al* 2021 *PRR* **3**, 023250

* E-mail: ofer.neufeld@mpsd.mpdg.de

Enhanced high-harmonic generation from Cr-doped MgO crystals

U Thumm[1]*, V Nefedova[3], F Navarrete[2,1], N Tancogne-Dejean[4], S Fröhlich[3], W Boutu[3], M F Ciappina[5,6,7], D Gauthier[3], A Hamdou[3], S Kaassamani[3], A Rubio[4], and Hamed Merdji[3]

[1]Department of Physics, Kansas State University, Manhattan, Kansas 66506, USA
[2]Institute of Physics, University of Rostock, 18051 Rostock, Germany
[3]Ultrafast Nanophotonics Group, LIDYL, CEA-CNRS-Université Paris-Saclay, 91191 Gif-sur-Yvette, France
[4]Max Planck Institute for the Structure and Dynamics of Matter and Center for Free-Electron Laser Science, Luruper Chaussee 149, 22761 Hamburg, Germany
[5]ICFO-Institut de Ciences Fotoniques, The Barcelona Institute of Science and Technology, Avenue Carl Friedrich Gauss 3, 08860 Castelldefels (Barcelona), Spain
[6]Physics Program, Guangdong Technion-Israel Institute of Technology, Shantou, Guangdong 515063, China
[7]Technion-Israel Institute of Technology, Haifa 32000, Israel

Synopsis We show the first experimental observation of impurity-enhanced HHG yields that is supported by our numerical solutions of the Semiconductor Bloch Equations.

RA

High-harmonic generation (HHG) from crystals is a new source of coherent extreme ultraviolet (XUV) attosecond radiation [1], which also allows the retrieval of band structure information [2]. Increasing the HHG yield and cutoff are fundamental to developing efficient XUV sources. We investigated experimentally and theoretically an alternative way of boosting the HHG yield based on doping [5].

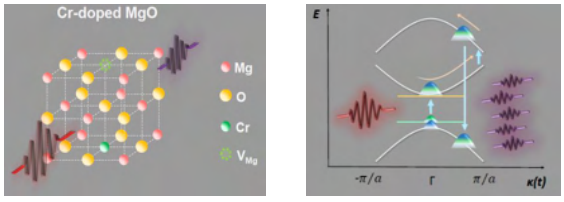


Figure 1. Schematic of HHG from MgO:Cr crystals in coordinate (left) and momentum space (right). The laser electric field excites an electron wave packet from the valence to a conduction band (blue up arrows), where it is accelerated (orange arrows). It then recombines with its residual hole (blue down arrow), emitting HHs. In MgO:Cr the occupied impurity-defect band and vacancy-defect band (horizontal lines) enable additional transitions that enhance the HH yield relative to MgO.

The presence of dopants results in new electronic states in the band gap, as well as lattice defects, which modify the minimum band gap. Since the interband HHG yield depends exponentially on the minimum band-gap energy (EG) of the solid [3], one can expect a substantial change of the HHG yield by reducing EG [4].

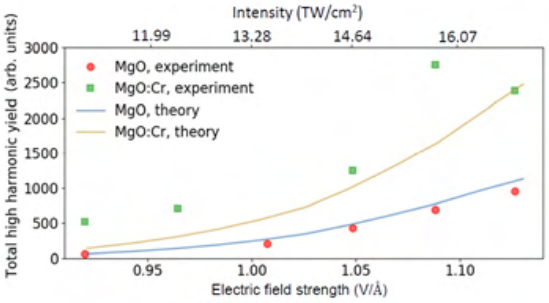


Figure 2. HHG yield for MgO and MgO:Cr as a function of the 1.55 μm driving-laser peak-electric-field strength.

We acknowledge support from the: AFOSR Grant N° FA9550-17-1-0369, NSF Grants N° 1464417 and N° 1802085, and PETACom FET Open H2020 Grant N° 829153.

References

[1] G Vampa *et al.*, IEEE J. Sel. Top. Quantum Electron. **21**, 8700110 (2015).
[2] N Tancogne-Dejean *et al.*, Phys. Rev. Lett. **118**, 087403 (2017).
[3] F Navarrete *et al.*, Phys. Rev. A **100**, 033405 (2019).
[4] T Huang *et al.*, Phys.Rev. A **96**, 043425 (2017).
[5] V Nefedova *et al.*, Appl. Phys. Lett. **118**, 201103 (2021).

*E-mail: thumm@phys.ksu.edu

1.5mJ, 30W OPA at 2um via spectrally selective amplification

B E Schmidt[1†], D Wilson[1,2], M Ivanov[1,2], P Abdolghader[1], A Raffray[1,2], T Balciunas[3], F Légaré[2], and H J Wörner[3]

[1] few-cycle Inc, 1650 Boulevard Lionel-Boulet, Varennes, J3X 1P7, QC, Canada
[2] Institut national de la recherche scientifique, 1650 Boulevard Lionel-Boulet, Varennes, J3X 1P7, QC, Canada
[3] ETH Zürich, Vladimir-Prelog-Weg 2, Zürich 8093, Switzerland

Synopsis To reach high average power operation combined with good conversion efficiency we utilize spectrally selective amplification with multiple nonlinear crystals to yield 12% conversion efficiency with 30W output at 2um wavelength.

RA

High power IR lasers are important tools for the ultrafast community. The advent of high average power Yb laser as the pump source for optical parametric amplifiers (OPAs) enabled the demonstration of unprecedented average power outputs [1]. In ref 1, a 660W pump laser was used to achieve 100W of IR output power at a shorter wavelength of 1.7um with a slightly more favorable quantum defect and heat management situation as compared to our >2µm target for the center wavelength. Short pulses around the much more challenging center wavelength of 2µm have been demonstrated at lower conversion efficiency of about 6% with a record average power of 27W very recently [2]. In this contribution, we present our first results towards a >50W IR laser at 2µm with 20kHz repetition rate where we have achieved so far an IR output power of 30W (signal only) for a pump power of 240W at 1030nm corresponding to 12.5% conversion efficiency (for uncompressed pulses).

To tackle the problem of excessive crystal heating especially for amplified wavelengths longer than 2µm, we employ the strategy of wavelength selective amplification. Following the concept of FOPA [3] where different spectral regions are amplified independently in a spatially extended Fourier plane, here we realize channel selective amplification in time domain, comparable to a traditional Optical Parametric Chirped Pulse Amplifier (OPCPA) scenario. In our approach, we stretch the seed temporally to match with the 1.5ps pump beam. Upon amplification, however, we narrow the gain bandwidth to a fraction of the entire seed bandwidth. This results in two advantages: (i) we can use potentially thicker crystals as the phase matching bandwidth is not a too strong concern anymore and (ii) by amplifying different wavelengths in different crystals, we can better control the heat dissipation at the problematic ranges, typically in the IR part of the spectrum. In this manner, we ca use BBO crystals to amply a spectral region from 1.92 µm up to 2.22 µm wavelength.

The resulting amplified spectrum (red curve) with a 4 channel amplifier (4 nonlinear crystals) is shown in Fig. 1(a). Due to the wavelength specific heat management, we are able to maintain the good spatial seed beam properties, shown in Fig. 1(b-c).

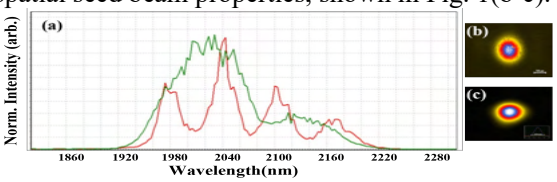


Figure 1. (a): The 30W output of the 4 channel amplified spectrum (red curve) covers the entire seed bandwidth (green curve) to yield a spectrum that supports 60fs pulses centred at 2060nm wavelength. Due to the wavelength selective heat management on the BBO crystals, we can maintain optimum spatial beam quality at 240W of incident pump which corresponds to 30W output (signal only). (b) shows the beam profile and (c) the corresponding focal spot.

At the conference, we plan to present different upgrades including the demonstration of preliminary bulk compression of the amplified output as well as operation at 450W pump power with a modified setup that utilizes 6 – 8 channels. The goal is to reach >50W of 50fs amplified pulses at 2 µm wavelength that can be subsequently compressed in a high efficiency hollow-core fiber (HCF) to sub 15fs pulse duration. Assuming an already demonstrated HCF efficiency of 80% [4], we are aiming for 40W (2mJ, 20kHz) sub-2 cycle pulses at 2 µm wavelength.

References

[1] M. K. R. Windeler, et al.,Opt.Lett.**44**, 4287-4290 (2019)
[2] T.Feng, et al., Opt. Express **28**, 8724-8733 (2020).
[3] B. E. Schmidt et al., Nature Communications **5** (2014).
[4] V. Cardin, et al., Appl. Phys. Lett. **107**, 181101 (2015)

† E-mail: schmidt@few-cycle.com

Polarization shaping of light for strong field valleytronics

I Tyulnev[1*], L Vamos[1] and J Biegert[1,2]

[1] ICFO - Institut de Ciencies Fotoniques, The Barcelona Institute of Science and Technology, Castelldefels (Barcelona), 08860, Spain
[2] ICREA, Pg. Lluís Companys 23, Barcelona, 08010, Spain

Synopsis We shape the polarization of mid-infrared light into a trefoil, to use it as a pump for valley polarization switching. With high harmonic spectroscopy we demonstrate its element specificity inside GaSe through selection rules which emerge from the combined crystal and field symmetries.

Strong field induced effects provide access to exotic phases and polarization states in crystals and 2D materials. With the growing number of recent interests ranging from valley polarization [1] to controlled emission in chiral media [2], the polarization tailoring of light is required to explore currently emerging areas such as optoelectronics, spintronics, field effect transistors and photo-electron catalysts [3].

In this work we demonstrate the first step towards building an all-optical valleytronic switch as proposed by [1]. Importantly, valley selectivity will be achieved, not by the handedness of circular light, but by the strong field interaction of a trefoil shaped laser polarization which is matched to the material's crystal structure.

We report on the experimental realization of the trefoil field at mid-IR wavelengths where the fundamental wavelength of 3.2 µm from our OPCPA system is combined with its second harmonic in a Mach-Zehnder polarization interferometer. The polarization vector draws a trefoil pattern when both beams are turned to circular polarization with opposite handedness. With this field, we generate high harmonics inside z-cut GaSe (EKSMA) which are highly sensitive to the polarization state of the driving field. For example, matching a linear polarized pump to any crystal axis leads to enhancement in the harmonic signal, as carriers are moved along the equivalent symmetry axis in reciprocal space. In Figure 1 we demonstrate this dependency as our crystal is rotated. For instance, a linearly polarized field results in a six-fold modulation of harmonic 5 (H5) for one full rotation, thus reflecting the six-fold symmetry of the hexagonal lattice. Circular polarization does not access any specific symmetry; thus, the six-fold modulation is lost, but selection rules dictate suppression of harmonic orders 3n; this is clearly observed in Fig. 1 H6. Lastly, the trefoil field accesses the three-fold symmetry of the crystal, where it aligns with the sublattice of either Ga or Se which have different contributions in the harmonic signal and result in a modulation of H5 at 120 degrees.

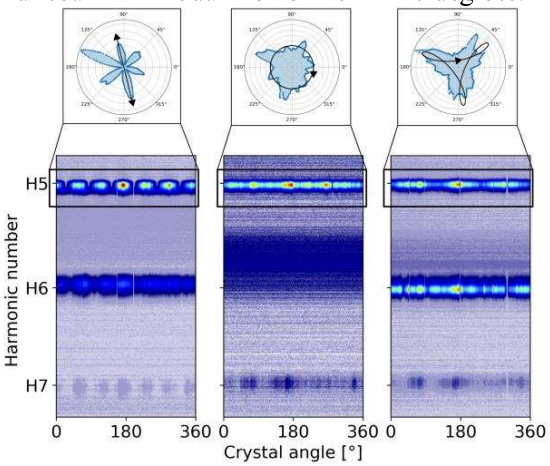


Figure 1. High harmonic yield as a function of the rotation angle between crystal and electric field for linear, circular, and trefoil polarization of the 3.2 µm pump. (Top) Lineouts for 5th harmonic and sketched driving field.

This unique response, which only appears for the trefoil field, proves its sensitivity to the atomic flavor. Meanwhile high harmonic spectroscopy gives direct microscopic access to the specific degree of valley polarization and a convenient characterization technique.

These results provide a first approach towards subcycle control over hexagonal materials for information encoding and processing at petahertz frequencies.

References

[1] Jiménez-Galán Á *et al. Nat. Phot. :* 14, 728, 2020
[2] Ayuso D *et al. Nat. Commun. :* 12, 3951, 2021
[3] Wang C & An Y. *Appl. Surf. Sci. :* 583, 152520, 2022

* E-mail: igor.tyulnev@icfo.eu

Poster Session III, Highlights B
Chair: **Jan Marcus Dahlström**, Lund University, Sweden

R01 **Attosecond Coherent Electron Motion in Molecules Measured with Attosecond X-ray Pulse Pairs**
Jordan O'Neal, LCLS Attosecond Campaign Collaboration 173

R02 **Decoherence and Revival of Attosecond Charge Migration Driven by Non-adiabatic Dynamics**
Danylo Matselyukh, Victor Despré, Nikolay Golubev, Alexander Kuleff, Hans Jakob Wörner 174

R07 **Optically forbidden inner valence excited state lifetimes in neon atoms measured by attosecond noncollinear four wave mixing spectroscopy**
Nicolette Puskar, Yen-Cheng Lin, James D Gaynor, Maximilian Schuchter, Ashley P Fidler, Clare Keenan, Daniel M Neumark, Stephen R Leone 175

R13 **Measurement of the Attoclock-Offset Angle and the Wigner Time Delay in a single experiment**
Nils Anders, Daniel Trabert, Angelina Geyer, Max Hofmann, Markus S. Schöffler, Till Jahnke, Lothar Ph. H. Schmidt, Maksim Kunitski, Reinhard Dörner, Sebastian Eckart 176

R18 **Application of the CHIP method to chiral recognition**
Nicolas Douguet, Luca Argenti 177

R19 **General scaling law of non collinear high harmonic generation and its applications**
Mekha Vimal, Martin Luttmann, David Bresteau, Fabien Lepetit, Olivier Tcherbakoff, Jean-François Hergott, Thierry Auguste, Thierry Ruchon 178

R24 **Optical measurement of photorecombination time delays**
Chunmei Zhang, Graham G Brown, Dong Hyuk Ko, Paul B Corkum 179

R28 **Time-resolved spectroscopy of Xe giant resonance by employing all-optical measurement of attosecond pulses**
Dong Hyuk Ko, Graham G Brown, Chunmei Zhang, Paul B Corkum 180

R29 **Probing electronic and vibrational dynamics in Furan with AttoXAFS**
Stefano Severino, Karl Michael Ziems, Maurizio Reduzzi, Adam Summers, Hung-Wei Sun, Ying-Hao Chien, Stefanie Gräfe, Jens Biegert 181

RB

Attosecond Coherent Electron Motion in Molecules Measured with Attosecond X-ray Pulse Pairs

J O'Neal[1,2 *], on behalf of the LCLS Attosecond Campaign Collaboration[3]

[1]Stanford PULSE Institute, Menlo Park, CA, USA
[2]Department of Physics, Stanford University, Stanford, CA, USA
[3]Linac Coherent Light Source, SLAC National Accelerator Laboratory, Menlo Park, CA, USA

Synopsis Attosecond soft X-ray pulse pairs from a free-electron laser [1] offer the opportunity to probe valence electron dynamics in molecules, with elemental specificity, on the natural timescale of coherent valence electron motion. We present measurements of attosecond electron dynamics probed with resonant Auger-Meitner spectroscopy. We observe a new resonance open just below the oxygen *K*-edge that signals the creation of inner valence holes. The resonance is linear in the pump pulse tuned below the carbon *K*-edge, decays rapidly within the first femtosecond, and shows a revival around 4.2 fs.

RB

Impulsive photoionization can prepare a superposition of valence-ionized electronic states in a molecule [2]. The coherent evolution of this electron wavepacket can cause the electron hole to move across the molecule on an attosecond timescale. The influence of this short-lived electronic coherence on subsequent chemical motion is an open question. Here we make use of subfemtosecond X-ray pulse pairs [1,3] to observe coherent electronic motion in a prototypical molecule, *para*-Aminophenol (NH_2-C_6H_4-OH).

A 260 eV X-ray pulse drives impulsive ionization of inner valence shell electrons. Sudden removal of an electron creates a non-stationary superposition of N-1 electron cationic eigenstates, since the attosecond ionization pulse is shorter than the timescale of electron rearrangement. We track the evolution of this inner valence hole with resonant Auger-Meitner (AM) spectroscopy [4,5].

Figure 1 a) shows the excess AM electron signal created by increasing the pump pulse energy at a pump/probe delay of 0.54 fs. A new AM resonance is found, which scales linearly with the pump intensity. In panel b), we choose probe photon energy bounds to capture this new resonance (blue solid line) and two background regions to capture inter-delay systematics. This AM resonance decays within the first femtosecond, and a small revival is seen around 4.2 fs, suggesting a coherent rephasing of the valence ionized wavepacket.

Use of the Linac Coherent Light Source (LCLS), SLAC National Accelerator Laboratory, is supported by the U.S. Department of Energy, Office of Science, Office of Basic Energy Sciences under Contract No. DE-AC02-76SF00515. This work was primarily supported by the U.S. Department of Energy (DOE), Office of Science, Office of Basic Energy Sciences (BES), Chemical Sciences, Geosciences, and Biosciences Division (CSGB)

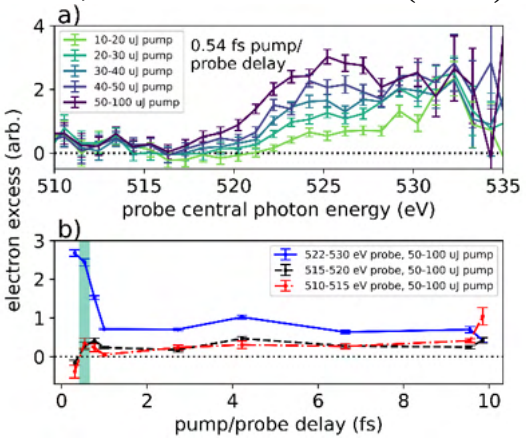


Figure 1. Auger-Meitner electron excess above pump intensity 2-10 uJ. a) At 0.54 fs pump/probe delay, electron excess as a function of pump intensity and probe photon energy. b) Delay dependence of electron excess, integrated over specified photon energy ranges. Shaded delay point is shown in more detail in panel a).

References

[1] Duris J *et al* 2020 *Nat. Photonics* **14** 30
[2] Cederbaum L S *et al* 1999 *Chem. Phys. Lett.* **307** 205-210
[3] Lutman A A *et al* 2013 *Phys. Rev. Lett.* **110** 134801
[4] Wolf T J A *et al* 2021 *Faraday Discuss.* **228**, 555
[5] Barillot T *et al* 2021 *Phys. Rev. X* **11** 031048

* E-mail: joneal2@stanford.edu

Decoherence and Revival of Attosecond Charge Migration Driven by Non-adiabatic Dynamics

D T Matselyukh[1]*, V Despré[2], N V Golubev[3], A I Kuleff[2], HJ Wörner[1]

[1]Laboratorium für Physikalische Chemie, ETH Zürich, 8093 Zürich, Switzerland
[2]Physikalisch-Chemisches Institut, Universität Heidelberg, 69120 Heidelberg, Germany
[3]Laboratory of Theoretical Physical Chemistry, EPF Lausanne, 1015 Lausanne, Switzerland

Synopsis
The effect of nuclear motion on electronic coherences in the electronically-excited states of silane (SiH_4) has been investigated using soft-X-ray attosecond transient absorption spectroscopy on the L2, 3 edge of silicon. With the support of Multi-Configurational Time-Dependent Hartree simulations, we find that the measured charge migration (with a period of 1.39 and 1.30 fs) decoheres in 15 fs and recoheres at a delay of 50 fs due to differences in the vibrational dynamics of different electronic states.

RB

Recent theoretical studies have predicted coherences between bifurcating wavepackets [1] and the dephasing and revival of charge migration [2]. Unfortunately, experimental techniques showing sensitive and robust probes of these phenomena have lagged behind, leading to key open questions in the field of attochemistry. Pioneering studies have shown experimental signatures of charge migration [3, 4], however, the influence of nuclear dynamics remains to be demonstrated. In this work, we will present experimental and theoretical results from X-ray attosecond transient absorption spectroscopy (ATAS) on silane (SiH_4) that show the dephasing and revival of charge migration and demonstrate the wealth of information that can be extracted by applying the ATAS technique to studying charge migration.

5 fs Vis/NIR pump pulses are used to strong-field excite the silane molecule into a superposition of electronically excited states. This electronic superposition is then probed using a delayed Soft-X-ray attosecond probe pulse covering the $L_{2,3}$ absorption edge of silicon at 100-110 eV. The charge migration resulting from the coherence is detected through quantum beats in the transient-absorption spectrum and, as opposed to isolated atoms, exhibits a rich temporal structure in which the initial quantum beat decays over the first 15 fs but then reappears between delays of 40 and 50 fs.

The interpretation of the electronic dynamics is achieved with the help of Multi-Configurational Time-Dependent Hartree (MCTDH) calculations in which the electronic and vibrational degrees of freedom of the system are treated fully quantum-mechanically. These calculations reproduce the temporal structure of the quantum beat in the experiment and assign them to a superposition of valence and Rydberg excited states separated by 3 eV (corresponding to a quantum beats with a period of 1.4 fs). The MCTDH simulations also allow us to identify the signature of possible non-adiabatic effects in the experimental results, giving evidence for the preservation of coherence upon passage through a conical intersection. Adiabatic dynamics are are found to be responsible for the modulation of the coherence between the electronic states. Specifically, we find that electronic coherence requires overlap in both position and momentum space of the associated vibrational wavepackets.

With this work we have obtained the first experimental evidence of dephasing and revival of attosecond charge migration, mediated by nuclear and non-adiabatic dynamics. Our work also demonstrates the exceptional potential of ATAS deriving from its element specificity.

References

[1] M Kowalewski et al., Phys. Rev. Lett. **115**, 193003 (2015).
[2] D Jia et al., J. Phys. Chem. **10**, 15 (2019).
[3] F Calegari et al. et al., Science. **346**, 6207 (2014).
[4] P M Kraus et al., Science. **350**, 6262 (2015).

*E-mail: mdanylo@ethz.ch

Optically forbidden inner valence excited state lifetimes in neon atoms measured by attosecond noncollinear four wave mixing spectroscopy

N G Puskar[1,2] *, Y-C Lin[1,2], J D Gaynor[1,2], M C Schuchter[1,2,3], A P Fidler[4], C Keenan[5], D M Neumark[1,2] and S R Leone[1,2,6]

[1]Department of Chemistry, University of California, Berkeley, California 94720, USA
[2]Chemical Sciences Division, Lawrence Berkeley National Laboratory, Berkeley, California 94720, USA
[3]Laboratory for Physical Chemistry, ETH Zürich, Zürich 8093, Switzerland
[4]Department of Chemistry, Princeton University, New Jersey 08544, USA
[5]Department of Chemistry, The University of Chicago, Illinois 60637, USA
[6]Department of Physics, University of California, Berkeley, California 94720, USA

Synopsis Attosecond noncollinear four wave mixing spectroscopy was used to measure the autoionization decay lifetimes of inner valence electronic excitations in Ne atoms. Broadband NIR pulses couple the $2s2p^6 3p$ XUV-bright state to neighboring $2s2p^6 3s$ and $2s2p^6 3d$ XUV-dark states. Lifetimes for the $3s$, $3p$, and $3d$ states were observed to be 15 ± 4 fs, 43 ± 5 fs, and 860 ± 40 fs, respectively, in agreement with literature expectations. This study shows that four wave mixing provides access to optically forbidden states, enabling explorations of wider regions of electronic dynamics in atoms and molecules.

RB

Attosecond pulses provide the time resolution needed to measure electronic dynamics such as autoionization directly in the time-domain [1]. Using high harmonic generation to produce attosecond XUV and soft X-ray pulses, tabletop laboratories can explore time-resolved electronic motion with the elemental specificity intrinsic to inner-valence and core-level excitations [2]. Attosecond four wave mixing (4WM) spectroscopy can utilize a noncollinear beam geometry between the generated XUV pulse and two few-cycle NIR pulses to yield background free, spatially isolated emission signals (Figure 1) [3]. This technique has previously elucidated the lifetimes of $^2P_{1/2}$ ns/d autoionizing states in Kr and the v=0 and v=1 $3s$ Rydberg states in O_2 [4,5].

In this study, attosecond 4WM spectroscopy is used to measure the autoionization decay lifetimes of optically allowed (bright) and forbidden (dark) inner valence electronic excitations in neon gas. XUV pulses excite an electron from the inner valence $2s$ state into the $2s2p^6 3p$ XUV-bright state [6]. Then, two few-cycle NIR pulses probe this state as it decays with a lifetime observed to be 43 ± 5 fs. The transient behavior of two neighboring XUV-dark states, $2s2p^6 3s$ and $2s2p^6 3d$, are accessible by coupling the $2s2p^6 3p$ transition with broadband NIR photons. Controllably delaying the NIR pulses reveals the temporal evolution of the dark states, with lifetimes for the $2s2p^6 3s$ and $2s2p^6 3d$ states observed to be 15 ± 4 fs and 860 ± 40 fs, respectively.

Our results suggest a direct relationship between orbital angular momentum and autoionization decay lifetime. As angular momentum increases, the probability amplitude of the electron near the nucleus decreases, and the autoionization lifetimes are therefore expected to increase [7]. The lifetimes reported in this work support this trend. As exemplified here, attosecond 4WM can provide time-domain insight into highly excited electronic dynamics with few-femtosecond temporal resolution in a background-free manner, facilitating a greater physical understanding of ultrafast relaxation processes.

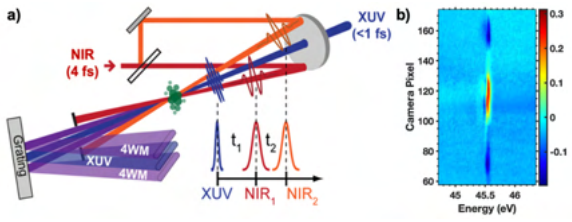


Figure 1. a) Attosecond noncollinear 4WM schematic. **b)** Spatially isolated upper and lower 4WM signals (dark blue emission regions) of neon's $2s2p^6 3p$ state.

References

[1] Ott C *et al* 2013 *Science* **340** 716
[2] Nisoli M *et al* 2017 *Chem. Rev.* **117** 10760
[3] Cao W *et al* 2016 *Phys. Rev. A* **94** 1
[4] Fidler *et al* 2019 *J. Chem. Phys.* **151** 114305
[5] Lin *et al* 2021 *Faraday Discuss.* **228** 537
[6] Schulz K *et al* 1996 *Phys. Rev. A.* **54** 3095
[7] Cooke W E *et al* 1978 *Phys. Rev. Lett.* **40** 178

* E-mail: nicolette.puskar@berkeley.edu

Measurement of the Attoclock-Offset Angle and the Wigner Time Delay in a single experiment

N Anders[1 *], D Trabert[1], A Geyer[1], M Hofmann[1], M S Schöffler[1], T Jahnke[1], L Ph H Schmidt[1], M Kunitski[1], R Dörner[1] and S Eckart[1 †]

[1]Institut für Kernphysik, Goethe-Universität, Frankfurt am Main, 60438, Germany

Synopsis We report on non-adiabatic tunnel ionization of Ne in co- [counter-] rotating two-color (CoRTC [CRTC]) laser fields. We apply the technique of holographic angular streaking of electrons (HASE). We demerge the interference pattern and the envelope of the measured electron momentum distribution. From the interference pattern, we infer the rotation angle of six above-threshold ionization peaks and six sideband peaks with unprecedented statistics. Interestingly, for low-energy electrons the rotation angle of the envelope and the interference pattern follow opposite trends.

RB

We report on the simultaneous investigation of the attoclock-offset angle [1] (the most probable emission angle) as well as the Wigner Time Delay [2] from a single experiment. We have measured the electron momentum distributions for the strong field ionization of neon using a co- [counter-] rotating two-color (CoRTC [CRTC]) laser field (see Fig. 1 (a), (b)). The measured data can be demerged into an interference pattern and its envelope to obtain two independent observables (see Fig. 1(c)-(f)).

In order to be able to apply the technique of holographic angular streaking of electrons (HASE) [3, 4], the two-color laser field consists of a weak 790 nm and a strong 395 nm laser pulse with a field ratio of 1/12. To measure the three-dimensional momenta of the electron and ion in coincidence a cold-target recoil-ion momentum spectroscopy (COLTRIMS) reaction microscope [5] was used.

Fig. 1 (a) [(b)] shows the measured electron momentum distribution in cylindrical coordinates for a CoRTC [CRTC] laser field. The envelope (Fig. 1 (c) [d]) was separated from the interference pattern (Fig. 1 (e) [(f)]) and the one- [three-] fold symmetry for each momentum bin was determined. It is visible that the phase of low energy electrons has an opposite trend for the envelope and the interference pattern.

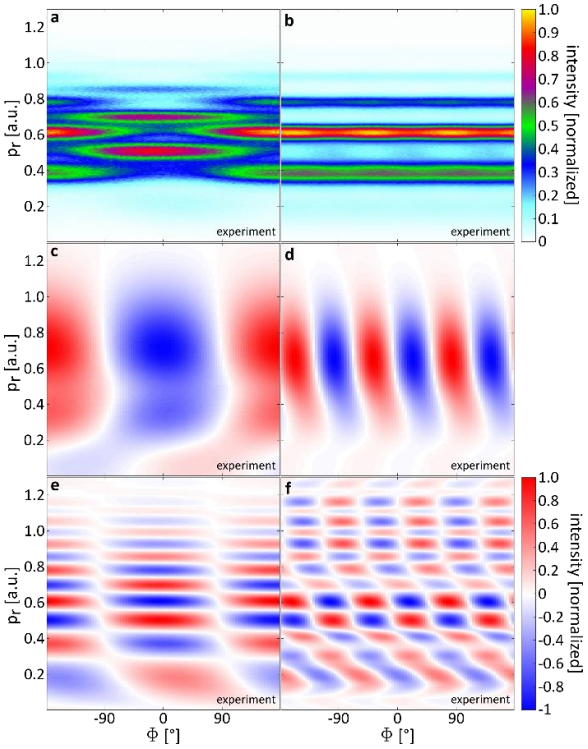


Figure 1. (a) [(b)] experimentally measured electon momentum distribution projected onto the laser's polarization plane in cylindrical coordinates for a CoRTC [CRTC] laser field. (c) [(d)] one- [three-] fold symmetry of the envelope for the CoRTC [CRTC] laser field. (e) [(f)] one- [three-] fold symmetry of the interference pattern for the CoRTC [CRTC] laser field.

* E-mail: anders@atom.uni-frankfurt.de
† E-mail: eckart@atom.uni-frankfurt.de

References

[1] Eckle P *et al* 2008 *Science* **322**, 1525-1529
[2] Wigner E P 1955 *Phys. Rev.* **98**, 145-147
[3] Eckart S 2020 *Phys. Rev. Research* **2**, 033248
[4] Trabert D *et al* 2021 *Nat. Commun.* **12**, 1697
[5] Ullrich J *et al* 2003 *Rep. Prog. Phys.* **66**, 1463

Application of the CHIP method to chiral recognition

N Douguet[1]* **and L Argenti**[2]

[1]Department of Physics, Kennesaw State University, Marietta, Georgia 30060, USA
[2]Department of Physics & CREOL, University of Central Florida, Orlando, Florida 32816, USA

Synopsis We consider the application of the circular holographic ionization-phase meter (CHIP) for the discrimination of chiral molecules. Because CHIP produces an interference in the angularly-resolved photoemission signal via a pair of counter-rotating consecutive harmonics, it has the potential to reveal chirality. Using the multi-photon complex Kohn (MPCK) method, we investigate the valence and oxygen K-shell photoionization of methyloxirane and show a strong photoelectron circular dichroism for randomly oriented molecules, thereby paving the way for new chiral recognition methods.

Chiral recognition is fundamental in resolving the puzzle of homochirality and has also important applications in the pharmaceutical industry. A recent technique, the photoelectron circular dichroism (PECD), considers the forward-backward asymmetry of photoelectrons emitted from randomly oriented chiral molecules ionized by circularly light and leads to a substantial effect when compared to conventional circular dichroism (CD). While PECD is an effect of only a few percent for randomly oriented molecules in the gas phase, a recent tour-de-force experiment [1] showed a PECD up to 50% for fixed-in-space molecules. The method requires the complete reconstruction of the molecular frame by detecting of at least three dissociative fragments in coincidence. Therefore, its systematic application to other molecules is far from straightforward and it is still highly desirable to develop novel protocols to efficiently discriminate randomly oriented enantiomers.

Here, we propose to study chirality by employing an attosecond interferometric XUV-pump-IR-probe photoionization protocol; the so-called CHIP method [2]. In CHIP, a pair of counter-rotating consecutive harmonics are combined with a circular IR field to produce an interference between one- and two-photon ionization pathways, leading to a photoemission anisotropy in the light polarization plane. Because CHIP offers a direct comparison between the signals produced from two counter-rotating harmonics, it is able to reveal chirality. We use the MPCK method [3] to study both the valence and oxygen K-shell photoionization of methyloxirane. We show that reverting the light helicity of the pulses in CHIP leads to a mirror image of the photelectron angular distribution in the light polarization plane for achiral molecules, while this symmetry is broken for a chiral system. We calculate a strong PECD for fixed-in-space molecule and show that survives when we average over the molecular orientation (see Fig. 1), demonstrating the potential of CHIP for chiral recognition of molecules in the gas phase.

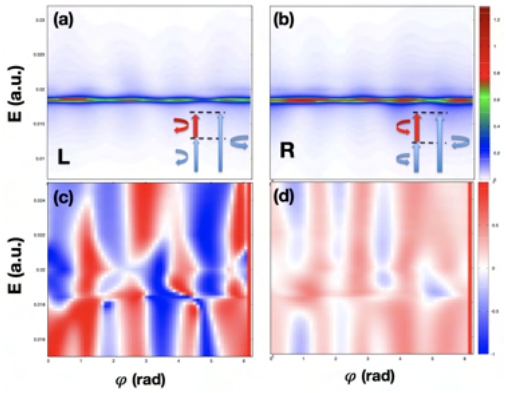


Figure 1. CHIP method in the valence photoionization of methyloxirane. Photoelectron signal in the light polarization plane for left (a) and right (b) schemes. The onset shows the light handedness. PECD signal when reverting light helicity for fixed-in-space (c) and randomly oriented (d) molecules.

References

[1] K Fehre *et al.*, Phys. Rev. Lett. **127**, 103201 (2021).
[2] S Donsa *et al.*, Phys. Rev. Lett. **123**, 133203 (2019).
[3] N Douguet, B. Schneider, and L Argenti, Phys. Rev. A **98**, 023403 (2018).

*E-mail: ndouguet@kennesaw.edu

RB

General scaling law of non collinear high harmonic generation and its applications

Mekha Vimal [*], Martin Luttmann, David Bresteau, Fabien Lepetit, Olivier Tcherbakoff, Jean-François Hergott, Thierry Auguste, Thierry Ruchon[†]

Université Paris-Saclay, CEA, CNRS, LIDYL, 91191 Gif-sur-Yvette, France

Synopsis High order harmonics driven by two non collinear beams constitutes an ideal testbed for theories, as it splits several channels of emission, usually degenerated, in a series of beamlets which may be analyzed separately. It also find many applications, to tailor high harmonics polarization, orbital angular momentum or generate them in cavities. We here introduce a classical theory that describes the yields of the beamlets as the ratio of the driving beams is varied. It is validated by both full quantum computations and experiments, and find unexpected interpretation in terms of photon channels.

RB

We investigate High order Harmonic Generation driven by two Non Collinear beams (NCHHG) theoretically and experimentally over a very large range of intensities ratios of the two beams, from the perturbative to the non perturbative regime [1-2]. By introducing the composite field which forms an "active optical grating" in an empirical model based on the Strong-Field Approximation (SFA), we could establish the scaling laws of the yields of the multiple beamlets generated. The theoretical and experimental results are in excellent agreement, and further match with a direct full 3D numerical model based on the resolution of the Schrödinger Equation within the strong field approximation. These results could also be interpreted in terms of photon channels associated to each beamlet, bridging the gap with previous interpretations restricted to the low perturbation regime. The establishment of this general description of NCHHG opens novel spectroscopic approaches. Thus we have identified specific spectroscopic signatures of strong field multiphoton processes in both the intermediate and strong perturbation regimes, which find straightforward interpretations within our active grating framework.

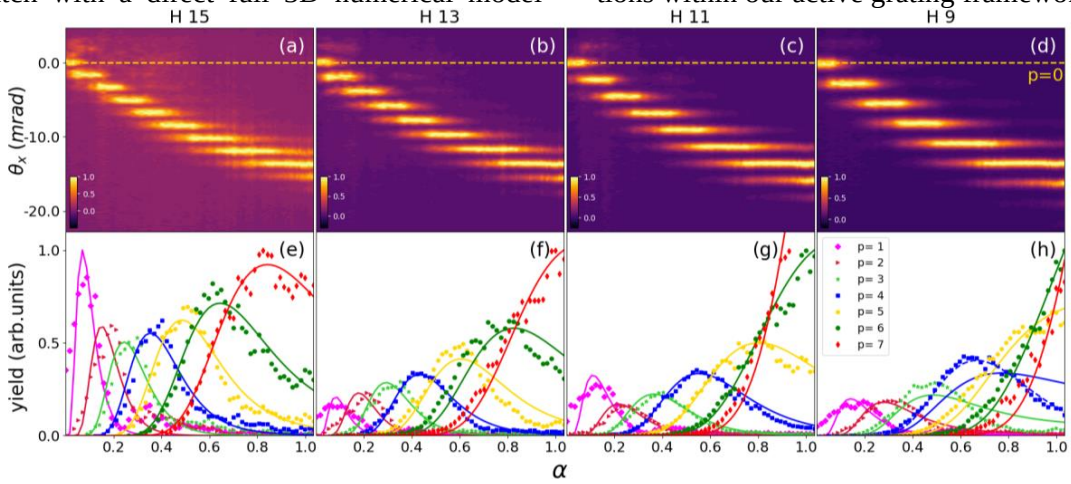


Figure 1. Experimental data for harmonics 15, 13, 11 and 9 for high perturbation levels are presented. The top panels (a-d) show the intensity of each order of diffraction of the active grating with increasing perturbation (α). The bottom panels (e-h) show emission yields of different diffraction orders of the corresponding harmonic order. The solid lines are the fits of the analytical model on the experimental data.

References

[1] C. Chappuis et.al, Phys.Rev. A, 99, 033806 (2019).
[2] M. Vimal et.al, submitted.

[*] E-mail: mekha.vimal@cea.fr
[†] E-mail: thierry.ruchon@cea.fr

Optical measurement of photorecombination time delays

C Zhang[1 *], G G. Brown[2 †], D H Ko[3], P B. Corkum[3]

[1]Beijing Institute of Technology, Beijing, China
[2]Max Born Institute, Berlin, Germany
[3]Joint Attosecond Science Laboratory, University of Ottawa,Ottawa, ON, Canada

Synopsis Recollision physics combines the ability to probe media structure through collisions and the precision of optics. We perform experimental and theoretical studies to investigate the dependence of the recollision electron wave packet on the transition moment phase. We show that, by perturbing recollision trajectories, photorecombination time delays in argon around the Cooper minimum can be measured entirely optically. In doing so, we demonstrated the link between the transition moment and recollision trajectories. Our approach paves the way for the optical study of ultrafast electron dynamics and photorecombination delays in gas-phase molecules and potentially in solids.

Understanding the recollision process is one of the most important accomplishments of attosecond science. In recollision physics, one of the common assumptions which had been widely used is that recollision trajectories are independent of the parent ion. The attosecond pulse spectra are expressed as the product of the system-free continuum wave packet and laser-free photorecombination differential cross sections (PRCS)[1]. Therefore the media undergoing recollision cannot be studied through recollision trajectories and attosecond measurements are typically done by photoionization-based methods, which are difficult to accomplish.

Here, we report an all-optical approach to studying the photorecombination time delays using recollision. We manipulate the electron-ion collision with a perturbing field and the group delay of the recollision electron wave packet is retrieved by observing the influence on the attosecond spectra of the perturbation optically. This approach permits us to determine photorecombination time delays that originate from many sources.

In the experiment, an isolated attosecond pulse is generated in argon. We then perturb recollision with a weak second-harmonic pulse. The perturbing field modulates the recollision trajectories, the near-field attosecond pulse wavefronts, and then the far-field attosecond pulse spectra. With a controlled phase shift on recollision trajectories, we obtain-spectrograms for all XUV energies. The phase information of spectrograms is related to emission time[2] allowing us to determine the group delay of the recollision electron for the whole spectrum.

In Fig.1, we show the group delay of unperturbed attosecond pulse from an *ab initio* simulation[3] of the experimental conditions. The red line is the reconstructed recollision electron group delay. The two group delay curves agree and they are linear until the cutoff with a delay ~150as near the Cooper minimum. The agreement between the simulation and experiment demonstrates that recollision trajectories are shaped by the transition moment phase.

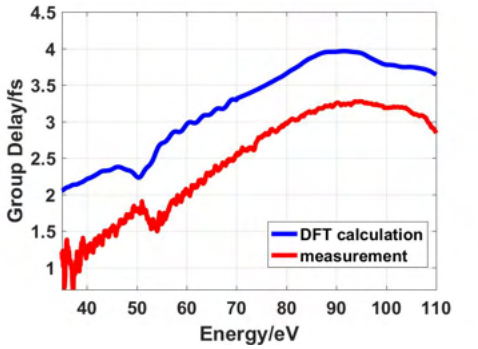


Figure 1. Group delay for the attosecond pulse generated in argon measured entire optically (red line) and calculated from an *ab initio* simulation of the experimental conditions(blue line).

Our results demonstrate an entirely optical way to study the ultrafast electron dynamics and photorecombination delays in gas-phase molecules and solids. Further, the dependence of recollision trajectories on the transition moment phase will affect both how to describe the recollision theoretically and how to measure and interpret measurements of recollision dynamics experimentally.

References

[1] Le , A.-T. *et al* 2009 *Phys. Rev. A* 80, 013401
[2] Kim, K.T.*et al* 2013 *Nature Phys* 9, 159 – 163
[3] Zhang C *et al* 2021 arXiv:2104.00844

* E-mail: chunmei.zhang@uottawa.ca
† E-mail: graham.brown@uottawa.ca

RB

Time-resolved spectroscopy of Xe giant resonance by employing all-optical measurement of attosecond pulses

D H Ko[1 *], G G. Brown[1], C Zhang[1 †] and P Corkum[1,2]

[1]Joint Attosecond Science Laboratory, University of Ottawa, Ottawa, ON K1N 6N5, Canada
[2]Joint Attosecond Science Laboratory, National Research Council of Canada, Ottawa, ON K1A 0R6, Canada

Synopsis We demonstrate time-resolved spectroscopy of multi-electron interaction by employing all-optical measurement of attosecond pulses. A strong resonance is observed using high harmonic spectroscopy of Xe due to the interaction between the recollision electron and the inner shell. By perturbing recollision trajectories, the dipole associated with the giant resonance is completely determined. Our result exhibits the feasibility of all-optical approaches in strong field physics for the real-time monitoring of multi-electron interaction, suggesting a new paradigm for attosecond science.

RB

Studying ultrafast multi-electron interactions on short time scales has been of great interest in strong field physics and attosecond science. It has been accomplished by well-established attosecond measurements that employ photoelectron streaking based on two-photon transition. Such measurements have led to the measurement of photoionization delays associated with different orbitals in Ne and of doubly excited states in He.

All-optical *in situ* measurement has been demonstrated as an alternative to traditional attosecond measurement. *In situ* measurement techniques utilize the XUV generation medium as a detection source by perturbing the recollision process with a weak infrared laser field. Recently, we demonstrated a highly efficient approach to *in situ* measurement by linking it with near-field imaging techniques to characterize an attosecond pulse using a single XUV spectral image [1]. Here, we extend this all-optical measurement to explore recollision-induced excitation of the Xe giant resonance [2].

Time-domain investigation of the Xe giant resonance is achieved by measuring an attosecond pulse generated in Xe. Xe atoms are driven by a strong few-cycle laser pulse with a polarization gating to create an isolated attosecond pulse with a broadband continuum spectrum up to 100 eV photon energy. A weak laser field is introduced at a small angle to perturb the XUV generation process at the center of the polarization gating. The two laser fields interfere and construct amplitude and phase modulations on the near-field dipole, inducing a non-stationary optical grating for measuring the attosecond pulse. By reimaging the dipole modulation with respect to wavelength using an X-ray focusing optic and a physical grating, we obtain a spectrally resolved XUV image to determine the spectral amplitude and phase of the attosecond pulse. As a result, we observe a large delay around the Xe resonance above 75 eV as shown in Fig. 1.

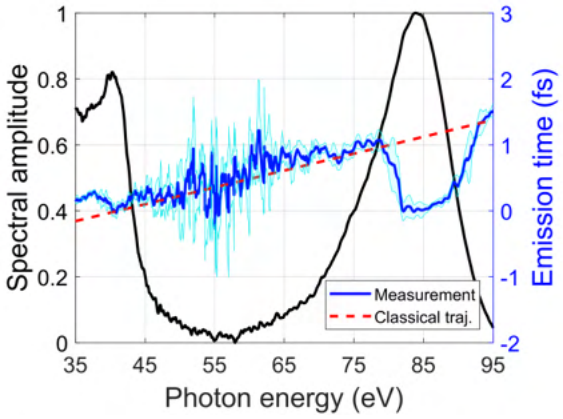


Figure 1. Spectral amplitude (black) and emission time (blue) of an attosecond pulse at the Xe giant resonance.

Our results tell the importance of multi-electron dynamics in shaping recollision trajectories and the possibility of all-optical approaches to probe multi-electron dynamics. It suggests a new paradigm for attosecond science, observing ultrafast phenomena by perturbing recollisional strong-field processes.

References

[1] Ko D H *et al* 2021 *Optica* **8** 1632-1637
[2] Shiner A *et al* 2011 *Nature Phys.* **7** 464-467

* E-mail: donghyuk.ko@uottawa.ca
† E-mail: Chunmei.Zhang@uottawa.ca

Probing electronic and vibrational dynamics in Furan with AttoXAFS

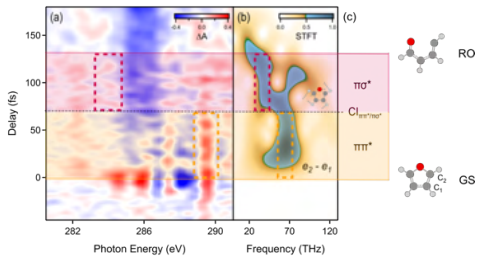
S Severino[1], K M Ziems[2], M Reduzzi[1], A Summers[1], H-W Sun[1], Y-H Chien[1], S Gräfe[2,3,4], J Biegert[1,5,*]

[1] ICFO - Institut de Ciencies Fotoniques, The Barcelona Institute of Science and Technology, Castelldefels, Spain
[2] Institute of Physical Chemistry and Max Planck School of Photonics, Friedrich-Schiller-Universität Jena, Germany
[3] Fraunhofer Institute for Applied Optics and Precision Engineering, Albert-Einstein-Str. 7, Jena, Germany
[4] Institute of Applied Physics and Abbe Center of Photonics, Friedrich-Schiller-Universität Jena, Germany
[5] ICREA, Pg. Lluís Companys 23, 08010 Barcelona, Spain

Synopsis We apply attosecond time-resolved carbon K-edge spectroscopy to investigate the ultrafast nonadiabatic relaxation pathways of furan after strong field excitation. The extreme temporal resolution along with state and conformal sensitivity of AttoXAFS allows to disentangle the intricate interplay between of the electronic and nuclear wavepackets and extract a detailed picture of the rich dynamics that involves several parallel pathways, multiple CIs, electronic coherences and transiently populated dark states.

RB

The interplay of the electron and nuclear wavepackets is at the heart of photoprotection mechanisms in a number of biologically relevant compounds like DNA nucleobases. A complete investigation of these dynamics requires a tool capable of disentangling the electron and nuclear degrees of freedom with atomic spatial resolution and sub-fs temporal sensitivity. Investigating the ultrafast nonadiabatic dynamics of furan (C_4H_4O) [1] we demonstrate how attosecond x-ray absorption fine structure spectroscopy with soft x-ray pulses [2,3] meets these requirements. Here, we excite furan via multi-photon absorption of a 17-fs pump beam at a photon energy of 0.7 eV and follow the subsequent relaxation dynamics measuring the time-dependent carbon K-edge absorption spectra with an isolated attosecond probe pulse. The differential absorption ΔA trace in Fig.a contains several characteristic features, which we analyze in combination with state-of-the-art simulations. Upon the excitation at time zero, we identify the initial transition to the ππ* excited state. After the first 20 fs, we observe a fast beating of the XAFS signal at 63 ± 9 THz (16 ± 2 fs) (see Fig.b) that originates from coherent electronic wavepacket dynamics as the nuclear wavepacket proceeds on several almost parallelly lying excited electronic states. The migration of the electron wavepacket corresponding to two distinct carbon atoms of furan is resolved in the experimental data as out-of-phase quantum beatings in two spectral regions due to the site-specificity of XAFS [4]. The method distinguishes the decay of the ππ* excited state in 65 ± 10 fs as passage through a second conical intersection, $CI_{\pi\pi^*/\pi\sigma^*}$, that transiently populates a dark state πσ* which ultimately leads to bond breaking. The signal between 70 fs and 140 fs, besides providing direct access of the electronic population in the πσ* state, results in a second Fourier component at 36 ± 9 (28 ± 7 fs) THz that is assigned to activation of the ring-opening (RO) vibrational mode (see Fig.b)). After 140 fs, the πσ* XAFS signature disappears and the emergence of a long-lasting component indicates the transition back into the ground state. Finally, we identify the RO pathway as the dominant relaxation pathway, in very good agreement with theory.



(a): Differential absorption. Marked in orange (magenta) is the relevant XAFS feature of the ππ* (πσ*) state; **(b)**: Short Time Fourier Transform of the 287eV signal; **(c):** the relevant electronic and nuclear configurations during the dynamics

In summary, we demonstrated the capability of core-level attosecond XAFS spectroscopy to disentangle the intricate pathways of coupled electronic and nuclear dynamics of a complex polyatomic system. The possibility to identify the exact evolution of such system across several non-adiabatic pathways provides a powerful tool to investigate the molecular building blocks of life.

References

[1] N. Gavrilov et al., Chemical Physics 349 (2008).
[2] S. M. Teichmann et al., Nat. Commun. 7, 11493 (2016).
[3] B. Buades et al., Optica 5, 502-506 (2018)
[4] Y. Kobayashi et al., arXiv:2112.10008v1 (2021).

* E-mail: jens.biegert@icfo.eu

Poster Session III, Highlights C
Chair: **Jiro Itatani**, The University of Tokyo, Japan

R34 **Stabilization of autoionizing polaritons in atomic ionization**
Coleman Cariker, Nathan Harkema, Eva Lindroth, Arvinder Sandhu, Luca Argenti . 183

R35 **First-Principles Simulations of Electron Dynamics Probed with Transient X-ray Absorption**
Min Chen, Mengqi Yang, Kenneth Lopata 184

R40 **The imaginary part of the high-order harmonic cutoff**
Emilio Pisanty, Marcelo Fabian Ciappina, Maciej Lewenstein 185

R41 **Strong-field chiral imaging with twisted photoelectrons**
Xavi Barcons, Andrés F. Ordóñez, Maciej Lewenstein, Andrew Maxwell 186

R45 **Role of Freeman resonances on spin polarization in strong field ionization of high angular momentum orbitals**
Felipe Morales, Serguei Patchkovskii, Zan Nie, Noa Nambu, Kenneth A Marsh, Chan Joshi, Olga Smirnova 187

R49 **Ultrafast non-adiabatic relaxation of XUV-excited molecules: Dynamics in correlation bands**
Alexander Kuleff 188

R50 **Probing Coherent Molecular Charge Migration with High-Harmonic Spectroscopy**
Kyle Hamer, Francois Mauger, Aderonke Folorunso, Kenneth Lopata, Robert Jones, Louis DiMauro, Kenneth J Schafer, Mette B Gaarde 189

R54 **Enantio-sensitive unidirectional light bending**
David Ayuso, Andrés F. Ordóñez, Piero Decleva, Mikhail Yu. Ivanov, Olga Smirnova 190

R55 **Theoretical study of attosecond order core-level photoionization time delay of heteronuclear diatomic molecules at high energies**
Yoshiaki Tamura, Kaoru Yamazaki, Fukiko Ota, Kiyoshi Ueda, Keisuke Hatada . . . 191

Stabilization of autoionizing polaritons in atomic ionization

C Cariker[1]*, N Harkema[2], E Lindroth[3], A Sandhu[2], and L Argenti[1,4]†

[1]Department of Physics, University of Central Florida, Orlando, FL 32816, USA
[2]College of Optical Sciences, University of Arizona, Tucson, Arizona 85721, USA
[3]Department of Physics, Stockholm University, Stockholm SE-106 91, Sweden
[4]CREOL, University of Central Florida, Orlando, FL 32816, USA

Synopsis We report *ab initio* calculations of attosecond transient absorption in argon, where the strong coupling between resonances in the continuum causes the $3s^{-1}4p$ to split into a pair of autoionizing polaritons, one of which exhibits stabilization against ionization. These predictions are in excellent agreement with experimental observations. We demonstrate that this stabilization phenomenon is caused by the interference between radiative and Auger decay paths, using an extension of the Jaynes-Cummings model to overlapping autoionizing states.

An intense laser pulse which couples resonances in the continuum can give rise to a split pair of autoionizing polaritons (AIPs) whose lifetime can be extended as a result of the interference between radiative and Auger decay channels [1]. We show how it is possible to reproduce this stabilization mechanism by extending to autoionizing states the Jaynes-Cummings model, which describes a two-level quantum system in interaction with a single-mode quantized radiation field [2]. We study the manifestation of this phenomenon in the attosecond transient absorption spectrum (ATAS) of the argon atom in the proximity of the $3s^{-1}$ threshold, where the most prominent autoionizing states appear as window resonances. For the model to quantitatively reproduce not only the stabilization phenomenon but also the complex profile of overlapping AIPs, we coupled the Jaynes-Cummings approach for the strong field coupling between autoionizing states with the Fano formalism for the coupling of bound states with multiple Auger and radiative decay channels. We compare the model predictions with full-fledged *ab initio* simulations of the system in a correlated close-coupling basis [3]. The transient-absorption spectra exhibit multiple avoided crossings between the $3s^{-1}4p$ resonance and the light-induced states originating from nearby metastable dark states. These avoided crossings, a hallmark of polaritonic multiplets, reveal that the dressing field couples several states through multiphoton resonant transitions, such as $3s^{-1}4f \longleftrightarrow 3s^{-1}3d \longleftrightarrow 3s^{-1}4p$. By switching off the coupling between selected resonances, we are able to fully assign the character of each avoided crossing. These theoretical predictions are in excellent agreement with recent experiments conducted in parallel [4]. This study indicates a new way to control the electronic structure in the continuum of polyelectronic systems.

*E-mail: ccariker@knights.ucf.edu
†E-mail: Luca.Argenti@ucf.edu

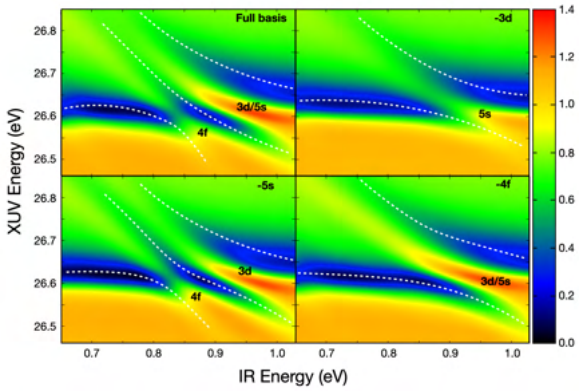


Figure 1. *Ab initio* spectrum of argon as a function of IR frequency, in the full basis (top left) as well as omitting selected resonances from the basis. By comparing the spectra obtained with different sets of states, we can assign all the avoided crossings observed in the full spectrum and identify the dominant radiative couplings between the $3s^{-1}n\ell$ states.

References

[1] P Lambropoulos and P Zoller, Phys. Rev. A **24**, 379 (1981).
[2] E T Jaynes and F W Cummings, Proceedings of the IEEE **51** 89 (1963).
[3] T Carette *et al.*, Phys. Rev. A **87**, 023420 (2013).
[4] N Harkema *et al.*, Phys. Rev. Lett. **127**, 023202 (2021).

RC

First-Principles Simulations of Electron Dynamics Probed with Transient X-ray Absorption

M Chen[1] M Yang[1] and K Lopata[1,2]*,

[1] Department of Chemistry, Louisiana State University, Baton Rouge, 70808, United States
[2] Center for Computation and Technology, Louisiana State University, Baton Rouge, 70808, United States

Synopsis Attosecond transient X-ray absorption spectroscopy (ATXAS) is a promising technique for probing electron dynamics in molecular systems, but interpreting experiments requires a means of relating spectra to the underlying dynamics. In this work we present first-principles simulated ATXAS computed using real time time-dependent density functional theory (RT-TDDFT) to determine the relationship between electron density and spectral modulations. Using both the case of neutral UV pumping and X-ray induced valence dynamics, we observe a universal trend: the optical density decreases at the times when there is an increased electron density around a particular absorbing atom. These results are expected to help guide and interpret X-ray free electron laser studies.

RC

Recent progress in the field of attosecond spectroscopy has opened the door to using short X-ray pulses to measure dynamics at the time scale of electron motion. Attosecond transient X-ray absorption spectroscopy (ATXAS) is particularly promising due to its high potential time resolution and spatial specificity. Reversing from time-delay to real-time, however, can be challenging, making it difficult to reconstruct the corresponding electron dynamics.

In this work, we simulate ATXAS using real time time-dependent density functional theory (RT-TDDFT) with hybrid functionals and Gaussian basis sets. These simulations uncover the relationship between local density around certain atom in a molecule, and the absorption energy shifts and intensity modulations. In the case of UV pumped aminophenol we observe that the main O K-edge absorption peak dims and blueshifts as the local electron density around oxygen atom increases, by ∼33% and +0.15 eV, respectively [1, 2]. An analogous effect is observed in the N K-edge ATXA spectrum (see Fig. 1). This relationship between local density and transient spectrum was likewise observed in a range of systems, including pumped CO, O_2, and a tetracyanoethylene/benzene dimer.

Additionally, we studied electron dynamics in impulsively ionized aminophenol, created by removing a 1s electron from either the nitrogen or oxygen atom. We find that the intensity of K-edge absorption in these systems is correlated with the local density modulations around the absorbing center, but is most sensitive when using different heteroatoms to pump and probe (e.g., pump@N, probe@O).

These findings and techniques are promising for interpreting AXTA spectra in ongoing and future X-ray free electron laser studies, as they allow prediction of modulated spectra without experimental inputs.

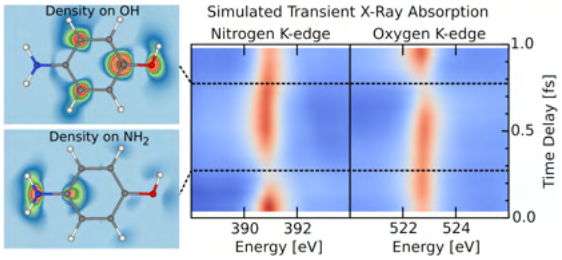


Figure 1. Simulated attosecond X-ray transient absorption in aminophenol following UV pump excitation. The optical density of the N K-edge absorption decreases with increasing electron density around N, and vice versa for the O K-edge [1].

References

[1] M Chen, K Lopata, Chem. Theory Comput. **16(7)**, 2020 (2020).
[2] M Yang, A Sissay, M Chen, K Lopata, Chem. Theory Comput. **18(2)**, 2022 (2022).

*E-mail: klopata@lsu.edu

The imaginary part of the high-order harmonic cutoff

E Pisanty[1,2,3]*, M F Ciappina[3,4] and M Lewenstein[3,5]

[1]King's College London, Department of Physics, WC2R 2LS London, UK
[2]Max Born Institute for Nonlinear Optics and Short Pulse Spectroscopy, 12489 Berlin, Germany
[3]ICFO – The Institute of Photonic Sciences, 08860 Castelldefels (Barcelona), Spain
[4]Guangdong Technion – Israel Institute of Technology, Shantou, 515063, Guangdong, China
[5]ICREA, Passeig de Lluís Companys, 23, 08010 Barcelona, Spain

Synopsis
We present a rigorous definition of the high-harmonic cutoff which is applicable to arbitrary driver waveforms. Our definition provides a natural meaning for the imaginary part of the cutoff energy, which controls the strength of quantum-path interference in the plateau. This construction radically simplifies quantum-orbit calculations. Using this definition, we build the Harmonic-Cutoff Approximation to calculate the exact location and brightness of the cutoff at a fraction of the cost of the state of the art – giving access to a much wider class of optimization tasks.

RC

The harmonic cutoff is one of the key concepts in high-harmonic generation, but it is also an elusive object which has long escaped a precise definition. In this work we provide the first natural definition for the harmonic cutoff; we show how to find it, in a simple and computationally effective way; and we show how it can be used.

We build our construction on a new type of quantum orbit, which recollides at the harmonic-cutoff times t_{hc} defined by a *second*-order saddle-point equation for the usual action S,

$$\frac{\mathrm{d}^2 S}{\mathrm{d}t^2}(t_{\mathsf{hc}}) = 0. \tag{1}$$

The cutoff energy is then given by the real part of $\Omega_{\mathsf{hc}} = \frac{\mathrm{d}S}{dt}(t_{\mathsf{hc}})$. This provides a natural value for $\mathrm{Im}(\Omega_{\mathsf{hc}})$, which controls the strength of quantum-path interference in the plateau. The quantum orbits emerge as different branches of a unified Riemann surface, which are united at branch points – the harmonic-cutoff times t_{hc}.

More practically, the times t_{hc} can be used to classify the solutions of saddle-point equations into quantum orbits in a simple and efficient way, making calculations more flexible and effective.

Last (but not least), the information at the times t_{hc} is enough to fully characterize the harmonic spectrum at the cutoff. This allows us to build a new approach – the Harmonic-Cutoff Approximation (HCA) – which gives a quantitatively accurate estimate of the location and brightness of the cutoff, and a qualitative estimate of the spectrum in the upper plateau. This requires solving a *single* saddle-point equation – as opposed to dozens or hundreds of equations, as in previous approaches.

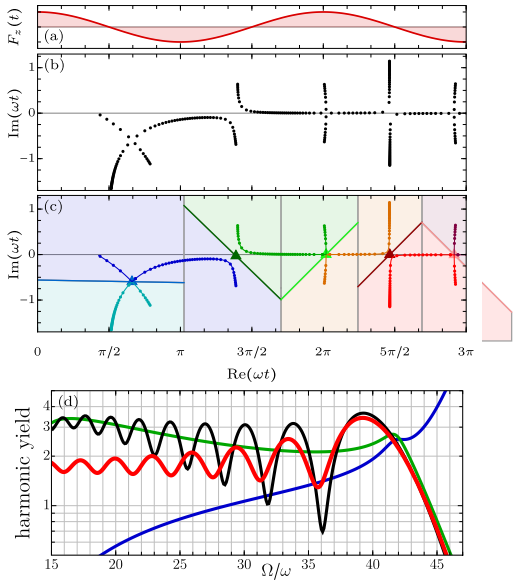


Figure 1. The saddle-point equations for HHG produce an unstructured cloud of solutions, shown in (b), which then need to be classified into quantum orbits. The harmonic-cutoff times t_{hc} (triangles, in (c)) simplify this classification. (d) The HCA (red line) matches the saddle-point approximation (black line, combining the short (blue) and long (green) trajectories) at the cutoff.

References

[1] E Pisanty *et al*, J. Phys.: Photon. **2** 034013 (2020)

*E-mail: emilio.pisanty@kcl.ac.uk

Strong-field chiral imaging with twisted photoelectrons

X Barcons[1], A F Ordóñez[1], M Lewenstein[1,2], and A S Maxwell[1,3]*

[1]ICFO-Institut de Ciencies Fotoniques, The Barcelona Institute of Science and Technology, 08860 Castelldefels (Barcelona), Spain. [2]ICREA, Pg. Lluís Companys 23, 08010 Barcelona, Spain.
[3]Department of Physics and Astronomy, Aarhus University, DK-8000 Aarhus C, Denmark.

Synopsis We present a new highly enantio-sensitive effect that exploits helicity in twisted photoelectrons ionized from a chiral target, dubbed photoelectron vortex dichroism (PEVD), which we proposed as a new ultrafast chiral imaging technique. PEVD displays huge forward-backwards asymmetry in orbital angular momentum (OAM)-resolved photoelectron emission, sensitive to molecular enantiomers.

RC

Molecular chirality plays a crucial role in biological systems, and distinguishing between molecular enantiomers is a highly important task. The most sensitive methods are those that directly use the electric-dipole interaction, which leads to strong chiral effects, such as in photoelectron circular dichroism (PECD) [1]. Recent progress in electron optics has allowed the production and measurement of vortex states carrying orbital angular momentum (OAM) [2]. The inherent chirality in vortex states, through a helical wavefront, makes them a direct probe of chirality [3]. Yet, the potential of photoelectrons carrying OAM as an enantio-sensitive probe remain unexplored. Using a recently developed theoretical framework for the photoelectron OAM in strong-field ionization [4], we reveal the connection between molecular chirality and photoelectron OAM.

We demonstrate, 'Photoelectron Vortex Dichroism' (PEVD), through strong-field ionization of a target of chiral hydrogen [5] with *linearly* polarized light, resulting in photoelectron vortices that encode the molecular chirality through conservation of helicity. Directly solving the time-dependent Schrödinger equation [6] and projecting onto electron vortex states, we demonstrate that the OAM-resolved momentum distribution is highly asymmetric, see Figure 1. This asymmetry is dependent on the chiral enantiomer employed as well as on the sign of the OAM. The asymmetry is quantified using the normalized difference, denoted $\mathrm{PEVD}^{\epsilon}_{l_v}$ (see Figure 1), which approaches the maximum value of 200%.

The asymmetry in PEVD is most visible after averaging over the carrier envelope phase of the laser, where it provides a clear enantio-sensitive observable. In contrast to PECD, PEVD is a direct chiral imaging probe, translating chirality from the target to the observable, without relying on a circularly polarized field. PEVD only scratches the surface of OAM-based techniques, with high enantiomer sensitivity and attosecond time resolution.

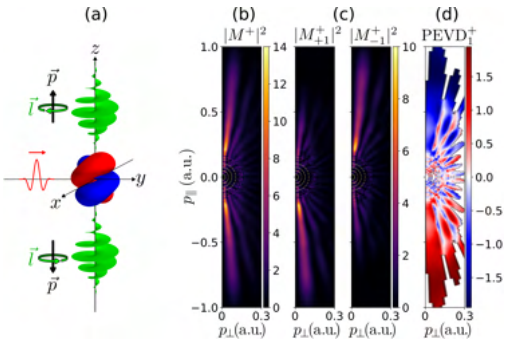


Figure 1. (a) Depiction of PEVD. (b) Standard photoelectron spectrum from strong-field ionization. Laser intensity $I = 10^{14}$ W/cm^2, wavelength $\lambda = 800$ nm and 2-cycle pulse. (c) OAM-resolved photoelectron spectra for OAM $l_v = \pm 1$. (d) Normalized difference between OAM or enantiomers.

References

[1] MHM Janssen et al, Phys. Chem. Chem. Phys. **16**, 856 (2013)
[2] KY Bliokh et al, Phys. Rep. **690**, 1 (2017)
[3] A Asenjo-Garciae et al, Phys. Rev. Lett. 113, 066102 (2014)
[4] AS Maxwell, et al, Faraday Discuss. **228**, 394 (2021) and Y Kang, et al, Eur. Phys. J. D **75**, 199 (2021)
[5] AF Ordonez et al, Phys. Rev. A **99**, 043416 (2019)
[6] V Tulsky et al, Comput. Phys. Commun. **251**, 107098 (2020)

*E-mail: andrew.maxwell@phys.au.dk

Role of Freeman resonances on spin polarization in strong field ionization of high angular momentum orbitals

F Morales,[1] S Patchkovskii,[1] Z Nie,[2,*] N Nambu,[2] K A Marsh,[2] C Joshi[2] and O Smirnova[1]

[1]Max Born Institute, Max-Born-Str. 2A, D-12489 Berlin, Germany
[2]University of California Los Angeles, Los Angeles, California 90095, USA

Synopsis Maximizing the amount of total spin polarization generated in strong, circularly polarized fields is essential for practical applications. Following the suggestion in [1] to use higher angular momentum orbitals, we present Time Dependent Schrödinger Equation calculations of total spin polarization for Yb III as a function of field strength for different wavelengths, and show that a total spin polarization of 50% is possible. We also discuss how Freeman resonances can affect total spin polarization.

The role of the magnetic quantum number and spin in strong field ionization of atoms and molecules was mostly ignored until about a decade ago, when the preference of tunnel ionization of counter rotating electrons of noble gases in a strong circularly polarized field was predicted [2]. The interplay of the sensitivity of ionization to the magnetic quantum number and the spin-orbit interaction leads to the generation of spin polarized electrons [3], which was demonstrated experimentally for Xenon [4].

Efficient and controlled generation of spin polarized electrons has a number of potential applications, as it may allow the probing of magnetic and chiral systems with a sub-femtosecond temporal and sub-Angstrom spatial resolution. Another possible application is the in-situ generation of spin polarized electron beams for the generation of high-energy, high-curent and low-emittance spin polarized electron beams [5], which would solve a long-stading scientific challenge for plasma-based accelerators.

Xenon has a predicted maximum spin polarization in strong field ionization with circularly polarized pulses of about 30% [4,5]. To improve this, it was suggested [1] to use atoms with higher angular momentum ground states. Following this suggestion we have developed an Yb III pseudo-potential and performed Time Dependent Schrödinger Equation simulations for different wavelengths and intensities. We find that for 400 nm, 10 fs pulses, a total spin polarization of 50% is possible.

However, the total spin polarization as a function of intensity for the case of 400 nm shows a peak structure, with lower total spin polarization at some intensities.

The reason behind this structure is the population of Freeman resonances, i.e. excited states Stark-shifted by the laser field. In atoms with a higher initial angular momentum, such as Yb III, it is easier to reach excited states compared to noble gases, due to the selection rules that apply to circularly polarized light. The population of these resonances affects the strong field ionization yields (Fig. 1) for a particular initial state, which, in this case, is responsible for the highest contribution to the total spin polarization.

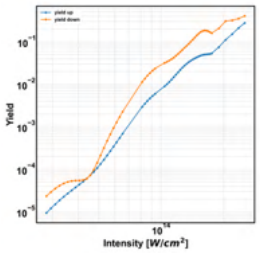


Figure 1. Intensity dependent spin up and spin down yields plotted against intensity, in log-log scale.

References

[1] J. Kaushal & O. Smirnova, JPB **51**, 174003 (2018).
[2] I. Barth & O. Smirnova, PRA **84**, 063415 (2011).
[3] I. Barth & O. Smirnova, PRA **88**, 013401 (2013)
[4] A. Hartung et al., Nat. Photonics **10**, 526 (2016).
[5] Z. Nie et al., PRL **126**, 054801 (2021).

* E-mail: felipe.morales@mbi-berlin.de

Ultrafast non-adiabatic relaxation of XUV-excited molecules: Dynamics in correlation bands

A I Kuleff*

Theoretische Chemie, PCI, Universität Heidelberg, Im Neuenheimer Feld 229, D-69120 Heidelberg, Germany

Synopsis The ultrafast non-adiabatic dynamics triggered by the ionization of a molecule with an XUV radiation will be analyzed with the help of quantum-dynamics calculations. The series of events occurring in the correlation band of the system, from the initial electron-correlation-driven charge migration to the final intramolecular vibrational-energy redistribution and eventual fragmentation, will be elucidated and discussed.

RC

Exposing molecules to XUV radiation populates typically highly-excited cationic states that triggers complex ultrafast dynamics in which both the electronic and the nuclear motions are strongly coupled. A fully quantum description of these dynamics in small polycyclic aromatic hydrocarbons (PAH) will be reported and compared to time-resolved experimental results [1, 2]. It will be shown that the non-adiabatic relaxation dynamics gets slower the closer the initial excitation is to the double-ionization threshold, as well as the larger the system is. Moreover, it will be demonstrated that these dynamics are general and governed by the so-called *correlation bands*, features created by the strong electron correlation in the inner valence, allowing to use a simple electron-phonon scattering model to explain and predict the relaxation dynamics of whole classes of molecules [3]. This ultrafast non-adiabatic relaxation in the correlation band is in competition with the first steps of a complete intramolecular vibrational-energy redistribution eventually leading to a fragmentation of the molecule [4]. Recent calculations [5] showing how the electron-correlation-driven charge migration occurring in the correlation band of ionized molecules can lead to a redistribution of the charge that increases the stability of the system will also be presented and discussed.

References

[1] A. Marciniak, *et al.,* Nature Commun. **6**, 7909 (2015).
[2] A. Marciniak, *et al.,* Nature Commun. **10**, 337 (2019).
[3] M. Hervé, *et al.,* Nature Phys. **17**, 327 (2021).
[4] A. Boyer, *et al.,* Phys. Rev. X **11**, 041012 (2021).
[5] V. Despré and A. I. Kuleff, arXiv:2111.00760 (2021).

*E-mail: alexander.kuleff@pci.uni-heidelberg.de

Probing Coherent Molecular Charge Migration with High-Harmonic Sideband Spectroscopy

K Hamer[1 *], F Mauger[1], A S Folorunso[2], K Lopata[2,3], R R Jones[4], L F DiMauro[5], K J Schafer[1] and M B Gaarde[1]

[1]Department of Physics and Astronomy, Louisiana State University, Baton Rouge, LA 70803, USA
[2]Department of Chemistry, Louisiana State University, Baton Rouge, LA 70803, USA
[3]Center for Computation and Technology, Louisiana State University, Baton Rouge, LA 70803, USA
[4]Department of Physics, University of Virginia, Charlottesville, VA 22904, USA
[5]Department of Physics, The Ohio State University, Columbus, OH 43210, USA

Synopsis Charge migration (CM), the coherent motion of electrons and holes in molecules, is currently attracting much theoretical and experimental interest. In this presentation, I will introduce high-harmonic sideband spectroscopy and show that it is a robust, all-optical, and background-free probe of attosecond CM.Taking the example of a halogenated carbon-chain molecule, I will show that monitoring the harmonic spectrum while varying the laser parameters (*e.g.*, the driving wavelength) allows for the extraction of detailed information about the CM process.

RC

Charge migration (CM), the coherent motion of electrons and holes in molecules is currently attracting much theoretical and experimental interest [1, 2]. In this presentation, I will introduce high-harmonic sideband spectroscopy (HHSS) and show that it can be a robust probe of attosecond CM in a halogenated carbon-chain molecule [3]. Using *ab initio* time-dependent density-functional theory to simulate both the CM and the HHG processes, I will show how the time-dependent, migration-induced, modulation of the harmonic signal induces sidebands in high-harmonic spectra. In turn, these sidebands robustly encode information about the nature of the migration dynamics, which makes HHSS an all-optical, background-free, and coherent probe. Monitoring the HHSS spectrum while varying the driving-laser parameters (*e.g.*, the wavelength) allows for the extraction of detailed information about the time-domain characteristics of the CM process. Finally, I will explore how HHSS could be demonstrated experimentally.

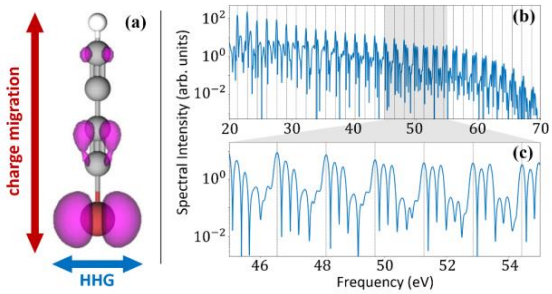


Figure 1. (a) Schematic of HHSS configuration to probe CM in BrC_4H. The HHG driving field is polarized perpendicular to the molecular backbone along which the periodic CM occurs. (b) HHG spectrum for a driving wavelength of 1575 nm. Thin grey lines denote the odd harmonics, while the other peaks are sidebands. (c) A zoomed-in portion of the HHG spectrum in (b).

Funding Acknowledgment
This work was supported by the U.S. Department of Energy, Office of Science, Office of Basic Energy Sciences, under Award No. DE-SC0012462. Portions of this research were conducted with high performance computational resources provided by Louisiana State University (http://www.hpc.lsu.edu) and the Louisiana Optical Network Infrastructure (http://www.loni.org).

References

[1] F. Mauger *et al.*, Phys. Rev. Research 4, 013073 (2022).
[2] A. Folorunso *et al.*, Phys. Rev. Lett. 126, 133002 (2021).
[3] K. Hamer *et al.*, under review arXiv: 2202.00730 (2022).

* E-mail: khamer3@lsu.edu

Enantio-sensitive unidirectional light bending

D Ayuso[1,2*], A Ordonez[2,3], P Decleva[4], M Ivanov[1,2,5] and O Smirnova[2,6]

[1]Department of Physics, Imperial College London, SW7 2BW London, United Kingdom
[2]Max-Born-Institut, 12489 Berlin, Germany
[3]ICFO, The Barcelona Institute of Science and Technology, 08860 Castelldefels, Spain
[4]Dipartimento di Scienze Chimiche e Farmaceutiche, Università degli Studi di Trieste, 34127 Trieste, Italy
[5]Institute für Physik, Humboldt Universität zu Berlin, 12489 Berlin, Germany
[6]Technische Universität Berlin, 10623 Berlin, Germany

Synopsis We show how to structure light's *local* handedness in space to realize an interferometer for efficient chiral recognition, which can be seen as a chiral version of Young's double slit experiment. Such chirality-structured light "bends" the nonlinear optical response of chiral molecules in a highly enantio-sensitive manner: opposite molecular enantiomers are forced to emit light at new optical frequencies in different directions. Our work exposes the immense potential of sculpting light's local chirality and creates novel opportunities for imaging molecular chirality on ultrafast time scales.

RC

Structured light [1] has key applications ranging from imaging and 3D micromanipulation to classical and quantum communication. However, its application to molecular chirality has been severely limited by the weakness of magnetic interactions [2]. Here we show how to structure the *local* handedness of *synthetic* chiral light [3] in space to realize a chiral version of Young's double slit experiment that leads to enantio-sensitive light bending [4].

The chiral double-slit experiment [4] involves two chiral emitters of opposite handedness, which emit light with the same intensity and opposite phase, see Fig. 1a. The combination of the achiral (left panel) and chiral (central panel) components of the emission leads to enantio-sensitive bending of the emitted light (right panel). The interference pattern is shifted to the right, or to the left, depending on the relative positions of the left- and right-handed slits.

We can realize the chiral double-slit experiment using synthetic chiral light [3] with structured handedness [4], which can be created using two non-collinear laser beams that carry cross-polarized ω and 2ω frequencies, see Fig. 1b. In the overlap region, the field becomes locally chiral: the tip of the electric-field vector draws a chiral (3D) Lissajous figure in time. By controlling the ω-2ω phase delays, we can structure the field's handedness h(r) in space, so that the field is left-handed at one point, right-handed at another, and achiral in between [4]. The nonlinear response randomly oriented chiral molecules captures the spatial distribution of h(r) and realizes the desired sequence of chiral emitters (slits).

Fig. 1c shows the nonlinear response of left- and right-handed randomly oriented fenchone molecules driven by this field. The total intensity is the same for left- and right-handed molecules, as the overall field is achiral. However, the direction of emission is highly enantio-sensitive: while the left-handed molecules emit harmonics preferentially to the left, the right-handed molecules emit harmonics preferentially to the right. The enantio-sensitive direction of bending can be fully controlled in our setup.

The possibility of structuring the local handedness of synthetic chiral light at will, endowing it with global handedness [3] or with polarization of chirality [4], creates exciting opportunities for ultrafast and highly enantio-sensitive imaging and control of ultrafast chiral dynamics.

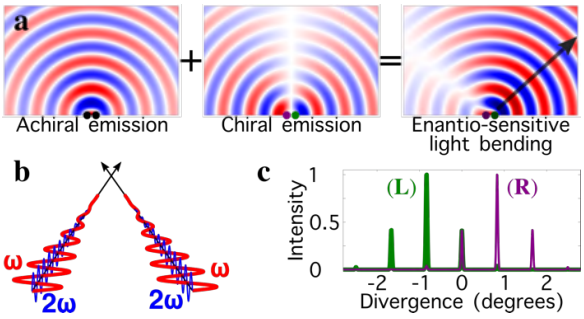


Fig. 1. a, Chiral double-slit Gedankenexperiment: the superposition of achiral and chiral emission leads to enantio-sensitive light bending. **b,** Synthetic chiral light with structured handedness can be created using two non-collinear laser beams that carry cross-polarized ω and 2ω frequencies. **c,** Far-field high-harmonic emission at frequency 12ω from L (green) and R (magenta) fenchone, see [4] for laser parameters and details of the calculations.

References

[1] Rubinsztein et al, *J Optics* **19**, 013001 (2016)
[2] Cameron et al, *J Phys Chem A* **118**, 3472 (2014)
[3] Ayuso et al, *Nat Photonics* **13**, 866-871 (2019)
[4] Ayuso et al, *Nat Commun* **12**, 3951 (2021)

* E-mail: d.ayuso@imperial.ac.uk

Theoretical study of attosecond order core-level photoionization time delay of heteronuclear diatomic molecules at high energies

Y Tamura[1]*, K Yamazaki[2], F Ota[1], K Ueda[3], K Hatada[1]†

[1]Department of Physics, University of Toyama, 3190 Gofuku, Toyama 930-8555, Japan
[2] RIKEN Center for Advanced Photonics, RIKEN, 2-1 Hirosawa, Wako, Saitama, 351-0198, Japan
[3]Graduate School of Science, Tohoku University, 6-3 Aramaki Aza-Aoba, Aoba-ku, Sendai 980-8578, Japan

Synopsis We derived analytical expressions of core level photoemission time delay from heteronuclear diatomic molecules within single scattering approximation. Resultant expressions reproduce the angular dependence in the high energy regime for C(1s) photoemission from CO molecules calculated with full multiple scattering theory.

Recent developments of attosecond light sources have enabled us to measure attosecond photoemission time delay in any form of matter in the range of extreme ultraviolet wavelengths, and the 1s core-level photoemission time delay measurements are becoming available. Here, molecular core-level photoemission time delay in a molecular frame is of particular interest. Molecular photoemission time delay exhibits a complex emission angle dependence in the molecular frame [1, 2, 3], which reflects the anisotropy of the molecular structure and potential. Core-level photoemission may give us the atom-resolved potential and geometrical information, and the entangled dynamics of nuclei and electrons in the photoemission process.

The core-level photoemission time delay which is defined by the energy derivative of photoionization amplitude from a unique atom can be divided into three contributions using multiple scattering theory within electric dipole, muffin-tin and some other approximations:

$$\tau(\mathbf{k},\hat{\boldsymbol{\varepsilon}}) = \tau_{\rm abs}(k) + \tau_{\rm path}(\mathbf{k},\hat{\boldsymbol{\varepsilon}}) + \tau_{\rm sc}(\mathbf{k},\hat{\boldsymbol{\varepsilon}})\,, \quad (1)$$

where $\hat{\boldsymbol{\varepsilon}}$ is polarization vector, $\mathbf{k}\,(|\mathbf{k}| = k)$ is momentum vector of photoelectrons. $\tau_{\rm abs}$ is a half of Wigner time delay for the absorbing atom. $\tau_{\rm path}$ and $\tau_{\rm sc}$ are time delays caused by propagation along the scattering paths and scattering at each atom, respectively. We derived an analytical expression $\tau^{(1)}_{\rm path}(k,\theta)$ with a single scattering approximation for heteronuclear diatomic molecules in the molecular frame, where the angle between $\mathbf{k}$ and the molecular axis is θ, with $\hat{\boldsymbol{\varepsilon}}_\parallel$ to be parallel to the molecular axis, hereafter, we rewrite the argument $(\mathbf{k},\hat{\boldsymbol{\varepsilon}}_\parallel)$ to (k,θ). We obtain (i) $\tau^{(1)}_{\rm path}(k,0) = 0$, which indicates that there is no delay caused, (ii)$\tau^{(1)}_{\rm path}(k,\pi/2) = (1/2)R/k$, indicating that it is just a traveling time of the photoelectrons over the bound length, and (iii) $\tau^{(1)}_{\rm path}(k,\pi)$ oscillates with a frequency of $2R$, due to interference between direct and scattered photoelectron waves. We found that $\tau^{(1)}_{\rm path}$ becomes dominant in the high-energy regime (k >3.5 a.u.) from its comparison with the full multiple scattering calculations, as illustrated in Fig. 1.

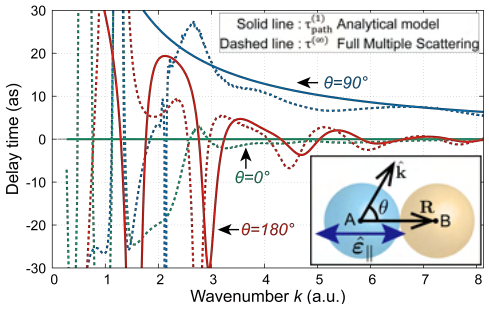


Figure 1. Comparisons of the analytical results $\tau^{(1)}_{\rm path}(k,\theta)$ (solid line) within single scattering approximation and with numerical results of total photoemission time delay $\tau^{(\infty)}(k,\theta)$ (dashed line) within full multiple scattering for C(1s) core-level photoemission in the CO molecule at $\theta = 0°$ (green), 90° (blue), and 180° (red). The inset depicts the coordinate in the molecular frame.

References

[1] J. Vos *et al.*, *Science* **360**, 1326-1330 (2018).
[2] S. Heck *et al.Sci. Adv.* **7**, eabj8121 (2021).
[3] X. Gong *et al.*, *Phys. Rev. X* **12**, 011002 (2022); and references cited therein.
[4] Y. Tamura *et al.*, *J. Phys. B: At. Mol. Opt. Phys.* **55**, 10LT01 (2022)

*E-mail: yoshiakitamura.susa@gmail.com
†E-mail: hatada@sci.u-toyama.ac.jp

RC

M01 **Entanglement of Orbital Angular Momentum in Non-Sequential Double Ionization**
Andrew Maxwell, Lars Bojer Madsen, Maciej Lewenstein 200

M02 **Direct inclusion of many-body effects in calculations of attosecond delays in atomic photoionisation**
Soumyajit Saha, Anton Ljungdahl, Eva Lindroth, Johanna Sörngård, Jimmy Vinbladh 201

M03 **Angle resolved, spin-orbit contributions to spectral phase in semi-relativistic RABBITT simulations.**
Luke Roantree, Andrew Brown, Hugo van der Hart, Connor Ballance, Jack Wragg . 202

M04 **Control of Parent-Ion Coherence in Helium Ion Ensemble**
Saad Mehmood, Eva Lindroth, Luca Argenti 203

M05 **Attosecond control of XUV multiphoton ionization**
M. Kretschmar, A. Hadjipittas, B. Major, J. Tümmler, I. Will, T. Nagy, M. J J Vrakking, A. Emmanouilidou, B. Schütte 114

M06 **Phase retrieval from angular streaking of XUV atomic ionization**
Anatoli Kheifets, Igor Ivanov, Anna Wang, James Cryan 115

M07 **Autoionizing states in atomic two-photon double-ionization: A virtual sequential finite-pulse model**
Siddhartha Chattopadhyay, Luca Argenti 204

M08 **Optimal density matrix extraction from attosecond spectrogram using ptychographic algorithms**
Jinhyeok Im, Pascal Salières and Charles Bourassin-Bouchet 205

M09 **Measuring two-photon transition delays using 'self-probing' of a resonance**
L Maëder, H J B Marroux, C Schouder, M Lejman, A Autuori, D Platzer, N Berrah, R Taïeb, J Caillat and P Salières 206

M10 **Under-threshold RABBITT: a novel probe of ionization dynamics and target electronic structure**
Anatoli Kheifets 207

M11 **Probing electronic decoherence with attosecond photoelectron interferometry**
D. Busto, H. Laurell, D. Finkelstein-Shapiro, C. Alexandridi, M. Isinger, S. Nandi, R. Squibb, M. Turconi, S. Zhong, C. Arnold, R. Feifel, M. Gisselbrecht, P. Salières, T. Pullerits, F. Martín, L. Argenti, A. L'Huillier 116

M12 **Ionization of co- and counter-rotating electrons in ultrashort circularly polarized laser pulses**
Spencer Walker, Lucas Kolanz, Joel Venzke, Andreas Becker 221

M13 **Control of Atomic Photoionization by Circularly Polarized Attosecond Chirped Pulses**
Nathaniel J. Strandsquist . . . 209

M14 **Theoretical Study of Vacuum Ultraviolet Pulse Characterization from Two-Photon Autocorrelation Signals**
Spencer Walker, Ran Reiff, Agnieszka Jaron-Becker, Andreas Becker . . . 210

M15 **Photoionization domains for Rabi oscillations at XUV wavelengths**
Edvin Olofsson, Mattias Bertolino, Saikat Nandi, Jan Marcus Dahlström . . . 211

M16 **Continuous variable quantum state tomography of photoelectrons**
Hugo Laurell, Daniel Finkelstein-Shapiro, Christoph Dittel, Chen Guo, Ron Demjaha, Robin Weissenbilder, Mattias Ammitzböll, Lana Neoricic, Sizuo Luo, Mathieu Gisselbrecht, Cord L. Arnold, Andreas Buchleitner, Tönu Pullerits, Anne L'Huillier, David Busto . . . 113

M17 **Multiphoton interaction phase shifts in attosecond science**
Mattias Bertolino, Jan Marcus Dahlström . . . 212

M18 **Volume effects in attosecond pulse reconstruction and photoemission time-delay retrieval**
Federico Vismarra, Rocio Borrego-Varillas, Yingxuan Wu, Daniele Mocci, Mauro Nisoli, Matteo Lucchini . . . 213

M19 **Ultra-stable and high spectral resolution attosecond beamline for photoelectron interferometry**
Robin Weissenbilder, Sizuo Luo, Anton Ljungdahl, Hugo Laurell, David Busto, Lana Neoricic, Mattias Ammitzböll, Chen Guo, Richard Squibb, Mathieu Gisselbrecht, Cord L. Arnold, Raimund Feifel, Luca Argenti, Eva Lindroth, Anne L'Huillier . . . 117

M20 **Ultrafast dynamics of multi-channel single photon ionization**
Jasper Peschel, David Busto, Marius Plach, Mattias Bertolino, Maria Hoflund, Sylvain Maclot, Jimmy Vinbladh, Hampus Wikmark, Felipe Zapata, Eva Lindroth, Mathieu Gisselbrecht, Jan Marcus Dahlström, Anne L'Huillier, Per Eng-Johnsson . . . 118

M21 **Complete reconstruction of an electron wavepacket generated by absorption of an attosecond pulse**
John Vaughan, Saad Mehmood, Coleman Cariker, Trevor Olsson, Swapneal Jain, Spenser Burrows, Eva Lindroth, Luca Argenti, Guillaume Laurent . . . 119

M22 **A Coupled Volterra Integral Equation Approach to Solving the Time-Dependent Schrödinger Equation (TDSE)**
Barry Schneider, Ryan Schneider, Heman Gharibnejad . . . 214

M23 **Studying the transition from the direct to sequential regime in the two-photon double ionization of Helium**

Adam prior, Lampros Nikolopoulos, Henri Bachau 215

M24 **Few- to multi-channel correlation effect on attosecond photoemission time de-lay**
Maia Magrakvelidze, Mohamed Madjet, Himadri Chakraborty 216

M25 **Theoretical studies of strong-field effects in atomic ionisation withultrashort radiation**
Andrew Forembski, Lampros Nikolopoulos 217

M26 **Nonadiabatic Strong Field Ionization of Atomic Hydrogen**
Daniel Trabert, Nils Anders, Simon Brennecke, Markus S. Schöffler, Till Jahnke, Lothar Ph. H. Schmidt, Maksim Kunitski, Manfred Lein, Reinhard Dörner, Sebastian Eckart 120

M27 **Angular anisotropy parameters for photoionization delays**
S. Saha, J. Vinbladh, J. Sörngård, A. Ljungdahl, E. Lindroth 121

M28 **Quantum Beat Spectroscopy of Bound Electrons in Helium**
Sara Mikaelsson, Dominik Hoff, Ann-Kathrin Raab, Chen Guo, Cord L Arnold, Anne L'Huillier, Mathieu Gisselbrecht 218

M29 **Coincidence studies of angle resolved XUV-IR RABBITT and photoionization time delays based on a general analysis framework**
Jennifer Joseph, fabian holzmeier, David Bresteau, Carlo Spezzani, Thierry Ruchon, Jean-François Hergott, Olivier Tcherbakoff, Pascal Doliveira, Jean-Christophe Houver, Danielle Dowek 219

M30 **Investigating photoionization by temporal Young-slit experiments**
Dominik Hoff, Sara Mikaelsson, Chen Guo, Ann-Kathrin Raab, Jan Vogelsang, Cord L. Arnold, Anne L'Huillier, Mathieu Gisselbrecht 220

M31 **Unraveling the transition between photoionization regimes via quantum trajectories**
Taylor Moon, Klaus Bartschat, and N. Douguet 221

M32 **The SYLOS COMPACT beam line at ELI-ALPS for intense High-Order Harmonic Generation**
Arjun Nayak, Mathieu Dumergue, Ioannis Orfanos, Emmanouil Skantzakis, Sergei Kühn, Paraskevas Tzallas, Dimitris Charalambidis, Subhendu Kahaly, Katalin Varju . 123

M33 **Resonant and Anti-Resonant Phases of Two- and Three-Photon Ionization of Helium**
Lorenz Drescher, Oleg Kornilov, Tobias Witting, Marc Vrakking 124

M34 **Simplified spectrogram reconstruction for the complete characterization of atto-second radiation**
Nicola Di Palo, Bruno Moio, Giacomo Inzani, Gian Luca Dolso, Fabio Medeghini, Rocio Borrego-Varillas, Mauro Nisoli, Matteo Lucchini 222

M35 **Attosecond circular-dichroism chronoscopy of photoelectron vortices**
Meng Han, Jia-Bao Ji, Hans Jakob Wörner 223

M36 **Laser-induced ionization of heavy metal and metalloid ions in intense and sculpted femtosecond laser fields**
Bo Ying, Frank Machalett, Matthias Kübel, A. Max Sayler, Thomas Stöhlker, Philipp Wustelt, Gerhard G. Paulus 224

M37 **NeXUS - first US attosecond user facility**
Vyacheslav Leshchenko, Timothy Scarborough, Theodore Ronningen, Louis DiMauro, Robert Baker 125

M38 **Sub-2-Cycle Carrier-Envelope-Phase–stabilized 110W, 1.1mJ Laser**
Steffen Hädrich, Maxim Tschernajew, Evgeny Shestaev, Nico Walther, Florian Just, Florian Karl, Sven Breitkopf, Christian Gaida, Oliver Herrfurth, Imre Seres, Zsolt Bengery, Barnabás Gilicze, Péter Jójárt, Zoltán Várallyay, Ádám Börzsönyi, Michael Müller, Christian Grebing, Dominik Hoff, Gerhard G. Paulus, Tino Eidam, Jens Limpert 126

M39 **Exploring symmetries in ultrafast photoelectron holography with two-color linearly polarized fields**
Thomas Rooke, Carla Faria 225

M40 **Electron choreography at the attosecond time scale**
Brady Unzicker, John Vaughan, Spenser Burrows, Morgan Tatum, Davis Arthur, Trevor Olsson, Swapneal Jain, Trevor Hart, Patrick Stringer, Guillaume Laurent . . 226

M41 **Data-Based Quantitative Characterization of the Multi-Resolution Cookiebox Instrument at LCLS**
Andrei Kamalov, Lars Funke, Razib Obaid, Dileep Bhogadi, Kurtis Borne, Nolan Brown, Jean-Charles Castagna, Xianchao Cheng, Taran Driver, Averell Gatton, Jack Hirschman, Justin James, Nelson Silke, Shi Hongliang, Audrey Therrien, Roger Trejo, Wolfram Helm, Markus Ilchen, Peter Walter, Ryan Coffee 227

M42 **Soft X-ray Generation with Ultrashort Pulses: The Krypton Surprise**
Pierre-Alexis Chevreuil, Fabian Brunner, Ursula Keller, Lukas Gallmann 127

M43 **A theoretical study on the dynamics of furan in tr-AttoXAFS**
Karl Michael Ziems, Stefano Severino, Maurizio Reduzzi, Adam Summers, Hung-Wei Sun, Ying-Hao Chien, Jens Biegert, Stefanie Gräfe 228

M44 **Strong Field Ionization and Fragmentation Dynamics of Molecular Nitrogen Probed by Femtosecond Soft X-ray Absorption Spectroscopy**
Carlo Kleine, Marc Oliver Winghart, Zhuang-Yan Zhang, Maria Ekimova, Sebastian Eckert, Marc J J Vrakking, Erik T J Nibbering, Arnaud Rouzée 229

M45 **Strong-field control of vibrational wave-packet revivals in molecular hydrogen**
Gergana D Borisova, Paula Barber Belda, Shuyuan Hu, Paul Birk, Veit Stooß, Maximilian Hartmann, Daniel Fan, Alejandro Saenz, Christian Ott, Thomas Pfeifer . 230

M46 **Towards Field Sampling of Ultrabroadband Continuum Radiation from deep-UV to NIR**
Amelie Schulte, Corinna Konrad, Matthew Weidman, Ferenc Krausz, Johannes Schötz 128

M47 **Multi-wave mixing in Neon to reveal dark-state quantum beats in attosecond transient emission**
Islam Shalaby, Sergio Yanez-Pagans, Nisnat Chakraborty, Arvinder Sandhu 231

M48 **Soliton self-compression based HHG driver for water-window transient absorption experiments**
Giuseppe Fazio, Tristan Kopp, Tadas Balciunas, Zhong Yin, Dmitry Zimin, Christian Brahms, John C. Travers, Hans Jakob Wörner 232

M49 **Compact, post-compressed high repetition rate ultrafast source for attoscience**
Ann-Kathrin Raab, Marcus Seidel, Ivan Sytcevich, Chen Guo, Anne L'Huillier, Cord L. Arnold, Anne-Lise Viotti 233

M50 **Photoinduced Charge Migration Studies using a 1.7um OPCPA Source**
Chase Geiger, Quynh Le, Zenghu Chang, Wendell Hill 234

M51 **Control of high harmonic spectral characteristics in a non-collinear generation geometry**
Lénárd Gulyás Oldal, Peng Ye, Zoltán Filus, Tamás Csizmadia, Tímea Grósz, Massimo De Marco, Zsolt Bengery, Imre Seres, Barnabás Gilicze, Péter Jójárt, Katalin Varjú, Subhendu Kahaly, Balazs Major 129

M52 **Unraveling the excited states dynamics in non-fullerene acceptor Y6**
Nisreen Alshehri, Safakath Karuthedath, Catherine De Castro, Julien Gorenflot, Frédéric Laquai 235

M53 **Relativistic Time-Dependent Configuration-Interaction Singles**
Felipe Zapata, Asimina Papoulia, Rezvan Tahouri, Jimmy Vinbladh, Anton Ljungdahl, Eva Lindroth, Jan Marcus Dahlström 236

M54 **Turning elliptically polarized light into a highly efficient chiro-optical tool**
Laura Rego, Olga Smirnova, David Ayuso 237

M55 **High repetition rate few-cycle short-wave infrared light source for strong-field experiments**
Ivan Sytcevich, Anne-Lise Viotti, Chen Guo, Ann-Kathrin Raab, Jan Vogelsang, Fabian Langer, Anne L'Huillier, Cord L. Arnold 130

M56 **Disentangling fundamental processes of a two-level wave packet in attosecond transient absorption spectroscopy**
Axel Stenquist, Felipe Zapata, Jan Marcus Dahlström . . . 238

M57 **Self-induced splitting of Zn $K\alpha$ emission line**
C A Schröder, M Pollanka, P Scigalla, M Mittermair, A Duensing, A S Landsman , L W Pi, R Kienberger . . . 239

M58 **Photoelectron – ion entanglement in streaked direct and shake-up photoemission: an ab initio approach**
Hongyu Shi, Uwe Thumm . . . 240

M59 **Accurate and complete atomic data set for Helium-Like ions using Relativistic Configuration Interaction approach for singly and doubly excited states**
S Manai, D E Salhi, H Jelassi . . . 241

M60 **First results from attosecond X-ray pump probe experiments in liquids**
S Li, K Li, L Young, C Pearce, S P Moeller, M Lin, E Nienhuis, G Doumy, G Dakovski, R Santra, A Marineili, J Cryan, D DePonte, T Orlando, A Clark, Z Loh, X Li and A Krylov . . . 242

M61 **The ELI-ALPS MIR-HE ATTO - design and status of the 1 keV attosecond beamline**
Filippo Campi, Torsten Golz, Jan Heye Buss, Sebastian Starosielec, Michael Schulz, Subhendu Kahaly, Eric Cormier, Sergei Kühn, Katalin Varjú . . . 131

M62 **TIXEL Detector Development at SLAC - the next generation charged particle detector for photon science applications.**
Peter Walter, Lorenzo Rota, Christopher Kenney, Mark McKelvey, Bojan Markovic, Angelo Dragone . . . 243

M63 **Ultrafast scanning tunneling microscopy**
Adi Goldner, Boyang Ma, Michael Krueger . . . 244

M64 **Ultrafast laser-driven dynamics in metal-insulator interface model**
Abdallah AlShafey, Gerard McCaul, Xuyan Gia, Shoushu Gong, Denys Bondar, Yuan-Ming Lu, Mohit Randeria, Alexandra S Landsman . . . 103

M65 **High-order harmonic generation in semiconductor quantum dots**
Harshitha Nandiga Gopalakrishna, Raktim Baruah, Christian Hünecke, Viacheslav Korolev, Alexander Croy, Martin Richter, Ingo Uschmann, Heike Marschner, Christian Reichardt, Andreas Undisz, Jan Dellith, Christian Spielmann, Ulf Peschel, Stefanie Gräfe, Maria Wächtler, Daniil Kartashov . . . 104

M66 **Emulation of high-numerical aperture extreme ultraviolet lithography using coherent 13.5 nm light**

Esben Larsen, Fabian Holzmeier, Kevin Dorney, Clayton Bargsten, Sayantani Santra, Shikhar Arvind, Dhirendra Singh, Daisy Raymondson, Rod Ward, Henry Kapteyn, Thomas Nuytten, Paul van der Heide, John Petersen 245

M67 **Ab Initio Study on Enhanced Energy Transfer from Intense Dual-Color Laser Fields to a Semiconductor**
Mizuki Tani, Kakeru Sasaki, Yasushi Shinohara, Kenichi L. Ishikawa 246

M68 **Attosecond Optical Switching by Synthesized Light Field**
Dandan Hui, Husain Alqattan, Simin Zhang, Vladimir Pervak, Enam Chowdhury, Mohammed Hassan 105

M69 **Mechanisms for Attosecond Carrier Thermalization in Metals**
Bethany R. de Roulet, Lorenz Drescher, Stephen R Leone 106

M70 **Tracking the melting of charge density wave and excitonic condensate in 1T-$TiSe_2$ with transient XUV spectroscopy**
A Zong, S-C Lin, Michael Zuerch 247

M71 **Towards extreme ultraviolet spectroscopy of two dimensional transition metal dichalcogenides**
Monalisa Mallick, Rudrakant Sollapur, Christian Spielmann, Michael Zuerch 248

M72 **Spatiotemporal characterization of few-cycle Bessel-Gaussian waveforms**
Yangyang Liu, Shima Gholam Mirzaeimoghadar, Tran-Chau Truong, Dipendra Khatri, Paul B Corkum, Michael Chini 107

M73 **Ultrafast electron-phonon relaxations in 2D carbide $Ti_3C_2T_x$ (MXene): A case study by attosecond transient absorption spectroscopy**
Sergej Neb, Dongbin Shin, Zeno Schumacher, Arthur Niedermayr, Denis A. Kuznetsov, Christoph R. Müller, Alexey Fedorov, Shunsuke Sato, Angel Rubio, Lukas Gallmann, Ursula Keller 108

M74 **Single-shot measurement of few-cycle mid-infrared waveforms on a chip**
Yangyang Liu, John E Beetar, Jonathan Nesper, Shima Gholam, Michael Chini . . . 249

M75 **Characterization of small polaron formation in $CuFeO_2$ with transient XUV spectroscopy**
Hanzhe Liu, Jonathan Michelsen, Isabel Klein, Finn Babbe, Jason Cooper, Scott Cushing 250

M76 **Tracing sub-cycle electron dynamics in two-color nearfields of nanometric metal tips**
Philip Dienstbier, Lennart Seiffert, Timo Paschen, Thomas Fennel, Peter Hommelhoff 109

M77 **Ultrafast exciton dynamics reconstruction via a new ptychographic approach**
Gian Luca Dolso, Bruno Moio, Giacomo Inzani, Nicola Di Palo, Rocío Borrego-Varillas, Mauro Nisoli, Matteo Lucchini 110

M78 **Ultrafast charge dynamics and optical spectra is strongly correlated materials**
Volodymyr Turkowski 251

M79 **Probing nanoplasma expansion dynamics from rare-gas clusters through NIR-wavelength Pump-Probe experiments**
Abraham Camacho Garibay, Bryan Smith, Vyacheslav Leshchenko, Li Fang, Pierre Agostini, Louis DiMauro 111

M80 **Coherence in the photoionization of xenon in weak or strong fields**
Stefanos Carlström, Mathieu Gisselbrecht, Anne L'Huillier, Jan Marcus Dahlström, Johan Mauritsson, Kenneth J Schafer, Mikhail Yu. Ivanov, and Serguei Patchkovskii 252

M81 **Superachromatic Reflective Phase Retarder for the Polarization Conversion of Attosecond Pulses**
Keisuke Sakata, Kengo Ito, and Taro Sekikawa 253

M82 **Femtosecond XUV–IR induced photodynamics in the methyl iodide cation**
Sonia Marggi Poullain, Marta L. Murillo-Sánchez, Geert Reitsma, Pedro Fernández-Milán, Jesús González-Vázquez, Rebeca De Nalda, Fernando Martín, Mark J J Vrakking, Oleg Kornilov, Luis Bañares 254

MP

Entanglement of Orbital Angular Momentum in Non-Sequential Double Ionization

A S Maxwell[1,3]*, L B Madsen[2], and M Lewenstein[1,2]

[1]ICFO-Institut de Ciencies Fotoniques, The Barcelona Institute of Science and Technology, 08860 Castelldefels (Barcelona), Spain. [2]ICREA, Pg. Lluís Companys 23, 08010 Barcelona, Spain.
[3]Department of Physics and Astronomy, Aarhus University, DK-8000 Aarhus C, Denmark.

Synopsis We demonstrate robust entanglement between the in the orbital angular momentum (OAM) of the two photoelectrons in the process of non-sequential double ionization (NSDI). Exploiting the discrete OAM allows for a simple analysis, that enables identification of targets that maximize the entanglement and a reduction in the number of measurements required to detect the entanglement.

Entanglement provides a computational resource, and the possibility of entanglement enhanced imaging processes [1]. Attosecond physics, deals with processes in matter on the scale of attoseconds (10^{-18}s) and has led to the development of a host of ultrafast imaging procedures, which often exploit quantum phenomena. However, the potential for entanglement to optimize or improve attosecond imaging is relatively unexplored. There is growing interest in entanglement in attoscience, with a focus on ion–electron entanglement. These studies almost always involve the calculation of a continuous variable density matrix and entanglement measures, which are challenging to compute and interpret, and often impossible to measure.

Recent rapid progress in the production and measurement of electron vortex states, carrying orbital angular momentum (OAM) [2], offers a solution to the above problems. We exploit the discrete degree of freedom, the OAM—inherent to all free particles, to clearly demonstrate the manifestation of entanglement in NSDI [3], a highly correlated two-electron ionization process, see Figure 1. Through known conservation laws [4] and the superposition of intermediate excited states, we demonstrate that the OAM in NSDI is entangled. Using the logarithmic negativity, the entanglement is quantified for a wide range of targets and parameters. We construct an entanglement witness, which provides a recipe for more simply detecting the entanglement in experiment, avoiding full tomographic measurements. The interplay of channels of excitation allows the photoelectrons to approach maximally entangled states. Furthermore, the entanglement is robust as it survives incoherent averaging over the focal volume of the laser. The use of OAM in attosecond processes provides a new avenue, to further the aim of imaging and controlling matter on ultrafast times scales. Furthermore, photoelectron-OAM entanglement demonstrates the fundamental non-classicality of NSDI.

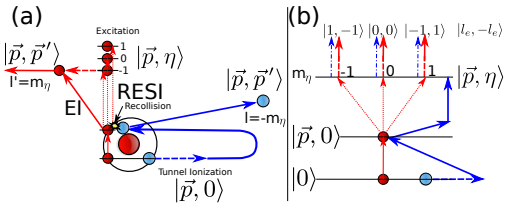


Figure 1. (b) NSDI process depicted for the EI and RESI mechanisms. Ionization via laser field is depicted by a dashed line and excitation in the singly charged ion is denoted by dotted lines. The two electron states are defined in [3]. (c) The RESI mechanism, which leads to final OAM states ($|l_e,-l_e\rangle$) in an entangled superposition. The numbers -1, 0, 1 refer to the values of the quantum magnetic number m_η of the intermediate excited state, $|\mathbf{p},\eta\rangle$.

References

[1] R Horodecki, et al, Rev. Mod. Phys. **81**, 865 (2009)
[2] KY Bliokh et al, Phys. Rep. **690**, 1 (2017)
[3] AS Maxwell et al, arXiv:2111.10148 [preprint] (2021).
[4] AS Maxwell, et al, Faraday Discuss. **228**, 394 (2021) and Y Kang, et al, Eur. Phys. J. D **75**, 199 (2021)

*E-mail: andrew.maxwell@phys.au.dk

Direct inclusion of many-body effects in calculations of attosecond delays in atomic photoionisation.

A Ljungdahl, J Vinbladh, S Saha, J Sörngård, and E Lindroth *

Department of Physics, Stockholm University, AlbaNova University Center, SE-106 91 Stockholm, Sweden

Synopsis We calculate attosecond delays in photoionisation by constructing the outgoing electron wave after two-photon interference. To accurately describe the atomic potential in many-electron systems it is necessary to include correlation effects. We present a method for including a class of such effects by direct solution of a system of linear equations. The method has a constant computational cost over a range of photon energies and enable resolution of resonances close to thresholds.

Attosecond science has enabled the study of the phase of an electron wave packet released due to photoabsorption in matter, for example in atomic photoionisation. When the electron is promoted to the continuum its phase changes due to the atomic potential. By taking the spectral derivative of the phase we obtain a quantity that represents a delay or advance of the wave packet. Interferometric techniques, such as the RABBIT scheme, can measure photoionisation delays using an attosecond pulse train in the extreme ultraviolet (XUV), and an infrared (IR) probe laser.

We perform many-electron numerical simulations of the full two-photon process, where we take a time-independent approach to constructing the outgoing electron wave. We present a new implementation of our approach that includes many-electron correlation to the level of the random phase approximation with exchange (RPAE), both relativistically and non-relativistically. Our earlier implementations included the RPAE effects by iteration when calculating the outgoing electron wave [1]. The new implementation solves a linear system of equations which includes all RPAE correlations "at once", avoiding problems with convergence. We also extend this approach to include higher order many-body effects.

The implementation has also been used as a validation tool for the development of new relativistic time-dependent methods [2], where we reproduce calculations of the one-photon cross section in neon, krypton and xenon, including also resonances close to thresholds.

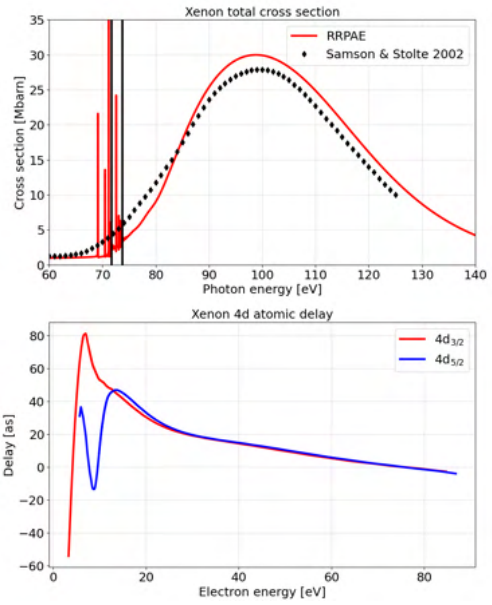


Figure 1. Example of relativistic calculations on xenon. Upper panel shows the total photoionisation cross section after absorption of an XUV photon, compared to measurements [3]. We see the resolution of resonances leading up to the $4d_{3/2}$- and $4d_{5/2}$-thresholds (vertical black lines). Lower panel shows the computed atomic delay in the separate $4d$ channels.

References

[1] J. Vinbladh *et al*, Phys. Rev. A **100** 043424 (2019).
[2] F. Zapata *et al*, Phys. Rev. A **105** 012802 (2022).
[3] J.A.R. Samson & W.C.Stolte, J. Electron. Spectroscopy and Related Phenomena **123** (2002).

*E-mail: Eva.Lindroth@fysik.su.se

MP

Angle resolved, spin-orbit contributions to spectral phase in semi-relativistic RABBITT simulations.

L. F. Roantree[1] *, J. Wragg[1], C. P. Ballance[1], A. C. Brown[1] †, and H. W. van der Hart[1].

[1]School of Mathematics and Physics, Queen's University of Belfast, Belfast, Northern Ireland

Synopsis We use R-Matrix with Time-dependence (RMT) to investigate relativistic effects in the "Reconstruction of Attosecond Beating By Interference of Two-photon Transitions" (RABBITT) technique. We extract phase information induced by the [Ne]$3s3p^6 4p\ ^1P$ resonance and use the direct access to the photoelectron wavefunction (PEW) offered by RMT to illustrate the individual Spin-Orbit contributions to this extracted phase, in addition to projecting the PEW onto a set of emission angles to angularly resolve the phase information.

Attosecond spectroscopy has enabled experiments to investigate how Fano resonance profiles build up over time [1]. Experimental techniques, underpinned by theory, have recently been developed in order to characterize phase relations within these profiles, for example the RABBITT approach [2, 3]. Through these, the phases of the associated ionization processes are shown to be of critical importance in the final resonance profile of an atomic state.

To obtain accurate ionization phases in multielectron systems, a good description of the atomic physics is essential. The RMT code suite has been designed specifically to describe the influence of atomic structure on ultrafast-atomic dynamics. Recently, the code has been extended to enable the inclusion of spin-orbit interactions using the Breit-Pauli approximation [4].

In this contribution, we use RMT to perform a numerical study of rainbow RABBITT, in which phase changes induced by an atomic resonance are traced as a function of energy across a RABBITT sideband [5, 6, 7]. Ar atoms are irradiated by an attosecond extreme ultraviolet (XUV) pulse train with a central frequency given by the 17th harmonic of a fundamental IR field with wavelength 786nm, combined with the weak, fundamental IR pulse.

We investigate the spectral phase across the lower sideband 'SB16', corresponding to either absorption of a $15\omega_{\mathrm{IR}}$ photon and an ω_{IR} photon, or absorption of a $17\omega_{\mathrm{IR}}$ photon and emission of an ω_{IR} photon. By isolating the ionization channels involving each Spin-Orbit (SO) split state of the resonance, we can build single SO component spectrograms, shown in Figure 1, and use them to analyze the SO contributions to the total energy-resolved spectral phase.

By projecting our photoelectron wavefunction onto a set of emission angles, we calculate the phase contribution along a given angle. Through this we obtain an angularly resolved picture of the phase across SB16, and a better understanding of the underlying dynamics.

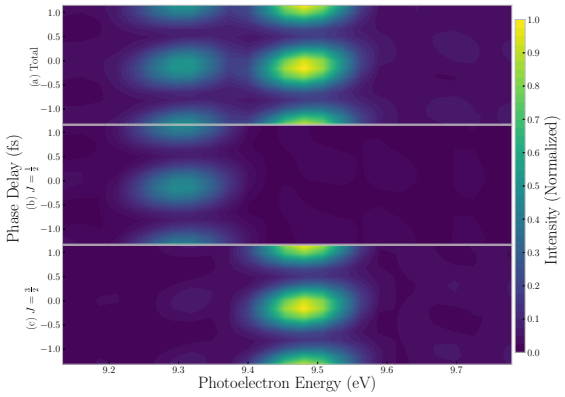


Figure 1. RABBITT spectrograms centered around SB16 showing a) the total sideband, b) the [Ne]$3s3p^6 4p\ ^1P_{\frac{1}{2}}$ channel contributions, c) the [Ne]$3s3p^6 4p\ ^1P_{\frac{3}{2}}$ channel contributions.

References

[1] A. Kaldun *et al* 2016 *Science* **354** 738-741
[2] Véniard V *et al Phys. Rev. A* **54** 721
[3] Muller H 2002 *Appl. Phys. B* **74** s17–s21
[4] Brown A C *et al* 2020 *Comput. Phys. Commun.* **250** 107062
[5] Kotur M *et al* 2016, *Nat. Commun.* **7** 10566
[6] Gruson V *et al* 2015, *Science 354* 734
[7] Turconi M *et al* 2020 *J. Phys. B: At. Mol. Opt. Phys.* **53** 184003

*E-mail: lroantree01@qub.ac.uk
†E-mail: andrew.brown@qub.ac.uk

Control of Parent-Ion Coherence in Helium Ion Ensemble

S Mehmood[1]*, E Lindroth[2] and L Argenti[1,3]†

[1] Dept. of Phys., University of Central Florida, Orlando, 32826, USA
[2] Dept. of Phys., Stockholm University, Stockholm, Sweden
[3] CREOL, University of Central Florida, Orlando, 32826, USA

Synopsis We present a theoretical study of the shake-up ionization of the helium atom in an attosecond XUV-pump IR-probe setup. We show how, by leveraging the beating between autoionizing states, the pump-probe delay can serve as a control knob to tune the coherence between either the N=2 or the N=3 states of the residual ion. From the picosecond dipole beating caused by relativistic interactions, we demonstrate that it is possible to reconstruct the polarization of the ion at the time of its inception.

Attosecond pulses can ionize atoms in a coherent process. Since the emerging fragments are entangled, however, each preserves only a fraction of the initial coherence [1], thus limiting the chance of guiding the ions subsequent evolution. In this work, we simulate the pump-probe ionization of the helium atom to demonstrate that the loss of ionic coherence of the ions with a same principal quantum number N can be controlled. This control is achieved by promoting multiphoton transitions from intermediate autoionizing states $N_L n_\ell$, below the N threshold, to the $N_{L'}\epsilon_{\ell'}$ continua [2, 3]. We also study the role played by the $(N+1)_L n_\ell$ resonances above the N threshold, which interact with the $N_{L'}\epsilon_{\ell'}$ channels due to correlation. The *ab initio* simulations of the attosecond pump-probe ionization of helium above the $N=2$ and $N=3$ thresholds are performed using the NewStock code [4]. Due to the fine splitting of the He^+ levels, the ionic dipole beats on a picosecond timescale. From the dipole beating, which is a measurable quantity, we reconstruct the polarization of the ion at its inception, and highlight the effect of resonant radiative continuum-continuum transitions on the coherence between ionic states of different parity. The reconstruction protocol, which can be applied to experimental data, also provides an estimate of the initial coherence between ionic states with different spin projections generated by the initial attosecond ionization event and can therefore reveal the role of spin-orbit interaction in ultrafast ionization processes. This research has been supported by NSF grant No. 1912507.

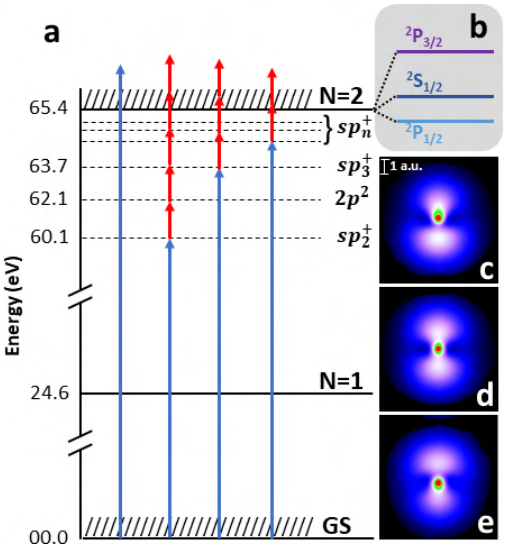


Figure 1. a) Several multi-photon paths interact to give rise to the $2s-2p$ coherence. c-e) The electron density in the He^+ ion at $\tau = 0$, 1, and 2 fs exhibits asymmetry due to ionization in the presence of polarized IR field. b) As a consequence of the fine-structure splitting of the $n=2$ He^+ level, the ionic dipole fluctuates, thus mapping the attosecond dependence of initial ionic coherence to the picosecond timescale.

References

[1] S Pabst *et al.*, Phys. Rev. Lett. **106**, 053003 (2011).
[2] S Mehmood, E Lindroth, L Argenti, Phys. Rev. Res. **3**, 023233 (2021).
[3] L Argenti and E Lindroth, Phys. Rev. Lett. **105** 053002 (2010).
[4] T Carette *et al.* Phys. Rev. A **87** 023420 (2013)

*E-mail: saadiphy@knights.ucf.edu
†E-mail: luca.argenti@ucf.edu

MP

Autoionizing states in atomic two-photon double-ionization: A virtual sequential finite-pulse model

S Chattopadhyay [1]*, **L Argenti**[1,2]†

[1]Department of Physics, University of Central Florida, Orlando, FL 32816.
[2]CREOL, University of Central Florida, Orlando, FL 32816

Synopsis The transition between non-sequential and sequential regime in the two-photon double ionization of helium can be qualitatively reproduced by a virtual sequential model (VSM). Little is known, however, about more complex atoms. Here, we present a finite-pulse extension of the VSM, which we apply to both the helium and neon atoms, starting from accurate *ab initio* multi-channel single photoionization amplitudes of the neutral atoms and of several excited states of their intermediate ions, which are computed with the NewStock code.

XUV-pump XUV-probe experiments made possible by new intense XUV sources [1,2] will allow us to directly observe correlated electron dynamics in atoms and molecules with attosecond time resolution. The quantitative description of two-photon double ionization (2PDI) dynamics entailed by these experiments requires expensive numerical simulations [3, 4] which solve directly the time-dependent Schrödinger equation. However, it has been shown that a simple virtual sequential model with only single-ionization intermediate states and no final-state interaction is able to capture several qualitative aspects of this process even below the sequential regime [5–7]. As a step towards the full *ab initio* description of time-dependent multi-photon double ionization processes, in this work, we extend the virtual sequential model to finite-pulse interactions [8] and to polyelectronic atoms.

The photoionization amplitudes of the initial neutral state and of the intermediate ionic states are computed *ab initio*, with the NewStock close-coupling code [9]. Although our model does not account for one-photon double-ionization amplitudes from the intermediate bound and autoionizing states, it does include the contribution of final autoionizing states as well as finite-pulse effects and the interference of multiple ionizing pulses. We will present detailed analysis of the joint energy distribution for the 2PDI of the helium and neon atom from the non-sequential to the sequential regime. Our results for helium compare favorably with *ab initio* pump-probe results in the literature. This work is supported by NSF grant No. PHY-1607588 and by the DOE CAREER grant No. DE-SC0020311.

*E-mail: Siddhartha.Chattopadhyay@ucf.edu
†E-mail: Luca.Argenti@ucf.edu

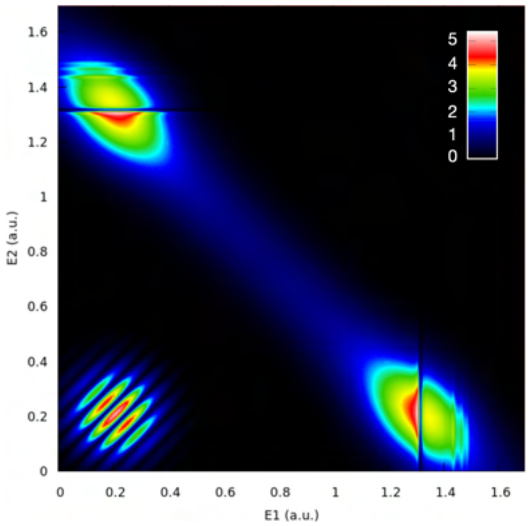


Figure 1. Photoelectron energy distribution for the 2PDI of He by two XUV pulses with central energy of 60 eV and 30 eV, duration of 400 as, peak inteansity of 8 GW/cm^2 and 0.1 GW/cm^2, respectively, and relative delay of 2 fs.

References

[1] J Duris *et al.*, Nat. Photonics **14**, 30 (2020).
[2] N Saito *et al.*, Optica **6** 1542 (2019).
[3] J Feist *et al.*, PRA **77** 043420 (2008).
[4] A Palacios *et al.*, PRL **103** 253001 (2009).
[5] D Horner *et al.*, PRA **76** 030701 (R) (2007).
[6] M Førre *et al.*, PRL **105** 163001 (2010).
[7] W Jiang *et al.*, PRL **115** 153002 (2015).
[8] A Jiménez Galán *et al.*, PRA **93** 023429 (2016).
[9] T Carette *et al.*, PRA **87** 023420 (2013).

Optimal density matrix extraction from attosecond spectrogram using ptychographic algorithms

J. Im[1,2]*, P. Salières[1]† and C. Bourassin-Bouchet[2]

[1]Universite Paris-Saclay, CEA, CNRS, LIDYL, Gif-sur-Yvette, 91191, France
[2]Universite Paris-Saclay, CNRS, Laboratoire Charles Fabry, Institut d'Optique Graduate School, Palaiseau Cedex, 91127, France

Synopsis We report the computational recovery of partially coherent electron density matrices extracted from photoelectron spectrograms using phase-retrieval algorithms. The reconstruction performances have been compared between several ptychographical algorithms considering different pulse types and various noise levels.

Laser-dressed photoelectron spectroscopy has played an important role in attoscience since the infancy of the domain. Especially laser-XUV cross-correlation has established itself as a reference approach for attosecond pulse metrology and for the measurement of photoemission time delays. This consists in measuring the photoelectron kinetic energy spectrum as a function of the laser-XUV delay. The resulting spectrogram must then be analyzed to extract the attosecond dynamics of the ionization process [1]. FROG-CRAB (Frequency-Resolved Optical Gating for the Complete Reconstruction of Attosecond Bursts) introduced the key idea that such traces could be processed with adapted algorithms to recover robustly the amplitude and phase of the electron wave packet [2]. Recently, we have shown that this approach could be extended to reconstruct partially coherent wavepackets described by an electron density matrix, a technique christened Mixed-FROG [3].

In this work, we look for the most reliable way to solve the Mixed-FROG inverse problem. To do so, we build upon the field of ptychography, a popular imaging technique that enables the reconstruction of nano-resolution images of samples from their x-ray diffraction patterns using algorithms [4]. Interestingly, the inverse problems behind ptychography and spectrogram measurements rely on common mathematics. Therefore the powerful algorithms developed for ptychography can in principle be used in attosecond science with equal success. Using the mixed-state formalism of ptychography [5], we adapted several of these algorithms to recover the density matrix from spectrograms. We then compared their performances on simulated data by monitoring the least-squares error ϵ between the original and retrieved spectrograms. The difference map (DM) algorithm and several variations of the Ptychographical Iterative Engine (PIE) algorithm were tested. Both isolated attosecond pulses, attosecond pulse trains and free-electron laser pulses were considered and the study was carried out for various noise levels on the spectrograms.

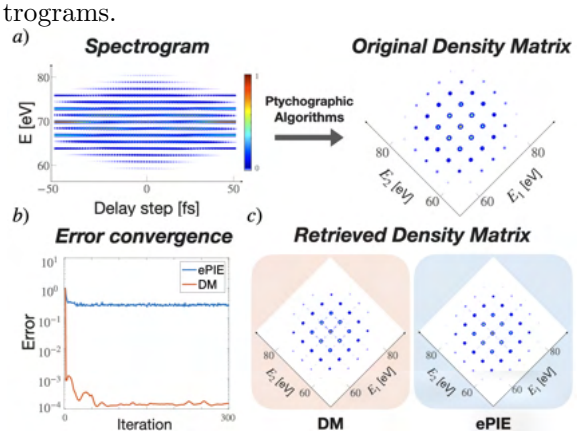


Figure 1. a) Density matrix extraction using ptychographic algorithms. b) Evolution of ϵ as a function of the iteration number for DM and ePIE. c) Corresponding retrieved density matrices.

References

[1] M. Schultze *et al.*, Science **328**, 1658 (2010).
[2] Y. Mairesse, F. Quéré Phys. Rev. A **71.1**, 011401 (2005).
[3] C. Bourassin-Bouchet *et al.* Phys. Rev. X **10**, 031048 (2020).
[4] J. Rodenburg, A. Maiden Springer Handbook of Microscopy **Ptychography**, 819-904 (2019).
[5] P. Thibault, A. Menzel Nature **494**, 7435 (2013).

*E-mail: jinhyeok.im@universite-paris-saclay.fr
†E-mail: pascal.salieres@cea.fr

Measuring two-photon transition delays using 'self-probing' of a resonance

L Maëder[1*], HJB Marroux[1], C Schouder[1], M Lejman[1], A Autuori[1], D Platzer[1], N Berrah[1,2], R Taïeb[3], J Caillat[3] and P Salières[1]

[1] Université Paris-Saclay, CEA, CNRS, LIDYL, 91191, Gif-sur-Yvette, France
[2] Physics Department, University of Connecticut, Storrs, CT, USA
[3] Sorbonne Université, CNRS, Laboratoire de Chimie Physique-Matière et Rayonnement, 75005 Paris, France

Synopsis We have developed an original interferometric technique that allows measuring the transition delay associated with a two-photon transition through a bound state with both high accuracy and spectral resolution.

The ionization dynamics in the vicinity of resonances are specifically interesting as they reveal the electronic behavior at energies particularly relevant for the quantum system. They have been studied using interferometric schemes such as the RABBIT technique where measurements of the spectral phase evolution allowed reconstructing the corresponding rich dynamics.

In the present study, we develop an alternative interferometric scheme to access the spectral phase of resonant transition amplitudes. It relies on reference single-photon transitions (rather than reference two-photon transitions as in RABBIT-like approaches) leading to a number of advantages. This is demonstrated in the case of the two-photon XUV+IR ionization of helium through the intermediate resonant state 1s3p.

We use a single harmonic beam (H15) overlapped with its generating IR field to induce two-photon transition towards the continuum, creating the free electron wavepacket (EWP) of interest. The latter is structured by the transient resonance with the intermediate 1s3p state that leads to a π rad spectral phase jump [1,2]. The 1s3p state is also coherently populated through a one-photon transition. After a variable delay τ, an additional IR field transfers some population from this state to the continuum, again by a one-photon transition, creating a reference EWP centered at the same energy. In contrast to the resonant two-photon transition, the sequential one-photon transitions produce an EWP with a smooth phase evolution providing an ideal reference. The interferences between the probed and reference EWPs encode their relative phase that has two contributions: i) the difference of phases accumulated during the delay τ by the 1s3p and the continuum states, and ii) the phase of the resonant two-photon transition. By measuring the τ-dependent photoelectron spectrum over hundreds of femtoseconds, we can access the latter phase with both high accuracy and high spectral resolution. A further advantage of this interferometric scheme is that the reference EWP has a similar partial wave decomposition as the studied EWP, which maximizes the contrast of the interferences regardless of the electron emission direction.

The spectrogram corresponding to the P_0 Legendre polynomial of the Abel inversion of the VMI images is shown in Fig. 1 (very similar spectrograms are obtained for P_2 and P_4). The clear difference in slope (inset) corresponds to a linear spectral phase of the probed two-photon transition around the resonance. It encodes the transition delay due to the transient trapping of the electron in the intermediate bound state before completing the transition.

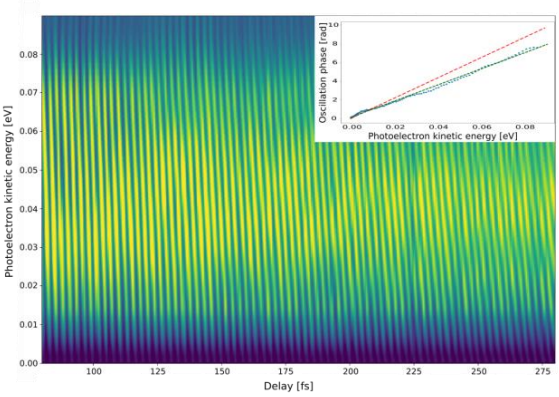


Figure 1. Photoelectron spectrogram showing highly contrasted interferences between the probed and reference EWPs. The inset shows the phase at the central oscillation frequency for each photoelectron energy (blue dots) compared to the simulated phases resulting purely from the accumulation delay τ (red dashed) and from the total calculation (green dashed).

References

[1] Swoboda M *et al* 2010 *Phys. Rev. Lett.* **104** 103003
[2] Autuori A *et al* 2022 *Sci. Adv.* **8** eabl7594

* E-mail: lucie.maeder@cea.fr

Under-threshold RABBITT: a novel probe of ionization dynamics and target electronic structure

A S Kheifets[1]*

[1]Research School of Physics, The Australian National University, Canberra ACT 2601, Australia

Synopsis When a harmonic energy of the attosecond pulse train submerges below the ionization threshold $(2q-1)\omega < I_p < (2q+1)\omega$, one quantum path of the RABBITT process (reconstruction of attosecond beating by interference of two-photon transitions) crosses the manifold of discrete atomic excitations. Not only does it change profoundly two-photon XUV + IR ionization dynamics, it opens the way for a faithful mapping of the target electronic structure in the form of the bound state energies and oscillator strengths.

Under threshold RABBITT (uRABBITT) has been demonstrated experimentally in He and Ne. In He, this process was detected by observing a resonant change of the uRABBITT phase [1]. In Ne, the photoelectron momentum distribution (PMD) was shown to acquire a very distinct symmetry [2]. Prompted by these earlier works, we study in depth uRABBITT in He and Ne by conducting an extensive set of numerical simulations. In result, we uncover the following properties: (i) a resonant change of the uRABBITT phase is only a part of a much broader phase transition across the ionization threshold [3], (ii) the uRABBITT amplitude maps faithfully the oscillator strength of the discrete transitions [4] and (iii) the symmetry of the PMD reflects the propensity rules that govern the discrete and continuous atomic transitions [5]. These discoveries make uRABBITT a powerful probe revealing ionization dynamics and the target structure.

In our numerical simulations, we solve the time-dependent Schrödinger equation (TDSE) for an atom ionized by XUV radiation from an attosecond pulse train in the presence of an IR dressing laser field. Our analytic model is based on the lowest order perturbation theory (LOPT) [6]. The uRABBITT magnitude and phase parameters are expressed via the direct and resonant two-photon ionization amplitudes. The latter depend sensitively on the bound state energies and oscillator strengths which are sourced from the software package ATOM [7]. Both the numerical TDSE and the analytic LOPT results agree well supporting our interpretation of the uRABBITT phase and amplitude. This is illustrated In the Figure where we map the uRABBITT parameters in Ne against the bound *nd* states energies and oscillator strength.

*E-mail: A.Kheifets@anu.edu.au

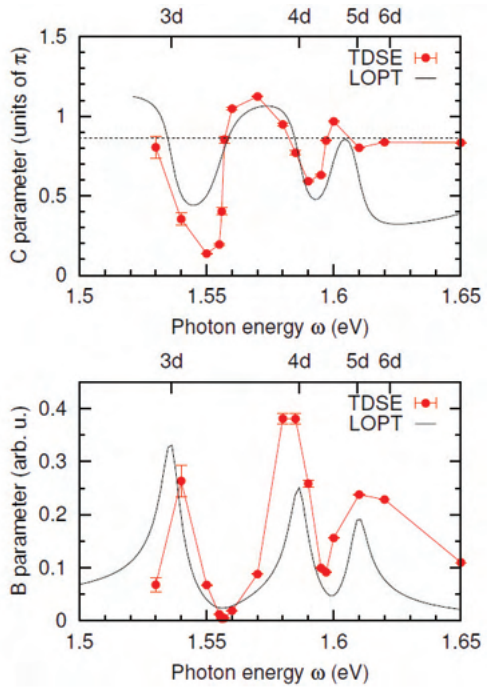


Figure 1. The uRABBITT phase (top) and magnitude (bottom) parameters in Ne as the functions of the IR photon frequency. The ticks *nd* mark the crossing of the submerged harmonic H13 with the corresponding energy levels. The dotted line marks the flat non-resonant phase parameter.

References

[1] M Swoboda *et al*, PRL **104**, 103003 (2010).
[2] D M Villeneuve *et al*, Science **356**, 1150 (2017).
[3] A S Kheifets and A W Bray. Phys. Rev. A **103**, L011101 Letter (2021).
[4] A S Kheifets, Atoms **9**, 66 (2021).
[5] A S Kheifets, Phys. Rev. A **105**, 013114 (2022).
[6] J M Dahlström *et al*, Chem. Phys. **414**, 53 (2013).
[7] M Ya Amusia and L V Chernysheva, Handbook for the ATOM programs. CRC Press (1997).

MP

Ionization of co- and counter-rotating electrons in ultrashort circularly polarized laser pulses

S Walker[1,†*], L Kolanz[1], J Venzke[1] and A Becker[1]

[1]JILA and Department of Physics, University of Colorado, Boulder, 80309-0440, USA

Synopsis We have found a surprisingly large change by two orders of magnitude in the emission probability of counter- over co-rotating electrons (P_+/P_-) in rare-gas-like atoms by ultrashort, intense, circularly polarized pulses in the few-photon ionization regime [1, 2]. To gain further insights, we use time independent Floquet formalism to determine the dependence of these ionization probabilities on Stark resonances associated with the magnetic quantum number of each initial state and predict the location and magnitude of this change in terms of the atomic potential.

We have studied ionization of atoms with non-zero orbital angular momentum by an intense circularly polarized laser as a function of wavelength [1, 2]. Numerical solutions of the time-dependent Schrodinger equation show a change by two orders of magnitude in the emission probability of counter- over co-rotating electrons in the few-photon ionization regime due to differences in the accessible ionization pathways and intermediate resonances (Figure 1).

To further understand this mechanism we transform into a system of coordinates that rotates with the applied circular field, which reduces the time-dependent Hamiltonian to a time-independent one which can be used to determine the dependence of the ionization probabilities on Stark resonances associated with the magnetic quantum number of an initial state. We will present predictions for how one might use physical properties of the atomic potential in order to predict where an by how much these emission ratios are maximised.

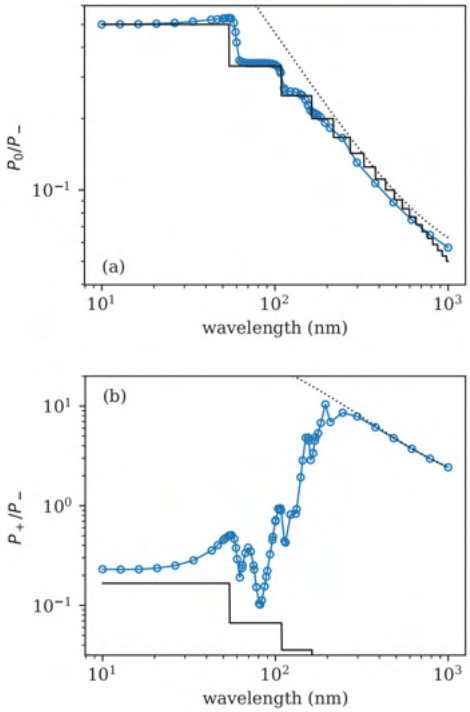


Figure 1. Emission ratio of (a) $m = 0$ to co-rotating electrons (P_0/P_-) and (b) counter- to co-rotating electrons (P_+/P_-) as function of wavelength for a neonlike atom at 5×10^{14} W/cm^2 interacting with a 10-cycle left-handed pulse. Dashed lines represent non-adiabatic tunneling theory and solid lines lowest order perturbation theory with $l \to l + 1$ photon processes only.

Acknowledgements

This work was primarily supported by a grant from the U.S. Department of Energy, Division of Chemical Sciences, Atomic, Molecular, and Optical Sciences Program (Award No. DE-SC0001771). We also acknowledge a grant from the U.S. National Science Foundation (Award No. 1734006) for computer resources used for part of the present calculations.

References

[1] S. Walker, L. Kolanz, J. Venzke, and A. Becker, Phys. Rev. A **103**, L061101 (2021).

[2] S. Walker, L. Kolanz, J. Venzke, and A. Becker, Phys. Rev. Research **3**, 043501 (2021).

*E-mail: Spencer.Walker@colorado.edu

Control of Atomic Photoionization by Circularly Polarized Attosecond Chirped Pulses

N J Strandquist and J M Ngoko Djiokap*

Department of Physics and Astronomy, University of Nebraska, Lincoln, Nebraska 68588-0299, USA

Synopsis We show how a pair of circularly polarized attosecond pulses linearly chirped can produce and control a new class of spiral pattern in the photoelectron momentum distribution (PMD) for pulses with zero time-delay, which is counter-intuitive for a linear process.

Our capability of using numerical and analytical tools to treat quite exactly the interaction of elliptically-polarized XUV attopulses with S-state atoms (with binding energy E_b) led to the 2015 discovery of electron matter-wave Archimedean spiral vortices in the PMD following single ionization by a pair of time-delayed, copropagating oppositely circularly-polarized (OCP) attopulses [1]. This prediction for one-photon, extended to single-color and two-color multiphoton ionization [2], not only have been confirmed experimentally using femtopulses [3]; but have stimulated numerous studies from several leading research groups for the occurrence and applications of this pattern in other systems and processes (see for instance [4]). In all these studies, the time delay τ between the two pulses was shown to play a crucial role since this basic pattern in the multiphoton regime originates from the linear (in energy E) Ramsey phase $(E + E_b)\tau$ accumulated between the creations of the two electronic wave packets delayed in time. In other words, spirals never occur for OCP pulses with $\tau = 0$. Although all these theoretical studies used transform limited pulses (TLPs), current techniques (either from HHG or FEL) for generating attosecond pulses introduce a chirp. In the unpublished work [5], we study how such chirp can affect the spiral production by photoionization. For two OCP attosecond pulses with identical chirp rates, the PMD obtained is identical to that produced by TLPs, meaning that information about the chirp is not reflected in the PMD. This intuitive result for linear processes holds for any τ. Whilst zero time delay leads to dipole patterns, nonzero time delays lead to spirals. The situation changes dramatically when the two pulses have equal but opposite chirp rates, $\xi \equiv \xi_1 = -\xi_2$. Counter-intuitively, the zero time delay case is shown to lead to a new kind of spirals, which is induced by an unusual chirp-dependent quadratic Ramsey phase. Moreover, the nonzero time delay case is shown to produce PMDs that are very sensitive to the chirp sign as a result of the mixture of the τ-dependent linear Ramsey phase and the ξ-dependent quadratic Ramsey phase. In the present work, we provide a full analytical description of this linear process using first-order perturbation theory (PT), with an emphasis on controlling the direction of emission of electron by tuning the chirp for the case of equal and opposite chirp rates. All our predictions from PT are demonstrated to be in excellent concert with our *ab initio* numerical results obtained by solving the full-dimensional time-dependent Schrödinger equation.

References

[1] J M Ngoko Djiokap, S X Hu, L B Madsen, N L Manakov, A V Meremianin, and A F Starace, Phys. Rev. Lett. **115**, 113004 (2015).

[2] J M Ngoko Djiokap, A V Meremianin, N L Manakov, S X Hu, L B Madsen, and A F Starace, Phys. Rev. A **94**, 013408 (2016).

[3] D Pengel, S Kerbstadt, D Johannmeyer, L Englert, T Bayer, and M Wollenhaupt, Phys. Rev. Lett. **118**, 053003 (2017). D Pengel, S Kerbstadt, L Englert, T Bayer, and M Wollenhaupt, Phys. Rev. A **96**, 043426 (2017).

[4] J M Ngoko Djiokap, Phys. Rev. A **104**, 013115 (2021).

[5] Nathaniel J Strandquist and J M Ngoko Djiokap, *"Attochirp Effects in Atomic Photoionization of Atoms" (to be submitted soon).*

*E-mail: marcelngoko@unl.edu

MP

Theoretical Study of Vacuum Ultraviolet Pulse Characterization from Two-Photon Autocorrelation Signals

S Walker[1,†,*], R Reiff[1], A Jaron-Becker[1] and A Becker[1]

[1]JILA and Department of Physics, University of Colorado, Boulder, 80309-0440, USA

Synopsis We introduce a two-photon autocorrelation technique based on multiple Gaussian pulses to characterize the time-dependent amplitude and phase variation of the electric field of a vacuum ultraviolet pulse.

In this work, we discuss and apply an extension of the single-Gaussian autocorrelation technique, which enables the characterization of an isolated ultrashort VUV pulse or a pulse train, i.e. the time-dependent amplitude and phase variation of the electric field. The extension is based on the analytical solution of the time-dependent Schrödinger equation (TDSE) for the perturbative two-photon ionization of an atom by a Gaussian laser pulse in the single-active-electron approximation [1]. Since the solution includes both resonant and non-resonant pathways, it can be used for the characterization of broadband pulses with photon energies in the regime of typical atomic excitation energies. The unknown pulse is approximated as a superposition of multiple Gaussian pulses about one or several frequencies, for which the amplitudes and temporal widths are determined via fitting to the two-photon autocorrelation signal generated by the unknown laser pulse. We demonstrate this extension of the single-Gaussian autocorrelation technique via applications based on results for ultrashort VUV pulses from numerical simulations of macroscopic high harmonic generation (HHG) [2]. Figure 1 shows exemplary results for the reconstruction of a single pulse (a-c) and a pulse train (d-e). Both amplitudes and phase variation of the original pulses (dashed lines) are reconstructed well using a few Gaussians (solid lines).

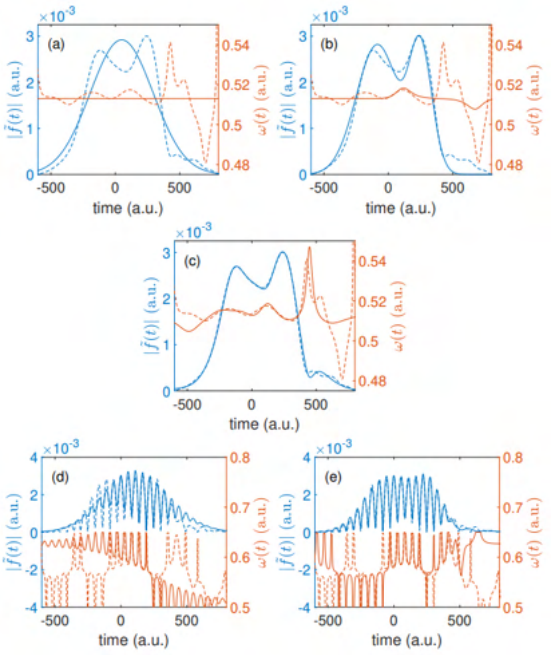


Figure 1. Comparison of time-dependent amplitude $|\tilde{f}(t)|$ (blue line) and phase variation $\omega(t)$ (red line) of the filtered 9th harmonic (dashed line) and reconstructed pulse (solid line) with (a) 1, (b) 2 and (c) 6 Gaussians for the 9th harmonic and (d) 1 and (e) 3 Gaussians per harmonic for an attosecond pulse train comprised of the 9th and 11th harmonics [1]. The harmonics are results of numerical simulations of HHG for a gas jet of hydrogen atoms interacting with a 20-cycle 800 nm pulse at peak intensity of 4×10^{13} W/cm^2 [2].

Acknowledgements

This work has been supported by grants from AFOSR MURI (Grant No. FA9550-16-1-0121) and the U.S. National Science Foundation (Award No. PHY-1734006).

References

[1] S Walker, R Reiff, A Jaron-Becker and A Becker, Opt. Lett. **46**, 3083 (2021).

[2] R Reiff, J Venzke, A Jaron-Becker and A Becker, OSA Continuum **4**, 1897 (2021).

*E-mail: Spencer.Walker@colorado.edu

Photoionization domains for Rabi oscillations at XUV wavelengths

E Olofsson[1], M Bertolino[1], S Nandi[2], and J M Dahlström[1] *

[1]Lund University, Lund, Box 118, SE-221 00 Lund, Sweden
[2]Université de Lyon, Université Claude Bernard Lyon 1, CNRS, Institut Lumière Matière, Villeurbanne, France

Synopsis Motivated by recent experimental results from the FERMI free-electron laser, we study photoionization from a Rabi-oscillating atom, and investigate at which intensities non-linear ionization processes become important. Additionally, we study the rates of relevant decay and ionization processes, that limit the parameter space where Rabi oscillations can take place.

When an atom is driven by a laser field with a photon energy that is nearly resonant with an atomic transition, it can undergo periodic population transfers between the ground and excited state, known as Rabi oscillations [1, 2]. The aim of this work is to study photoionization from atoms using a free-electron laser tuned to a specific resonance [3]. Using time dependent perturbation theory to model photoionization from a Rabi oscillating atom, we have shown that in addition to the expected pathway of ionization from the excited state, non-resonant two-photon ionization will have a comparable amplitude at intensities on the order of 10^{13} W/cm^2 [3].

The Rabi oscillations lead to an Autler-Townes-like doublet structure in the resulting photoelectron spectrum [2, 3]. When the non-resonant pathway becomes important, there will be a detuning-dependent asymmetry between the two components of the doublet, which is not present when the first-order amplitude dominates [3]. Our model is able to explain observations made at FERMI for the 1s^2-1s4p resonance in He, and agrees with simulations performed using the time-dependent configuration interaction singles method [3].

Here, we study the transition from one-photon ionization to non-resonant two-photon ionization, for different excited states in the He Rydberg series over a wide parameter space. Our results show that the transition to the two-photon regime occurs at lower intensities as we go up in the Rydberg series.

In Fig. 1 we show our prediction of different domains for photoionization from a Rabi oscillating atom at XUV wavelengths. The colored regions in Fig. 1 indicate for which combinations of intensity and pulse duration it should be possible to observe an Autler-Townes doublet in the photoelectron spectrum. The red region indicates where one-photon ionization from the excited state is dominant, and the blue region indicates where the non-resonant two-photon process is stronger. The diamond in Fig. 1 corresponds to the FEL parameters for the experiment described in Ref. [3], and shows that the experiment was performed in a region where both resonant and non-resonant processes are important.

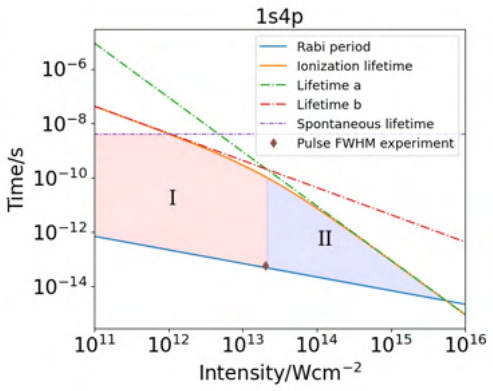


Figure 1. Relevant timescales as a function of intensity for the Rabi oscillating 1s^2-1s4p transition in He.

References

[1] I I Rabi, Phys. Rev. **51**, 652 (1937).
[2] S H Autler and C H Townes, Phys. Rev. **100**, 703 (1955).
[3] S Nandi *et al.*, arXiv:2201.10950 (2022).

*E-mail: marcus.dahlstrom@matfys.lth.se

MP

Multiphoton interaction phase shifts in attosecond science

M Bertolino[1] *, **J M Dahlström**[1] †

[1] Department of Physics, Lund University, Box 118, SE-221 00 Lund, Sweden

Synopsis We use ab initio simulations of interferometric experiments in attosecond and free-electron laser sciences to find a dependence on multiphoton phase shifts in above-threshold ionization. A simple rule of thumb is devised that is able to explain general phase and amplitude effects on an *absolute* scale, relative to known reference experiments. For instance, we show why interferometric ATI experiments are shifted by $\pi/4$ relative to RABBIT-like experiments, and why there is no 2ω-phase modulation (RABBIT-modulation) in laser-assisted photoionization with odd and even harmonics.

In Ref. [1] we study three recent attosecond and free-electron laser experiments from Ref. [2, 3, 4], using an *ab initio* method based on the time-dependent configuration interaction singles [5] (TDCIS). We find that the dependence on the carrier-envelope phase can partly be understood based on accumulation of *interaction phase* in multiphoton processes. We derive the following rule of thumb, valid in the limit of a small ponderomotive energy, which expresses the nth laser-assisted photoionization process as

$$c_{\mathbf{k}}^{(n)} \approx (-i)^{|n|} J_{|n|} \exp(in\varphi) f_{\mathbf{k}}^{(\mathrm{pump})}, \qquad (1)$$

where $f_{\mathbf{k}}^{(\mathrm{pump})}$ is the elementary photoionization amplitude, φ the CEP difference between pump and probe fields, $J_{|n|}$ a Bessel function and $(-i)^{|n|}$ an *interaction phase* which accumulates for each included interaction.

This rule of thumb is used to provide an explanation to why laser-assisted photoionization experiments with mixed parity express no RABBIT modulation [2, 3], and why interferometric above-threshold ionization experiments are shifted relative to RABBIT experiments [4]. In Figure 1 we show the modulation of twin sidebands measured along the polarization axis as reported in Ref. [3]. That the two sidebands are out of phase by $-\pi/2$ is directly related to the interaction phase shift.

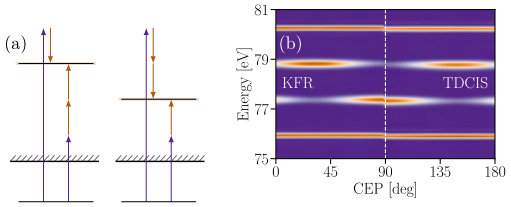


Figure 1. (a) Photoionization pathways included in the rule of thumb for the twin SB experiment in Ref. [3]. (b) Photoelectron peaks along the polarization axis calculated using KFR and TDCIS.

References

[1] M Bertolino, J M Dahlström, Phys Rev Research **3** (2021) 013270.
[2] G Laurent, et al., Phys Rev Lett **109** (2012) 083001.
[3] P K Maroju, et al., Nature **578** (2020) 386-391.
[4] L J Zipp, A, Natan, P H, Bucksbaum, Optica **1** (2014) 013270.
[5] L Greenman, et al., Phys Rev A **82** (2010) 023406.

*E-mail: mattias.bertolino@matfys.lth.se
†E-mail: marcus.dahlstrom@matfys.lth.se

Volume effects in attosecond pulse reconstruction and photoemission time-delay retrieval

F. Vismarra[1,2]*, R. Borrego-Varillas[2], Y. Wu[1,2], D. Mocci[1], M. Nisoli[1,2] and M. Lucchini[1,2]

[1]Department of Physics, Politecnico di Milano, 20133 Milano, Italy
[2]Institute for Photonics and Nanotechnologies, IFN-CNR, 20133 Milano, Italy

Synopsis We investigate numerically the effect of a finite spatio-temporal distribution of the fields in streaking spectroscopy. We characterize their impact on pulse reconstruction and on the retrieval of photoemission time-delays.

Attosecond streaking spectroscopy is one of the most extended approaches for measuring photoemission time delays [1]. So far all discussions and experimental data analysis have assumed a single atom-fields interaction, namely 1D-approximation. However, in a real attosecond experiment an ensemble of atoms interacts with fields that are confined in space (3D fields). To study the effect of a finite 3D distribution we averaged over a grid of single-point 1D-streaking traces, $W^{1D}_{x,y,z}$ in Eq.1, accounting for IR and XUV intensity variation along the radial coordinate (2D effects, x, y plane) and the propagation direction (3D effects, z):

$$W^{3D}(\epsilon,\tau) = \sum_{x,y,z} W^{1D}_{x,y,z}(\epsilon,\tau)\Delta V \qquad (1)$$

where ΔV is the volume of a single grid point.
We tested several fields configurations by changing the IR-XUV spot size ratio, η, IR-intensitiy and focalization conditions. For each scenario considered, we quantified 2D and 3D ensemble effects on the retrieval of the attosecond pulse duration and the IR-field intensity. We found that the impact of 2D and 3D effects can be severe, leading to an important trace variation up to 60-80% with respect to a 1D-trace, as shown in Fig.1. We also found that the relevance of these effects scales up with intensity: for the same IR-XUV spot size ratio value, differences from the ideal 1D-trace become more pronounced as the IR intensity increases. This error propagates in the evaluation of XUV pulse duration and IR-intensity reconstruction.
We then simulated the streaking traces in two gases (argon and neon) using the same formalism to evaluate the photoemission time delay.

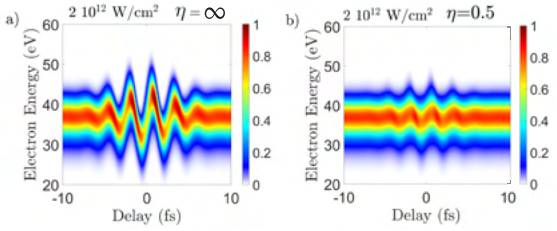


Figure 1. Simulated streaking traces in argon using a 5-fs, 2×10^{12}-W/cm^2 IR pulse and a 250 as XUV pulse for η values of a) infinite (plane wave) and b) 0.5.

By exploiting an opportunely modified version of the ePIE algorithm [3] we reconstructed in parallel the two traces. The retrieved attosecond chirp is automatically subtracted, allowing for the retrieval of the relative photoemission time delay between the two species. In spite of the weak nature of the photoemission time delay, (10-100 as) [2] we found a surprisingly robust and accurate reconstruction in all considered scenarios, with only minor deviation from the theoretical value. As the ensemble average has a similar effect on the two streaking traces, the parallel reconstruction delivers the correct photoelectron phase difference, despite the severe distortion caused on each individual trace. Our results thus demonstrate the robustness of this approach for the investigation of photoemission delays.

References

[1] L. Gallmann, Struct. Dyn.,**4**, 061502, (2017).
[2] R. Pazourek, Rev. Mod. Phys.,**87**, 765, (2015).
[3] M. Lucchini, Opt. Express, **23**, 29502, (2015).

*E-mail: federico.vismarra@polimi.it

MP

A Coupled Volterra Integral Equation Approach to Solving the Time-Dependent Schrödinger(TDSE) Equation

B. I. Schneider[1] *, **R. Schneider**[2] **and H. Ghartibnejad**[1]

[1]National Institute of Standards and Technology, Gaithersburg, MD 20899
[2]University of California San Diego, 9500 Gilman Dr, San Diego, CA 92093

Synopsis A coupled Volterra integral equation method is described to solve the TDSE which avoids the short-time approximation used in many other approaches. The method is similar in spirt but not detaila to [1], allowing large time-steps, with high accuracy and efficiency.

Most approaches to solving the time-dependent Schrödinger (TDSE) involving time dependent interactions invoke the short-time approximation. In essence, one propagates the TDSE over a sufficiently short time interval that one can ignore the time dependence of the interaction. It is possible to improve these approaches, for example, as is done in the Magnus expansion, but they often require the evaluation of commutators which are not always easy to compute. A new and simple approach to overcome both of the aforementioned problems, is based on rewriting the TDSE as;

$$|\Psi(t)\rangle = \exp(-iH_0(t-t_0))\,|\Psi(t_0)\rangle \\ -i\exp(-iH_0t)\int_{t_0}^{t}\exp\big(iH_0t'\big)V(t')\,\big|\Psi(t')\big\rangle \qquad t_0 \le t \le t_f \tag{1}$$

where $H = H_0 + V(t)$ and the spatial variables have been surpressed for notational convemience. Since we have chosen H_0 to be time independent, the problem reduces to an exact propagation of the TDSE when $V(t) = 0$. If the time step is sufficiently small so that the integral may be ignored, the equation reduces to the calculation of the action of a matrix exponential on a known vector which may be evaluated a using a variety of well known methods. Using Lagrange interpolation of the integrand on a set of Gauss-Lobatto grid points, we compute a set of integration weights $w_{p,i}$ and perform the integration to get,

$$|\Psi(t_p)\rangle = \exp(-iH_0(t_p-t_0))\,|\Psi(t_0)\rangle \\ -i\exp(-iH_0t_p)\sum_q w_{p,q}\exp(iH_0t_q)V(t_q)\,|\Psi(t_q)\rangle \tag{2}$$

A direct solution of Eq (2) would be prohibitive in realistic problems because the size of the linear system is the product of the spatial basis times the number of time points. Fortunately, both the Jacobi and Gauss-Seidel iterative methods have been successfully employed in practice to solve Eq. (2) with the former converging more rapidly than the latter. The number of iterations needed for convergence was far less than the number of time points for the problems considered to date. The method has been applied to an exactly soluble two state problem found in the literature [2] using the so-called block-by-block technique. Those authors required 1200 points to produce a solution whose accuracy on average was six orders of magnitude less accurate than ours using 10 points. More realistic examples will be presented at the conference,

References

[1] Ndong, M., Tal-Ezer, H., Kosloff, R. and Koch, C. P. , J. Chem. Phys., **132** (6), 064105 (2010)

[2] Wang, W. and Wang, X., Wuhan University Journal of Natural Sciences, **16**(6) (2011)

*E-mail: bis@nist.gov

Studying the transition from the direct to sequential regime in the two-photon double ionization of Helium

A Prior[1]*, H Bachau[2], and L A A Nikolopoulos[1]

[1]School of Physical Sciences, Dublin City University, Collins Ave, Dublin 9, Ireland.
[2]Université de Bordeaux, Centre des Lasers Inteses et Applications, France.

Synopsis In this research we examine the dynamics of two-photon double ionization of the Helium atom and of particular interest is the transition from the direct to sequential double ionization mechanism by varying the photon energy from 45 eV to 70 eV for an attosecond laser pulse of intensity 10^{14}W/cm^2.

The two-photon double ionization (DI) of the Helium atom is investigated and of particular interest is the dynamics of electrons upon interaction with an intense and ultrashort laser pulse. The photoionization dynamics is studied numerically via the *ab initio* direct solution of time-dependent Schrödinger equation (TDSE). More specifically, the joint spectral and angular distributions the ejected electrons have been calculated following the interaction with a pulse at an intensity of 10^{14}W/cm^2 and of 1 as (1 as = 10^{-18} s) duration. We have focused on here in the study of excitation of two electrons into the continuum states and in the role of the correlation between electrons during the DI process. With the existence of more than one double ionization mechanism present, namely the direct and sequential double ionization mechanisms, we have examined these different mechanisms by varying the photon energy to reach the energies required. In this study, we focus on the transition from the direct to sequential regime as we vary the photon energy (45 eV - 70 eV) across the transition threshold energy of 54.4 eV. We have published a similar study for the case of two-electron spherical quantum dots [1]. We have confirmed our results using two different calculational methods, developed independently from the Dublin and Bordeaux groups. These methods are specially designed atom-laser interaction codes tested thoroughly over the years [2, 3], successfully implemented to two-electron outer-valence atoms and more recently extended to two-electron quantum dots [4, 5].

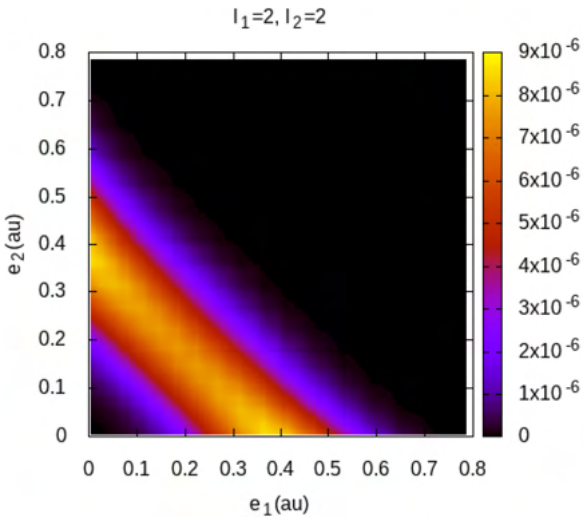


Figure 1. Two-electron joint-energy spectrum representing a weak double ionization channel ($\ell_1 = 2$, $\ell_2 = 2$) for a 45 eV pulse.

References

[1] A Prior, L A A Nikolopoulos, and H Bachau, Atoms **8**, 38 (2020).
[2] L A A Nikolopoulos, Comput. Phys. Comm. **150**, 2 (2003).
[3] H Bachau *et al.*, Rep. Prog. Phys. **64**, 1815 (2001).
[4] H Bachau and L A A Nikolopoulos, J. Phys. Chem. A **122**, 1574 (2018).
[5] L A A Nikolopoulos and H Bachau, Phys. Rev. A. **94**, 053409 (2016).

*E-mail: adam.prior6@mail.dcu.ie

MP

Few- to multi-channel correlation effect on attosecond photoemission time delay

M Magrakvelidze[1,2 *], M E Madjet[2,3] and H S Chakraborty[2 †]

[1]Science Department, Cabrini University, Radnor, Pennsylvania 19087, USA
[2]Department of Natural Sciences, D L Hubbard Center for Innovation, Loess Hills Research Center, Northwest Missouri State University, Maryville, Missouri 64468, USA
[3]Bremen Center of Computational Materials Science, University of Bremen, Bremen, Germany

Synopsis We present a landscape of our recent studies on the time delay of photoemission (PI) and photorecombination processes in the Ar atom, and the PI process in the C_{60} molecule. The computations are conducted in a framework of linear-response time-dependent density functional theory. Stark differences in magnitudes and mechanisms between few-electron correlations in the case of atoms and many-electron correlations in the case of fullerenes are showcased. Beautiful agreements with ultrafast measurements are the strength of the study.

A corridor to rich explorations of electron correlations is the ultrafast access to photoabsorption dynamics. Abilities to produce attosecond (as) laser pulses have instigated pump-probe measurements of ultrafast photoprocesses. These experiments are broadly classified into the streaking and RABITT chronoscopy. In this, the initial time delay induced by the XUV pump pulse derives solely from the correlation.

One simple, fundamental route to this intrinsic delay in photoemission is the Eisenbud-Wigner-Smith (EWS) approach. The fact that the probe pulse modify the correlated and uncorrelated emission signals roughly equally, the difference between the corresponding EWS delays captures pure correlation effects.

We applied a framework of linear-response time-dependent density functional theory (TDDFT) to compute EWS time delays. The result for Ar 3*s* and 3*p* relative emission agreed well with two, out of three, measured RABITT data near the 3*s*-3*p* interchannel-correlation imposed 3*s* Cooper minimum (CM) [1]. Further, a similar notion of 3*s*-3*p* interchannel coupling is applied to explain the delay of Ar 3*p* photorecobination process near the 3*p* CM. Recombination results have shown good agreement with RABITT measurements [2].

In atomic cases, binary-channel interactions cover dominant correlations. Near the giant plasmon (GP) resonance energies of C_{60}, the correlation is multi-channel with a large scale coherence. Thus, results at C_{60} GP show a far larger delay trend over a very broad energy range (Figure 1). The occurance of a XUV-energy windowed attractive field (shown) provides a pathology of the underlying mechanism. An excellent agreement with streaking data is obtained [3].

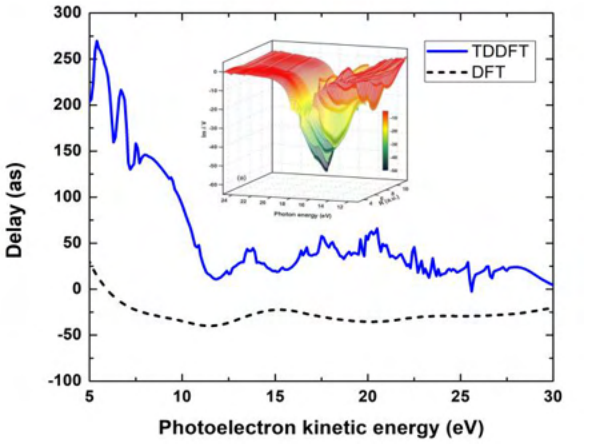


Figure 1. DFT (uncorrelated) and TDDFT (correlated) delays of photoelectrons from C_{60} in electron kinetic energy near the giant plasmon resonance. Inset: The imaginary part of the plasmon driven induced density.

Research is supported by the US NSF grant PHY-1806206 and PHY-2135107.

References

[1] Dixit G *et al* 2013 *Phys. Rev. Lett.* **111** 203003
[2] Magrakvelidze M *et al* 2015 *Phys. Rev. A* **91** 063415
[3] Biswas S *et al* 2022 arXiv:2111.14464 [physics.atom-ph]

* E-mail: mm12133@cabrini.edu
† E-mail: himadri@nwmissouri.edu

Theoretical studies of strong-field effects in atomic ionisation with ultrashort radiation

A Forembski[1]* **and L A A Nikolopoulos**[1]†

[1]Dublin City University, School of Physical Sciences, Collins Ave, Dublin 9, Ireland

Synopsis We aim to present theoretical studies of few-photon atomic ionisation with strong broadband sub-femtosecond pulses as well as an efficient computational approach to the problem. At present our studies involve helium but the general conclusions should be of more generality.

During the last decade the building and installation of large-scale laser facilities worldwide (ELIs/FELs) have allowed experimental groups to perform non-linear atomic ionisation schemes, triggered by intense ultrashort radiation in the (sub)femtosecond time-scale [1]. These radiation sources are operating in the UV or soft x-ray wavelength regime and as such ionisation with a single- or few-photon(s) is energetically possible. While both experimentally and theoretically, strong-field ionisation with long-wavelength, narrow-band, Ti:Sapphire has been studied extensively and many phenomena are well understood, this is not the case with ultrashort pulses with an extended frequency spectrum.

The present work focuses on the study of few-photon ionisation of noble gases with high intensity short pulses of extended bandwidth. We utilise an ab-initio calculational code [2] to examine the role of different phenomena in photoionisation under pulse durations and photon energies that have recently become experimentally achievable. An example of our work can be found in [3], where we study AC-Stark shifts in the photoelectron energy spectrum of Helium under two-photon absorption from a few hundred atto-second high intensity XUV laser pulse. An example of AC-Stark shifts in Helium is shown in Fig. (1).

Using the same theoretical framework we also examine the differences in the response of the 2s2p He autoionising state when driven with radiation from an isolated pulse versus a train of attosecond light pulses; for example how the exciting population, transient absorption spectra and time-delayed decay are affected in these two types of attosecond-scale radiation.

As a compliment to the above studies, we have been working on developing a computational framework, which, based on the modern paradigms of parallel and heterogeneous computing will provide greater performance in future simulations. We hope that some preliminary results and perspectives for this newly developed software will be available for presentation.

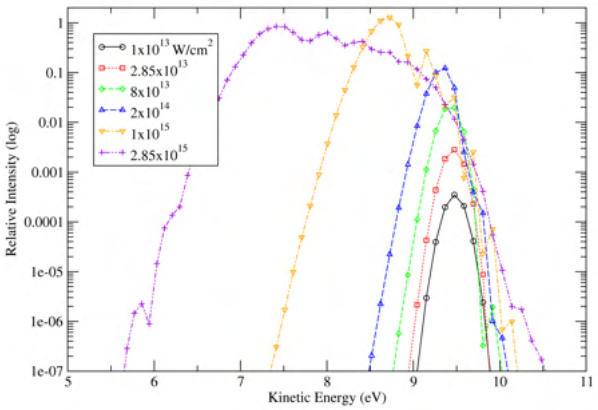


Figure 1. First ATI peak of He irradiated by the 11th harmonic of an 800 nm IR laser with a $\sim$ 15fs envelope and $\sim$ 500as pulse duration. The peak shifts towards lower kinetic energy with greater pulse intensity.

References

[1] P Tzallas *et. al.*, Nature Physics **7**, 781–784 (2011)
[2] L A A Nikolopoulos, Comp. Phys. Comm. **150**, 2 (2003)
[3] I Makos *et. al.*, High Power Laser Sci. Eng. **8**, 2020.

*E-mail: andrew.forembski2@mail.dcu.ie
†E-mail: lampros.nikolopoulos@dcu.ie

MP

Quantum Beat Spectroscopy of Bound Electrons in Helium

S Mikaelsson[†1], D Hoff[1], C Guo[1], A-K Raab[1], C L Arnold[1], A L'Huillier[1], and M Gisselbrecht[*1]

[1]Department of Physics, Lund University, P.O. Box 118, SE-221000 Lund, Sweden

Synopsis Quantum Beat Spectroscopy is a universal method for studying excited states in matter. We apply it in helium using a short attosecond pulse train to simultaneously ionize and excite high lying states and then ionize the bound electron wave-packets with a broadband infrared probe. The resulting interference pattern in the low kinetic energy region of the photoelectron spectrum is measured as a function of emission angle and delay between the extreme ultraviolet pulses and the infrared field.

The advent of broadband extreme ultraviolet sources makes it possible to investigate electron wave-packets of high lying bound states in atoms [1,2]. The dynamics of these states can be mapped out in the ionization continuum with an infrared field, which may also uncover new, light induced, dressed states [3]. Here, we carry out a complete characterization of these electron wave-packets using a small number of attosecond pulses.

We use a short attosecond pulse train generated by a 200 kHz CEP-stable OPCPA at 800 nm [4]. The high harmonic spectrum with energies from 20 eV to 50 eV simultaneously generates a superposition of high lying bound and continuum states in helium. The near IR probe pulse then ionizes the bound part of the electron wave packet after a variable delay. The photoelectrons are recorded with a coincidence 3D momentum spectrometer [5]. The resulting delay dependent photoelectron spectrum exhibits rich oscillations originating from interferences between one and two photon ionization, as well as quantum beating between the different exited states. These interferences contain information about the electron wave-packets and the resonant ionization dynamics.

Figure 1a) shows the photoelectron signal in the low kinetic energy region along the polarization axis of the electrical field as a function of delay. Figure 1b shows the corresponding Fourier analysis. The two 45° lines are characteristic of 'direct-indirect' interference, originating from the 3p and 4p states [1,6]. Several quantum beats between photoelectrons originating from different p-states can be observed, indicating a coherent superposition of several high-lying states. Additionally, the angle and energy resolved spectra allows us to determine the phase of the electron wave-packets for the different ionization pathways. Hence, we can disentangle pathways leading to final states with the same or mixed parity.

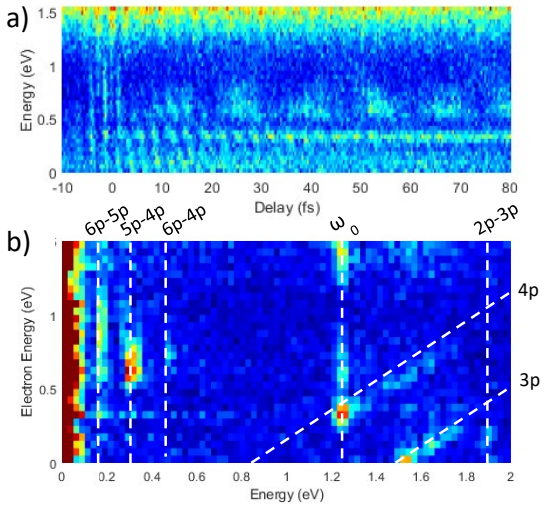


Figure 1: a) Pump-probe trace in the low kinetic energy region. b) Fourier analysis of a) with features assigned to the originating states of the helium atom.

In conclusion, we perform attosecond quantum beat interferometry with a short attosecond pulse train and a broadband near IR probe with full angular resolution. By extracting the phase of the features originating from high lying bound states, we can study their preparation, their time evolution, and their ionization dynamics near threshold.

References

[1] Mauritsson M *et al* 2010 *PRL* **105** 053001
[2] Lucchini M *et al* 2015 *PRA* **91** 063406
[3] Swodoba M *et al* 2010 *PRL* **104** 1033003
[4] Harth A *et al* 2018 *J. Opt.* **20** 014007
[5] Gisselbrecht M *et al* 2005 *RSI* **76** 013105
[6] Klünder K *et al* 2013 *PRA* **88** 033404

[†] E-mail: sara.mikaelsson@fysik.lth.se
[*] E-mail: mathieu.gisselbrecht@sljus.lu.se

Coincidence studies of angle resolved XUV-IR RABBITT and photoionization time delays based on a general analysis framework

J Joseph[1], F Holzmeier[1], D Bresteau[2], C Spezzani[3], T Ruchon[2*], J F Hergott[2], O Tcherbakoff[2], P D'Oliveira[2], J C Houver[1], and D Dowek[1†]

[1]Université Paris-Saclay, CNRS, Institut des Sciences Moléculaires d'Orsay, 91405, France
[2]Université Paris-Saclay, CEA, CNRS, LIDYL, Gif Sur Yvette, 91191, France
[3]Elettra-Sincrotrone, Trieste, Basovizza, 34149, Italy

Synopsis We investigate photoionization dynamics of atoms and molecules at the attosecond time scale to access angle resolved time delays in atomic and molecular photoionization within the XUV-IR RABBITT scheme, using electron-ion coincidence momentum spectroscopy at the ATTOLab laser facility, Université Paris-Saclay. For photoionization of atoms, a unifying description of the photoelectron angular distribution in terms of Legendre polynomial functions of the polar emission angle and the cosine dependence of the XUV-IR delay is proposed. It is illustrated by new results for n*p* ionization of Ar and Ne.

Recent investigations on time-resolved photoionization dynamics of atoms and molecules take advantage of the XUV-IR two-photon RABBITT scheme [1,2]. Here, an XUV attosecond pulse train (APT) consisting of a comb of odd-order harmonics of an 800 nm IR laser ionizes the target and a probe IR field induces continuum-continuum transitions producing sidebands (SBs) in the photoelectron spectra. Relying on an expansion in Legendre polynomials, the photoelectron angular distribution (PAD) of the oscillating SB signal $I_{SB}(\theta,\tau)$ is written as a function of the electron emission angle (θ) and delay (τ) between the XUV and IR fields as follows [3]:

$$I_{SB}(\theta,\tau) = h_0(\tau) + h_2(\tau)P_2(cos\theta) + h_4(\tau)P_4(cos\theta)$$

In this unified formalism, each of the $h_i(\tau)$ functions is developed in the form $h_i(\tau) = a_i + b_i \cos(2\omega\tau + \phi_i)$, ($i$ = 0, 2, 4). This complete description of the $I_{SB}(\theta,\tau)$ signal enables determination of the nine relevant parameters characterizing the static (a_i) and dynamic (b_i,ϕ_i) components of the PADs, which are expressed in terms of the partial wave dipole matrix elements involved in the two-photon transition at play in the RABBITT scheme [3].

In our study, we present new results on n*p* ionization of Ar and Ne in the (0-18 eV) electron energy range, performed using electron-ion coincidence momentum spectroscopy at the 10 kHz FAB-10 beamline of the ATTOLab laser facility, Université Paris-Saclay [3]. Similarities and differences between the two photon ionization dynamics of Ar and Ne are emphasized. In particular, we observe an enhancement of the PAD asymmetries in the presence of the IR probe field, which are more prominent for the Ne target. We also report on the angular dependence of the atomic delays and delay dependence of the PAD anisotropy across the studied SBs. Based on the proposed formalism, an extensive comparison of these results with the existing theoretical and experimental studies on RABBITT scheme is achieved [3].

Relying on a similar methodology, we performed preliminary XUV-IR studies on inner valence ionization of NO and O_2 aiming at the extraction of angle resolved emission delays in molecular frame. It will be interesting to compare these results with recently reported results for NO [4], as well as with the recent one-photon ionization time delays obtained from spectrally resolved measurements at Synchrotron SOLEIL [5].

References

[1] Paul P M *et al* 2001 *Science* **292** 1689
[2] Klünder K *et al* 2011 *Phys. Rev. Lett.* **106** 143002
[3] Joseph J *et al* 2020 *J. Phys. B: At. Mol. Opt. Phys.* **53** 184007
[4] Gong X *et al Phys. Rev. X* **12** 011002
[5] Holzmeier F *et al* 2021 *Nat Commun* **12** 7343

* E-mail: thierry.ruchon@cea.fr
† E-mail: danielle.dowek@universite-paris-saclay.fr

MP

Investigating photoionization by temporal Young-slit experiments

D. Hoff[1†], S Mikaelsson[1†], C Guo[1], A.-K. Raab[1], J Vogelsang[1,2], C L Arnold[1], A L'Huillier[1] and M Gisselbrecht[1*]

[1]Department of Physics, Lund University, P. O. Box 118, SE-22100 Lund, Sweden
[2]Institut für Physik, Carl von Ossietzky Universität Oldenburg, 26129 Oldenburg, Germany

Synopsis Photoionization with a small number of attosecond pulses opens a new way to control the interference of electron wave-packets with a dressed field. Under these conditions, the interaction with the dressing field can result both in a classical momentum kick of the electron and in the absorption/emission of a discrete quantum of energy. To understand this behavior we employ state-of-the art 3D momentum spectroscopy and fully characterize the electron wave-packets in time, frequency and space.

Single-photon photoionization is one of the fundamental processes in nature, whose temporal aspects have attracted much attention the recent years [e.g. 1]. We recently demonstrated the ability to carry out photoionization studies in a regime where only a small number of attosecond pulses are produced, which can be interpreted as a Young-slit experiments in time [2]. Under these conditions, photoemission in the presence of a dressing laser field is no longer ruled by energy quantization and parity conservation. Instead, the emission is asymmetric with respect to the polarization axis and the kinetic energy spectrum can be manipulated. We present here our progress in controlling the photoionization dynamics with a few attosecond pulses.

The experiment was carried out using high order harmonic generated from a 200 kHz optical parametric chirped pulse amplification laser emitting CEP-stablized few-cycle pulses (≤6-fs) around 800 nm. The resulting attosecond pulse trains consist of 2-3 pulses with controllable phase difference [3]. When the ultrashort XUV light pulses impinge on atoms together with a weak IR dressing field (<10^{11} W/cm^2) , multiple coherent ultrabroadband electron wave packets are created. The IR field allows to modulate the individual phases of the electron wave-packets, and to control how they interfere in the frequency domain. The photoelectrons are analysed with a 3D momentum electron-ion spectrometer [4].

We study this unexplored regime of light matter interaction by measuring photoionization in different rare gases. As shown in Figure 1, the spectrograms representing the photoelectron signal as function of the kinetic energy and the delay between the attosecond pulses and the dressing field for electrons emitted along the polarization axis exhibit a non trivial behaviour. Depending on the number of pulses in the train, one can identify continuous energy shifts ("streaking-like"), or the formation of discrete energy peaks ("sideband-like")

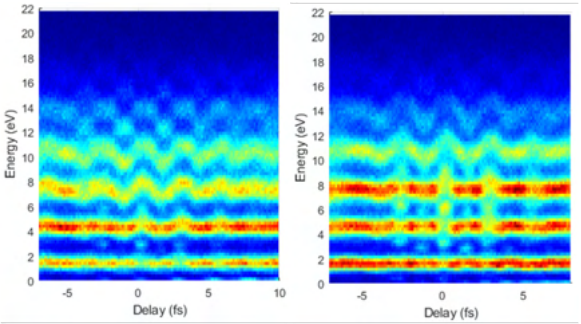


Figure 1. Spectrograms recorded in helium with two attosecond pulses (left) and three attosecond pulses (right)

To analyse these spectrograms, we implement iterative methods in the form of a generalized projections algorithm based on the strong field approximation [5], including their angular denpendance. This allows us to achieve an accurate characterization of the amplitude and the phase of electron wave-packets.

References

[1] Pazourek R *et al* 2015 *Rev. Mod. Phys*. **87** 765
[2] Cheng Y-C, Mikaelsson S *et al* 2020 *Proc. Nat. Am. Sci.* **117**, 10727
[3] Guo C *et al* 2018 *J. Phys. B.* **51** 034006
[4] Mikaelsson S *et al* 2021 *Nanophotonics* **10**, 117
[5] P.D. Keathley *et al* 2016 *New J. Phys.* **18**, 073009.

† E-mail: dominik.hoff@sljus.lu.se
* E-mail: mathieu.gisselbrecht@sljus.lu.se

Unraveling the transition between photoionization regimes via quantum trajectories

Taylor Moon[1], Klaus Bartschat[2], and N. Douguet[1]*

[1]Department of Physics, Kennesaw State University, Marietta, Georgia 30060, USA
[2]Department of Physics and Astronomy, Drake University, Des Moines, Iowa 50311, USA

Synopsis We use quantum trajectories to investigate the complex photoionization dynamics of atoms in intense and ultra-short laser pulses. The time-dependent energy of the trajectories makes it possible to characterize the nature of the emission process. In particular, a new adiabatic parameter, which is sensitive to the details of the photoionization process, is introduced to quantify and map in space the competition between multi-photon and tunneling ionization. We analyze the variation of this parameter for different atoms, light intensity, light frequency, and we compare with the Keldysh parameter.

The photoionization dynamics of atoms and molecules subjected to intense laser fields depends strongly on the pulse characteristics and target structure. The ionization mechanism is commonly classified in two different, but possibly co-existing, ionization regimes [1]. In the multi-photon regime (*vertical* ionization channel), the fast oscillations of the barrier heats up the electron that gains energy until it is eventually free to escape. In the tunneling regime (*horizontal* ionization channel) the wavefunction adapts to the slowly-varying (quasi-static) barrier, and the electron traverses the classically forbidden region without significant change in energy.

The Keldysh adiabatic parameter γ compares the time scale for tunneling and the pulse period. While it provides an indication on the conditions of the ionization process, it is based on general assumptions and only provides an averaged and limited information Moreover, it is insensitive to the details of the target structure, pulse shape, and the onset of over-the-barrier ionization. Finally, defining a borderline between ionization regimes at $\gamma \sim 1$ remains questionable.

In this work, we compute quantum trajectories [2] in simple atoms ionized by few-cycle laser pulses. The time-dependent energy of the trajectories, starting from different initial positions of the atoms, reveals the exit time and exit position from the barrier, consistently with the ionization dynamics. By comparing the exit position to the adiabatic exit point for a static barrier, we deduce the level of tunneling ionization $0 \leq \beta \leq 1$ of the ionization process. The spatial dependence of β is presented in the onset of Fig. 1 for a high-intensity one-cycle optical pulse. We introduce a Bohmian adiabatic parameter $0 \leq \gamma_B < \infty$, averaged over the trajectories, which compares the rate of *horizontal* and *vertical* ionization. This numerical parameter provides a robust quantitative description of the onset of the tunneling regime and contains rich information, e.g., role of excited states, range of binding potential, and initial electronic angular momentum. Fig. 1 shows that the tunneling regime for an 800-nm pulse is reached at lower intensity than predicted by the Keldysh parameter.

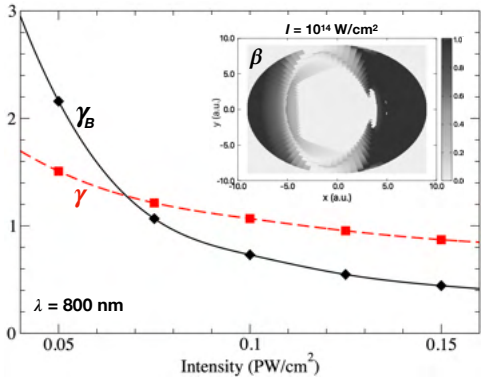


Figure 1. Keldysh (dashed red) and Bohmian (solid black) adiabatic parameters for a 800-nm one-cycle pulse in the photoionization of atomic hydrogen. The inset shows β at $I = 10^{14}\mathrm{W/cm}^2$.

References

[1] M Ivanov, M Spanner, and O. Smirnova, J. Mod. Opt. **52**, 165 (2005).
[2] N Douguet and K. Bartschat, Phys. Rev. A **97**, 013402 (2018).

*E-mail: ndouguet@kennesaw.edu

MP

Simplified spectrogram reconstruction for the complete characterization of attosecond radiation

N Di Palo[1,2]*, B Moio[1,2], G Inzani[1], G L Dolso[1], F Medeghini[1,2], R Borrego-Varillas[2], M Nisoli[1,2], M Lucchini[1,2]

[1] Department of Physics, Politecnico di Milano, 20133 Milano, Italy
[2] Institute for Photonics and Nanotechnologies, IFN-CNR, 20133 Milano, Italy

Synopsis We present a novel method, named Simplified Trace Reconstruction in the Perturbative Regime (STRIPE), for the complete temporal characterization of ultrashort light pulses based on two-color photoionization of a noble gas target. By applying STRIPE to both simulated and experimental data, we demonstrate its superior performances against other established reconstruction algorithms.

Following ultrafast phenomena in nature like charge carrier excitation in solids or ultrafast nuclear motion in molecules requires the use of extremely short light sources, whose temporal characterization is of paramount importance.

An established method for the characterization of attosecond to few-femtosecond (fs) pulses employs a two-color photoemission scheme, where an extreme-ultraviolet (XUV) pulse excites electrons from a gas target while a few-cycle, infrared (IR) electric field dresses the photoelectron distribution [1]. Phase-retrieval algorithms can be used to extract both electric fields from the photoelectron trace, like the extended ptychographic iterative engine (ePIE) [2]. However, these methods are time consuming, they are limited by experimental non-idealities (i.e., noise, background, instrumental response), and often their use lacks generality. With STRIPE we propose a novel method, based on a simplified version of the strong field approximation formula describing the two-color photoemission process [3], which aims at providing a more reliable and faster solution for ultrashort pulse characterization.

To test its performances, we used STRIPE for the reconstruction of simulated data with several XUV pulse configurations (e.g., isolated attosecond pulse, attosecond pulse train (APT), few-fs single-harmonic pulse). The results nicely compare to the ones obtained with other algorithms, proving the reliability of STRIPE.

Then, we tested STRIPE capabilities with experimental data (see Fig.1 for the case of a trace produced by an APT). By applying STRIPE to the differential spectrogram (difference between photoelectron spectra with and without the IR pulse), we obtain a perfect reconstruction of the trace despite an appreciable noise. At the same time, by imposing the measured spectrum as a constraint, STRIPE returns a larger and more reliable estimation of the satellite pulses compared to ePIE, limited in this case by the distortion of the photoelectron spectrum due to the instrumental response function.

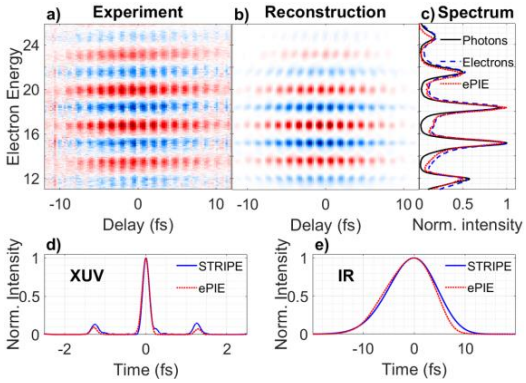


Figure 1. The differential spectrogram is shown in **a)**, while **b)** presents the STRIPE reconstruction. Panel **c)** shows the XUV spectrum (shifted by the ionization potential, black), the photoelectron spectrum (blue-dashed), and the ePIE reconstruction (red-dotted). **d)**, **e)** Reconstructed temporal profiles for both XUV and IR pulses.

In conclusion, we propose a novel, faster, and more reliable solution for the characterization of ultrashort XUV and IR pulses, showing its superior performances with respect to other established methods when applied to both simulated and experimental data. Our results pave the way for a more precise and faster calibration of ultrafast spectroscopy experiments.

References

[1] Orfanos I *et al* 2019 *APL Photonics* **4** 080901
[2] Lucchini M *et al* 2015 *Optics Express* **23** 23
[3] Moio B *et al* 2021 *J. Phys. B* **54** 154003

* E-mail: nicola.dipalo@polimi.it

Attosecond circular-dichroism chronoscopy of photoelectron vortices

M Han[1]*, J Ji[1] and H Wörner[1]

[1]Laboratorium für Physikalische Chemie, ETH Zürich, Zürich, 8093, Switzerland

Synopsis We introduce a novel plug-in apparatus for generating circularly polarized attosecond pulses, fully characterize these pulses and develop attosecond circular-dichroism chronoscopy. We apply this new metrology to characterize amplitude and phase dichroisms in the creation and manipulation of photoelectron vortices.

In a recent advance[1], we established attosecond metrology in circular polarization and demonstrated a plug-in apparatus to simplify the generation of circularly polarized attosecond XUV pulses based on the non-collinear high-order harmonic generation (HHG) process[2, 3]. We characterized the circular attosecond pulses using the circular-RABBIT (circular-XUV + circular-IR) measurements. Here, we employ this novel metrology to study and manipulate the chiral dynamics of electron vortices on attosecond time scales. As illustrated in Figure 1, a circularly polarized attosecond pulse train is used to photoionize argon atoms, preparing electron vortices with well-defined helicity in the continuum state. We then probe the electron vortices with a synchronized co-rotating or counter-rotating near-infrared (IR) laser pulse through circular-RABBIT measurements. We observe that the sideband (SB) yield in the co-rotating geometry is remarkably enhanced compared with that in the counter-rotating case with a CD signal ranging up to 35%. More importantly, when switching the helicity of the IR probe, we demonstrate that the phase of the SB photoelectrons has dichroic structures and opposite bending directions along the light propagation direction, and the corresponding photoionization time delays can differ by several hundreds of attoseconds. Our findings are supported by solving the time-dependent Schrödinger equation (TDSE) in three dimensions. The insights gained from the calculation are then used to retrieve a complete set of partial-wave amplitudes and phases from the experimental data, resulting in a quantum-mechanically complete description of the photoionization and continuum dynamics.

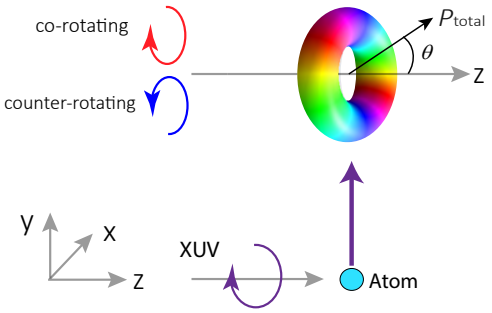


Figure 1. Average July Climate in Orlando, Florida, USA.

References

[1] Han Meng, Ji Jia-Bao, and Wörner Hans Jakob. Attosecond metrology in circular polarization, 2022. submitted.

[2] Daniel D. Hickstein, Franklin J. Dollar, Patrik Grychtol, Jennifer L. Ellis, Ronny Knut, Carlos Hernández-García, Dmitriy Zusin, Christian Gentry, Justin M. Shaw, Tingting Fan, Kevin M. Dorney, Andreas Becker, Agnieszka Jaroń-Becker, Henry C. Kapteyn, Margaret M. Murnane, and Charles G. Durfee. Non-collinear generation of angularly isolated circularly polarized high harmonics. *Nature Photonics*, 9:743–750, 11 2015.

[3] Pei-Chi Huang, Carlos Hernández-García, Jen-Ting Huang, Po-Yao Huang, Chih-Hsuan Lu, Laura Rego, Daniel D. Hickstein, Jennifer L. Ellis, Agnieszka Jaron-Becker, Andreas Becker, Shang-Da Yang, Charles G. Durfee, Luis Plaja, Henry C. Kapteyn, Margaret M. Murnane, A. H. Kung, and Ming-Chang Chen. Polarization control of isolated high-harmonic pulses. *Nature Photonics*, 12:349–354, 6 2018.

*E-mail: meng.han@phys.chem.ethz.ch

MP

Laser-induced ionization of heavy metal and metalloid ions in intense and sculpted femtosecond laser fields

B Ying[1,2], F Machalett[1,2], M Kübel[1], A M Sayler[3], T Stöhlker[1,2], P Wustelt[1], G G Paulus[1,2] *

[1]Institute of Optics and Quantum Electronics, Friedrich Schiller University Jena, 07743 Jena, Germany
[2]Helmholtz Institute Jena, Fröbelstieg 3, 07743 Jena, Germany
[3]Deptartment of Physics & Astronomy, Benedictine College, Atchison, KS 66002, USA

Synopsis First experiments on time-resolved multiple ionization of gold ions by 3D coincidence momentum spectroscopy are presented. We introduce a liquid-metal ion source as a new target source with unique properties. It features an extremely small emittance and can produce targets covering half the periodic table, plus an uncounted number of respective compounds. Considering the fact that up to 50% of all proteins of an organism contain metal atoms, a focus on their behavior under conditions relevant in attosecond science appears to be timely.

A large region of the periodic table, which so far has hardly been considered in strong-field laser physics, is represented by metals and metalloids. From a theoretical point of view, modeling such complex many-electron systems is a challenge, but gives access to light-driven dynamics in multi-electron systems. Specifically, the ionization of electrons from the f(fundamental)-shell is largely unexplored to date. Further, higher charge states of heavier targets may require the inclusion of relativistic effects in the theoretical description. Another central issue for understanding strong-field light-matter interactions are effects beyond the single-active-electron approximation or the dipole approximation. In addition, the behavior of molecules consisting of heavy elements or heavy and light elements is largely unexplored.

We report on the implementation of a liquid metal ion source into a 3D coincidence momentum spectroscopy setup in order to fill these gaps. In a first experiment, the interaction of ionic silicon and gold with intense laser pulses is studied. Laser intensities of up to $4 \times 10^{16}\,\mathrm{W/cm^2}$ allow for the observation of up to ten-fold ionization of Au^+ ions and double ionization of Si^{2+} ions. Further, by utilizing two-color sculpted laser fields to control the ionization process on the attosecond time scale, we demonstrate the capability to resolve the recoil ion momenta of heavy metal atoms. Simulations based on a semiclassical model assuming purely sequential ionization reproduce the experimental data well. This work opens up the use of a range of metallic and metalloid ions, which have hardly been investigated in strong-field laser physics so far.

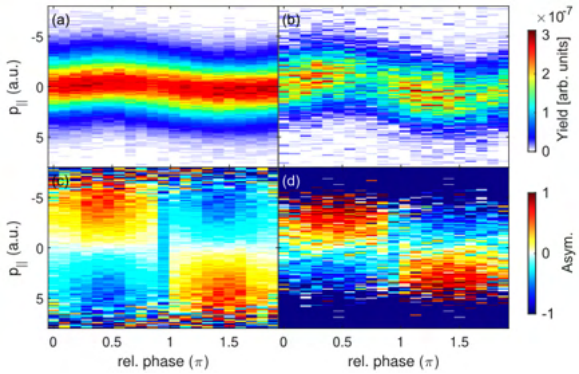


Figure 1. Measured momentum distribution in laser polarization direction for ionization of Au^+ ions with a laser peak intensity of $4 \times 10^{14}\,\mathrm{W/cm^2}$ and a pulse duration of 40 fs. (a) Relative phase-dependent momentum distribution $p_\parallel$ of Au^{2+} produced by single ionization (SI), (b) same as (a) for Au^{3+} produced by double ionization (DI), (c) and (d) the asymmetry maps for SI and DI.

References

[1] B Ying *et al.*, J. Phys. B: At. Mol. Opt. Phys. **54**, 174002 (2021).

*E-mail: gerhard.paulus@uni-jena.de

Exploring symmetries in ultrafast photoelectron holography with two-color linearly polarized fields

T. Rook anc C. Figueira de Morisson Faria*

University College London, Gower Street, London WC1E 6BT, UK

MP

Synopsis We investigate ultrafast photoelectron holography in bi-chromatic linearly polarized rω-sω fields of commensurate frequencies and relative phase ϕ, focusing on the existing symmetries and for which parameters they are kept or broken. Using group theory, saddle-point methods and the Coulomb quantum-orbit strong-field approximation, we discuss the symmetries of the ionization times and of the driving field for r+s even and odd, provide general expressions and analyze the consequences on the prominence and contrast of specific holographic patterns, such as the fan, the spider and the spiral.

Due to the high electron currents and ultrafast time scales involved, photoelectron holography has established itself as a powerful imaging tool [1]. However, there are several open questions about how different types of holographic interference behave in the presence of tailored fields and/or more complex targets, especially in the presence of residual binding potentials. In this work, we investigate photoelectron holography in bichromatic linearly polarized fields using group-theoretical methods, with emphasis on existing symmetries and for which parameters they are kept or broken [2].

We show that, for a rω-sω field, there are three relevant symmetries: the well-known half-cycle symmetry, which is broken for r+s odd, and reflections around the field crossings and maxima, which may or may not be kept depending on how both waves are dephased. The three symmetries are always present for monochromatic fields, while for bichromatic fields this is not guaranteed, even if r+s is even and the half-cycle symmetry is retained. Breaking the half-cycle symmetry automatically breaks one of the other two, while if it is retained, the other two symmetries are either both kept or broken. We analyze how this affects the ionization times and saddle-point equations. We provide a general expression for what relative phases ϕ the symmetries are retained, for an arbitrary (r,s) field, which can be generalized to n-color fields.

As an application, we compute photoelectron momentum distributions for bichromatic fields with the Coulomb Quantum Orbit Strong-Field Approximation (CQSFA) [3] and assess how holographic structures such as the fan, the spider and interference carpets behave, focusing on the reflection symmetries. We discuss how the Coulomb distorted orbit classification changes with the inclusion of the weak second driving wave, taking into consideration the field gradient, extrema and their relation with the broken symmetries. The features encountered can be traced back to the field gradient and amplitude affecting ionization probabilities and quantum interference in different momentum regions.

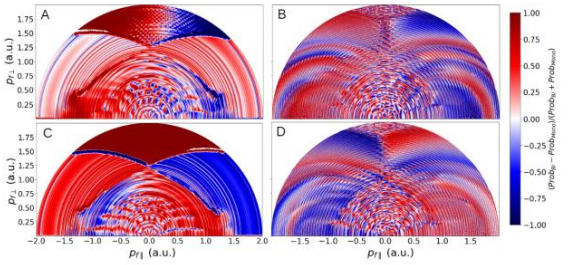


Figure 1. Normalised difference between the transition probability for a (1,2) bichromatic field and its monochromatic counterpart, computed for hydrogen. The monochromatic field has wavelength 800m and intensity 7.0 x 10^{14}W/cm^2. The upper and the bottom row were calculated for the relative phases ϕ = 0 and ϕ = π/4 respectively, and the left and the right columns correspond to the CQSFA and the time-dependent Schrodinger equation (TDSE), respectively.

We hope our study will pave the way for orbit-based investigations in tailored fields for which the residual binding potential and the driving laser field are included on equal footing.

References

[1] Figueira de Morisson Faria C and Maxwell A S 2020 *Rep. Prog. Phys*. **83** 034401
[2] Rook T and Faria C, in preparation
[3] Lai X *et al*, 2015 *Phys. Rev. A* **92** 043407

* E-mail: c.faria@ucl.ac.uk

MP

Electron choreography at the attosecond time scale

B Unzicker, J Vaughan, S Burrows, B Tatum, D Arthur, T Olsson , S Jain, T Hart, P Stringer and G M Laurent *

Department of Physics, Auburn University, 380 Duncan Drive, Auburn, AL 36849, USA

Synopsis In this work, we report on coherent control of electron dynamics in atoms via attosecond pulse-shaping. We show that the photoelectron emission from argon gas produced by absorption of an attosecond pulse train (APT) made of odd and even harmonics can be manipulated along the direction of polarization of the light by tuning the spectral components (amplitude and phase) of the pulse.

With the recent development of XUV light sources with attosecond duration, new capabilities emerge for controlling quantum dynamics in matter down to the natural timescale of electron motion. So far, attosecond control has been mostly achieved with pump/probe schemes where an attosecond-pump pulse triggers a given electronic process, and a phase-locked femtosecond-probe field is used to steer its dynamics [1]. The system under scrutiny is thus controlled by varying the time delay between the two pulses.

An alternative approach consists of shaping the spectral components of the attosecond pulse to control the dynamics. Within the widely accepted three-step model describing attosecond pulse generation via HHG, the spectral components are defined by the electron wavepacket trajectories (also referred to as quantum orbits) in the driving laser field. By tailoring the temporal waveform of the femtosecond driving field, the quantum orbits can then be tuned giving some control over the spectral components of the attosecond pulse train (APT). Two-color femtosecond waveforms, for example, have proved to be very efficient in manipulating quantum orbits in the HHG process. The literature is rich with experimental and theoretical studies reporting the dependence of both the spectrum and the polarization of the resulting APT on the temporal profile of such synthetized waveforms [2].

In this work, we show how the APT's spectral phases can be manipulated by varying the intensity ratio r and the relative phase ϕ between the two components of the driving field. As an application for such a spectral pulse shaping technique, we also report on a coherent control experiment where the photoelectron emission from atoms generated by tailored attosecond pulses in presence of relatively weak IR field is manipulated along the direction of polarization of the light by tuning the spectral phases of the APT [3]. Emission patterns where photolelectrons are emitted in the same direction or, conversely, are emitted in opposite directions depending on their energy can be obtained by tuning the spectral components of the pulse, as shown in Fig. 1.

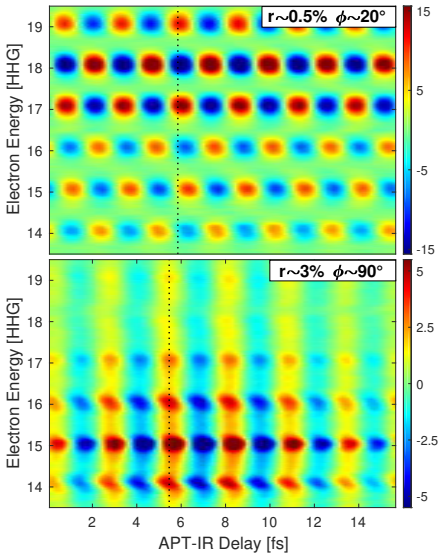


Figure 1. Density plots of the asymmetric components of the photoelectron emission as a function of the time delay between the APT and IR fields and the photoelectron energy.

References

[1] Mauritsson J *et al* 2008 *Physical Review Letters* **100** 073003
[2] Mauritsson J *et al* 2006 *Physical Review Letters* **97** 013001
[3] Unzicker B *et al* 2021 *New Journal of Physics* **23** 013019

*E-mail: glaurent@auburn.edu

Data-Based Quantitative Characterization of the Multi-Resolution Cookiebox Instrument at LCLS

A. Kamalov[1]*, L. Funke[2], R. Obaid[1], D. Bhogadi[1], K. Borne[3], N. Brown[1], J. Castagna[1], X. Cheng[1], T. Driver[14], A. Gatton[1], J. Hirschman[1], J. James[1], S. Nelson[1], H. Shi[1], A.C. Therrien[5], R. Trejo[1], W. Helmi[2], M. Ilchen[67], P. Walter[1] and R. Coffee[1]

[1] - LCLS, SLAC National Accelerator Laboratory, 2575 Sand Hill Road, Menlo Park, CA 94025, USA
[2] - Technische Universita ̈t Dortmund, Maria-Goeppert-Mayer-Strasse 2, 44227 Dortmund, Germany
[3] – J.R. Macdonald Laboratory, Department of Physics, Kansas State University, Manhattan, KS 66506, USA
[4] - The Stanford PULSE Institute, 2575 Sand Hill Road, Menlo Park, CA 94025, USA
[5] - Université de Sherbrooke, Sherbrooke, Quebec J1K 2R1, Canada
[6] - Institut fur Physik und CINSaT, Universitat Kassel, Heinrich-Plett-Strasse 40, D-34132 Kassel, Germany
[7] - European XFEL, Holzkoppel 4, 22869 Schenefeld, Germany

Synopsis We present the first measurements taken with the new 'cookiebox' concentric electron spectrometer array that is under development at the LCLS Time-resolved AMO (TMO) Instrument. Ar, Ne, and N_2O data are inspected to characterize the instrument's performance and demonstrate some of the electron spectroscopy capabilities under development for the user community.

The LCLS-II upgrade at SLAC will revolutionize the XFEL capabilities available for the ultrafast physics user community. Part of the facility upgrade is the development of end-stations that will enable users to take full advantage of LCLS-II's high repetition rate (1 MHz) and sub-femtosecond pulse duration [1] capabilities. One such end station is the Multi-Resolution COokiebox (MRCO) [2] : a 'cookiebox' type concentric array of eletron Time of Flight (eToF) detectors [3] that can simultaneously measure photoelectron angular distributions at multiple highly-resolved energy regions, all within a magnetic field-free environment. A MRCO prototype equiped with eight of the full 20 eToF detector units was commissioned in a series of experiments designed to benchmark the instrument's performance.

Photoionization of the neon K-edge is performed to characterize MRCO's angular resolution capability. Furthermore, second-step autoionization spectra of Rydberg excited neon demonstrate MRCO's high energy resolution, shown in Figure 1. $L_{2,3}MM$ Auger-Meitner spectra of argon are collected for multiple electrostatic lens settings, quantifying electron spectroscopy resolution and collection efficiency as functions of photon energy and retardation potential. Experimental data are compared to SIMION calculations to benchmark how well the real eToF instrument performs as an ideal ToF detector. Temporal signals from unique eToF detectors are studied to verify the absence of artificial RF-mediated correlations between independent eToF detectors. Finally, a preliminary attempt to reconstruct single-shot XFEL spectra from collected photoeletron spectra is presented.

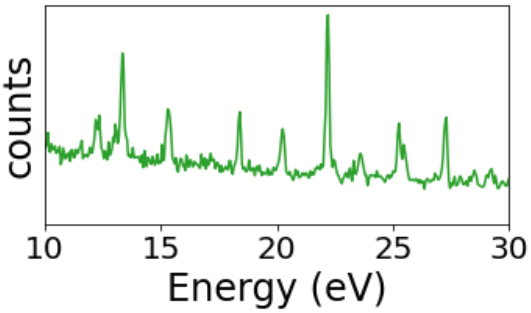


Figure 1: Second-step Auger-Meitner electron peaks from 1s→3p photoexcitation of Neon [4]. Peaks with FWHM of less than 0.25 eV are recorded.

References

[1] Duris J. *et al* 2020 *Nature Photonics* **14** 30-36
[2] Walter P. *et al* 2021 *J. Synch. Radiation* **28** 1364-1376
[3] Viefhaus J. *et al* 2013 *Nucl. Instrum. Methods Phys. Res. A* **710** 151-154
[4] Hentges R. *et al* 2004 *J. Phys. B: At. Mol. Opt. Phys.* **37** L267

* E-mail: akamalov@slac.stanford.edu

MP

A theoretical study on the dynamics of furan in tr-AttoXAFS

K M Ziems[1,5*], S Severino[2], M Reduzzi[2], A Summers[2], H-W Sun[2], Y-H Chien[2], J Biegert[2,3], S Gräfe[1,4,5]

[1]Friedrich-Schiller-Universität Jena, 07743 Jena, Germany
[2]Institut de Ciencies Fotoniques, The Barcelona Institute of Science and Technology, 08860 Castelldefels, Spain
[3]ICREA, 08010 Barcelona, Spain
[4]Fraunhofer Institute for Applied Optics and Precision Engineering, 07745 Jena, Germany
[5]Max Planck School of Photonics and Abbe Center of Photonics, 07743 Jena, Germany

Synopsis We employ a multi-physics approach comprised of on-the-fly surface hopping dynamics and quantum chemical methods to examine the ultrafast relaxation dynamics of furan induced by strong-field excitation and probed by attosecond carbon K-edge spectroscopy. The emergence and interplay of electronic and vibrational coherence during the dynamics is assessed and compared to experimental results. Furthermore, general trends and computational tools are derived.

Non-adiabatic relaxation pathways through conical intersections (CIs) have been subject to numerous theoretical and experimental investigations that demonstrated the relevance of such ultrafast phenomena for chemical and biological processes. The interplay of electron and nuclear wavepackets is not only at the heart of these relaxation processes but also poses a substantial experimental challenge. Time-resolved attosecond x-ray absorption fine structure (tr-AttoXAFS) spectroscopy is capable of meeting these requirements. Here, we report on the extensive theoretical study performed to unravel the ultrafast non-adiabatic relaxation process of furan and aid the analysis of the experimental investigation. Moreover, we describe general trends and theoretical procedures for tr-AttoXAFS.

We employ on-the-fly surface hopping including non-adiabatic and laser coupling [1] based on electronic structure calculations on the time-dependent density functional theory level. X-ray spectra were calculated for specific nuclear and electronic configurations using the core-valence-separation scheme in the frozen-core equation-of-motion model on the coupled cluster singles and doubles level of theory [2].

Upon strong-field excitation into the $\pi\pi^*$ (S_2) excited state, furan undergoes ultrafast dynamics through Ring-Opening (RO) or Ring-Puckering (RP) pathways [3]. In the first 20fs after excitation, we observe partial population transfer via CI to the S_1 state, resulting in a coherent electronic wavepacket as the evolution of the nuclear wavepacket proceeds on several almost parallelly lying excited electronic states. For RO, the $\pi\pi^*$ excited state decays through a second CI that transiently populates a dissociative dark $\pi\sigma^*$ state leading to CO bond breaking, and subsequently an energetic separation of electronic states and a dephasing of the electronic wavepacket. At later times, a CI leads to relaxation to the electronic ground state. Both, theory and experiment, identify the RO pathways as dominant. Simulated x-ray spectra are used to resolve the dynamics in the experiment. For the semi-classical dynamics, the influence of the strong-field laser pulse and its polarization are discussed together with the influence on the initial ground state geometry. Moreover, different approaches to analyze the structural dynamics and coherences are proposed that are applicable to other larger systems to be studied with tr-AttoXAFS.

In summary, we present the theoretical study for the tr-AttoXAFS experiment of furan, which provides a rich and detailed picture of the coupled electronic and nuclear dynamics of this prototype complex polyatomic system.

References

[1] Richter M 2011 *J. Chem. Theory Comput.* **7** 11493
[2] Tsuru S 2019 *J. Chem. Phys.* **151** 124114
[3] Stenrup M 2011 *Chemical Physics* **379**

* E-mail: karl-michael.ziems@uni-jena.de

Strong Field Ionization and Fragmentation Dynamics of Molecular Nitrogen Probed by Femtosecond Soft X-ray Absorption Spectroscopy

C Kleine[1], M-O Winghart[1], Z-Y Zhang[1], M Ekimova[1], S Eckert[1], M J J Vrakking[1], E T J Nibbering[1] and A Rouzée[1,*]

[1]Max Born Institute, Berlin, 12489, Germany

Synopsis The strong field ionization dynamics of molecular nitrogen induced by intense, 800 nm laser pulses is investigated with femtosecond soft x-ray absorption spectroscopy (XAS) at the N K-edge. Specific core-shell transitions are observed in the transient soft x-ray spectrum and used to retrieve, after the interaction with the strong laser field, population distribution of the electronic-ground and excited states of the N_2^+.

With its element-specificity and state-sensitivity, X-ray absorption spectroscopy has increasingly become a method of choice to investigate the local electronic structure of molecules, both in the gas phase and in solution. The growing development of Free Electron Lasers (FELs) [1] and high-order harmonic sources [2] over the last two decades providing ultrashort X-ray pulses with unprecedented flux and pulse duration reaching the attosecond timescale, has moreover enabled to directly monitor in real-time the local transient electronic structure of photoexcited molecules, as these are mapped onto X-ray absorption changes for specific atomic elements [3].

In our study, a broadband soft x-ray pulse obtained from high-order harmonic generation in helium and covering a photon energy range from 250 eV to 450 eV [4] is used to probe the electronic-state population distribution of N_2^+ ions formed by strong field ionization by an intense, 800 nm laser pulse. The transient population numbers for the N_2^+ in the X, A and B states are directly retrieved by monitoring the XAS changes around the N K-edge (see Fig. 1). Our measurements indicate a remarkably low population of the A state already at early pulse delay, whereas the X and B states have a population number of similar magnitude, in contrast to what is expected using standard models based on tunneling ionization rates. In addition, the transient XAS signal recorded on a time scale of tens of picoseconds show that the N_2^+ ions are converted into atomic N and N^+. This effect is attributed to significant collisional dynamics leading to dissociative excitation in the plasma resulting from the laser-molecule interaction.

Our measurements suggest that direct electronic population inversion between the ground and the second electronic state of N_2^+ ions can be achieved in strong field ionization experiments, which is particularly relevant to the recent observation of lasing components in filaments produced in air by intense laser pulses [7].

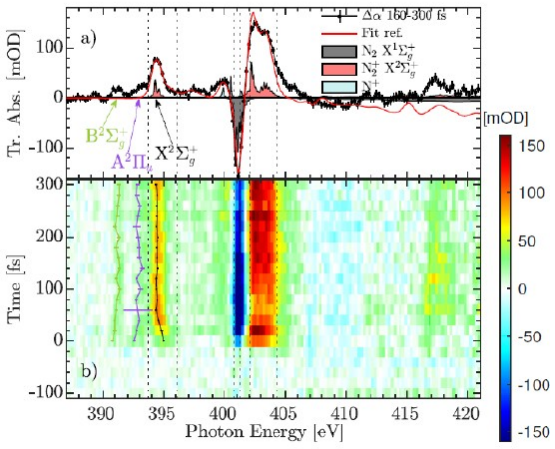


Figure 1. a) Transient XAS integrated between 160 fs and 300 fs (black curve), N_2 ($X^1\Sigma^+_g$) (grey area) and N_2^+ ($X^2\Sigma^+_g$) (red area), soft x-ray absorption spectra taken from [5] and [6] are shown as well. The two peaks at 391.2 eV and 392.9 eV are assigned to the lowest core resonances of N_2^+ in the B and A electronic states. b) Transient XAS of strong field ionized N_2 in the time-window between -100 fs and 300 fs.

References

[1] Emma P *et al* 2010 *Nat. Phot.* **4** 641
[2] Paul P M *et al* 2001 *Science* **292** 1689
[3] Attar A R *et al* 2017 *Science* **356** 54
[4] Kleine C *et al* 2019 *J. Phys. Chem. Lett.* **10** 52
[5] Chen C T *et al* 1989 *Phys. Rev. A* **40** 6737
[6] Lindblad R *et al* 2020 *Phys. Rev. Lett.* **124** 203001
[7] Yao J *et al* 2011 *Phys. Rev. A* **84** 021802

* E-mail: rouzee@mbi-berlin.de

MP

Strong-field control of vibrational wave-packet revivals in molecular hydrogen

G D Borisova[1*], P Barber Belda[1], S Hu[1], P Birk[1], V Stooß[1], M Hartmann[1], D Fan[1], A Saenz[2], C Ott[1] and T Pfeifer[1†]

[1]Max-Planck-Institut für Kernphysik, 69117 Heidelberg, Germany
[2]Institut für Physik, Humboldt-Universität zu Berlin, 12489 Berlin, Germany

Synopsis In an XUV (extreme ultraviolet) transient-absorption experiment with molecular hydrogen we excite transitions from the molecular ground state to electronically excited states in the spectral range 13-17 eV. Absorption lines corresponding to the C and D vibration bands change in line-shape and intensity under the influence of the dressing near-infrared (NIR) field, both with time-delay and for inceasing NIR intensity. For the D vibrational band we reconstruct the real-time strong-field-driven molecular dipole response and observe the revival of the vibrational wave packet to shift in time as a function of the NIR intensity.

Attosecond transient absorption spectroscopy has been widely used to access electron dynamics in atoms and, additionally, nuclear dynamics in molecules. Here, we use strong few-fs NIR pulses of tunable intensity, temporally set right after the attosecond-pulsed excitation, and study their influence on the electronic and nuclear degrees of freedom in the hydrogen molecule. Employing the technique of real-time reconstruction of the strong-field-driven dipole response [1] we extract time information about the molecule from the measured absorption spectra.

We used XUV light spanning between 13 and 17 eV to spectrally resolve the vibrational bands of the electronically excited C and D states in H_2, Fig. 1(a). Concentrating on the spectral region of the D band between 14 and 16.5 eV, we reconstruct the dipole response of the D-band vibrational wave packet, launched by the XUV pulse, Fig. 1(b). For zero NIR intensity we can directly observe the revival of the vibrational wave packet around 270 fs. Increasing the NIR intensity modifies the free evolution of the wave packet shifting its revival to earlier times. We thus identify the NIR intensity as a knob to coherently control the nuclear dynamics, which persist much longer than the timing and duration of the used laser pulses. We support our findings with a multi-level model simulation of the H_2 molecule, where we have full control over the included states and couplings between them.

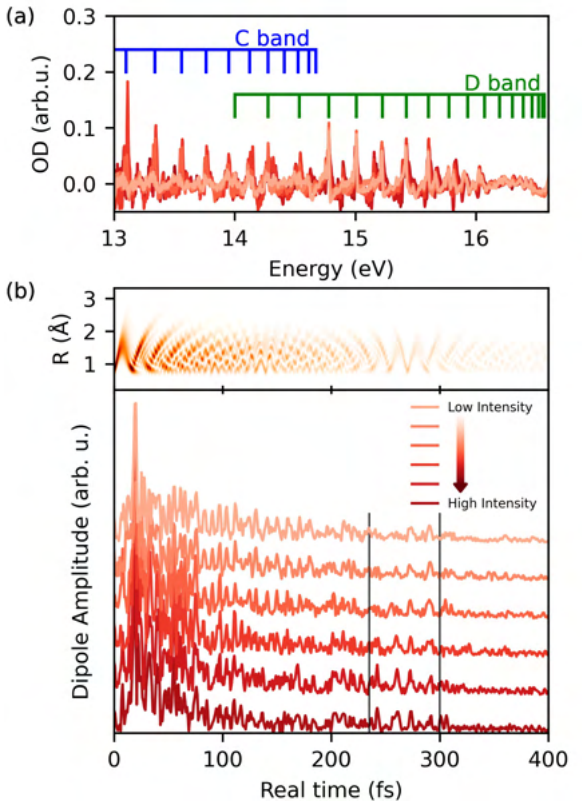


Figure 1. (a) Absorption spectrum of H_2 for different NIR intensities. **(b)** Reconstruction of the time-dependent dipole emitted by the excited vibrational wave packet of the D band. Revivals of the dipole take place in the time region between the vertical black lines. To illustrate the field-free revival, the upper part of (b) shows the calculated time evolution of the D vibrational wave packet for zero NIR intensity.

References

[1] Stooß V *et al* 2018 *PRL* **121** 173005

* E-mail: borisova@mpi-hd.mpg.de
† E-mail: thomas.pfeifer@mpi-hd.mpg.de

Multi-wave mixing in Neon to reveal dark-state quantum beats in attosecond transient emission

I Shalaby[1 *], S Yanez-Pagans[1], N Chakraborty[1], and A Sandhu[1 **]

[1]Department of Physics, University of Arizona, Tucson, Arizona, 85721, USA

Synopsis We report a new approach of multi-wave mixing between XUV and optical fields, which extends the conventional four-wave-mixing and attosecond transient absorption studies to a new regime. In a multi-color, multipulse transient absorption scheme, we use XUV, NIR, and MIR field to induce electronic couplings between multiple bound and continuum states in neon through four-wave and six-wave mixing pathways. Resulting transient emission spectrum shows a long-lived quantum beat due to the resonant excitation of a dark-state wavepacket, and we observe an interesting phase dependence between different pathways.

Tunable attosecond transient absorption [1,2] is used to study non-linear mixing processes in neon. Multi-color pulses provides new transition pathways and photon energy tunibility optimizes the resonant electronic couplings.

The XUV pulse in the form of 13th harmonic is acompanyed by the driver 800-nm NIR pulse to access the 3p dark states of neon. The variable wavelength (1300-1600 nm) MIR is used a as third delayed pulse and absorption/emission spectrum is collected and analyzed. Various emissions are observed corresponding to four-wave and six-wave mixing pathways (Fig. 1).

In a previous study [3], time-dependent variation wa sobserved in the four-wave emission spectrum of Neon due to pressure modulations of the harmonic intensity. In this work quantum beats are observed in six-wave emissions involving the spin-orbit split 3p dark states (Fig. 1).

Specifically, with the 1540 nm MIR probe, a long-lived emission with sustained beating is observed in the final 6s state. Beats are also observed for MIR probe wavelengths of 1400 and 1500 nm corresponding to different final states. Importantly, we observe a phase difference between the beats corresponding to the 6s [3/2] and 6s [1/2] final states.

This work extends the previous non-linear mixing studies to a new regime of multi-wave mixing with multi-color fields. The flexibility and tunability of this approach will allow probing a wide range of systems using the attosecond transient absorption and emission experimental schemes.

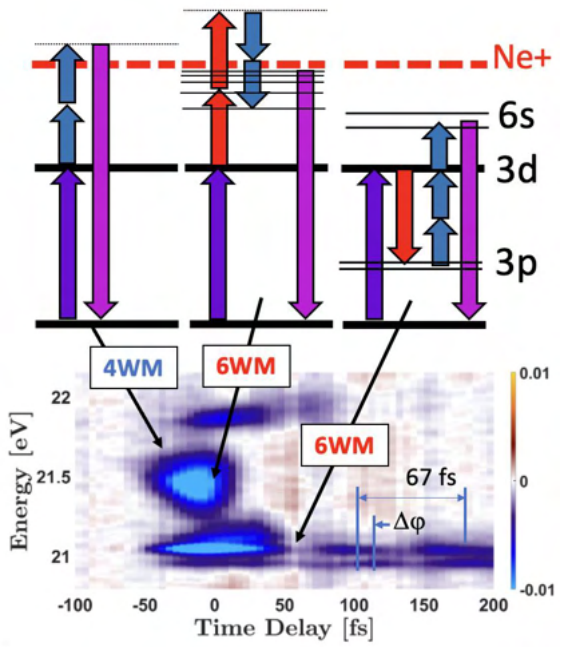


Figure 1. Emission |OD| of 6s spin-orbit split states around 21 eV. Negative delay when probe NIR arrives earlier. Quantum beats with 67 fs period (0.06 eV) are observed with an ~20 fs phase difference between beats in different 6s states.

This work was supported by the U.S. Department of Energy, Office of Science, Basic Energy Sciences, Award #DE-SC0018251.5.

References

[1] Nathan H *et al* 2018 *Opt. Lett.* **43** 3357-3360
[2] Nathan H *et al* 2021 *Phys. Rev. Lett.* **127** 023202
[3] Wei C *et al* 2016 *Phys. Rev. A* **94** 021802®

* E-mail: ishalaby@email.arizona.edu
** E-mail: asandhu@email.arizona.edu

MP

Soliton self-compression based HHG driver for water-window transient absorption experiments

G Fazio[1]*, T Kopp[1], T Balčiūnas[1], Z Yin[1], D Zimin[1], C Brahms[2], J C Travers[2] and H J Wörner[1]

[1]ETH Zürich, Vladimir-Prelog-Weg 2, 8093 Zürich (Switzerland)
[2]School of Engineering and Physical Sciences, Heriot-Watt University, Edinburgh (UK)

Synopsis We present the generation of a supercontinuum soft-X-ray spectrum generated by high-harmonic generation driven by self-compressed 1450 nm pulses using the soliton effect. The compression of 2.8 mJ, 30 fs pulses down to sub 10-fs (supporting 7.2 fs duration) is achieved in a hollow-core fiber and delivered to the HHG target under vacuum using no additional dispersive optics.

Table-top high-harmonic-generation (HHG) based soft X-ray (SXR) sources offer the best temporal resolution to study the most biologically relevant elements (C, N, S) in the energy window where water is transparent [1, 2, 3, 4]. Since the HHG spectrum cut off is proportional to $lambda^2$, optical parametric amplification is often used to extend it; however, due to the drop of the generation efficiency at longer wavelengths ($\eta \propto \lambda^{-6}$ [5]), there have been efforts in development of short-wave IR (1-1.4 μm) sources [6]: such possibility is given by the signal pulses obtained by a Ti:Sa laser-pumped OPA, but the further shortening of the pulses is hindered by to the lack of sufficiently broadband chirped mirrors.

In this contribution, we demonstrate few-cycle pulse generation in the spectral range centered at 1450 nm based on soliton self-compression in hollow-core fibers [7] and its coupling to a HHG beamline. Under optimal conditions, for a pulse propagating through a gas-filled hollow-core fiber (HCF), the negative dispersion and the positive nonlinearity compensate each other, yielding pulses characterized by a super-continuum spectrum and a duration of a few femtoseconds without any need for additional dispersive optics[7]. We employ the signal wave from a Ti:Sa laser-pumped OPA into a 4 m long HCF with a bore diameter of 530 μm, filled with gas at the input and pumped at the output, as shown in figure a. The emerging self-compressed pulses are delivered directly to a HHG beamline under vacuum, yielding the HHG spectrum shown in figure b. The setup is designed for time-resolved (TR) XAS experiments: the sample is excited by a pulse of 400-200nm, and it is then investigated by the SXR probe obtained by HHG. The current cut off at the C K-edge will be extended for TR-XAS experiments, that will be presented. Figure c and d shows the preliminary pulse characterization and spectral broadening results. We observed pulse shortening from 30 fs down to 9.8 fs by filling the fiber with $\approx$ 1 bar of neon. Note that the pulse characterization has been performed in air with pulses transmitted through an output port of a vacuum chamber thus preventing us from measuring even shorter pulse durations.

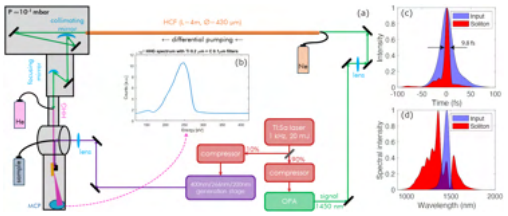


Figure 1. (a) Experimental setup. (b) HHG spectrum obtained. (c) Temporal and (d) spectral profiles compare the pulses with no broadening (evacuated fiber) and soliton-self-compressed pulses.

*E-mail: giuseppe.fazio@phys.chem.ethz.ch

References

[1] K S Zynchenko et al., Science **371**, 489 (2021).
[2] Y Pertot et al., Science **355**, 264 (2017).
[3] A R Attar et al., Science **356**, 54 (2017).
[4] A D Smith et al., J. Phys. Chem. Lett. **11**, 1981 (2020).
[5] A D Shiner et al., Phys. Rev. Lett. **103**, 073902 (2009).
[6] L Barreau et al., Sci. Rep. **10**, 5773 (2020).
[7] J C Travers et al., Nat. Photon. **13**, 547 (2019).

Compact, post-compressed high repetition rate ultrafast source for attoscience

A-K Raab[1], M Seidel[2], I Sytcevich[1], C Guo[1], A L'Huillier[1], C L Arnold[1] and A-L Viotti[1,2] *

[1]Department of Physics, Lund University, P.O. Box 118, SE-22100 Lund, Sweden
[2]Deutsches Elektronen-Synchrotron DESY, Notkestraße 85, D-22607 Hamburg, Germany

Synopsis We compress the output of a 200 kHz, 34 W, 300 fs Yb amplifier down to 31 fs with > 87 % power efficiency to reach 2.5 GW peak power in a single-stage bulk multi-pass cell built only from off-the-shelf equipment, showing long-term power and spectral stability. A detailed spatial-temporal characterization was performed and the preservation of CEP stability was shown. This multi-pass cell setup constitutes a promising driver for HHG and ultrafast applications.

For applications at the attosecond time scale, laser sources with high stability and good spatial-spectral properties are essential, together with a high-repetition rate and high peak-powers. To achieve such pulses, for example as a driver for high harmonic generation (HHG), complex set-ups like optical parametric chirped pulse amplifiers are often used [1]. An alternative, often more efficient approach is the direct post-compression of a laser amplifier output, by spectral broadening in a Kerr-medium and adequate dispersion management. While different broadening methods exist [2], we focus on multi-pass cells (MPCs) due to their outstanding power handling capabilities [3]. For instance, MPCs with multiple thin Kerr media were demonstrated at 80 MW input peak power [4].
Here, we spectrally broaden pulses with 330 MW peak power, i.e. more than 80 times the critical power of the nonlinear media. Neither vacuum, nor high pressure equipment is required. We implemented a bulk MPC with 15 roundtrips in a Kerr-medium consisting of two thin fused silica plates. The output of a 300 fs Ytterbium (Yb) rod-type amplifier at 200 kHz and 34 W average power is compressed down to 31 fs with a high efficiency of > 87 % in a single stage, as depicted in Fig. 1. A peak power of 2.5 GW is reached, constituting a record value for bulk MPCs and competing with capillary-based post-compression in this power range. This compact setup has a footprint of less than 0.3 m^2 and is built solely from off-the-shelf components, making it extremely cost- and space-efficient.

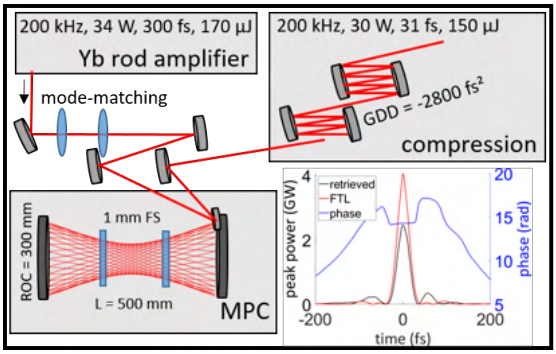


Figure 1. Experimental setup and compressed output pulses measured via an home-built frequency-resolved optical gating setup.

For the planned applications towards HHG, the compressed MPC output is thoroughly characterized with high fidelity, including a detailed investigation of the optimum input pulse parameters. For the output a detailed pulse duration characterization is performed. Long-term power and spectral stability, preserved spatial beam quality, spectral-temporal homogeneity as well as short-term carrier-envelope phase (CEP) stability are measured. In conclusion, we present a space- and cost-efficient ultrafast source with good output characteristics at peak-powers in the GW range suitable for HHG and time-resolved applications towards few femtosecond and attosecond time-scales.

References

[1] S. Mikaelsson et al., Nanoph. **10, 117** (2021).
[2] T. Nagy et al., Adv. in Phys. **X, 6:1, 184579** (2021).
[3] A.-L. Viotti et al., Optica **9** (2022).
[4] M. Seidel et al., Laser & Phot. Rev. **2100268** (2021).

*E-mail: anne-lise.viotti@fysik.lth.se

MP

Photoinduced Charge Migration Studies using a 1.7μm OPCPA Source

C Geiger[1,2]*, Q Le[2], Z Chang[1,2] and W T Hill III[3]

[1]CREOL, University of Central Florida, Orlando, Florida 32816, USA
[2]Department of Physics, University of Central Florida, Orlando, Florida 32816, USA
[3]Institute for Physical Science and Technology, University of Maryland, College Park, Maryland, USA

Synopsis We study the motion of electrons and nuclei with sub-femtosecond temporal resolution for atoms and molecules whose binding energy is 284-543eV. The tabletop 1.7-micron Optical Parametric Chirped Pulse Amplifier (OPCPA) source acts to generate X-ray attosecond pulses and is simultaneously used as an infrared pump in Attosecond Transient Absorption Spectroscopy (ATAS) experiments. It is planned to use this source in an ATAS setup to study photoinduced charge migration in propiolic acid molecules, which will provide valuable information about the coupling between electrons and nuclei.

Studying photoinduced charge separation in molecules is essential to understanding many chemical, physical, and biological processes such as photocatalysis, photovoltaics, and photosynthesis. This involves observing charge migration – an ultrafast electronic process occurring before electron-neutron coupling – which requires both the preparation of superposed electronic states and experimental tools with sub-femtosecond temporal resolution. Charge migration is responsible for the slower process of charge transfer, which is a permanent relocation of charge from a donor to an acceptor. Since the fundamental physics that drives charge migration dynamics is the same as that which drives population oscillation in two-level quantum systems, these studies can reveal important details of coherent states, such as timing, pathways, and correlation. By advancing our understanding of electron-neutron coupling and coherent processes, it may be possible to control molecules' chemical reactions by manipulating their electronic states.

In this work, a tabletop, broadband, Carrier-Envelope Phase (CEP)-stable, femtosecond pulsed 1.7-micron infrared source was developed to generate attosecond pulses through High Harmonic Generation (HHG) in a target gas. These X-ray attosecond pulses have sufficient photon energy to perform studies at the Carbon and Nitrogen K-edge, and have been used to observe vibrational, rotational, and electronic dynamics in atoms, molecules, and condensed matter systems on attosecond, femtosecond, and picosecond timescales in nitric oxide molecules [1]. Recently, a theoretical paper has shown that it is possible to observe charge migration in a propiolic acid molecule, HC_2CO_2H, through ATAS experiments in the water window (282-533eV) [2]. Their simulations have shown that strong absorption at the C K-edge at $\tau = 0$ indicate that the hole of the ionized molecule is initially located at the triple-bonded carbon atoms. When these absorptions drop to a minimum at $\tau = 2$ fs, absorptions at the O K-edge reach a maximum, indicating that the charge has migrated to the carboxyl group of the molecule. We plan to use propiolic acid as an organic test molecule for monitoring charge migration by ATAS at the C and O K-edge, which may validate the theoretical predictions.

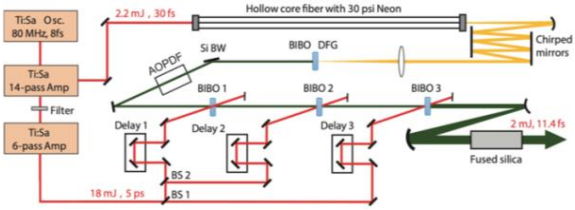


Figure 1. Schematic Setup of the 1.7-micron OPCPA. Adapted from [3].

This work was supported by the NSF grant N^0 PHY-1806575 and N^0 PHY-1806584.

References

[1] N Saito *et al*., Optica 6, 1542-1546 (2019).
[2] N Golubev and J Vaníček, Phys. Rev. Lett. 127 123001 (2021).
[3] Y Yin *et al*., Opt. Lett., vol. 41, pp 1142-1145 (2016).

* E-mail: geiger@knights.ucf.edu

Unraveling the excited states dynamics in non-fullerene acceptor Y6

N Alshehri*, S Karuthedath, CSP De Castro, J Gorenflot, and F Laquai

KAUST Solar Center, Physical Sciences and Engineering Division (PSE), King Abdullah University of Science and Technology (KAUST), Thuwal, 23955, Kingdom of Saudi Arabia

Synopsis In non-fullerene-based organic solar cells (OSCs), both donor and acceptor harvest photons, leading to a high charge generation yield that enhances the power conversion efficiencies. In particular, using the small molecule Y6 as an acceptor achieves a high power conversion efficiency above 17%. Herein, we use ultrafast transient spectroscopy to investigate the dynamics of Y6 excited states since it strongly absorbs in the near IR region. Upon excitation, an ultrafast formation of singlet and triplet charge-transfer states was observed.

Non-fullerene-based organic solar cells have driven tremendous attention due to their promising performance that exceeds their fullerene counterparts. In fullerene-based OSCs, the donor polymers mainly govern exciton dynamics whereas non-fullerene-based OSCs (NFA), both acceptor and donor harvest photons. Consequently, the NFA-based OSCs show high yield of charge generation that enhances the organic solar cells performance. Among other NFAs, a recently emerged small molecule Y6 (molecular structure shown in Figure 1) shows superior power conversion efficiency above 17% in single junction devices namely because it strongly absorbs in the near-IR region [1, 2].

This alone, however, does not explain its high performance hence, the importance of unveiling the dynamics of Y6's excited states. Here, we use ultrafast transient absorption (TA) to investigate the excited states dynamics of Y6 at timescale ranging from femtoseconds to a few nanoseconds along with other methods including photo, chemical-induced and electroabsorption spectroscopies. These complimentary methods were used to identify the excited states signatures.

So far, we observed an ultrafast formation of singlet charge-transfer (CT) state from optically generated excitons. At later time, the singlet CT decays to triplet CT state via intersystem crossing (Figure 1).

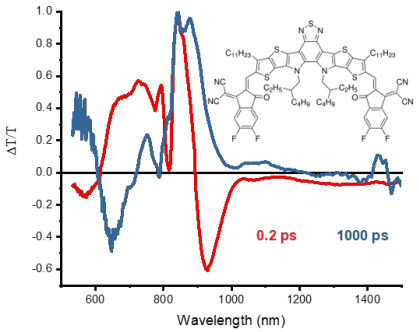


Figure 1. TA spectra of neat Y6 thin film excited at $\lambda = 600$ nm. The red line is assigned to singlet charge transfer (CT) whereas the blue line to triplet CT states.

References

[1] G Zhang, Nat Commun **11**, 2020 (2020).
[2] R Wang, J. Am. Chem. Soc. **142**, 2020 (2020).

*E-mail: nisreen.alshehri@kaust.edu.sa

MP

Relativistic time-dependent configuration-interaction singles

F Zapata[1]*, A Papoulia[1], R Tahouri[1], J Vinbladh[1,2], A Ljungdahl[2], E Lindroth[2] and J M Dahlström[1]†

[1]Department of Physics, Lund University, Lund, 22100 Sweden.

[2]Department of Physics, Alba Nova University Center, 10691 Stockholm, Sweden.

Synopsis A derivation of the relativistic time-dependent configuration-interaction singles (RTDCIS) method is presented. Diagrammatic many-body perturbation theory, based on the relativistic random phase approximation, is used as a benchmark with excellent agreement between RTDCIS reported at the Tamm-Dancoff level.

Attosecond chemistry aims to unravel the electron motion and coherence in atoms and molecules. A major contribution to this field was the real-time observation of the motion of valance-shell electrons in krypton ions made by Goulielmakis *et al.* in 2010 [1]. Since then, ATAS has been widely used in different scenarios [2]. Despite the great success of ATAS, all studies so far are based on non-relativistic ATAS theory [3], although the importance of spin-orbit coupling was demonstrated already by the first ATAS experiment [1]. Regarding the lack of a relativistic theory, our aim is to develop a general relativistic attosecond transient absorption spectroscopy method for studying atoms far beyond the perturbative regime [4]. In order to achive our goal, the N-electron time-dependent Dirac equation (TDDE) must be solved. As a compromise between computational cost and accuracy, the relativistic time-dependent configuration-interaction singles (RTDCIS) method is proposed as an efficient option to solve this complicated task [5]. In oder to validate RTDCIS, different observables has been computed for krypton and xenon, such as the photoionization cross sections. RTDCIS results have been compared with other relativistic calculations and experimental data, *see* Figure 1. As expected, RTDCIS results are similar to RRPA within the Tamm-Dancoff approximation (RRPA(TD)). This novel method opens the possibility to describe the electron spin dynamics by means of spin-resolved ATAS experiments far beyond the perturbative regime. Similarly, it can be applied to other strong-field processes, such as high-order harmonic generation, above-threshold ionization and laser-assisted photoionization.

*E-mail: felipe.zapata@matfys.lth.se
†E-mail: marcus.dahlstrom@matfys.lth.se

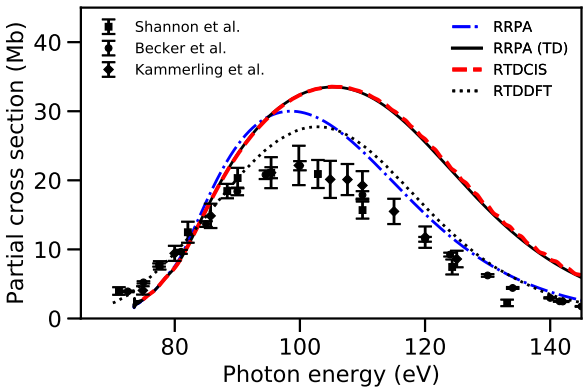


Figure 1. Xenon partial $4d$ photoionization cross section. Comparison of different relativistic calculations with experimental results. RTDCIS, RRPA and RRPA(TD) from Ref. [5]. RTDDFT from Ref. [6]. Experimental data form Ref. [7, 8, 9].

References

[1] E Gaulielmakis *et al.* Nature **466** 739 (2010)
[2] C Ott *et al.* Nature **516** 374 (2014); C Ott *et al.* Science **340** 716 (2013)
[3] M Wu *et al.* J. Phys. B: At. Mol. Opt. Phys. **49**, 062003 (2016)
[4] F Zapata, J Vinbladh, E Lindroth and J M Dahlström, Electron. Struct. **3** 014002 (2021)
[5] F Zapata, J Vinbladh, A Ljungdahl, E Lindroth and J M Dahlström, Phys. Rev. A **105** 012802 (2022)
[6] D Toffoli, M Stener and P Decleva, J. Phys. B: At. Mol. Opt. Phys. **35** 1275 (2002)
[7] S P Shannon *et al.* J. Phys. B : At. Mol. Opt. Phys. **10** 825 (1977)
[8] U Becker *et al.* Phys. Rev. A **39** 3902 (1989)
[9] B Kammerling *et al.* J. Phys. B: At. Mol. Opt. Phys. **22** 841 (1989)

Turning elliptically polarized light into a highly efficient chiro-optical tool

L Rego[1] *, O Smirnova[2,3] and D Ayuso[1,2]

[1]Department of Physics, Imperial College London, London, SW7 2BW, United Kingdom
[2]Max-Born-Institut, Berlin, Germany
[3]Technische Universität Berlin, Berlin, Germany

MP

Chiral recognition is both vital and hard. Circularly and elliptically polarized light, the standard chiro-optical tools, are poor chiral photonic reagents: the enantio-sensitive response of the molecules to such light is only a small fraction of the total optical response. Here we show that tight focusing can turn an ultrashort elliptically polarized pulse into a highly efficient chiro-optical tool that leads to enantio-sensitive *bending* of the nonlinear optical response, creating new opportunities for ultrafast and efficient imaging of molecular chirality and atto-second chiral dynamics.

Distinguishing between the two opposite versions (enantiomers) of a chiral molecule is vital in organic chemistry, materials science or biomedicine, but also challenging, as they behave identically unless they interact with another chiral object. Standard chiral light, i.e. circularly or elliptically polarized light, is a convenient chiro-optical tool [1], but it is highly inefficient: the enantio-sensitive response of the molecules arises beyond the electric-dipole approximation and is only a small fraction of the total optical response.

Here we show that the longitudinal components that naturally arise upon tight focusing [2] can turn elliptically polarized light into an extremely efficient chiro-optical tool. When an elliptically polarized laser is tightly focused, the laser polarization plane tilts towards the propagation direction, as depicted in Fig. 1a. This tilt is opposite at opposite sides of the beam axis and is locked to the propagation direction. In an ultrashort laser pulse, the combination of the tilted electric-field vector with the propagation direction creates a chiral structure that allows us to distinguish between opposite enantiomers via purely electric-dipole interactions.

Figs. 1b,c show that the proposed optical configuration leads to enantio-sensitive bending [3] of the nonlinear optical response of randomly oriented chiral molecules: opposite molecular enantiomers emit harmonic light in opposite directions, and thus the enantio-sensitive direction of bending records the molecular handedness with high efficiency. Interestingly, this strongly enantio-sensitive effect is driven by purely electric-dipole interactions, even though the optical field is not *locally* chiral, making this optical driving field fundamentally different from our previous proposals [3,4] and, to our knowledge, from any other optical setup for chiral recognition.

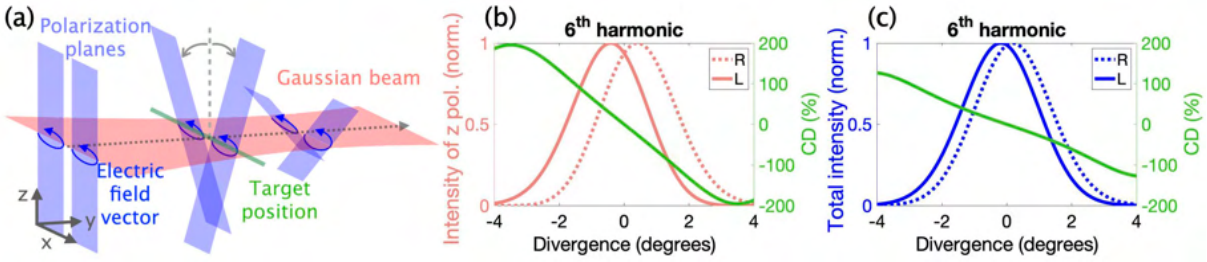


Fig. 1. (a) Forward polarization tilt (blue) in an elliptically polarized gaussian beam (pink), tightly focused into a chiral medium (green). (b,c) Intensity of the z-polarized component (b) and total intensity (c) of the 6th harmonic emitted by the right- (dotted lines) and left-handed (solid lines) propylene oxide, and spatially-dependent chiral dichroism (green), $CD=2(I_L-I_R)/(I_L+I_R)$; TDDFT simulations, $I=6\cdot10^{13}W\cdot cm^{-2}$, focal diameter 5μm, λ=780 nm, and pulse duration 7 fs.

[1] Berova *et al* 2013 978-1-118-01293-2 Wiley
[2] Bliokh K Y & Nori F 2015 *Phys. Rep.* **592** 1
[3] Ayuso D *et al* 2021 *Nat. Commun.* **12** 1-9
[4] Ayuso D *et al* 2019 *Nat Photon* **13**, 866–871

* E-mail: l.rego@imperial.ac.uk

MP

Disentangling fundamental processes of a two-level wave packet in attosecond transient absorption spectroscopy

A Stenquist[*], **F Zapata**[†] **and J M Dahlström**[‡]

Department of Physics, Lund University, Lund, 22100 Sweden.

Synopsis Attosecond transient absorption of a two-level wave packet coupled to both bound and continuum states is studied theoretically by the construction of an analytical model. This allows for disentanglement of fundamental absorption and emission processes of resonant and non-resonant nature.

Attosecond transient absorption spectroscopy (ATAS) is used to study electron dynamics with the aim of unravelling ultra-fast phenomena in atoms and molecules. There have been many investigations on ATAS between bound states [1, 2], but few works has focused on the coupling of a prepared bound wave packet to both bound and continuum states [3]. A recent experimental investigation of the physical phenomena in this regime is presented in Ref. [4]. In order to disentangle the fundamental processes in this rich transient absorption regime, we have developed an analytical model which is able to account for the resonant (bound and continuum) and the off-resonant contribution. In the present work [5], we consider a hydrogen atom in an initial superposition state, comprised of two non-degenerate states, impinged upon by an attosecond pulse. We study the absorption depending on the relative wave packet phase of the prepared superposition. The analytical model, based on Coulomb functions, was compared with numerical simulations, conducted by solving the time-dependent Schrödinger equation, showing good agreement. The model allows us to explain that off-resonant contributions have a significant impact when lower energy states can be reached from the prepared wave packet, see for instance the transition to $1s$ from the prepared p wave packet in Fig. 1. The off-resonant contribution results in alternating absorption and emission structures over the relative wave packet phase, not present for the s wave packet. Thus, we have identified the mechanism causing emission structures from p wave packets. Using the model we have fully disentangled the complex ATAS spectra of two-level wave packets in atoms.

[*]E-mail: axel.stenquist@matfys.lth.se
[†]E-mail: felipe.zapata@matfys.lth.se
[‡]E-mail: marcus.dahlstrom@matfys.lth.se

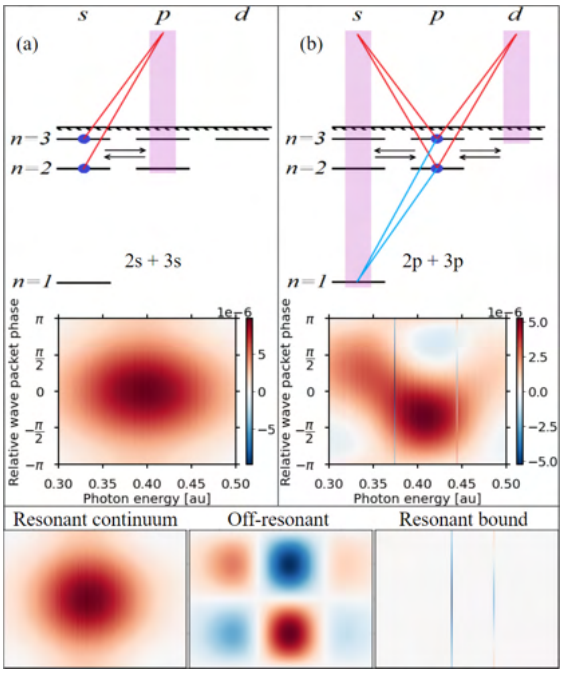


Figure 1. (a) and (b) shows the schematic of the transitions handled by the model for the prepared superpositions 2s+3s and 2p+3p respectively as well as the corresponding absorption profiles resolved over wave packet phase and photon energy. The bottom figures show the contribution of the three absorption processes presented in the schematic, these are the resonant continuum (red lines), off-resonant (purple area) and resonant bound (blue lines) contributions.

References

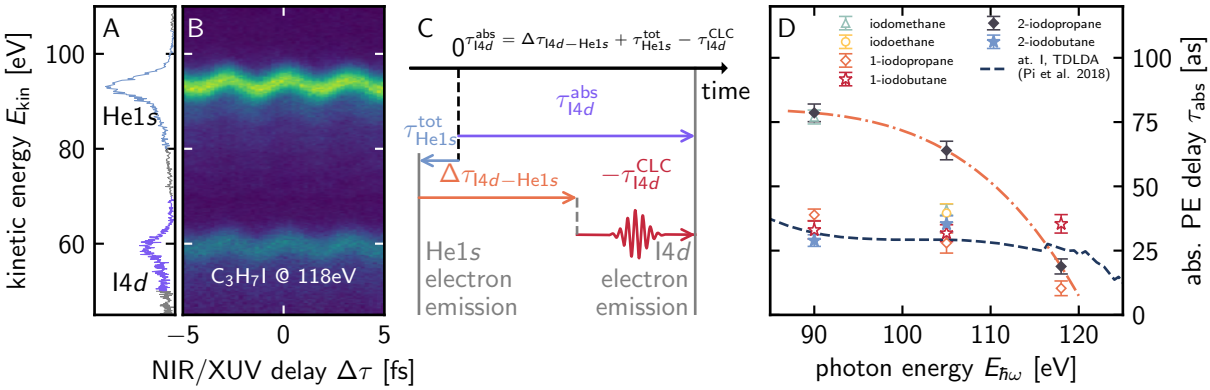
[1] M Wu *et al.* J. Phys. B **49**, 062003 (2016)
[2] A R Beck *et al.* Chem. Phys. Lett. **624**, 119 (2015)
[3] J M Dahlström *et al.* J. Opt. **19**, 114004 (2017)
[4] P Birk *et al.* J. Phys. B **53**, 03 (2020)
[5] A Stenquist *et al.* Publication in progress

Photoemission Chronoscopy of the Iodoalkanes

C A Schröder[1]*, M Pollanka[1], P Scigalla[1], M Mittermair[1], A Duensing[1], A S Landsman[2] , L W Pi[3], R Kienberger[1]

[1] Physik Department, Technische Universität München, 85748 Garching, Germany
[2] Department of Physics, Columbus, Ohio, The Ohio State University
[3]State Key Laboratory of Transient Optics and Photonics, Xi'an Institute of Optics and Precision Mechanics of the Chinese Academy of Sciences, Xi'an 710119

Synopsis Recent theoretical simulations of several iodoalkanes (S Biswas et al., Nature Physics **16** (2020)) suggest that the absolute I4*d* photoemission delay time increases with the size of the attached functional group. We find experimentally that this observation does not generalize to other iodoalkanes with implications for the use of these molecules for absolute photoemission timing experiments on condensed matter systems.



Expanding the available experimental data (cf. [7, 1]) by studying primary iodoalkanes from iodomethane to 1-iodobutane and the secondary iodoalkanes 2-iodopropane and 2-iodobutane a surprising bifurcation of the excitation-energy dependence of the absolute photoemission times is found, that so far lacks explanation (panel **D**).

Photoemission timing of the I4*d* electrons for 90 eV, 105 eV and 118 eV is assessed via attosecond streaking (panels **A**, **B** and [4]) where the giant resonance in the I4$d \rightarrow \varepsilon f$ channel at 94 eV [6] serves as an intra-molecular time zero which we clock against the accurately known He1*s* [8] calculated with [3, 2, 5]. Absolute photoemission times, isolated by subtracting the measurement induced Coulomb laser coupling delay [9] (panel **C**), are shown in panel **D** in comparison to a theoretical prediction τ_{at} for atomic Iodine [10]. No clear correlation between the size of the functional group and the observed deviation of τ_{I4d} from τ_{at} is found where one might expect an increase. This is most evident for the case of 2-iodopropane versus 2-iodobutane at 90 eV and 105 eV (black diamonds vs. blue stars in **D**, red line was drawn as a guide to the eye) where the larger functional group exhibits a smaller delay. The currently available data on iodomethane furthermore suggests that even in the smallest iodoalkanes significant deviations from τ_{at} can occur, which has far-reaching implications for the use of Iodine for the purpose of absolute photoemission timing in condensed matter systems [7].

*E-mail: christian.schroeder@tum.de

References

[1] S Biswas et al., Nature Physics **16, (2020)**.
[2] F A Gianturco et al., The Journal of Chemical Physics **100, (1994)**.
[3] G M J Barca et al., The Journal of Chemical Physics **152, (2020)**.
[4] J Itatani et al., Phys. Rev. Lett. **88, (2002)**.
[5] A P P Natalense et al., The Journal of Chemical Physics **111, (1999)**.
[6] T N Olney et al., Chemical Physics **232, (1998)**.
[7] M Ossiander et al., Nature **561, (2018)**.
[8] M Ossiander et al., Nature Physics **13, (2017)**.
[9] R Pazourek et al., Rev. Mod. Phys. **87, (2015)**.
[10] L-W Pi et al., Applied Sciences **8, (2018)**.

MP

Photoelectron-ion entanglement in streaked direct and shake-up photoemission: an *ab initio* approach

U Thumm* **and H Shi**

Department of Physics and J. R.Macdonald Lab., Kansas State University, Manhattan, KS 66506, USA

Synopsis By comparing direct with shake-up streaked photoionization of helium, we explore the effects of electronic correlation on attosecond time- and angle-resolved photoemission based on *ab initio* calculations.

We applied our FE-DVR code for the *ab initio* calculation of single- and double-ionization of gaseous helium atoms [1] to explore the effects of electronic correlation on attosecond time- and angle-resolved photoemission. Our calculated spectra and relative photoemission time delays for IR streaked direct and He^+ ($n = 2$) shake-up XUV emission agree well with experimental and theoretical data in [2].

To scrutinize the influence of the transient induced oscillating residual excited He^+ ($n = 2, 3$) charge distribution, we compare our *ab initio* streaking calculations with single active electron (SAE) calculations. By adjusting effective multipole SAE potentials to ab initio calculated He^{+*} charge distributions, we assess the role of individual multipole components of the residual He^{+*} ion on spectra and photoemission delays.

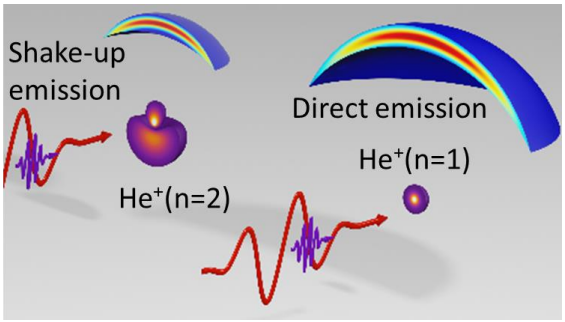


Figure 1. *Ab initio* calculated electron probability densities for direct (left) and He+(n=2) shape-up (right) streaked photoemission.

Supported by US DOE grant N° DEFG02-86ER13491 and US NSF grant N° PHY 2110633.

References

[1] A Liu and U Thumm, Phys. Rev A **91**, 043416 (2015).
[2] M Ossiander *et al.*, Nat. Phys. **13**, 280 (2017).

*E-mail: thumm@phys.ksu.edu

Accurate and complete atomic data set for Helium-Like ions using Relativistic Configuration Interaction approach for singly and doubly excited states

S Manai [1,2]*, D E Salhi [1] and H Jelassi [1]

[1]Research laboratory on Energy and Matter for Nuclear Science Development, LR16CNSTN02, Tunisia. National Center for Nuclear Science and Technologies, Sidi Thabet Technopark 2020 Ariana Tunisia.
[2]Faculty of Sciences of Bizerte, University of Carthage, Tunisia.

Synopsis Accurate atomic data are required for many ions to estimate the power loss from the impurities in the forthcoming fusion reactors, such as the International Thermonuclear Experimental Reactor project. In our study, the atomic data calculations were provided using the relativistic configuration interaction method implemented in the Flexible Atomic Code. Transition probabilities are reported for all E1, E2, M1 and M2 transitions. Breit interactions and QED effects were included. Comparisons were made with other available theories reported in the literature and a good agreement was found.

Accurate atomic data is considered to be the principal way to effectively solve the future energy problem as a clean and infinite energy resource and it is being developed internationally via the International Thermonuclear Experimental Reactor ($ITER$) Project [1]. Then, extensive spectroscopic studies both experimental and theoretical have been performed in the last few years in order to estimate the power loss from the impurities in the forthcoming fusion reactors. Furthermore, accurate values of wavelengths and their errors are required for the interpretation of a wealth of high-resolution data obtained in the last two decades by the Chandra X-ray Observatory and the European Space Agency's X-ray Multi-Mirror Mission. As previously published [2, 3], we continue to focus on Helium-like ions. In this work, energy levels, wavelengths and transitions rates have been calculated for the lowest singly excited 70 levels among $1snl(n \leq 6, l \leq (n-1))$ configurations and the lowest doubly excited 250 levels arising from the K-vacancy $2ln'l'(n' \leq 6,\ l' \leq (n'-1))$ configurations of helium-like ions with $Z = 5-9$. The calculations were performed using the Relativistic Configuration Interaction (RCI) method implemented in the Flexible Atomic Code (FAC) [4]. Comparisons were made with other available theories reported in the literature [5, 6, 7, 8]. Finally, the accuracy of the present calculations is enough to facilitate the identification of many observed spectral lines, plasma modelling as well as diagnostics of astrophysical plasma and controlled thermonuclear fusion.

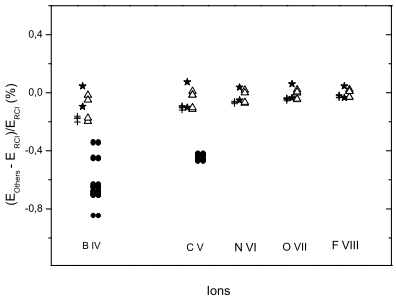


Figure 1. Comparisons of our RCI energy levels values with other theoretical and experimental results.

References

[1] A J H, Donne et al, Nucl. Fusion. **47**, 337 (2007).
[2] S Manai and H Jelassi, Pramana. **95**, 1-9 (2021).
[3] S Ben Nasr, S Manai, D E Salhi, P Quinet and H Jelassi, Atomic Data and Nuclear Data Tables. **135**, 101346 (2020).
[4] M. F. Gu, Canadian Journal of Physics. **86**, 675-689 (2008).
[5] G. W. Drake, Canadian Journal of Physics. **66**, 586611 (1988).
[6] D A Verner, E M Verner and G J Ferland, Atomic Data and Nuclear Data Tables. **64**, 1180 (1996).
[7] K M Aggarwal, T Kato, F P Keenan and I Murakami, Physica Scripta. **83**, 015302 (2010).
[8] B Sow, M Sow, Y Gning, A Traore, A S Ndao and A Wague, Radiation Physics and Chemistry. **123**, 2530 (2016).

*E-mail: manai.soumaya12@gmail.com

MP

First results from attosecond X-ray pump probe experiments in liquids

S Li[1 *], K Li[1,2], L Young[1,2 †], C Pearce[3], S P Moeller[4], M Lin[4], E Nienhuis[3], G Doumy[1], G Dakovski[4], R Santra[5], A Marineili[4], J Cryan[4], D DePonte[4], T Orlando[6], A Clark[7], Z Loh[8], X Li[9] and A Krylov[10]

[1]Argonne National Laboratory, Lemont, 60439, US
[2] University of Chicago, Chicago, 60637, US
[3] Pacific Northwest National Laboratory, Richland, 99354, US
[4] SLAC National Accelerator Laboratory, Menlo Park, 94025, US
[5]CFEL/ University of Hamburg, Hamburg, 22607, Germany
[6]Georgia Institute of Technology, Atlanta, 30332, US
[7]Washington State University, Washington, 99164, US
[8]Nanyang Technological University, 50 Nanyang Ave, 639768, Singapore
[9] University of Washington, Seattle, 98195, US
[10]University of Southern California, Los Angeles, 90089, US

Synopsis The radiation-induced electronic and nuclear dynamics in liquid water were investigated by the x-ray transient absorption following an x-ray ionization pump in a liquid sheet jet using sub-fs X-ray pulses on the ChemRIXS beamline at LCLS. The pump X-ray photon energy is scanned from 255 eV to 275 eV, while the corresponding probe photon energy range is 510 to 550 eV, which covers the valence/inner-valence hole absorption band in the water window below the Oxygen K-edge. A set of time delay points are applied for each photon energy scan, aiming to capture the dynamics including Auger decay, intermolecular coulombic decay (ICD), electron transfer mediated decay (ETMD), and proton transfer processes after valence ionization.

Understanding the elementary steps following ionization in aqueous systems will provide a framework for radiation-matter interactions in chemistry and biology. However, a microscopic understanding of the reaction mechanisms in the relevant physico-chemical time regime is missing as typical techniques, EPR and UV spectroscopies, lack either time resolution or spectral clarity. A powerful two-color sub-femtosecond time-resolved X-ray pump/X-ray probe scheme developed at LCLS provides qualitatively new window to systematically understand the electronic and nuclear dynamics following valence, inner-valence, and core ionization in aqueous systems.

Very recently those radiation-induced reactions in liquid water were investigated by the x-ray transient absorption in the water window following an x-ray ionization pump in a liquid sheet jet using sub-fs pulses from X-ray laser-enhanced attosecond pulse generation (XLEAP) on the ChemRIXS beamline at LCLS. The pump X-ray photon energy is scanned from 255 eV to 275 eV, while the corresponding probe photon energy range is 510 to 550 eV, which covers the valence/inner-valence hole absorption band in the water window below the Oxygen K-edge. Starting from 0.6 fs, a set of time delay points are applied for each photon energy scan, aiming to capture the ultrafast dynamics including Auger decay, intermolecular coulombic decay (ICD)[1], electron transfer mediated decay (ETMD)[2], and proton transfer processes after valence ionization.

References

[1] Jahnke, T. et al., "Experimental Observation of Interatomic Coulombic Decay in Neon Dimers", Phys. Rev. Lett. 93 (16): 163401–163404 (2004).

[2] Aziz, E.F., et al., "Interaction between liquid water and hydroxide revealed by core-hole deexcitation", Nature 455 (7209): 89–91 (2008).

* E-mail: shuai.li@anl.gov
† E-mail: young@anl.gov

TIXEL Detector Development at SLAC - the next generation charged particle detector for photon science applications.

P. Walter[1] *, L. Rota[1], C. Kenney[1], M. McKelvey[1], B. Markovic[1], and A. Dragone[1]

[1]SLAC National Accelerator Laboratory, 2575 Sand Hill Road, Menlo Park, California 94025, USA.

MP

Synopsis Momentum spectroscopy has enabled a new class of experiments in both laser based ultrafast sciences, and x-ray spectroscopy. The fundamental concept of these spectrometers is that the arrival time and position of each fragment is measured. We would like to present the next generation of multi-coincidence electron and ion momentum spectroscopy experiments detector.

With their brightness, energy and rate, new generation light sources, storage rings and FEL require novel detectors with unprecedented performance. Along with the birth of LCLS and now with the LCLS-II upgrade, SLAC has been developing new families of integrating PAD detectors required to exploit the new capabilities of SLAC sources and to enable new science. Along with the general-purpose ePix family with aiming at full frame readouts at 100 kHz, a new family, SparkPix, capable of extracting information at the full MHz repletion rate available at LCLS-II is under development. SparkPix detectors are tweaked for specific classes of experiments where characteristic features in the data can be exploited to minimize data rates out of the detectors. The first member of the SparkPix family is Tixel a Time-of-flight detector with high segmentation capable to detect directly electrons and ions with a time resolution down to 100 ps. Tixel is optimized for COLd Target Recoil Ion Momentum Spectroscopy (COLTRIMS) experiments at MHz rate planned at TMO [1] at LCLS-II. Segmentation in pixels of 100umx100um will allow the possibility to resolve momenta of large number of concurrent fragments.

This time resolving pixelated detector will provide the time of arrival and time over threshold. This new development is supposed to work without a MCP in front of the TIXEL detector. With such a pixelated charged particle detector based on silicon technology and with > 300 hits at a repetition rate of up to 1 MHz it will be possible to perform for the first time massive coincidence experiments. Since the number of combinations grows exponentially with the number of hits this detector it will be possible to detect and analyze large densities of hits with high repetition rate.

We will present the planned experiments and science enabled by the new TIXEL detector at LCLS and the characteristics of the this new detector. Status and timeline of the RD project will be presented tighter with the results of a first small prototype of the tPix ASIC designed to demonstrate critical performance metrics and validate the concept.

Table 1. Key Performance Parameters

Mode of Operation	TOT and TOA
Time resolution	$<$ 100ps
Pixel size	100x100 μm
Energy range	1-10 keV
Array	176x192
Si technology	0.13 μm
Full matrix readout	5 kfps

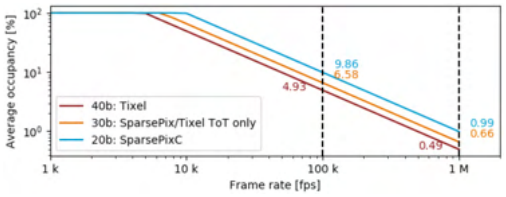


Figure 1. Tixel readout architecture is based on a sparse readout engine designed for the new SparkPix family of Experiment Specific X-ray Cameras tailored to exploit the full potentials of LCLS-II. Shown is the maximum occupancy versus frame rate.

References

[1] P. Walter et. al. The Time-resolved Atomic, Molecular and Optical Science Instrument at the Linac Coherent Light Source, arxiv.org.

*E-mail: pwalter@slac.stanford.edu

Ultrafast scanning tunneling microscopy

A Goldner[1] *, B Ma[1] and M Krüger[1]

[1]Physics Department and Solid State Institute, Technion – Israel Institute of Technology, Haifa 32000, Israel

Synopsis Integrating a conventional scanning tunneling microscope (STM) with an ultrafast laser pulses promises attosecond and sub-nanometer imaging of ultrafast electron dynamics. Here we drive STM tunneling currents using low-power 6fs phase-stable infrared laser pulses and isolate the laser-induced current from the static DC tunneling current using continuous polarization modulation. We observe tunneling currents on the order of pAs and achieve STM operation solely driven by the laser field. Numerical simulations show that the laser-driven tunneling current consist of single attosecond bursts.

Attosecond science can reach the intrinsic time scale of electronic dynamics in atoms and molecules. Their observation calls for novel approaches that combine ultrafast temporal resolution with extremely small spatial resolution in the sub-nanometer regime. Conventional STM, based on DC tunneling, has a poor temporal resolution due to electronic limits, which is slower than a few nanoseconds. Building on recent advances [1,2], we introduce time resolution in STM by combining the conventional STM with an ultrashort femtosecond laser pulse. Based on our simulations, the duration of the induced tunneling current can be confined to hundreds of attoseconds. Simultaneous Angstrom spatial resolution and attosecond temporal resolution are within reach.

One of the challenges combining ultrashort laser pulses with STM tips is the thermal instability. In order to minimize laser-induced tip expansion and deformation and reduce thermal contributions to the net current, the laser power has to be kept at a minimum. Another challenge is to isolate the laser-induced current from the static STM tunneling current. In order to overcome those challenges we devised an experimental setup that combines a commercial ambient room-temperature STM with phase-stable 6fs laser pulses generated by a Ti:Sapphire oscillator with central wavelength 830nm (see Fig. 1(a)). The high-repetition rate source (80 MHz) allows for the generation of sizable currents on the order of pA for laser powers in the mW regime. A parabolic mirror (f = 50mm) focuses the laser onto the STM nanotip made from Pt/Ir alloy, which is in close proximity to a flat gold sample. In order to distinguish the laser-induced current from the static STM tunneling current, we continuously modulate the polarization of the laser pulse using a piezo-controlled interferometer which generates a lock-in current in the STM tunneling gap.

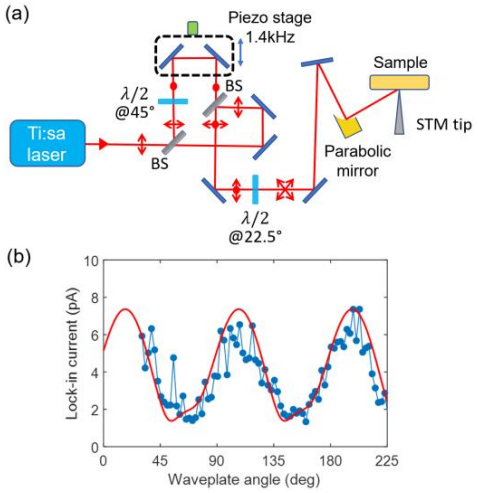


Figure 1. (a) Sketch of the experimental setup. (b) Laser current vs waveplate angle (blue: data, red: model).

Our experiment was carried out at low power (3mW). We measured the lock-in current as a function of the angle of the waveplate after the interferometer and found a strong modulation (see Fig. 1(b)). Our results agree with predictions describing a linear mechanism of laser-driven STM current. At higher laser powers on the order of 20mW, we are able to generate sizable currents in a nonlinear regime of laser-driven STM and achieve STM operation solely with the laser-driven current. Efforts are currently underway to demonstrate optical waveform control, which will open the door to true attosecond control of electron tunneling.

References

[1] Cocker T L *et al.* 2013 *Nature Photonics* **7** 620
[2] M Garg and K Kern 2020 *Science* **367** 411

* E-mail: adigold@technion.ac.il

Emulation of high-numerical aperture extreme ultraviolet lithography using coherent 13.5 nm light

Esben W. Larsen[1*], Fabian Holzmeier[1], Kevin M. Dorney[1], Clayton Bargsten[2], Sayantani Santra[1], Shikhar Arvind[1], Dhirendra P. Singh[1], Daisy Raymondson[3], Rod Ward[2], Henry Kapteyn[2,3], Thomas Nuytten[1], Paul van der Heide[1], and John Petersen[1]

[1]imec, Kapeldreef 75, 3001 Leuven, BE
[2]KM Labs, 4775 Walnut St. #102, Boulder, CO 80301, USA
[3]JILA, Department of Physics, University of Colorado Boulder and NIST, Boulder, CO, 80309, USA

Synopsis We demonstrate the use of 92-eV photons produced by high-order harmonic generation to perform interference lithography at ~20-nm pitch patterns in a metal oxide photoresist by the utilization of a split mirror interference lithography tool. Analysis of scanning electron microscope images enables us to identify potential sources of image blur, which we attribute to out-of-sync vibrations, flare, spectral purity, and laser stability. Nevertheless, these results confirm the ability of tabletop, high-harmonic extreme ultraviolet sources to print dense lithographic patterns.

Photolithography using lithographic scanners lies at the heart of the semiconductor industry. The smallest feature printable by an industrial lithography machine (e.g. a scanner) is largely determined by the wavelength of the light source and it's optical arrangement. Until recently the workhorse of the industry has been excimer lasers operating in the deep ultraviolet (193 nm and 248 nm), but with the ever-growing need for smaller and faster electronics shorter wavelength light is needed.

The state-of-the-art extreme ultraviolet (EUV) lithography tool is the NXE:3400C operate at 13.5 nm and has a numerical aperture (NA) of 0.33. The NXE:3400C has recently been deployed in high volume manufacturing for the 5-nm technology node with producing pitches (lines and spaces) with periods down to 28 nm, while lithographic research has demonstrated features down to 24 nm pitches using this tool in single exposures. The theoretical minimum pitch allowed by this tool is 21 nm. Going to even smaller features a higher NA is required.

To this end ASML have been developing the EXE:5000 series over the last few years, and the first of its kind is currently under installation at a new joint facility between imec and ASML. These scanners will have a NA of 0.55, thus having an optical limit of ~13 nm pitches.

As a consequence of the high photon energy utilized in EUV scanners the initial steps of the photolithography process are now driven by photoionization and there is an urgent need to explore and understand the limits of photoresist performance to harness the full power of these advanced machines. However, the high costs associated with EUV scanners (>150M$ for the NXE:3400C and >300M$ for the EXE:5000) necessitate the need for accessible sources of 13.5 nm EUV light that can emulate the lithographic process.

To these ends, imec has recently installed and commissioned the first industrial, ultrafast EUV metrology and lithography lab with a primary aim to explore the limits of photoresist performance and their associated ultrafast chemistries.

Here, we demonstrate the use of a tabletop, high-harmonic EUV system to perform interference lithography of ~20-nm pitch patterns. Despite the ultrashort duration of EUV pulses at 13.5 nm (~1-3 fs), we still achieve line-and-space patterns over a 1-micron exposure field.

* E-mail: Esben.WittingLarsen@imec.be

MP

Ab Initio Study on Enhanced Energy Transfer from Intense Dual-Color Laser Fields to a Semiconductor

M. Tani[1], K. Sasaki[1], Y. Shinohara[1,2], and K. L. Ishikawa[1,2,3] *

[1]Department of Nuclear Engineering and Management, the University of Tokyo, Tokyo, 113-8656, Japan
[2]Photon Science Center, The University of Tokyo, Tokyo, 113-8656, Japan
[3]Research Institute for Photon Science and Laser Technology, The University of Tokyo, Tokyo 113-0033, Japan

Synopsis Using the time-dependent density-functional theory, we investigate how energy transfer to crystalline silicon from intense two-color laser pulses depends on the mixing ratio while keeping the total intensity constant. The energy absorption is substantially enhanced when two colors are approximately equally mixed, compared to single-color cases. Our analysis based on a 1D independent-electron model shows that this effect is mainly because the intraband motion by the longer wavelength assists interband transition by the shorter wavelength.

In recent years, the interaction between ultrashort intense lasers and semiconductors or dielectrics has been attracting significant attention in terms of high-order harmonic generation [1] or laser ablation without the heat-affected zone [2]. The energy transfer from lasers to electrons is a key process here. Several experimental and theoretical studies have reported that the use of two-color laser pulse pairs enables highly efficient laser ablation of transparent materials compared to single color one [3,4]. In the present work, to elucidate how dual-color femtosecond laser pulses deposit energy to electrons in semiconductor and dielectric materials, we use the time-dependent density functional theory (TDDFT) and examine the energy absorption of bulk silicon under two-color [ultraviolet (UV) and infrared (IR)] intense femtosecond laser fields as a function of relative intensity with the total fluence conserved.

We use an open-source software SALMON [5] for TDDFT simulations and consider various combinations of photon energies ($\hbar\omega_1, \hbar\omega_2$). Figure 1 shows the results for $\hbar\omega_1$=0.2, 0.8, 1.6 eV and $\hbar\omega_2$=3.2 eV. Note that $\hbar\omega_1$ is smaller than the direct bandgap (3.1eV) and $\hbar\omega_2$ slightly larger. The common pulse width is 14.4 fs in FWHM, and the total peak intensity is fixed to 1 TW/cm^2.

The absorbed energy as a function of the $\hbar\omega_1$ (IR) laser field fraction $\eta = I_1/(I_1 + I_2)$ is plotted in this figure, where I_1 (I_2) denotes the peak intensity of the $\hbar\omega_1$ ($\hbar\omega_2$) component. We find that the deposited energy by simultaneous irradiation is significantly enhanced in comparison with the single-color cases ($\eta = 0,1$) and takes maximum value at η~0.5 for each $\hbar\omega_1$ while the enhancement does not occur when the two pulses are temporally separated. The enhancement is more prominent for smaller $\hbar\omega_1$ (i.e., longer wavelength), which indicates an essential role of the intraband motion induced by the $\hbar\omega_1$ field. Detailed analysis based on a 1D independent-electron model originally presented in Ref. 1 reveals that its role is indeed two-fold, i.e., to increase the interband transition kicked by the $\hbar\omega_2$ field and to promote conduction electrons to higher energy. Especially, the former effect plays a dominant role. The benefit of this effect could be enjoyed more with a THz laser field.

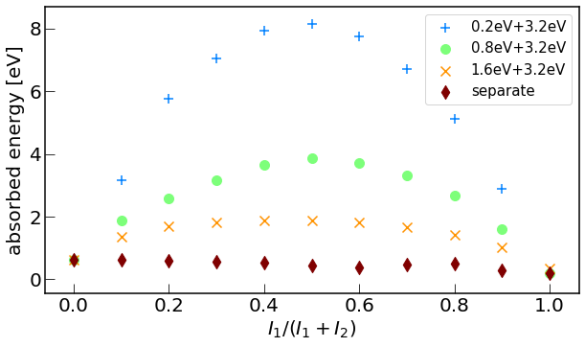


Figure 1. Blue +, lime circle, orange x, and brown diamond dots denote absorbed energy at each η with $\hbar\omega_1 = 0.2, 0.8, 1.6$ eV (simultaneous irradiation with $\hbar\omega_2$) and 0.2 eV (temporally delayed from $\hbar\omega_2$).

References

[1] T. Ikemachi *et al* 2017 *Phys. Rev. A* **95** 043416
[2] R. R. Gattass *et al* 2008 *Nat. Photonics* **2** 219
[3] X. Yu *et al* 2013 *Opt. Express* **39** 19
[4] P. G. de A. Martínez *et al* 2021 *Phys.Rev. A* **103** 033107
[5] M. Noda *et al* 2019 *Comput. Phys. Commun.* **235** 356

* E-mail: ishiken@n.t.u-tokyo.ac.jp

Tracking the melting of charge density wave and excitonic condensate in 1T-$TiSe_2$ with transient XUV spectroscopy

A Zong[1,2], S-C Lin[1,2] and M Zuerch[1,2]*

[1]University of California at Berkeley, Department of Chemistry, Berkeley, 94720, USA
[2]Lawrence Berkeley National Laboratory, Materials Sciences Division, Berkeley, 94720, USA

Synopsis Transient XUV spectroscopy in a cryogenic sample environment is key to studying light-induced phase transitions in the ground state of many quantum materials. Here we examine the ultrafast melting of the charge-density-wave (CDW) phase in 1T-$TiSe_2$, which is also a putative excitonic insulator. The CDW suppression is evidenced by characteristic phonon oscillations that selectively modulate the Ti and Se absorption edges. The role of excitonic correlations in this nonequilibrium transition is revealed by the dependence of the initial edge response on the transient free carrier density.

1T-$TiSe_2$ provides a rich platform to investigate nonequilibrium transitions [1] and light-induced states [2, 3], thanks to its rich phase diagram as a result of the interplay among excitonic correlation, strong electron-phonon coupling, as well as domain structures. In equilibrium, 1T-$TiSe_2$ undergoes a CDW transition around 200 K, which is accompanied by excitonic condensation due to interactions between Ti 3d electrons and Se 4p holes. It was shown that a low-fluence femtosecond pulse can selectively break the exciton condensate without destroying the CDW superlattice [4]. We further demonstrated that the exciton melting governs a light-induced dimension crossover of the CDW modulation, leading to a transient 2D CDW above a threshold pump pulse fluence [5]. Despite the critical role of exciton correlation in mediating this phase transition, there lacks a microscopic understanding of how excitons are broken within the first tens of femtosecond after excitation.

Here we measured the photoinduced changes of the Ti $M_{2,3}$ and Se $M_{4,5}$ edges in order to understand how Ti 3d electrons and Se 4p holes are dissociated. Critical to the experiment is the construction of a new table-top attosecond XUV spectroscopy beamline fitted with a cryogenic sample environment, which is capable of detecting transient transmission changes down to 0.1 mOD in routine operations. We observed clear oscillatory signals corresponding to the 6-THz A_{1g} phonon in the normal state (Fig. 1), indicative of light-induced melting of the CDW. Notably, the Ti $M_{2,3}$ edge shows pronounced oscillation although only the Se atoms oscillate in space. By varying the incident pump fluence, we find that sub-100-fs changes in the Ti and Se edges display markedly different initial response times, providing direct evidence for the carrier-induced screening of the electron-hole Coulomb attraction that initiates the exciton unbinding.

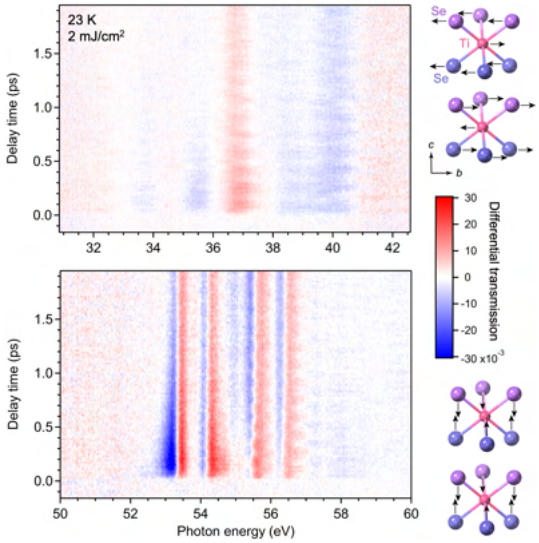


Figure 1. XUV transmission changes near the Ti $M_{2,3}$ edge (*upper*) and Se $M_{4,5}$ edge (*lower*) recorded in the CDW phase. Schematics on the right show the CDW soft phonon (*upper*) and the A_{1g} phonon (*lower*) in the undistorted lattice.

References

[1] T. Rohwer *et al.*, Nature **471**, 490 (2011).
[2] S. Duan *et al.*, Nature **595**, 239 (2021).
[3] S.-Y. Xu *et al.*, Nature **578**, 545 (2020).
[4] M. Porer *et al.*, Nat. Mater. **13**, 857 (2014).
[5] Y. Cheng *et al.*, Nat. Commun. **13**, 963 (2022).

*E-mail: mwz@berkeley.edu

MP

Towards extreme ultraviolet spectroscopy of two dimensional transition metal dichalcogenides

M Mallick[1 *], R Sollapur[1,2], C Spielmann[1,2,3] and M Zürch[1,4]

[1]Institute of Optics and Quantum Electronics, Friedrich Schiller University, Jena, 07743, Germany
[2]Abbe Center of Photonics, Friedrich Schiller University, Jena, 07743, Germany
[3]Helmholtz Institute, Jena, 07743, Germany
[4]Department of Chemistry, University of California, Berkeley, 94720, USA

Synopsis Understanding the ultrafast photo-response in two-dimensional transition metal dichalcogenides semiconductors will pave the way for new energy-efficient photonic devices. When these nanomaterials are scaled down from bulk to monolayer, the screening of electrons leads to strong enhancement in excitonic transitions that can be studied using element-specific extreme ultraviolet spectroscopic methods. Our work involves investigating the out-of-equilibrium dynamics on the electronic time scale and identifying electronic and structural couplings.

The two dimensional (2D) transition metal dichalocgenides (TMDCs) has shown tremendous potential in optoelectronic applications. The dimensionality of TMDCs plays an important role in their band structure, inversion symmetry, exciton's lifetime, spin-valley coupling of the charge carriers etc. [1]. So far, the majority of the time-resolved out of equilibrium studies for these semiconductors are based on optical spectroscopic methods. These techniques have major drawbacks like overlapping spectral signatures, incapable of tracking the dynamics across a material junction unambiguously because of lack of atomic sensitivity and inherently limited temporal resolution [2]. When these nanomaterials are scaled down from bulk to monolayer, the screening of electrons changes drastically affecting valence electronic structure. This leads to strong enhancement in excitonic transitions that can be studied using element-specific extreme ultraviolet (XUV) spectroscopic methods. This spectroscopy provides excellent time and energy resolution as well [3]. In our work, we are interested in observing carrier dynamics on the electronic time scale and identify their structurals couplings. These TMDCs will be pumped by few-cycle near-infrared (NIR) pulses and probed by broadband attosecond XUV pulses. We record the transient absorption changes around absorption edges of the transition metals. To generate few-cycle pulses, we have compressed a long NIR pulse from a commercial Ti:Sapphire femtosecond laser system using a gas filled hollow core fiber (HCF).Then the pulses are passed through dielectric chirped mirrors for dispersion compensation[4]. To date, we were able to achieve ~ 3 fs at ~0.6 mJ pulse energy, which is well-suited for broadband XUV generation using high harmonic generation [5].

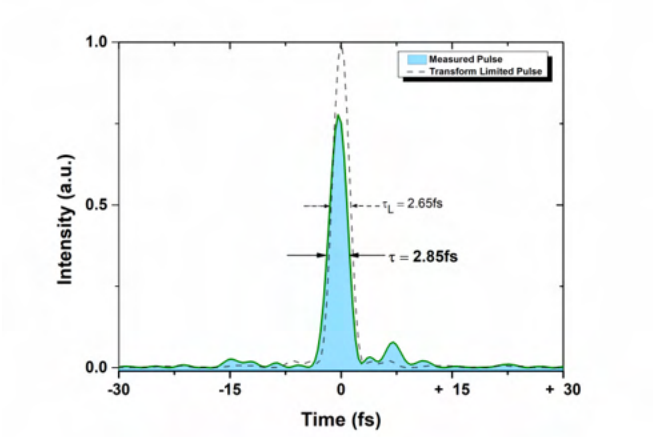


Figure 1. Sub-femtosecond (~3fs) pump pulse obtained.

References

[1] Kin F M *et al* 2016 *Nature Photon.*10 216
[2] Philipp S *et al* 2017 *Nano Lett.* 17 3 1455
[3] Lauren J B *et al* 2016 *JOSA B.* 33 C57
[4] De Silvestri S. *et al* 2008 *Springer.*3 chp.1 3
[5] P B Corkum 1993 *Phys. Rev. Lett.*. 71 1994

* E-mail: monalisa.mallick@uni-jena.de

Single-shot measurement of few-cycle mid-infrared waveforms on a chip

Y Liu[1], J E Beetar[1], J Nesper[1], S Gholam-Mirzaei [1,2], and M Chini[1,3 *]

[1]Department of Physics, University of Central Florida, Orlando FL 32816
[2]Joint Attosecond Science Laboratory (JASLab), National Research Council of Canada and University of Ottawa, Ottawa, Ontario K1A 0R6, Canada
[3]CREOL, the College of Optics and Photonics, University of Central Florida, Orlando FL 32816

Synopsis The characterization of transient optical waveforms requires an 'optical oscilloscope' with sub-cycle temporal resolution and single-shot operation. Here, we show that strong-field multiphoton excitation of photocurrents in a silicon-based image sensor can provide the sub-cycle temporal gate for waveform measurements in the mid-infrared. By mapping the time delay between a strong fundamental and weak perturbation pulse onto a transverse spatial coordinate of the image sensor, the few-cycle mid-infrared waveforms are characterized in a single-shot geometry.

Controlling and recording optical waveforms (including the carrier-envelope phase, CEP) are critical tools for generating isolated attosecond pulses and studying strong-field interactions. Complete characterization of optical waveforms, however, requires a sub-cycle temporal gate capable of sampling the electric field oscillations. In the past, several techniques, such as attosecond streaking and electro-optic sampling, have allowed waveform measurements. However, all waveform characterization techniques so far require scanning-geometry measurements which average over multiple laser shots. Our recent work showed that nonlinear excitation in solids can provide a sub-cycle temporal gate [1], in analogy to gas phase ionization in the TIPTOE (tunneling ionization with a perturbation for the time-domain observation of an electric field) technique [2]. Here, we show that the solid platform can also allow operation in a single-shot geometry, by using a silicon-based image sensor as the nonlinear medium and by mapping the time delay onto a transverse spatial coordinate of the two-dimensional sensor. Using this technique, we demonstrate single-shot measurements of few-cycle mid-IR waveforms [3].

In our experiment, CEP-stable 2.1-cycle mid-IR pulses are generated by nonlinear compression of multi-cycle mid-infrared pulses from an optical parametric amplifier. The pulses are then split into an intense fundamental and weak perturbing beam, and recombined in a Mach-Zehnder interferometer geometry. The single-shot waveform measurement is enabled by cylindrical focusing of the fundamental and perturbing pulses onto a CMOS camera in a small-angle crossed-beam geometry. Completely characterizing the optical waveforms further requires that the fundamental pulse has CEP of zero, which is achieved by copropagating a weak second-harmonic field with the perturbing pulse [2, 3]. After setting the fundamental CEP to be zero, the complete optical waveforms (including CEP) of the perturbation pulse can be characterized directly. By varying the CEP of the perturbation pulse by ~π rad, we observe that the signal modulations transform from a positive to a negative sine-like waveform, as shown in Fig. 1.

In conclusion, we demonstrate single-shot characterization of few-cycle mid-IR waveforms using a simple Si-based image sensor as the nonlinear optical medium. Using other sensors, it is likely that the technique can be extended to near-IR or even visible wavelengths.

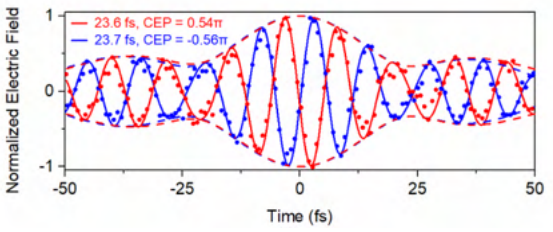


Figure 1. Complete characterization of optical waveforms of the perturbation pulse. The perturbation pulse CEP is varied by changing the insertion of a CaF_2 wedge.

References

[1] Liu Y *et al* 2021 *Photon. Res.* **9** 929
[2] Park S B *et al* 2018 *Optica* **5** 402
[3] Liu Y *et al* 2022 *Nat. Photonics* **16** 109

* E-mail: michael.chini@ucf.edu

MP

Characterization of small polaron formation in $CuFeO_2$ with transient XUV spectroscopy

H. Liu[1], J. M. Michelsen[1], I. M. Klein[1], F. Babbe[2], J. K. Cooper[2] and S. K. Cushing[1] *

[1]Division of Chemistry and Chemical Engineering, California Institute of Technology, Pasadena, CA 91125, USA
[2]Joint Center for Artificial Photosynthesis, Lawrence Berkeley National Laboratory, Berkeley, CA 94720, USA

Synopsis Small polaron formation at sub-picosecond timescales limits the mobility of photo-injected carriers and is the limiting factor for many photoactive materials. We use transient XUV reflection spectroscopy to characterize the small polaron formation in $CuFeO_2$, a photoelectrode material for CO_2 reduction. The signature of small polarons is identified as an enhanced spectral splitting occurring within 500 fs after photoexcitation, which is attributed to the enhanced anisotropic local field effects associated with lattice distortions from small polaron formation. We apply theory based on the Bethe-Salpeter equation to relate photoexcited electron and hole occupations to polaron formation.

First-row transition metal oxides have long been proposed for various clean energy conversion applications such as solar water splitting and CO_2 reductions. However, despite their suitable band gaps and earth abundance, the wide applications of transition metal oxides as photoelectrode materials have largely been hindered by its limited photoconversion efficiency. Recent experiments have observed the evidence of small polaron formation at sub-picosecond timescale [1, 2]. During small polaron formation, photoexcitation causes charge transfer from oxygen to metal atoms, followed by local lattice expansion that traps photoinjected carriers at metal sites, reducing their mobilities.

In this work, we use tabletop femtosecond extreme ultraviolet (XUV) reflection spectroscopy to track the small polaron formation dynamics in $CuFeO_2$, a potential photocathode material for CO_2 reduction. Experimentally, a rhombohedral $CuFeO_2$ thin film is photoexcited by a femtosecond 400 nm pulse. The resulting coupled carrier and structural dynamics are probed by monitoring the transient reflectivity changes around the Fe $M_{2,3}$ edge, as shown in Figure 1. In $CuFeO_2$, initial photoexcitation promotes electrons from valence bands, which primarily consists of Cu 3d and O 2p states, to Fe 3d states in the conduction band. This charge transfer process changes the Fe oxidation states and is observed as the emergence of multiple peaks immediately after photoexcitation. Followed by charge transfer, spectral splittings are observed around 55 eV and 52 eV. The spectral splittings grows immediately after photoexcitation and forms a metastable state after ~ 1 ps. To understand the relationship between polaron formation and carrier recombination, we measure dynamics from fs to device-relevant timescales. Applying a theoretical approach based on density functional theory and the Bethe-Salpeter equation, the observed spectral splittings are attributed to small polaron formation around Fe atoms. During the small polaron formation, the local anisotropic lattice expansion further lifts the energy degeneracy of Fe 3p core states through the anisotropic crystal field effects, giving rise to the observed large spectral splitting energy around 1 eV. In addition, anti-correlated intensity modulations at 50 eV and 52 eV are observed and can be understood by highly damped Fe-O bond length oscillations during the small polaron formation.

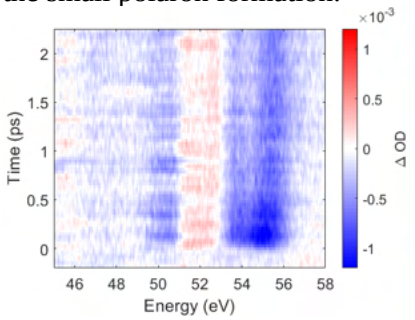


Figure 1. Transient XUV reflection at Fe $M_{2,3}$ edge.

References

[1] Carneiro, L. *et al.*, Nature Mater 2017, 16, 819-825
[2] Husek, J. et al., 2018 J. Phys. Chem. C 2018, 122, 21, 11300-11304

* E-mail: scushing@caltech.edu

Ultrafast charge dynamics and optical spectra in strongly correlated materials

V Turkowski *

Department of Physics, University of Central Florida, Orlando, Florida 32816, USA

Synopsis Strong electron-electron correlations, i.e. interactions between electrons when they occupy the same atom, play a very important role in static and nonequilibrium, including ultrafast, properties of many materials. In the ultrafast case, to describe these effects accurately one needs an ab initio approach of TDDFT with an appropriate exchange-correlation (XC) potential. We describe our proposed algorithm to obtain such a potential from many-body theory and show applications of the obtained potential to different types of materials in the case of ultrafast optical response.

Strong electron-electron correlations define static and nonequilibrium properties of many materials. In particular, signs of these correlations can be seen in the optical absorption and emission spectra. In order to describe the properties of such materials one needs to use special many-body or *ab initio* tools. For instance, in the *ab initio* case one needs an exchange-correlation (XC) potential that properly takes into account the effects of electron-electron correlations. In this work, we give details of our Time-Dependent Density-Functional Theory (TDDFT) approach for strongly correlated materials, where the XC kernel is derived from the charge susceptibility by solving an effective Hubbard model within Dynamical Mean-Field Theory. We show applications of the theory to different types of materials (ferromagnetic metals, band and Mott insulators). In particular, we demonstrate how the effects of correlations are revealed in the absorption and emission spectra, including the case of High Harmonic Generation. We summarize the remaining challenges for the theory, including the cases of non-local correlations and very strong perturbations.

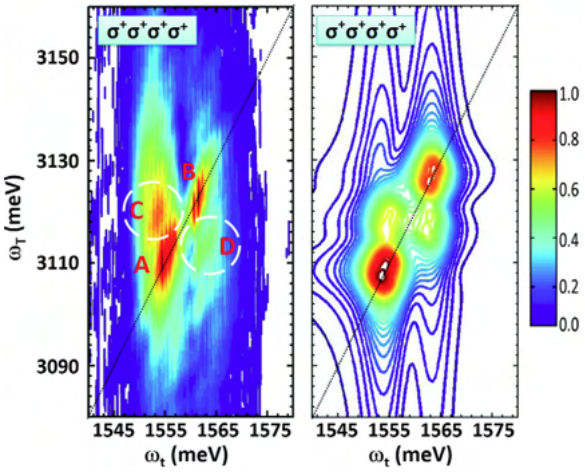


Figure 1. Experimental (left) and theoretical (right) 2DFS spectra for a GaAs quantum well. Nondiagonal peaks correspond to coherent coupling between different exciton states [3].

References

[1] N U Din, V Turkowski, and T S Rahman, 2D Mater **8**, 025018 (2021).
[2] V Turkowski *"Dynamical Mean-Field Theory for Strongly Correlated Materials"*, Springer (2021).
[3] J Paul *et al.*, Phys. Rev. Lett. **116**, 157401 (2016).

*E-mail: Volodymyr.Turkowski@ucf.edu

MP

Coherence in the photoionization of xenon in weak or strong fields

Stefanos Carlström[1,2]*, Mathieu Gisselbrecht[1]†, Anne L'Huillier[1], Jan Marcus Dahlström[1], Johan Mauritsson[1], Kenneth J Schafer[3], Misha Yu Ivanov[2,4,5], and Serguei Patchkovskii[2]

[1] Department of Physics, Lund University, Box 118, SE-221 10 Lund, Sweden
[2] Max-Born-Institut, Max-Born-Straße 2A, 12489 Berlin, Germany
[3] Department of Physics and Astronomy, Louisiana State University, Baton Rouge, LA 70803, USA
[4] Department of Physics, Imperial College London, South Kensington Campus, SW72AZ London, UK
[5] Institut für Physik, Humboldt-Universität zu Berlin, Newtonstraße 15, 12487 Berlin, Germany

Synopsis We investigate two different ways of preparing coherences between the xenon ion spin-orbit-split ground state (5p J=3/2 and 1/2), between which the transition is dipole-forbidden. They can be thought of as "which way" experiments, since we cannot tell which way the photoelectron took to end up in its final state.

The development of attosecond science in the last decades relies on the interaction of light pulses either in the extreme ultraviolet in the weak-field regime, or in the near infrared in the strong-field regime. At this ultra-short timescale, different ionization pathways cannot always be disentagled, thus losing information on which-way the electron was emitted. We study here how this lost of information affects the coherence of ionic states in xenon.

The first case is in the weak-field regime [1], where a bichromatic (or polychromatic) field with an energy separation of the components equalling the spin-orbit splitting is used to ionize the system. Due to the difference in ionization potential between the spin-orbit channels, there will be at least two pathways where the photoelectrons overlap energetically, and we can impart coherence between the ionic states indefinitely, regardless of the pulse duration.

The second case is instead in the strong-field regime [2], where rescattering trajectories in above-threshold ionization are used to drive transitions between the ion cores. The rescattering trajectories are in fact equivalent to highly excited Rydberg state wavepackets, which are very good at absorbing photons from the external field, not necessarily to become further excited, but to channel the energy into the ion; they act as an "atomic antenna" [3]. Through this mechanism, we are able to achieve degrees of coherence exceeding 10 %, in a regime where would expect zero, due to the dipole transition between the ion core states being forbidden.

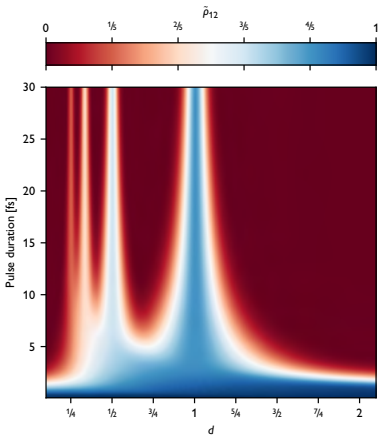


Figure 1. Degree of coherence between different spin–orbit channels, for different detunings of a five-photon field, i.e., photon energies $\hbar q\omega$ for five consecutive values of q, with $\hbar\omega = d\Delta E_{\mathrm{S-O}}$.

References

[1] S Carlström, J Mauritsson, K J Schafer, A L'Huillier, and M Gisselbrecht, Journal of Physics B: Atomic, Molecular and Optical Physics, **51(1)**, 015201 (2018).

[2] S Carlström, J M Dahlström, M Y Ivanov, and S Patchkovskii, arXiv:2204.14082 [physics.atom-ph] (2022).

[3] M Y Kuchiev, Soviet Journal of Experimental and Theoretical Physics Letters, **45(7)**, 404 (1987).

*E-mail: stefanos.carlstrom@matfys.lth.se
†E-mail: mathieu.gisselbrecht@sljus.lu.se

Superachromatic Reflective Phase Retarder for the Polarization Conversion of Attosecond Pulses

Keisuke Sakata, Kengo Ito, and Taro Sekikawa *

Department of Applied Physics, Hokkaido University, Kita 13 Nishi8, Kita-ku, Sapporo 060-8628, Japan

Synopsis A reflective superachromatic phase retarder for extreme ultraviolet attosecond pulses was developed using SiC mirrors. The polarizations of the 17th and 19th harmonic were converted to nearly circular polarization. The phase retardation provided by the retarder at 27.7 eV is 90° with a deviation less than $\pm\lambda/50$ for a bandwidth of 3.1 eV, which is broad enough for the polarization conversion of attosecond pulses.

Circularly polarized extreme ultraviolet (EUV) light makes it possible to investigate magnetic and chiral properties, to which linearly polarized light is insensitive. Circularly polarized high harmonics are promising as a coherent EUV light source because of ultrashort pulse duration, breaking into the attosecond temporal regime. Here, as a simple approach to generate circularly polarized attosecond pulses, we developed a superachromatic reflective quarter-wave ($\lambda/4$) phase retarder for attosecond pulses at 27.7 eV [1]. The phase retarder consists of three SiC mirrors. The differences in the phase retardations between *s*- and *p*- polarizations on the mirror surface transform the polarization of the incident light. The sequential incident angles to three mirrors are 74°, 58°, and 74°, determined by Fresnel coefficients using the complex refractive index. It is found that the phase retardation is 90° at 27.7 eV and that the deviation is within $\pm\lambda/50$ for a bandwidth of 3.1 eV, which is broad enough to support the attosecond pulses. Therefore, the phase retarder proposed here could convert the linearly polarized attosecond pulses into the circular.

Experimentally, we characterized the developed phase retarder in the following procedures : The linearly polarized 17th (=26.4 eV) or 19th (=29.5 eV) harmonics were selected by a toroidal grating and was used for the characterization of the phase retarder. The polarization of the beam passing through the retarder was characterized by measuring the angle dependence of the transmittance of the linear polarizer consisting of three gold mirrors with the incident angles set at 70°, 50° and 70° sequentially. Because the reflectance of gold highly anisotropic in the EUV region, a set of gold mirrors works as the linear polarizer.

Figures 1a and 1b show the transmittance of the 17th and 19th harmonics after inserting the phase retarder. The linear polarization was converted to the elliptical polarization. The ellipticities of the polarization were 0.94 and 0.88, respectively. These values are high enough for the application to polarimetry. The phase retardations provided by the retarder were determined by the fitting analysis of the experimental data using Muller matrices and were found to be 93° and 84° for 17th and 19th harmonics, respectively. They are consistent with the theoretical reflectance using the complex indices. Therefore, the developed phase retarder has a phase retardation of 90° at a photon energy at 27.7 eV. The deviation from $\lambda/4$ is less than $\pm\lambda/50$ at the 17th and 19th harmonic. Therefore, the phase retarder supports ±1.55-eV bandwidth, which is broad enough to convert the polarization of the attosecond pulses with a center photon energy of 27.7 eV [1]. Because the theoretical throughput of the retarder is 15 percent, the converted attosecond pulses are applicable to spectroscopic and imaging investigations. The phase retarder will be a useful optical element for attosecond science.

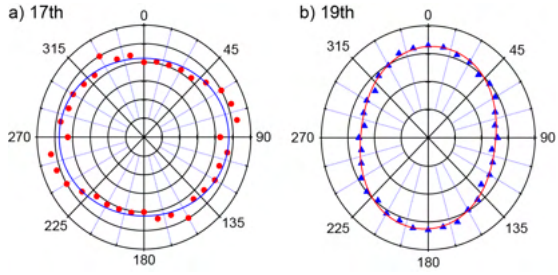


Figure 1. a) and b) Angle dependence of the transmittance of the 17th (●) and 19th (▲) harmonics after the phase retarder, respectively. The solid lines are the fitting results to obtain the phase retardations.

References

[1] T. Sekikawa et al., Nature **432**, 605 (2004).

* E-mail: sekikawa@eng.hokudai.ac.jp

Femtosecond XUV–IR induced photodynamics in the methyl iodide cation

S. Marggi Poullain[1*], M. L. Murillo-Sánchez[1] , G. Reitsma[2], P. Fernández-Milán[3], J. González-Vázquez[3] , R. de Nalda[4] ,F. Martín[3,5,6], M. J J Vrakking[2] , O. Kornilov[2] and L. Bañares[1,5]

[1]Departamento de Química Física, Facultad de Ciencias Químicas, Universidad Complutense de Madrid, 28040, Madrid, Spain
[2]Max-Born-Institute, Max Born Strasse 2A, D-12489 Berlin, Germany.
[3]Departamento de Química, Módulo 13, Facultad de Ciencias, Universidad Autónoma de Madrid, 28049 Madrid, Spain
[4]Instituto de Química Física Rocasolano, Consejo Superior de Investigaciones Científicas, Serrano 119, 28006 Madrid, Spain
[5]Instituto Madrileño de Estudios Avanzados en Nanociencia (IMDEA-Nanoscience), Cantoblanco, 28049 Madrid, Spain
[6]Condensed Matter Physics Center (IFIMAC), Universidad Autónoma de Madrid, 28049 Madrid, Spain

TP

Synopsis The time-resolved photodynamics of the methyl iodide cation (CH_3I^+) are investigated by means of femtosecond XUV–IR pump–probe spectroscopy. A time-delay-compensated XUV monochromator is employed to isolate specific harmonics for one-photon ionizing the methyl iodide molecule, while VMI is employed to detect selected fragment ions —CH_3^+ and I^+— as well as photoelectrons. The experimental results in combination with *ab initio* calculations provide a detailed picture of the CH_3I^+ dissociation and show how a moderately strong IR pulse can control and modify the photodynamics.

The development of light sources in the extreme ultraviolet (XUV) based on high harmonic generation has opened new avenues for the investigation of time-resolved photodynamics in cationic excited electronic states of polyatomic molecules. Here, an XUV pump - infrared (IR) probe scheme with femtosecond time resolution is employed in order to demonstrate how a moderately strong IR pulse can control and modify the photodynamics following one-photon XUV single ionization of methyl iodide (CH_3I) [1].

A time-delay-compensated XUV monochromator is employed to isolate a specific harmonic, the 9th harmonic of the fundamental 800 nm (13.95 eV, 88.89 nm) [2], which is used as a pump pulse to prepare the cation in several electronic states. A time-delayed IR probe pulse is used to probe the dissociative dynamics on the first excited $\tilde{A}\ ^2A_1$ state potential energy surface. Photoelectrons and photofragment ions—CH_3^+ and I^+—are detected by velocity map imaging. The experimental results are complemented with high level *ab initio* calculations for the potential energy curves of the electronic states of CH_3I^+ as well as with full dimension on-the-fly trajectory calculations on the first electronically excited state $\tilde{A}\ ^2A_1$, considering the presence of the IR pulse. The CH_3^+ and I^+ pump–probe transients reflect the role of the IR pulse in controlling the photodynamics of CH_3I^+ in the $\tilde{A}\ ^2A_1$ state, mainly through the coupling to the ground state $\tilde{X}\ ^2E_{3/2,1/2}$ and to the excited $\tilde{B}\ ^2E$ state manifold. Oscillatory features are observed and attributed to a vibrational wave packet prepared in the $\tilde{A}\ ^2A_1$ state. The IR probe pulse induces a coupling between electronic states leading to a slow depletion of CH_3^+ fragments after the cation is transferred to the ground $\tilde{X}\ ^2E_{3/2,1/2}$ states and an enhancement of I^+ fragments by absorption of IR photons yielding dissociative photoionization.

References

[1] Murillo-Sánchez M L *et al* 2021 *New J. Phys.* **23** 073023
[2] Eckstein M *et al* 2015, *J. Phys. Chem. Lett.* **6** 419

* E-mail: smarggi@ucm.es

T01 **Probing molecular dynamics using ultrafast XUV transient spectroscopy**
John E Beetar, Sonia Marggi Poullain, Kristina Chang, Yuki Kobayashi, Stephen R Leone 143

T02 **Imaging intramolecular hydrogen migration via polarization-averaged molecular-frame photoelectron angular distributions**
Keisuke Hatada, Shigeru Abe, Soki Goto, Yoshiaki Tamura, Fukiko Ota, Hao Xue, Manabu Kanno, Naoki Kishimoto, Kiyoshi Ueda, Sergio Díaz-Tendero, Fernando Martín 144

T03 **Effect of the shot-to-shot variation on charge migration induced by sub-fs X-Ray free-electron laser pulses**
Gilbert Grell, Zhaoheng Guo, Taran Driver, Piero Decleva, Etienne Plésiat, Antonio Picón, Jesús González-Vázquez, Peter Walter, Jon Marangos, James Cryan, Agostino Marinelli, Alicia Palacios, Fernando Martín 263

T04 **Photochemical dynamics of gaseous CH_2I_2 induced by an intense UV pulse**
Yijue Ding, Loren Greenman, Brett Esry, Daniel Rolles, Artem Rudenko 264

T05 **Photoelectron and ion momentum imaging of molecules excited by ultrashort vacuum ultraviolet pulses**
Daniel Slaughter, Kirk Larsen, Roger Bello, Niranjan Shivaram, C. William McCurdy, Predrag Ranitovic, Robert Lucchese, Thorsten Weber 265

T06 **Photoelectron spectroscopy using a synthetically chiral laser pulse**
Zack Dube, Georgios Katsoulis, Yonghao Mi, Tian Wang, Guilmot Ernotte, Andrei Yu Naumov, David M Villeneuve, Paul B Corkum, Agapi Emmanouilidou, Andre Staudte 266

T07 **Attosecond coincidence spectroscopy of CH_4 and CD_4**
Dominik Ertel, David Busto, Hamed Ahmadi, Jakub Benda, Marvin Schmoll, Matteo Moioli, Ioannis Makos, Fabio Frassetto, Luca Poletto, Robert Moshammer, Claus Dieter Schröter, Thomas Pfeifer, Zdeněk Mašín, Serguei Patchkovskii, Giuseppe Sansone 145

T08 **State-resolved attosecond photoionization of molecular nitrogen**
Mikhail Osolodkov, Tobias Witting, Federico Furch, Claus Peter Schulz, Vicent Borràs, Jesús González-Vázquez, Fernando Martín, Marc Vrakking 146

T09 **Few-femtosecond dynamics of nitroanilines resolved by XUV-NIR spectroscopy**
Rocio Borrego-Varillas, Federico Vismarra, Yingxuan Wu, Daniele Mocci, fabian holzmeier, Maurizio Reduzzi, Pedro Recio, Javier Cachon, Jesús González-Vázquez, Alicia Palacios, Jose Santos, Matteo Lucchini, Nazario Martin, Fernando Martín, Luis Bañares, Mauro Nisoli 267

T10 **Molecular spin-orbit delays from attosecond photoionization**
Anna Wang, Jun Wang, Erik Isele, Philip Bucksbaum, James Cryan 269

T11 **Multi-resolution 'CookieBox' electron time-of-flight spectrometer for spectral diagnostics and molecular dynamics in the attosecond regime at LCLS**
Razib Obaid, Andrei Kamalov, Averell Gatton, Taran Driver, Xianchao Cheng, Justin James, Jean-Charles Castagna, Dileep Bhogadi, James Cryan, Wolfram Helm, Markus Ilchen, Peter Walter, Ryan Coffee 270

T12 **Direct observation of transient excitation and dissociation dynamics of methyl iodide by two-color time resolved photo-electron spectroscopy**
Mariusz Lejman, Dominique Platzer, Alice Autuori-Génaud, David Bresteau, Thierry Ruchon, Jérôme Palaudoux, Francis Penent, Pascal Lablanquie, Gildas Goldsztejn, Loïc Journel, Renaud Guillemin, Oksana Travnikova, Tatiana Marchenko, Denis Cubaynes, Marc Simon, Pascal Salières, Basile Wurmser, Richard Taïeb, Jérémie Caillat 147

T13 **Rotating the rotationless: Laser-induced dynamics of the 4He dimer**
Jan Kruse, Maksim Kunitski, Qingze Guan, Dörte Blume, Reinhard Dörner 148

T14 **Carbon KLL normal Auger induced femtosecond nonradiative decay cascade in tropone dication ($C_7H_6O_2^+$)**
Kaoru Yamazaki, Katsumi Midorikawa 271

T15 **Molecular photoionization time delays**
Adrián Jesús Suñer Rubio, Roger Bello, Alicia Palacios, Fernando Martín 272

T16 **Capturing correlation effects in molecular XUV ionisation**
Karl Michael Ziems, Jakob Bruhnke, Volker Engel, Stefanie Gräfe 273

T17 **Young's type formula for p-s wave interference of core-level PA-MFPADs of hetero-diatomic molecules based on multiple scattering theory**
Fukiko Ota, Kaoru Yamazaki, Didier Sébilleau, Kiyoshi Ueda, Keisuke Hatada 274

T18 **Recent advances in the first principle simulation of attosecond XUV pump - XUV probe ionization spectra**
Gilbert Grell, Jesús González-Vázquez, Piero Decleva, Alicia Palacios, Fernando Martín 275

T19 **A Polarization-Consistent R-matrix Model for molecular photoionization and electron scattering**
Thomas Meltzer, Zdeněk Mašín 276

T20 **Probing autoionization and dissociation at conical intersections with photoelectron spectroscopy and interferometry**
Dipayan Biswas, James K. Wood, Alexander Plunkett, Arvinder Sandhu 149

T21 **Femtosecond-resolved chiroptical switching in methyl-lactate**

Vincent Wanie, Etienne Bloch, Erik P. Månsson, Lorenzo Colaizzi, Krishna Saraswathula, Sergey Ryabchuk, François Légaré, Andrea Trabattoni, Valérie Blanchet, Marie-Catherine Heitz, Nadia Ben Amor, Yann Mairesse, Bernard Pons, Francesca Calegari 150

T22 **Attosecond time delays in the body frame for photodetachment of polyatomic anions**
C. William McCurdy, Robert Lucchese, Thomas Rescigno 277

T23 **Strong-field dissociation of CO_2^+**
Hung Hoang, Uwe Thumm 278

T24 **On-the-Fly Ab Initio Semiclassical Evaluation of Electronic Coherences in Polya-tomic Molecules Reveals a Simple Mechanism of Decoherence**
Nikolay Golubev, Tomislav Begusic, Jiri Vanicek 279

T25 **Attosecond Intramolecular Scattering and Vibronic Delays**
Luca Argenti, Bejan Ghomashi, Nicolas Douguet 280

T26 **Search for long-lasting electronic coherence using on-the-fly ab initio semiclassical dynamics**
Alan Scheidegger, Jiri Vanicek, Nikolay Golubev 281

T27 **Ultrafast dynamics in the photoionization of chiral molecules**
Loren Greenman, Esteban Goetz, Isaac Yuen 282

T28 **Ion-Photoelectron Entanglement Controlled with Attosecond Pulse Pairs**
Jun Wang 151

T29 **On the use of the weak-field asymptotic theory to simulate strong-field ionization of molecules including excited state effects**
Imam Wahyutama, Denawakage Jayasinghe, Francois Mauger, Mette B Gaarde, Kenneth Lopata, Kenneth J Schafer 283

T30 **Ab initio simulation of photoelectron energy spectra emitted from molecules based on the time-dependent configuration-interaction-singels method**
Yuki Orimo, Teramura Takuma, Takeshi Sato, Kenichi L. Ishikawa 284

T31 **Mapping Static Core-Holes and Ring-Currents with X-ray Scattering**
Andrés Carrascosa, Mengqi Yang, Haiwang Yong, Lingyu Ma, Adam Kirrander, Peter Weber, Kenneth Lopata 285

T32 **On the generation of electronic ring currents by circularly polarized light**
Oriol Vendrell 286

T33 **Time-dependent multicomponent optimized coupled-cluster method for nonadiabatic electro-nuclear dynamics**
Takeshi Sato, Yuki Orimo, Yang Li, Kenichi Ishikawa 287

T34 **Revisiting the Born approximation in the context of electron energy loss spectroscopy**
Marin Sapunar, Zdeněk Mašín . . . 288

T35 **Electron-ion interaction for the strong field ionization of H_2**
Angelina Geyer, Ofer Neufeld, Daniel Trabert, Umberto De Giovannini, Max Hofmann, Nils Anders, Lothar Schmidt, Markus S. Schöffler, Angel Rubio, Till Jahnke, Maksim Kunitski, Reinhard Dörner, Sebastian Eckart . . . 289

T36 **Characterization of light-induced potentials in the strong-field dissociation of O_2^+**
Uwe Thumm, Paul Abanador . . . 153

T37 **Attosecond dynamics in O_2 with ASTRA, a transition-density-matrix approach to molecular ionization**
Carlos Marante, Juan Martín Randazzo, Heman Gharibnejad, Barry I. Schneider, Jeppe Olsen, Luca Argenti . . . 154

T38 **Coherent Control of Extreme Ultraviolet Emission Generated Through Frustrated Tunneling Ionization**
Yang Hwan Kim, Hyeok Yun, Seong In Hwang, Chang Hee Nam, Kyung Taec Kim . . . 290

T39 **Universal enhancement of high-order above threshold ionization across laser wavelengths**
Abraham Camacho Garibay, Kenneth Talbert, Cosmin Blaga, Kenneth J Schafer, Pierre Agostini, Louis DiMauro . . . 291

T40 **Imaging photo-induced dynamics using Laser-Induced Electron Diffraction**
Matthew Robinson, Evangelos Karamatskos, Joss Wiese, Jolijn Onvlee, Arnaud Rouzee, Jochen Küpper . . . 292

T41 **Attosecond pump-probe spectroscopy of quantum electronic coherence**
Marco Ruberti . . . 155

T42 **Theory behind the real-time imaging of resonant photoemission dynamics**
Alice Autuori-Génaud, Dominique Platzer, Mariusz Lejman, Guillaume Gallician, Lucie Maëder, Antoine Covolo, Lea Bosses, Malay Dalui, David Bresteau, Jean-François Hergott, Olivier Tcherbakoff, Hugo J B Marroux, Vincent Loriot, Franck Lepine, Lionel Poisson, Pascal Salières, Jérémie Caillat . . . 156

T43 **Temporal characterization of two color laser fields using tunneling ionization**
Kyung Taec Kim, Jeong-uk Shin, Wosik Cho, Rajaram Shrestha . . . 293

T44 **Strong field ionization of chiral molecules in co- and counter-rotating two-color laser fields**

Max Hofmann, Daniel Trabert, Jan Kruse, Jonas Rist, Angelina Geyer, Nils Anders, Lothar Ph. H. Schmidt, Till Jahnke, Maksim Kunitski, Markus S. Schöffler, Reinhard Dörner, Sebastian Eckart 294

T45 **Dissociation dynamics of HeH^+ isotopologues in intense laser fields**
Saurabh Mhatre, Florian Oppermann, Manfred Lein, Stefanie Gräfe 297

T46 **Stationary molecular R-matrix approach for above-threshold multi-photon ionization and the coupling delay in RABITT processes**
Jakub Benda, Zdeněk Mašín, Jimena Gorfinkiel 157

T47 **Three-Sideband RABBITT in Argon: Experiment and Theory**
Divya Bharti, Hemkumar Srinivas, Farshad Shobeiry, Robert Moshammer, Thomas Pfeifer, Kathryn Hamilton, Klaus Bartschat, Anne Harth 158

T48 **Strong-field ionization and a practical approach to molecular tunneling ionization theory: a case study of butadiene**
Anh-Thu Le, Vu Ngoc Tuoc 300

T49 **Analysis of correlations in strong field ionization**
Igor Ivanov, Kyung Taec Kim 301

T50 **Angle-resolved phases in photoemission: from atomic to molecular systems**
Roger Bello, Fernando Martín 159

T51 **Attosecond electron dynamics near the ionization threshold in Ne**
Kathryn Hamilton, Klaus Bartschat, Matteo Moioli, Hamed Ahmadi, David Busto, Dominik Ertel, Ioannis Makos, Marvin Schmoll, Maria M. Popova, Elena V. Gryzlova, Alexei N. Grum-Grzhimailo, Maxim D. Kiselev, Sergey N. Yudin, Claus Dieter Schröter, Robert Moshammer, Thomas Pfeifer, Giuseppe Sansone 160

T52 **Complexity of the holographic structures induced by strong field laser pulses in atomic targets**
Abdelmalek Taoutioui, Károly Tőkési 302

T53 **Non-dipole effects in strong-field detachment from negative ions**
Resad Kahvedzic, Stefanie Gräfe 303

T54 **Modeling molecular break-up processes under short and intense laser pulses**
C-H Yuen, P Modak, C-D Lin 304

T55 **Spectral Signature of Molecular Charge Migration**
Rubén Fernández Carbón, Luca Argenti 161

T56 **Frustrated tunneling dynamics in ultrashort laser pulses**
Edvin Olofsson, Stefanos Carlström, Jan Marcus Dahlström 305

T57 **High-resolution time-of-flight electron spectrometry with time-dependent retarding potentials**

Gabriel Granveau and Charles Bourassin-Bouchet 307

T58 **Petahertz optical valley switches**
Alvaro Jimenez Galan, Rui Silva, Giulio Vampa, Mikhail Yu. Ivanov 133

T59 **Observation of light driven band structure via multi-band high harmonic spectroscopy**
Ayelet Uzan, Nirit Dudovich 134

T60 **Competition of anomalous and interband polarization contributions to high-harmonic generation in solids**
Lun Yue, Mette B Gaarde 308

T61 **Two-color-driven enhanced high-order harmonic generation in solids**
Francisco Navarrete, Uwe Thumm 309

T62 **Tracing dissociation dynamics and ultrafast cooling in liquid pyridine using time-resolved X-ray absorption spectroscopy**
Tadas Balciunas, Yi-Ping Chang, Zhong Yin, Cedric Schmidt, Vit Svoboda, Thomas Penfold, Jean-Pierre Wolf, Hans Jakob Wörner 135

T63 **Uncovering the mechanism of high-harmonic generation in liquids**
Angana Mondal, Ofer Neufeld, Zhong Yin, Zahra Nourbakhsh, Vit Svoboda, Angel Rubio, Nicolas Tancogne-Dejean, Hans Jakob Wörner 136

T64 **Spatial phase shifts in the near-field of plasmonic nanoparticles play a key role for the direct photoexcitation of dark states in aggregates**
Fabian Dröge, Klaus Renziehausen, Ulf Peschel, Alexander Schubert, Stefanie Gräfe 310

T65 **Light-wave coherent control of the Mott transition.**
Eduardo B. Molinero, Rui E.F. Silva 311

T66 **Photoexcited electron and hole dynamics in ZnTe and $ZnTe_xSe_{1-x}$ alloys**
Jonathan Michelsen, Hanzhe Liu, Isabel Klein, Sage Bauers, Andriy Zakutayev, Scott Cushing 137

T67 **Dynamical band imaging of simultaneous light-dressed Volkov state and pho-to-induced carrier state in WSe_2 using high-harmonic-based Tr-ARPES**
Ryo Yoshioka, Yasushi Shinohara, Takuya Okamoto, Yoji Kunihashi, Keiko Kato, Hiroki Mashiko, Yoshiaki Sekine, Hiroki Hibino, Ikufumi Katayama, Jun Takeda, Katsuya Oguri 138

T68 **Many-body effects during high harmonic generation in 1D solids**
Ethan Winchester, Rachel Cooper, Jeremy Gulley 313

T69 **Ultrafast XUV Magnetic Circular Dichroism: Observing Spin Transport at Interfaces**

Robert Baker, Martin Schutlze, Harshad Gajapathy, Savini Bandaranayake, Emily Hruska, Stephen Londo 139

T70 **Attosecond pulse and crystal band reconstruction with symmetry-aware deep neural networks**
Nikolai Klimkin, Álvaro Jiménez Galán, Rui Silva, Mikhail Yu. Ivanov 140

T71 **Wavelength dependence of high-order haronic generation in a single atomic layer and bulk semiconductors**
Viacheslav Korolev, Vipin Krishna, Mohammad Monfared, Thomas Lettau, Amin Sadeghifaraz, Elnaz Irani, Christian Hünecke, Giancarlo Soavi, Christian Spielmann, Ulf Peschel, Stefanie Gräfe, Daniil Kartashov 141

T72 **Development of Two-Color Sub-Femtosecond Pump/Probe Techniques with X- ray Free-Electron Lasers**
Zhaoheng Guo 314

T73 **Isosteric molecules in the time-domain**
M Pollanka, C A Schröder, P Scigalla, M Mittermair, A Duensing, and R Kienberger 315

T74 **Electron Correlation Effects in High Harmonic Generation in ZnO Studied with Dynamical Mean-Field Theory and Time-Dependent Density-Functional Theory**
Didarul Alam, N Ud Din, Michael Chini, Volodymyr Turkowski 316

T75 **A Stereo-ATI approach for few-cycle pulse characterization and control**
Dominik Hoff 317

T76 **Improved initial conditions of the strong-field ionized electron and their reconstruction from the detected momentum of the electron**
Szabolcs Hack, Szilárd Majorosi, Mihály Benedict, Sándor Varró, Attila Czirják . . . 318

T77 **Quantum interference in strong-field ionization by a linearly polarized pulse explains non-zero tunnel exit momentum**
Attila Czirják, Szabolcs Hack, Szilárd Majorosi, Mihály Benedict, Sándor Varró . . . 319

T78 **Coherent diffractive extreme-ultraviolet generation from nanostructured silica $CIPe_4$**
Sylvianne Roscam Abbing, Radoslaw Kolkowski, Zhuang-Yan Zhang, Filippo Campi, Lars Lötgering, Femius Koenderink, Peter Kraus 320

T79 **Intra- and intercycle interferences in ω-2ω strong field ionization: Phase delays**
Diego Arbó, Sebastián López 321

T80 **Phase delays in ω-2ω above-threshold ionization of atomic argon**
Sebastián López, Stefan Donsa, Joachim Burgdörfer, Diego Arbó 322

T81 **Self-induced splitting of Zn $K\alpha$ emission line**
Špela Krušič, Andrej Mihelič, Klemen Bučar, Matjaž Žitnik 323

T82 **Petahertz-bandwidth amplifier for the XUV/X-ray attosecond pulses based on IR-field-dressed plasma-based X-ray laser**
Vladimir Antonov, Ilias Khairulin, Mikhail Ryabikin, Olga Kocharovskaya 324

T83 **High-Harmonic Spectroscopy of Dynamical Symmetries in Graphene**
Navdeep Rana, Mrudul MS, Gopal Dixit 325

Effect of the shot-to-shot variation on charge migration induced by sub-fs X-Ray free-electron laser pulses

G Grell[1,2]*, Z Guo[3,4], T Driver[4,5], P Decleva[6,7], E Plésiat[1,2], A Picón[2], J González-Vázquez[2,8], P Walter[4], J P Marangos[9], J P Cryan[4,5], A Marinelli[3,4], A Palacios[2,8] and F Martín[1,2,10]†

[1]Instituto Madrileño de Estudios Avanzados en Nanociencia (IMDEA), Madrid, 28049, Spain
[2]Departamento de Química, Módulo 13, Universidad Autónoma de Madrid, Madrid, 28049, Spain
[3]Stanford University, Stanford, 94305, CA, USA
[4]SLAC National Accelerator Laboratory, Menlo Park, 94025, CA, USA
[5]Stanford PULSE Institute, SLAC National Accelerator Laboratory, Menlo Park, 94025, CA, USA
[6]Istituto Officina dei Materiali (CNR-IOM), 34149 Basovizza - Trieste, Italy
[7]Dipartimento di Scienze Chimiche e Farmaceutiche, Universitá di Trieste, 34127 Trieste, Italy
[8]Institute for Advanced Research in Chemistry (IAdChem), Universidad Autónoma de Madrid, Madrid, 28049, Spain
[9]The Blackett Laboratory Extreme Light Consortium, Imperial College London, London, SW7 2AZ, United Kingdom
[10]Condensed Matter Physics Center (IFIMAC), Universidad Autónoma de Madrid, Madrid, 28049, Spain

TP

Synopsis Theoretical study regarding the attosecond charge migration in para-aminophenol following sub-fs soft X-Ray ionization at 260 eV. The relative importance of the shot-to-shot variation of the XFEL pulses as well as the inclusion of ground state nuclear effects has been assessed based on ionization calculations carried out with the static-exchange B-spline DFT method.

Recently, X-Ray free electron lasers (XFELs) have been demonstrated to be capable of producing sub-fs soft X-Ray pulses, using the method of X-Ray laser-enhanced attosecond pulse generation implemented at the LCLS facility [1]. This finally grants access to tunable soft X-Ray pulses, carrying a much higher intensity than their respective high harmonic generation (HHG) counterparts, to conduct nonlinear X-Ray spectroscopies of attosecond electron dynamics. However, most XFELs build up their pulses from noise via self-amplified spontaneous emission, which introduces a stochastic shot-to-shot variation of the fields in terms of temporal envelope, phase, and intensity. This characteristic is absent in the more conventional HHG sources and its impact on studies of molecular attosecond charge migration is not yet known.

We address this problem with a first principles theoretical study of the ultrafast charge dynamics induced in the para-aminophenol molecule (NH_2-C_6H_4-OH) by ionization with an ensemble of 100 sub-fs 260 eV X-Ray pulses generated from start-to-end simulations of the XFEL at the LCLS. The ionization amplitudes for each of these pulses have been evaluated with the static-exchange B-spline DFT method that has been successfully applied in previous studies at lower photon energies [2, 3].

For a single molecular geometry we find that the shot-to-shot variation reduces the amplitudes of the charge fluctuations by up to 35 % during the first 10 fs after the pump ionization. This is much weaker than the damping introduced by the nuclear zero point energy spread that is modeled by sampling over a set of geometries according to the nuclear Wigner distribution of the molecule. The latter effect leads to a considerable damping of the charge dynamics, in particular beyond the first 3 fs after the ionization by the pump.

These results show that the shot-to-shot variation does not significantly affect the charge migration induced by 260 eV pulses in para-aminophenol. In a broader picture these findings may suggest that attosecond soft X-Ray spectroscopies, as those available at the LCLS [1], can be reliably used to investigate charge dynamics at their early stages.

References

[1] Duris J *et al. Nat. Phot.* **14**, 30 (2020)
[2] Calegari F *et al. Science* **346**, 336 (2014)
[3] Lara-Astiaso M *et al. J. Phys. Chem. Lett.* **9**, 4570 (2018)

*E-mail: gilbert.grell@imdea.org
†E-mail: fernando.martin@imdea.org

Photochemical dynamics of gaseous CH_2I_2 induced by an intense UV pulse

Y Ding[1], L Greenman, B D Esry, D Rolles, and A Rudenko

J. R. Macdonald Laboratory, Kansas State University, Manhattan, KS 66506

TP

Synopsis The ultrafast UV-induced dynamics of gas-phase CH_2I_2 are studied by coincident ion momentum imaging in combination with molecular dynamics calculations. Both experiment and theory show a dominance of direct dissociation after C-I bond cleavage along with a minor pathway leading to transient geometries that resemble the ground-state CH_2I-I isomer.

We conduct a joint experimental-theoretical study on CH_2I_2 in the gas phase[1]. The experiment is conducted using an ultrafast UV pump - IR probe strategy with different delays to study the time-dependent dynamics of CH_2I_2 molecule. A Coulomb explosion measurement indicates multiple reaction channels after UV absorption.

To calculate the dynamics, we build accurate CH_2I_2 potential energy surfaces based on more than 200,000 grid points. We identified several conical intersections between the lowest three surfaces as well as a metastable isomer on the ground surface[2].

Assuming a Franck-Condon transition to the first- and second-excited surfaces, we then carry out trajectory calculations using initial conditions sampled from a classical partition function for the ground surface in the harmonic approximation. These trajectory calculations show while most molecules directly dissociate with one photon absorption, a small fraction leads to geometries resembling the ground-state isomer. The extent to which the results can be compared with experiment will be discussed along with some of the limitations of the calculations themselves.

This work is supported by the Chemical Sciences, Geosciences, and Biosciences Division, Office of Basic Energy Sciences, Office of Science, US Department of Energy under Award No. DE-FG02-86ER13491.

References

[1] B. Kaderiya, Y. Ding, F. Ziaee, E. Wang, K. Borne, S. Bhattacharyya, N. Marshall, T. Severt, P. Kanaka Raju, I. Ben-Itzhak, B. D. Esry, L. Greenman, D. Rolles, A. Rudenko, *unpublished*.

[2] V. A. Borin *et al.*, Phys. Chem. Chem. Phys., 18, 28883 (2016).

[1]E-mail: dingy@ksu.edu

Photoelectron and ion momentum imaging of molecules excited by ultrashort vacuum ultraviolet pulses

D S Slaughter[1]*, K A Larsen[1,2], R Y Bello[1], N Shivaram[1], C W McCurdy[1,3], P Ranitovic[1], R R Lucchese[1], and Th Weber[1]

[1]Chemical Sciences Division, Lawrence Berkeley National Laboratory, Berkeley, California 94720, USA
[2]Graduate Group in Applied Science and Technology, University of California, Berkeley, California 94720, USA
[3]Department of Chemistry, University of California, Davis, California 95616, USA

Synopsis Competing vacuum ultraviolet photoexcitation paths, populating identical electronic states but producing discrete or continuous reaction product energies depend strongly on the molecular orientation. The paths are distinguished by ion fragment momentum imaging, using cross-polarized ultrashort two-color near infrared and vacuum ultraviolet laser pulses. Reactions driven by the absorption of two vacuum ultraviolet photons, including resonant and non-resonant ionization are also investigated by electron-ion coincidence momentum imaging and ab initio theory.

We report recent advances in ion momentum imaging, and electron-ion coincidence momentum imaging, using ultrashort vacuum and extreme ultraviolet pulses produced by high-order harmonic generation (HHG).

By momentum imaging of ion fragments produced in a 2-color cross-polarized ultrashort laser pulse absorbed by D_2, two different four-step dissociative ionization pathways after four-photon absorption were found to produce dissociative D^+ with very low kinetic energies and rich angular structure (Figure 1), with both pathways being excitation by one vacuum ultraviolet (VUV, 13.95 eV) and three near infrared (NIR, 1.55 eV) photons. Ab initio electronic structure and time-dependent Schrödinger equation calculations, and angular momentum, energy and parity conservation allowed the identification of the excited neutral molecular states and molecular orientations relative to the polarization vectors in these different photoexcitation and dissociation sequences. One sequential photodissociation pathway selects molecules aligned parallel to the light propagation direction. The other pathway dominates for molecules aligned perpendicular to the light propagation direction but not along either of the two light polarization vectors.

Using ultrashort near-ultraviolet pulses to drive HHG, we investigate 2-photon excitation of high-lying electronic states, including dissociative ion pair states in O_2 that compete with autoionization, and we demonstrate photoelectron momentum imaging with ion detection in coincidence. Future prospects for ultrafast time-resolved molecular-frame photoelectron imaging experiments will be discussed.

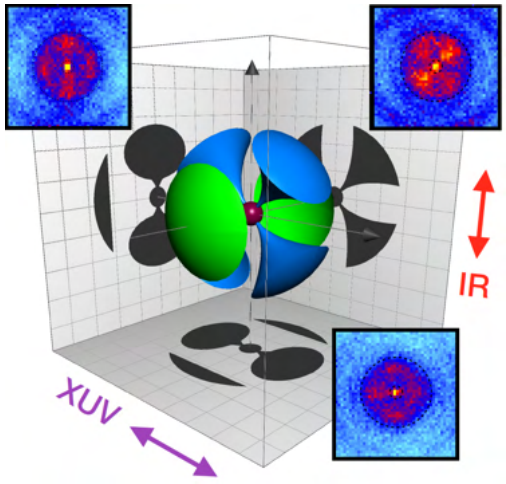


Figure 1. 3-dimensional D^+ ion momentum distribution measured from dissociative photoionization of D_2 by a 2-color cross-polarized ultrashort laser pulse.

References

[1] D S Slaughter, F P Sturm, R Y Bello, K A Larsen, N Shivaram, C W McCurdy, R R Lucchese, L Martin, C W Hogle, M M Murnane, H C Kapteyn, P Ranitovic, and TH Weber Phys. Rev. Research **3**, 033191 (2021).

*E-mail: DSSlaughter@lbl.gov

Photoelectron spectroscopy using a synthetically chiral laser pulse

Z Dube[1]*, G Katsoulis[2], Y Mi[1], T Wang[1], G Ernotte[1], A Yu Naumov[1], D M Villeneuve[1], P B Corkum[1], A Emmanouilidou[2], and A Staudte[1]†

[1]National Research Council Canada, Ottawa, 100 Sussex Drive, Ottawa, Canada
[2]University College London, London, WC1E 6BT, UK

Synopsis Using a four-pulse, synthetically chiral pulse scheme, we study the photoelectron distributions to compare simple and complex responses in Cold Target Recoil Ion Momentum Spectroscopy: argon atoms and propylene oxide, a chiral molecule.

Chiral enantiomers are notoriously difficult to differentiate as they have the same chemical and physical properties, yet they often have dramatically different biochemical functionality. Circularly polarized light has been shown to be able to distinguish between them, but the sensitivity is low, on the order of a few percent signal difference [1]. The reason for the weak optical response is that the wavelength is large compared to the molecule, and therefore the field appears two-dimensional. In 2019, Ayuso et al proposed a multi-pulse scheme to create an optical field with a locally chiral, i.e., a 3-dimensional electric field component. This scheme was predicted to yield a 100% signal difference between enantiomers in the high harmonic signal [2]. The predicted giant effect in the high harmonic spectrum so far remains untested by experiment. On the other hand, it is also unclear how sensitive the photoelectron response will be to the above scheme. In this work, we present the preliminary results of photoelectron measurements taken with a Cold Target Recoil Ion Momentum Spectroscopy (COLTRIMS) machine using this scheme, observing both a simple atom and a chiral molecule.

References

[1] R Cireasa *et al.*, Nat Phys, **11**, 654 (2015).
[2] D Ayuso *et al.*, Nat Phot, **13**, 866 (2019).

*E-mail: zack.dube@gmail.com
†E-mail: andre.staudte@nrc.ca

Few-femtosecond dynamics of nitroanilines resolved by XUV-NIR spectroscopy

R. Borrego-Varillas[1]*, F. Vismarra[1,2], Y. Wu[1,2], D. Mocci[1,2], F. Holzmeier[2,3],M. Reduzzi[1,2], P. Recio[4], J. Cachón[4], J. González-Vázquez[5], A. Palacios[5], J. Santos[6,7], M. Lucchini[1,2], N. Martín[6,7], F. Martín[5,7], L. Bañares[4,7] and M. Nisoli[1,2]

[1]IFN-CNR, Piazza Leonardo da Vinci 32, 20133 Milano (Italy)
[2]Department of Physics, Politecnico di Milano, Piazza Leonardo da Vinci 32, 20133 Milano (Italy)
[3]imec, 3001, Leuven (Belgium)
[4]Departamento de Química Física, Universidad Complutense de Madrid, 28040 Madrid (Spain)
[5]Departamento de Química, Universidad Autónoma de Madrid, Cantoblanco 28049 Madrid (Spain)
[6]Departamento de Química Orgánica I, Universidad Complutense de Madrid, 28040 Madrid (Spain)
[7]IMDEA-Nanoscience, C/ Faraday, 9, Campus de Cantoblanco, 28049 Madrid (Spain)

TP

Synopsis The dynamics triggered by photo-ionization in nitroanilines, the simplest donor/ acceptor systems, are investigated with unprecedented temporal resolution. We resolve the role of the donor charge density, the position of the acceptor group and the length of the aromatic chain.

The full comprehension of photoinduced electron transfer (ET) and charge transfer (CT) in molecules requires real-time imaging of the electronic motion, which takes place on attosecond to few-femtosecond time scales [1]. By using time-resolved photo-ion spectroscopy, we here investigate the ultrafast dynamics initiated by a short train of attosecond pulses (<2 fs) and probed with a 5-fs near-infrared (NIR) pulse in nitroanilines, the simplest prototype donor and acceptor systems.

Figure 1 shows the investigated systems: p-nitroaniline (PN), m-nitroaniline (MN), N,N-dimethyl-4-nitroaniline (DN), 4-amino-4'-nitrobiphenyl (ANB) and 4-dimethylamino-4'-nitrobiphenyl (DANB). Ions related to the fragmentation of the benzene rings, with a mass/charge ratio m/z = 63 ($C_5H_3^+$) and m/z = 50 ($C_4H_2^+$), show a clear dependence on the length of the chromophoric chain with the smaller molecules presenting a faster decay. Methylated samples (DN and DANB) show a similar trend for the CH_3^+ fragment (m/z = 15). Figure 1 shows as an example the time-of-flight spectrum of the fragment NO^+ (m/z=30). Due to the broad kinetic energy distribution of the fragment, the spectrum is composed by a central peak (KE_0 in Fig. 1) and two side peaks (KE_- and KE_+). Ultrafast dynamics (Fig. 1b) with a decay time constant of about 30 fs are observed in all cases for the side peaks. Instead, PN does not exhibit any dynamics at the central peak. Similar dynamics are observed for the NO_2^+ fragment (m/z=46) for all the molecules.

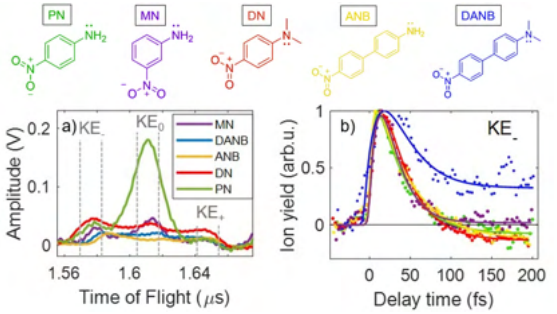


Figure 1. Chemical structures. NO^+ photofragment: a) mass spectra and b) ion yield as a function of the delay (fits in solid lines).

The NO^+ and NO_2^+ dynamics can be interpreted in terms of two different dissociation processes. A first fragmentation channel, responsible for the central peak, involves the generation of NO^+ and the radical $C_6H_4NH_2$. The side peaks, instead, are assigned to Coulomb explosion of the NO fragment coming from a double ionization process and it is therefore an imprint of the dication dynamics. This interpretation is in agreement with experiments performed with synchrotron radiation in nitrobenzene[2].

Our results open the way to the investigation and control of ET and CT in push-pull molecules at the electronic time scale.

References

[1] M. Nisoli, et al., Chem. Reviews 117, (2017).
[2] L. Cooper, Int. J. Mass Spectrometry 207, (2001).

*E-mail: rocio.borregovarillas@cnr.it

Ultrafast dissociation in C_2H_4 and C_2D_4 induced by XUV attosecond pulse trains

M Vacher[1], A Boyer[2], V Loriot[2], F Lépine[2] and S Nandi[2] *

[1]Nantes Université, CNRS, CEISAM UMR 6230, F-44300 Nantes, France
[2]Univ de Lyon, Univ Claude Bernard Lyon 1, CNRS, Institut Lumière Matière, F-69622, Villeurbanne, France

TP

Synopsis Following ionization by a few-femtosecond extreme-ultraviolet pulse, a polyatomic molecule can be left into highly excited cationic states, making the ensuing relaxation process hard to decipher. Here, we show that a molecule and its isotopologue reacts differently to the incident radiation, despite no difference in their ground electronic state. The observed difference in relaxation timescales between the two systems, which is supported by non-adiabatic dynamics simulations, allows us to obtain a mechanistic view of the underlying process.

Following the pioneering works of A. H. Zewail, femto-chemistry experiments have provided many important insights about light-induced dynamics in complex molecules. These experiments usually involve resonantly exciting a particular electronic state in a molecule using ultraviolet or, visible laser pulses, and following its relaxation in the neutral system. With the advent of high-order harmonic generation (HHG) based sources providing ultrashort coherent pulses in the extreme ultraviolet (XUV) domain, it is now possible to investigate dynamical processes in highly excited *photo-ionized* species. Pioneering examples include small diatomic molecules [1] as well as large polyatomic molecules [2,3].

Here, we used an attosecond pulse train, produced via HHG in Kr, as pump to ionize and excite ethylene molecule (C_2H_4) and its deuterated counter-part (C_2D_4). A near infrared (NIR) pulse was used to probe the subsequent relaxation dynamics. We collected the resulting ionic fragments as a function of the delay between the XUV-pump and NIR-probe. The H^+ and D^+ fragments display a fast decay of a few tens of femtoseconds in their delay-dependent yields. However, the extracted time-constants (τ) show that τ_{H^+} is faster by almost 7±2 fs compared τ_{D^+} [see Fig. 1(a)], irrespective of the NIR-probe intensity. Our findings are supported by advanced trajectory surface hopping based calculations, which show that the number of H-loss trajectories increases at a much faster rate compared to the number of D-loss trajectories [see Fig. 1(b)]. This is because the heavier D-atom takes longer time compared to the lighter H-atom to dissociate completely. Utilizing the observed isotope effect, we could identify the relevant nuclear co-ordinate governing the relaxation pathway in the XUV-ionized molecules [4].

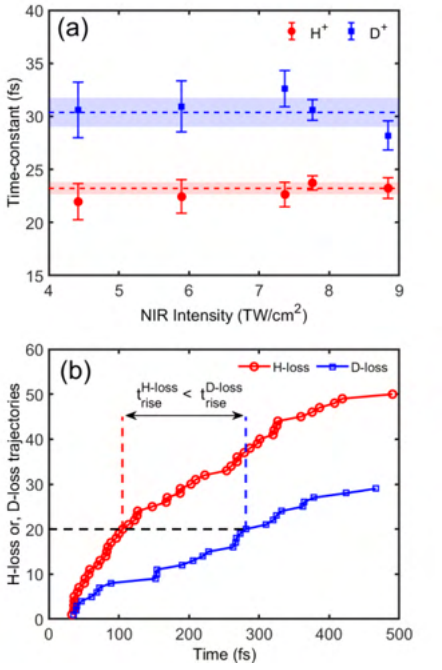


Figure 1. (a) Time-constants for H^+ and D^+ fragments at different probe intensities. (b) The number of trajectories for H-loss in C_2H_4 and D-loss in C_2D_4 following ionization by an ultrashort XUV pulse.

References

[1] Sansone G *et al* 2010 *Nature* **465** 763
[2] Calegari F *et al* 2014 *Science* **346** 336
[3] Hervé M *et al* 2021 *Nature Physics* **17** 327
[4] Vacher M *et al* 2022 *submitted*

* E-mail: saikat.nandi@univ-lyon1.fr

Molecular spin-orbit delays from attosecond photoionization

A. L. Wang[1,2]*, J. Wang[1,2], E. R. Isele[1,2], P. H. Bucksbaum[1,2,3], and J. P. Cryan[1,4]

[1]Stanford PULSE Institute, SLAC National Accelerator Laboratory, Menlo Park, California 94025, USA
[2]Department of Applied Physics, Stanford University Stanford, California 94305, USA
[3]Department of Physics, Stanford University Stanford, California 94305, USA
[4]Linac Coherent Light Source, SLAC National Accelerator Laboratory, Menlo Park, California 94025, USA

TP

Synopsis We study the effect of molecular dynamics on spin-orbit delays in photoionization of methyl-iodide. The photoemission delays are measured using RABBITT, an interferometric technique that uses an attosecond pulse train to interrogate photoionization dynamics. We compare the photoemission delays of methyl-iodide to delays in xenon, which has similar spin-orbit structure, to isolate the effects of attosecond molecular physics on spin-orbit channel coupling.

Photoemission delays can help us determine the limits of our models and approximations for photoionization of molecules. Here we use RABBITT measurements of photoemission delays [1] to examine how spin-orbit delays, which have been previously observed in Xe [2], are altered by attosecond molecular physics. Comparing measurements of the photoemission delay from CH_3I to those from Xe can help us identify and separate the molecular physics of CH_3I as opposed to effects common to both targets.

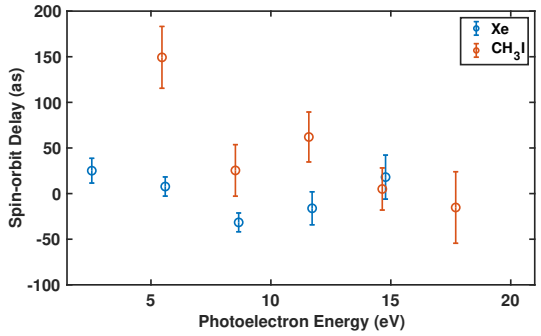


Figure 1. Comparison of spin-orbit delays, defined as $\tau^{(2)}_{3/2} - \tau^{(2)}_{1/2}$. The measurements from this study, Xe and CH_3I, are in blue and orange circles.

The results of our measurements in Xe and CH_3I are shown in the figure. All values are spin-orbit delays, which are the difference between delays to the $X_{3/2}$ and $X_{1/2}$ states of the cation. Spin-orbit delays from Xe have been studied previously [2], and our results agree well with those findings. Our measurements show a clear difference in spin-orbit delays between Xe and CH_3I, particularly for delays between 5 eV and 12 eV. The observed behavior in the different targets could result from the differing nuclear charge between the Xe and I atoms, but it is more likely due to molecular effects. The effect of the molecular potential, as opposed to the centrosymmetric Coulomb-like potential of an atom, can be seen in the increase of delay in higher energy photoelectrons in CH_3I compared to Xe, marking an increase in the reach of the short-range potential scattering contribution. In addition to the overall shape of the scattering potential, adding molecular bonding alters the electronic structure and spin-orbit states of CH_3I compared to Xe, and introduces nuclear motion. All of these would affect channel coupling during photoionization, which is imprinted on the photoemission delay. Our future work in photoemission delays from electronically excited, dissociating CH_3I may shed light on the extent of these effects on spin-orbit delays.

This work was supported by the U.S. Department of Energy (DOE), Office of Science, Office of Basic Energy Sciences (BES), Chemical Sciences, Geosciences, and Biosciences Division (CSGB).

References

[1] P. M. Paul, E. S. Toma, P. Breger, G. Mullot, F. Augé, Ph. Balcou, H. G. Muller and P. Agostini, Science **292** 1689-1692 (2001).
[2] I. Jordan, M. Huppert, S. Pabst, A. S. Kheifets, D. Baykusheva, H. J. Wörner, Phys. Rev. A , **95**, 013404 (2017).

*E-mail: annaliw@stanford.edu

Multi-resolution 'CookieBox' electron time-of-flight spectrometer for spectral diagnostics and molecular dynamics in the attosecond regime at LCLS

R Obaid[1]*, A Kamalov[1], A Gatton[1], T Driver[1], D Bhogadi[1], J-C Castagna[1], X Cheng[1], J Cryan[1], W Helml[2], M Ilchen[3], P Walter[1], and R Coffee[1]

[1]SLAC National Accelerator Laboratory, Menlo Park, 94025, USA. [2]Technische Universitat Dortmund, Dortmund, Germany. [3]European XFEL GmbH, Schenefeld, Germany.

TP

Synopsis
In this presentation, we report the commissioning of an angular array of electron time-of-flight spectrometer and its corresponding attosecond science outlook in terms of shot-by-shot diagnostics and photochemistry.

We report the commissioning of an angular array of electron time-of-flight spectrometer intended for non-invasive spectral, temporal, and polarization characterization of single shots of high-repetition rate, short wavelength Free-Electron Lasers (FELs), such as the LCLS-II at SLAC National Accelerator Laboratory. LCLS-II is the next generation FEL capable of providing multi-color, multi-polarization, and multiple x-ray pulses with temporal control in the attosecond timeframe. Thus, there is a significant need for single shot diagnostics of such pulses with attosecond temporal resolution well below the expected LCLS-II energy bandwidth that will allow for wide and adjustable energy acceptance windows. Such a resolution for instance would allow the single shot identification of well seeded shots versus SASE background. With such diagnostics, we can train an inference model running on a shot-by-shot basis with unstreaked measurement in the front-end-enclosure (FEE) of the FELs providing ground truth for downstream science case measurement.

Furthermore, with this multi-resolution capable spectrometer array, we are addressing the need for an instrument to provide high repetition rate science for attosecond resolution electron spectroscopy using angular streaking and multi-color x-ray pulses. Given that correlated electron motion is a core topic for LCLS-II, the attosecond resolution of single-shot photo and Auger electron time-dependent emission spectra is sure to reveal the atto-science proposed for the future of FELs, and easily covers the chemical science in the few femtosecond regime.

The array of spectrometers and the end-station are specifically designed for the Time-resolved Atomic, Molecular and Optical science end station (TMO) at LCLS-II. The designed spectrometers are capable of providing minimally chromatic electrostatic lensing and independently controlled retardation enabling simultaneous angle-resolved photo-electron and Auger electron spectroscopy with high energy resolution. Moreover, they are designed to ensure energy resolution of 0.25 eV across an energy window of up to 75 eV which can be individually centered via the adjustable retardation to cover ranges of electron kinetic energies relevant to soft x-ray regime. Additionally, by interleaving detector retardation we are able to analyze angular emission patterns of both photo-electrons and Auger electrons in the same shot. As designed, this spectrometer array is able to provide non-invasive and online spectral-polarimetry measurements, polarization-sensitive attoclock spectroscopy for characterizing the full time–energy structure of SASE or seeded LCLS-II pulses, while supporting emerging trends in molecular frame spectroscopy measurements.

References

[1] P Walter et al., J. Sync. Rad. 28, 5 (2021).
[2] G Hartmann et al., Rev. Sci. Inst. 87 (2016).
[3] N Hartmann et al., Nat. Phot. 12 (2018).
[4] J Viefhaus et al., Nucl. Instrum. Meth. 710 (2013).

*E-mail: robaid@slac.stanford.edu

Carbon *KLL* normal Auger induced femtosecond nonradiative decay cascade in tropone dication ($C_7H_6O^{2+}$)

K. Yamazaki[1,2]*, and K. Midorikawa[1]

[1]RAP, RIKEN, Wako, 351-0198, Japan; [2]PRESTO, JST, Kawaguchi, 332-0012, Japan

Synopsis We found that tropone dications ($C_7H_6O^{2+}$) created by carbon KLL normal Auger decay undergo nonradiative decay cascade via 10-10^2 dicationic states with time constant $\tau_{\rm NRD} \sim 10^2$ fs using surface hopping nonadiabatic reaction dynamics simulations. The value of $\tau_{\rm NRD}$ strongly depends on the initial dicationic states.

TP

The excited dications of organic molecules created by x-ray induced core photoemission and subsequent Auger decay [1, 2] undergo nonradiative decay (NRD) to lower-lying states via many intermediate states, and result in fragmentation [3, 4, 5]. The time scale and number of electronic states involved in the NRD in x-ray generated dication are the keys to clarify the early stage of such multi-state x-ray induced nonadiabatic reaction dynamics both experimentally and theoretically[4, 5]. In this study, We simulated the carbon KLL normal Auger induced NRD in tropone dication ($C_7H_6O^{2+}$) via surface hopping nonadiabatic reaction dynamics simulations.

The diabatic population of two-hole dicationic states in tropone dication $\{|\Psi_{\rm d}\rangle\}$ generated by carbon KLL normal Auger decay (time constant $k_{\rm Auger}^{-1} = 5.8$ fs [6]) process in incoherent limit $\mathbf{P}(t)$ is written as a function of time t [7],

$$\mathbf{P}(t) = g(t, s_{\rm pu}) \star \Theta(t)[1 - \exp(-k_{\rm Auger}t)]\tilde{\mathbf{P}}(t), \quad (1)$$

where $g(t, s_{\rm pu})$ is the envelope function of a Gaussian pump pulse with the full width half maximum (FWHM) of $s_{\rm pu} = 10$ fs, "$\star$" represents convolution, $\Theta(t)$ is the Heaviside step function, and $\tilde{\mathbf{P}}(t)$ is the diabatic population of $\{|\Psi_{\rm d}\rangle\}$ in sudden ionization limit. The $\tilde{\mathbf{P}}(t)$ were evaluated by the surface hopping nonadiabatic reaction dynamics simulation using the linear-vibronic coupling (LVC) model Hamiltonian [8, 9]. The initial population $\tilde{\mathbf{P}}(t = 0)$ is set to be proportional to relative intensity of the Auger decay calculated by the two-hole population analysis [1, 2, 10]. The Auger intensities and parameters of LVC model Hamiltonian were evaluated by the state-averaged CASSCF theory.

The carbon KLL normal Auger decay dominantly creates singlet dications by $t = 20$ fs (Figure 1). The cascade of NRD immediately starts just after the ionization processes. Tropone dications ionized to the band **I** located at two-electron binding energy of $E_{\rm 2eb}$ = 30-40 eV at the Franck-Condon geometry decay to the lower-lying band via $\sim$ 30 states with the NRD time constant of $\tau_{\rm NRD}$ = 206 fs, and those ionize to band **II** at $E_{\rm 2eb}$ = 40-50 eV decay to band **I** via $\sim$ 100 dicationic states with $\tau_{\rm NRD}$ = 266 fs according to our global fitting analysis on $\tilde{\mathbf{P}}(t)$.

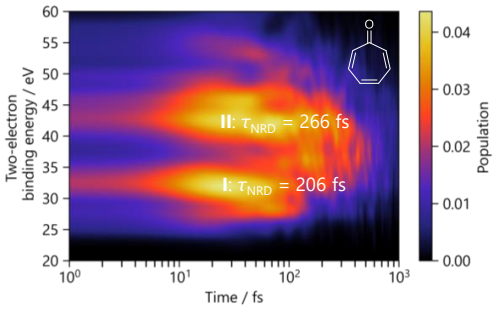


Figure 1. The diabatic population $\mathbf{P}(t)$ of tropone dication as a function of t and $E_{\rm 2eb}$.

References

[1] Li Z *et al* 2017 *Phys. Rev. Lett.* **115** 143002
[2] Inhester L. *et al* 2018 *J. Phys. Chem. Lett.* **9** 1156-1163
[3] Liekhus-Schmaltz C *et al* 2015 *Nat. Commun.* **6** 8199
[4] Li Z *et al* 2017 *Nat. Commun.* **8** 453
[5] Kukk E *et al* 2021 *Phys. Rev. Res* **3** 013221
[6] Epshtein M *et al* 2020 *J. Phys. Chem. A* **124** 9524–9531
[7] Fukuzawa H et al 2019 *Nat. Commun.* **10**, 2186
[8] Plasser F *et al* 2019 *Phys. Chem. Chem. Phys.* **21**, 57-69
[9] May S *et al* 2014 *J. Chem. Phys.* **140** 204302
[10] Mitani M et al 2003 *J. Electron Spectros. Relat. Phenomena.* **128** 103–111

*E-mail: kaoru.yamazaki@riken.jp

Molecular photoionization time delays

A J Suñer-Rubio[1]*, R Y Bello[1,2], A Palacios[1,3]† and F Martín[1,2,4]

[1]Departamento de Química, Módulo 13, Universidad Autónoma de Madrid, 28049 Madrid, Spain
[2]Instituto Madrileño de Estudios Avanzados en Nanociencia, Cantoblanco, 28049 Madrid, Spain
[3]Institute of Advanced Research in Chemical Sciences, Universidad Autónoma de Madrid,28049 Madrid, Spain
[4]Condensed Matter Physics Center, Universidad Autónoma de Madrid, 28049 Madrid, Spain

TP

Synopsis Attosecond electron streaking and Reconstruction of Attosecond Beating By Interference of Two-photon Transitions (RABBITT) are the most succesfull experimental strategies to extract photoionization time delays. In this work, full dimensional simulations have been performed to extract molecular photoionization time delays, investigating the dependencies with the nuclear degrees of freedom. The hydrogen molecular ion has been employed as benchmark system.

The observation of electronic motion in real time remained a challenge over the years, since it opens unforeseen ways to track and manipulate matter. In the last decades, the first light pulses with durations comparable to the time scale of electronic motion, *i.e.* a few attoseconds (1 as $= 10^{-18}$ s), were generated [1, 2, 3]. Thus, it is nowadays possible to obtain real-time images of the formation and breaking of chemical bonds or to quantify the electron dynamics upon excitation or ionization processes. In a photoionization event, the electron is ejected from an atom or a molecule after the interaction with an electromagnetic field. However, the emission is not instantaneous. How long does the electron wave packet require to escape? This is defined as photoionization time delay. The most successful experimental strategies to extract these photoionization time delays in atoms are the attosecond electron streaking [4, 5, 6] and the RABBITT technique [7, 8]. Both techniques use a pump-probe scheme, combining attosecond pulses with IR fields, to characterize the electronic wave packet, accessing the ultrafast dynamical information. The former uses a single pulse as a pump, while the latter uses a train of pulses.

However, scarce works have been performed in molecules [9, 10, 11, 12, 13] and a solid theoretical ground to understand the physical meaning of a photoionization time delay when the electron is coupled to the nuclear degrees of freedom is still to be developed. We employ as benchmark system the simplest molecule, the hydrogen molecular ion. The dependencies with the nuclear degrees of freedom are investigated by performing, for the first time, full dimensional simulations to extract molecular photoionization time delays using the above-mentioned techniques.

References

[1] P Agostini and L F DiMauro, Rep. Prog. Phys. **67**, 813 (2004).
[2] P Corkum and F Krausz, Nat. Phys. **3**, 381 (2007).
[3] F Krausz and M. Ivanov, Rev. Mod. Phys. **81**, 163 (2009).
[4] E Constant et al., Phys. Rev. A **56**, 3870 (1997).
[5] J Itatani et al., Phys. Rev. Lett. **88**, 173903 (2002).
[6] E Goulielmakis et al., Science **305**, 1267 (2004).
[7] P M Paul et al., Science **292**, 1689 (2001).
[8] H G Muller, Appl. Phys. B **74**, s17 (2002).
[9] G Sansone et al., Nature **465**, 763 (2010).
[10] F Calegari et al., Science **346**, 336 (2014).
[11] R Pazourek et al., Rev. Mod. Phys. **87**, 765 (2015).
[12] D Baykusheva and H J Wörner, J. Chem. Phys. **146**, 124306 (2017).
[13] S Nandi et al., Sci. Adv. **6**, eaba7762 (2020).

*E-mail: adrian.sunner@uam.es
†E-mail: alicia.palacios@uam.es

Capturing correlation effects in molecular XUV ionisation

K M Ziems[1,2] *, J Bruhnke[1] †, V Engel[3] and S Gräfe[1,2,4]

[1] Friedrich-Schiller-Universität Jena, 07743 Jena, Germany
[2]Max Planck School of Photonics and Abbe Center of Photonics, 07743 Jena, Germany
[3]Bayerische Julius-Maximilians-Universität Würzburg, 97074 Würzburg, Germany
[4]Fraunhofer Institute for Applied Optics and Precision Engineering, 07745 Jena, Germany

TP

Synopsis We employ a molecular model system to investigate electron-nuclear correlation effects in XUV ionisation and their impact on the post-ionisation dynamics and photoelectron distribution by means of numerically solving the time-dependent Schrödinger equation. Commonly applied approximations are tested for their potential to resolve the exact dynamics.

Understanding the correlated electronic motion on its intrinsic, attosecond timescale and the interplay with nuclear degrees of freedom is at the heart of attosecond science that strives to deepen our fundamental understanding of chemical systems [1]. Ionisation by attosecond XUV pulses induces complex correlated dynamics: firstly, the creation of coherent electron wavepackets in the parent ion comprised of electronic states in a large energy window; secondly, the correlation of electronic and nuclear wavepackets during and after the ionisation process; thirdly, the continuum dynamics of the emitted photoelectron. Additionally, the bound dynamics prior to ionisation have to be assessed. Finally, the question of how these processes are imprinted on observables is of utmost importance to experimentally resolve and analyse these complex dynamics in real-time.

Since the complete description of the ionisation and coherent post-ionisation dynamics of molecules is a many-particle problem dominated by electron and nuclear correlation, it demands the highest level of theory. However, solving the time-dependent nuclear-electronic Schrödinger equation is only feasible for few electron atoms or small molecular model systems. Here, we aim at providing a systematic study of the attosecond XUV-induced ionisation dynamics in molecules by means of numerically solving the time-dependent Schrödinger equation for a quantum model system, consisting of two electrons and one nucleus, restricted to move in one dimension each (the polarisation direction of the XUV pulse) (see Fig. 1) [2].

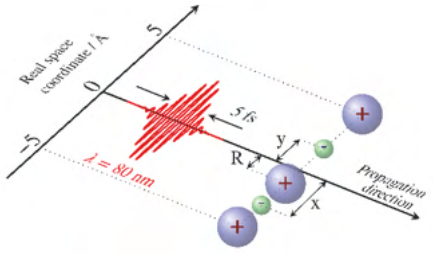


Figure 1: Extended Shin-Metiu model system comprised of two fixed outer and one moving nucleus, and two moving electron interaction wih a XUV pulse

Our work is divided in two topics. Firstly, we report on the effect of nuclear-electron correlation pre, during, and post ionisation. Upon ionisation, the nuclear momentum is conserved in the post-ionisation dynamics and imprinted on the photoelectron spectrum's asymmetry, thus, yielding an observable to measure the correlated nuclear and electron momentum behavior [3]. Secondly, we aim to give methodological guidance for future simulations by carefully dissecting which approximations can be introduced while still recovering the full picture of the coherent electron and nuclear dynamics. To this end, we employ time-dependent perturbation theory, semiclassical dynamics, treating the nuclei classically or even frozen, different continuum approximations, Condon approximation, and the sudden approximation.

To summarize, using a model system we describe nuclear-electron correlation effects for XUV ionisation and assess the capabilities of commonly applied approximations.

References

[1] Corkum B 2007 *Nature Physics* **3** 381
[2] Fröbel F 2020 *J. Phys.B.* **53** 14405
[3] Falge M 2012 *J. Phys. Chem. Lett.* **18** 2617

* E-mail: karl-michael.ziems@uni-jena.de
† E-mail: jakob.bruhnke@uni-jena.de

TP

Young's type formula for p-s wave interference of core-level PA-MFPADs of hetero-diatomic molecules based on multiple scattering theory

F Ota[1]*, K Yamazaki[2,3], D Sébilleau[4], K Ueda[5], K Hatada[1]†

[1]Department of Physics, University of Toyama, 3190 Gofuku, Toyama 930-8555, Japan
[2] Institute for Materials Research, Tohoku University, 2-1-1 Katahira, Aoba-ku, Sendai 980-8577, Japan
[3] RIKEN Center for Advanced Photonics, RIKEN, 2-1 Hirosawa, Wako, Saitama, 351-0198, Japan
[4] Institut de Physique de Rennes, UMR UR1-CNRS 6251, Université de Rennes, F-35000 Rennes, France
[5]Graduate School of Science, Tohoku University, 6-3 Aramaki Aza-Aoba, Aoba-ku, Sendai 980-8578, Japan

Synopsis We derived a p-s wave interference variation of Young's double-slit formula for the polarization-averaged molecular frame core-level photoelectron angular distribution (PA-MFPADs) of hetero-diatomic molecules, which may be used to extract bond lengths. The C-O bond lengths retrieved from the PA-MFPADs via this formula reproduce the original bond length used in the reference *ab-initio* PA-MFPADs within the relative error of 5 %. We expect it to be used to retrieve the bond length for time-resolved PA-MFPADs.

The PA-MFPADs, obtained by coincidence measurements of photoelectrons emitted from a K shell in a molecule by linearly polarized x-ray irradiation and fragment ions, contain structural information of the molecule. Therefore, the measurements of PA-MFPADs using an x-ray free electron laser, which delivers extremely short x-ray pulses down to hundreds of attoseconds, allow us to visualize ultrafast temporal variations of structure. Here, we report our theoretical studies of PA-MFPADs of hetero-diatomic molecules, that undergo ultrafast dissociation [1].

Employing the multiple scattering theory with the plane wave, muffin-tin, and single-scattering approximations, the pattern which appears in the photoemission angle dependence of PA-MFPADs can be interpreted to be originated by the interference of the direct- and single-scattered photoelectron wave, similar to p- and s-wave. According to this theoretical model, we obtain the following Young's type formula,

$$R \sim \frac{(\Delta N - 1)\pi}{k\,(\cos\theta_F - \cos\theta_B)} + \beta, \qquad (1)$$

where R is the bond length, k is the wavenumber of the photoelectron, and θ_F and θ_B are the angles of either the peaks or valleys in the PA-MFPADs that are closest to the forward or backward, respectively. ΔN is the difference between the numbering of the peaks or valleys at θ_F and θ_B from the forward. The constant β depends on k but not on R. In Coulomb scattering model, it becomes $\beta = -Z/k^2$, where Z is the atomic number of the scattering atom.

Figure 1 shows that the C-O bond lengths estimated from the *ab-initio* PA-MFPADs by Eq. (1) reproduce the original ones within a relative error of 5%. Eq. (1) is expected to be used for bond length analysis for PA-MFPADs obtained by femtosecond time-resolved measurements.

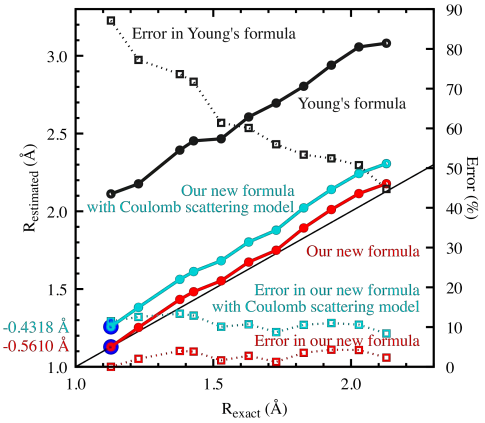


Figure 1. Bond lengths estimated with Young's formula (black), Eq. (1) with β by Coulomb scattering model (light blue), and fitting at the equilibrium distance (red). Corresponding errors from the exact values of the straight black line are also shown with the same combination of colors.

References

[1] Ota F *et al* 2021 *J. Phys. B* **54** 024003, *ibid.* 084001, *ibid.* 244002.

*E-mail: oofukiko@gmail.com
†E-mail: hatada@sci.u-toyama.ac.jp

Recent advances in the first principle simulation of attosecond XUV pump - XUV probe ionization spectra

G Grell[1,2]*, J González-Vázquez[2,3], P Decleva[4], A Palacios[2,3] and F Martín[1,2]†

[1]Instituto Madrileño de Estudios Avanzados en Nanociencia (IMDEA), Madrid, 28049, Spain
[2]Departamento de Química, Módulo 13, Universidad Autónoma de Madrid, Madrid, 28049, Spain
[3]Institute for Advanced Research in Chemistry (IAdChem), Universidad Autónoma de Madrid, Madrid, 28049, Spain
[4]Istituto Officina dei Materiali (CNR-IOM), 34149 Basovizza - Trieste, Italy

Synopsis We present recent advances in the development of a protocol for the first principles simulation of attosecond pump – attosecond probe spectroscopies in the regimes of XUV and soft X-Ray photon energies. The protocol combines the CASPT2 method to treat the bound molecular states and the static exchange B-spline DFT method to model the pump and probe photoionization amplitudes with the trajectory surface hopping method to simulate the coupled electron nuclear motion between the pump and probe ionization steps. The protocol is scrutinized for several molecules and different pump-probe setups.

Recently, tunable sub-fs soft X-Ray (SXR) pulses became available at the LCLS X-Ray free electron laser (XFEL) at intensities that exceed those of current SXR high harmonic generation (HHG) sources by several orders of magnitude [1]. This overcomes the current intensity restriction of HHG based attosecond XUV pump-probe experiments to using XUV or SXR pulses as either the pump *or* the probe fields and thus paves the way for attosecond nonlinear X-Ray spectroscopic experiments that employ sub-fs SXR pulses for both pumping *and* probing ultrafast electron dynamics in molecules.

To identify these dynamics in transient spectra high level simulations covering (i) the ionization by the sub-fs SXR pump, (ii) the ensuing coupled electron-nuclear dynamics, and (iii) the interaction with the sub-fs SXR probe are desirable tools. However, each of the steps (i)-(iii) marks a formidable challenge already on its own. Their combination in a single study severely limits the tractable system size, in particular if the transient probe photoionization spectrum is sought after, which mandates an additional, more involved, ionization calculation for the probe step.

In this contribution we report an approach that marks a trade-off between computational cost and accuracy to facilitate the complete treatment (i)-(iii) in simulating sub-fs pump-probe photoionization spectra from XUV to SXR photon energies for small organic molecules. To this end, we employ complete active space wave functions with perturbative correlation energy correction (CASPT2) to describe the molecular bound states of the neutral, cationic and dicationic species, respectively. Further, the pump and probe ionization amplitudes are evaluated by a Dyson orbital approach, where the continuum states of the outgoing electron are obtained with the static exchange B-spline DFT method based on respective CASPT2 densities. Finally, the coupled electron-nuclear dynamics between the pump and probe interactions is modeled with the fewest switches trajectory surface hopping method, where an ensemble of trajectories represents the nuclear zero point energy spread.

The performance of the outlined protocol will be scrutinized for different molecules and various spectroscopic setups. Facilitating sub-fs XUV and SXR pulses, the dynamics induced by the pump ionization of valence orbitals are interrogated by probing either valence ionization, or core ionization, respectively. In addition to that we are going to study the performance of further simplifications to the outlined protocol, such as neglecting the motion of the nuclei and disregarding the explicit evaluation of the continuum states for the probe ionization step, i.e., the sudden approximation.

References

[1] Duris J *et al. Nat. Phot.* **14**, 30 (2020)

*E-mail: gilbert.grell@imdea.org
†E-mail: fernando.martin@imdea.org

TP

A Polarization-Consistent R-matrix Model for molecular photoionization and electron scattering

T Meltzer and Z Mašín *

Institute of Theoretical Physics, Faculty of Mathematics and Physics, Charles University, V Holešovičkách 2, 180 00 Prague 8, Czech Republic

Synopsis We have developed a new R-matrix model, polarization-consistent coupled Hartree-Fock (PC-CHF), for studying photoionization and electron-molecule scattering processes in a wide range of molecules. We find that our new model provides significantly improved results compared to standard Static Exchange plus Polarization (SEP) calculations, and furthermore, that the results demonstrate acceptable agreement with more expensive Close-Coupling calculations. This allows us to study increasingly larger systems.

Photoionization and electron-molecule collisions are important processes that occur throughout our Universe. We are interested in describing these processes in biological systems. One system of interest is the formic acid dimer which is a likely precursor to life on Earth and one of the simplest prototypes for a dihydrogen bonded system.

Photoionization and electron scattering are distinct but related phenomena that can both be aptly described using the R-matrix method, as implemented in the UKRMol+ code [1]. To date, most R-matrix calculations using the UKRMol+ codes have largely focused on small and intermediate-sized molecules, for which we have a set of well established models – ranging from simple Static-Exchange (SE) to more sophisticated Close-Coupling (CC) models. For larger molecules, however, or systems comprising of several monomers we are typically restricted to SE or SEP calculations.

In our most recent work [2] we find that the SEP model is completely inappropriate for describing photoionization due to a large amount of spurious resonances that occur in the low-energy region. A similar effect is observed in electron-scattering calculations but it is usually less severe [3]. Our PC-CHF model eliminates the spurious resonances of the SEP model by explicitly coupling all of the polarization configurations to their corresponding final ionic states, as can be seen in Figure 1.

The PC-CHF model is designed to sit conceptually between SEP and CC calculations. Whilst the CC model is capable of producing very accurate results it can quickly become unwieldy for larger systems. In addition it requires non-trivial optimization of several parameters which is not the case of the PC-CHF model. In this work, we present our latest results for electron-scattering and photoionization for the formic acid dimer using the PC-CHF model.

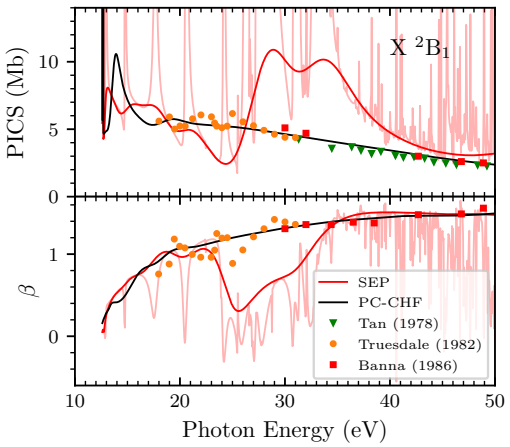


Figure 1. H_2O photoionization cross-section (top) and asymmetry parameter (bottom) for transition into the ground ionic state X $^2B_1$. Smoothed (red solid) and raw (light red) R-matrix calculation using the SEP model compared with PC-CHF results (black solid) and experimental data (see [2] and references therein).

References

[1] Mašín Z *et al* 2020 *CPC* **249** 107092
[2] Meltzer T *et al* 2022 *J. Phys. B* (accepted)
[3] Morgan L A *et al* 1997 *J. Phys. B* **30** 4087–4096

*E-mail: zdenek.masin@utf.mff.cuni.cz

Attosecond time delays in the body frame for photodetachment of polyatomic anions

C W McCurdy[1,2]*, **T N Rescigno** [1] **and R R Lucchese**[1]

[1]Chemical Sciences Division, Lawrence Berkeley National Laboratory, Berkeley, 94720, USA
[2]Department of Chemistry, University of California, Davis , Davis, CA, 95616, USA

Synopsis Attosecond time delays in the photodetachment of molecular anions, where molecular features are not obscured by an overall Coulomb phase, are explored in *ab initio* multichannel electron scattering calculations.

TP

The measurement of attosecond time delays in photoionization [1] has become a well-established probe of the interaction of the emitted electron with the residual ion. Observations of the delay, $\tau = \hbar \frac{\partial}{\partial E} \arg \left\{ \langle \Phi_{\mathbf{k}}^{(-)} | \sum_i \hat{\epsilon} \cdot \mathbf{r}_i | \Phi_0 \rangle \right\}$, measure the phase of the photoionization amplitude, and can reveal signatures of resonances and their interference with background scattering in the body frame [2]. However, the Coulomb phase, $\eta_l = \arg \Gamma(l + 1 + iZ/k)$, dominates photoionization time delays below photoelectron energies of a few eV and commonly obscures intrinsically molecular aspects of the delay.

Although few if any experiments have addressed time delays in photodetachment of polyatomic anions, we predict they will display time delays unobscured by Coulomb scattering and are therefore sensitive to the details of the correlated electron-neutral molecule scattering continuum. In the body-frame those delays can show signatures of the long range dipole potential as well as short range interactions. Measuring time delays for the photoemission of core or inner valence electrons would allow their observation in the body frame, because the neutral molecule produced with a core vacancy will undergo Auger decay and subsequently dissociate into at least one charged fragment. Coincidence measurements of the emmited electron and charged fragment could reveal the delays in the body frame of diatomics or linear molecules, and in the recoil frame for polyatomics.

We present *ab initio* calculations of time delays in the body frame for a range of ions including C_2^-, CN^-, BN^- and $HOCO^-$ together with analytical models showing how the long range dipole potential can be revealed in time delays at energies away from resonances.

*E-mail: cwmccurdy@ucdavis.edu

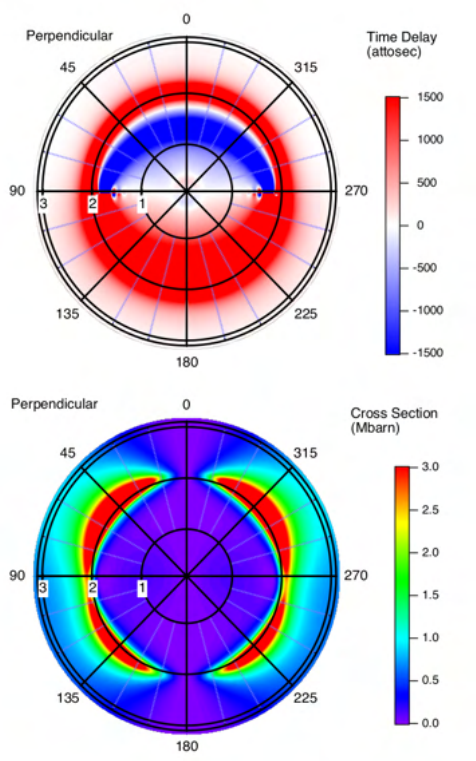


Figure 1. Time delay and electron angular distribution for photodetachment with polarization horizontal of CN^- (vertical) to produce $CN(1s^{-1})$.

The figure shows results of Complex Kohn Variational calculations for photodetachment of an N 1s electron, displaying a π d-wave resonance and dipole scattering effects as functions of energy (in eV) and angle.

References

[1] R Pazourek, S Nagele and J Burgdörfer, Rev. Mod. Phys. **87**, 765 (2015).
[2] F Holzmeier, J Joseph, J C Houver, M Lebech, D Dowek and R R Lucchese, Nature Comm. **12**, 7343 (2021).

Strong-field dissociation of CO_2^+

U Thumm* **and V-H Hoang**

Department of Physics, Kansas State University, Manhattan, Kansas 66506, USA

TP

Synopsis We theoretically investigated strong-field XUV-IR pump-probe dissociative ionization of CO_2.

We theoretically investigated strong-field XUV-IR pump-probe dissociative ionization of CO_2. Employing the multi-configurational self-consistent-field quantum-chemistry code GAMESS to *ab initio* calculate CO_2^+ adiabatic potential energy surfaces and dipole couplings, we numerically propagated the time-dependent Schrödinger equation for the nuclear motion. Distinguishing the effects of (velocity-dependent) non-adiabatic and external IR-field dipole couplings, we (A) calculated the population of the predissociative C $^2\Sigma_g^+$ state and kinetic energy release (KER) in $O+CO^+$ dissociation channel and (B) investigated the imprint on KER spectra of the nuclear dynamics near the A $^2\Pi_u$ and B $^2\Sigma_u^+$ conical intersection. Accounting for all vibrational normal modes (bending, symmetrical and anti-symmetrical stretch), our simulated fragment KER spectra and pump-probe-delay dependent CO^+ yield oscillation period are in good agreement with the experiment of Timmers et al. [1]. This agreement persists for reduced-dimensionality calculations with linear molecules (disregarding bending).

Supported under grant DEFG02-86ER13491 by the U.S. Department of Energy, Office of Science.

References

[1] H Timmers *et al.*, Phys. Rev. Lett. **113**, 113003 (2014).

*E-mail: thumm@phys.ksu.edu

On-the-Fly Ab Initio Semiclassical Evaluation of Electronic Coherences in Polyatomic Molecules Reveals a Simple Mechanism of Decoherence

N V Golubev*, T Begušić and J Vaníček†

Laboratory of Theoretical Physical Chemistry, Institut des Sciences et Ingénierie Chimiques, Ecole Polytechnique Fédérale de Lausanne (EPFL), CH-1015 Lausanne, Switzerland

TP

Synopsis Understanding the interplay between the nuclear rearrangement and ultrafast electronic motion requires a concerted description of the electron-nuclear dynamics. In this work, we show that a simple, single-trajectory semiclassical scheme can evaluate the electronic coherence time in polyatomic molecules accurately. The presented technique describes the decoherence with just two semiclassical parameters—the phase space distance and signed area between the trajectories moving on two electronic surfaces and thus reveals the physical mechanism of the process.

The recent progress in laser technologies has stimulated investigations of fundamental physics lying behind the electronic and nuclear dynamics of molecules. Many methods ranging from fully quantum multi-configurational time-dependent Hartree (MCTDH) to more approximate mixed quantum-classical and semiclassical techniques have been developed and applied for simulating polyatomic molecules.

Here, we use the thawed Gaussian approximation (TGA) [1], one of the simplest semiclassical approaches for molecular dynamics, to evaluate the influence of nuclear motion on the ultrafast electronic dynamics and to find a simple, yet detailed mechanism of decoherence, which is not available in basis set methods such as MCTDH.

We simulate coupled electron-nuclear dynamics taking place after outervalence ionization of propiolic acid (HC_2COOH). Figure 1 shows the electronic coherence evaluated by five different schemes where the dynamics was performed with the full quantum MCTDH method ("quantum") or with the semiclassical vertical Hessian TGA ("semiclass."), and either with the vibronic coupling ("VC") or on-the-fly ("OTF") Hamiltonian, both obtained at the *ab initio* many-body Green's function ADC(3) level of theory. All simulations except the "quantum VC" calculation employed the diabatic approximation ("diab."), which neglects nonadiabatic couplings between the diabatic states, or the adiabatic approximation ("adiab."), which neglects nonadiabatic couplings between adiabatic states.

Our simulations demonstrate that on the short timescale the TGA gives results almost identical to the full quantum MCTDH calculations [2]. In contrast to numerical quantum methods, the semiclassical TGA reveals the physical mechanism of decoherence beyond the general blame on nuclear motion. In addition, TGA can help breaking the "curse of dimensionality" appearing in the treatment of large systems and thus should be useful for preselecting molecules for experimental studies [3].

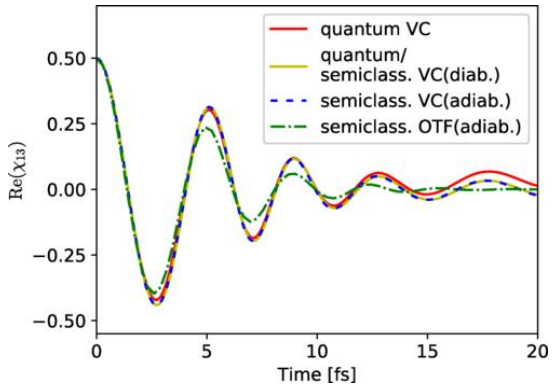


Figure 1. Comparison of various techniques for computing the electronic coherence measured by the time-dependent overlap $\chi_{13}(t)$ of the nuclear wave packets propagated on the first and third cationic states of propiolic acid after removal of a HOMO electron.

References

[1] Heller E J 1975 *J. Chem. Phys.* **62** 1544
[2] Golubev N V *et al* 2020 *Phys. Rev. Lett.* **125** 083001
[3] Scheidegger A *et al* 2022 *J. Chem. Phys.* **156** 034104

* E-mail: nik.v.golubev@gmail.com
† E-mail: jiri.vanicek@epfl.ch

Attosecond Intramolecular Scattering and Vibronic Delays

L Argenti[1]*, B Ghomashi[2], and N Douguet[3]

[1]Department of Physics & CREOL, University of Central Florida, Orlando, Florida 32816, USA
[2]University of Colorado at Boulder, Boulder, Colorado 80309, USA
[3]Department of Physics, Kennesaw State University, Marietta, Georgia 30060, USA

TP

Synopsis We study the temporal and vibrational signature of the nuclear recoil in the emission and intramolecular scattering of a photoelectron emerging from a localized orbital. We illustrate these phenomena in the ionization of the CO molecule from the C-1s orbital using an analytical model that reproduces the entangled character of the nuclear and electronic motion. We decompose the photoemission delay in its localization and resonant-confinement components. Photoionization by a short pulse results in a coherent vibrational ionic state delayed compared to the classical sudden-photoemission limit.

Understanding the interplay between the electron dynamics initiated by sudden photoionization and the slower nuclear motion that ensues is essential to describe the evolution of a molecule in the few femtoseconds that follow its ionization by an attosecond pulse. When a molecule is ionized by an x-ray photon from a localized core orbital, in particular, the emerging photoelectron collides with nearby nuclei giving rise to the well-known interference patterns of EXAFS spectroscopy [1]. Vibrationally resolved spectra bear the signature of the energy transferred to the nuclei by the intramolecular scattering process [2]. XFELS, make it now possible to study this phenomenon resolved in time.

In this work, we simulate the real-time dynamics of the CO molecule following the C-1s ionization induced by a coherent soft-x-ray pulse using a simplified 1D theoretical model. The vibrationally resolved photoemission delay results from the interplay between two different phenomena: the localization of the photoelectron at its birth and its resonant confinement by the two nuclei. A short pulse creates ions in partially coherent vibrational states, either in compression or in expansion, depending on the pulse central energy relative to confinement resonances. The vibrational delay, due to intramolecular scattering, is imprinted in the deviation of the nuclear Wigner distribution (WD) from the sudden-photoemission limit.

At selected energies, adjacent confinement resonances can be entangled via the vibrational state resulting in either negative or positive photoemission delay peaks. Moreover, ultrashort pulses result in controllable coherent ionic vibrational states that exhibit a delay with respect to the sudden-photoemission approximation, due to intramolecular photoelectron scattering.

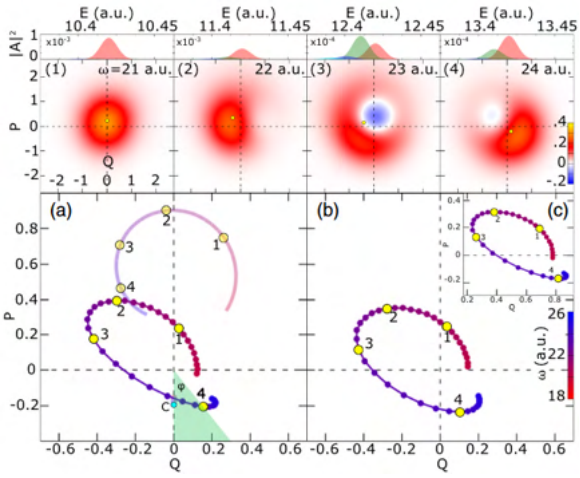


Figure 1. Photoelectron probability (top) and nuclear Wigner distributions (1-4) for the electron leaving from the carbon side. The central pulse frequency, ω, is scanned across a resonance ($\omega_{\rm res} \sim 22$ a.u.). The trajectory of the (Q,P) expectation value as a function of ω computed numerically (a), or analytically with the Fano model (b). The light colored arc is the resonant intramolecular-scattering component.

This work was supported by the NSF Grant N° PHY-1607588 and N° 1912507, and by the DOE CAREER Grant N° DE-SC0020311.

References

[1] B. Zimmermann *et al.*, Nat. Phys. 4, 649 (2008).
[2] E Plésiat *et al.*, Phys. Rev. A **85**, 023409 (2012).
[3] B Ghomashi, N Douguet, and L Argenti, Phys. Rev. Lett. **127**, 203201 (2021).

*E-mail: Luca.Argenti@ucf.edu

Search for long-lasting electronic coherence using on-the-fly ab initio semiclassical dynamics

A Scheidegger[1], J Vaníček[1], and N Golubev[1] *

[1]Laboratory of Theoretical Physical Chemistry, Institut des Sciences et Ingenierie Chimiques, Ecole Polytechnique Federale de Lausanne (EPFL), CH-1015 Lausanne, Switzerland

Synopsis Using a combination of high-level ab initio electronic structure methods with efficient on-the-fly semiclassical evaluation of nuclear dynamics, we performed a massive scan of small polyatomic molecules searching for a long-lasting oscillatory dynamics of the electron density triggered by the outer-valence ionization. We observed that in most of the studied molecules, either the sudden removal of an electron from the system does not lead to the appearance of the electronic coherence or the created coherences become damped by the nuclear rearrangement on a time scale of a few femtoseconds. However, we report several so far unexplored molecules with the electronic coherences lasting up to 10 fs, which can be good candidates for experimental studies. In addition, we present the full-dimensional simulations of the electronic coherences coupled to nuclear motion in several molecules which were studied previously only in the fixed nuclei approximation.

TP

Exposing a molecule to a short light pulse may bring this molecule to a nonstationary quantum state, thus launching a coupled dynamics of electronic and nuclear wave packets. Coherent superposition of multiple electronic states often results in ultrafast evolution of molecular observables, such as the electron density.

Our screening procedure consists of the following four steps: (I) the molecule of interest is downloaded from the PubChem database; (II) the ionic spectrum of the molecule at a fixed reference geometry is computed utilizing the non-Dyson version of the ADC scheme; (III) if the molecule has an appropriate ionic spectrum, namely, both sufficient energy gaps between ionic states and strong hole-mixing, an initial prescreening of the electronic coherences is performed using the TGA combined with the TDDFT; and (IV) the best candidates showing a long lasting coherence are verified by the TGA using the EOM-CC-IP.

As an example we show the results for but-3-ynal for which we simulated the ionization of the HOMO [Fig. 1(a)], populating the first and the third electronic states in proportion ≈81%/19%, respectively, according to the hole-mixing weights [Fig. 1(b)]. The evolution of electronic coherence created by such a superposition is shown in Fig. 1(c). The oscillations of the coherence gradually dephase within 10 fs. The hole density computed along the molecular axis of the but-3-ynal is shown in Fig. 1(d). The charge performs a couple of clear oscillations before being trapped by the nuclear motion and distributed along the molecular chain.

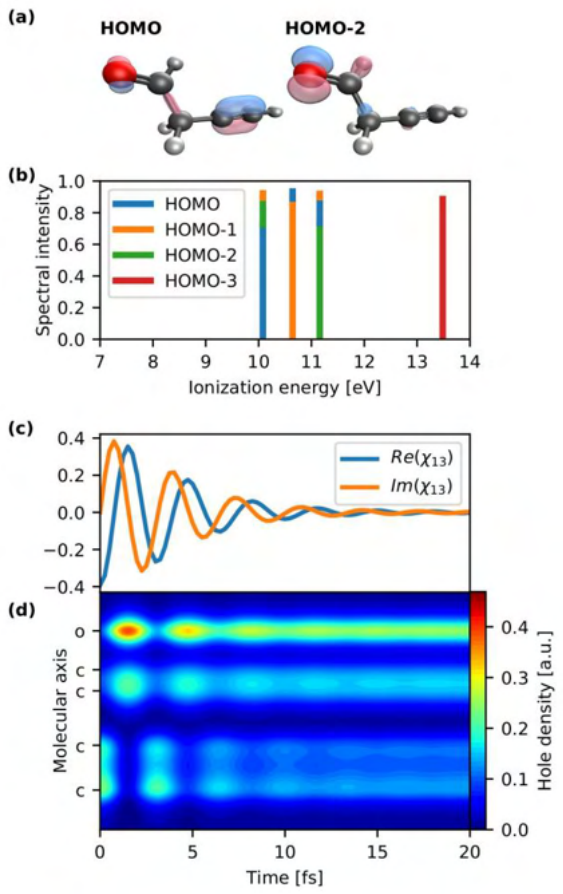


Figure 1. Ionization spectrum and the coupled electron–nuclear dynamics triggered by the ionization out of the HOMO of the but-3-ynal molecule. (a) HF molecular orbitals involved in the hole-mixing. (b) First four cationic states. (c) Time evolution of the electronic coherence between the first and the third cationic states created after removal of the HOMO electron. (d) Time evolution of the hole density along the molecular axis.

* E-mail: nik.v.golubev@gmail.com

Ultrafast dynamics in the photoionization of chiral molecules

L Greenman[1]*, R E Goetz[2], C-H I Yuen[1] and C P Koch[3]

[1]Kansas State University, Manhattan KS, 66503, USA
[2]Drake University, Des Moines IA, 50311, USA
[3]Freie Universität Berlin, Berlin, 14195, Germany

Synopsis Chiral molecules, those which break mirror symmetry, display their asymmetries in the photoelectron spectra. By time-resolving these effects, the ultrafast dynamics of these molecules can be examined.

Chirality is a property that distinguishes molecular physics from atomic physics. The mirror symmetry breaking of chiral molecules also gives them distinct fingerprints in photoelectron spectra. Photoelectron circular dichroism (PECD), the difference between the photoionization angular distributions of left- and right-circularly polarized light, is a key example. With ultrafast and attosecond laser sources, PECD can be addressed in a time-resolved manner. We have explored using this to enhanced PECD measurements, to differentiate whether chiral effects occur from bound or continuum states, and to examine the dependence of PECD measurements on the nuclear geometry of chiral molecules. In order to calculate PECD effects, we combine quantum chemistry with scattering theory using the ePolyScat code [1, 2] and time-dependent perturbation theory. Perturbed states are expanded in Gaussians, while the continuum states are expanded on spatial grids, allowing convergence to be captured for effects considered to be "in the continuum". The extent of the ability to converge such calculations will be presented.

References

[1] F A Gianturco, R R Lucchese, and N Sanna, J. Chem. Phys. **100**, 6464 (1994).
[2] A P P Natalense and R R Lucchese, J. Chem. Phys. **111**, 5344 (1999).

*E-mail: lgreenman@phys.ksu.edu

On the use of the weak-field asymptotic theory to simulate strong-field ionization of molecules including excited state effects

I S Wahyutama[1]*, D D Jayasinghe[2], F Mauger[1], M B Gaarde[1], K Lopata[2,3], and K J Schafer[1]

[1]Department of Physics and Astronomy, Louisiana State University, Baton Rouge, Louisiana 70803, USA
[2]Department of Chemistry, Louisiana State University, Baton Rouge, Louisiana 70803, USA
[3]Center for Computation and Technology, Louisiana State University, Baton Rouge, Louisiana 70803, USA

Synopsis We study weak-field asymptotic theory (WFAT) as an alternative to the time-dependent density functional theory (TDDFT) for simulating angle-resolved strong-field ionization. We show that WFAT is able to reproduce the general features of the TDDFT angle-dependent yield for molecules such as NO and OCS. The absence of limitations that TD methods using Gaussian basis sets have, such as long computation time and ionization leakage, makes WFAT an attractive option for qualitative studies of ionization. Additionally, we report the development of many-electron WFAT based on integral representation.

The intense interest in strong field ionization in molecules stems not just from recollision processes but also from the prospect that the observed photoelectron distributions can be associated with specific ultrafast electron dynamics occurring within a molecule. To understand the connection between the experimentally observed angle-resolved ionization yields and the electron dynamics within a molecule requires accurate computations of molecular strong field ionization, often over a wide range of molecular orientations and geometries.

In this work, we concern ourselves with a method of computing molecular tunnel ionization in strong, quasi-static fields called weak-field ionization theory (WFAT) [1]. We compare it to simulations using time-dependent density functional theory (TDDFT), which has been used to simulate strong field ionization in, for example, halomethanes [2]. Our motivation is the observation that calculating angle-resolved ionization yields with TDDFT, while accurate, is both time-consuming and, at low field amplitude, plagued by ionization leakage through the absorbing boundaries that must be used.

In WFAT the angular-resolved ionization rate is calculated as a function of the strong field amplitude and direction, and as such is not inherently time-dependent. It does not, however, suffer from either of the above limitations (long simulation times and leakage at low intensities). In this work, we show that angle-dependent ionization yield produced by WFAT can be used to represent the same quantity produced by time-dependent propagation with comparable results in many cases. In particular, we study a set of molecules, including NO and OCS, and compare the angle-dependent ionization yields obtained through TDDFT and WFAT.

An additional feature of strong field ionization is the excitation of some fraction of the molecules before ionization. In this regard, the experimental ionization yields must also include the angle-dependent yield from these excited states. To handle these excited state effects, we have extended the many-electron WFAT (MEWFAT) [3], that has been derived under the so-called *tail representation*, to the *integral representation*. In the tail representation, one is limited to diatomic and simple linear molecules. The integral representation of WFAT removes this limitation and thus allows access to the analysis of larger molecules and excited state effects using MEWFAT.

References

[1] A. I. Dnestryan and O. I. Tolstikhin, Phys. Rev. A **93**, 033412 (2016).
[2] P. Sandor, *et al.*, J. Chem Phys.**151**, 194308 (2019).
[3] O. I. Tolstikhin, L. B. Madsen, and T. Morishita, Phys. Rev. A **89**, 013421 (2014).

*E-mail: wahyutama1@lsu.edu

Ab initio simulation of photoelectron energy spectra emitted from molecules based on the time-dependent configuration-interaction-singels method

Y Orimo[1 *], T Teramura[1], T Sato[1,2,3], K L Ishiakwa[1,2,3]

[1] Graduate School of Engineering, The University of Tokyo, 7-3-1 Hongo, Bunkyo-ku, Tokyo, 113-8656, Japan
[2] Photon Science Center, School of Engineering, University of Tokyo, 7-3-1 Hongo, Bunkyo-ku, Tokyo 113-8656, Japan
[3] Research Institute for Photon Science and Laser Technology, University of Tokyo, 7-3-1 Hongo, Bunkyo-ku, Tokyo 113-0033, Japan

TP

Synopsis We present *ab initio* simulations of angle-resolved photoelectron energy spectra (ARPES) from molecules based on the time-dependent configuration interaction singles (TDCIS) method. To extract ARPES from real-time simulations, the time-dependent surface flux (tSURFF) method, an efficient computational scheme to extract angle-resolved photoelectron energy spectra, is applied to the TDCIS method.

In attosecond science, angle-resolved photoelectron energy spectra (AEPES) are one of the most important observables to experimentally investigate strong field and ultrafast phenomena induced by the light-matter interaction. To theoretically explore such phenomena, we have developed and implemented various *ab initio* approaches for simulations of multielectron dynamics in laser fields [1]. Among them, the time-dependent configuration interaction singles (TDCIS) method [2,3], which describes a total wavefunction by the configuration interaction (CI) expansion truncated at the singly-excited electronic configuration, has an advantage that it can consider multielectron dynamics including multichannel effects with a small computational cost. We have already successfully computed high harmonics generation from polyatomic molecules such as acetylene and propane with this method.

In this study, we realize *ab initio* simulations of photoelectron ARPES emitted from molecules by applying the time-dependent surface flux [4,5] method, which calculates photoelectron energy spectra by integrating flux of the wave function on a surface, to the TDCIS method. As a numerical application, we have simulated photoionization process of a nitrogen molecule exposed to a $\omega - 2\omega$ two-color laser pulse ($\hbar\omega = 12.4$ eV) and computed the photoelectron momentum distribution (Figure 1). In this simulation, the 3 highest occupied orbital energies are 16.9 eV, 17.3 eV, and 21.3 eV, and thus the photoelectron energies are expected to be 7.9 eV, 7.5 eV, and 3.5 eV based on Koopmans' theorem. These values are consistent with our result. This indicates that our implementation can successfully simulate the photoionization process and extract PES from the real-time simulation.

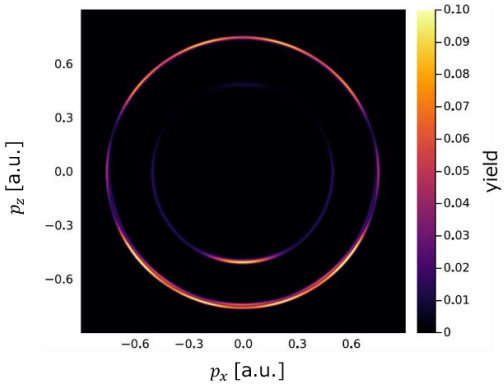


Figure 1. Photoelectron momentum distribution on the xz plane from a nitrogen molecule exposed to a $\omega - 2\omega$ two-color pulse with $\hbar\omega = 12.4$ eV. The photoelectron energies of the outer and inner peaks are 7.7 eV and 3.4 eV.

References

[1] Ishikawa K L, Sato T 2015 *IEEE J. Sel. Top. Quantum Electron.* **21**, 8700916
[2] Sato T, Teramura T, K L Ishikawa 2018 *Appl. Sci.* **8**, 433
[3] Teramura T, Sato T, Ishikawa K L 2019 *Phys. Rev. A* **100** 043402
[4] Tao L, Scrinzi A 2012 *New J. Phys.* **14**, 013021
[5] Orimo Y, Sato T, Ishiawa K L 2019 *Phys. Rev. A* **100**, 013419

* E-mail: ykormhk@atto.t.u-tokyo.ac.jp

Mapping Static Core-Holes and Ring-Currents with X-ray Scattering

A M Carrascosa[1], M Yang[2], H Yong[1], L Ma[1], A Kirrander[3], P M Weber[1] and K Lopata[2,4]*

[1] Department of Chemistry, Brown University, Providence, 02912, USA.
[2] Department of Chemistry, Louisiana State University, Baton Rouge, 70803, USA.
[3] EaStCHEM, School of Chemistry, University of Edinburgh, Edinburgh, EH9 3FJ, UK.
[4] Computation and Technology, Louisiana State University, Baton Rouge, 70803, USA.

TP

Synopsis X-ray scattering-based methods are promising to monitor the attosecond electronic dynamics with high temporal and spatial resolutions. However, the sensitivity of the scattering signals to changes in density and the interpretation of the dynamics with the scattering response are poorly understood. In this work, the simulations of stationary core-holes and the electron dynamics induced by the inner-shell ionization of the oxazole molecule are presented. With a combination of time-dependent density functional theory simulations and X-ray scattering theory, we demonstrate that the sudden ionization of the inner-shell electron results in significant change in the X-ray scattering signal. Additionally, time-dependent ring currents of a rapidly ionized molecule can be qualitatively mapped into the scattering signal modulations, which suggests that X-ray scattering can be a practical tool to probe attosecond electron dynamics.

With the advance of X-ray free-electron lasers (XFELs), atto-second X-ray scattering becomes a promising tool to capture the ultra-fast electron dynamics and investigate the structure evolution in complex reactions. In scattering experiments on gas phase molecules, the signal can be sensitive to changes in the electronic structure, as demonstrated in a recent experiment [1], and theoretical predictions play an important role in quantifying such effects [2]. Mapping the intriguing scattering signals to the real-time electronic dynamics is also a challenging topic both experimentally and theoretically. Recent theoretical studies have shown that instead of the instantaneous density, the time-dependent scattering is mainly sensitive to the electronic currents and dominated by the change of the inelastic scattering [3, 4, 5].

In this work [6] we simulate how electron dynamics in the conjugated ring-shaped oxazole molecule can be probed with X-ray scattering. A combination of real-time time-dependent functional theory (RT-TDDFT) and X-ray scattering theory was used to calculate the signal changes for both static core-holes, as well as X-ray pump-induced attosecond ring-currents. The simulated scattering signals show that different electronic states have distinct scattering patterns that are sensitive to the removal of an inner-shell electron. For the attosecond dynamics, the scattering signal is approximated by the absolute value of the electron density derivative, which has been previously shown to be a qualitative mapping between these two. The resulting time-delay dependent scattering patterns show a strong dependence on the instantaneous ring currents in the molecule. These results suggest that attosecond X-ray scattering is promising for probing electron dynamics in molecules, especially for the case where the currents involve a large spatial divergence.

References

[1] H Yong *et al.*, Nat. Commun. **11**, 2157 (2020).
[2] N Zotev, A M Carrascosa, M Simmermacher, A Kirrander, J. Chem. Theory Comput. **16**, 2594 (2020).
[3] G Hermann, V Pohl, G Dixit, and J C Tremblay, Phys. Rev. Lett. **124**, 013002 (2020).
[4] M Kowalewski, K Bennett, and S Mukamel, Struct. Dyn. **4**, 054101 (2017).
[5] M Simmermacher, N E Henriksen, K B Møller, A M Carrascosa, and A Kirrander, Phys. Rev. Lett. **122**, 073003 (2019).
[6] A M Carrascosa, M Yang, H Yong, L Ma, A Kirrander, P M Weber, and K Lopata, Faraday Discuss. **228**, 60 (2021).

*E-mail: klopata@lsu.edu

On the generation of electronic ring currents by circularly polarized light

O Vendrell[1] * **and K R Nandipati**[1]

[1]Theoretische Chemie, Physikalisch-Chemisches Institut, Universität Heidelberg, Im Neuenheimer Feld 229, 69120 Heidelberg, Germany

TP

Synopsis We consider the generation of electronic ring currents by circularly polarized laser light in the presence of vibronic coupling effects. Dynamical Jahn-Teller distortions result in the surprising effect that the same light polarization triggers either clockwise or anti-clockwise electronic currents depending on the spectral region of the molecule targeted by the pulse.

Circularly polarized light generates electronic ring currents in ring-shaped molecules, potentially enabling the control of the flow of electrons in optoelectronic devices. Theoretical descriptions have previously not considered the inevitable dynamic Jahn-Teller distortions of the molecular geometry and focused on the electrons alone. We find that, due to the vibronic coupling, different vibronic states resonant with light of a specific circular polarization can feature opposite electronic circulation directions [1, 2]. This phenomenon results in the hitherto unrecognized effect that the laser frequency alone can determine the direction of the electronic current by targetting different spectral regions of a molecule.

In this contribution, we consider the theory of photo-induced molecular ring currents under nuclear-electronic couplings and we then apply this theory to the general $(E \times e)$ JT Hamiltonian, where the vibronic coupling results in a conical intersection (CI) between the corresponding adiabatic potential energy surfaces. Numerical simulations show how long laser pulses targeting a narrow spectral region of the vibronic spectrum result in quasi-stationary ring currents. In contrast, short laser pulses result in highly oscillatory currents with strong nuclear-electronic couplings. The observations made on JT systems are general and have consequences for laser-generated currents and their control in complex molecules at the crossroads of chemistry, optoelectronics, and ultrafast science.

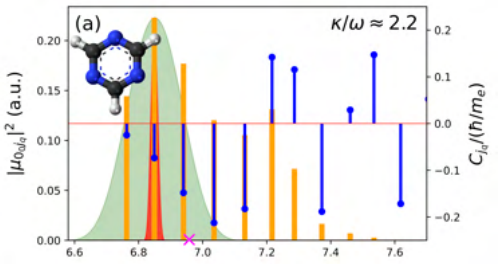


Figure 1. Absorption spectrum ($\propto |\mu_{0_0 j_q}|^2$) for the 2D sym-triazine $(E \times e)$ JT Hamiltonian (orange, left y-scale) and vibronic ring currents ($\mathcal{C}_{j_q}/(\hbar/m_e)$) (blue, middle y-scale) as a function of the eigenstates' energy. Superimposed is the spectral representation of the τ=30 fs pulse (shaded in green) resonant with the lower band of the absorption spectrum below the conical intersection.

References

[1] K R Nandipati, O Vendrell, J. Chem. Phys. **153**, 224308 (2020).

[2] K R Nandipati, O Vendrell, Phys. Rev. Research **3**, L042003 (2021).

*E-mail: oriol.vendrell@uni-heidelberg.de

Time-dependent multicomponent optimized coupled-cluster method for nonadiabatic electro-nuclear dynamics

T Sato[1,2,3] *, Y Orimo[1], Y Li[1], and K. L. Ishikawa[1,2,3]

[1] Department of Nuclear Engineering and Management, School of Engineering, The University of Tokyo, Tokyo, 113-8656, Japan
[2] Photon Science Center, School of Engineering, The University of Tokyo, Tokyo, 113-8656, Japan
[3] Research Institute for Photon Science and Laser Technology, The University of Tokyo, Tokyo, 113-0033, Japan

Synopsis We report successful formulation and implementation of the time-dependent multicomponent optimized coupled-cluster (TD-MC-OCC) method for nonadiabatic electro-nuclear dynamics. The TD-MC-OCC method is based on the multicomponent coupled-cluster expansion of the total wavefunction with time-dependent electronic and nuclear orbital functions. The method is size extensive, gauge invariant, and polynomial cost-scaling, achieving a uniformly accurate description of electro-nuclear dynamics independent of the number of particles. Numerical applications to intense-laser driven ionization/dissociation dynamics in one-dimensional model molecules are presented.

We have developed time-dependent multiconfiguration self-consistent-field (TD-MCSCF) [1] and time-dependent optimized coupled-cluster (TD-OCC) [2] methods for simulating intense laser-driven electron dynamics. These methods are based on the configuration-interaction (CI) or coupled-cluster (CC) expansion of the total wave function using time-dependent orbitals for efficiently describing ionization dynamics. In particular, the size-extensivity of the TD-OCC method guarantees a uniformly accurate description of the multielectron dynamics independent of the number of electrons.

On the other hand, one needs to treat both electrons and nuclei in a molecule quantum mechanically to describe nonadiabatic molecular dynamics. Various methods have been developed to this end as summarized in a recent review [3], including the general TD-MCSCF method for electro-nuclear dynamics [4], which can treat an arbitrary multicomponent system consisting of different kinds and numbers of interacting fermions and bosons, based on the general CI expansion using time-dependent orbitals.

In this work, we formulate the time-dependent multicomponent optimized coupled-cluster (TD-MC-OCC) method for electro-nuclear dynamics. It uses the multicomponent CC expansion with time-dependent electronic and nuclear orbitals. The present method is size extensive, gauge invariant, and polynomial cost-scaling, achieving a uniformly accurate description of electro-nuclear dynamics independent of the number of particles. Numerical applications of the method to intense-laser driven ionization/dissociation dynamics of molecules will be presented (Fig. 1).

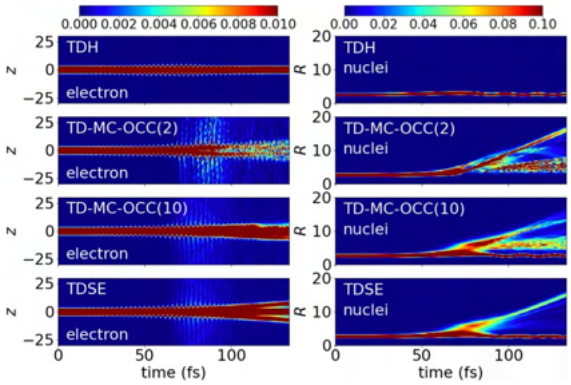


Figure 1. Contour plot of the time-dependent electronic (left) and nuclear (right) density of a one-dimensional hydrogen molecular ion model [4] exposed to a laser pulse with an intensity of 2×10^{14} W/cm^2, a wavelength of 800 nm, and a duration of 50 optical cycles. Numerical results with time-dependent Hartree (top), TD-MC-OCC with two and 10 orbitals each for the electron and nuclei (middles), and numerically exact time-dependent Schrödinger equation (bottom).

References

[1] Ishikawa K L, Sato T 2015 *IEEE J. Sel. Top. Quantum Electron.* 21, 8700916
[2] Sato T *et al* 2018 *J. Chem. Phys.* **148** 051101
[3] A. U. J. Lode *et al* 2020 *Rev. Mod. Phys.* **92** 011001
[4] Anzaki R, Sato T, Ishikawa K L 2017 *Phys. Chem. Chem. Phys.* **19** 22008

* E-mail: sato@atto.t.u-tokyo.ac.jp

Revisiting the Born approximation in the context of electron energy loss spectroscopy

M Sapunar[1,2], **Z Mašín**[1*]

[1]Institute of Theoretical Physics, Charles University, Prague 8, 18000, Czech Republic
[2]Department of Physical Chemistry, University of Chemistry and Technology, Prague 6, 16628, Czech Republic

TP

Synopsis Calculations of nuclear dynamics in molecules following the impact of an electron require knowledge of accurate relative populations of the excited electronic states. We show that a quick and a suprisingly accurate estimate of the relative populations can be obtained by the Born approximation for multi-electron targets despite significantly overestimating the absolute values of the cross sections.

An electron beam interacting with matter will excite some molecules through inelastic scattering. In our work we focus on electronic excitation. The energy imparted on the system can be measured through electron energy loss spectroscopy (EELS) with a signal analogous to photoelectron spectroscopy, but with an electron instead of a photon initiating the process. This allows EELS to probe optically forbidden transitions such as singlet-triplet excitations due to relaxed selection rules.

Simulating electron initiated processes is significantly more difficult than photon initiated processes. In the latter the probability of exciting the system to a particular initial state can be reasonably approximated simply from its oscillator strength while the former requires an expensive scattering calculation.

The aim of our work is to develop a cheap method for calculating electron impact cross sections which would bypass scattering calculations but would retain sufficient accuracy to represent well the ratios of the cross sections. These will be used as the initial condition for the followup calculations of nuclear dynamics.

With this goal in mind, a natural starting point is the Born approximation in which the scattering amplitude $f(\theta,\phi)$ can be obtained directly as a matrix element of the potential between the target and the electron represented by a plane wave

$$f(\theta,\phi) = -\frac{\mu}{2\pi\hbar^2}\langle \boldsymbol{q}_f \Phi_f | \hat{V} | \Phi_i \boldsymbol{q}_i \rangle \ .$$

This calculation removes the problem of modelling of the continuum making it applicable even to very large systems which are untractable by ab initio scattering codes. The required integrals have been implemented in the UKRmol+ suite of programs [1] based on the formalism developed by Kuang and Lin [2].

Here we benchmark the cross sections obtained using the Born approximation against scattering calculations performed with the R-matrix method for H_2 [3] and pyrimidine [4]. In both cases the electronic structure method employed for the target states was the same as the one employed in R-matrix calculations

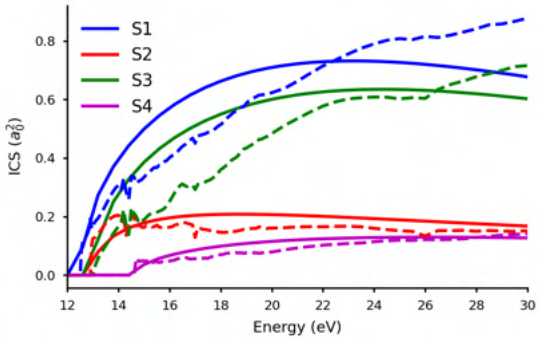


Figure 1. Integrated electron impact cross-sections for the four lowest singlet states of H_2 using an R-matrix (dashed) and renormalized Born approach (full lines).

As expected, the absolute cross sections given by the Born approximation are significantly overestimated, but their relative magnitudes are represented quite well.

We are working on inclusion of electron exchange to calculate optically forbidden (singlet-triplet) transitions.

References

[1] Mašín Z *et al* 2020 *Comput. Phys. Commun.* **249** 107092
[2] Kuang J *et al* 1997 *J. Phys. B* **30** 2549
[3] Meltzer T *et al* 2020 *J. Phys. B* **53** 145204
[4] Regeta K *et al* 2016 *J. Phys. Chem* **144** 024302

* E-mail: zdenek.masin@utf.mff.cuni.cz

Electron-ion interaction for the strong field ionization of H_2

A Geyer[1 *], O Neufeld[2], D Trabert[1], U De Giovannini[2], M Hofmann[1], N Anders[1], L Ph H Schmidt[1], M Schöffler[1], A Rubio[2], T Jahnke[1], M Kunitski[1], R Dörner[1] and S Eckart[1 †]

[1]Institut für Kernphysik, Goethe-Universität, Frankfurt am Main, 60438, Germany
[2]Max Planck Institute for the Structure and Dynamics of Matter and Center for Free-Electron Laser Science, Hamburg, 22761, Germany

TP

Synopsis We report on the strong field ionization of molecular hydrogen using a co-rotating circularly polarized two-color laser field. The three-dimensional momentum distributions of the charged fragments are measured in coincidence using cold target recoil ion momentum spectroscopy (COLTRIMS). For the dissociation channel we observe the well-expected half-moon structure and, in addition, low energy electrons in coincidence with high kinetic energy release (KER) of the ions. We speculate that the low energy electrons are a fingerprint of an interaction between the outgoing electron and the ion.

The strong field ionization of molecular hydrogen is experimentally investigated using a co-rotating circularly polarized two-color (CoRTC) field. The two-color field (central wavelengths of 390 nm and 780 nm) is generated in an interferometric two-color setup [1] and the single color intensities are I_{390} = 6.2 x 10^{13} W/cm^2 and I_{780} = 3.8 x 10^{13} W/cm^2 (preliminary intensity calibration). The three-dimensional momentum distributions of the charged fragments are measured in coincidence using cold target recoil ion momentum spectroscopy (COLTRIMS) [2].

Fig. 1(a) shows the Lissajous curve of the laser electric field and the corresponding vector potential. Fig. 1(b) shows the measured electron momentum distribution for the dissociation of H_2 for the laser parameters that are given above. These laser parameters and the corresponding electron momentum distribution are similar to prevous measurements of atoms in CoRTC fields [3]. For the dissociation of H_2 we are able to generate the electron momentum distribution as a function of the kinetic energy release (KER) of the ions. In Fig. 1(c) and Fig. 1(d) the energy of the electron is shown as a function of the KER. In Fig. 1(d) each column of the distribution from Fig. 1(c) is normalized to a maximum of 1. It is found that low-energy electrons are very pronounced at a KER of about 3 eV.

We argue that the correlation of low-energy electrons and KER is a fingerprint of an energy transfer between the outgoing electron and the H_2^+ ion. However, for the chosen field parameters recollisions are unlikely. Thus, we speculate that the outgoing electron can transfer energy to the H_2^+ ion if the electron's energy is resonant to the transition between the $1s\sigma_g$ and the $2p\sigma_u$ state of the H_2^+ ion. Since, the energy splitting of the $1s\sigma_g$ and the $2p\sigma_u$ state depends on the internuclear distance this might explain the experimental findings.

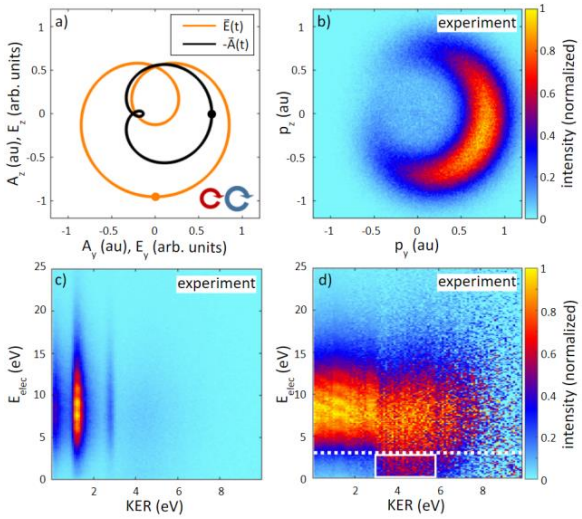


Figure 1. (a) The Lissajous curve of the laser electric field and the corresponding vector potential. The arrows indicate the temporal evolution of the laser's elecric field. (b) Measured electron momentum distribution of the laser parameters that are shown in (a). (c) shows the energy of the electron as a function of the KER. In (d) each column of the distribution in (c) is normalized to a maximum of 1. The dashed line in (b) guides the eye and the rectangle highlights the low-energy electrons that are observed in coincidence with 3 eV < KER < 6.5 eV.

References

[1] Eckart S *et al* 2016 *Phys. Rev. Lett.* **117** 133202
[2] Ullrich J *et al* 2003 *Rep. Prog. Phys.* **66** 1463
[3] Eckart S *et al* 2018 *Phys. Rev. Lett.* **121** 163202

* E-mail: geyer@atom.uni-frankfurt.de
† E-mail: eckart@atom.uni-frankfurt.de

Coherent Control of Extreme Ultraviolet Emission Generated Through Frustrated Tunneling Ionization

Y H Kim[1], H Yun[1], S I Hwang[1], C H Nam[1,2] and K T Kim[1,2*]

[1]Center for Relativistic Laser Science, Institute for Basic Science, Gwangju, 61005, Korea
[2]Department of Physics and Photon Science, Gwangju Institute of Science and Technology, Gwangju, 61005, Korea

TP

Synopsis We demonstrate experimental and theoretical analysis on the phase of coherent extreme ultraviolet emission generated through frustrated tunneling ionization (FTI). The FTI emission generated at various target positions shows an intensity modulation due to the interference of the electron wave packets tunneled at multiple half-cycles of a driving laser pulse. The intensity modulation is pronounced before the focus, while it is relatively slower after the focus. These behaviors explain the phase matching of the FTI emission, which is similar to that of high harmonic generation.

An electron liberated from an atom through tunneling moves along different quantum trajectories depending on its timing of birth. The electron that borns at the peak of the laser field can stop near the parent ion with zero kinetic energy at the end of the laser field. The electron can recombine to the excited states of the parent atom. This strong-field excitation process is called frustrated tunneling ionization (FTI) [1,2].

A coherent light can be emitted from the FTI excited atom by a transition to the ground state. The wavelength of the light lies in the range of extreme ultraviolet (EUV). Since The FTI excitation process is fully coherent, a subtle change of the driving laser field alters the phase of the FTI emission. In this work, we study the phase dependence of the FTI emission on the target position to understand the phase-matching property of the FTI emission.

In the experiment, a few-cycle laser pulse (5-fs in duration, 800 nm in wavelength) was focused at a He gas jet target to generate an FTI emission (I_0=5.0*10^{14} W/cm^2). The position of the gas jet target was moved along the optic axis of the focused beam near the focal plane (z=0). Angle-resolved spectra of the FTI emission were recorded using a EUV spectrometer. One of the experimental results is shown in Figure 1(a), showing a strong position dependence and interference patterns.

To understand the origin of the target position dependence, we developed the four-step semi-classical model [2], and the result is shown in Figure 1(b). Both results show that the FTI emission is rather brighter behind the focal plane (z>0) than before the focal plane (z<0). This behavior is similar to that in high-order harmonic generation [3] in which the phase shift caused by the Gouy phase of the focused laser beam is compensated by the phase accumulated through the FTI electron trajectory that strongly depends on the laser intensity. These results explain the phase-matching condition of the FTI emission.

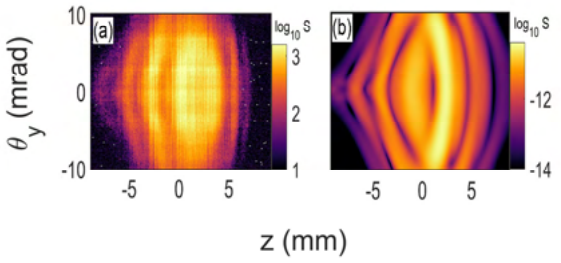


Figure 1. Spatial distribution of FTI emission obtained at different target positions. (a) Experimental results. (b) Four-step model results.

References

[1] H Yun *et al* 2018 *Nat. Photon.* **12** 620
[2] J H Mu *et al* 2018 *Phy. Rev. A* **98** 063429
[3] P Saliéres *et al* 1995 *Phys. Rev. Lett.* **74** 3776

* E-mail: kyungtaec@gist.ac.kr

Universal enhancement of high-order above threshold ionization across laser wavelengths

A Camacho Garibay[1] *, K Talbert[1] , C Blaga[2], K Schafer[3], P Agostini[1] , L F DiMauro[1]

[1]The Ohio State University, Columbus, 43210, United States
[2]Kansas State University, Manhattan, 66506, United States
[3]Louisiana State University, Baton Rouge, 70803, United States

Synopsis Through a combination of experimental and theoretical studies, we are to identify the existence of leading intensities, characterized by an important increase in high-energy photoelectron yield accompanied by distinctive features in the spectra. These features are found to be common across multiple wavelengths, when spectra are presented in terms of the ponderomotive energy.

Above threshold ionization, one of the fundamental discoveries that gave rise to strong field physics, is a multi-photon process in which an electron absorbs more photons than the minimum required to ionize. The semiclassical three-step model, where electrons are considered classical particles following well defined trajectories as they propagate through the field after undergoing tunneling ionization, has successfully explained the main characteristics observed in the photoelectron spectra [1]. However, additional features have been observed that cannot be accounted for by the three-step model, such as enhancements of up to an order of magnitude at intermediate regions of the ATI spectrum for relatively small changes in the peak intensity of the laser pulse [2].

Here, with the help of laser pulses of tunable wavelength in the visible regime, we uncover the existence of leading intensities. These are particular laser peak intensities capable of producing a significant increase in the ionization yield while at the same time providing distinctive and dominating features in the final measured spectra. These features include the appearance of a yield enhancement at intermediate energies around 6Up energy (therefore requiring a rescattering event), additionally display an ATI comb whose position remains stable even after a further increase in intensity. Additional careful measurements provide evidence of the existence of another stable comb of ATI peaks around 10Up suggesting they both belong to a single comb, allowing for an estimation of the leading intensity directly from the experiment.

The experimental photoelectron spectra can be entirely reproduced by focal averaged TDSE calculations with flat-top pulses in the SAE approximation. We find that the ionization rate of high energy photoelectrons shows periodic enhancements separated by one photon. We also demonstrate the existence of a very stable wavepacket that persists in the combined potential of the field and the atom for many cycles.

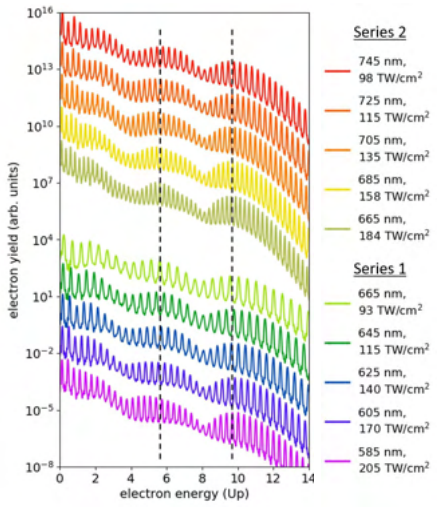


Figure 1. TDSE calculated spectra for argon at different leading intensities and wavelengths.

Once the leading intensities are identified at different wavelengths, both theory and experiment show that a universal spectrum is obtained when expressing the individual spectra in terms of their corresponding ponderomotive energy (Figure 1). This is found to be true not only across wavelengths, but also for multiple target atoms and potentially even molecules.

References

[1] Schafer K *et al* 1993 *Phys Rev Lett.* 15 70(11)
[2] Paulus *et al* 2001 *PRA* 64 021401(R)

* E-mail: camachogaribay.1@osu.edu

TP

Imaging photo-induced dynamics using Laser-Induced Electron Diffraction

M S Robinson[1,2*], E T Karamatskos[1,2,3], J Wiese[1,2,4], J Onvlee[1,2], A Rouzee[5], and J Küpper[1,2,3,4†]

[1]Center for Free-Electron Laser Science, Deutsches Elektronen-Synchrotron DESY, Hamburg, Germany
[2]Center for Ultrafast Imaging, Universität Hamburg, 22761 Hamburg, Germany
[3]Department of Physics, Universität Hamburg, 22761 Hamburg, Germany
[4]Department of Chemistry, Universität Hamburg, 20146 Hamburg, Germany
[5]Max-Born-Institut für Nichtlineare Optik und Kurzzeitspektroskopie, 12489 Berlin, Germany

Synopsis Laser-Induced Electron Diffraction (LIED) is a rapidly progressing technique with the potential to image the structures of gas-phase molecules on the sub-femtosecond timescale. In this report, we detail recent successes that we achieved, in which we imaged molecules to within a precision of ~5 pm using LIED, as well as our advances in theoretical modelling to predict the rescattering of electrons after strong-field ionisation. We also detail our next steps as we move towards performing full pump-probe experiments to observe the photo-induced chemical dynamics of molecules using LIED.

With its increased scattering cross sections, compared to contemporary diffraction methods, and its ability to provide picometer-resolved images of molecules with sub-femtosecond time-resolution, laser-induced electron diffraction (LIED) has the potential to provide us with clear structural information on the early-stage photo-induced dynamics of molecules like no other technique that has come before.

Within the Controlled Molecule Imaging group at CFEL in Hamburg, in collaboration with colleagues from the Max-Born Institute Berlin, we have been able to demonstrate the power of LIED to image structures of highly-controlled molecules. Using a combination of ultra-cold molecular beams and electrostatic deflectors, we are able to produce a well-defined low-energy gas-phase sample that can be used for precise LIED experiments [1].

With this set-up, we have successfully recovered the structure of carbonyl sulfide (OCS) using LIED, to within a precision and accuracy of less than 5 picometers when compared to measurements from more established structural techniques [2]. Additionally, as LIED induces an inherent ionisation of the system that one is probing, we were also able to unravel and appropriately take into account the subtle changes in the scattering signal due to the location of the charge on the ion. In comparison to the typical approach of extracting the structural information based on the assumption of neutral-molecule scattering cross-sections, this yielded improved agreement with the experimental data and thus more accurate structural information.

As we move to investigating more complex systems, we also focus on developing advanced analysis tools and theoretical models to better understand the scatting images recorded after strong-field ionisation, including a custom semi-classical approach that utilises ADK tunnel ionisation theory [3].

For our next step, we focus on applying LIED to imaging the structural changes corresponding to the chemical dynamics that occur in a system after photo excitation, i.e., in a pump-probe approach. As a proof-of-principle experiment, we plan to look at the photo-induced dissociation of the prototypical micro-solvated biomolecular system indole-water, for which work has already started. The methods for performing this experiment will be detailed in this presentation.

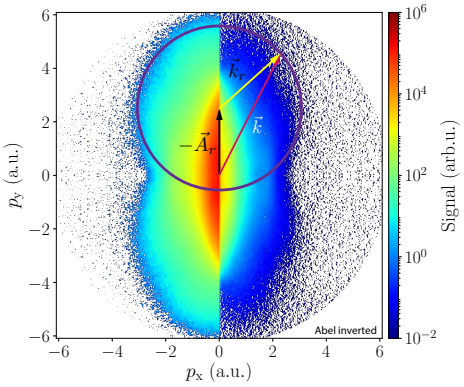


Figure 1. Projected 2D electron momentum distribution (left) and slice through the 3D electron momentum distribution after Abel inversion (right) from OCS after ionization by an intense laser pulse (Image adapted from ref. 1)

References

[1] Trippel, S *et al* 2018 *Rev. Sci. Instrum.* **89, 5–8**
[2] Karamatskos, E T *et al.* 2019 *J. Chem. Phys.* **150, 244301**
[3] Wiese, J *et al*. 2021 *Phys. Rev. Res.* **3, 013089**.

* E-mail: matthew.robinson@cfel.de
† E-mail: jochen.kuepper@cfel.de

Temporal characterization of two color laser fields using tunneling ionization

K T Kim[1,2*], J Shin[1,2], W Cho[2], R Shrestha[1,2]

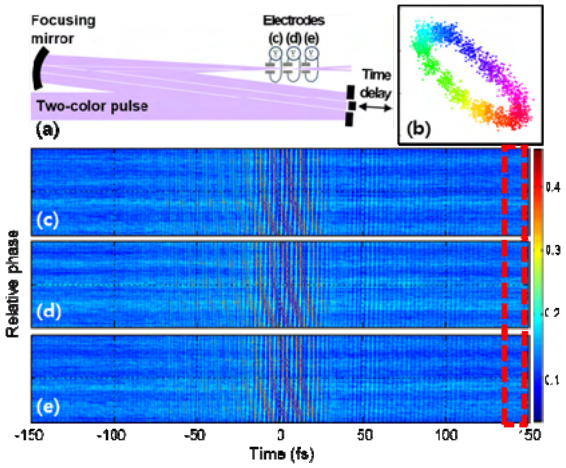
[1]Center for Relativistic Laser Science (CoReLS), Institute for Basic Science, Gwangju, 61005, Korea
[2]Department of Physics and Photon Science, Gwangju Institute of Science and Technology, Gwangju, 61005, Korea

Synopsis We demonstrate the temporal characterization of a two-color laser field using the TIPTOE (tunneling ionization with a perturbation for the time-domain observation of an electric field) method. The two-color laser fields are completely characterized, including the relative phase between the fundamental and its second harmonics. The reconstruction results show good consistency, supporting the validity of the measurement.

The superposition of a fundamental laser field and its second harmonic field can form an asymmetric electric field which is useful in various applications [1, 2]. In these applications the temporal characterization of the two-color laser field, including the relative phase between the two-color laser field, is required. However, it is challenging due to the broad spectral range of the two-color laser field. In addition, most conventional pulse characterization techniques rely on the second harmonic generation of an input laser pulse [3]. Therefore, the two-color laser pulse made by the superposition of the fundamental and its second harmonic field can cause measurement issues.

Recently, a pulse characterization technique called TIPTOE (tunneling ionization with a perturbation for the time-domain observation of an electric field) and its reconstruction algorithm has been successfully demonstrated [4, 5]. In this work, we demonstrate that the two-color laser field, including the relative phase between the fundamental and its second harmonic fields, can be accurately reconstructed using the TIPTOE method.

The temporal profile of an input laser field is directly sampled using tunneling ionization in the TIPTOE technique. The modulation of ionization yields is measured using the experimental setup shown in Fig. 1(a) We measured ionization yields at three different places along the beam path near the focus. In this way, the ionization yields can be obtained at three different relative phases, as shown in Fig. 1(c)-(e). The ionization yields obtained at a large delay (marked by red dashed lines) are modulated. This modulation contains information on the relative phase between the fundamental and its second harmonic field. The relative phase can be determined by a single laser shot by mapping the ionization yields obtained at the three positions as shown in Fig. 1(b). The reconstruction is performed using the Adam algorithm including these information. The temporal profile of the two-color laser pulse was successfully reconstructed using the three ionization yield modulation data in a single scan.



[Fig.1] (a) Experiment setup for the temporal characterization of two-color laser fields. (b) A map of relative phase extracted from data (c)-(e). (c)-(e) Ionization yield as a function of time delay and relative phase measured at the three electrodes.

References

[1] Kim K Y *et al.* 2008 *Nat. Photonics* 2 605
[2] De S *et al.* 2009 *Phys. Rev. Lett.* 103 153002
[3] Trebino R *et al.* 1997 *Rev. Sci. Instrum.* 68 3277
[4] Park S B *et al.* 2018 *Optica* 5 402
[5] Cho W *et al.* 2021 *Sci. Reports* 11 13014

* E-mail: kyungtaec@gist.ac.kr

TP

Strong field ionization of chiral molecules in co- and counter-rotating two-color laser fields

M Hofmann*, D Trabert, J Kruse, J Rist, A Geyer, N Anders, L Ph H Schmidt, T Jahnke, M Kunitski, M S Schöffler, R Dörner and S Eckart†

Institut für Kernphysik, Goethe Universität, Frankfurt am Main, 60438, Germany

Synopsis We report on our recent findings on fragmentation channel resolved PECD of propyleneoxide with two-color femtosecond laser pulses. We will use co- and counter-rotating laser fields with different field ratios. We measure photoelectrons and ions in coincidence. We thereby hope to elucidate the influence of sub-cycle dynamics on the PECD for the parent ion and also fragmentation channels.

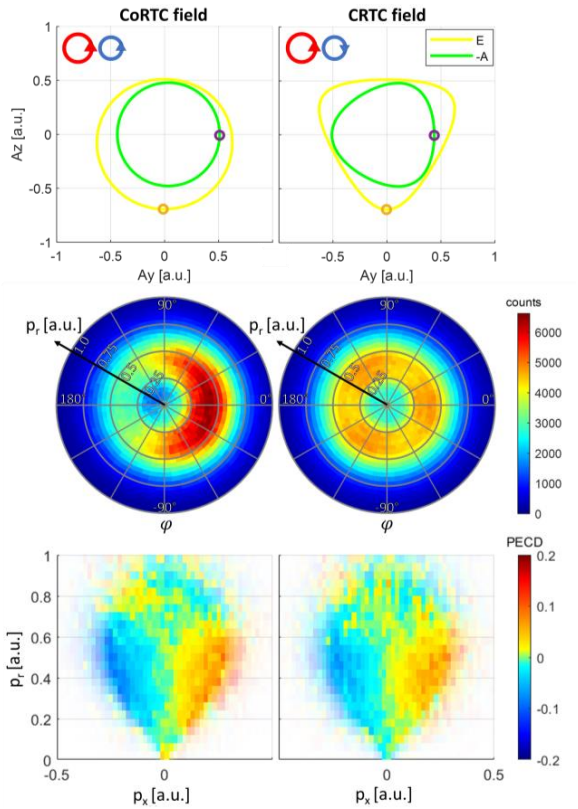


Figure 1. Field ratio $E_{790}/E_{395} \approx 7$, $E_0 \approx 6{,}32 \cdot 10^{13}$ W/cm. Left column: CoRTC laser field. Right column: CRTC laser field. The blue and red arrows in the top left corners illustrate the rotation and the field ratios of the two color laser pulse. First row: Simulated Lissajous figures of the electric fields and the corresponding vector potentials. The small circles denote the negative vector potential at the most probable instance of tunneling (peak electric field). Second row: Photoelectron momenta projected onto the laser's polarization plane in cylindrical coordinates. Third row: p_x and p_r dependant PECD. Countrates define the opacity of the bins.

It has been shown that the PECD (Photo Electrical Circular Dichroism) can vary within one cycle of the laser field. This allows one to access to dynamics on the attosecond timescale [1,2]. In order to inverstigate the role of non-adiabatic tunneling for PECD, we studied the fragmentation channel resolved PECD [3] of propyleneoxide with co-rotating (CoRTC) and counter-rotating (CRTC) two color fields in the strong field regime [4].

We expect that the PECD in CoRTC-fields is higher than for CRTC-fields due to its higher angular frequency at the instance of tunneling (peak electric field) [5,6]. First findigs for propyleneoxide (electron detected with the parent ion without molecular breakup) shown in Fig. 1 support this perspective: As it can be seen in the third row, the PECD of the CoRTC field is higher than for thr CRTC field.

The three-dimensional electron momenta have been measured in coincidence with ions using cold-target recoil-ion momentum spectroscopy (COLTRIMS) [7].

References

[1] Demekhin P *et al* 2018, *Phys. Rev. Lett.* **121** 253201
[2] Bloch E *et al* 2021, *Phys. Rev. X* **11**, 041056
[3] Fehre K *et al* 2019, *J. Phys. Chem. A*, **123** 6491-6495
[4] Ivanov M *et al* 2005, *J. of Mod. Opt.* **52** 165-184
[5] Eckart S *et al* 2018, *Phys. Rev. Lett.* **121** 163202
[6] Barth I *et al* 2011, *Phys. Rev. A* **84**, 63415
[7] Jagutzki O *et al* 2002, *IEEE Tr. on N. Sc.*, **49** 2477-2483

* E-mail: hofmann@atom.uni-frankfurt.de
† E-mail: eckart@atom.uni-frankfurt.de

Femtosecond intramolecular rearrangement of the CH_3NCS radical cation

S Li[1], B Jochim[1], J Stamm[1], Swati S Priyadarsini[1], S Yuwono[1], P Piecuch[1,2] and M Dantus[1,2]

[1]Department of Chemistry, Michigan State University, East Lansing, MI 48824, USA
[2] Department of Physics and Astronomy, Michigan State University, East Lansing, MI 48824, USA

Synopsis We report on the reaction dynamics of CH_3SCN and CH_3NCS following strong-field ionization. Both molecules generate the ion CH_3S^+ with different timescales, with CH_3NCS exhibiting coherent oscillations in the CH_3S^+ yield as a function of pump-probe delay.

Methyl isothiocyanate (MITC), CH_3NCS, is of relevance due to its generation from the decomposition of sodium metam, an important fungicide [1]. Studies of the photodissociation of MITC and its isomer methyl thiocyanate, CH_3SCN (MTC) suggest the two compounds share an excited state potential energy surface because both can produce CH_3S^+, the ion of interest in this paper [2]. For MTC, the generation of this ion is due to a single bond breaking, while for MITC, this involves an intramolecular rearrangement.

The reaction dynamics of MITC and MTC after strong-field ionization were studied using pump-probe spectroscopy. Strong-field ionization was initiated with 40-fs, 800-nm pulses with a peak intensity of 1×10^{14} W cm^{-2}. These parameters correspond to a Keldysh parameter of ~0.9, hence favoring tunnel ionization. The probe pulse was polarized at "magic angle" relative to the pump pulse, and was attenuated to ~3×10^{13} W cm^{-2}.

In the time-resolved traces (Figure 1), CH_3S^+ yield from MITC has a separate timescale of depletion and regeneration compared to CH_3S^+ from MTC. This difference in timescale indicates that the CH_3S^+ yield from MITC is not caused by contamination by MTC in the sample. In the case of MITC, coherent oscillations in the ion yield of CH_3S^+ were observed, but no oscillations were observed in MTC. The oscillations in the yield of CH_3S^+ as a function of pump-probe delay are due to vibrational modes in the precursor ion, CH_3NCS^+.

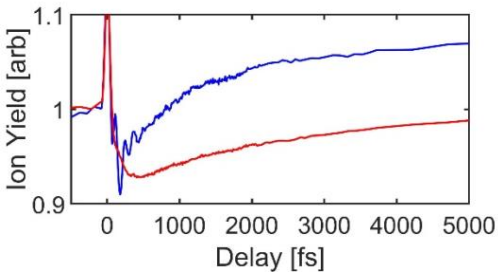


Figure 1. Normalized ion yield of CH_3S^+ from MITC (blue) and MTC (red) after ultrafast tunnel ionization. Yield of the ion of interest is recorded as a function of pump-probe delay.

These oscillations were analyzed using the maximum entropy technique [3]. This analysis, combined with the Fourier transformation, revealed two beating frequencies at ~130 cm^{-1} and ~250 cm^{-1}. We carried out high-level calculations and molecular dynamics simulations to determine that these beating frequencies in the ion yield correspond to normal modes in the parent CH_3NCS^+ ion. These bending motions in the parent ion are caused by a change in geometry upon tunnel ionization of the neutral MITC molecule.

References

[1] R. A. Alvarez, C. B. Moore, "Quantum Yield for Production of CH3NC in the Photolysis of CH3NCS," Science **263**, 205–207 (1994)

[2] E. A. Wade, J. L. Pore, "Infrared Emission Following Photolysis of Methylisothiocyanate and Methylthiocyanate," *J. Phys. Chem. A* **115**, 5319–5323 (2011).

[3] W. H. Press, S. A. Teukolsky, W. T. Vetterling, and B. P. Flannery, Numerical Recipes in C (Cambridge University Press, New York, 1992).

Dissecting intra-cycle quantum interference in photoelectron holography

C. Figueira de Morisson Faria*
University College London, Gower Street, London WC1E 6BT, UK

TP

Synopsis We provide a summarizing account of a series of investigations in ultrafast photoelectron holography, in which, using the Coulomb Quantum Orbit Strong-Field Approximation (CQSFA), we assess how specific holographic patterns form in an orbit-based, quantum mechanical framework. This includes well-known structures, such as the fan and the spider, as well as overlooked holographic patterns such as the spiral, and applications to parity measurement and detecting multipath interference. The latter work has been a joint effort with experimental groups, whose results back up our theory.

Similarly to traditional holography, ultrafast photoelectron holography explores quantum phase differences between qualitatively different electron pathways to extract information about a target [1]. Unfortunately, however, the residual binding potential is neglected in most theoretical models of the interference patterns encountered. This is problematic as its presence radically alters the electron dynamics. In this presentation, we will analyze a myriad holographic patterns, known and overlooked, in terms of electron trajectories using an orbit-based method developed at UCL that includes the binding potential and the laser field on equal footing: the Coulomb Quantum-orbit Strong-Field Approximation (CQSFA) [2].

Subsequently, we will provide applications and illustrate how photoelectron holography may be used to detect the parity of atomic and molecular orbitals [3] and introduce a novel spiral-like holographic structure highly sensitive to phase differences [4], in joint work with several experimental groups. We also discuss how one can overcome the obstacle posed by inter-cycle interference, in form of above-threshold ionization (ATI) rings, in order to investigate subtle multi-path interference by using filtering techniques in experiment and theory, such as unit-cell averaging [5]. We also show how the presence of the Coulomb potential leads to twisted holographic patterns in elliptically polarized driving fields, which can be traced back to quantum interferences between particular orbit types [6].

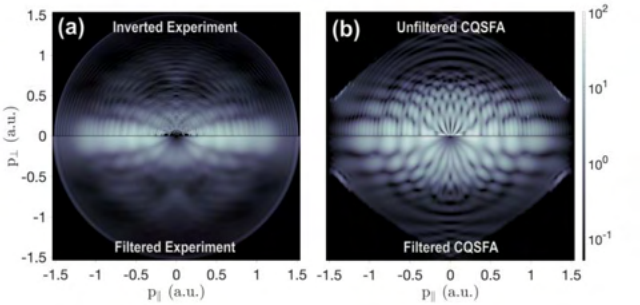


Figure 1. : Photoelectron momentum dependent yield for argon for a laser intensity of 2×10^{14}W/cm^2 and wavelength $\lambda = 800$ nm. : Panels (a) shows the application of the time-filtering technique to the experimental data, while panel (b) shows it being applied to the CQSFA calculations. (a) The top half shows the raw experimental data after it has been inverted via polar onion-peeling. (b) The top half shows the CQSFA calculation with just unit-cell averaging applied. The bottom halves of both panels display the result of the time-filtering upon the top halves. The ATI rings and the fine modulations of the ATI rings and the fine modulations of the CQSFA have both been removed, without disrupting underlying structure. From [5].

References

[1] Figueira de Morisson Faria C and Maxwell A S 2020 *Rep. Prog. Phys*. **83** 034401
[2] Maxwell A S *et al*, 2017 *Phys. Rev. A* **96**, 023420; 2018 *J. Phys. B* **51**, 124001
[3] Kang H *et al*, 2020 *Phys. Rev. A* **102**, 013109
[4] Maxwell A S *et al*, 2020 *Phys. Rev. A* **102**, 03311
[5] Werby N, Maxwell A S, Forbes R *et al*., 2021 *Phys. Rev. A* **104,** 013109
[6] Kim G, Hofmann C, et al, in preparation.

* E-mail: c.faria@ucl.ac.uk

Dissociation dynamics of HeH^+ isotopologues in intense laser fields

S Mhatre[1]*, F Oppermann[2], M Lein[2] and S Gräfe[1]

[1] Institute of Physical Chemistry, Friedrich-Schiller-University Jena, Helmholtzweg 4, 07743 Jena, Germany
[2] Institute of Theoretical Physics, Leibniz University Hannover, Appelstraße 2, 30167 Hannover, Germany

Synopsis The dissociation dynamics of HeH^+ in short infrared laser pulses is theoretically and numerically investigated. Fixing the reduced mass and systematically changing the nuclear-mass ratio allows us to focus on the effects caused by the mass asymmetry alone. From our classical and quantum mechanical calculations, we find that at a certain mass ratio, the dipole interaction with the field is strongly suppressed, which in turn suppresses the dissociation probability.

HeH^+ constitutes an ideal system for studying isotope effects due to its wide-ranging isotopologue availability, which varies from the highly asymmetric $^4HeH^+$ to the symmetric $^3HeT^+$ in terms of mass. Although the electronic configuration is identical, their nuclear (reduced) masses are different from each other. As a consequence, the vibrational level structure of the isotopologues differs. Strong-field dissociation dynamics induced by intense mid-infrared fields depends sensitively upon the vibrational level spacing, and therefore, these dissociation dynamics may strongly differ for various isotopologues.

In our theoretical study, we disentangle contributions originating from the difference in the reduced mass from those originating from the mass asymmetry between two individual atoms by artificially fixing the reduced mass (i.e. the resonance condition) and systematically varying the nuclear mass ratio. For simplicity, we approximate the masses of proton and neutron (m_n) to be equal and ignore the nuclear mass defects.

In a charged asymmetric system such as HeH^+ ion, the permanent dipole moment depends on the center of the mass (origin of the coordinate system). We shift this center of mass position according to the mass ratio parameter $r = m_H/(m_{He} + m_H)$, where m_H and m_{He} are the masses of hydrogen and helium nuclei respectively. As r goes from 0 to 1, the center of mass shifts from He to H and the dipole moment changes with it (see figure 1).

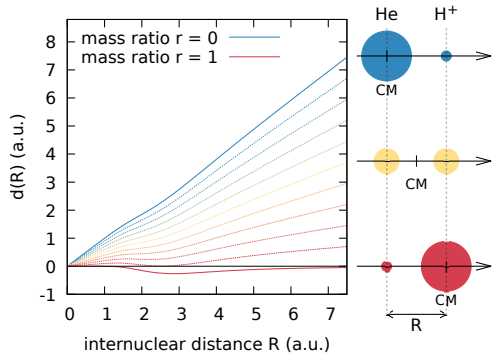


Figure 1. Changes in permanent dipole $d(R)$ with respect to the position of the center of mass

Our calculations based on the 1D TDSE [1] and classical trajectories show a pronounced minimum in the dissociation yield at a certain mass ratio for a given wavelength. In the quantum dynamical picture, this occurs as important vibrational transitions become "forbidden" or suppressed, which is mimicked in the classical case, as the driving force (the derivative of the dipole moment) effectively goes to zero, thereby strongly suppressing the dipole interaction strength, which renders the influence of the field negligible at that mass ratio. We believe this study improves our understanding of the role of the mass asymmetry in strong-field dissociation dynamics.

Table 1. Selected HeH^+ isotopologues with identical reduced mass $\mu = 1.5m_n$ and different mass ratios

Isotopologue	Total mass	Mass ratio
$^3HeT^+$	6	0.5
$^6HeD^+$	8	0.25

References

[1] F Oppermann et al, J. Phys. B: At. Mol. Opt. Phys. **53**, 174001 (2020).

*E-mail: saurabh.mhatre@uni-jena.de

Adiabatic expressions for the wave function of electron in a finite-range potential and an intense low-frequency laser pulse

A V Flegel[1], N L Manakov[1], Ia V Breev[1,2], and M V Frolov[1,2] *

[1]Department of Physics, Voronezh State University, Voronezh 394018, Russia
[2]Department of Radiophysics, University of Nizhny Novgorod, Nizhny Novgorod 603950, Russia

TP

Synopsis Within the adiabatic approximation, the closed analytic form for the wave function of electron interacting with a finite-range potential and an intense low-frequency laser pulse is obtained with quasiclassical accuracy. We discuss the parametrizations of amplitudes of fundamental strong-field processes in terms of laser and binding-potential parameters. The perturbation theory in an additional weak extreme ultraviolet (XUV) pulse is developed. The XUV-induced modification of high-order harmonic generation amplitude is discussed.

There is no doubt that analytical approaches are in demand for deeper understanding of strong-field phenomena in terms of specific properties of the wave function (WF) in an intense laser field (see, e.g., Refs. [1, 2]). In this work, we extend our recently developed adiabatic approach for description of the above-threshold detachment (ATD) [3] to explore the analytical structure of the WF for an electron interacting with a finite-range potential $U(r)$ and an intense low-frequency infrared (IR) laser pulse [4]. In our analysis we consider two cases, when an electron is initially in a bound (i) or scattering (ii) state of $U(r)$. The obtained closed analytical forms for the WF comprise a sum of the initial bound state for the case (i) or the initial scattering state with the laser-modified (kinematic) momentum for the case (ii) and a rescattering correction, which is a superposition of scattering states of $U(r)$ with time-dependent momenta, whose directions and magnitudes are determined by the classical "rescattering" condition. The time-dependent coefficients in the superposition of scattering states in the case (i) are presented as a product of the tunneling exponential (describing the electron appearance in the continuum) and the time-dependent propagation factor, while in the case (ii), these coefficients involve the amplitude of electron-core scattering with the energy transfer from the laser pulse instead of the tunneling factor in the case (i).

Based on the analytic expressions for the WFs including the rescattering corrections, we obtained the parametrizations for transition matrix elements and cross sections for fundamental strong-field processes [i.e., for ATD for high-energy electrons, high-order harmonic generation (HHG), laser-assisted electron scattering, laser-assisted radiative attachment, and laser-assisted bremsstrahlung] in terms of laser and binding-potential parameters with the exact account of effects of $U(r)$ and quasiclassical accuracy for the account of electron-laser interaction. These parameterizations include either tunneling factors or scattering amplitudes and propagation factors involved in the laser-dressed WFs.

In order to describe the laser-dressed state in the presence of an additional weak field, we formulate the perturbative result for the WF in terms of the Green's function, whose approximate expression is obtained within the analytic expressions for the adiabatic WFs in the intense IR field [4]. The developed perturbation theory is used to calculate the HHG amplitude in an intense IR field and a weak extreme ultraviolet (XUV) perturbation. We found that the additional perturbative interaction of the XUV field with an atomic system in an intense IR field induces the HHG channels with the absorption of the XUV photons. The interference between different HHG channels carries an information about the nonlinear interaction of an atomic system with the laser field in the XUV range, which is of the growing interest nowadays due to increasing intensities of XUV sources.

*E-mail: frolov@phys.vsu.ru

References

[1] A de Bohan et al, Phys. Rev. Lett. **89**, 113002 (2002).
[2] M V Frolov et al, J. Phys. B **39**, S283 (2006).
[3] A V Flegel et al, Phys. Rev. A **102**, 063119 (2020).
[4] A V Flegel et al, Phys. Rev. A **104**, 033109 (2021).

Photoelectron distributions after ionization of hydrogenlike ions in superstrong electromagnetic fields

D A Telnov[1] * **and S I Chu**

[1]Department of Physics, St. Petersburg State University, St. Petersburg 199034, Russia

Synopsis Ionization probabilities and photoelectron distributions of the hydrogen atom and hydrogenlike ions He^+ and Ne^{9+} in superstrong electromagnetic fields are obtained by solving the time-dependent Dirac equation with the help of the generalized pseudospectral method in spherical coordinates, both within and beyond the dipole approximation. The photoelectron spectra exhibit above-threshold ionization peaks and a low-energy structure. In the superstrong field regime, the low-energy structure builds up with increasing field strength while the above-threshold ionization peaks decrease.

For the wavelength of the external electromagnetic field exceeding the atomic size to a great extent, the electric dipole approximation has been a common approach to describe the interaction of the atom or ion with the field. However, nondipole effects due to magnetic fields may be important even at long wavelengths, depending on the field intensity. Here we report the calculations of the photoelectron energy and angle distributions of the H atom as well as hydrogenlike ions He^+ and Ne^{9+} in superstrong electromagnetic field both within and beyond the dipole approximation [1]. The time-dependent Dirac equation is solved with the help of the generalized pseudospectral method in spherical coordinates. A simple transformation of the original Dirac Hamiltonian is suggested that removes the spurious states. For He^+ and Ne^{9+}, the external field parameters such as the peak field strength, carrier frequency, and pulse duration are scaled with respect to the nuclear charge, so all three hydrogenlike targets have identical ionization probabilities if treated nonrelativistically within the dipole approximation. Then the deviation from the scaling law can be attributed to relativistic and nondipole effects. In the set of the hydrogenlike ions with scaled external field parameters, the nondipole corrections to the ionization probabilities are larger for the targets with higher nuclear charges. For the light hydrogenlike ions and field parameters used in the calculations, the key role is played by the nondipole effects rather than kinematic relativistic corrections.

Figure 1 shows the energy–angle photoelectron spectra for He^+ both within and beyond the dipole approximation, in the polarization–propagation plane (the vertical axis is in the polarization direction). The spectra manifest the features, which are not prominent in weaker fields: the satellite structure in the above-threshold ionization (ATI) peaks and the low-energy structure (LES). With increasing the peak field strength, the LES builds up while the ATI peaks decrease.

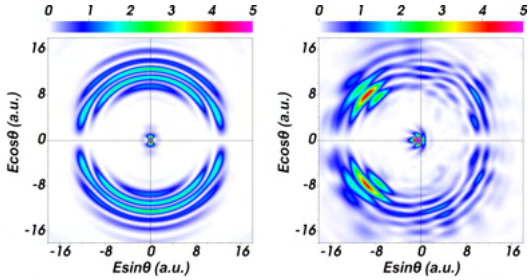


Figure 1. Energy–angle differential ionization probabilities of He^+ at the peak field strength $F = 3200$ a.u., carrier frequency is $\omega = 14$ a.u., and pulse duration $\tau = 3.75$ optical cycles. Left panel: dipole approximation. Right panel: beyond the dipole approximation.

The nondipole effects in the energy–angle distributions break the rotational symmetry about the polarization direction of the electromagnetic field. In the angular distributions within the LES, a prominent lobe opposite to the propagation direction shows up [2] and becomes dominant in stronger fields.

References

[1] D A Telnov and S I Chu, Phys. Rev. A **104**, 023111 (2021).
[2] M Førre *et al*, Phys. Rev. Lett. **97**, 043601 (2006).

*E-mail: d.telnov@spbu.ru

Strong-field ionization and a practical approach to molecular tunneling ionization theory: a case study of butadiene

Anh-Thu Le[1*], Vu Ngoc Tuoc[2 †] and Pham Nam Phong[2]

[1]Department of Physics, University of Connecticut, Storrs, 06269 Connecticut, USA
[2]Institute of Engineering Physics, Hanoi University of Science and Technology, 1 Dai Co Viet Rd., Hanoi, Vietnam

TP

Synopsis We present calculations of strong-field ionization based on numerical solutions of the time-dependent density functional theory (TDDFT). With the structure coefficients extracted from the time-independent calculations within the same approach, ionization from the molecular tunneling ionization (MO-ADK) theory can be obtained and benchmarked against the TDDFT results. We illustrate our method on the example of channel- and angle-resolved strong-field ionization of the polyatomic molecule 1,3-butadiene. We compare our theoretical results with recent measurements by Mikosch *et al*, Phys. Rev. Letts. **110**, 023004 (2013), and discuss the origin of the discrepancies with their experiment.

Strong-field ionization of molecules has been one of the most important research directions in intense laser-molecules interaction. This process is at the heart of many exciting processes in attosecond physics such as high-harmonic generation, laser-induced electron diffractions, non-sequential double ionization. Despite great progress in experimental [1,2] and theoretical [3-6] investigation, channel-resolved and angle-resolved ionization of molecules, especially polyatomic molecules is still rather semi-quantitative. In fact, recent experiment with 1,3-butadiene [2] revealed significant discrepancies between measured channel- and angle-resolved ionization yields and the quite popular molecular tunneling ionization (MO-ADK) theory [3]. This result is intriguing since angle-dependent ionization from the MO-ADK theory has been largely found to be quite satisfactory for majority of molecules so far. Furthermore, this theory has been frequently used in simulations for other strong-field processes, in which ionization can serve as the first step of the whole process.

In this work we performed detailed investigation of numerical solutions of the time-dependent density functional theory (TDDFT) and the MO-ADK theory on an example of 1,3-butadiene, for typical laser parameters used in the experiment by Mikosch *et al* [2]. The calculations were carried out using *Octopus* code [7]. To check the stability of our results, we used different exchange-correlation functionals in the TDDFT. As for the MO-ADK theory, we extracted the structure coefficients by using the same DFT functionals. This method allows accurate extraction of the structure coefficients since accurate wavefunctions at large distance can be obtained from *Octopus*. This also guarantees the consistency of the method and its comparisons with the TDDFT results.

We found overall good agreements between the TDDFT and MO-ADK results for all cases. Furthermore, our results also agree with the angle-dependent ionization from the HOMO (or the D_0 channel), measured by Mikosch *et al* [2] for the ionization from the HOMO. For the HOMO-1 (the D_1 channel), we found some discrepancies with the experiment. Based on these results, we speculate that the discrepancies with experiments could be due to the coexistence of an conformer of 1,3-butadiene molecule. This research is currently under progress.

References

[1] Agaki H et al 2009 Science **325**, 1364
[2] Mikosch J *et al* 2013 *Phys. Rev. Letts.* **110,** 023004
[3] Tong X M *et al* 2002 *Phys. Rev. A* **66,** 033402
[4] Muth-Bohm J *et al* 2000 *Phys. Rev. Letts.* **85,** 2280
[5] Tolstikhin O *et al* 2011 *Phys. Rev. A* **84,** 053423
[6] Hoerner P and Schlegel H B 2017 *J. Phys. Chem. A* **121,** 5940
[7] Tancogne-Dejean N *et al* 2020 *J. Chem. Phys.* **152,** 124119

* E-mail: thu.le@uconn.edu
† E-mail: tuoc.vungoc@hust.edu.vn

Analysis of correlations in strong field ionization

I A Ivanov[1]*, **K T Kim**[2]†

[1]Center for Relativistic Laser Science, Institute for Basic Science (IBS), Gwangju 61005, Republic of Korea
[2]Department of Physics and Photon Science, GIST, Gwangju 61005, Republic of Korea

Synopsis We propose to use correlation function analysis as a tool for the study of strong field ionization. We show, in particular, that the study of the correlations of electron's coordinate and velocity reveals patterns which can be naturally interpreted as manifestations of the electron's exit point (the spatial point where the electron exits the tunneling barrier). This analysis provides an unambiguous definition of the exit point in the tunneling ionization process. The location of the exit point thus determined agrees well with the estimates used in the semiclassical simulations.

TP

In the framework of the standard semiclassical picture of ionization based on the Keldysh theory and its modifications, known as the two-step model, [1, 2], an electron emerges into the continuum with zero or near zero velocity at a certain point in space (the tunnel exit), setting up initial conditions for the subsequent classical or semiclassical electron motion. An initial value of the coordinate is defined either by the Field Direction Model (FDM) [3] or (for Coulomb systems) by an estimate based on the use of the parabolic coordinate system [4], as a point at which the electron exits the barrier. Despite the great deal of success which had the trajectory based calculations employing these initial conditions defining the subsequent electron motion, the notions of the initial conditions are not easy to reconcile with quantum mechanics (QM). We cannot assign direct meaning to the initial electron's coordinates and velocity using the wave-function provided by the solution of the conventional TDSE, such a possibility being excluded by the very basic principles of the QM. What we can do, however, using the TDSE and the framework of the conventional QM, is to study *correlations* between different observables at different moments of time. We show that studying correlation function $C(z,t;v,t_m)$ describing correlations between the probabilities to locate electron in particular regions of the coordinate and momentum spaces reveals patterns which can be naturally interpreted as manifestations of the electron's ionization event, providing information about spatial location of the exit point, where electron exits the tunneling barrier.

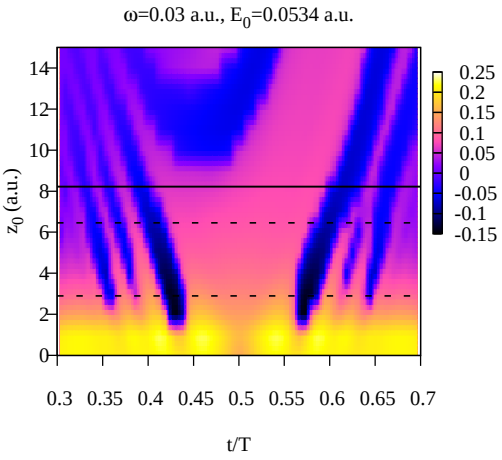


Figure 1. Correlation function $C(z,t;v,t_m)$ for a Coulomb potential for a single-cycle driving laser pulse. Black dash lines show locations of the tunnel entry and exit points obtained using the FDM formula [3], solid black lines show location of the tunnel exit point based on the estimate using parabolic coordinates [4].

References

[1] L V Keldysh, Sov. Phys. -JETP. **20**, 1307 (1965).
[2] H R Reiss, Phys. Rev. A **22**, 1786 (1980).
[3] A S Landsman and U Keller, Physics Reports **547**, 1 (2015).
[4] N I Shvetsov-Shilovski, D Dimitrovski and L B Madsen **85**, 023428 (2012).

*E-mail: igorivanov@ibs.re.kr
†E-mail: kyungtaec@gist.ac.kr

Complexity of the holographic structures induced by strong field laser pulses in atomic targets

A Taoutioui [1] *, **K Tőkési** [1] †
[1]Institute for Nuclear Research, Debrecen, 4026, Hungary

TP

Synopsis Photoelectron holographic structures in momentum distributions of ionised electrons by few-cycle strong laser pulses are investigated for hydrogen atom target by solving numerically the full-dimensional time-dependent Schrödinger equation. We present results on how the number of optical cycles, the intensity, and the wavelength of the laser pulse influence the holographic structures. We found that the density of the interference stripes in the holographic structures can be increased either by increasing the laser intensity or by using longer laser wavelengths.

Nowadays, the laser-induced electron diffraction (LIED) imaging technique uses the self-imaging of the molecular target by its own re-scattered electrons liberated by strong-field interaction to image the nuclei motion in molecules[1,2]. Those electrons must be sufficiently energetic to induce a possible structure retrieval from the diffraction pattern. On the other hand, the re-scattered electrons are also the backbone of the strong-filed attosecond photoelectron holography (SFAPH) imaging technique because they represent the probe electron beam of the target structure. This latter is based on the interference scenarios between the scattered and unscattered electrons liberated in the same optical cycle. Along this line an intensive work has been devoted to understand the sub-cycle electron dynamics from the momentum distributions of photoelectrons (holograms) [3,4]. The principle of photoelectron holography is based on the presence of two coherent electron wave packets (the re-scattered and direct electron wave packets) which interfere between each other due to their phase difference forming holographic structures in the PMD.

We found that the formation of the most known holographic structures strongly depend on the number of optical cycles (see Fig. 1.). In particular for the case of the three-cycle pulse, the PMD shows an interesting features, i.e. one can see the coexistence the fishbone-like, shield like and fanlike holographic structures in the same holographic pattern (see Fig. 1c). Thus, the three-cycle pulse could be a good pulse candidate to investigate the holographic structures. In addition, we can also note that the ATI rings are less pronounced and will not wash out the holographic patterns unlike the multi-cycle pulses (see Fig. 1d). The effects of the intensity and wavelength of the laser pulse to the PMD show that they are responsible for the interference fringes density in the holographic structures. We found in particular, that the fan-like structure is very sensitive to the wavelength variation. It is interesting to note that this fan-like structure can disappear by applying longer wavelengths [5].

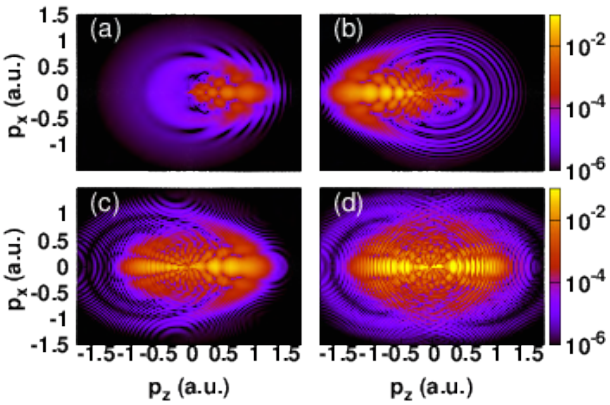


Figure 1. PMDs corresponding to the ionisation of hydrogen atom induced by a strong laser pulse of a carrier wavelength of 800nm . The panels correspond to different number of optical cycles N of the pulse. (a): N=1; (b): N=2; (c): N=3 ; (d): N=8. The laser intensity and the carrier envelope phase are fixed at $1 \times 10^{14} cm^2$ and 0 degree respectively.

Acknowledgement

This work was support by the Bilateral relationships between Morocco and Hungary in science and technology (S&T) under the project number 2018-2.1.10-TÉT-MC-2018-00008.

References

[1] Blaga, C. I. et al., Nature (2012) 483, 194–197.
[2] Pullen, M. G. et al., Nat. Commun. (2015) 6,1–6.
[3] Krasniqi, F. et al., Phys. Rev. A (2011) 81, 033411.
[4] de Morisson Faria et al. Rep. on Prog. Phys. (2020) 83, 034401.
[5] Taoutioui A et al., Sci Rep (2022) **12,** 2877.

* E-mail: abdelmalek.taoutioui@atomki.hu
* † E-mail: tokesi@atomki.hu

Non-dipole effects in strong-field detachment from negative ions

R Kahvedžić[1,2]*, **S Gräfe**[1,2,3,4]†

[1]Institute of Physical Chemistry, Friedrich Schiller University Jena, Jena, 07743, Germany
[2]Max Planck School of Photonics, Jena, 07745, Germany
[3] Abbe Center of Photonics, Friedrich Schiller University Jena, Jena, 07745, Germany
[4]Fraunhofer Institute for Applied Optics and Precision Engineering, Jena, 07745, Germany

TP

Synopsis We analyze the process of electron detachment from negative ions in intense mid-infrared light fields by applying our non-relativistic approach to strong-field approximation with the first-order non-dipole correction. The approach allows us to compute the photoelectron momentum spectra including the non-dipole correction and using the dipole approximation, thereby enabling a direct comparison and identification of differences, which is used to study the non-dipole effects.

Our approach is based on the single-active electron strong-field approximation (SFA) with non-dipole corrections. The Volkov wave functions are solutions of the length gauge time-dependent Schrödinger equation (TDSE) with the Hamiltonian

$$H = \frac{\mathbf{p}^2}{2} + \underbrace{\left(\mathbf{r} + \frac{\hat{\mathbf{k}}\cdot\mathbf{r}}{c}\mathbf{p}\right)\cdot\mathbf{E}(t)}_{H_{\rm int}(t)}, \qquad (1)$$

obtained by retaining terms up to first order in the expansion of the vector potential in powers of the inverse speed of light c [1]. These non-dipole Volkov states are of the form

$$\psi^{\rm V}_{\mathbf{p}}(\mathbf{r},t) = \frac{1}{(2\pi)^{3/2}} e^{i\boldsymbol{\pi}(\mathbf{p},t)\cdot\mathbf{r} - \frac{i}{2}\int^t dt'[\boldsymbol{\pi}(\mathbf{p},t')]^2}, \quad (2)$$

with the modified canonical momentum $\boldsymbol{\pi}(\mathbf{p},t) = \mathbf{p} + \mathbf{A}(t) + \frac{\hat{\mathbf{k}}}{c}\left[\mathbf{p}\cdot\mathbf{A}(t) + \frac{1}{2}\mathbf{A}^2(t)\right]$. Within the SFA, the transition amplitude from the initial bound state ψ_i to the Volkov state is $M_{\mathbf{p}i} = M^{(0)}_{\mathbf{p}i} + M^{(1)}_{\mathbf{p}i}$, with [2]

$$M^{(0)}_{\mathbf{p}i} = -i\int_{t'}^{t} dt_0 \langle\psi^{\rm V}_{\mathbf{p}}(t_0)|H_{\rm int}(t_0)|\psi_i(t_0)\rangle, \quad (3)$$

$$M^{(1)}_{\mathbf{p}i} = -\int_{t'}^{t} dt_1 \int_{t'}^{t_1} dt_0 \int d^3\kappa \langle\psi^{\rm V}_{\mathbf{p}}(t_1)|V(\mathbf{r}) \times |\psi^{\rm V}_{\boldsymbol{\kappa}}(t_1)\rangle\langle\psi^{\rm V}_{\boldsymbol{\kappa}}(t_0)|H_{\rm int}(t_0)|\psi_i(t_0)\rangle, \quad (4)$$

where $M^{(0)}_{\mathbf{p}i}$ describes the direct transition, whereas $M^{(1)}_{\mathbf{p}i}$ accounts for rescattering with the parent core via the effective potential $V(\mathbf{r})$. The differential detachment probability for a given momentum $\mathbf{p}$ is proportional to the modulus squared of the transition amplitude. Numerically evaluating the integrals appearing in the transition amplitude, we compute the momentum spectra of photoelectrons originating from strong-field photodetachment of the F^- ion (see the figure below). Comparing spectra computed with the first-order non-dipole correction to their dipole approximation counterparts, we identify and analyze the non-dipole effects on momentum distributions of photoelectrons. We find that the non-dipole correction accounts for the forward-backward asymmetry along the pulse propagation direction in intense mid-IR fields.

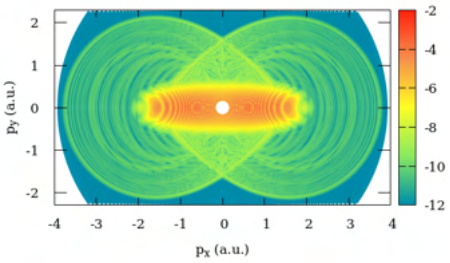


Figure 1. Photodetachment spectrum of F^- ion in a linearly polarized long pulse of wavelength 3200 nm and intensity 2.0×10^{13} W/cm^2.

References

[1] N J Kylstra et al., J. Phys. B **34**, 2001 (2001)
[2] D B Milošević et. al Phys. Rev. A **68**, 2003 (2003)

*E-mail: resad.kahvedzic@uni-jena.de
†E-mail: s.graefe@uni-jena.de

Modeling molecular break-up processes under short and intense laser pulses

C-H Yuen[1]*, **P Modak**[1] , **and C-D Lin**[1]

[1] Kansas State University, Manhattan, 66506, USA

TP

Synopsis Intense short laser pulses (a few femtoseconds) have been used in recent years to study the breakup dynamics of molecules. However, observable such as kinetic energy release and branching ratios of molecular fragments are often difficult to predict by theory. In this work, we develop a simple model for sequential double ionization and apply it to the case of nitrogen molecule.

In pump-probe experiments, population of pumped states is generally less than 10% of the population of the initial state. Probing the dynamics with a weak laser therefore results in weak signal. To enhance the probe signal, it is desirable to use an intense short laser field.

One of the possible process for strong field probe is double ionization. In recent years, there are numerous studies on breakup dynamics of molecules using short and intense IR laser field [1, 2]. Momenta of charged fragments from double ionization have been measured in coincidence. Angle-integrated quantities, such as kinetic energy release (KER) and branching ratios, can then be obtained. These observables may be less sensitive to the details in modeling, such that it is possible to simulate the results with a simple model.

In this work, we utilize a fixed-nuclei density matrix approach to model the sequential double ionization process. The model includes tunneling ionization of the neutral and the ion as well as laser couplings between the ionic states. Population of different doubly charged states can be obtained at a low computational cost. To benchmark our model, we apply it to the nitrogen molecule. A good agreement on the KER spectra with a previous experiment [3] is obtained.

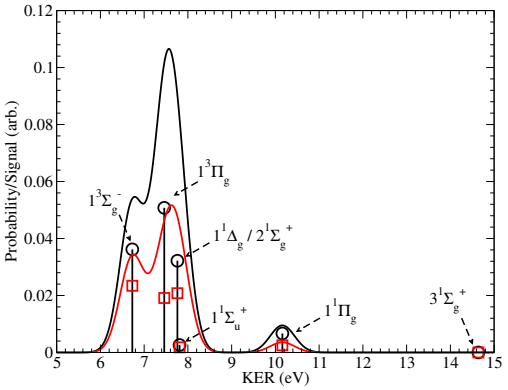


Figure 1. Angular-averaged probabilities for forming different N_2^{2+} states with non-zero KER, obtained with (circle) and without (square) including the laser couplings of different N_2^+ states. Black and red solid lines are the convoluted results with 0.28 eV energy resolution. The laser used is linear polarized and has a peak intensity of 1.2 $\times 10^{15}$ W/cm^2, pulse duration of 8 fs, and 800 nm wavelength.

References

[1] S Zhao et al, Phys. Rev. A **99**, 053412 (2019).
[2] C Cheng et al, Phys. Rev. A **104**, 023108 (2021).
[3] S Voss et al, J. Phys. B: At. Mol. Opt. Phys. **37**, 4239 (2004).

*E-mail: iyuen@phys.ksu.edu

Frustrated tunneling dynamics in ultrashort laser pulses

E Olofsson[1], S Carlström[1] and J M Dahlström[1]*

[1]Lund University, Lund, Box 118, SE-221 00 Lund, Sweden

Synopsis We study the process of frustrated tunneling in ultrashort laser pulses with a model based on the strong-field approximation, and investigate the modulations in the final state populations as the carrier-envelope phase of the pulse is varied. The results of the model are compared to results obtained by the solving the time dependent Schrödinger equation.

TP

In addition to the process of tunneling ionization, one also finds a nonzero Rydberg state population, when an atom is subjected to an intense, low frequency laser pulse. This process is known as frustrated tunneling ionization, and has been explained with a classical model where the electron tunnels close to the peaks of the electric field, and is later captured by the atomic potential [1]. We have studied frustrated tunneling in Hydrogen with ultrashort pulses using a model based on the strong-field approximation (SFA) [2], and compared it to results obtained by solving the time-dependent Schrödinger equation (TDSE) [3]. We used pulses of 800 nm wavelength, a 2, 3, or 4 cycle pulse duration and intensities on the order of 10^{14} W/cm^2.

The SFA model that was used relies on a saddle-point approximation that is supplemented with additional constraints to ensure that the trajectory associated to a solution of the saddle-point equation will have have an energy and angular momentum that corresponds to a particular Rydberg state. We find that there are two classes of trajectories that can lead to frustrated tunneling: the first branch has recolliding trajectories that are born after the peaks of the electric field (α), while the second branch consists of trajectories that are born before the electric field peaks (β). Since we are dealing with short laser pulses, the carrier-envelope phase (CEP) becomes important. The solutions to the modified SFA equations show an intricate dependence on CEP and angular momentum l. As the CEP is varied in our TDSE simulations, we see a modulation in the total population of states with different principal quantum numbers n, see Fig. 1, that the SFA theory can qualitatively reproduce for $n \geq 5$. However, for $n = 2, 3$ we do not see agreement between the TDSE and SFA results. Additionally, when we resolve the CEP variations in l, we do not find agreement between TDSE and SFA for any n.

In conclusion, we have showed that population transfer to Rydberg states in ultrashort, intense pulses can be interpreted by frustrated tunneling. To support this conclusion, we have also performed TDSE simulations where the continuum states are damped during propagation, and find that this leads to an incorrect excited state distribution, which suggests that the continuum states play an important role in populating the Rydberg states.

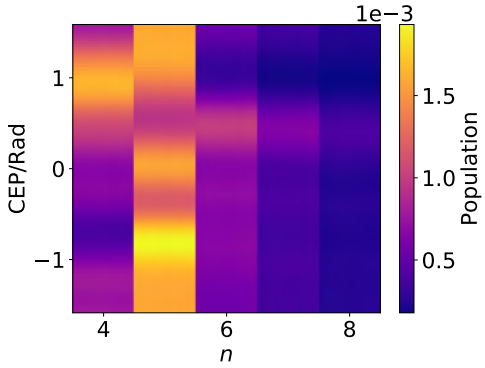


Figure 1. CEP dependence of the Rydberg population with principal quantum number n, calculated with the TDSE.

References

[1] T Nubbermeyer *et al.*, Phys. Rev. Lett. **101**, 233001 (2008).
[2] S V Popruzhenko, J. Phys. B: At. Mol. Opt. Phys. **51**, 014002 (2017).
[3] E Olofsson, S Carlström, and J M Dahlström, J. Phys. B: At. Mol. Opt. Phys. **54**, 154002 (2021).

*E-mail: marcus.dahlstrom@matfys.lth.se

Signatures of multi-band effects in high-harmonic generation in monolayer MoS_2

B R Nebgen[1,2 *], L Yue[3 †], R Hollinger[1,2], C B Uzundal[1,2], Z Gan[4], E Najafidehaghani[4], A George[4], C Spielmann[5,6,7], D Kartashov[5,6], A Turchanin[4,6], D Y Qiu[8], M B Gaarde[3], M Zuerch[1]

[1]Department of Chemistry, University of California, Berkeley, 94720, USA; [2]Lawrence Berkeley National Laboratory, Materials Science Division, Berkeley, 90720, USA; [3]Department of Physics and Astronomy, Louisiana State University, Baton Rouge, 70803, USA; [4]Institute of Physical Chemistry, Friedrich Schiller University, Jena, 07743, Germany; [5]Institute of Optics and Quantum Electronics, Friedrich Schiller University, Jena, 07743, Germany; [6]Abbe Center of Photonics, Friedrich Schiller University, Jena, 07743, Germany; [7]Helmholtz Institute, Jena, 07743, Germany; [8]Department of Mechanical Engineering and Materials Science, Yale University, New Haven, 06520, USA

TP

Synopsis Experimental observation of high harmonic generation (HHG) in monolayer MoS_2 reveals high-harmonic yield dependence on crystal orientation due to spatial symmetry as well as recombination from multiple conduction bands. Observation of such specific material properties through HHG paves the way for using solid-state HHG spectroscopy to probe ultrafast dynamics and trace phase transitions in condensed matter.

High-harmonic generation (HHG) from intense laser pulses in solids is increasingly attracting attention as a probe of ultrafast electronic processes and crystalline symmetries in condensed matter systems [1]. HHG from atomically thin semiconductors provides an opportunity to investigate the microscopic origin of HHG due to the absence of laser propagation effects [2]. In addition, few-layer transition metal dichalcogenides (TMDs) offer a tunable material platform with unique properties to interrogate with solid-state HHG and diverse applications in optoelectronics and spintronics [3].

Here, we investigate the polarization properties of high-order harmonics generated in monolayer MoS_2 as a function of crystal orientation relative to the mid-IR laser field polarization [4]. We experimentally observe that crystal symmetries impose constraints on harmonic emissions, leading to pronounced nodes in the HHG spectra at certain angles (dots in Fig 1a). These symmetry constraints have been explored previously in MoS_2 [5]. Building on previous studies, we additionally find an angular shift such that for several mid-IR wavelengths, the parallel-polarized odd-order harmonics below (above) 3.5 eV are enhanced for driver polarization along the armchair (zigzag) direction (Fig 1a). By solving the time-dependent density matrix equations involving a valence band and two conduction bands, we trace these angular shifts to electron-hole recombinations from different conduction bands, mapping lower energy harmonics to recombinations involving the first conduction band and higher energy harmonics to recombinations involving the second conduction band (see theory results in Fig 1b). This measurement effectively probes the vectorial nature of recombination dipoles from different bands in MoS_2, building up from the single conduction band picture of solid-state HHG that has been considered previously. This material specific analysis paves the way for solid-state HHG as a detailed probe of ultrafast dynamics in condensed matter systems.

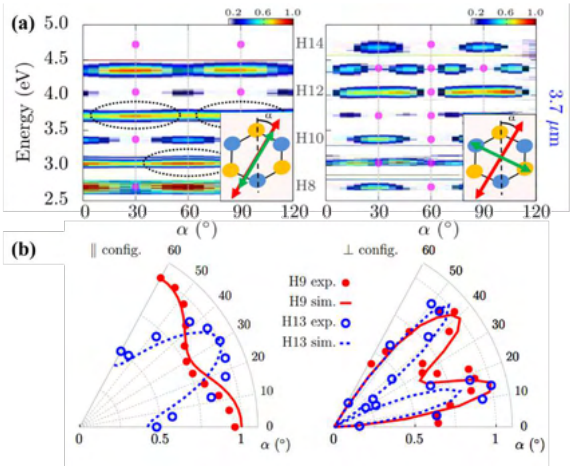


Figure 1. (a) Orientation dependent HHG spectra of MoS_2 with a 3.7 μm driver highlighting the angular shift in parallel-oriented odd harmonics at 3.5 eV (dotted ovals). (b) Comparison of experimental and simulated orientation-dependent HHG yields with a 3.7 μm driver.

References

[1] S Ghimire and D A Reis, Nat. Phys. 90, 10-16 (2019). [2] S Manzeli, et. al., Nat. Rev. Mater. 2, 17033 (2017). [3] I Kilen, et. al., Phys. Rev. Lett. 125, 083901 (2021). [4] L Yue, et. al., arXiv:2112.13032v2 [cond-mat.mtrl-sci] (2022). [5] H Liu, et. al., Nat. Phys. 13, 262-265 (2017).

* E-mail: bailey_nebgen@berkeley.edu
† E-mail: lyue3@lsu.edu

High-resolution time-of-flight electron spectrometry with time-dependent retarding potentials

Gabriel Granveau[1] **and Charles Bourassin-Bouchet**[1]*

[1]Université Paris-Saclay, CNRS, Laboratoire Charles Fabry, Institut d'Optique Graduate School, Palaiseau Cedex, 91127, France

Synopsis We propose to enhance the performances of electron Time-of-Flight spectrometers by using a dynamical retarding potential instead of a static one. This allows one to adapt the retarding potential as a function of the electrons' kinetic energy and therefore to control their flight time. Simulations show that this could dramatically improve the energy resolution of Time-of-Flight spectrometers over a wide energy range.

Time-of-Flight (ToF) spectroscopy was first used by Thomson in 1913 [1], and was then further developed through the XXth century. The technology has been widely adopted by the attosecond community for measuring photoelectron kinetic energy spectra, and improved for example by adding a magnetic bottle [2]. However such ToF spectrometers cannot maintain a high resolution over broad energy spectra which are yet inherent to attosecond photoionization. While the energy resolution is very good at low energy, it rapidly worsens as the energy increases, see Fig. 1 a). A usual improvement consists in adding a retarding potential in order to slow down and better resolve the fastest electrons. As a counterpart, electrons with an energy lower than the potential step are irremediably lost.

In this work, we propose to replace the static retarding potential with a dynamical one. By adapting the height of the potential step as the electrons arrive on it, one can selectively slow down or accelerate electrons with a given energy. Through this new degree of freedom, it becomes possible to control the electron flight time at each energy, thus opening new possibilities such as bunching the electrons or increasing the energy resolution. Although related approaches have been developed for controlling ion beams [3], this idea has never been applied to ToF electron spectroscopy to our knowledge. Moreover this concept can in principle be implemented on existing ToF spectrometers by simply replacing the static retarding potential generator with an arbitrary waveform generator. We have validated this approach numerically with the softwares SIMION and COMSOL. In Fig.1 (b-c), the potential is chosen to optimize the energy resolution over the 5-150 eV range. On existing spectrometers, our simulations show that the resolution is then improved up to a factor of 4 at 140 eV compared to the situation without retarding potential, see Fig.1 b). This improvement increases up to a factor of 9 when the position of the potential step in the flight tube is also optimized, see Fig.1 c).

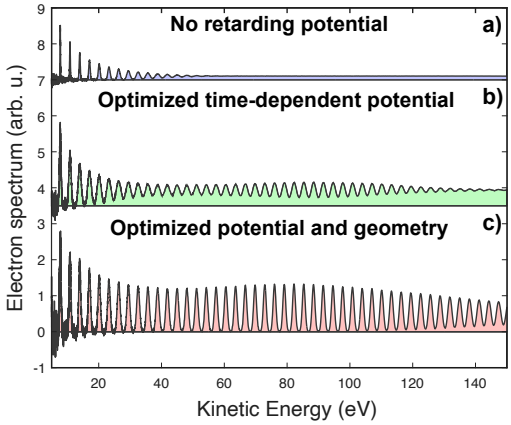


Figure 1. Simulation of the energy response of different spectrometers to a comb of equi-intense infinitly narrow high-order harmonics spaced by 3.1 eV: a) without retarding potential, b) with a dynamical retarding potential, c) with a dynamical potential and an optimized geometry. In the three cases, the total flight tube length is 2.2m.

References

[1] J. Thomson, *Rays of Positive Electricity and their Application to Chemical Analysis.*, Longmans, Green and Co. (1913).

[2] P. Kruit and F. H. Read, J. Phys. E: Sci. Instrum. 16 313 (1983).

[3] F. J. Lynch et al., Nucl. Instr. and Meth. 159, 245-263 (1979).

*E-mail: charles.bourassin-bouchet@institutoptique.fr

Competition of anomalous and interband polarization contributions to high-harmonic generation in solids

Lun Yue* **and Mette B. Gaarde**

Department of Physics and Astronomy, Louisiana State University, Baton Rouge, Louisiana 70803, USA

TP

Synopsis High-harmonic generation (HHG) has been touted as a potential all-optical probe of the Berry curvature in solids. Here, we theoretically investigate the competition between the Berry curvature and interband contributions to HHG in MoS_2. Results from our ab-initio current-decomposition approach show that while the anomalous current, involving the Berry curvature, often dominates for the lowest-order harmonics, the interband current dominates for higher harmonics, even well below the band gap.

A pertubative external electric field irradiating a solid with nonvanishing Berry curvatures (BCs) can induce an anomalous current perpendicular to the driving field. Recently, it has been suggested that an intense mid-infrared laser can induce nonperturbative anomalous high harmonics [1, 2], and that such harmonics could be used as an all-optical probe of the BCs of a material [2]. At the same time, the interband current can also induce harmonics polarized perpendicular to the driving laser [3]. The aim of our work is to shed light on the competition between the anomalous and the interband harmonics.

We investigate HHG in monolayer MoS_2, due to the extensive recent interest in atomically thin semiconductors, as well as the lack of propagation effects. Density-functional theory is used to obtain the relevant bands and couplings, and HHG is calculated using a time-dependent density-matrix formalism in the velocity gauge. A novel implementation involving the dressed bands and couplings allows us to decompose the total microscopic current into four contributions: intraband, interband, anomalous and mixture currents. The figure shows an example of a decomposed spectrum, and it is clearly observed that the anomalous harmonics involving the BCs dominate at low harmonic orders, while interband harmonics dominate at higher harmonic orders, even well below the band gap energy (vertical line).

The intraband and mixture harmonics have negligible contributions. Further simulations show that increasing the driving laser wavelength will increase the anomalous-to-interband yield ratios of the low-order harmonics, which can potentially lead to the experimental disentangling of the anomalous and interband harmonics. Finally, we show that the anomalous harmonics depend on the BCs of all the valence bands in MoS_2, not only the bands near the band gap.

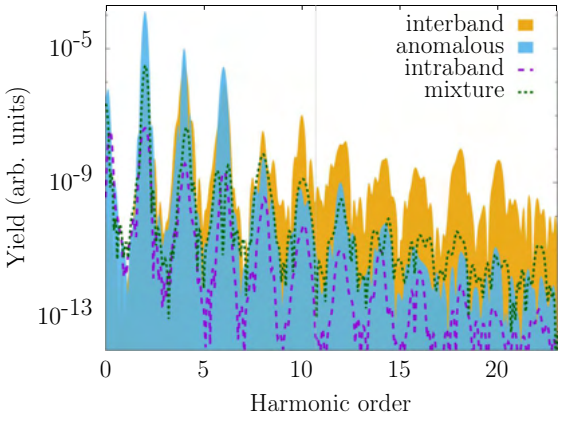


Figure 1. HHG spectrum for driving laser polarized perpendicular to the MoS_2 mirror axis, and harmonics emitted along the mirror axis. Pulse parameters are 7400 nm, 0.05 TW/cm^2 and 148 fs.

References

[1] H. Liu, Y. Li, Y. S. You, S. Ghimire, T. F. Heinz, and D. A. Reis, Nat. Phys. **13**, 262 (2017).

[2] T. T. Luu and H. J. Wörner, Nat. Commun. **9**, 916 (2018).

[3] N. Yoshikawa, K. Nagai, K. Uchida, Y. Takaguchi, S. Sasaki, Y. Miyata, and K. Tanaka, Nat. Commun. **10**, 3709 (2019).

*E-mail: lyue3@lsu.edu

Two-color-driven enhanced high-order harmonic generation in solids

U Thumm[1]* **and F Navarrete**[1,2]

[1]Department of Physics, Kansas State University, Manhattan, Kansas 66506, USA; [2]Institute of Physics, University of Rostock, 18051 Rostock, Germany

Synopsis For suitable amplitude ratios and delays of a fundamental pulse and its coherently superimposed second harmonic driving pulse, we find for high-harmonic generation (HHG) in MgO crystals an up to fivefold enhancement of the spectral HH yield and significant shifts of the HH cutoff frequency.

We theoretically investigate the emission of high-harmonic (HH) radiation in model crystals [1] by bichromatic few-cycle driving pulses that are composed as the phase-coherent superposition of a mid-infrared fundamental pulse and its second harmonic [2]. Adjusting the model-crystal parameters to reproduce the lowest band gap of MgO, we examine the extent to which distinct domains of the HH spectrum can be controlled and enhanced by tuning the temporal profile of the bichromatic driving laser electric field. We change the driving-pulse shape by varying its fundamental-versus-second-harmonic pulse amplitude ratio and delay, while keeping the energy of the driving laser pulse fixed.

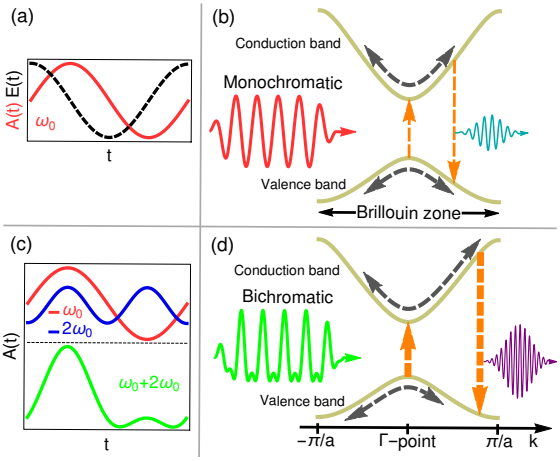


Figure 1. Mechanisms of HHG in solids by (a), (b) monochromatic and (c), (d) bichromatic pulses.

Figure 1(a) shows the vector potential $A(t)$ (solid red line) and electric field $E(t)$ (dashed black line) of a monochromatic driving laser pulse with carrier frequency ω_0. A schematic of HHG by a monochromatic driver (red line) interacting with a two-band model solid represented by the dispersion curves of its valence and conduction bands as a function of the crystal momentum k in the first BZ is shown in Fig.1(b). The induced intraband motion in both bands is indicated as dashed gray arrows. Laser-driven interband excitation and recombination are represented as orange arrows. Electronic intraband and interband currents contribute to the emission of HH radiation (cyan line).

Figure 1(c) depicts the vector potentials for one period of the fundamental pulse (red line) and phase-coherent harmonic pulse (blue line) with frequencies ω_0 and $2\omega_0$, and their bichromatic superposition pulse (green line) with harmonic-conversion ratio $R = 0.5$ and chromatic delay $\tau = \pi/4$. HHG in by bichromatic driver (green line) in sketched in Fig.1(d). The asymmetry and non-sinusoidal shape of the driver modify intraband and interband currents, as compared to a monochromatic driver of identical pulse energy. This changes the HHG spectrum (purple line) and can increase the HHG yield and cutoff frequency.

Supported by AFO-SR Award N° FA9550-17-1-0369 and NSF Grant N° PHY-1802085.

References

[1] F Navarrete, M F Ciappina, and U Thumm, Phys. Rev. A **100**, 033405 (2019).

[2] F Navarrete and U Thumm, Phys. Rev. A **102**, 063123 (2020).

*E-mail: thumm@phys.ksu.edu

TP

Spatial phase shifts in the near-field of plasmonic nanoparticles play a key role for the direct photoexcitation of dark states in aggregates

F Dröge[1], K Renziehausen[1]*, U Peschel[1], A Schubert[1,2], S Gräfe[1,3]

[1]Institute of Physical Chemistry & Abbe School of Photonics, Friedrich Schiller University Jena, Helmholtzweg 4, 07743 Jena, Germany
[2]Present address: Merck KGaA, 64293 Darmstadt, Germany
[3]Fraunhofer Institute for Applied Optics and Precision Engineering IOF, Albert-Einstein-Str. 7, 07745 Jena, Germany

Synopsis By means of quantum dynamical simulations we explain how to control the dynamics of an excitonic system in the vicinity of a plasmonic nanoparticle: The aggregate is excited with the combined electric field of both the laser pulse and an additional field generated by the nanoparticle. The combined field is spatially inhomogeneous, so each individual monomer unit experiences a different field, with differences in both field strength and phase. Our analysis shows that this phase shift is an important tool to influence the direct photoexcitation of electronic dark states of the aggregate.

Nanoplasmonics[1] have emerged to be a hot research topic. Here, we present results of our recent work on the dynamics of plasmonic-excitonic model systems[2]. When the electric field E_L of an incident laser pulse interacts resonantly with a metallic nanoparticle, it induces a collective oscillating motion of the particle's electrons. This oscillation causes a coherent electric field E_{NP} which is strongly localized within the vicinity of the nanoparticle and falls off exponentially as a function of distance. In the model system considered here, a molecular aggregate is in this vicinity (see Fig. 1 for the case that the aggregate is a quadrumer). The aggregate experiences the combined field $E_\Sigma = E_L + E_{NP}$, comprised of the incident laser, E_L, and the spatially inhomogeneous near field E_{NP}. As a consequence, both the amplitude $E_{0,\Sigma}$ and the phase ϕ_Σ of this field E_Σ will depend on the distance R from the nanoparticle. Thus, the different monomer units are affected by different field strengths of the superposed field E_Σ. Neighboring electronic excited states $|e_n\rangle$ of the aggregate are coupled by a static coupling, lifting the degeneracy. From these new states, some states are optically accessible, while others are dark (see also Fig. 1B). However, even these small differences in the interaction of each monomer with the field lead to a breaking of the aggregate's symmetry, so that the electronic states being formerly dark can be directly photoexcited. Our quantum dynamical simulations illustrate that this population of the formerly dark states both for a dimer and a quadrumer is primarily due to the variation in the distance-dependent phase ϕ_Σ. For the dimer, the monomer unit which is further away from the nanoparticle is preferentially excited.

*E-mail: klaus.renziehausen@uni-jena.de

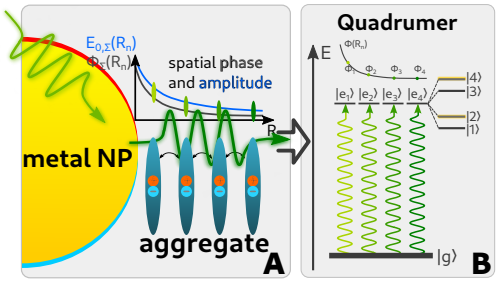


Figure 1. Schematic representation of the analyzed system for a quadrumer aggregate. Panel **A**: Full system including the plasmonic nanoparticle, the quadrumer, the incident laser pulse (light green), the resulting superposed field (dark green), and the spatial depencency of the amplitude $E_{0,\Sigma}$ and the phase ϕ_Σ. Panel **B**: Energy levels with one common ground state $|g\rangle$ and four degenerate states $|e_n\rangle$. An intra-aggregate coupling splits these states into the states $|n\rangle$, where the states $|2\rangle$ and $|4\rangle$ are dark states in case of a homogenous illumination.

References

[1] S A Maier. *Plasmonics: fundamentals and applications*, Springer (2007).
[2] F Dröge, K Renziehausen, U Peschel, A Schubert, S Gräfe. (2022) (in preparation).

Light-wave coherent control of the Mott transition.

E B Molinero[1]*, **R E F Silva**[1,2]†

[1]Instituto de Ciencia de Materiales de Madrid, Consejo Superior de Investigaciones Científicas (ICMM-CSIC), Madrid, E-28049, Spain

[2]Max-Born-Institut, Max Born Strasse 2A, D-12489 Berlin, Germany

Synopsis In the present work, we show that the phase transition in Mott-like systems under presence of a field, can be effectively controlled by a proper engineer of the laser. We also find that it can be experimentally characterize based on the optical response of the system.

TP

The discovery of high-harmonic generation in bulk solids [1] enabled the encounter of two (previously) non-overlapping areas of physics: condensed matter and attosecond physics. Since then, there has been an increasing interest in this newborn field because it allows us to elucidate the ultrafast dynamics of electrons. In ref. [2], it was found that when a strong laser field is applied to a Mott system, a phase transition (from insulator to metal) will take place if the amplitude of the field surpass a certain threshold. This transition occurs because the electrons are able *to tunnel* through the Coulomb interaction assisted by the laser and therefore, doublons begin to appear.

The main purpose of this work is to show that one can take advantage of this tunneling mechanism in order to acquire a *coherent control* over the Mott transition by engineering the laser. To achieve that goal, we will superimpose two different lasers: a mid-IR and a train of short pulses. They are chosen so neither of them reaches the threshold on their own; only when they sum coherently, the amplitude of the total field will be higher than the threshold and thus, the Mott phase breaks down. Then, one would expect that the phase transition can be forced by tuning the laser parameters. Indeed, we show that by varying the delay δ (between the two lasers) and also varying the carrier-envelope phase ϕ_{CEP} of the short pulses, the transition only takes place for specific values of the pair $(\delta, \phi_{\mathrm{CEP}})$.

Solving the time-dependent Schrödinger equation confirms this statement. We also find that all the dynamics can be predicted by computing the doublon total production rate Γ [3], a quantity which *only* depends on the laser shape and the threshold amplitude. In Fig. 1 we compare the production rate versus the mean number of doublons D. There, one can appreciate that a maximum in the production rate is translated to an increase in the number of doublons, signaling the appearance of the phase transition. Therefore, the transition can be effectively controlled by first, making a prediction based on Γ and afterwards, engineer the laser parameters accordingly. Lastly, we show that the Mott transition can be optically characterized thanks to its emission spectra. Interestingly, we find that the *integrated spectrum* I also resembles the prediction made by Γ, which makes I a suitable figure of merit of the phase transition.

Our work has shown how one can take advantage of the tunneling phenomenon in strongly correlated systems to control their insulator-to-metal phase transition. We expect this could facilitate the generation of such phases experimentally.

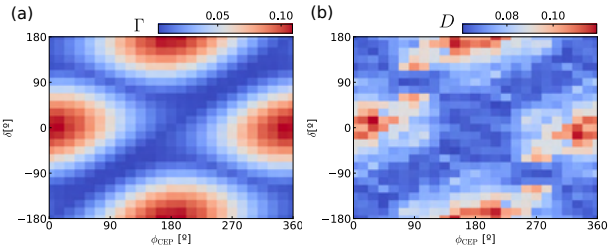


Figure 1. (a): Total production rate Γ. (b): Average number of doublons D.

References

[1] S Ghimire et al, Nature Phys **7**, 138–141 (2011).
[2] R E F Silva et al, Nature Photon. **12**, 266–270 (2018).
[3] T Oka, Phys. Rev. B **86** 075148 (2012).

*E-mail: ebmolinero@gmail.com
†E-mail: ruiefdasilva@gmail.com

First-principles simulation for attosecond transient spectroscopy of solids and its application to magnetic materials

S A Sato[1,2] *

[1]Center for Computational Sciences, University of Tsukuba, Tsukuba, Ibaraki 305-8577, Japan
[2]Max Planck Institute for the Structure and Dynamics of Matter, Luruper Chaussee 149, 22761 Hamburg, Germany

TP

Synopsis We study the transient optical properties of laser-excited magnetic materials with the first-principles calculation. As a result, we find a significant reduction of the photoabsorption of bulk Co and Ni around the $M_2, 3$ absorption edge, reflecting the light-induced demagnetization and reduction of exchange-splitting. The discovered correlation between magnetic and optical properties of solids would enable us to study the light-induced ultrafast spin-dynamics in the time domain via transient optical spectroscopy.

We have been developing the first-principles electron dynamics calculations to simulate the attosecond spectroscopy for solids [1] based on the time-dependent density functional theory (TDDFT). The first-principles calculations have been a powerful tool to analyze complex electron dynamics in solids, and we studied the microscopic mechanism of ultrafast phenomena in the attosecond regime. In the recent work for bulk Ti [2], we combined the first-principles calculations with the attosecond transient absorption spectroscopy and clarified that optical properties of laser-excited transition metals can be modified due to the light-induced ultrafast electron localization.

In this work, we apply the first-principles calculations to magnetic materials in order to find a correlation between transient magnetic and optical properties of light-driven systems [3]. For this purpose, we analyze the transient optical properties of laser-excited bulk Co and Ni as a prototype of magnetic materials. Figure 1 (a) shows the computed absorption spectrum of bulk Co. The $M_{2,3}$ absorption edge is located at around 56 eV. We then compute the absorption coefficient μ by changing the electron temperature T_e to study the laser-excited materials in the hot-electron state. Figure 1 (b) shows the change of the absorption spectrum from the room temperature. As seen from Fig. 1 (b), the photoabsorption significantly decreases around the absorption edge with the increase in the electron temperature. We further analyzed the local magnetization of Co atoms and their exchange split for different electron temperatures. As a result, we found that the electronic excitation reduces the local magnetization and the exchange-split of core states, causing the blue shift of the absorption edge. The blue shift further causes the decrease of photoabsorption around the absorption edge. The observed connection between transient magnetic and optical properties would offer a novel opportunity to study the light-induced ultrafast spin-dynamics with the transient optical spectroscopy technique.

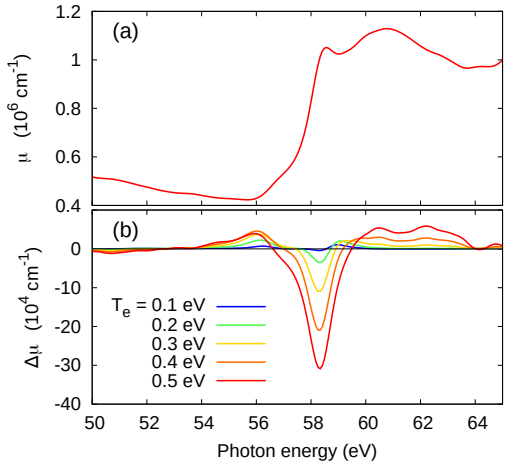


Figure 1. (a) Static photoabsorption spectrum of bulk Co. (b) Photoabsropiton change by changing the electron temperature T_e.

References

[1] S A Sato, Comput. Mater. Sci. **194**, 110274 (2021).
[2] M Volkov *et al.*, Nature Physics **15**, 1145 (2019)
[3] S A Sato, Electronic Structure (in press).

*E-mail: ssato@ccs.tsukuba.ac.jp

Many-body effects during high harmonic generation in a 1D solids

E Winchester, R Cooper, and J R Gulley*

Department of Physics, Kennesaw State University, Kennesaw, GA 30144, USA

Synopsis We characterize the role of many-body collisions during high harmonic generation (HHG) from a multi-subband semiconductor nanowire. The nanowire is exposed to ultrashort IR radiation polarized along the nanowire axis, allowing for both interband and intraband excitations. Our calculations suggest that, for 1D solids, the role of many-body effects are not negligible when the applied laser field is strong enough to drive Bloch oscillations.

TP

Modeling light interaction with 1D solids is important for understanding the dynamics of optoelectronic sensors containing semiconductor nanowires and nanowire arrays [1]. It is commonly assumed that many-body effects (MBEs) (*i.e* Coulomb scattering, dephasing, and carrier-phonon scattering) are unimportant in modeling HHG coupled to the behavior of laser-generated electron-hole plasmas in solids [2, 3]. However, when a strong bias voltage or an intense ultrashort IR laser pulse interacts with a semiconductor nanowire, our calculations show that MBEs do affect the dynamics of HHG in a 1D solid.

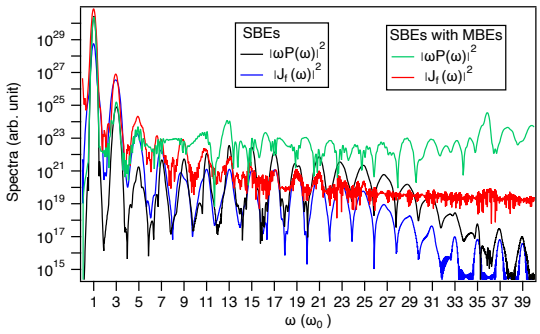


Figure 1. Spectra of the polarization current density and the free current density from the 10 μm wavelength, 70-fs pulsewidth laser field in a GaAs nanowire. Results are shown for solving the SBEs without any MBEs (black and blue), and with MBEs (green and red).

Our simulations solve the semiconductor Bloch equations (SBEs) [2, 3] with MBEs [1] for IR pulse interactions with a GaAs nanowire using a fully fitted band-structure. The laser pulse has a wavelength of 10 μm and a pulsewidth of 70 fs. The field strength was chosen so that the excited electrons may traverse the width of the Brillouin zone during an oscillation cycle of the field. We compare the results with and without Coulomb collisions and demonstrate the regimes where such corrections are not negligible. In this work we have included Coulomb collisions as well as many-body Coulomb dephasing of the quantum coherence between electron states.

Figure 1 shows the spectra of the polarization current and free-current density for two cases: (i) solving the semiconductor Bloch equations (SBEs) for electron-hole populations and coherences without any MBEs included, thereby excluding the all scattering and Coulomb correction terms in the SBEs, and (ii) the full SBEs in which all MBEs included. We can see that excluding the MBEs makes for a cleaner spectra and that adding MBEs moves the noise threshold upward while keeping discernible high harmonics. In all cases, HHG spectra is seen up to 20 orders of the fundamental frequency.

References

[1] J R Gulley and D Huang, Opt. Express **27**, 17154 (2019).
[2] D Golde, T Meier, and S W Koch, Phys. Rev. B **77**, 075330 (2008).
[3] I Kilen, M Kolesik, J Hader, J V Moloney, U Huttner, M K Hagen, and S W Koch, Phys. Rev. Lett. **125**, 083901 (2020).

*E-mail: jgulley@kennesaw.edu

Development of Two-Color Sub-Femtosecond Pump/Probe Techniques with X-ray Free-Electron Lasers

Z Guo[1,2] *, on behalf of the LCLS Attosecond Campaign Collaboration[3]

[1]Department of Applied Physics, Stanford University, Stanford, CA, USA
[2]Stanford PULSE Institute, LAC National Accelerator Laboratory, Menlo Park, CA, USA
[3]Linac Coherent Light Source, SLAC National Accelerator Laboratory, Menlo Park, CA, USA

TP

Synopsis We demonstrate the generation of gigawatt-level attosecond 2-color pump/probe pulse pairs with tunable subfemtosecond delays at the Linac Coherent Light Source (LCLS). Pump/probe delays measured by the angular streaking technique are in good agreement with start-to-end XFEL simulations.

The natural time scale of quantum mechanical motion of electrons in molecules and solids is usually on the order of hundreds of attoseconds. Probing time-dependent dynamics with atomic-site specificity on such timescales requires the generation of soft X-ray attosecond pulses pairs with variable delay and synchronization down to the sub-femtosecond level. We report the generation of GW-level attosecond pump/probe pulse pairs with tunable sub-femtosecond delays at the Linac Coherent Light Source (LCLS). The attosecond 370 eV pump pulse is first generated via the Enhanced Self-Amplified Spontaneous Emission (ESASE) method [1, 2], then the attosecond 740 eV probe pulse is produced by re-amplifying the electron beam microbunching after the magnetic chicane, as shown in Fig. 1(a). Due to the harmonic amplification, the minimal delay between pump-probe pulse pairs (limited by slippage between the light field and the electron bunch) can be shorter than 0.5 femtoseconds. We use the angular streaking technique [3] to measure temporal delays between pump/probe pulse pairs at multiple beamline configurations, as shown in Fig. 1(b-c). When the delay chicane is turned off, the averaged delay is increased by ~150 attoseconds by adding one undulator module for probe pulses. Long delays can be set up by turning the delay chicane on. These experimental results are in agreement with start-to-end XFEL simulations. Looking toward future experiments, our sub-femtosecond pump/probe technique can be applied to observe electronic charge dynamics in molecular systems.

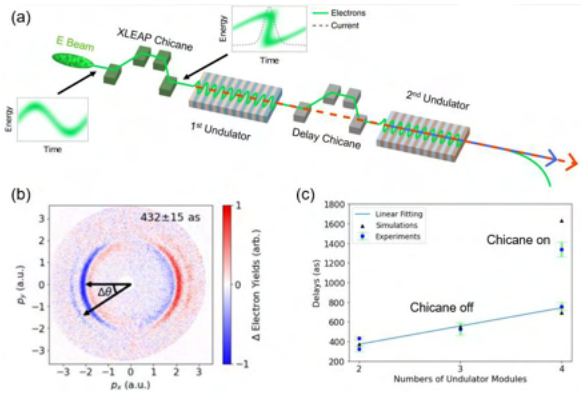


Figure 1. Schematic representation of the two-pulse technique. (a) Attosecond pump/probe pulse pairs generated from the split undulator mode. (b) The angular streaking measurement of 432±15 as delay with delay chicane off and 2 undulator modules in the 2nd stage. (c) Simulated and measured delays at multiple beamline configurations.

References

[1] Zholents A A. *Physical Review Special Topics-Accelerators and Beams* 8.4 (2005): 040701.
[2] Duris J *et al. Nature Photonics* 14.1 (2020): 30-36.
[3] Li S *et al. Optics Express* 26.4 (2018): 4531-4547.

* E-mail: zhaoheng@stanford.edu

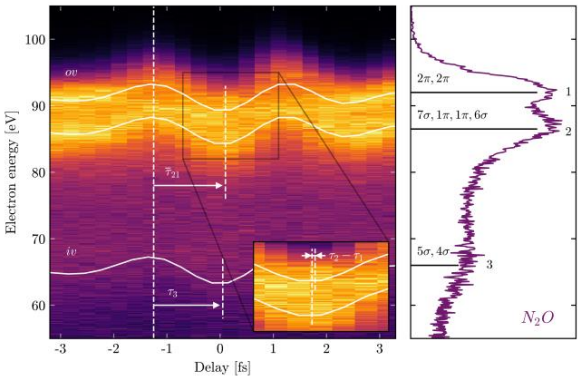
Isosteric molecules in the time-domain

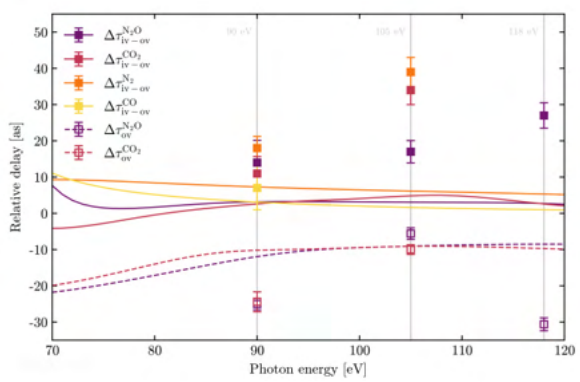
M Pollanka*, C A Schröder, P Scigalla, M Mittermair, A Duensing, R Kienberger

Physik Department, Technische Universität München, Garching, 85748, Germany

Synopsis In this work, we report on photoemission timing measurements performed on small isosteric molecules in the gas phase on an attosecond timescale. By comparing the photoemission time delay between the respective σ and π orbitals in the inner (iv) and outer (ov) valence states of CO_2 and N_2O we expect to find deeper insight into the characteristics of isosterism in the time-domain. Furthermore, the isoelectronicity of CO and N_2 is investigated in detail as a complementary study.

TP





Due to the similarities in molecular structure (isostericity) and electronic configurations (isoelectronicity) the pure effect of the specific molecular/orbital characteristics is expected to be probed. The results regarding similarities and differences in photoemission dynamics can serve as a stepping stone for isosteric characteristics in these molecules and may bear the potential to draw conclusions from these simple systems to unknown or unexplored isosteric molecular bonds in general. The measurement campaign so far provided interband ($\Delta\tau_{iv-ov}$) as well as intraband ($\Delta\tau_{ov}$) relative photoemission time delays for N_2O, CO_2, N_2 and CO via attosecond streaking spectroscopy. Exemplary for all molecules, the figure on the left shows the streaking trace for N_2O together with its static spectrum and the marked orbital groups for extracting the inter- and intraband delays [1]. Scattering calculations help us to gain a greater understanding of the correlations between molecular geometry and photoemission time and therefore the isosteric influence, with the focus on assessing the differences between modelling and experimental findings. The figure on the right shows the corresponding ePolyScat [2, 3, 4] calculation results (solid and dashed lines) together with the extracted delays from the streaking measurements (squares) via diffrTDSE [5]. The experimental data show great correspondence and consistency but also overall deviations from the calculated expected values, which are determined but not completely understood up to now. As the calculations are only taking the Eisenbud Wigner-Smith delay and the addition of the laser induced Coulomb-laser coupling delay contribution into account, the aim is to determine the missing further delay contribution. Absolute photoemission timing via the atomic chronoscope method [1] in order to gain a deeper insight into the isosteric/isoelectronic comparability in the time-domain together with the verification of a relation to Yijie Liao et.al's [6] findings of an photon energy dependent oscillation in the photoemission time delay of asymmetric molecules are two further steps on the path of completing the picture.

References

[1] M Ossiander et al., Nature 561 (2018).
[2] F A Gianturco et al., The Journal of Chemical Physics 100, (1994).
[3] A P P Natalense et al., The Journal of Chemical Physics 111, (1999).
[4] G M J Barca et al., The Journal of Chemical Physics 152, (2020).
[5] C Brunner et.al., Optics Express Vol. 30, Issue 9 (2022).
[6] Y Liao et.al., Phys. Rev. A 104, (2021).

* E-mail: maximilian.pollanka@tum.de

Electron Correlation Effects in High Harmonic Generation in ZnO Studied with Dynamical Mean-Field Theory and Time-Dependent Density-Functional Theory

D Alam[1 *], N Ud Din[1], M Chini[1], V Turkowski[1]

[1]Department of Physics, University of Central Florida, Orlando, 32816, USA

TP

Synopsis High harmonic generation (HHG) is an efficient experimental method to study the effects of the interaction of electrons with a strong laser pulse and the dynamics of excited charges in solids and other systems. In most of the previous theoretical studies of the HHG in solids, the effects of electron-electron interaction in the many-body dynamics were either neglected or included with uncontrollable approximations. We include these effects by taking into account the on-site Coulomb interaction between charges and perform an *ab initio* analysis of their role in the HHG in ZnO.

After first being observed in the condensed phase in 2011 [1], high harmonic generation (HHG) has become a field of active research in solid-state physics. Despite many important findings, the role of electron-electron correlations in HHG was up to now an open question, in particular, due to the lack of reliable theoretical tools. In this work, we address the problem with a combined accurate dynamical mean-field theory and time-dependent density-functional theory (DMFT-TDDFT) approach, where the TDDFT equations are solved with the exchange-correlation kernel obtained from the charge susceptibility of the effective Hubbard model solved with DMFT [2]. We apply the tool to ZnO, probably the most studied solid-state HHG system.

To find the effect of correlations, we compare our results in the cases without and with local Coulomb repulsion between electrons (energy U = 4eV). We have found that the correlation dramatically affects the HHG, most notably by shifting the center-of-mass of the HH spectrum to higher harmonics (see Figure 1). Both effects become even more pronounced as the strength of the pulse and the number of optically-active bands increase. We also analyzed the dependence of the HH spectrum on the pulse duration in presence of correlations and found that with increasing pulse duration, some harmonics become suppressed. These results may shed more light on the understanding of the role of correlation effects in HHG in solids at different strengths and durations of the pulse.

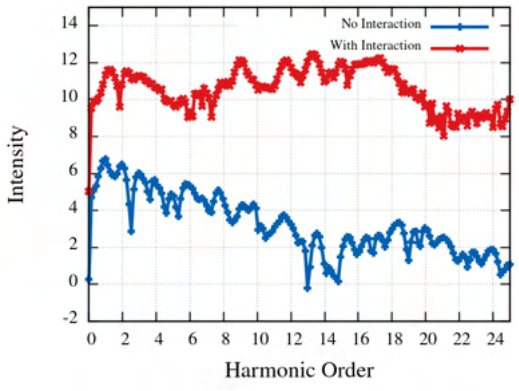


Figure 1. Change of the interband HH spectrum in ZnO when the correlation (interaction) effects are taken into account in the case of pulse duration ~ 66 fs, electric field strength 0.07 V/Å, and frequency 0.3 eV.

References

[1] Ghimire S et al Nature Physics 2011: **7(2):138-141**

[2] V Turkowski "Dynamical Mean-Field Theory for Strongly Correlated Materials", Springer (2021)

* E-mail: dalam@knights.ucf.edu

A Stereo-ATI approach for few-cycle pulse characterization and control

D Hoff[1 *]

[1]Single Cycle Instruments UG (haftungsbeschränkt) & Co. KG, Jena, 07745, Germany

Synopsis The detection of signature electron spectra emerging from above threshold ionization to determine the CEP and laser pulse asymmetry/duration has proven over the years to be a reliable, robust, real-time and single shot technique to characterize few-cylce laser pulses. Latest developements enable diagnosing the very same pulses that are applied later on in experiments downstream by measuring in-line of the laser beam. Moreover improved electronics allow for employing it for direct CEP stabilization of oscillators and amplifier chains.

After the first detection of CEP effects in above threshold ionization by Paulus et al. [1] the emerging rescattered electrons were successfully used as a probe for the electric field of few-cycle laser pulses [2]. Based on this observation, a diagnostic technique measuring the electron spectra to the left and right of a horizontally polarized laser pulse in a stereo time-of-flight spectrometer scheme was developed, Fig. 1 [2-5].

This approach has proven to be able to measure the key parameters CEP and asymmetry/pulse duration of individual few-cycle laser shots in real time and for hundreds of kHz repetition rate [5,6].

By employing fast electronics it is possible to use this device also to control and stabilize the CEP of high repetition rate laser amplifiers [6,7]. Moreover, the detected values for CEP and asymmetry can be tagged to events taking place in laser-matter interactions in an experiment of interest [8].

By further development of the device design it is now possible to detect these parameters CEP and pulse duration of the same pulse that is effective in laser matter interactions downstream by measuring the ATI signal in-line of the beam.

Additionally improved and faster electronics allow for high speed CEP control at hundreds of kHz repetition rate which enables even the direct control over oscillator CEP outputs.

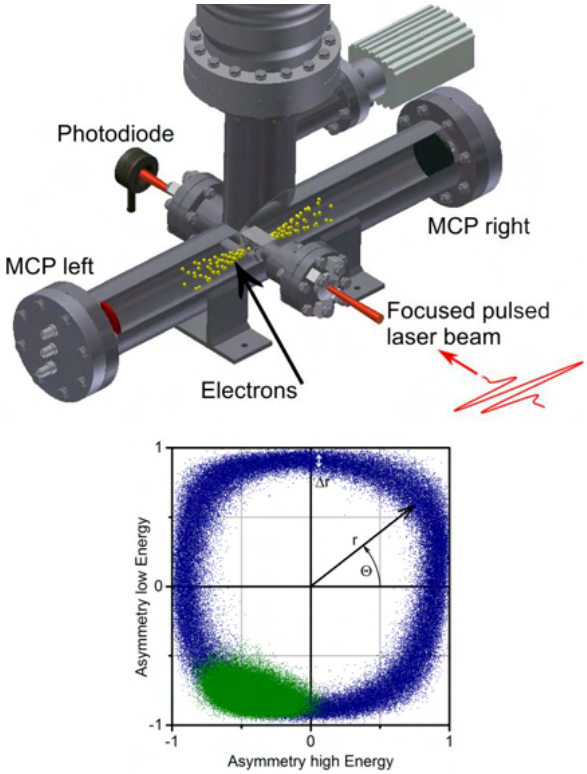


Figure 1. Top: Stereo ATI time of flight spectrometer for in-line detection of few-cycle pulses. Bottom: Resulting asymmetry plot providing access to CEP and pulse duration [5].

References

[1] Paulus G et al, 2001 Nat. **414**, 182.
[2] Wittmann T et al, 2009 Nat. Phys. **5** , 357.
[3] Sayler A. M. et al, 2011 Opt. Lett. **36** , 0146-9592.
[4] Sayler A. M. et al, 2011 Op. Ex. **36**, 3639.
[5] Hoff D. et al, 2018 Opt. Lett. **43**, 3850.
[6] Hädrich S. et al, 2022 Opt. Lett. **47**, 1537.
[7] Adolph et al, 2011 Opt. Lett. **36**, 18, 3639
[8] Johnson et al, 2011, Phys. Rev. A. **83**, 013412

* E-mail: info@sci-phi.de

Improved initial conditions of the strong-field ionized electron and their reconstruction from the detected momentum of the electron

Sz Hack[1]*, Sz Majorosi[1], M G Benedict[2], S Varró[1] and A Czirják[1,2]

[1]ELI-ALPS, ELI-HU Non-Profit Ltd., Szeged, H-6728, Hungary
[2]Department of Theoretical Physics, University of Szeged, Szeged, H-6720, Hungary

TP

Synopsis We reveal the real classical picture associated with the exact quantum process of strong-field ionization in parameter range relevant to state-of-the-art experimental techniques. This model follows the quantum evolution very well; it accounts for direct ionization, rescattering and the blurred nature of the liberation process; it solves and explains the problem of the non-zero initial momentum in models assuming traditional tunneling. Using the improved initial conditions, we show a simple procedure for reconstruction the starting time from the detected momentum of a directly escaped electron.

Tunneling time and exit momentum are of great significance regarding both quantum theory and attosecond metrology. Several research groups published relevant experimental results related to tunneling time and nonzero exit momentum of the ionized electron [1]. The explanatory theoretical models often employ classical dynamics, where the choice of proper initial conditions is an important open question with controversies regarding, e.g., conservation of energy.

We investigate the liberation of the electron of a model hydrogen atom by a linearly polarized single-cycle near-infrared laser pulse having a peak intensity that ensures tunneling. We introduce properly chosen initial conditions for the trajectories of the escaping electron [2]. A suitably chosen set of these trajectories follow the quantum evolution very well and they also reflect that the liberation process is blurred both in space and time. To connect the quantum and classical dynamics of the liberated electron we define the initial condition of the possible trajectories with the quantum momentum function $q(z,t)$, which is the position-dependent average momentum of the electron, and with the outermost inflection point of a suitable stationary phase space trajectory of the instantaneous potential, $p_z\left(z_\mathrm{i}, t_\mathrm{s}; E_\mathrm{s}\right) = \sqrt{2\left(E_\mathrm{s} - V\left(z_\mathrm{i}, t_\mathrm{s}\right)\right)}$ depending on the energy of the electron E_s. We introduce the novel initial conditions by the solution of the following equation:

$$q(z_\mathrm{i}, t_\mathrm{s}) = p_z\left(z_\mathrm{i}, t_\mathrm{s}; E_\mathrm{s}\right). \qquad (1)$$

It has only a single solution for every realistic starting time at E_s which is in the over-the-barrier (OB) regime.

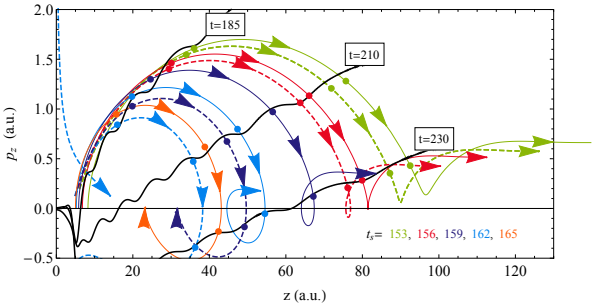


Figure 1. Classical phase space trajectories of the liberated electron according to Eq. 1 (dashed lines) in comparison with simple man trajectories (solid lines) for the indicated starting time instants. Snapshots of the classical and the quantum propagation at marked instants, represented by the dots and by $q(z,t)$ (black solid lines), respectively, show a good match for all of the different outcomes.

On Fig. 1 we can see that the new model accounts both for direct ionization and rescattering depending on the starting time despite the initial energy of the trajectories are in the OB energy range. Using the improved initial conditions, we show a simple procedure to reconstruct the starting time from the detected momentum of a directly escaping electron. We tested this method with numerical experiments resulting the accuracy of the reconstructed starting time less than 5 as for the most probable trajectories.

References

[1] C Hofmann *et al.*, J. Mod. Opt. **66**, 1052 (2019).
[2] Sz Hack *et al.*, Phys. Rev. A **104**, L031102 (2021).

*E-mail: Szabolcs.Hack@eli-alps.hu

Quantum interference in strong-field ionization by a linearly polarized pulse explains non-zero tunnel exit momentum

A Czirják[1,2]*, Sz Hack[1,2], Sz Majorosi[1], M G Benedict[2], and S Varró[1,3]

[1]ELI-ALPS, ELI-HU Non-Profit Ltd., Szeged, H-6728, Hungary
[2]Department of Theoretical Physics, University of Szeged, Szeged, H-6720, Hungary
[3]Wigner Research Centre for Physics, Budapest, H-1121, Hungary

TP

Synopsis Phase space analysis and accurate tracking of the energy distribution reveals that quantum interference between tunneling and over-the-barrier pathways of escape plays an important role during the liberation of an atomic electron by a linearly polarized single-cycle near-infrared laser pulse, despite that the peak laser intensity corresponds to tunnel ionization. This naturally leads to a new non-zero tunnel exit momentum for the electron, based on the quantum momentum function, and in a good agreement with recent experimental results.

We theoretically and numerically investigate the liberation of an atomic electron by a linearly polarized single-cycle near-infrared laser pulse with a peak intensity corresponding to tunnel ionization. This process is of fundamental importance in attosecond physics, with open questions regarding e.g. the tunnel exit momentum [1].

Based on a phase space analysis with the Wigner function [2] and by tracking the energy distribution in the instantaneous (Coulomb + laser) potential, we reveal the importance of quantum interference between tunneling and over-the-barrier pathways of escape [3]. We highlight the Wigner function's natural connection to the quantum momentum function (QMF), which enables us to use the QMF as the fundamental quantity to represent the true time-dependent quantum dynamics, including quantum interference. We define a suitable value of the QMF as a novel tunnel exit momentum, without any contradiction to energy conservation, and in a good agreement with recent experimental results [4, 1].

We give more insight into the onset of the electron's escape process by studying a wave packet which is obtained as the positive momentum and positive energy (PMPE) part of the electron's quantum state at the final instant of the laser pulse [3] (thus, it is able to reach a detector at a macroscopic distance without recollision). By quantum propagating this PMPE wave packet backwards in time and comparing its Wigner function with classical phase space trajectories, we can demonstrate that our novel tunnel exit momentum values initiate classical dynamics in excellent agreement with the quantum evolution.

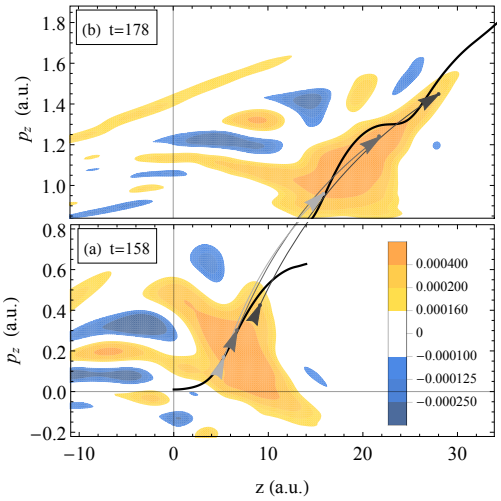


Figure 1. Comparison of quantum evolution to classical dynamics, starting with our novel tunnel exit momentum, before (a) and after (b) the peak of the driving laser pulse (at $t = 165$ a.u.). Colored contour plot of the Wigner function which represents the PMPE part of the electron's quantum state [3]; plot of the QMF (solid black line); classical phase space trajectories (thin gray lines) starting shortly before the peak of the driving laser pulse (having 800 nm carrier wavelength).

References

[1] M Li et al., Phys. Rev. Lett. **122**, 183202 (2019).
[2] A Czirják et al., Opt. Commun. **179**, 29 (2000).
[3] Sz Hack et al., Phys. Rev. A **104**, L031102 (2021).
[4] N Camus et al., Phys. Rev. Lett. **119**, 023201 (2017).

*E-mail: attila.czirjak@eli-alps.hu

Coherent diffractive extreme-ultraviolet generation from nanostructured silica

Sylvianne D.C. Roscam Abbing[1*], Radoslaw Kolkowski[2], Zhuang-Yan Zhang[1], Filippo Campi[1], Lars Lötgering[1], A. Femius Koenderink[2], Peter M. Kraus[1*]

[1]Advanced Research Center for Nanolithography (ARCNL), Science Park 106, 1098 XG Amsterdam, The Netherlands

[2]Center for Nanophotonics, AMOLF, Science Park 104, 1098XG Amsterdam, The Netherlands

TP

Synopsis We demonstrate high-harmonic generation inside nanostructured silica, enabling control over the phase, amplitude and polarization of the generated extreme-ultraviolet wavefront. We use these emitted patterns for height metrology of the generating structure, probing the near-field confinement inside the nanostructured silica and demonstrate imaging of complex structures.

High-Harmonic Generation (HHG) is driving the research field of attosecond science through the generation of coherent extreme-ultraviolet (XUV) pulses, and enables lensless imaging and metrology with high resolution. More recently, HHG from a solid medium was demonstrated [1], and specifically silica is shown to generate harmonics extending into the XUV regime [2]. However, tailoring complex spatial amplitude, phase, and polarization properties of XUV pulses is made non-trivial by the lack of efficient optical elements. Here, we have overcome this limitation through the generation from structured solids [3], which enable direct control over amplitude and phase patterns of nonlinearly generated extreme-ultraviolet pulses.

Generation from micron-structured silica allows to imprint phase and amplitude on either the generated harmonics or on the fundamental wavefront, both leading to diffraction of the XUV pulses. In addition, we demonstrate height metrology of the structures and characterize the thickness of the sample. Moreover, we generate harmonics inside nanometer-sized structures and use HHG to probe the near-field confinement of the fundamental radiation inside these nanostructures. By changing the polarization of the fundamental radiation, we control the fundamental near-field distribution inside the nanostructures, and influence the amplitude and polarization of the structured HHG emission. Using classical diffraction theory and near-field simulations, we model the experimental results quantitatively. Finally, we also generate from complex aperiodic structures, and can replicate the obtained diffraction pattern very well with simulations, see Fig. 1. In addition, the iterative reconstruction of the recorded diffraction patterns, demonstrates the use of solid-state HHG from structured materials for imaging and metrology purposes. In conclusion, we have demonstrated the generation of structured XUV pulses. Our results pave the way for introducing super-resolution imaging, direct manipulation of beams through nano-engineered samples, and metrology of nanostructures into the extreme-ultraviolet spectral range.

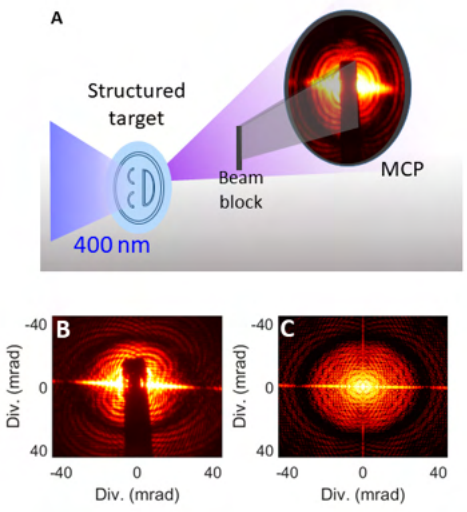


Figure 1. A) Schematic of experimental setup. B) Measured diffraction of target in A. C) Simulated diffraction pattern of target in A.

References

[1] Ghimire S *et al* 2011 *Nature physics* 7(2) 138-141
[2] Luu TT *et al* 2015 *Nature* 521(7553) 498-502
[3] Sivis M *et al* 2017 *Science* 357(6348) 303-306

Intra- and intercycle interferences in ω-2ω strong field ionization: Phase delays

D G Arbó[1,2 *] **and S D López**[1†]

[1] Institute for Astronomy and Space Physics - IAFE (CONICET-UBA), C1428ZAA, Buenos Aires, Argentina and
[2] Universidad de Buenos Aires, Facultad de Cs. Exactas y Naturales y Ciclo Básico Común, Buenos Aires, Argentina

Synopsis We characterize the phase delays for a typical ω-2ω configuration for hydrogen ionization. A splitting of the maximum of the forward ionization as a function of the relative phase exhibits the preclusion of the perturbative regime.

TP

Strong-field ionization by laser fields with commensurate frequencies and well-defined relative phase permits the tune and control of the emission processes [1,2]. The concepts of phase shifts and time delays in RABBIT have been extended for two-color (ω-2ω) lasers with controlled relative phase [3]. Very recently, we have theoretically explored the extraction of ω-2ω phase delays by means of the *ab initio* solution of the TDSE and through the development of a perturbation theory for atomic argon [4].

We develop a strong-field non-perturbation theory of the electronic photoemission process in atomic hydrogen due to a ω-2ω [Ti:Sapphire laser (800 nm) and its harmonic (400 nm)] linearly polarized short laser pulse. We introduce a general theory based on the saddle point approximation (SPA) to study phase delays of photoelectrons. We focus on the extraction of the phase shifts using directional emission in the forward direction. We calculate the ionization time of each interfering electron trajectory and study the dependence of the electron emission as a function of the relative phase within the strong field approximation (SFA).

We consider the vector potential $A(t) = -\lfloor F_{2\omega}/(2\omega)\sin(2\omega t) + F_{\omega}/\omega \sin(\omega t + \phi)\rfloor$. Within the SPA, electron yield stem from the coherent superposition of semiclassical trajectories. The energy spectrum in the forward direction as a function of the relative phase ϕ between the two colors is depicted. All multiphoton peaks (ATIs and sidebands) are present in the intercycle factor in Fig. 1a with separation of one ω photon energy, which is independent ϕ. The interhalfcycle factor can be observed as a 2π-periodic function in Fig. 2b. The separation between interhalfcycle maxima corresponds to a 2ω photon energy and the amplitude of the oscillation increases with energy. The interplay between the inter- and interhalfcycle interferences is plotted in Fig. 2c where both ATI peaks and sidebands are present. We see that the first multiphoton peak just above the threshold is an ATI peak with $\phi_0=\pi/4$ and $5\pi/4$. In turn, the first sideband maximizes at $\phi_0=3\pi/4$ and $7\pi/4$.

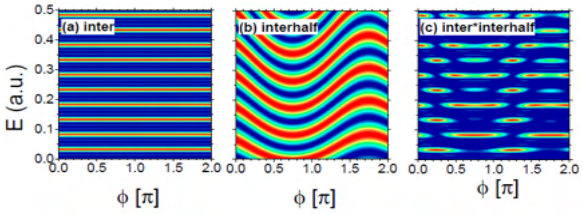


Figure 1. SPA energy distribution (normalized) in the forward direction as a function of ϕ. (a) Intercycle factor, (b) interhalfcycle factor, (c) multiplication of (a) and (b).

Phase delays calculated within our SPA agree not only with our SFA calculations (not shown) but also with previous perturbation theories [3,4] if the probe field amplitude is much weaker than the pump pulse, or photoelectron energies are close to the threshold (perfurbative regime). The extension of perturbative theories to the strong-field approximation gives rise to novel effects for intermediate and high electron energies like the departure of the sinusoidal behavior of the intensity of ATIs and sidebands as a function of the relative phase ϕ, which forces us to revise the extraction method of phase delays for SFA.

References

[1] Arbó D G *et al* 2014 *Phys. Rev. A* **89**, 043414
[2] Xie X *et al* 2012 Phys. *Rev. Lett.* **108**, 193004
[3] Zipp L J et al 2014 *Optica* **1**, 361
[4] López S D *et al* 2021 *Phys. Rev. A* **104**, 043113

* E-mail: diego@iafe.uba.ar
† E-mail: sebastlop@iafe.uba.ar

Phase delays in ω – 2ω above-threshold ionization of atomic argon

S D López[1], S Donsa[2], J Burgdörfer[2], and D G Arbó[1,3] †

[1]Institute for Astronomy and Space Physics IAFE (CONICET-UBA), C1428ZAA, Buenos Aires, Argentina
[2]Institute for Theoretical Physics, Vienna University of Technology, A-1040 Vienna, Austria, EU
[3]Universidad de Buenos Aires, Facultad de Cs. Exactas y Naturales and Ciclo Básico Común, Buenos Aires, Argentina

TP

Synopsis We theoretically explore the extraction of information on the ionization phases from argon atoms subject to a linearly polarized laser field with a ω – 2ω setting. We find a very good agreement between our ab initio results of the time dependent Schrödinger equation and measured phase delays [L. J. Zipp, A. Natan, and P. H. Bucksbaum 2014, *Optica* **1**, 361] but significant differences with the strong field approximation even at energies well above the ionization threshold.

Since the 1990's, two-color ω-2ω laser fields with well-controlled relative phases have been studied experimentally and theoretically. One key feature is that the broken inversion symmetry of the ω-2ω field allows for interference between odd and even partial waves of the outgoing photoelectron. Recently, Zipp *et al* [1] extended the measurement of ionization phases and attosecond time delays to the strong-field multiphoton regime. In this novel ω-2ω interference protocol the role of electron wavepackets emitted by absorption of subsequent harmonics in the RABBIT protocol is replaced by adjacent ATI peaks generated by a strong driving field of frequency 2ω. The concomitant weaker field opens up interfering pathways to sidebands in between neighboring ATI peaks by absorbing or emitting one ω photon. This approach of measuring the ionization as a function of the relative phase between the ω and the 2 ω fields somewhat resembling the original RABBIT protocol promises to offer insight into the ionization phase and, possibly, timing information of multiphoton processes [2].

We present a theoretical study of the ionization phase in the multiphoton regime accessible by two collinearly polarized laser fields of the form $\vec{F}(t)=\left[F_{2\omega}\cos(2\omega t)+F_{\omega}\cos(\omega t+\phi)\right]\hat{z}$. In Fig. 1 we show *ab initio* results of the energy spectrum calculated within the time dependent Schrödinger equation (TDSE) in the forward direction as a function of the relative phase ϕ. Phase delays have been extracted by fitting the ATI and sideband with the perturbative prediction [4]. We find a very good agreement between our TDSE calculations and the experiments [1] but strong deviations from the predictions of the strong field approximation (SFA) in dashed vertical lines, clearly indicating that the atomic potential has a crucial influence on the ionization phase of ATI peaks even at energies well above the ionization threshold.

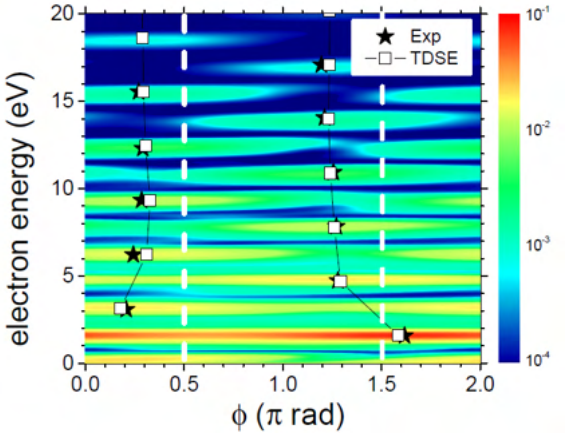


Figure 1. TDSE energy spectrum in the forward direction as a function of the relative phase ϕ. Squares: calculated phase delays and the stars: experiments in [1]. vertical dashed lines: SFA.

Unlike RABBIT, the present ω-2ω protocol opens up a multitude of competing quantum paths, turning the extraction and interpretation of interference phases more complex.

References

[1] L J Zipp *et al* 2014 *Optica* **1** 361-364
[2] J Fuchs *et al* 2020 *Optica* **2** 154
[3] S Donsa *et al* 2019 *Phys. Rev. Lett.* **123** 133203
[4] López S D *et al* 2021 *Phys. Rev. A* **104**, 043113

† E-mail: diego@iafe.uba.ar

Self-induced splitting of Zn Kα emission line

Š Krušič[1]*, A Mihelič[1], K Bučar[1] and M Žitnik[1]

[1]Jožef Stefan Institute, Jamova cesta 39, SI-1000 Ljubljana, Slovenia

Synopsis

This work presents a theoretical study of x-ray superfluorescence in zinc after K-shell photoionization with intense attosecond free-electron laser pulses. The developed model predicts a splitting of the $K\alpha_1$ emission line, which is a consequence of strong amplification of spontaneously emitted radiation as it propagates through the core-excited medium. This spectral feature could be observed with standard high-resolution x-ray spectrometers. Since the K-hole lifetime in zinc is only 394 as, subfemtosecond pulse duration is crucial for the manifestation of this phenomenon in the hard x-ray spectral region.

TP

The development of free-electron lasers (FELs) [1] has opened the way for studying nonlinear processes in the interaction of x-ray light with matter. One of such processes is superfluorescence [2], where spontaneously emitted radiation is amplified as it propagates through a target with inverted population. While in the optical regime, where superfluorescence has been extensively studied, this process is usually observed by detecting the characteristic temporal profile of the amplified spontaneous radiation, this is not feasible in the x-ray domain, where the excited state lifetime, and with that the duration of the emitted pulse, is well below one picosecond.

Another difficulty in studying x-ray superfluorescence lies in the lack of reliable theoretical modeling. A successful model of superfluorescence must describe both the spontaneously emitted field, as well as its interaction with matter after strong amplification [2]. However, both the most widely used model based on Maxwell-Bloch equations [3], as well as the more recently developed approach formulated in terms of quantum two-point correlation functions [4], have proven to be inadequate when dealing with multilevel systems and competing decay channels, which is the situation generally encountered in realistic systems.

We present a theoretical model of superfluorescence in extended multilevel targets based on a combination of the above mentioned approaches [5], which overcomes some of the deficiencies of the individual constituent sets of equations. The model is employed to study the spectral properties of $K\alpha_{1,2}$ emission in zinc at ~ 8630 eV, after photoionization by 9750 eV FEL pulses with a duration of a few hundred attoseconds (Fig. 1). Numerical simulations predict a splitting of the amplified $K\alpha_1$ emission line at high pump intensities due to a self-induced Autler-Townes effect, which could be observed with the present-day resolution of x-ray spectrometers. We also show that the short pump pulse duration with respect to the excited state lifetime is crucial for the manifestation of this effect. Experimental realization of the presented scheme has only recently become feasible with the demonstration of attosecond x-ray FEL pulses [6].

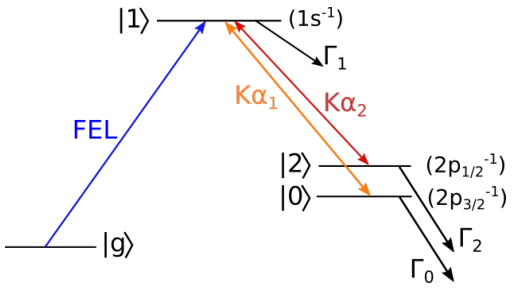


Figure 1. Schematic representation of the processes following K-shell photoionization of zinc by a short FEL pulse.

References

[1] P Emma *et al.*, Nat. Photon. **4**, 641 (2010).
[2] M Gross and S Haroche, Phys. Rep. **93**, 301 (1982).
[3] O Larroche *et al.*, Phys. Rev. A **62**, 043815 (2000).
[4] A Benediktovitch *et al.*, Phys. Rev. A **99** 013839 (2019).
[5] Š Krušič *et al.*, Phys. Rev. A **102**, 013102 (2020).
[6] J Duris *et al.*, Nat. Photon. **14**, 30 (2019).

*E-mail: spela.krusic@ijs.si

TP

Petahertz-bandwidth amplifier for the XUV/X-ray attosecond pulses based on IR-field-dressed plasma-based X-ray laser

V A Antonov[1 *], I R Khairulin[1,2], M Yu Ryabikin[1,2] and O Kocharovskaya[3]

[1]Institute of Applied Physics of the Russian Academy of Sciences, Nizhny Novgorod, 603950, Russia
[2]Lobachevsky State University of Nizhny Novgorod, Nizhny Novgorod, 603950, Russia
[3]Department of Physics and Astronomy, Texas A&M University, College Station, 77843-4242, USA

Synopsis The possibility to amplify the attosecond pulses, produced via the high-harmonic generation (HHG) of an infrared (IR) laser field, either maintaining their polarization, or increasing the elliptisity is shown. A plasma-based X-ray laser dressed by a replica of the fundamental frequency IR laser field, is suggested to be used as a sufficiently broadband amplifier.

High-order harmonic generation (HHG) of infrared (IR)/optical laser fields in gases led to formation of the attosecond pulses of the extreme ultraviolet (XUV)/X-ray radiation and opened the way for the experimental study and control over the electronic processes in atoms, molecules, and solids at their intrinsic time scales. However, the HHG process is quite inefficient, whereas amplification of the attosecond pulses is a formidable problem, since none of the existing amplifiers can support the corresponding petahertz bandwidth. We discuss a possible solution of this problem, that is, the possibility to amplify an attosecond pulse train, based on modulation of a plasma-based X-ray laser with a replica of the IR field used for HHG.

Plasma-based X-ray lasers are capable of producing relatively high energy pulses in the XUV/X-ray range in compact setup. Ordinarily, X-ray laser emission is narrowband and has picosecond duration. However, as we have shown in [1], under the action of a strong IR field, which induces sub-laser-cycle Stark shift of the energy levels of the active medium, the gain of an X-ray laser is redistributed from the resonance to a set of equidistant sidebands in petahertz amplification bandwidth, making it possible to amplify pulses of attosecond duration.

In this talk, we discuss the possibilities for the attosecond pulse amplification in different wavelength ranges from tens of nanometers to the "water window" range (2.3–4.4 nm) in either collisional or recombination plasma-based X-ray lasers. In particular, we have shown the possibility to achieve a high gain on the order of a few tens for circularly polarized pulses and even higher gain on the order of a hundred for the linearly polarized pulses. The possibility to increase the ellipticity during the amplification is also shown [2], see Fig. 1.

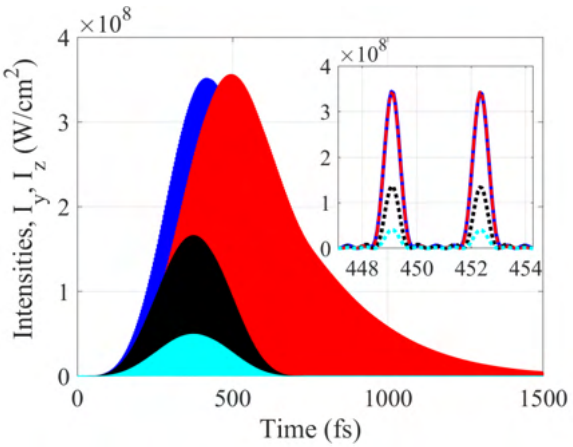


Figure 1. Time dependences of the intensities of two orthogonal linear polarization components of the high-harmonic field with 24.85 nm central wavelength at the input (black and cyan) and the output (blue and red) from Ne-like Ti^{12+} X-ray laser dressed by the fundamental frequency 3.9 μm IR field. An inset shows the form of individual sub-fs pulses at the peak of the total intensity envelope. The phase difference between the polarization components is preserved during the amplification.

References

[1] Antonov V A *et al* 2019 *Phys. Rev. Lett.* **123** 243903
[2] Khairulin I R *et al* 2021 *Research Square* 1131350, DOI: 10.21203/rs.3.rs-1131350/v1

* E-mail: antonov@appl.sci-nnov.ru

High-Harmonic Spectroscopy of Dynamical Symmetries in Graphene

N Rana[1 *], **M S Mrudul**[1] **and G Dixit**[1 †]

[1]Department of Physics, Indian Institute of Technology Bombay, Powai, Mumbai 400076, India

Synopsis Interaction of intense laser light with solids may lead to changes in the symmetry of the solids. The interplay between transiently-evolving dynamical symmetry and electronic dynamics dictates several physical, optical and chemical properties of solids. Thus, probing the dynamical symmetries is essential for our microscopic understanding of several ubiquitous phenomena and predicting new concepts in solids. In this contribution, we demonstrate that high-harmonic spectroscopy is sensitive to the transiently-evolving dynamical symmetry in vibrating graphene.

Interaction of intense laser light with solids may lead to changes in the symmetry of the solids. It is known that the interplay between transiently-evolving dynamical symmetry and electronic dynamics dictates several physical, optical and chemical properties of solids. Thus, probing the dynamical symmetries is essential for our microscopic understanding of several ubiquitous phenomena and predicting new concepts in solids.

In this contribution, we demonstrate that high-harmonic spectroscopy is sensitive to the transiently-evolving dynamical symmetry in vibrating Graphene with subcycle temporal resolution. It is found that the dynamical symmetries lead to the generation of higher-order sidebands in the high-harmonic spectrum, which is modulated by the frequency of the coherent vibration. Also, time-frequency map of the spectrum yields the snapshots of the transiently-evolving dynamical symmetry in vibrating Graphene. The interaction between intense laser and vibrating graphene is modelled by solving the density matrix based using the semiconductor Bloch equation [1, 2]. Present work opens a platform to probe phonon-driven processes in solids and nonlinear phononics with subcycle temporal resolution.

References

[1] Mrudul M S *et al* 2021 Optica 8, 422-427

[2] Mrudul M S *et al* 2021 Phys. Rev. B. 103, 094308

* E-mail: navdeeprana@iitb.ac.in
† E-mail: gdixit@phy.iitb.ac.in

R01 **Attosecond Coherent Electron Motion in Molecules Measured with Attosecond X-ray Pulse Pairs**
Jordan O'Neal, LCLS Attosecond Campaign Collaboration . . . 173

R02 **Decoherence and Revival of Attosecond Charge Migration Driven by Non-adiabatic Dynamics**
Danylo Matselyukh, Victor Despré, Nikolay Golubev, Alexander Kuleff, Hans Jakob Wörner . . . 174

R03 **Strong Field Simulator: Attosecond Study of Strong Field Ionization in Noble Gas Atoms**
Qiaoyi Liu, Andrew Piper, Dietrich Kiesewetter, Yaguo Tang, Pierre Agostini, Kenneth J Schafer, Louis DiMauro . . . 334

R04 **Verifying the Frequency Resolved Optical Switching Technique to Accurately Characterize Multi-Octave IR Pulse**
Adrien Longa, Mayank Kumar, Philippe Lassonde, Antoine Laramée, Heide Ibrahim, François Légaré, Adrien Leblanc . . . 335

R05 **Generation of femtosecond multi-millijoule pulse at 3 μm through a 2-mm pumped OPCPA**
Fangjie Zhou, Yi Wu, Zenghu Chang . . . 336

R06 **Nonlinear pulse compression via multipass cell and contrast enhancement via nonlinear ellipse rotation of a thin-disk regenerative amplifier**
Yanik Pfaff, Gaia Barbiero, Michael Rampp, Sandro Klingebiel, Haochuan Wang, Catherine Y. Teisset, Robert Jung, Abel H. Woldegeorgis, Jasna Jaksic, Clara J. Saraceno, Thomas Metzger . . . 337

R07 **Optically forbidden inner valence excited state lifetimes in neon atoms measured by attosecond noncollinear four wave mixing spectroscopy**
Nicolette Puskar, Yen-Cheng Lin, James D Gaynor, Maximilian Schuchter, Ashley P Fidler, Clare Keenan, Daniel M Neumark, Stephen R Leone . . . 175

R08 **Weak pre-ionization for phase-matched high harmonic generation in absorp-tion-limited long media**
Ondrej Finke, Jan Vábek, Michal Nevrkla, Nadezhda Bobrova, Ondřej Hort, Matej Jurkovič, Martin Albrecht, Alexandr Jančárek, Fabrice Catoire, Stefan Skupin, Jaroslav Nejdl . . . 338

R09 **10mJ Hollow-Core Fiber operation at 250W average power with 90% efficiency**
Maksym Ivanov, Derrek Wilson, Alexis Labranche, Gabriel Tempea, Alicia Ramirez, François Légaré, Clement Paradis, Arvid Hage, Torsten Mans, Carlos Trallero, Bruno E. Schmidt . . . 339

R10 **High-energy multidimensional solitary states in hollow-core fibers**

Reza Safaei, Guangyu Fan, Ojoon Kwon, Katherine Légaré, Bruno E. Schmidt, Philippe Lassonde, Heide Ibrahim, François Légaré 340

R11 **In Situ Sub-50-Attosecond Active Stabilization of the Delay Between Infrared and Ultraviolet Light Pulses**
Martin Luttmann, David Bresteau, Jean-François Hergott, Olivier Tcherbakoff, Thierry Ruchon 341

R12 **Attosecond delays of high harmonic emissions from isotopes of molecular hydrogen measured by Gouy phase XUV interferometer**
M H Mustary, Liang Xu, Wanyang Wu, Nida Haram, Han Xu, Feng He, R T Sang, I Litvinyuk 342

R13 **Measurement of the Attoclock-Offset Angle and the Wigner Time Delay in a single experiment**
Nils Anders, Daniel Trabert, Angelina Geyer, Max Hofmann, Markus S. Schöffler, Till Jahnke, Lothar Ph. H. Schmidt, Maksim Kunitski, Reinhard Dörner, Sebastian Eckart 176

R14 **High Flux High Harmonic Generation at the Sylos Long Beamline at ELI-ALPS**
Balázs Nagyillés, Zsolt Diveki, Balazs Farkas, Robin Weissenbilder, Cord L. Arnold, Per Eng-Johnsson, Sergei Kühn, Anne L'Huillier, Katalin Varjú, Subhendu Kahaly . . . 343

R15 **>45-fold pulse compression using molecular gas-filled hollow-core fiber**
John E Beetar, Nrisimha Murty Madugula, Tran-Chau Truong, Yangyang Liu, Michael Chini 344

R16 **Spectrally tuneable ultrashort monochromatized extreme ultraviolet pulses at 100 kHz**
Tamás Csizmadia, Zoltán Filus, Tímea Grósz, Peng Ye, Lénárd Gulyás Oldal, Massimo De Marco, Péter Jójárt, Imre Seres, Zsolt Bengery, Barnabás Gilicze, Matteo Lucchini, Mauro Nisoli, Fabio Frassetto, Fabio Samparisi, Katalin Varjú, Subhendu Kahaly, Balazs Major 345

R17 **Ultrafast dynamics in large molecular ions following XUV ionization**
Alexie Boyer, Marius Hervé, Richard Brédy, Isabelle Compagnon, Franck Lepine . . 346

R18 **Application of the CHIP method to chiral recognition**
Nicolas Douguet, Luca Argenti 177

R19 **General scaling law of non collinear high harmonic generation and its applications**
Mekha Vimal, Martin Luttmann, David Bresteau, Fabien Lepetit, Olivier Tcherbakoff, Jean-François Hergott, Thierry Auguste, Thierry Ruchon 178

R20 **Guiding of Laser Pulses at the Theoretical Limit – 97% Throughput Hollow-Core Fibers – with subsequent compression to 1.3 cycles**

Young-Gyun Jeong, Alexis Labranche, Riccardo Piccoli, Andrea Rovere, Luca Zanotto, Gabriel Tempea, Derrek Wilson, Maksym Ivanov, Alicia Ramirez, Roberto Morandotti, François Légaré, Luca Razzari, Bruno E. Schmidt 347

R21 **Dual-Crystal Setup for 2 m, sub-3-cycle Pulse Amplification in OPCPA Pumped by High Energy Nd:YAG lasers**
Rimantas Budriūnas, Vytenis Girdauskas, Tomas Stanislauskas 348

R22 **High-flux, 100-kHz, user-oriented attosecond beamline driven by a high-average-power annular laser beam**
Peng Ye, Lénárd Gulyás Oldal, Tamás Csizmadia, Zoltán Filus, Tímea Grósz, Massimo De Marco, Péter Jójárt, Imre Seres, Zsolt Bengery, Barnabás Gilicze, Katalin Varjú, Subhendu Kahaly, Balazs Major 349

R23 **Electric-field sampling at near-petahertz frequencies and megahertz repetition rates**
Anchit Srivastava, Andreas Herbst, Daniel Schade, Mahdi M Bidhendi, Max Kieker, Francesco Tani, Hanieh Fattahi 350

R24 **Optical measurement of photorecombination time delays**
Chunmei Zhang, Graham G Brown, Dong Hyuk Ko, Paul B Corkum 179

R25 **User Facility for Attosecond Soft x-rays and THz at University of Central Florida**
Biridiana Rodriguez, Michael Chini, Tran-Chau Truong, Mihai Vaida, Zenghu Chang, Li Fang 351

R26 **CEP-stable infrared OPCPA sources**
Yoann Pertot, Nicolas Thiré, Raman Maksimenka, Simone Bux, Gregory Gitzinger, José Villanueva, Thomas Pinoteau, Nicolas Forget 352

R27 **Experiments with upgraded XUV source at ELI Beamlines facility**
Ondrej Hort, Matej Jurkovič, Ondřej Finke, Martin Albrecht, Jan Vábek, Jaroslav Nejdl 353

R28 **Time-resolved spectroscopy of Xe giant resonance by employing all-optical measurement of attosecond pulses**
Dong Hyuk Ko, Graham G Brown, Chunmei Zhang, Paul B Corkum 180

R29 **Probing electronic and vibrational dynamics in Furan with AttoXAFS**
Stefano Severino, Karl Michael Ziems, Maurizio Reduzzi, Adam Summers, Hung-Wei Sun, Ying-Hao Chien, Stefanie Gräfe, Jens Biegert 181

R30 **Focusing properties of high-order harmonics**
Marius Plach, Maria Hoflund, Jasper Peschel, Sylvain Maclot, Hugo Dacasa, Kevin Veyrinas, Eric Constant, Hampus Wikmark, Chen Guo, Cord L. Arnold, Anne L'Huillier, Per Eng-Johnsson 354

R31 **Construction of a Femtosecond Field Synthesizer**
James Turner, Allan Pettipher, Hortense Allegre, Mary Matthews, John Tisch . . . 355

R32 **Spectral phase of attosecond pulse trains generated by intense femtosecond two-color fields**
Trevor Olsson, Swapneal Jain, Jody Davis, Scott Chumley, Will Medlin, Guillaume Laurent . . . 356

R33 **General Characterization of Odd-Even Harmonic Generation by Power Terahertz Pulse**
Ngoc-Loan Phan, Doan-An Trieu, Van-Hoang Le . . . 357

R34 **Stabilization of autoionizing polaritons in atomic ionization**
Coleman Cariker, Nathan Harkema, Eva Lindroth, Arvinder Sandhu, Luca Argenti . 183

R35 **First-Principles Simulations of Electron Dynamics Probed with Transient X-ray Absorption**
Min Chen, Mengqi Yang, Kenneth Lopata . . . 184

R36 **Numerical calculation of composite light-matter quantum states in strong-field interactions**
Matan Even Tzur, Oren Cohen . . . 358

R37 **Microscopic wavefront imaging of multi-wavelength high-harmonic beams**
X Liu, M. Du, A. Pelekanidis, F Zhang, K S E Eikema, S Witte . . . 359

R38 **Quantum path interference in HHG for bi-elliptical drivers**
Anne Weber, Birger Böning, Björn Minneker, Stephan Fritzsche, Emilio Pisanty . . 360

R39 **Three ways to select from two attosecond pulses**
Katalin Kovács, Valer Tosa . . . 361

R40 **The imaginary part of the high-order harmonic cutoff**
Emilio Pisanty, Marcelo Fabian Ciappina, Maciej Lewenstein . . . 185

R41 **Strong-field chiral imaging with twisted photoelectrons**
Xavi Barcons, Andrés F. Ordóñez, Maciej Lewenstein, Andrew Maxwell . . . 186

R42 **Control of N_2^+ lasing: Rotational coherence and propagation effects**
Maria Richter, Marianna Lytova, Felipe Morales, Stefan Haessler, Olga Smirnova, Michael Spanner, Mikhail Yu. Ivanov . . . 362

R43 **Control of achiral and chiral media with synthetic chiral vortex beams**
Nicola Mayer, David Ayuso, Mikhail Yu. Ivanov, Olga Smirnova . . . 363

R44 **Effects of Dynamic Core-Electron Polarization on High-Order Harmonic Generation from Multielectron Molecules**
Van-Hoang Le, Ngoc-Loan Phan, Cam-Tu Le . . . 364

R45 **Role of Freeman resonances on spin polarization in strong field ionization of high angular momentum orbitals**
Felipe Morales, Serguei Patchkovskii, Zan Nie, Noa Nambu, Kenneth A Marsh, Chan Joshi, Olga Smirnova . . . 187

R46 **Modelling intensity volume averaging in ab initio calculations of High Harmonic Generation**
Lynda Hutcheson, Hugo van der Hart, Andrew Brown . . . 365

R47 **Extended optimization laws for high harmonic generation in gases**
Balazs Major, Katalin Varjú . . . 366

R48 **Ultrafast Electron Dynamics in the Strong Field Regime**
Lisa Ortmann, Brock Grafstrom, Alexandra S Landsman . . . 367

R49 **Ultrafast non-adiabatic relaxation of XUV-excited molecules: Dynamics in correlation bands**
Alexander Kuleff . . . 188

R50 **Probing Coherent Molecular Charge Migration with High-Harmonic Spectroscopy**
Kyle Hamer, Francois Mauger, Aderonke Folorunso, Kenneth Lopata, Robert Jones, Louis DiMauro, Kenneth J Schafer, Mette B Gaarde . . . 189

R51 **Tailoring Alignment and Orientation of Poly-atomic Molecules for Enhanced HHG Yield: A Non-Perturbative Laser-Matter Interaction-based Perspective**
Kalyani Chordiya, Mousumi Upadhyay Kahaly . . . 368

R52 **High-harmonic generation using driving pulses at 10^{16} W/cm^2**
E Svirplys, K Kovács, M Anus, O Ghafur, K Varjú, M J J Vrakking, V Tosa, B Major, and B Schütte . . . 369

R53 **High-Harmonic Generation in the Water Window from mid-IR Laser Sources**
Keegan Finger, David Atri-Schuller, Nicolas Douguet, Klaus Bartschat, Kathryn Hamilton . . . 370

R54 **Enantio-sensitive unidirectional light bending**
David Ayuso, Andrés F. Ordóñez, Piero Decleva, Mikhail Yu. Ivanov, Olga Smirnova 190

R55 **Theoretical study of attosecond order core-level photoionization time delay of heteronuclear diatomic molecules at high energies**
Yoshiaki Tamura, Kaoru Yamazaki, Fukiko Ota, Kiyoshi Ueda, Keisuke Hatada . . . 191

R56 **Radiative transition properties for In XLVIII using the Ab initio MCDHF-RCI method**
D E Salhi, S Manai, S Ben Nasr, and H Jelassi . . . 371

R57 **Nonresonant Coherent Population Transfer in Argon Rydberg Wavepackets**

J. D. Gaynor, Y. Kobayashi, A. P. Fidler, Y.-C. Lin, C. Keenan, D. M. Neumark, Stephen R Leone 372

R58 **Development of a Time-Resolved Solid-State High-Harmonic Generation Spectrometer for Probing Ultrafast Dynamics in Strongly Correlated Materials**
J. A. Spies, F. Kohrell, B. R. Nebgen, M. Zuerch 373

R59 **Measurement of nonlinear signal electric field from a femtosecond four-wave mixing interaction in molecules and materials**
Francis Walz, Siddhant Pandey, Niranjan Shivaram 374

R60 **Laser-driven Bloch electrons in the almost-strong-field regime**
Adrian Pfeiffer 375

R61 **Carrier-Envelope Phase Dependent Harmonics in Solids using a Few-Cycle IR Pulse**
Hortense Allegre, James Turner, Katarzyna Kowalczyk, Allan Pettipher, Mary Matthews, John W G Tisch 376

R62 **Signatures of multi-band effects in high-harmonic generation in monolayer MoS_2**
B R Nebgen, L Yue, R Hollinger, C B Uzundal, Z Gan, E Najafidehaghani, A George, C Spielmann, D Kartashov, A Turchanin, D Y Qiu, M B Gaarde, M Zuerch 306

R63 **A 4.1 μm Fe:ZnSe-based CPA for Driving High-Order Harmonics beyond the Water Window**
Alphonse Marra, Arnold Banner, Zenghu Chang 164

R64 **Passively phase-locked 2 um intense few-cycle optical parametric amplifier at 100 kHz repetition rate**
Takayuki Kurihara, Tianqi Yang, Tomoya Mizuno, Teruto Kanai, Jiro Itatani 377

R65 **Generation of annular few-cycle pulses by self-compression and spatial filtering in solid thin plates**
Xiaoxian Zhu, Yitan Gao, Yabei Su, Siyuan Xu, Kun Zhao, Shaobo Fang, Jiangfeng Zhu, Zhiyi Wei 378

R66 **Time evolution of the high harmonics spectra from the liquid water driven by double MIR pulses**
Tianqi Yang, Takayuki Kurihara, Tomoya Mizuno, Teruto Kanai, Yoshihisa Harada, Jiro Itatani 165

R67 **Attosecond electron pulse trains from metal nanotips**
Avraham Eitan, Maor Eldar, Salma Abo-Toame, Adi Goldner, Michael Krueger . . . 166

R68 **Elucidating the Role of Surface States Through High-Harmonic Generation (HHG) Spectroscopy**

Isabelle Tigges-Green, Somnath Biswas, Nicholas Fasano, Matthew Edwards, Nicholas Karpowicz, Gregory Scholes, Julia Mikhailova 379

R69 **Few-cycle short-wave infrared pulse generated via bulk compressions**
T-C Truong, J E Beetar, and M Chini 380

R70 **Carrier-envelope phase effects in high harmonic generation from thin-film ZnO**
Yangyang Liu, Christian Cabello, Troie Journigan, Sasha Berriel, Tran-Chau Truong, Dipendra Khatri, Parag Banerjee, Michael Chini 381

R71 **Sub-cycle control of valley polarization in WSe_2 monolayer**
Arqum Hashmi, Shunsuke Yamada, Atsushi Yamada, Kazuhiro Yabana, Tomohito Otobe 167

R72 **Multi-dimensional HHG-spectroscopy of ultrafast phonon dynamics via CEP**
Ofer Neufeld, Jin Zhang, Umberto De Giovannini, Hannes Huebener, Angel Rubio . 168

R73 **Elliptically Polarized and Structured Harmonics in Reflection from Plasma Mirrors**
Nicholas Fasano, Matthew Edwards, Julia Mikhailova 382

R74 **Symmetry Effects in Carrier-Envelope Phase-Dependent Harmonics from ZnO**
Troie Journigan, Yangyang Liu, Christian Cabello, Dipendra Khatri, Tran-Chau Truong, Michael Chini 383

R75 **Enhanced high-harmonic generation (HHG) from Cr-doped MgO crystals**
Uwe Thumm, Viktoria Nefedova, Francisco Navarrete, Sven Fröhlich, Nicolas Tancogne-Dejean, Willem Boutu, Marcelo Fabian Ciappina, David Gauthier, Aimrane Hamdou, Shatha Kaassamani, Angel Rubio, Hamed Merdji 169

R76 **Measuring the non-linear susceptibility of a semiconductor by polarization resolved high-order harmonic generation spectroscopy**
Davide Faccialà, Andrea Annunziata, Nicolas Tancogne-Dejean, Aditya Pusala, Eugenio Cinquanta, Gabriele Crippa, Michele Devetta, Giovanni Isella, Monica Bollani, Umberto De Giovannini, Hannes Huebener, Angel Rubio, Salvatore Stagira, Caterina Vozzi . 384

R77 **1.5mJ, 30W OPA at 2um via spectrally selective amplification**
Bruno E. Schmidt, Derrek Wilson, Maksym Ivanov, Pedram Abdolghader, Antoine Raffray, Tadas Balciunas, François Légaré, Hans Jakob Wörner 170

R78 **Polarization shaping of light for strong field valleytronics**
Igor Tyulnev, Lenard Vamos, Jens Biegert 171

R79 **Strong-field photoelectron (PE) emission of plasmonic nanoparticles (NPs)**
Uwe Thumm, Erfan Saydanzad, Jeffrey Powell, Artem Rudenko 385

RP

R80 **Quantification and analysis of spectral broadening of femtosecond pulses in solid medium**
Yitan Gao, Xianzhi Wang, Xiaoxian Zhu, Kun Zhao, Heyuan Liu, Z H Wang, Shaobo Fang, Zhiyi Wei 386

R81 **On-chip polarization-sensitive time-domain spectroscopy in the near-infrared using plasmonic nanoantenna arrays**
M Turchetti, M R Bionta, F Ritzkowsky, M Yeung, K K Berggren and P D Keathley 387

R82 **Tracking electron dynamics in wide-bandgap semiconductors by transient grating solid-state high harmonic spectroscopy.**
Sylvianne D.C. Roscam Abbing, Filippo Campi and Peter M. Kraus 388

Strong Field Simulator: Attosecond Study of Strong Field Ionization in Noble Gas Atoms

Q Liu[1 *], A Piper[1], D Kiesewetter[1], Y Tang[1], P Agostini[1], K J Schafer[2] and L F DiMauro[1]

[1] Department of Physics, The Ohio State University, Columbus, Ohio 43210, USA

[2] Department of Physics & Astronomy, Louisiana State University, Baton Rouge, Louisiana 70803, USA

Synopsis We demonstrate the strong field simulator (SFS), an attosecond method capable of decoupling ionization from acceleration and recollision in strong field processes. Our SFS method employs an extreme ultraviolet attosecond pulse train to ionize the target dressed by a strong mid-infrared pulse that accelerates the electron and drives recollision. We present a functional SFS by simulating strong field recollision in noble gas atoms. Our work shows the promise of the SFS method for studying strong field processes and providing unprecedented control of strong field phenomena.

RP

The dynamics of an electron photoionized by an intense laser field is commonly understood using the semi-classical three-step model: the electron first tunnels out of the atomic potential, then it is accelerated in the strong field, and finally it recollides with its parent ion [1]. One complication of studying strong field processes, particularly recollision, is that tunneling can occur at times within the infrared field cycle that are weighted by the instantaneous ionization probability proportional to field strength, thus only a limited phase space of all possible trajectories contributes to the measurement [2]. In order to study the individual quantum trajectories in strong field recollision, we introduce the strong field simulator (SFS) method.

The SFS method investigates strong field processes by decoupling ionization from the acceleration and recollision steps through a phase locked extreme ultraviolet (XUV) attosecond pulse train (APT) with photon energies at or above the ionization threshold synchronized to a strong mid-infrared (MIR) pulse, as is shown in Figure 1. In this scheme, the tunneling ionization step is replaced by single-photon XUV ionization, while the MIR pulse accelerates the electron and drives recollision. A variable delay between the XUV and MIR pulse enables the control of the electron's release time in the strong field, accessing a well-defined set of trajectories [3]. By controlling different experimental parameters such as the MIR wavelength, intensity, target species and polarization, the SFS method can allow for a robust multi-dimensional study of strong field recollision.

Here, we demonstrate a functional SFS by simulating strong field recollision in noble gas atoms. In the XUV-seeded photoelectron spectrum averaged over all delays, a large enhancement in photoelectron yield is observed that cannot be thought of as simply the sum of the MIR-only and XUV-only spectra. Furthermore, the ionization yield of double ions is also measured, and a clear oscillation in yield as a function of delay at twice the MIR frequency is observed, a strong piece of evidence that the ionization is recollision driven. This is the first observation of two-color, recollision driven, double ionization between a MIR laser and a tabletop XUV APT source.

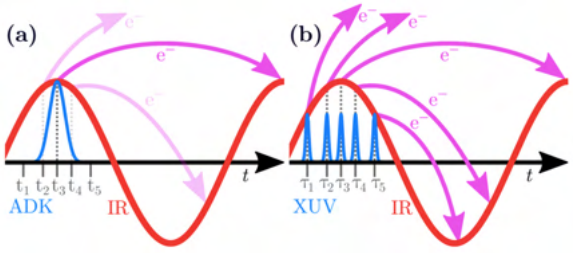


Figure 1. Comparison between (a) ordinary strong field processes and (b) the strong field simulator.

Our work shows the promise of the SFS method for studying strong field processes and providing control of strong field phenomena with unprecedented breadth and sensitivity.

References

[1] Schafer K *et al* 1993 *Phys. Rev. Lett.* **70 1599**
[2] Walker B *et al* 1994 *Phys. Rev. Lett.* **73 1227**
[3] Schafer K *et al* 2004 *Phys. Rev. Lett.* **92 023003**

* E-mail: liu.6530@osu.edu

Verifying the Frequency Resolved Optical Switching Technique to Accurately Characterize Multi-Octave IR Pulse

A Longa[1]*, M Kumar[1], P Lassonde[1], A Laramée[1], H Ibrahim[1], F Légaré[1], and A Leblanc[2]

[1]Institut National de la Recherche Scientifique, Centre EMT, ALLS laboratory, 1650 Boulevard Lionel-Boulet, Varennes, Qc, J3X1S2, Canada

[2]Lab. d'Optique Appliquée, Ecole Polytechnique, ENSTA, CNRS, Université Paris Saclay, Palaiseau, France

Synopsis We present advanced features of the frequency resolved optical switching (FROSt) technique: (i) temporal characterization of an IR supercontinuum spanning over two octave of bandwidth, (ii) a high precision characterization of the spectral phase with less than 10 fs^2 of error on group delay dispersion, (iii) characterization of pulses independently of their polarization direction. These attributes allow the use of the FROSt technique for the precise characterization and control of the spectral phase of ultrashort few-cycle pulses down to single-cycle.

RP

With the progress in ultrafast laser technologies, major efforts have been made to generate and characterize high energy ultrashort laser pulses down to sub-cycle duration. The access to such pulses allows, for instance, to generate high harmonic radiation with photon energy in the water window, ultrashort electron bunches, or to measure ultrafast dynamics in atoms and molecules. The characterization and control of the spectral phase of such pulses is a key step in the outgrowth of these techniques. Nevertheless, the temporal characterization of ultra-broadband IR pulses remains challenging. Techniques relying on a $\chi^{(2)}$ nonlinear process such as second-harmonic generation frequency resolved optical gating (SHG-FROG) or dispersion scan (D-scan) are inherently limited in bandwidth by the phase matching conditions. More complex techniques were developed, such as tunnel ionization in the air (TIPTOE) or electro-optical sampling (EOS) that not only measure the temporal profile but directly its electric field. However, they are much more complex to implement. We use an alternative pulse characterization technique, the frequency resolved optical switching (FROSt), free of phase matching, based on transient absorption in solids. The pulse to be characterized probes the ultrafast switch of the transient optical transmission of a solid triggered by a pump pulse. Its versatility was demonstrated by characterizing different ultrashort pulses with central wavelengths from 0.77 to 10 μm and various energies down to a few nanojoules [1]. In principle, this technique is only spectrally limited by the sensitivity of the spectrometer and the transparency range of the material used for the switch. First, we demonstrate on FROSt's capability to characterize ultra-broadband infrared pulses up to more than two octaves of bandwidth. The broaden pulses center at 1.75 μm were generated using a standard commercial Ti-Sa pumped OPA and a cascade of two hollow core fibers. The pulses exhibit wide spectral broadening with spectra spanning from 0.55 to 2.5 μm and are completely characterized using FROSt [2]. On another experiment, we have characterized the precision limit of the FROSt measurement. The experimental spectral phases are compared with the phase shifts calculated using the Sellmeier equation. The agreement is excellent between the theory and the experiment for all fused silica (FS) thicknesses, even for the phase shift induced by the 0.2 mm window, corresponding to a change of 10 fs^2 in the group delay dispersion (GDD) of the probe pulse making the FROSt a suitable technique to characterize single-cycle pulses. At last, we show the simultaneous characterization of three pulses spanning over two octaves of spectral bandwidth, regardless of their polarization. In this particular case, the OPA is tuned to optimize the signal and idler pulses to central wavelengths of ∼1.25 and ∼2.2 μm. The signal pulse is frequency-doubled to ∼615 nm. The three pulses are characterized simultaneously using FROSt [3]. These attributes allow the use of FROSt technique for the precise characterization and the control of the spectral phase of ultrashort few-cycle pulses down to single-cycle.

References

[1] A Leblanc *et al.*, Opt Express **27**, 28998 (2019).
[2] A Leblanc *et al.*, Journal of Physics: Photonics **3**, 045002 (2021).
[3] P Lassonde *et al.*, Opt Express **29**, 23225 (2021).

*E-mail: adrien.longa@inrs.ca

Generation of femtosecond multi-millijoule pulse at 3 µm through a 2-µm pumped OPCPA

F Zhou[1], Y Wu[1], and Z Chang[1*]

[1]Institute for the Frontier of Attosecond Science and Technology, The College of Optics and Photonics (CREOL) and Department of Physics, University of Central Florida, Orlando, FL, 32816

Synopsis 3 mJ pulses at 3 µm are generated by a three-stage, $ZnGeP_2$-based optical parametric chirped pulse amplifier pumped by a 2 µm, thermoelectrically cooled Ho:YLF laser. The output pulses are compressed to 150 fs, though the spectrum supports 50 fs transform-limited pulses.

RP

An Optical Parametric Chirped Pulse Amplifier (OPCPA) that outputs millijoule, femtosecond pulses at 3 µm has been developed. The high-power mid-infrared pulses pave the way for generating attosecond X-ray pulses with photon energies extending beyond the water window via high harmonic generation. The OPCPA is pumped by a high-energy picosecond Ho laser at 2 µm, a more efficient scheme than pumping by Yb lasers at 1 µm.

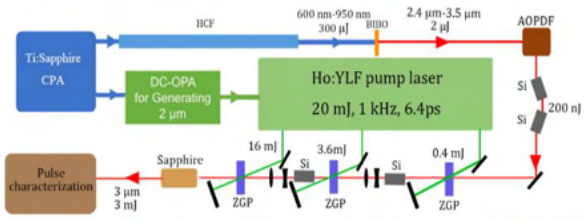


Figure 1. Optical layout of the OPCPA

The optical layout of the OPCPA is shown in Figure 1. 2 mJ pulses from the Ti:Sapphire CPA are divided equally. Half of the energy is sent to a dual-chirped OPA to generate the seed for the Ho:YLF CPA that pumps the OPCPA [1]. The seed is stretched by a chirped volume Bragg grating (CVBG) to 470 ps and amplified through a four-stage amplifier. The first two stages employ a double-pass configuration and amplify the 5 µJ seed to 8 mJ. Each stage is pumped by a 35 W CW laser at 1.94 µm. Two 5 mm-diameter, 50 mm-long, 0.75% at.-doped, cylindrical Ho:YLF crystals are used and are water cooled to 15°C. The output is then amplified to 60 mJ by two single-pass booster amplifiers, both pumped by 110 W. Two thermoelectric cooling modules are used for each stage to cool the 8 mm × 8 mm × 50 mm rectangular crystals to -20°C. The same CVBG is used for the compressor as for the stretcher to compress the pulse to 6.4 ps. The entire laser system is purged with dry nitrogen to reduce the water absorption of the 1.94 µm pump and to prevent the formation of ice on the crystals.

The other half of the energy from the Ti:Sapphire is spectrally broadened to 600-950 nm by a hollow-core fiber. This pulse then generates the 2.5-3.5 µm signal of the OPCPA via intra-pulse difference frequency generation in a 0.8 mm-thick BIBO [2]. The signal is stretched by a 60 mm long silicon block and an acousto-optic programmable dispersive filter (AOPDF) to 6 ps. To prevent damage to the ZGP crystals and to reduce the beam distortion of the pump caused by the thermal lensing effect of the Ho:YLF, the total pumping energy is currently limited to 20 mJ. 0.4 mJ, 3.6 mJ and 16 mJ pulses are sent to the 1st, 2nd, and 3rd stages of the OPCPA respectively. All 3 stages employ a non-collinear configuration, and a 30 mm-long piece of silicon is placed after the 1st and the 2nd stages to further stretch the pulse. The 200 nJ signal is amplified to 24 µJ, 280 µJ and 3 mJ in the 1st, 2nd and 3rd stages respectively. The final output is compressed by 150 mm-long piece of bulk sapphire to 150 fs with 75% efficiency. The spectrum of the final output spans from 2.8 µm to 3.2 µm supporting 50 fs Fourier transform-limit pulses. The peak power will be further increased by optimizing the pulse compression and by taking advantage of the full energy of the Ho:YLF amplifier.

References

[1] Murari K *et al* 2020 *Appl. Phys. Lett.* 117, 141102
[2] Yin Y *et al* 2017 *Sci Rep* **7**, 11097

* E-mail: Zenghu.Chang @ucf.edu

Nonlinear pulse compression via multipass cell and contrast enhancement via nonlinear ellipse rotation of a thin-disk regenerative amplifier

Y. Pfaff[1,2]*, G. Barbiero[1], M. Rampp[1], S. Klingebiel[1], H. Wang[1], C. Y. Teisset[1], R. Jung[1], A. H. Woldegeorgis[1], J. Jaksic[1], C. J. Saraceno[2] and T. Metzger[1]

[1]TRUMPF Scientific Lasers GmbH + Co. KG, Unterföhring, 85774, Germany
[2]Photonics and Ultrafast Laser Science, Ruhr University Bochum, Bochum, 44801, Germany

Synopsis We report on the nonlinear pulse compression of 10 mJ, 840 fs pulses at 3kHz repetition rate to 38 fs via gas-filled multipass cell. Moreover, the temporal-intensity contrast is enhanced via nonlinear ellipse rotation of more than a factor 50 in the same experiemtal setup.

The fronted for the experimental setup outlined below is a commercial Yb-doped thin-disk regenerative amplifier (DIRA 200-5) [1]. The system provides pulses with 10 mJ pulse energy and a pulse duration of 840 fs at a repetition rate of 3 kHz.

The nonlinear spectral broadening is performed inside a Herriott-type multipass cell. The chamber is equipped with dielectric mirrors (radius of curvature 1.2 m) and is filled with 650 mbar of argon. The total number of passes in the cell is 37.

Following a chirped mirrors compressor providing a total dispersion of -3500 fs², the pulses were compressed down to 38.4 fs, strikingly close to the supported Fourier transform limit. The laser beam quality remained excellent with a measured M^2=1.17.

In order to achieve a short pulse duration with higher pulse contrast, we additionally combined nonlinear ellipse rotation (NER) to the nonlinear spectral broadening. Due to the similar nature of self-phase modulation and NER, it was possible to carry out this experiment adding few elements to the existing broadening setup [2].

The polarization rotation from linear to elliptical polarization is performed by a broadband achromatic λ/4 wave plate, which is positioned in the collimated beam before the cell. A second broadband achromatic λ/4 wave plate is placed after the cell in the recollimated beam to compensate the introduced ellipticity. The orthogonal polarizations are split by a Glan-Taylor calcite polarizer after attenuation.

Under an angle of θ_{NER} = 5° for the first λ/4 wave plate, the temporal contrast with NER is improved by more than a factor of 50. Through the implementation of NER, the contrast enhanced pulse contains 56% of the input energy [3], without affecting the pulse duration after recompression (Fig. 1). Because of the additional optical components, the number of bounces on the chirped mirror compressor are increased to reach a total dispersion of -5000 fs².

The beam quality factor of the gaussian shaped laser output is preserved and is measured to be M^2 = 1.19.

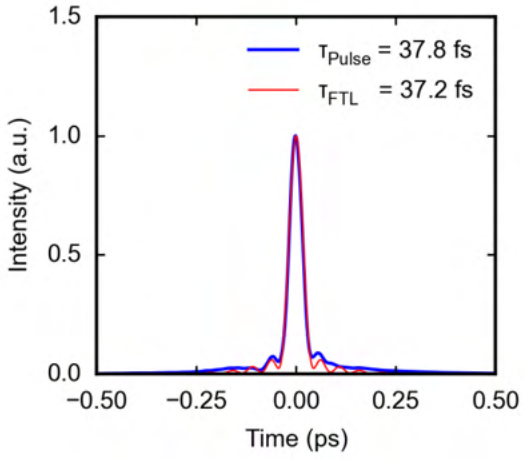


Figure 1. Retrieved temporal profile of the compressed pulse and the calculated Fourier transform limited profile after NER. The pulse duration is measured via second-harmonic frequency-resolved optical gating.

References

[1] Teisset C. Y. *et al* 2013 in *Advanced Solid-State Laser Congress*, paper JTh5A.1.
[2] Homoelle D. *et al* 2002 *Opt. Lett.* **27** 1646
[3] Pajer V. *et al* 2021 *Laser Phys. Lett.* **18** 065401

* E-mail: yanik.pfaff@trumpf.com

RP

Weak pre-ionization for phase-matched high harmonic generation in absorption-limited long media

O Finke[1,2], J Vábek[1,2,3], M Nevrkla[1,2], N Bobrova[2], O Hort[1], M Jurkovič[1,2], M Albrecht[1,2], A Jančárek[1,2], F Catoire[3], S Skupin[4] and J Nejdl[1,2,*]

[1]ELI Beamlines Centre, Institute of Physics of the Czech Academy of Sciences, Na Slovance 2, 182 21 Prague, Czechia
[2]Faculty of Nuclear Sciences and Physical Engineering CTU, Břehová 7, 115 19 Prague 1, Czechia
[3]Centre des Lasers Intenses et Applications, Université de Bordeaux-CNRS-CEA, 33405 Talence Cedex, France
[4]Institut Lumière Matière, UMR 5306 Université Lyon 1 - CNRS, Université de Lyon, 69622 Villeurbanne, France

Synopsis We have discovered that ionization-induced defocusing is the main reason for inefficient harmonic generation in long absorption-limited media. To overcome this issue, a novel method utilizing pre-ionization is validated both experimentally and numerically.

RP

Applications that require high-energy XUV pulses are usually performed with sources of high-order harmonic generation (HHG) driven by high peak power laser systems. The scaling of the efficient generation process calls for generation in long media.

Simulations of non-linear laser propagation have revealed a strong impact of defocusing on the efficiency of the generation. We show that pre-ionization of the medium to a certain level increases the XUV signal significantly.

The ionization-induced defocusing substantially affects the laser pulse in the gaseous medium [1]. Numerical simulations that use cylindrically symmetric unidirectional solver [2] show that IR intensity drastically drops in the first part of the medium (region I) and stabilizes in the second part (region II) along the propagation axis. The Value of the stabilized intensity in region II is almost independent of the IR intensity at the entrance and pressure in the long krypton medium.

During absorption-limited generation (absorption length is much shorter than the medium length), the absorption plays a critical role, therefore region II is crucial as most of the detected XUV radiation originates there.

The pulse intensity in region II is too low to ionize the medium enough to suppress the phase mismatch between the laser field and its q-th harmonic $\Delta k = k_q - qk_1$.

Considering only the dominant processes for each wave (dispersion of the neutrals for both waves and effect of plasma for the laser field), we can find the optimal degree of ionization η as a function of atomic density ρ and the coherent length $L_{coh} = 1/|\Delta k|$ as

$$\eta = \frac{\omega_1 \varepsilon_0 m_e}{e^2}\left(\Delta\chi \mp \frac{2\pi c}{q\omega_1 \rho L_{coh}}\right), \qquad (1)$$

where $\Delta\chi = \chi_1^{(n)} - \chi_q^{(n)}$ is the difference of susceptibilities of neutrals at laser and its q-th harmonic frequency (at standard temperature and pressure). We assume that for optimal phase-matching, the coherent length needs to be the same as medium length or longer. Equation (1) reveals the interval of η, where optimal phase-matching is achieved.

By pre-ionizing the medium into the optimal interval of η, phase mismatch is minimized. In the case of the 17th harmonic of 800 nm laser generated in krypton, homogeneous pre-ionization to 8% shows a decrease of phase mismatch by an order of magnitude.

We have employed a weak capillary discharge with a 15 mm long and 1 mm wide target to generate a pre-ionized medium. We observed an enhancement of the harmonic signal (by a factor 3 in H17 in krypton and five times in the case of H21 in argon).

The analytical model we developed and comprehensive numerical simulations of the whole generation process confirm our experimental findings. We believe our method will help the HHG sources to match the requirements of many photon-hungry applications.

* E-mail: nejdl@fzu.cz

References

[1] Rivas D E *et al* 2018 *Optica:* ***5****, 1283-1289*
[2] Bergé L *et al* 2007 *Rep. Prog. Phys.:* ***70*** *1633*

10mJ Hollow-Core Fiber operation at 250W average power with 90% efficiency

M Ivanov[1,2], D Wilson[1,2], A Labranche[1], G Tempea[1], A Ramirez[1], F Légaré[2], C Paradis[3], A Hage[3], T Mans[3], C Trallero[4], B E Schmidt[2] *

[1]few-cycle Inc, Varennes, J3X 1P7, Canada
[2]Institut national de la recherche scientifique, Varennes, J3X 1P7, Canada
[3]Amphos GmbH, Herzogenrath, 52134, Germany
[4]University of Connecticut, Storrs, 06269, US

Synopsis We developed a high transmission Hollow-core fiber (HCF) with 1mm ID that supports 97% absolute transmission. We were able to achieve about 30 times spectral broadening of 11mJ, 1.5ps pulses from a 275W, 25 kHz InnoSlab multi-pass amplifier with 90% fiber transmission. The spectrum achieved with Kr at 1 bar supports a 50fs TL bandwidth.

In this contribution we demonstrate the so far highest average power HCF output of 250W for 10mJ of output pulse energy.

The driving laser is Amphos GmbH delivering up to 11mJ of <1.5ps pulses at 25kHz (275W average power). The laser repetition rate is tunable to 200kHz, 300 W, 1.5 mJ. The beam is coupled in a loose focusing condition to a newly developed high throughput HCF from few-cycle Inc of 1mm ID that has proven to enable up 97% transmission [1]. Figure 1a) shows that transmission remains nearly constant up to 273W input for the air cooled fiber. Figure 1b) shows the spectral broadening as red curve which corresponds to a TL pulse duration of about 50fs with good long term and short term (std. dev. 0.58%) stability. We will present the latest results of our ongoing peak power and average power scaling development.

We designed a passive heat transfer system to evacuate the directly from the fiber tip. By improving the ceramic material and shape of the tapered fiber protection the fiber tip has been able to withstand >500mJ of coupled pulse energy.

Regarding the average power scaling, we follow a dual strategy of (i) reducing the heat load by achieving very high transmission and (ii) by increasing the cooling efficiency of the fiber and fiber tip. We have successfully tested the evacuation of 120W by an upgraded air cooling setup.

The final goal is the develop a system capable of handling 1J of energy combined with 1kW of average power, since such ps Yb lasers are now available [2].

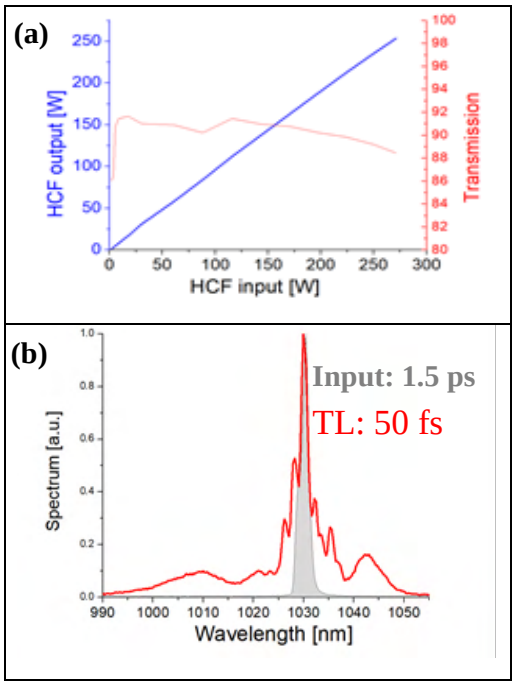


Figure 1. (a) The power transmission as a function of incident power remains fairly constant up to a maximum input of 273W with 11mJ per pulse. (b) spectral broadening at 1 bar Kr shown as the red curve overplayed with the input spectrum as shaded grey.

References

[1] Jeong Y *et al* 2020 *Ultrafast Phen.*: Th4A.6
[2] Wang Y *et al* 2020 *Opt. Lett.* 45, 6615

* E-mail: schmidt@few-cycle.com

High-energy multidimensional solitary states in hollow-core fibers

R. Safaei[1], G. Fan[1], O. Kwon[1], K. Légaré[1], B. E. Schmidt[2], P. Lassonde[1], H. Ibrahim[1] and F. Légaré[1,*]

[1]Advanced Laser Light Source, INRS-EMT, Varennes, J3X1P7, Quebec, Canada
[2]*few-cycle* Inc., 1650 Boulevard Lionel-Boulet, Varennes, J3X 1S2, Canada

Synopsis Using sub-picosecond pulses, we report the first time observation of the formation of highly-stable multidimensional solitary states (MDSS) in molecular-filled hollow-core fibers. The MDSS have broadband red-shifted spectra with an uncommon negative quadratic spectral phase at output. This approach paves the route to compress sub-picosecond Ytterbium laser systems to few-cycle pulse duration using a compact setup. These few-cycle pulses have been used to drive high harmonic generation, and the generated XUV pulses were used for X-ray resonsant magnetic scattering measurements.

RP

Optical solitons (solitary states) are self-sustained, localized wave packets that exhibit confinement in one or multiple dimensions (spatial and temporal) and have attracted substantial theoretical and experimental investigations [1]. In this work, we demonstrate the generation of multidimensional solitary states (MDSS) in a large core hollow-core fiber (HCF) filled with nitrogen (N_2) [2].

The physical concept of this work is illustrated and explained in Fig.1(a). As a starting reference point, the focal spot size at the HCF input pulses was chosen for obtaining high coupling efficiency into the fundamental mode. Under the weak guiding condition in the HCF, modes fall into groups of linearly polarized modes (LP_{mn}). Self-focusing in the HCF is interpreted as the transfer of energy from the fundamental mode (LP_{01}) to other LP_{0n} modes which have rotational symmetry with the maximum intensity in the central part. In the high-energy regime, the effects of self-focusing and diffraction become significant and multiple LP_{0n} modes are created at the beginning of the fiber. These extended multidimensional pathways lead to an enhancement of the Raman process, which provides sufficient nonlinearity to balance the potential diffraction. This nonlinear self-trapping mechanism, together with the ultra-low modal dispersion inherent to large core HCFs, make the generated MDSS undergo efficient red-shifted spectral broadening through cascaded SRS. In the experiment, 700 fs, high-energy pulses (5mJ/pulse) with a central wavelength of 780 nm were launched into a 3 m long hollow-core (500 µm) fiber filled with N_2. The 700 fs pulses are obtained by positively chirping 40 fs pulses from a Titanium-Sapphire amplifier. At the HCF output, the coherent solitary states are located at the leading edge of the initial driver pulse with a negative quadratic spectral phase. These solitary states are experimentally separated from the pump part by placing a long pass filter (above 830 nm) at the HCF output (the pump part is selected by a band-pass filter (760nm-790nm)). The broadband MDSS pulses are subsequently compressed using a simple piece of fused-silica (FS) to 10.9 fs, and used to drive high harmonic generation for X-ray resonant magnetic scattering experiments.

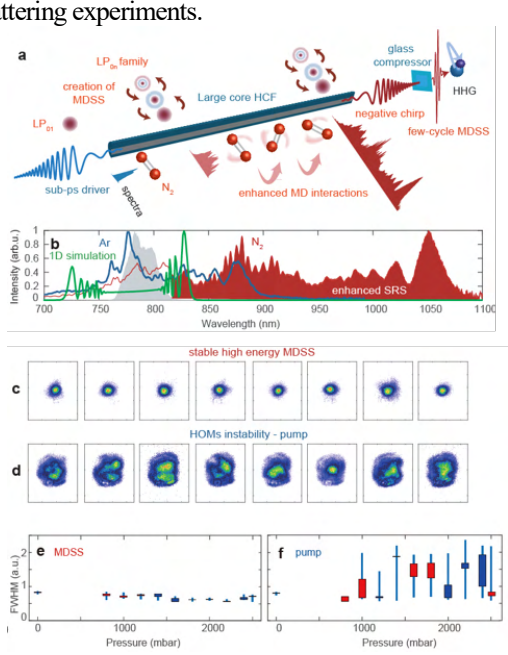


Figure 1 Conceptual illustration (a) and experimental observation of MDSS (b)-(f). Statistical changes for the full-width at half-maximum (FWHM) of the spatial profile are shown for the MDSS beam (e) and the pump (f) for 20 single-shot images per pressure. Panel 3 (candlestick chart) shows that the FWHM of the MDSS have negligible fluctuations, which further confirms the self-trapping effect of the MDSS beam through its propagation in the HCF.

References

[1] P. Knight and A. Miller, *Optical solitons: theory and experiment* (Cambridge University Press, 1992), Vol. 10.

[2] R. Safaei et *al.* Nature Phot. **14**, 733-739 (2020).

* E-mail: francois.legare@inrs.ca

In Situ Sub-50-Attosecond Active Stabilization of the Delay Between Infrared and Ultraviolet Light Pulses

M. Luttmann*, D. Bresteau, J.-F. Hergott, O. Tcherbakoff, and T. Ruchon†

Université Paris-Saclay, CEA, CNRS, LIDYL, 91191 Gif-sur-Yvette, France

Synopsis We introduce a robust technique, named LIZARD (Laser-dressed IoniZation for the Adjustment of the pump-pRobe Delay), allowing *in situ* active stabilization of the pump-probe delay between a near-infrared pulse, and an extreme-ultraviolet pulse. The important feature of the method is the use of an error signal calculated from a two-photon photoelectron signal obtained by photoionizing a gas target with the two superimposed beams. The resulting delay stability (below 30 as) makes LIZARD a promising tool for attosecond pump-probe experiments.

Attosecond pump-probe experiments require to control, with sub-femtosecond precision, the delay between two ultrashort light pulses. One of them is usually intense and in the Vis-IR spectral range, while the second is weak and in the XUV spectral range. In order to perform experiments asking for high statistics, such a stability should be maintained over hours, while scanning the delay. This can only be achieved through active stabilization schemes, usually relying on the live measurement of interferences from an additional continuous laser beam co-propagating in the interferometer [1]. Such techniques have drawbacks: they require many additional optics, and most importantly do not provide an in situ control of the delay. Indeed, what is actually stabilized is the optical path difference accumulated by the continous laser, which may differ from the XUV / IR optical path difference. We recently introduced a new technique, named LIZARD (Laser-dressed IoniZation for the Adjustment of the pump-pRobe Delay), which does not require any such additional laser beam and allows an *in-situ* delay control [2].

The principle of LIZARD is to extract the correction signal from two-photon photoelectron spectra obtained by photoionizing a gas target in an electronic spectrometer, with the two superimposed beams. It was implemented on the FAB10 beamline at the ATTOLab facility (CEA Saclay). Despite an interferometer length of several meters, we achieved a long term stability of 28 as RMS of our pump-probe setup and could record RABBIT (Reconstruction of Attosecond Beatings By Interference of Two-photons transitions) traces over hours (Fig. 1). The high degree of stability enables long averaging times, making LIZARD a promising technique for the stabilization of pump-probe experiments requiring high statistics, such as coincidence spectroscopy or photoemission from surfaces. In the case of RABBIT, we show that the measurement of spectral phases is more precise with LIZARD, especially at energies where the signal to noise ratio is very low. Moreover, it does not require any additional laser or even additional optical elements but a refocusing optic that is common to both beams.

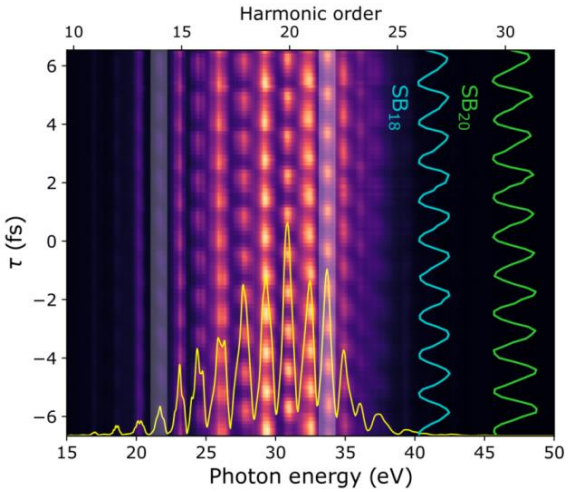


Figure 1. A RABBIT scan in Ar gas, stabilized by the LIZARD technique. The scan lasted approximately two hours. The two energy bands highlighted in white were used as the two phase quadrature input signals for the delay control. In blue and green, lineouts of two other sidebands not used for the LIZARD stabilization.

References

[1] F. Böttcher et al, Applied Physics B 91, 287–293 (2008)

[2] M. Luttmann et al, Phys. Rev. Applied 15, 034036 (2021)

* E-mail: martin.luttmann@cea.fr

† E-mail: thierry.ruchon@cea.fr

Attosecond delays of high harmonic emissions from isotopes of molecular hydrogen measured by Gouy phase XUV interferometer

M H Mustary[1], Liang Xu[2,3], Wanyang Wu[2], Nida Haram[1], Han Xu[1], Feng He[2,4], R T Sang[1] and I V Litvinyuk[1,*]

[1]Centre for Quantum Dynamics, Griffith University, Brisbane, Queensland 4111, Australia
[2]Key Laboratory for Laser Plasmas (Ministry of Education) and School of Physics and Astronomy, Collaborative Innovation Center for IFSA (CICIFSA), Shanghai Jiao Tong University, Shanghai 200240, China
[3]Shanghai Key Lab of Modern Optical System, University of Shanghai for Science and Technology, 200093 Shanghai, People's Republic of China
[4]CAS Center for Excellence in Ultra-intense Laser Science, Shanghai, 201800, China

Synopsis We present a precise measurement of HHG phase difference between two isotopes of molecular hydrogen using the advanced extreme-ultraviolet (XUV) Gouy phase interferometer [1]. The measured phase difference is about 200 mrad, corresponding to ~3 attoseconds time delay which is nearly independent of harmonic order. The measurements agree very well with numerical calculations of a four-dimensional time-dependent Schödiner equation. Numerical simulations also reveal the effects of molecular orientation and intra-molecular two-centre interference on the measured phase differences. This technique enables the observation of subtle effects of molecular structures and nuclear motion on electron dynamics in strong laser fields.

RP

High harmonic spectroscopy can access structural and dynamical information on molecular systems encoded in amplitude and phase of high harmonic generation (HHG) signals4. However, measurement of the harmonic phase is a daunting task. Building an interferometer in the XUV region is quite challenging for two reasons: firstly, it is challenging to control the delay of the XUV pulses precisely between the two arms with sub-cycle precision; secondly, the highly reflective XUV optics is yet to be developed. Our passively stabilized Gouy phase interferometer [1,2], on the other hand, is an all-optical direct XUV interferometric technique. It does not require calibration of gas pressures to ensure the same number densities. Additionally, it does not require any XUV optics. The tecnique provides an elegant way to generate two coherent high harmonic pulses without splitting the driving laser and XUV beams. The two mutually coherent XUV pulses are generated by exploiting the inherent properties (Gouy phase) of a single Gaussian focused laser beam. Its unprecedented resolution of 300 μrad (~100 zeptoseconds) is a result of any instability in the distance between the two arms (the gas jets in this case) of the interferometer being determined relative to the Rayleigh length, z_R of the fundamental laser beam as opposed to the XUV wavelength in a conventional optical interfeometer.

Here, we apply the technique to investigate the effect of nuclear dynamics on the electron motion in molecular hydrogen by precise measurement of high harmonic phase difference (and corresponding HHG phase delays) produced in H_2 and D_2. Since the ionization potentials of H_2 (Ip =15.43 eV) and D_2 (Ip = 15.46 eV) are almost identical, the difference in the phase accumulated by electron in the continuum is considered to be negligible. However, due to the nuclear mass difference, the evolution of nuclear wave packet while electron propagates in the continuum and then recombines to the ground state may differ substantially. The harmonic intensity from the heavy isotope was shown tobe higher compared to the lighter molecule as harmonic emission is sensitive to the nuclear motion, though for D_2 the ionization probability is less than for H_2. The aim of this work is to measure a small phase difference of HHG signals and to gain an insight into the correlated electron–nuclear dynamics for the two isotopes of molecular hydrogen.

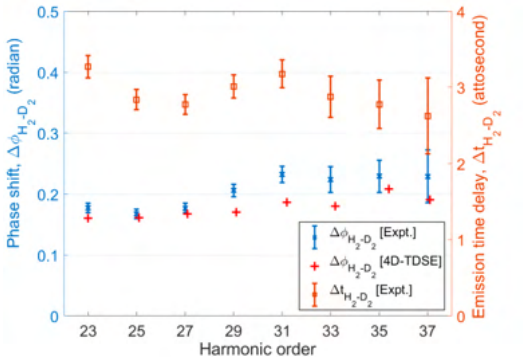


Figure 1. Phase differences and delays between H_2 and D_2.

References

[1] Mustary M H et al. *J. Phys. B: At. Mol. Opt. Phys*. 51, 094006 (2018).
[2] Laban, D. E. et al. *Phys. Rev. Lett.* 109, 263902 (2012).

*E-mail: *i.litvinyuk@griffith.edu.au*

High Flux High Harmonic Generation at the Sylos Long Beamline at ELI-ALPS

B Nagyillés[1 *], Z Diveki[1 †], B Farkas[1], R Weissenbilder[2], C. L. Arnold[2], P Eng-Johnsson[2], S Kühn[1],

A L'Huillier[2], K Varjú[1], and S Kahaly[1]

[1]ELI-ALPS, Wolgang Sandner street 3, 6728 Szeged, Hungary
[2]Department of Physics, Lund University, Professorsgatan 1, 223 63 Lund, Sweden

Synopsis The realization and first results are presented from and upscaled High-order Harmonic beamline designed to efficiently harness the power of TW class, 1 kHz, two-cycle lasers. We give first insight into the vast parameter space offered by the beamline toward the generation of powerful attosecond pulses and discuss their applicability to experiments at the ELI-ALPS User Facility.

RP

High-order Harmonic Generation in Gases (GHHG) remains the state-of-the-art method to produce light pulses that are able to capture and eventually manipulate the fastest processes down to the attosecond time scale. It has been the core technology of the field of attosecond sciences since its discovery. Despite the development of sophisticated techniques such as phase-locked XUV-IR pump-probe able to retrieve electron dynamics with few ten attosecond resolution, the dream of pure XUV pulse experiments (i.e. nonlinear interaction schemes) has not quite materialized. The main obstacle is the intrinsically low conversion efficiency of GHHG preventing the production of sufficiently high XUV pulse energies.

With the advent of modern OPCPA technology, TW class lasers with kHz repetition rates and few-cycle duration are now available, promising to overcome this obstacle. While the path of upscaling has been described in theory [1,2], only an experiment can tell how these goals can be reached in practice.

The ELI-ALPS Research Institute and User Facility [3] houses one of the first implementation in this direction by combining the SYLOS laser with the GHHG LONG beamline. The upscaling approach taken here relies on loose focusing into long, low pressure gas targets. Emphasis is put on flexibility since a largely unknown space of laser and beamline parameters needs to be explored. To this end, two configurations are available: one with 19 m focusing into a 30-60 cm variable gas cell, and another with 55 m focusing into an array of 15 independent, consecutive 40 cm long gas cells.

We will report here our first results with the 19 m focusing setup. Guided by extensive simulation work [4] we explore how the pertinent XUV pulse properties such as spectrum, divergence, pulse energy, behave under these novel generation conditions. Fig. 1 shows as just one example the conversion efficiency of the 23rd harmonic as function of cell length and pressure.

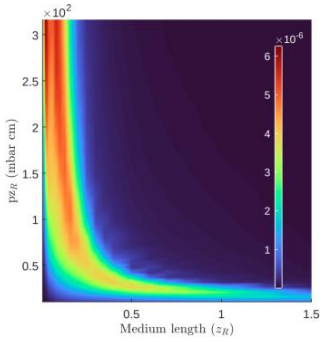


Figure 1. Conversion efficiency (in color) as a function of medium length (in unit of the Rayleigh length) and pressure times Rayleigh length for the 23rd harmonic in Ar. The laser intensity is 2.5x10^{14} W/cm^2, wavelength 810 nm and pulse duration, 22 fs. The medium is centered at the focus.

References

[1] Heyl C M *et al* 2016 *Optica* **3** 75
[2] Rudawski P *et al* 2013 *Rev. Sci. Instrum.* **84** 073103
[3] Kühn S et al 2017 J. Phys. B: At. Mol. Opt. Phys. **50** 132002
[4] Weissenbilder R et al 2022 arXiv:2202.08202

* E-mail: balazs.nagyilles@eli-alps.hu
† E-mail: diveki.zsolt@eli-alps.hu

>45-fold pulse compression using molecular gas-filled hollow-core fiber

J E Beetar[1,2], M Nrisimhamurty[1], T C Truong[1], Y Liu[1] and M Chini[1,3] *

[1]Department of Physics, University of Central Florida, Orlando FL 32816
[2]Department of Chemistry, University of California, Berkeley, California 94720
[3]CREOL, the College of Optics and Photonics, University of Central Florida, Orlando FL 32816

Synopsis The implementation of high average power Yb-based lasers for attosecond science requires the development of efficient techniques for nonlinear post-compression to few optical cycles. Here, we show how the delayed rotational nonlinearity of linear molecular gases can enhance the nonlinear phase shift accumulated by pulses with long input duration. We demonstrate the generation of sub-two-cycle pules using an N_2O-filled hollow-core fiber compressor and investigate the thermal effects that will need to be overcome in order to scale this technique to high-average powers.

RP

The temporal compression of laser pulses, and their conversion into extreme ultraviolet and x-ray wavelengths through the process of high-order harmonic generation (HHG), has enabled measurement and control of ultrafast processes down to attosecond timescales. Compression to few-cycle durations is now becoming routine for Ti:sapphire laser amplifiers outputting mJ-level pulses with durations below ten cycles. However, reliance on mJ-level Ti:sapphire lasers can limit repetition rates to the few kHz regime, restricting their application to time-resolved spectroscopies that demand high data acquisition rates. Toward this end, nonlinear compression of Yb-doped laser systems, for which small quantum defect allows for high average powers, has garnered considerable attention. However, the narrower gain-bandwidths of Yb-doped crystals results in pulses hundreds of femtoseconds in duration, making their implementation as few-cycle drivers for attosecond science still a challenging task.

Here, we show how the delayed rotational nonlinearity of linear molecular gases can significantly enhance the nonlinear phase shift accumulated by pulses with long input durations, resulting in the generation of multi-octave supercontinua [1] (Fig 1). We employ a Yb:KGW laser amplifier outputting pulses 280 fs in duration with an energy of 400 μJ to demonstrate post-compression to below two optical cycles (< 6 fs) using a 3.5-m-long N_2O-filled hollow-core fiber and chirped mirrors. The complex phase associated with the Raman-enhanced supercontinuum is analyzed through complementary pulse characterizations using a second harmonic-based frequency resolved optical gating device and with a field sampling technique based on tunneling in a solid [2]. The fidelity of the compressed pulses is demonstrated by driving HHG in argon, where the observation of a supercontinuum structure provides evidence for the temporal confinement of the XUV emission.

Additionally, we investigate changes in the spectral broadening that arise at high input average powers associated with repetitive laser interactions [3]. We track the change of the supercontinuum spectrum and estimate the gas temperature as a function of pulse number using a density matrix formalism to simulate the effects of nonequilibrium rotational state distributions in a high-temperature gas. These measurements illustrate how the thermal excitation of the gas medium must be overcome in order to efficiently harness the delayed nonlinearity of molecular gases for compression of high-repetition-rate sources.

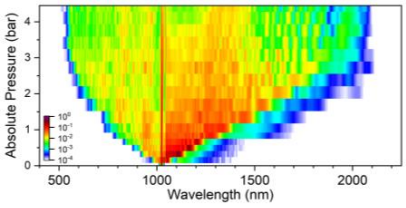


Figure 1. Pressure-dependent spectrum obtained after propagating in N_2O-filled hollow-core fiber

References

[1] Beetar J E *et al* 2020 *Sci Adv* **6** eabb5375
[2] Liu Y *et al* 2021 *Photon. Res.* **9** 929
[3] Beetar J E *et al* 2021 *Opt Lett* **46** 2437

* E-mail: michael.chini@ucf.edu

Spectrally tuneable ultrashort monochromatized extreme ultraviolet pulses at 100 kHz

T Csizmadia[1]*, Z Filus[1], T Grósz[1], P Ye[1,†], L Gulyás Oldal[1], M De Marco[1], P Jójárt[1], I Seres[1], Zs Bengery[1], B Gilicze[1], M Lucchini[2,3], M Nisoli[2,3], F Frassetto[4], F Samparisi[4], L Poletto[4], K Varjú[1,5], S Kahaly[1,6], and B Major[1]

[1]ELI ALPS, ELI-HU Non-Profit Ltd., Szeged, H-6728, Hungary
[2]Institute for Photonics and Nanotechnologies, IFN-CNR, Milano, 20133, Italy
[3]Department of Physics, Politecnico di Milano, Milano, 20133, Italy
[4]Institute for Photonics and Nanotechnologies, IFN-CNR, Padova, 35131, Italy
[5]Department of Optics and Quantum Electronics, University of Szeged, Szeged, H-6720, Hungary
[6]Institute of Physics, University of Szeged, Szeged, H-6720, Hungary

Synopsis We generated spectrally tuneable ultrashort quasi-monochromatic extreme ultraviolet (XUV) pulses with 100 kHz repetition rate at a user-oriented beamline (*HR GHHG Condensed*) of the Extreme Light Infrastructure - Attosecond Light Pulse Source (ELI ALPS). The beamline is equipped with an asymmetric, double-grating, time-preserving monochromator. The monochromatic high harmonic (HH) source is characterized in terms of imaging properties, transmission efficiency, overall photon flux, spectral characteristics and temporal response.

RP

This work reveals the latest progress and experimental capabilities of a user-oriented XUV beamline based on high harmonic generation (HHG) extended with compensated (TDC) monochro The monochromatization with u sponse [1] has been realized in metric arrangement of the two c of the TDC design. Such config suited for tabletop high avera beamlines employing an annula ometry [2], because it simultar long first stage input arm for f residual generating field from t tion [3], and — with a shorter s sor stage — tight focusing condit target region, as well as reduced laboratory space.

The current driving laser is system at ELI ALPS, deliveri to 6 fs duration (present experi formed with ≈ 40 fs pulses) at a r 100 kHz and with pulse energies

The detailed characterizatio ated HH radiation shows mono pulses down to 100 meV spec that can be focused to a 70 µn width at half maximum) in the target region [5]. The temporal duration of the pulses was estimated between 13 and 27 fs that are coherent with the measured duration of the driving laser pulses. Significantly longer pulse durations

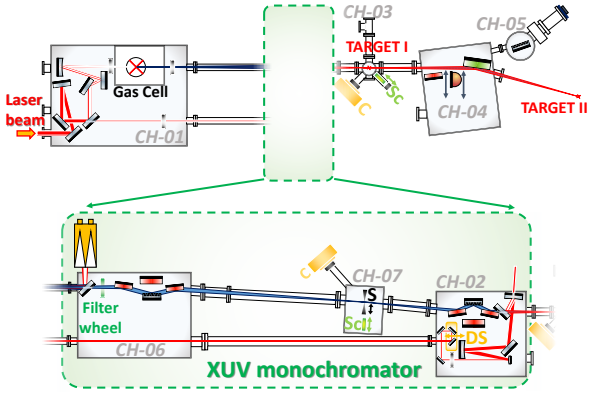


Figure 1. Schematics of the *HR GHHG Condensed* beamline with the XUV monochromator (enclosed with a dashed green line). C: camera; S: slit; Sc: scintillator; DS: delay stage.

References

[1] Poletto L, and Frassetto F 2018 *Appl. Sci.* **8, 5**
[2] Ye P *et al* 2020 *J. Phys. B* **53**, 154004
[3] Ye P *et al* 2022 *Ultrafast Science*, in press
[4] Shestaev E *et al* 2020 *Opt. Lett.* **45 6350**
[5] Csizmadia T *et al* 2022, in preparation

*E-mail: tamas.csizmadia@eli-alps.hu
†Current address: Université Paris-Saclay, CEA, CNRS, LIDYL, Gif-sur-Yvette, 91191, France

Ultrafast dynamics in large molecular ions following XUV ionization

A Boyer[1]*, M Hervé[1], R Brédy[1], I Compagnon[1] and F Lépine[1]

[1] Univ Lyon, Université Claude Bernard Lyon 1, CNRS, Institut Lumière Matière, Villeurbanne, F-69622, France

Synopsis We present experiments using a new instrument combining XUV High Harmonic Generation source with electrospray ionization methods. This offers new opportunities to study dynamics induced by an ultrashort XUV pulse excitation in very large molecular ions. First time-resolved measurements in molecular ions are discussed. This demonstrates the possibility to extend ultrafast XUV and attosecond science to other research field such as biochemistry where polypeptides and entire proteins are studied.

RP

The development of attosecond technologies has brought new tools to study in real time electron and nuclear dynamics in atoms and molecules. Since the first experiments performed on atoms, the domain has significantly evolved in terms of sophistications of available methods to study small systems, allowing to investigate complex effects such as hole migration or electron scattering [1]. More recently, the complexity of the studied systems has also been increased to larger molecules, addressing new questions such as the role of electron correlation [2,3]. However, all these experiments were performed on neutral molecules while the majority of molecules carry a charge in their natural environment. Since the charge modifies the electronic landscape of the molecule and their properties, there is real need to extend the attosecond technologies to molecular ions. Moreover, the current technics are limited to the investigation of "model" systems with a relatively small number of atoms.

In this context, we have developed a new experimental set-up combing XUV-IR pump-probe scheme with electrospray sources (ESI) and mass spectrometer. In this experiment the density of molecules interacting with the laser pulses is very low and the High Harmonic Generation source and the entire experiment has to be optimized to overcome this experimental challenge.

Using this set-up, we were able to observe ultrafast dynamics of few tens of femtoseconds following the XUV photoionization of a large protonated molecule. Showing the importance of charge and energy dynamics on ultrashort timescale even in complex systems. Since electrospray sources offer the possibility to study large molecules without size restrictions, we also studied molecular ions as large as proteins. In Fig.1.a) the example of Cytochrome C (CytC) is presented. CytC is composed by more than hundred amino acids. Fig.1.b) presents the measured ions corresponding to the interaction of CytC carrying 15 protons with the ultrashort XUV pulses (purple line). These masses correspond to the ionization and subsequent dissociation of the multiply-charged protein.

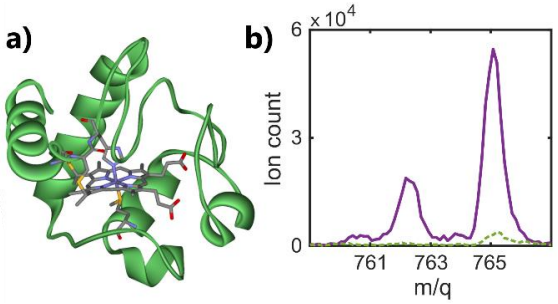


Figure 1. a) Schematic representation of CytC. **b)** Zoom of mass spectra of CytC obtained by collision (dashed green line) or after interacting with the XUV pulses (purple line).

Our results open new perspectives for the development of attochemistry in complex molecular systems.

References

[1] Nisoli M *et al* 2017 *Chem. Rev.* **117** 10760-10825
[2] Hervé M *et al* 2021 *Nature Physics* **17** 327-331
[3] Calegari F *et al* 2014 *Science* **346** 336-339

* E-mail: alexie.boyer@univ-lyon1.fr

Guiding of Laser Pulses at the Theoretical Limit – 97% Throughput Hollow-Core Fibers – with subsequent compression to 1.3 cycles

Y Jeong[1], A Labranche[2], R Piccoli[1], A Rovere[1], L Zanotto[1], G Tempea[2], D Wilson[1,2], M Ivanov[1,2], A Ramirez[2], R Morandotti[1,3], F Légaré[1], L Razzari[1] and B Schmidt[2] *

[1]Institut national de la recherche scientifique, Varennes, J3X 1P7, Canada
[2]few-cycle Inc, Varennes, J3X 1P7, Canada

Synopsis We demonstrate Yb laser (170fs) propagation in large a core hollow-core fiber (HCF) with 97.4% transmission. It serves as a pre-compression stage to achieve 1.3 cycle pulses in a second step with 70% overall efficiency.

We present pulse compression of Yb laser achieved a commercial Yb:KGW regenerative amplifier (Pharos, Light Conversion) delivering 1 mJ, 175 fs pulses at 1 to 6 kHz. This beam is precisely matched to the fundamental mode of a large core HCF (few-cycle Inc.) of 1 mm inner diameter.

The HCF was first set up at lower power and without vacuum enclosure. The transmission for a 0.5-m-long fiber was measured to be as high as 97.4%. Remarkably, these values are virtually equal to the analytically calculated 97.6%. This value is obtained multiplying the overlap integral of a Gaussian input beam and the fiber fundamental mode (98%) [1] by the power propagation loss over 1 m (99.6%) [2]. Including vacuum beam routing for compactness and at an Ar operation pressure of 3.2 bar the transmission dropped to 95%. Subsequent compression with chirp mirrors (few-cycle Inc.) yielded 25fs pulses (fig. 1a) with very good spatio-spectral homogeneity with 92% total efficiency after this first stage, an energy stability of 0.6% RMS and an M2 parameter of about 1.05.

These pulses were further compressed in a more conventional fiber of 500um ID with 1m length and a different set of chirp mirrors that support single cycle compression. The Gaussian fit of the autocorrelation in fig. 1d shows a FWHM of 4.5fs which corresponds to 1.3 optical cycles at 1030nm center wavelength. The overall efficiency for this two stage, close to 40-fold pulse compression down to the single cycle regime is 70%.

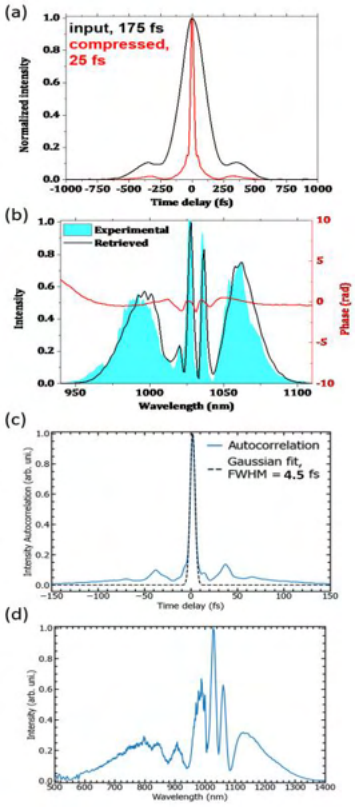


Figure 1. (a) autocorrelation of input, 175 fs, and compressed, 25 fs, pulses after the first compression stage; (b) spectrum and phase of the 25 fs pulse after the first compression stage; (c) autocorrelation of compressed, 4.5 fs, pulse after the second compression stage; (d) spectrum of the 4.5 fs pulse after the second compression stage.

References

[1] Nisoli M *et al* 1998 *IEEE JSTQE* **4**, 414
[2] Marcatili E *et al* 1964 Bell System Technical Journal 43, 1783

* E-mail: schmidt@few-cycle.com

Dual-Crystal Setup for 2 µm, sub-3-cycle Pulse Amplification in OPCPA Pumped by High Energy Nd:YAG lasers

R Budriūnas[1,2] *, V Girdauskas[1], T Stanislauskas[1]

[1]Light Conversion, Vilnius, LT-10233, Lithuania
[2]Vilnius University Laser Research Center, Vilnius, LT-10223, Lithuania

Synopsis We present a scheme for amplifying broadband pulses at 2 µm with picosecond Nd:YAG lasers. The scheme involves using different nonlinear crystals in sequence to amplify adjacent wavelength regions with thick crystals and pump intensities that can be safely used with 30 ps pump pulses. As a proof-of-concept, amplification of pulses with bandwidth supporting <3 optical cycles to 300 µJ is demonstrated with 3.6 mJ, 30 ps pump pulses. Further scaling towards 10 mJ pulse energy is underway.

RP

High power, few-cycle pulse sources at 2 µm are receiving a lot of interest because of the enticing possibility of high harmonic generation in the water window. Recently, several record-breaking 2 µm optical parametric chirped pulse amplification (OPCPA) systems based on high power Yb:YAG pump lasers were demonstrated [1-3]. Conversely, Nd:YAG lasers are widely used in high-energy OPCPA [4,5], but their pulse durations (tens of ps) limit intensity applicable on nonlinear crystals to ~10 GW/cm^2, requiring thick crystals and reducing amplification bandwidth in typical 2 µm OPCPA setups based on degenerate Type-I phase matching. We overcome this limitation by designing gain stages with two crystals selected to amplify different wavelength ranges.

Our OPCPA setup is depicted schematically in Fig. 1(a). A femtosecond Yb:KGW laser system (Pharos, Light Conversion) is used to pump a parametric amplifier that produces ultrabroadband, CEP-stabilized pulses tunable through 1.7-3 µm, tuned to 2 µm for this case, where 50 µJ pulse energy is achieved. The seed pulses are sent to a bulk material stretcher and an acousto-optic filter for spectral phase control. Stretched seed pulses are amplified in multiple amplification stages based on a sequence of KTA and MgO:LN crystals, pumped by a multi-beam Nd:YAG laser (Ekspla) delivering total 105 mJ energy in 3 beams. Amplified pulses will be compressed in bulk fused silica.

Here we present results from the first amplification stage using 3.6 mJ pump energy. Fig. 1(b) shows how MgO:LN (Type-I, 6 mm thick) and KTA (Type-II, 6 mm thick) crystals amplifying different adjacent spectral bands, maintaining sub-20fs bandwidth. Fig. 1(c) shows the variation of amplified signal energy with pump energy. With 3.6 mJ pump energy (intensity 15 GW/cm^2), signal is amplified to 294 µJ (8% efficiency) without saturation.

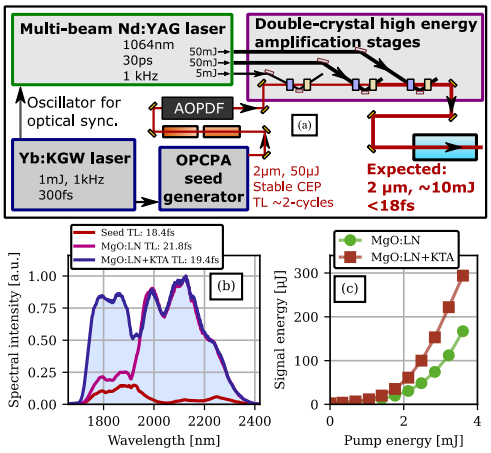


Figure 1. (a) OPCPA setup (AOPDF: acousto-optic programmable dispersive filter) (b) Spectra of pulses amplified in the first amplification stage at 3.6 mJ pump energy. Legend indicates transform limited pulse durations (c) Signal energy as a function of pump energy

With current Nd:YAG lasers, the scheme could be readily scaled to produce multi-TW 2 µm pulses at kHz repetition rate, enabling high-energy water window high harmonic generation.

High energy amplification and pulse compression will be presented at the conference.

References

[1] Pupeikis J *et al* 2020 *Optica* **7** 168
[2] Feng T *et al* 2020 *Opt. Express* **28** 8724
[3] Neuhaus M *et al* 2018 *Opt. Express* **26** 16074
[4] Rivas D E *et al* 2017 Sci. Rep. **7** 5224
[5] Budriūnas R *et al* 2017 Opt. Express **25** 5797

* E-mail: rimantas.budriunas@lightcon.com

High-flux, 100-kHz, user-oriented attosecond beamline driven by a high-average-power annular laser beam

P Ye[1,*], L Gulyás Oldal[1], T Csizmadia[1], Z Filus[1], T Grósz[1], M De Marco[1], P Jójárt[1], I Seres[1], Z Bengery[1], B Gilicze[1], K Varjú[1,2], S Kahaly[1] and B Major[1,2,†]

[1]ELI ALPS, ELI-HU Non-Profit Ltd., Szeged, H-6728, Hungary
[2]Department of Optics and Quantum Electronics, University of Szeged, Szeged, H-6720, Hungary

Synopsis We present the status of the HR GHHG beamline of the ELI ALPS user facility, a high-flux, 100-kHz attosecond source providing extreme-ultraviolet – infrared pump-probe capabilities. To remove the residual high-average-power driving laser after generation, we shape the driving laser beam to be annular. The infrared probe beam is also reshaped to be annular, thus it can be combined with the high-harmonics with low loss. We also provide a detailed discussion on the effect of nonlinear propagation in the generation medium on the concept of high-harmonic generation with annular beams.

RP

We obtained a high attosecond pulse train energy (~50 pJ/shot on target) with our 100-kHz, user-oriented attosecond beamline at the Extreme Light Infrastructure Attosecond Light Pulse Source (ELI ALPS) [1]. This was achieved by forming the driving laser beam to an annular shape, by utilizing a uniquely designed high-harmonic generation (HHG) gas cell [2], and by performing an extensive parametric optimization of generation conditions. The use of the annular beam allows us to handle high-average-power laser beams in a more efficient way [3], reducing the requirements of filtering the generating infrared (IR) from the collinear extreme-ultraviolet (XUV) beam. This results in a 19% transmission of the generated XUV to target [1]. We demonstrate and describe in details, the advantages of building an HHG beamline with XUV-IR capabilities by using an annular-central splitting of the laser beam. .

Specifically, in this presentation we focus on aspects of the traditional concept of HHG using annular driving beams [4], which – to our knowledge – has not been studied so far in systems using high-average-power lasers. We show ─ using simulations and experiments ─ that modifications of the laser field due to the ionized medium has a minimal effect on the far-field properties of the IR field after generation in our experimental conditions (see Fig. 1). At the same time, there is an additional aspect of similar relevance: the beam profile is slightly changed due to diffraction effects on the gas target aperture [1]. In our analysis, both effects are considered and proved to have a manageable contribution to beam reshaping.

In parallel, we show that the IR probe beam is also reshaped to an annular form and, with smart positioning of a holey recombination mirror, the XUV and the IR probe beam can be recombined with minimal losses.

In summary, we demonstrated the performance and the pump-probe ability of the high-repetition-rate laser based gas HHG beamline for gas targets (HR GHHG Gas) of ELI ALPS.

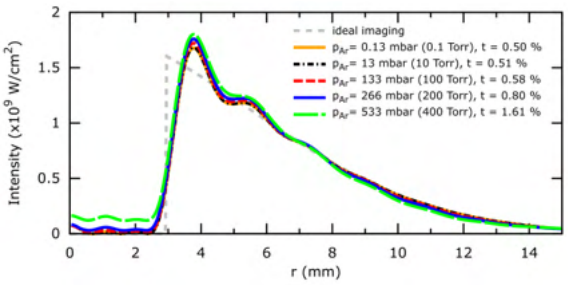


Figure 1. Simulated far-field beam profile of the driving annular laser beam after the generation at different pressures of argon gas (p_{Ar}). The 'ideal imaging' case stands for a fully undisturbed propagation, i.e. a perfect imaging of the beam at the holey splitting mirror. The transmission (t) shows the ratio of the energy passing through the center of a holey mirror with respect to input beam energy.

References

[1] Ye P *et al* 2022 *Ultrafast Science*, in press.
[2] Filus Z *et al* 2022, in preparation
[3] Klas R *et al* 2018 *Opt. Express* **26** 19318
[4] Peatross J *et al* 1994 *Opt. Lett.* **19** 942

* Current address: LIDYL, CEA, CNRS, Université Paris-Saclay, CEA Saclay 91191, Gif-sur-Yvette, France
† E-mail: balazs.major@eli-alps.hu

Electric-field sampling at near-petahertz frequencies and megahertz repetition rates

A Srivastava[1,2], A Herbst[1,2], D Schade[1,2], M M Bidhendi[1,2], M Kieker[1,2], F Tani[1], and H Fattahi[1, 2,*]

[1]Max Planck Institute for the Science of Light, Erlangen, Staudstrasse 2, 91058, Germany
[2]Friedrich-Alexander University, Erlangen, Staudstrasse 7, 91058, Germany

Synopsis We report on efficient external pulse compression of 255 fs, 20 µJ, 1 MHz pulses of a Yb:YAG amplifier to 4.7 fs in a two-stage gas-filled photonic crystal fiber. 80% of the energy of the nearly single-cycle pulses was down-converted to octave-spanning pulses at 2 µm via intra-pulse difference frequency generation. The remaining 20% of the energy was used to sample the electric field of the carrier-envelope-phase stable pulses at 2 µm in ambient air. To the best of our knowledge, this is the first megahertz frontend for near-petahertz field-sampling in ambient air. This system is ideal for broadband field-resolved NIR spectroscopy.

RP

Near-infrared (NIR) spectroscopy is a powerful tool for acquiring information on molecular composition and concentration. However, broadband frequency-domain measurements in this spectral region have been limited in detection sensitivity and dynamic range. Direct detection of the electric field of the molecular response in the time domain holds promise to mitigate these shortcomings. Here, an ultrashort, phase-coherent pulse excites the molecules at their resonance frequencies, while a second ultrashort pulse is used to resolve the transmitted electric field with, the molecular response imprinted.

Such measurement requires the centre frequency of the two pulses to be at least separated by one octave. In this abstract, we report on the development of a laser system that fullfills this requirements and demonstrates the first ambient-air, electric field sampling at near petahertz frequencies and megahertz repetition rates.

20 µJ, 255 fs, 1 MHz pulses of a Yb:YAG amplifier (CARBIDE-Light Conversion) were compressed in a cascaded system of gas-filled single-ring photonic crystal fibers, consisting of eight thin-walled capillaries surrounding a hollow core. In the first nonlinear stage, the input pulses are spectrally broadened based on self-phase-modulation and compressed to 26 fs at full width at half maximum (FWHM) in a chirped-mirror compressor. The second nonlinear stage is designed for soliton-effect self-compression to near single-cycle pulses. Additional chirped mirrors are used to pre-compensate for the beam path's induced dispersion and to recompress the pulses to 4.7 fs (FWHM).

80% of the energy of the 4.7 fs pulses is down-converted to short wavelength infrared (SWIR) in a 1 mm thick BiBO crystal. The generated octave-spanning spectrum is centered at 2 µm. The remaining 20% of the energy is used as a probe in a nonlinear electro-optic sampling setup [1-3]. Fig.1 shows the field-resolved detection of the SWIR pulses in ambient air. The detection bandwidth covers the entire molecular combination band and overtone excitations, and is ideal for broadband field-resolved NIR spectroscopy.

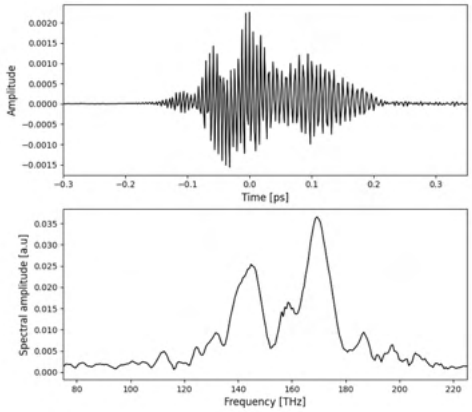


Figure 1. The sampled electric field (top) and its corresponding spectrum (bottom).

References

[1] Alismail A et al 2020 Science Advances, **6**
[2] Keiber S et al 2016 Nature Photonics **10**, 159
[3] Bidhendi M.M, *Master Thesis*, Friedrich-Alexander University, March (2021)

* E-mail: hanieh.fattahi@mpl.mpg.de

User Facility for Attosecond Soft x-rays and THz at University of Central Florida

B Rodriguez[1], M Chini[1], T C Truong[1], M Vaida[1], Z Chang[1,2], L Fang[1*]

[1]Department of Physics, University of Central Florida, Orlando, Florida 32816
[2]CREOL, University of Central Florida, Orlando, Florida 32816

Synopsis A User Facility for Attosecond Soft x-rays and Terahertz (UFAST) is being designed and will be constructed at University of Central Florida. The facility will provide a variety of light sources, from <2-cycle femtosecond laser pulses at 2 μm central wavelength, isolated attosecond XUV/X-ray pulses, to few-cycle infrared laser pulses and single-cycle terahertz light. UFAST will be equipped with endstations of reaction microscope for ion-electron measurement, reflective transient absorption spectroscopy, high harmonic generation from solids, and time-angle-resolved photoemission spectroscopy. UFAST is expected to become in operation in 2023. We will present the light source parameters and the instrumental capabilities and discuss future opportunities for users.

RP

The User Facility for Attosecond Soft x-rays and Terahertz (UFAST) is located on University of Central Florida campus. The goal of UFAST to provide an instrumental platform for time-resolved investigations of charged particle dynamics during or induced by photointeractions, as well as applications of ultrafast technology in laser machining and ultrafast spectroscopy in planetary science [1].

The facility delivers a variety of light sources with wavelength spanning from soft x-rays, XUV, long-wave infrared (LWIR), to terahertz (THz) and pulse durations in the femto-atto-second range. The consortium of these light sources provides a versatile tool for in-depth understanding of photo-induced phenomena at the atomic spatial level and the natural timescale of electron and ion motion. Particularly, the generation of several-tens of attosecond pulses in the water-window range (250eV – 530eV) is a unique capability for electron dynamics studies with atomic site specificity and attosecond temporal resolution. Figure 1 shows the overall layout of the instruments at UFAST.

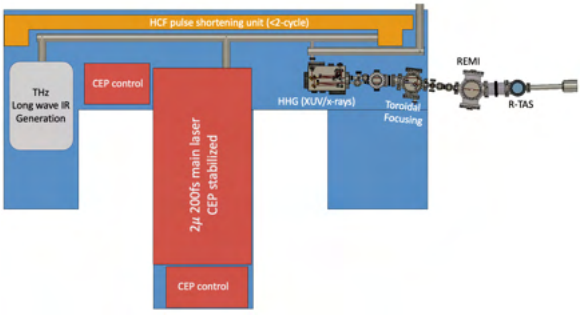


Figure 1. Instrument layout of UFAST, including base laser, secondary light sources and endstations. HHG: high harmonic generation. CEP: carrier envelope phase. REMI: reaction microscope. R-TAS: reflective transient absorption spectrometer. (tr-ARPES is not shown.)

The base laser is comprised of a thulium-doped fiber amplifier and a hollow-core-fiber (HCF) pulse sharenting unit. The thulium fiber laser delivers pulses of 2μm central wavelength, ~200fs duration, and 2mJ pulse energy at a repetition rate of 100 kHz (200W average power). The HCF unit shortens the 200fs pulses from the Tm-fiber laser to 14 fs (aiming at ~12 fs) with a through put of >45%. The final output of the base laser is, at the best effort, <2 cycle pulse duration, 120W average power at 100 kHz. This system is carrier envelope phase stabilized.

This base laser will be used to drive multiple secondary light sources, including (1) an XUV/x-ray light source that delivers isolated XUV/x-ray attosecond pulses generated via high harmonic generation (HHG); (2) a LWIR source based on frequency differencing; and (3) THz source generated from plasma interaction.

UFAST will be equipped with a reaction microscope and a reflective transient absorption spectrometer, which are adapted to the attosecond beamline; and a time-resolved angle-resolved photoemission spectrometer (tr-ARPES) and a setup for HHG-from-solids, to which the base laser beam will be sent. The 200 fs laser pulses and THz pulses will be used for laser machining and planetary science applications.

Grant: NSF 2117826.

References

[1] Kraus, P M *et al* 2018 *Nature Reviews Chemistry.* **2** 82-94

* E-mail: li.fang@ucf.edu

CEP-stable infrared OPCPA sources

Y Pertot[1]*, N Thiré[1], R Maksimenka[1], S Bux[1], G Gitzinger[1], J Villanueva[1], T Pinoteau[1] and N Forget[1]

1. Fastlite, 165 rue des cistes, pôle euro 95, Bât D, 06600 Antibes, France

Synopsis: We review several schemes to generate CEP-stabilized pulses based on a single supercontinuum generation followed by a difference frequency generation process, and their impact on CEP stability performances out of OPCPA systems.

RP

Because of the intrinsically low conversion efficiency of nonlinear processes, parametric sources were essentially limited by the available energy/power of the so-called "pump" lasers. The advent of kW-class picosecond Ytterbium lasers delivering multi-mJ pulses at high repetition rate (10-100 kHz) has removed the long-lasting power bottleneck of ultrashort optical parametric amplifiers (OPAs) and opened the path to a large set of applications, among which are the generation of few-cycle optical pulses, high-flux mid- and far-infrared pulses, intense THz fields but also X-UV and soft X-Rays secondary sources through high-harmonic generation [1,2].

One of the key parameters of such sources is their ability to provide control of the carrier envelope phase (CEP). Usually, the latter is achieved by the generation of a passively stable CEP pulse, through a difference frequency generation process, with an active correction loop. However, depending on the central wavelength of the source, different schemes have to be used in order to generate a CEP stable seed, thus creating strong performance variations in terms of CEP stability.

We review the different generation schemes developed at Fastlite, all based on a single supercontinuum generation followed by a difference frequency generation process, and their consequences on the CEP stability through the presentation of several OPCPA systems. This scheme has the great advantage to be implemented with the same pump laser than the amplification stages. The supercontinuum generation step is based on filamentation in a bulk dielectric medium.

It is important to identify how this highly non-linear process affects the determinism of the generated wave phase, and how this "loss" of determinism is distributed over the bandwidth. Pump energy distribution and its impact on the CEP is also investigated, as shown in figure 1.

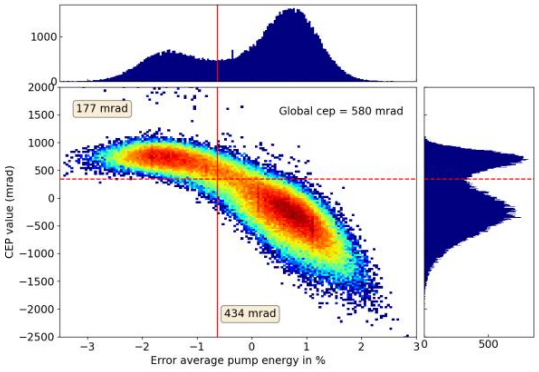


Figure 1: Correlation map between pump laser energy and output CEP measured by the mean of a f to 2f setup. Up and right plots shows the histogram distribution.

References:

[1] T. Popmintchev et al.,"Bright coherent ultrahigh harmonics in the keV X-ray regime from mid-infrared femtosecond lasers", Science 336, 1287-1291 (2012).
[2] H.Fattahi et al., "Third-generation femtosecond technology," Optica 1, 45-63 (2014)

* E-mail: yoann.pertot@fastlite.com

Experiments with upgraded XUV source at ELI Beamlines facility

O Hort[1,*], M Jurkovič[1,2], O Finke[1,2], M Albrecht[1,2], J Vábek[1,2,3], and J Nejdl[1,2]

[1]ELI Beamlines Centre, Institute of Physics of the Czech Academy of Sciences, Na Slovance 2, 182 21 Prague, Czechia
[2]Faculty of Nuclear Sciences and Physical Engineering CTU, Břehová 7, 115 19 Prague 1, Czechia
[3]Centre des Lasers Intenses et Applications, Université de Bordeaux-CNRS-CEA, 33405 Talence Cedex, France

Synopsis We report on our pursuit for a more versatile and powerful high harmonic generation (HHG) based XUV source. Using high-energy laser pulses require a long generating medium resulting in issues with nonlinear propagation effects. Furthermore, applications of narrowband XUV radiation require monochromatization that alters the XUV wavefront significantly. We present novel approaches to tackle these issues with shaping the driver laser pulses and the generation medium; as well as new capabilities of the HHG beamlines that are of interest to users.

High harmonic generation (HHG) in gases is a well-established process to reliably produce ultrashort XUV pulses [1]. These pulses have many applications, such as revealing ultrafast atomic and molecular dynamics. The challenge lies in achieving a high XUV photon number and the spectral content matching a target's energetic structure for efficient interaction.

The HHG nowadays benefit from high power OPCPA laser drivers, such as the L1 laser at ELI Beamlines that delivers pulses of 50 mJ, 15 fs at 1 kHz. To exploit the potential of such a laser, one has to adhere to scaling laws [2] that result in a low pressure long generating medium. Seeking a high XUV signal with such kind of gas target leads inevitably to nonlinear effects during the laser pulse propagation.

When an intense laser pulse enters a long gaseous medium, an intensity clamping manifests as a significant intensity drop to a level not high enough to ionize the medium to efficiently generate the HHG. We numerically show that this behaviour is linked to self-focusing, and it is a general mechanism of the intense pulse interaction with a long medium.

To crack this fundamental problem, we preionize the medium to a few percents, reaching optimal phase matching. Experimentally, we use a capillary discharge to preionize a rare gas and reach a 5 fold XUV signal enhancement.

Another challenge is to match the generated XUV lines to target energetic levels and the generation of a single harmonic line for certain applications. Driving pulses chirping and sophisticated methods were employed to tune the XUV frequency, and grating monochromators are typically used to select a single harmonic.

We propose to conveniently produce tunable single harmonic frequency via control between the driving laser and second harmonic generation. We demonstrate the tunability of 2 eV of harmonic 7. By adapting the generating medium length, we can suppress higher harmonics than 7^{th}, and the 5^{th} harmonic is cut away by a state-of-the-art aluminium filter. This way, we obtained only an XUV line of the 7^{th} harmonic.

The HHG beamline is also open for external users. As the spatio-temporal coupling of the XUV pulses is currently a hot topic [3], the HHG beamline was upgraded to fit the needs of a very short HHG medium in different geometries. An Even-Lavie supersonic valve was installed and is easily swappable with a variable-length motorized gas cell. We also included the focusing length of 2 m, which can be easily changed to 5 m geometry and a 14.5 m mirror will be installed during upcoming months.

In conclusion, we have upgraded the HHG beamline with new HHG geometry and demonstrated an XUV signal enhancement with a controlled pre-ionized medium. We also developed an XUV source of a single harmonic line tunable over 2 eV bandwidth.

References

[1] Paul P M *et al* 2001 *Science* **292** 3
[2] Heyl C M *et al* 2016 *Optica* 3 75-81
[3] Wikmark H *et al* 2019 *PNAS* 116 11

* E-mail: Ondrej.Hort@eli-beams.eu

RP

Focusing properties of high-order harmonics

M Plach[1]*, M Hoflund[1], J Peschel[1], H Dacasa[1], K Veyrinas[2], E Constant[3], H Wikmark[1], Sylvain Maclot[1], C Guo[1], C Arnold[1], A L'Huillier[1] and P Eng-Johnsson[1]

[1] Department of Physics, Lund University, P.O. Box 118, SE-22100 Lund, Sweden
[2] Université de Bordeaux , CNRS, CEA, Centre Laser Intenses et Applications (CELIA), 43 Rue P. Noailles, 33400 Talence, France
[3] Univ Lyon, Univ Claude Bernard Lyon 1, CNRS, Institut Lumière Matière, F-69622 Villeurbanne, France

Synopsis We generate high-order harmonics in argon, and refocus them to few microns spots. A knife-edge measurement technique shows that the harmonic foci longitudinal positions vary strongly with the harmonic order but can be minimized by controlling the generation position.

RP

The investigation of ultrafast electron dynamics using nonlinear extreme ultraviolet (XUV)-pump XUV-probe spectroscopy requires light sources with high flux and high intensity. High-order harmonic generation (HHG) can provide this, but tight spatial focusing is needed. Hereby, the longitudinal overlap of harmonic foci is critical [1, 2]. We present experimental and simulated results on the focusing properties of harmonics in the spectral range between 17-45 eV for different generation conditions [3].

A terawatt laser system delivers 40 fs pulses with 45 mJ pulse energy at 806 nm at a repetition rate of 10 Hz. The infrared (IR) beam is wavefront corrected by a deformable mirror (DM). The DM allows us to add a curvature to the beam, changing the IR focus position relative to the pulsed Ar gas cell used for HHG. After propagation and IR-filtering, the XUV is refocused to a few micrometers focal spot by two toroidal mirrors in a Wolter configuration, with a high demagnification factor. A knife-edge is inserted into the beam at different positions along the propagation axis close to the geometrical focus. From this measurement, we determine the focal spot size and longitudinal position for each harmonic and compare the results with simulations (Fig. 1). We show that the focusing properties depend on the harmonic order and the position of the IR focus relative to the gas cell. We conclude that, even when the total HHG yield is rather constant, the spatial and temporal profiles and thereby the XUV intensity change strongly with the generation conditions.

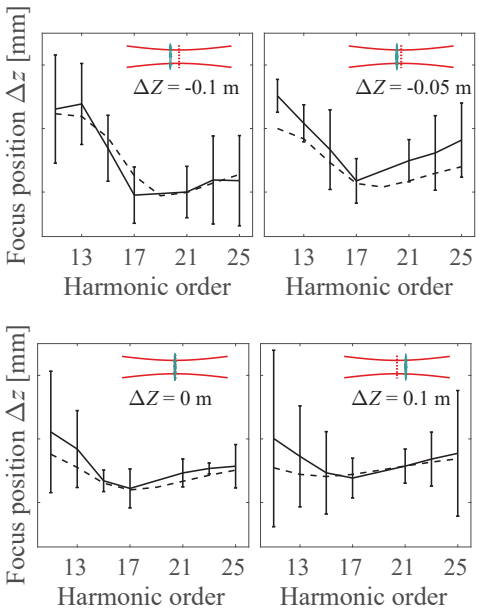


Figure 1. Measured (solid line) and simulated (dashed line) focus position of harmonic orders 11-25 at different generation position ΔZ relative to the IR focus. The subfigure indicates the IR focus position (vertical dashed line) with respect to the generation medium position (vertical solid line).

References

[1] L Quintard, Science Advances 5, 2019 (2019)
[2] H Wikmark, Proceedings of the National Academy of Sciences 2019, 116, 4779-4787 (2019)
[3] M Hoflund, Ultrafast Science, 9797453, 2021 (2021)

*E-mail: Marius.Plach@fysik.lth.se

Construction of a Femtosecond Field Synthesizer

J Turner[1] * , A Pettipher[1], H. Allegre[1], M Matthews[1], J WG Tisch[1]

[1]Imperial College London, London, SW7 2BX

Synopsis High-harmonic generation (HHG) is a path to the generation of isolated extreme ultraviolet (XUV) attosecond pulses. The cut-off energy and harmonic flux of XUV photons generated by the HHG process can be enhanced through the use of sub-cycle shaping that optimizes the recollision energy and trajectory of the elctron wavepacket in the continuum. A 'perfect' waveform can be approximated through the coherent combination of three laser fields of different colours. We present a femtosecond field synthesizer, currently under construction, that temporally and spatially combines 400, 800 and 1350 nm optical pulses.

RP

High Harmonic Generation (HHG) is the primary table-top optical process allowing access to isolated attosecond (as, 10^{-18} sec) pulses and coherent photon sources in the extreme ultraviolet (XUV) spectral region. The use of attosecond XUV pulses as an imaging tool (for example, to probe molecular dynamics) is greatly enhanced by increasing the electron recombination energy [1].

The production of high-energy, high-flux XUV photons is a challenge as the HHG scaling law predicts a falling off of the harmonic flux with approximately λ^{-6} [2]. Furthermore, an increase in the driving field intensity has a limited effect due to the saturating effect of ionization of the gas target. Shaping the driving field is, therefore, an effective way to enhance both the harmonic yield and energy of the generated photons by controlling the dynamics of ionized electrons before recombination with the parent ion**.**

L Chipperfield et. al. [3] have shown the 'perfect' waveform for the efficient driving and recollision of freed electrons in the HHG process. This waveform optimizes the ionization, displacement from the core and returning kinetic energy of the ionized electron, all of which have a bearing on the resultant harmonic yield and cut-off energy of XUV photons. The photons produced are calculated to potentially have a kinetic energy over 3 times larger than those produced by a monochromatic driving wave [1]. A close approximation of the perfect waveform is achievable using a driving field comprising of three commensurate wavelength contributions from the same laser source.

A femtosecond (fs) field synthesizer (FFS), capable of approximating this waveform is under construction at Imperial College that combines three fields: 400 nm, 800 nm and a short-wave infrared (SWIR) component at 1300 nm. All of these colours are seeded by a Ti:Sapphire chirped-pulse amplification system. A few-cycle pulse of 4 femtoseconds is generated in one of the arms by spectral broadening in a home-built, differentially-pumped hollow-core fibre before temporal compression by a set of chirped mirrors. The remainder of the amplifier pulse energy is sent to a commercial optical parametric amplifier system which is tunable in the range 1200-2100nm. The residual pump passing out of the TOPAS is frequency doubled in a BBO crystal, producing a 400 nm field. A schematic of the experimental set-up is shown in Fig. 1.

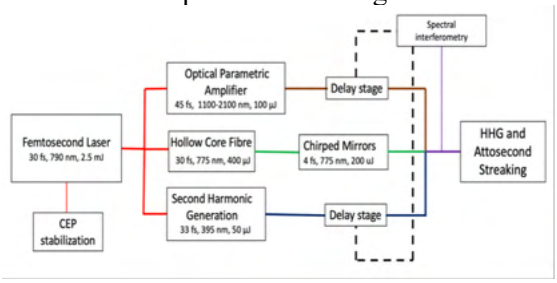


Figure 1. Schematic of the Femtosecond Field Synthesizer.

Using a two-colour version of this system we have demonstrated [4], using attosecond streaking, a two-fold enhancement of the flux of isolated attosecond pulses and shown their duration was minimally effected by the presence of the second harmonic field.

References

[1] Chipperfield L *et al* 2010 *J Mdrn. Opt.*. ***57*** *992-998*

[2] Colosimo P *et al* 2008 *Nature Physics* ***4*** 386-389

[3] Chipperfield L *et al* 2009 *Phys. Rev. Lett.* .**102** 063001

[4] Greening D *et al* 2020 *Opt. Exp.* ***28*** 23329

* E-mail: j.turner19@imperial.ac.uk

Spectral phase of attosecond pulse trains generated by intense femtosecond two-color fields

T A Olsson*, S Jain, S Burrows, J Davis, S Chumley, W Medlin, and G M Laurent†

Department of Physics, Auburn University, 380 Duncan Drive, Auburn, AL 36849, USA

Synopsis The spectral phases of attosecond pulse trains (APTs) generated by intense, two–color, femtosecond fields ($\omega + 2\omega$) via the high harmonic generation (HHG) process are investigated within the Strong Field Approximation (SFA). We show that the spectral phases exhibit high tunability for an intensity ratio between the two colors of the driving field in the range of 0.1 to 5%. By varying both the phase and the intensity ratio between the two colors, we show that the spectral phases can be manipulated in order to produce either one or two attosecond pulses per optical cycle of the driving field.

RP

The development of attosecond light sources based on the high-harmonic generation process has offered new possibilities to probe dynamics in matter down to the natural timescale of electron motion. So far, attosecond measurements have been generally performed through the generation of an electron wavepacket by absorption of the attosecond pulse. The dynamics under scrutiny can then be unravelled from the attributes of the electron wavepacket assuming that the spectral components of the attosecond pulse encoded in the measurement are known.

The spectral characteristics of APTs generated by an one-color driving field have been reported extensively in the literature. In particular, it is well known that the frequency-dependence of the spectral phase (namely the attochirp) limits the achievable level of synchronization of the frequencies making up the pulse [1]. On the contrary, studies on the spectral phases of APTs generated by a multi-color field have been sparse, despite the potential such APTs could have for attosecond experiments [2].

In this work, we show that the spectral phases of APTs generated by intense two–color femtosecond fields ($\omega + 2\omega$) can be tuned by varying both the intensity ratio and the phase between the two components of the driving field. The spectral phases have been computed within the Strong Field Approximation theory, which has proved to be successful at qualitatively reproducing the characteristics of the HHG radiation generated with single- and multi-color fields. As shown in Fig. 1, we found that the spectral phases exhibit high tunability for an intensity ratio between the two colors of the driving field in the range of 0.1 to 5%. In particular, we show that the spectral phases can be manipulated in order to produce either one or two attosecond pulses per optical cycle of the driving field [3].

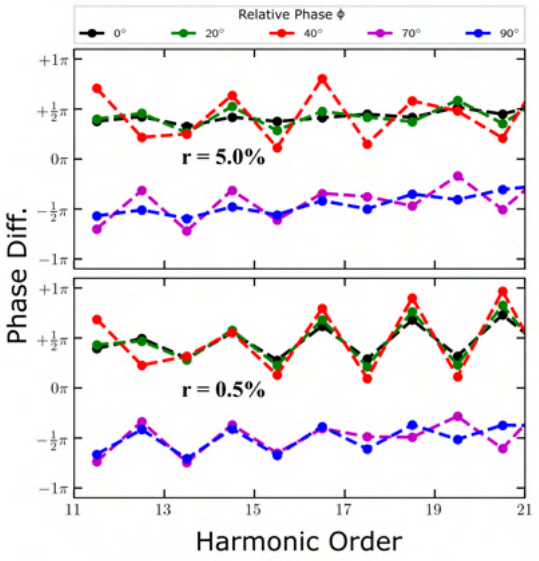


Figure 1. Calculated phase difference between consecutive odd and even harmonics for various intensity ratios r and relative phases ϕ between the 2ω and ω components of the two-color driving field.

References

[1] Maitresse Y *et al* 2003 *Science* **302** 1540
[2] Mitra S *et al* 2020 *Journal of Physics B* **53** 134004
[3] Unzicker B *et al* 2021 *New Journal of Physics* **23** 013019

*E-mail: tzo0018@auburn.edu
†E-mail: glaurent@auburn.edu

General Characterization of Odd-Even Harmonic Generation by Power Terahertz Pulse

Ngoc-Loan Phan[1*], Doan-An Trieu[1], Van-Hoang Le[1†]

[1] *Department of Physics, Ho Chi Minh City University of Education, Ho Chi Minh City, 72711, Vietnam*

Synopsis The relative intensity of odd-even harmonics from an atom in near- and mid-infrared (NIR and MIR) driven laser field combined with terahertz (THz) pulse is studied. The intensity of even harmonics linearly takes off by increasing the THz pulse's electric field until it reaches the critical point. Interestingly, this critical point is almost universal within the scaling of the wavelength of a driven laser. This phenomenon reveals potential applications in exactly retrieving the electric field of THz pulse and controlling the phase matching of the high-order harmonic generation (HHG).

HHG emitted from an asymmetric laser-target system has been paid much attention to because the rich structural information encoded in and its broadband plateau with high conversion efficiency, essential for generating attosecond pulse trains. Specifically, the HHG for this system contains both odd and even harmonics due to the symmetry breaking. Controlling the successive odd and even harmonics is an essential task for generating attosecond pulse trains and solving the phase-matching problem.

One easy way to break the laser-target symmetry is to modify the waveform of the laser field by adding a static electric field into the linearly polarized driven laser. This action enhances the intensity of low-order harmonics, stretches the plateau, and forms multiple plateaux [1,2], which benefit in generating attosecond pulse trains and isolated attosecond pulse. These studies mostly focus on the intense region of the additional static electric field (more than 100 MV/cm) where the emerged even harmonics have the same intensity as the odd harmonics. Investigating the manifestation of odd-even HHG in the weaker static electric field receives less attention, although the correlation between the even and odd harmonics is still questionable in this region.

It should be noted that such a strong static electric field mentioned above is difficult to archive in HHG experiments. Fortunately, the fast development of intense broadband THz pulse with stable carrier-envelope phase [3,4] has emerged as a candidate to replace a static electric field in the HHG studies.

In this report, we discuss the response of the even and odd harmonics emitted from different atoms in the combination of a NIR (or MIR) laser pulse to the presence of a THz laser. It is shown that with gradually increasing the electric field of THz laser, the intensity of odd harmonics is unchanged, while that of even harmonics rapidly takes off. After a critical point, the intensities of the odd and even harmonics meet each other and fluctuate around the stable value. These behaviors occur for all harmonics below the cutoff.

The critical points are almost insensitive to the driven laser's intensity but strongly depend on the driven laser's wavelength. For more convenience, we scale the THz intensity by the factor ω_0^3/E_0, where ω_0 and E_0 are the carrier frequency and the driven laser's electric field, respectively. Surprisingly, the scaled critical point is the same regardless of the driven laser parameters and atomic targets. Furthermore, we explain this universality by analyzing the quantum orbit theory and then discuss the application of this universality in the extraction of macroscopic parameters such as the THz's electric field.

References

1. V. D. Taranukhin and N. Y. Shubin, J. Opt. Soc. Am. B **17**, 1509 (2000).
2. S. Odzak and D. B. Milosevic, Phys. Rev. A **72**, 033407 (2005).
3. D. Daranciang *et al.*, Appl. Phys. Lett. **99**, 141117 (2011).
4. A. D. Koulouklidis *et al.*, Nat. Commun. **11**, 2041 (2020).

* loanptn@hcmue.edu.vn

† hoanglv@hcmue.edu.vn

RP

Numerical calculation of composite light-matter quantum states in strong-field interactions

M Even Tzur*[†1] and O Cohen[1]

1. Department of Physics and Solid-State Institute, Technion – Israel Institute of Technology, 32000 Haifa, Israel

Synopsis We develop a non-perturbative, non-Hermitian, Floquet formalism for strong-field interactions, within the framework of quantum-electrodynamics (QED). Our formalism captures high harmonic generation (HHG) and above-threshold ionization (ATI), allowing for a numerical calculation of composite light-matter quantum states without relying on light-matter separability assumptions at any stage. Hence, our approach captures entanglement in HHG, as well as QED corrections to semi-classical electronic wavefunctions, associated with the emission of photons.

RP

Phenomena such as high harmonic generation [1] (HHG) and above-threshold ionization (ATI) [2] are often referred to as strong-field interactions because they occur when strong laser fields (encompassing 10^{12}-10^{15} photons) interact with matter. Theoretical treatments of such interactions often rely on a semi-classical approximation, solving the time-dependent Schrodinger equation for an electronic wave packet interacting with a classical electromagnetic (EM) field [3], rather than with a macroscopic photonic state. While these theoretical approaches are perfectly adequate to describe the majority of strong-field experiments, recent advances in quantum-optical HHG [4] call for the development of new theoretical approaches, where the light and matter are placed on equal (quantum) footing. Here we develop a non-perturbative, non-Hermitian, Floquet formalism for strong-field interactions, within the QED framework. Our formalism employs the complex-scaled (t,t') method [5] to initially calculate the semi-classical resonant Floquet states governing the dynamics, when the light is not yet quantized. Then, upon quantization of the multimode EM field, the classically driven electron couples to the quantized modes. The composite light-matter state is corrected by Floquet perturbation theory from an initial uncoupled product state (classically driven electron ⊗ EM vacuum state), to a composite light-matter state, which is not necessarily separable. Performing a partial trace on the EM degrees of freedom, we obtain quantum optical corrections to the electronic wavefunction density (as shown by the exemplary calculation in Figure 1).

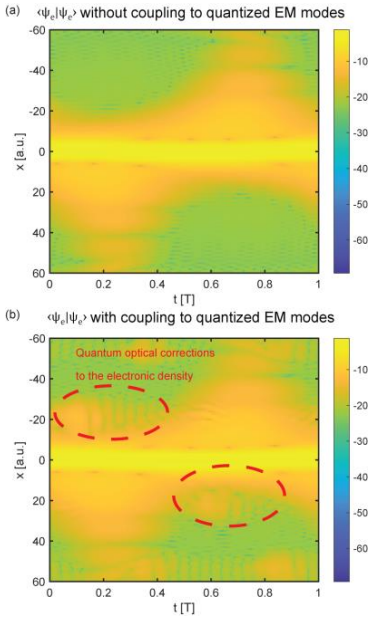


Figure 1: time dependent electronic density of an initially bound electron, irradiated by a coherent-state light field **(a)** without coupling to quantized electromagnetic modes **(b)** with coupling to quantized electromagnetic modes.

References

[1] Pherson, A. et al., *JOSA B* **4**, 595 (1987).

[2] Agostini, P. et al., *Phys.Rev.Lett* **42**, 1127 (1979).

[3] Yu, C. et al, *Adv.Phys.X* **4**, 1562982 (2019).

[4] Gorlach, A. et al. *Nat. Comm.* **11**, 4598 (2020).

[5] Peskin, U, *J.Phem.Phys* **99**, 4590 (1993)

* E-mail: matanev@campus.technion.ac.il

Quantum path interference in HHG for bi-elliptical drivers

A Weber[1,2]*, B Böning[3,4], B Minneker[2,3,4], S Fritzsche[2,3,4], E Pisanty[1]

[1] King's College London, London, WC2R 2LS, United Kingdom
[2] Theoretisch-Physikalisches Institut, Friedrich-Schiller-Universität Jena, D-07743 Jena, Germany.
[3] Helmholtz-Institut Jena, D-07743 Jena, Germany.
[4] GSI Helmholtzzentrum für Schwerionenforschung GmbH, D-64291 Darmstadt, Germany.

Synopsis
High-harmonic generation driven by complex laser fields, such as bi-elliptical two-color fields, involves electron trajectories starting from multiple ionization bursts during the laser cycle. We show that the quantum path interference of those different trajectories leads to a rapidly changing ellipticity of the harmonics.

RP

If a bi-elliptical two-color laser field (Fig. 1(a)) is used to drive high-harmonic generation (HHG), the emitted harmonics are – in general – elliptically polarized. However, the ellipticity seems unpredictable and unrelated to the driving beams' ellipticities. Using the quantum orbit approach, we can explain this behaviour by the quantum path interference between the various trajectories involved in the process of HHG.

When employing rather complex laser fields to drive HHG, the multiple ionization bursts yield electron trajectories of different shapes (Fig. 1(b)). Those trajectories of the liberated electron in the continuum barely change from one harmonic order to its neighbour. The polarization ellipse of the harmonic field induced by each trajectory can be predicted from the electron's velocity at recombination. Therefore, for simple fields, where the trajectories within one laser cycle have the same shape, the field ellipse of the harmonics can be easily deduced.

However, for driving laser fields with more complex structure, like bi-elliptical two-color laser fields, the trajectories recombining within one laser cycle may have very different shapes and phases. When combining their contributions to the field of the harmonic, their interference causes the harmonic ellipticity to be rapidly changing for subsequent orders.

We will also report on recent and ongoing work regarding the coalescence of trajectories at the harmonic cutoff.

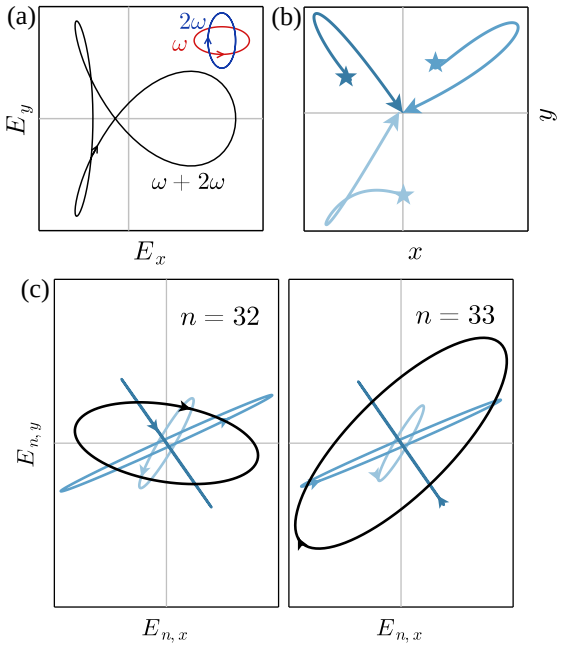


Figure 1. Driving HHG by a bi-elliptical ω-2ω laser field, shown in (a), yields multiple electron trajectories of different shapes (b). The overall harmonic field (black curves in (c)) then collects contributions from all the possible trajectories. (The lightest shaded harmonic field ellipse is scaled up by a factor of 10 for better visibility.)

References

[1] A Weber et al., Phys. Rev. A **104**, 063118 (2021).

*E-mail: anne.weber@kcl.ac.uk

Three ways to select from two attosecond pulses

K Kovács[1 *], V Tosa[1]

[1]National Institute for Research and Development of Isotopic and Molecular Technologies, Cluj-Napoca, 400289, Romania

Synopsis We demonstrate that two successive attosecond pulses can be obtained from naturally separated spectral domains formed during high-order harmonic generation and propagation in gas medium. We propose a feasible experimental configuration in which one can obtain one pulse in a lower energy domain (<300 eV), or another pulse in a higher energy domain (>300 eV). Without filtering, a double attosecond pulse emission with fixed temporal separation is obtained. The gap between the two spectral domains is close to the onset of the water window.

Based on numerical calculations, we propose a new experimental setup for high-order harmonic generation (HHG) of **mid-infrared** few-cycle laser pulses [1]. The advantage of the proposed configuration is that it allows the generation of **two successive** attosecond pulses having **separate spectral content**, both in the XUV regime. We demonstrate that the spectral separation results from macroscopic propagation effects in Helium gas.

With the proposed experimental parameters the spectral gap is close to the onset of the water window (282 eV). Coherent light sources in the water window are important for the ultrafast dynamic imaging of biological samples in water medium.

The experimentally feasible parameters are based on the setup presented in [2]: = 1700 nm, = 6 fs, L_{med} = 9 mm filled with He at p = 200 Torr pressure placed in the converging beam such that it ends in the nominal laser focus position (f = 50 cm). A pulse of 1 mJ, creates 9×10^{14} W/cm^2 peak intensity at the beginning of the gas cell.

In Fig. 1. we show that at the end of the interaction region one has two consecutive attosecond bursts (upper panel) with separated spectral content as identified in the lower panel.

We propose here three scenarios:

(1) With the use a low-pass spectral filter the attosecond pulse below 300 eV is kept with its total flux; this pulse is labeled 2 on the figure and it is generated mostly off-axis.

(2) With a high-pass filter the attosecond pulse above 300 eV is kept; this is pulse labeled 1 on the figure and it is generated close to the propagation axis.

(3) Without spectral filtering a double attosecond pulse emission with fixed temporal separation is obtained.

The spectral separation of successive attosecond pulses is an example of space-time coupling in nonlinear optics, good candidate to be further explored and exploited both theoretically and experimentally.

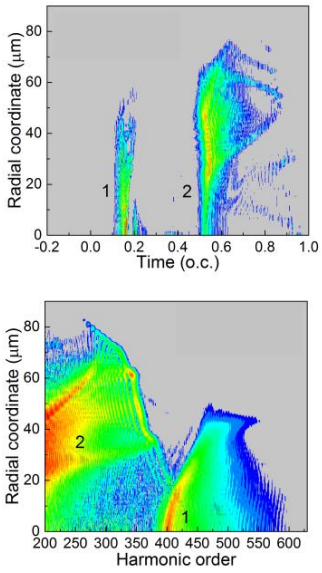


Figure 1. Upper panel: Temporal–radial maps of the two attosecond pulses in the 146–460 eV spectral domain (H200-H630). Lower panel: Spectral-radial maps of the harmonic radiation at the exit of the interaction region. Color scale spans two orders of magnitude, logarithmic scale, arbitrary units.

References

[1] Kovacs K and Tosa V 2020 *Scientific Reports* **10** 7392

[2] Cardin V et al. 2018 *J. Phys. B.* **51** 174004

* E-mail: kkovacs@itim-cj.ro

Control of N_2^+ lasing: Rotational coherence and propagation effects

M Richter[1]*, M Lytova[2], F Morales[1], S Haessler[3], O Smirnova[1], M Spanner[2], and M Ivanov[1]

[1]Max-Born-Institute, Max-Born Straße 2A, 12489 Berlin, Germany
[2]National Research Council of Canada, 100 Sussex Drive, Ottawa K1A 0R6, Canada
[3]Labo. d'Optique Appliquée, Inst. Polytechnique de Paris, 181 Chemin de la Hunière, 91120 Palaiseau, France

Synopsis We show that lasing without inversion arises naturally during propagation of intense femtosecond laser pulses in air. It is triggered by the combination of molecular ionization and molecular alignment, both unavoidable in intense light fields. We also present control methods to optimize the lasing, taking comprehensive account of the relevant laser-molecule interactions and pulse propagation effects.

RP

We present a lasing without inversion scheme [1, 2, 3] that uses only the natural dynamics of a multi-level quantum system and requires no coherence between the excited and the lower electronic states; effectively, lasing without inversion comes "for free".

We also show that this mechanism is active in the highly efficient generation of 391 nm radiation during propagation of intense femtosecond laser pulses in air [1, 2, 3], under standard conditions where the process known as "laser filamentation" leads to self-guiding of light. Identifying the mechanism responsible for the coherent emission at this line, corresponding to the $X^2\Sigma_g^+(\nu''=0) \leftarrow B^2\Sigma_u^+(\nu'=0)$ transition in the molecular nitrogen ion, has been a long-standing puzzle. The main difficulty in resolving this puzzle stems from the apparent lack of a general physical mechanism capable of generating population inversion between X and B in N_2^+ for standard filamentation conditions, including intensity clamping around $I \sim 100$ TW/cm^2. We will show that our inversionless amplification mechanism provides a key missing component of this puzzle.

Our pump-probe simulations show [1, 2] that neither electronic nor rotational population inversion in the medium is necessary, see Fig. 1. Amplification is possible thanks to the coherent rotational dynamics in the ion. The proposed amplification mechanism is completely general. The only necessary ingredients are non-negligible population in the excited (B) state and molecular rotations, both unavoidable during the interaction with an intense laser pulse.

*E-mail: maria.richter@mbi-berlin.de

In this mechanism, the gain window travels with the group velocity of the pump pulse so that amplification occurs only in the forward direction. To achieve lasing in the backward direction, highly desirable for remote sensing, one would greatly benefit from creating electronic or at least rotational population inversion. To this end, well-timed control pulses can be used to steer the ro-vibronic dynamics in the ion. We show that optimization of such control pulses, including their carrier frequencies, energies, time delays and propagation modifications could open a route for achieving backward lasing in open air.

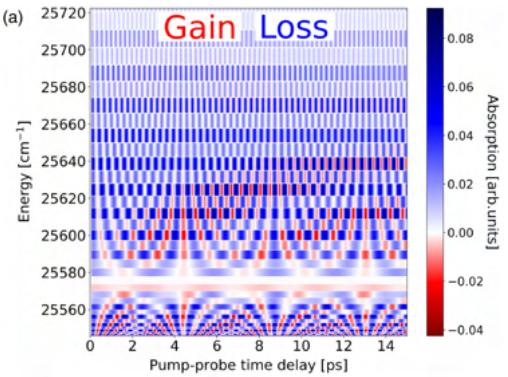


Figure 1. Simulated frequency-resolved gain and loss of the weak, time-delayed probe interacting with the pumped, but inversionless N_2^+ [1].

References

[1] M Richter et al., Optica **7**, 586 (2020).
[2] M Lytova et al., Phys. Rev. A **102**, 013111 (2020).
[3] D. Kartashov et al., Research in Optical Sciences, OSA Technical Digest (online) (Optica Publishing Group), paper HTh4B.5 (2014).

Control of achiral and chiral media with synthetic chiral vortex beams

N Mayer[1]*, D Ayuso[2], M Ivanov[1,2,3], and O Smirnova[1,4]

[1]Max-Born-Institut, Max-Born-Str. 2A, Berlin, 12489, Germany
[2]Department of physics, Imperial College London, London, SW7 2AZ, United Kingdom
[3]Institut für Physik, Humboldt-Universität zu Berlin, Newtonstr. 15, Berlin, 12489, Germany
[4]Technische Universität Berlin, Hardenbergstr. 33A, Berlin, 10623, Germany

Synopsis We combine bicircular vortex beams to create a synthetic chiral vortex beam that displays chirality in the dipole approximation and azimuthally varying handedness. We use numerical simulations to show that the vortex can imprint its local chirality on the single atom or molecule as well as its orbital angular momentum (OAM) on the macroscopic response of an isotropic atomic or molecular ensemble. The enantio-sensitive response can be tuned both locally and globally by tuning the OAM of the two beams.

RP

Light displaying chirality in the dipole approximation can be created by combining two or more beams with commensurate frequencies and suitable polarization in a non-collinear or tightly-focused setup, leading to highly-sensitive and controllable enantio-sensitive response in chiral media [1]. However, the connection between synthetic chiral light, a spin angular momentum (SAM) based concept, with vortex beams, an orbital angular momentum (OAM) based one, has not been made yet. Here, we bridge this gap by showing how the interplay between the SAM and OAM degrees of freedom in tightly-focused vortex beams gives rise to the concept of a chiral vortex.

In particular, we consider two bicircular Laguerre-Guassian beams with frequencies ω and 2ω and OAM ℓ_ω and $\ell_{2\omega}$ in the tight focus regime. Due to the presence of a longitudinal component along the beams' propagation axis, the polarization of the light at a given point draws a chiral Lissajous curve, whose handedness is described by the chiral correlation function [1]

$$h^{(5)} = \mathbf{E}^*_{2\omega} \cdot (\mathbf{E}^*_{\omega} \times \mathbf{E}_{\omega})\,(\mathbf{E}_{\omega} \cdot \mathbf{E}_{\omega})\,. \qquad (1)$$

We demonstrate that for particular combinations of OAM beams the spatial distribution of the light's handedness is arranged in a vortex fashion around the beam propagation axis, describable by a integer topological charge

$$\chi = \ell_{2\omega} + m_{2\omega} - 2(\ell_\omega + m_\omega), \qquad (2)$$

where $m_{r\omega}$ and $\ell_{r\omega}$ are the SAM and OAM of the $r\omega$ field. In this contribution we show using time-dependent Schrödinger equation simulations that chiral vortices can be used to imprint chirality on a gas jet of achiral atoms [2]; moreover, we model High-Harmonic Generation using a DFT-based Strong-Field Approximation to show how chiral vortices can be used to shape the near- and far-field response of an ensemble of chiral molecules. In conclusion, we describe a new type of light that displays chirality both locally, through its SAM, as well as globally, through its OAM, allowing one to control the enantio-sensitive response microscopically as well as macroscopically by tuning the angular momentum of the two beams.

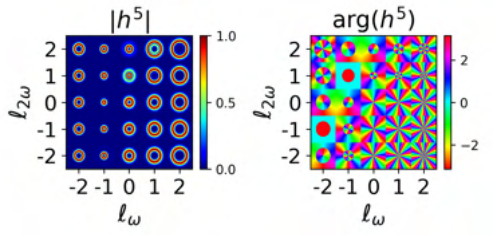


Figure 1. Absolute value and phase of the chiral correlation function for combinations of OAM $(\ell_\omega, \ell_{2\omega})$ and counter-rotating SAM $(m_\omega, m_{2\omega}) = (1, -1)$.

References

[1] D Ayuso et al., Nat. Photon. **13**, 866–871 (2019).
[2] N Mayer, M Ivanov and O Smirnova, arXiv:2112.02658 (2021).

*E-mail: mayer@mbi-berlin.de

Effects of Dynamic Core-Electron Polarization on High-Order Harmonic Generation from Multielectron Molecules

Van-Hoang Le[1*], Ngoc-Loan Phan[1†], Cam-Tu Le[2‡]

[1] *Department of Physics, Ho Chi Minh City University of Education, Ho Chi Minh City, 72711, Vietnam*
[2] *Advanced Institute of Materials Science, Ton Duc Thang University, Ho Chi Minh City, 72915, Vietnam*

Synopsis The unambiguous effect of the dynamic core-electron polarization (DCeP) on different aspects of the high-order harmonic generation (HHG) is reported systematically. Particularly, the origin of DCeP imprints in HHG is clarified by considering each step of the harmonic generation (ionization, propagation, and recombination). Then, the weight of the DCeP to the HHG spectra in each step is estimated carefully by the electron-trajectories analysis. Interestingly, the DCeP is involved in the propagation step besides the ionization and recombination ones.

RP

In the past few decades, the nonlinear laser-interaction has attracted unprecedented advances in both experimental and theoretical studies. The simplest model is popularly used, called single-active electron (SAE) approximation, where the core electrons are frozen but not the outermost electron. However, the SAE theory significantly deviates from the experimental observation for atoms and molecules with large polarizability; thus, its validation needs to be reconsidered.

The core-electron polarization is, in fact, large in a strong laser field, raising a question about the DCeP role. A recent study on the harmonic process has demonstrated the DCeP effect on the dynamic minimum of HHG from CO molecule [1]; however, a comprehensive investigation of the DCeP impact in different aspects of HHG is still desirable.

Our recent studies show that the DCeP strongly affects different characteristics of HHG emitted from CO_2 and CO molecules in a linearly polarized laser pulse. Firstly, we indicate that the DCeP can shift and sharpen the structural minima in the HHG from CO_2 molecules [2]. Then, we demonstrate the significant DCeP effect on the intensity and shape of HHG from CO molecules at harmonics near the cutoff [3]. Finally, we find out that the DCeP dramatically modifies the even-to-odd ratio, i.e., the ratio between the intensities of the even and the average of the two adjacent odd orders [4,5]. The discrepancy between the two cases of including and neglecting DCeP is especially large, as much as one order. This strong effect of DCeP makes the simulated even-to-odd ratio nicely matches the available experimental data [6,7]. In Ref. [5], we also find out the DCeP impact on the harmonic phase besides the harmonic intensity found in previous studies [1,3,4].

It is natural to ask whether the DCeP effects on different aspects of HHG have the same origin. This report systematically discusses the physical underlying of DCeP imprints in HHG by considering each step of harmonic generation according to the three-step model. We show that the DCeP effect on HHG not only originates from the ionization and recombination steps but also from the propagation one. The propagation step influences the phase of harmonic bursts whose coherence dramatically impacts harmonic intensity. A further electron-trajectories analysis is adopted to detect which step plays an essential role in the DCeP effect on harmonic generation. It is indicated that depending on the laser parameter, the weight of each step is differently contributed to the DCeP effect on HHG.

References

1. B. Zhang *et al.*, Phys. Rev. A **90**, 035402 (2014).
2. C.-T. Le *et al.*, Phys. Rev. A **100**, 053418 (2019).
3. C.-T. Le *et al.*, Phys. Rev. A **97**, 043405 (2018).
4. N.-L. Phan *et al.*, Phys. Chem. Chem. Phys. **21**, 24177 (2019).
5. H.T. Nguyen *et al.*, Phys. Rev. A **105**, 023106 (2022).
6. E. Frumker *et al.*, Phys. Rev. Lett. **109**, 233904 (2012).
7. P.M. Kraus *et al.*, Phys. Rev. Lett. **113**, 023001 (2014).

* hoanglv@hcmue.edu.vn
† loanptn@hcmue.edu.vn
‡ lethicamtu@tdtu.edu.vn

Modelling intensity volume averaging in ab initio calculations of High Harmonic Generation

L Hutcheson*, H W van der Hart and A C Brown†

Centre for Theoretical Atomic, Molecular and Optical Physics, School of Mathematics and Physics, Queen's University Belfast, Belfast BT7 1NN, United Kingdom

Synopsis We present a method to estimate the effect of the focal volume averaging on high harmonic spectra obtained from *ab initio* calculations. While accounting for the phase of harmonics produced at different locations in the focal volume gives the most accurate results, a simplified approach, using a smaller number of calculations allows for a satisfactory assessment of which features of the experimental spectrum may be traced directly to single-atom effects. We show results demonstrating this approach using the R-Matrix with Time method.

RP

High Harmonic Generation (HHG) experiments probe the coherent response of many atoms (or molecules) in a target when illuminated by a focused laser beam. This macroscopic response can be exploited to measure HHG as the coherent build-up of many single atom emissions [1].

Insight into the the single atom response is often obscured in experiment, but can be provided by *ab initio* calculations which model a single atom (or molecule) irradiated by a laser at a single intensity. The most straightforward way to replicate the intensity volume effect with theoretical simulations is to perform thousands of calculations over the full-range of intensities observed in the laser focal spot and compute the gross response. However, this method is not tractable with detailed, computationally demanding *ab initio* methods. A more appropriate technique would take a small subset of intensities, weight the contribution from each intensity and thereby compute the gross response.

This contribution will outline three methods (of increasing complexity) for approximating the intensity volume effect on high harmonic spectra obtained from *ab initio* calculations, which consider both the geometry of the experiment and the phase of the harmonic response. The 'naive' method simply calculates a weighted intensity average. The 'intermediate' method also accounts for the difference between the near field harmonics obtained in simulations and the far field harmonics observed in experiment and a 'full' method which also accounts for the geometry of the detector.

Using the *ab initio* R-Matrix with Time (RMT) method [2], we look at two different experimental schemes to assess these approaches to intensity averaging. We find that all three methods can approximate the intensity averaging effect with only a small computational cost.

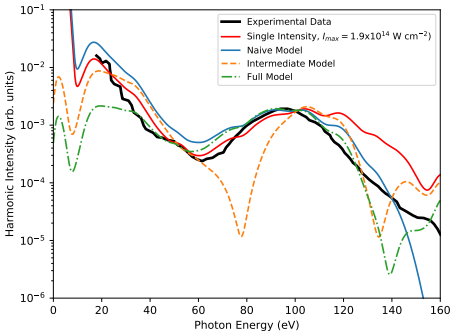


Figure 1. HHG spectrum produced by xenon irradiated by a 1800nm, 1.9×10^{14} Wcm^{-2} pulse. Agreement between experimental [3] and theoretical data is improved when accounting for intensity averaging using the three proposed methods.

References

[1] C Vozzi *et al*, New J. Phys. **13**, 073003 (2011).
[2] A C Brown *et al*, Comp. Phys. Commun. **250**, 107062 (2020).
[3] A D Shiner *et al*, Nat. Phys. **7**, 464-467 (2011).

*E-mail: lhutcheson02@qub.ac.uk
†E-mail: andrew.brown@qub.ac.uk

Extended optimization laws for high harmonic generation in gases

B Major[1,2] * **and K Varjú**[1,2]

[1] ELI ALPS, ELI-HU Non-Profit Ltd., Wolfgang Sandner utca 3., Szeged 6728, Hungary
[2] Department of Optics and Quantum Electronics, University of Szeged, Dóm tér 9., Szeged 6720, Hungary

Synopsis We extend the one-dimensional model proposed by Constant and co-workers [Phys. Rev. Lett 82(8), 1668 (1999)] to analyze phase matching of high-order harmonic generation in absorbing medium; and provide new rule-of-thumb guidelines for harmonic-flux optimization. We show, for example, that having a generation gas medium that ends abruptly with a steep pressure gradient is required for achieving high flux.

RP

Almost 25 years ago, a one-dimensional phase-matching (PM) model for high-harmonic generation (HHG) in gases was proposed by E. Constant and co-workers [1]. This lead to very simple laws for flux optimization, and it also shed light on general properties of PM in gases. It became so successful that its guidelines are still followed by scientist when designing HHG beamlines [2]. At the same time, due to its simplicity, it does not allow for full understading of the complex mecahnisms of PM, and there is still a continuous effort to look for optimum generation media for HHG in gases [3,4].

Here we try to extend the capabilities of the model of Constant et al. by having less simplistic assumptions on the generation properties, but still keeping the same mathematical and physical basis [5]. The analytical approach of the original expressions simplifies the description of the macroscopic HHG process where all parameters (atomic number density, single-atom response, phase mismatch, absorption) related to the harmonic build-up are constant along the generation medium. In our approach, most of these parameters vary linearly with propagation distance in the generation volume. This still allows for an analytical treatment of the situation, while allowing to reach general guidelines on what pressure gradients can optimize the HHG flux in a gaseous medium [5].

One of the advantages of our extended model, for example, is that the effect of the pressure gradient at the end of the medium for more general pressure profiles (like a trapezoidal, serving as a simple model for gas targets of different kind, like gas cell or gas jet) can also be analyzed. The results of such a study is shown in Fig. 1. The curves of Fig. 1 suggest that under any phase matching condition ($R = 2\pi\, L_{abs} / L_{coh}$ describing the relation of coherence L_{coh} and absorption lengths L_{abs}, as in the original model [1]), it is important to have a steep pressure gradient at the medium end (describd by the dimensionless variable θ^2 [5]) for no loss of flux.

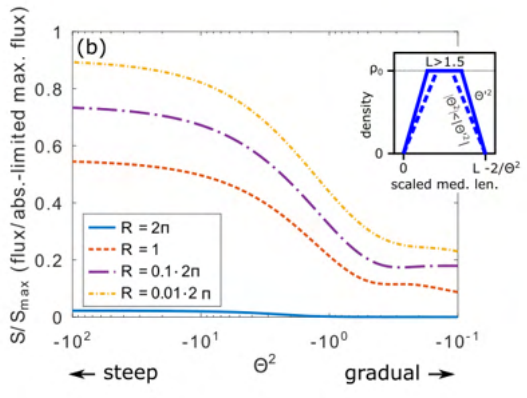


Figure 1. The high-harmonic flux S normalized to the absorption-limited maximum flux S_{max} for a gaseous generation medium having a trapezoidal pressure profile (see inset) for different pressure gradients θ^2 and phase matching conditions R.

Further analytical formulas are also derivable, allowing for the study of the pressure gradient through which the generating laser beam enters the medium, and how it can be tuned in a smart way to increase harmonic flux.

References

[1] Constant E *et al* 1999 *Phys. Rev. Lett* **82** 1668
[2] Heyl C M *et al* 2017 *J. Phys. B: At. Mol. Opt. Phys.* **50** 013001
[3] Weissenbilder R *et al* 2021 *Conference on Lasers and Electro-Optics (CLEO)* SW3Q.6
[4] Weissenbilder R *et al* 2022 arXiv:2202.08202
[5] Major B *et al* 2021 *J. Phys. B: At. Mol. Opt. Phys.* **54** 224002

* E-mail: balazs.major@eli-alps.hu

Ultrafast Electron Dynamics in the Strong Field Regime

L Ortmann[1,2], B Grafstrom[2 *], and A Landsman[2]

[1]Max Planck Institute for the Physics of Complex Systems, Dresden, 01187, Germany
[2]The Ohio State University: Department of Physics, Columbus, 43210, United States

Synopsis Classical Trajectory Monte Carlo (CTMC) methods were used to simulate the dynamics of photoionized electrons due to a strong field attosecond laser pulse. Two nonadiabatic models have been proposed to explain the behavior and subsequent dynamics of the ionized electrons, yet both theories offer two different physical descriptions about the initial momenta of the ionized electron. This present study is aimed at determining the physical validity of the two theories in the strong field and nonadiabatic regime.

Multiple theorectical models have been proposed to describe the behavior of strong field ionization in isolated atomic systems due to an attosecond laser pulse [1-4]. In the nonadiabatic and strong field regime, there are two models which make different assumptions about the initial conditions of the ionized electron during ionization, with the first [3] assuming a broad spread in ionization times and zero initial longitudinal velocity. And the second [4] assuming a narrow spread in ionization times and non-zero initial longitudinal velocity.

In this work, the two models were compared by simulating the trajectories of ionized electrons in helium atoms by an attosecond laser pulse and by looking at the final longitudinal velocity distribution produced by each theory. The parameters of the pulse (e.g. intensity, wavelength, and number of cycles) were varied for different test simulations and despite their different initial conditions, the two models were found to produce similar final velocity distributions across a range of laser parameters. It was determined that the broad spread in ionization times offsets the assumption of zero initial momenta in YI theory, which explains why the two final velocity distributions appear identical in nature.

Yet, it was also realized that under certain laser parameters, the two theories will produce two distinct final velocity distributions.

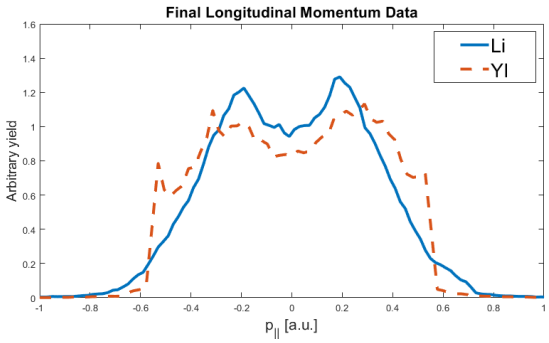


Figure 1. Simulated final velocities of ionized electrons by a 5-cycle, 400nm attosecond laser pulse.

The final velocity distrubutions were then compared to the results of a Time Dependent Schrodinger Equation (TDSE) calculation [5,6] and it was determined that the Li theory was the more accurate of the two models. A result that was found to be in agreement with the work done by Dr. Ortmann in her doctoral thesis [7].

References

[1] Keldysh L *et al* 1965 *Sov. Phys. JETP* **20** 1307-1314
[2] Reiss H 1980 *Phys. Rev. A* **22** 1786
[3] Yudin G and Ivanov M 2001 *Phys. Rev. A* **64** 013409
[4] Li M *et al* 2016 *Phys. Rev. A* **93** 013402
[5] Ivanov I *et al* 2018 *Comm. Phys.* **81** 1
[6] Ivanov I *et al* 2014 *Phys. Rev. A* **89** 021402
[7] Ortmann L 2019 *Trajectory-based Analyses of Ultrafast Strong Field Phenomena* [Doctoral Dissertation, Technische Universität Dresden] 41-51

* E-mail: grafstrom.1@osu.edu

RP

Tailoring Alignment and Orientation of Poly-atomic Molecules for Enhanced HHG Yield: A Non-Perturbative Laser-Matter Interaction-based Perspective

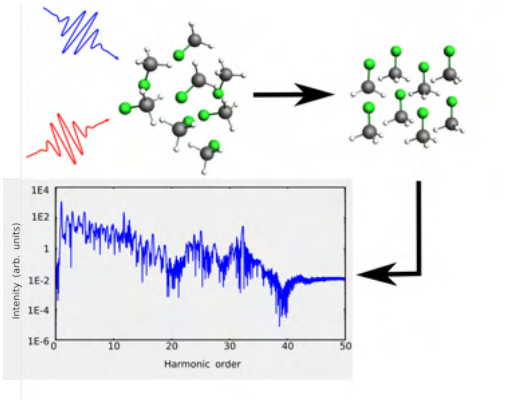
K Chordiya[1,2]*, and M U Kahaly[1,2]†

[1]ELI-ALPS, ELI-HU Non-Profit Ltd., Szeged, Hungary
[2]Institute of Physics, University of Szeged, Dóm tér 9, H-6720 Szeged, Hungary

Synopsis Demonstration of improved laser induced field free molecular alignment and orientation (A&O) of a poly-atomic molecule using the pulse frequency resonant geometry. To achieve high molecular A&O experimentally feasible pulse parameters are studied and correlation with rotational states excitation is revealed. On determining the high A&O laser parameters the high harmonic signal is simulated using time dependent density functional theory and strong field approximation. Identification of possible control parameters in laboratory conditions for efficient high harmonic yield.

RP

Increasing interest in the fields of ultrafast science such as femto-second chemistry, high-harmonics generation, and attosecond streaking using gaseous targets demands high molecular "alignment" and "orientation" (A&O). Multiple techniques are being investigated to increase high harmonic conversion efficiency. In this presentation, we will demonstrate the critical role of varying pulse parameters for (two pulse) on the A&O dynamics of an poly-atomic molecule, in its equilibrium ground and field resonant vibrational state. The field parameters used are identified to be experimentally feasible. By analyzing the interplay between laser pulse parameters and the resulting rotational population distribution, the origin of specific A&O dynamics was addressed. On achieving the high alignment and orientation of the molecules we simulate the high harmonics spectra using similar laser parameters, time dependent density functional theory and strong field approximation. The high harmonic generation in the poly-atomic molecules is further investigated with using different level of theoretical approximations. Effect of different beam profiles are also understood. We identify possible optimized conditions in laboratory environment, how harmonic generation can be amplified significantly in polyatomic molecules, suggesting an effective approach for increasing the HHG yield. Ramifications under high intensity field, and strategies to tackle those would also be discussed.



Acknowledgement

ELI-ALPS is supported by the European Union and co-financed by the European Regional Development Fund (GI-NOP-2.3.6-15-2015-00001). The authors acknowledge Project no. 2019-2.1.13-TÉT-IN-2020-00059 which has been implemented with the support provided from the National Research, Development and Innovation Fund of Hungary, financed under the 2019-2.1.13-TÉT-IN funding scheme. All authors acknowledge funding from PaNOSC European project. The authors acknowledge COST (European Cooperation on Science and Technology) for funding the Action CA17126 "Toward Understanding and Modelling Intense Electronic Excitation (TUMIEE)" supporting this work. This work benefited from networking activities carried out within the EU funded COST Action TUMIEE (CA17126) and represents a contribution to it.

*E-mail: Kalyani.Chordiya@eli-alps.hu
†E-mail: Mousumi.UpadhayayKahaly@eli-alps.hu

High-harmonic generation using driving pulses at 10^{16} W/cm^2

E Svirplys[1 *], K Kovács[2], M Anus[1], O Ghafur[1], K Varjú[3,4], M J J Vrakking[1], V Tosa[2], B Major[3,4] and B Schütte[1]

[1]Max Born Institute, Berlin, 12489, Germany
[2]National Institute for Research and Development of Isotopic and Molecular Technologies, Cluj-Napoca, 400293, Romania
[3]ELI-ALPS, ELI-HU Non-Profit Ltd., Szeged, 6728, Hungary
[4]Department of Optics and Quantum Electronics, Szeged, 6720, Hungary

Synopsis We present an unusual High-harmonic generation (HHG) scheme where relatively long 50-fs near-infrared (NIR) laser pulses with peak intensities up to 10^{16} W/cm^2 were focused into a high-pressure gas jet. Our experimental and numerical study indicates that NIR pulses experienced rapid spatio-temporal reshaping inside the gas target which caused a sharp decrease in the peak intensity until good phase-matching conditions for HHG were reached. This resulted in a ten-fold NIR spectrum broadening and generation of continuous HHG spectra ranging from 18 to 140 eV when using different gas species.

RP

In high-harmonic generation (HHG) good phase matching between the driving and generated extreme-ultraviolet (XUV) pulses is crucial. This necessitates careful tuning of many experimental parameters such as the laser intensity or gas pressure [1].

Here, we present a novel scheme that shows self-regulatory behavior of the driving laser intensity allowing for phase-matched HHG. The setup is similar to a compact intense XUV setup that was recently demonstrated [2]. Near-infrared (NIR) laser pulses obtained from a Ti:sapphire amplifier were focused into a high-pressure (>1 bar) atomic jet, leading to peak intensities of about 10^{16} W/cm^2 (in the absence of the gas), which is 1-2 magnitudes higher than the usual optimal intensity for the HHG. Significant reshaping of the 50-fs long driving NIR laser pulses was observed in each atomic gases investigated (Xe, Kr, Ar, Ne, He), resulting in a blue-shift and a ten-fold increase of the initial NIR bandwidth.

Our numerical calculations suggest that ionization-induced self-phase modulation is responsible for the spectral broadening, while plasma-induced defocusing results in a substantial decrease of the NIR intensity until a phase-matching condition is reached. Such rapid NIR pulse reshaping inside the HHG medium may be referred to as a strongly overdriven regime. Simulations show that during propagation through the jet NIR pulse reshaping is followed by the build-up of short attosecond pulse trains. This resulted in the observation of continuous XUV spectra ranging from 18-140 eV when using different gas species (Fig. 1). It can be seen that in a strongly overdriven regime the harmonic spectra are substantially broadened.

This flexible and compact HHG scheme is ideally suited for absorption and reflection spectroscopy, allowing to access XUV and soft X-ray spectral ranges without the need for tedious optimization procedures.

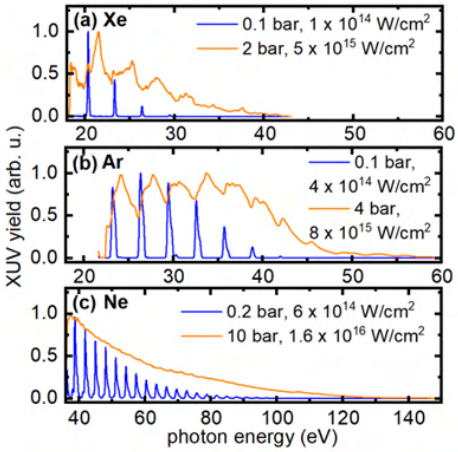


Figure 1. HHG spectra obtained using various gas species. The blue and orange curves correspond to a standard and strongly overdriven HHG regimes respectively.

References

[1] Constant E *et al* 1999 *Phys. Rev. Lett. 82, 1668*
[2] Major B *et al* 2021 *Optica* 8, 960

* E-mail: svirplys@mbi-berlin.de

High-Harmonic Generation in the Water Window from mid-IR Laser Sources

K Finger[1], D Atri-Schuller[1,2], N Douguet[3], K Bartschat[1], and K R Hamilton[1]*

[1]Department of Physics and Astronomy, Drake University, Des Moines, IA 50311, USA
[2]Department of Applied Physics, Stanford University, Stanford, California 94305, USA
[3]Department of Physics, Kennesaw State University, Marietta, GA 30060, USA

Synopsis Using both a single-active electron (SAE) model and the multi-electron R-Matrix with Time-dependence (RMT) method, we investigate the response of neon atoms to near-IR laser fields, which results in the production of high-order harmonics within the water window.

RP

Light sources with frequencies in the water window, which spans the K-edges of carbon and oxygen, can be used to image biological molecules in aqueous environments [1]. These soft X-rays can be produced, e.g., by synchrotron radiation, X-ray free-electron lasers, or high-harmonic generation (HHG) from mid-IR lasers, with the latter demonstrating the most promise for live-cell imaging with femtosecond time resolution [2].

However, describing harmonic generation in the mid-IR regime is a computationally difficult task, particularly if multi-electron effects are to be included in the calculation. We investigate the harmonic response of neon atoms to mid-IR laser fields (2000 – 3000 nm) using both a single-active electron (SAE) model [3] and the fully *ab initio* all-electron R-Matrix with Time-dependence (RMT) method [4]. The laser peak intensity and wavelength are varied to find optimal parameters for high-harmonic imaging in the water window. Comparison of the SAE and RMT results [5] shows very good qualitative agreement between the resulting spectra parameters, such as the cut-off frequency predicted by the classical three-step model [6].

Both the SAE and RMT methods can therefore be used to describe HHG in intense, near-IR laser pulses schemes. While more computationally demanding than the SAE model, RMT captures the multi-electron dynamics of the system. Since these have been shown to influence the detailed appearance of the harmonic spectrum [7], we are currently investigating these effects.

This work is supported by the United States National Science Foundation under PHY-1803844, PHY-2012078, OAC-1834740, and XSEDE PHY-090031, and by the Frontera Pathways allocation PHY20028.

*E-mail: kathryn.hamilton@drake.edu

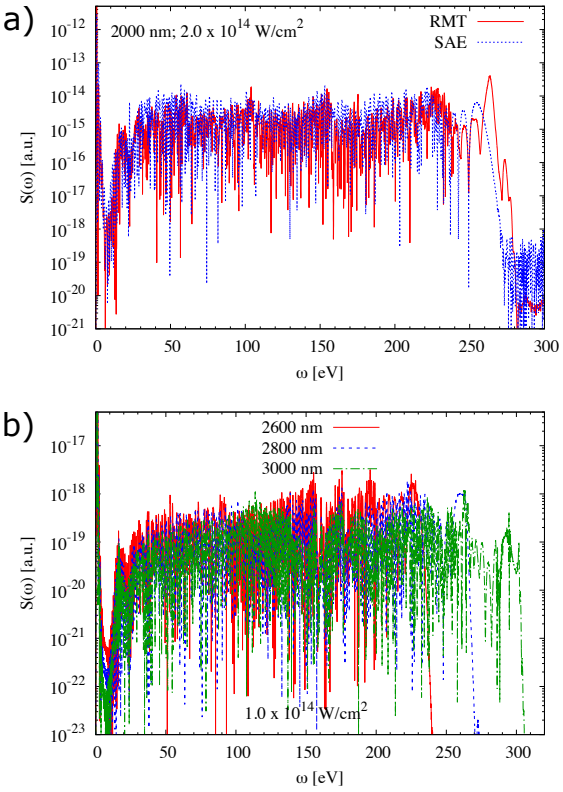


Figure 1. (a) Harmonic spectra for neon in a 2000 nm laser pulse with a peak intensity of 2×10^{14} W/cm^2. (b) Spectra determined by the RMT method in a 1×10^{14} W/cm^2 laser pulse with wavelengths ranging from 2600 nm to 3000 nm.

References

[1] R Neutze *et al.*, Nature **406** 752 (2020).
[2] Y Fu *et al.*, Commun. Phys **3** 92 (2020).
[3] T Pauly *et al.*, Phys. Rev. A **102** 013116 (2020).
[4] A C Brown *et al.*, Comp. Phys. Commun. **250** 107062 (2020)
[5] K Finger et al., arXiv:2101.10547 (2021).
[6] P B Corkum, Phys. Rev. Lett. **71** 1994 (1993).
[7] T Mazza *et al.*, Nat. Commun. **6** 6799 (2015).

Radiative transition properties for In XLVIII using the Ab initio MCDHF-RCI method

D E Salhi[1]*, S Manai[1,2], S Ben Nasr[1] and H Jelassi[1]

[1]Laboratory on Energy and Matter for Nuclear Sciences Development, LR16CNSTN02, National Center for Nuclear Sciences and Technologies, Sidi Thabet Technopark 2020 Ariana Tunisia
[2]Faculty of Sciences of Bizerte, University of Carthage, Tunisia

Synopsis The calculations for the He-like In ion were carried out using the GRASP2018 code based on the multiconfiguration Dirac-Hartree-Fock (MCDHF) following by the RCI calculation. Transition probabilities are reported for all types of transitions ($E1$, $E2$, $M1$ and $M2$ transitions). Breit interactions and quantum electrodynamics effects are included in the RCI calculation. Comparisons were made with other available data found in the literature and a good agreement was found which confirms the reliability of our results.

Atomic data have received a great deal of attention, due to their need for the upcoming ITER project (International Thermonuclear Experimental Reactor). So, extensive spectroscopic studies both experimental and theoretical have been performed in the last years in order to estimate the power loss from the impurities in the forthcoming fusion reactors. Accurate values of wavelengths and their errors are required for interpretation of a wealth of high-resolution data obtained in the last two decades by the Chandra X-ray Observatory and the European Space Agency's X-ray Multi-Mirror Mission [1].

As previously published [2, 3, 4, 5, 6], we continue to focus on He-like ions. Energy levels, wavelengths, weighted oscillator strengths, transition probabilities and lifetimes are calculated for all levels of $1s^2$ and $1snl$ ($n = 2 - 6$) configurations of He-like indium ion.

The calculations were carried out using the GRASP2018 code based on the multiconfiguration Dirac-Hartree-Fock (MCDHF) [7]. Transition probabilities are reported for all types of transitions ($E1$, $E2$, $M1$ and $M2$ transitions). Breit interactions and quantum electrodynamics effects are included in the RCI calculations. Comparisons were made with other data found in the literature and a good agreement was found which confirms the reliability of our results. We identified some new data that are calculated for the first time.

This computational approach enables us to present a consistent and improved data set of all important transitions of the In XLVIII spectrum, which are useful for identifying transition lines in further investigations.

RP

References

[1] V A Yerokhin and A Surzhykov, J. Phys. Chem. Ref. Data **48**, 033104 (2019).
[2] D E Salhi and H Jelassi, Canadian Journal of Physics **96**, 3 (2017).
[3] D E Salhi and H Jelassi, Orient. J. Phys. Sciences. **2**,2 (2017).
[4] D E Salhi, P Quinet and H Jelassi, Atomic Data and Nuclear Data Tables **126**, 70-157 (2019).
[5] D E Salhi, S Ben Nasr and H Jelassi, Radiation Physics and Chemistry **177**, 108817 (2020).
[6] D E Salhi, S Ben Nasr, S Manai, H Jelassi, Results in Physics **23**, 103960 (2021).
[7] C Froese Fischer, G Gaigalas, P Jönsson, J Bieron, Computer Physics Communications **237**, 184 (2019).

*E-mail: salhidhiaelhak@gmail.com

Nonresonant Coherent Population Transfer in Argon Rydberg Wavepackets

J. D. Gaynor[1,2], Y. Kobayashi[5], A. P. Fidler[1,2,4], Y.-C. Lin[1,2], C. Keenan[1,2,6], D. M. Neumark[1,2], S. R. Leone[1,2,3,†]

[1]Department of Chemistry, University of California, Berkeley, CA, 94720, U.S.A.
[2]Chemical Sciences Division, Lawrence Berkeley National Laboratory, Berkeley, CA, 94720, U.S.A.
[3]Department of Physics, University of California, Berkeley, CA, 94720, U.S.A
[4]Department of Chemistry, Princeton University, Princeton, NJ, 08544, U.S.A.
[5]SLAC National Accelerator Laboratory, 2575 Sandhill Road, Menlo Park, CA, 95024, U.S.A.
[6]Department of Chemistry, University of Chicago, Chicago, IL, 60637, U.S.A.

Synopsis Noncollinear attosecond four-wave mixing spectroscopy of Ar $3s^{-1}np$ Rydberg wavepackets are reported here. Emission from individual Rydberg states in the wavepacket have apparent lifetimes different from those that linewidth data and the n^3 proportionality would predict. The observations are understood by wave packet component analysis that shows coherent population transfer primarily from *(n+1)p* to *np* Rydberg states driven nonresonantly through *(n+1)s* and *(n-1)d* dark states during the four-wave mixing process.

RP

Coherently exciting a series of nondegenerate Rydberg eigenstates creates a non-stationary superposition of states known as a Rydberg wavepacket. Rydberg wavepacket dynamics are of fundamental and applied interest as convenient platforms for exploring coherent control and quantum information processing. Many efforts have sought to characterize [1], control and extend the lifetime of Rydberg wavepackets [2] in atomic gases. Precise atto- and femtosecond (fs) time-domain experiments are needed to characterize Rydberg wavepacket dynamics of lower principal quantum numbers and core-excited states.

We use attosecond four-wave mixing (FWM) spectroscopy to explore the wavepacket dynamics of an inner valence $3s^{-1}np$ autoionizing Rydberg series in Ar. An attosecond extreme ultraviolet (XUV) pulse excites the 3s electron into the *np* (n>3) autoionizing Rydberg series, creating a Rydberg wavepacket. Two few-cycle near-IR pulses, aligned noncollinearly with respect to the XUV excitation pulse, arrive temporally coincident with each other and controllably delayed from the XUV pulse to probe the evolution of the Rydberg wavepacket. The phase-matched FWM signal emits in a unique direction and is spectrally resolved. The time-resolved FWM emissions from different members of the Rydberg series in the wavepacket are analyzed and fit to a wavepacket model to decompose the amplitudes and phase of the superposition components.

† E-mail: srl@berkeley.edu

The *np* emissions decay on longer timescales than linewidth measurements of the $3s^{-1}np$ states indicate [3] and they do not follow the well-known n^3 proportionality for autoionizing Rydberg state lifetimes. For example, the 6p emission and analysis is shown in Fig. 1; the expected 6p lifetime is 52 fs, while the observed is ~200 fs. A reason is disclosed by the *np* emission being dominated by *(n+1)p* character. Calculations and time-dependent Shrödinger equation simulations reveal that coherent population transfer from the *(n+1)p* to *np* states is nonresonantly driven by the near-IR pulses, aided by *(n+1)s* and *(n-1)d* dark states.

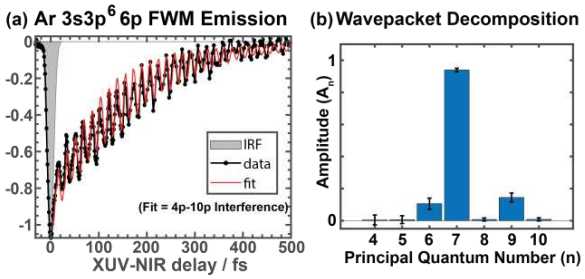


Figure 1. (a) Attosecond four-wave mixing emission from Ar $3s^{-1}$6p state reporting on wavepacket of autoionizing $3s^{-1}$np Rydberg states; instrument response (grey), data (black), wavepacket model fit (red) including Rydberg states 4p≤np≤10p. (b) Component amplitudes of the coherent superposition retrieved from wavepacket fit.

References

[1] Weinacht, T.C., *et al.*, 1998 *Phys. Rev. Lett.* **80** 5508.
[2] Ivanov, M.Y., *et al.*, 1997 *Chem. Phys. Lett.* **265** 231.
[3] Madden, R.P., *et al.*, 1969 *Phys. Rev.* **177** 136.

Development of a Time-Resolved Solid-State High-Harmonic Generation Spectrometer for Probing Ultrafast Dynamics in Strongly Correlated Materials

J. A. Spies[1,2,*], F. Kohrell[1,2], B. Nebgen[1,2], M. Zuerch[1,2]

[1]University of California at Berkeley, Department of Chemistry, 237 Hildebrand Hall, CA-94720 Berkeley, USA
[2]Lawrence Berkeley National Laboratory, Materials Sciences Division, 1 Cyclotron Road, CA-94720 Berkeley, USA

Synopsis Time-resolved solid-state high-harmonic generation (TR-sHHG) is an emerging table-top technique that enables the study of ultrafast electronic structural dynamics in materials. A TR-sHHG spectrometer was developed incorporating cryogenic temperature control and pump wavelengths ranging from UV to THz, well suited to study strongly correlated materials with coupled electronic, magnetic, and lattice degrees of freedom.

Strongly correlated materials (SCMs) are an emerging class of materials with unique coupled electronic, magnetic, and lattice degrees of freedom that have potential applications in energy as well as quantum computing and information [1]. Despite the high technological relevance, little is known about exploiting coupled degrees of freedom to reach new nonequilibrium phases with unique properties. Solid-state high-harmonic generation (sHHG) is a method that is well poised to study material properties (e.g., electronic and structural phase transitions, charge-spin couplings, etc.), electronic band structure, and symmetry in SCMs [2]. Coupling photoexcitation into sHHG experiments enables the measurement of ultrafast processes, providing insight into the nonequilibrium properties of SCMs. This technical contribution focuses on the development of a versatile instrument for performing time-resolved sHHG (TR-sHHG) at various excitation wavelengths, each well adopted to access different collective excitations resonantly, in a cryogenic environment tailored for studying coupled degrees of freedom in SCMs (Figure 1a).

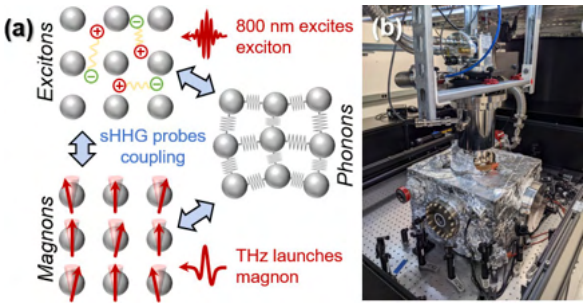


Figure 1. (a) Pump-probe of coupled collective excitations in a solid. (b) Cryogenic TR-sHHG spectrometer.

The TR-sHHG instrument (shown in Figure 1b) is built around a He cryostat capable of temperatures ranging from ~4-350 K. The sHHG probe is driven by a tunable mid-infrared (MIR) field (typically 3-5 μm, ~100 fs) with detection in the UV-visible range using a high-sensitivity spectrometer. Polarization optics for the MIR driver and sHHG emission enable polarization-resolved measurements for symmetry studies. The instrument currently incorporates an optical pump (800 nm, 400 nm, etc.) and a high-field THz pump (~0.2-5 THz bandwidth, peak at ~1 THz) generated by optical rectification in *N*-benzyl-2-methyl-4-nitroaniline (BNA) [3] is currently in development. The optical pump allows for selective excitation of electronic degrees of freedom (e.g., excitons) while the high-field THz pump allows for selective excitation of magnetic and lattice degree of freedom (e.g., magnons and phonons). The instrument is also versatile in that it can be easily reconfigured for traditional transient absorption measurements (e.g., using a white light continuum probe).

Initial measurements in commissioning focus on temperature-resolved studies of metal oxides and strongly correlated magnetic materials. Preliminary studies show the ability of cryogenic TR-sHHG to access the ultrafast dynamics of coupled collective excitations and their symmetry at temperatures where phenomena such as antiferromagnetic ordering occurs.

References

[1] J. Puebla, Commun. Mater. 1, 24, (2020)
[2] S. Ghimire, Nat. Phys. 15, 10, (2018)
[3] M. Shalaby, Opt. Lett. 41, 1777, (2016)

* E-mail: jacobaspies@berkeley.edu

RP

Measurement of nonlinear signal electric field from a femtosecond four-wave mixing interaction in molecules and materials

F Walz[1], S Pandey[1], and N Shivaram[1,2] *

[1]Department of Physics and Astronomy, Purdue University, West Lafayette, 47907, USA
[2]Purdue Quantum Science and Engineering Institute, Purdue University, West Lafayette, 47907, USA

Synopsis We measure the third order nonlinear response in molecules and materials, by fully reconstructing the temporal amplitude and phase of the emitted signal electric field. This is achieved by combining a spectral interferometry-based technique for measuring ultraweak femtosecond pulses, called TADPOLE, with Degenerate Four-Wave Mixing. The signal electric field measured as a function of real-time and time delay between the interacting pulses provides detailed information on ultrafast dynamics.

RP

The third-order nonlinear optical response, $\chi^{(3)}$ is a tensor quantity that, when measured in a time-resolved manner, can offer deep insight into the transient electronic character of a dynamically evolving system. The emitted signal electric field in a four-wave mixing nonlinear interaction, such as Degenerate Four-wave Mixing (DFWM), is directly related to the nonlinear response. Thus, a direct measurement of the signal electric field (amplitude and phase) provides complete information on the transient nonlinear response. In this work, we use the ultraweak femtosecond pulse reconstruction technique of TADPOLE [1] to measure the emitted nonlinear signal electric field from carbon dioxide and ethylene molecules and wide band-gap materials such as MgO and ZnO.

Near infrared pulses centered at 800 nm, with a pulse width of 50 fs and a repetition rate of 1 KHz are split to form the gate and probe pulses. The probe pulse is delayed with respect to the gate pulse using a delay stage. The gate pulse polarization can be rotated relative to the probe polarization. A reference pulse is derived from the probe pulse for spectral interferometry. The gate pulse is further split into two pulses with a mask and all three pulses are focused onto the target (gas cell or solid sample) with a lens. Spatial and temporal overlap are achieved using second harmonic generation in a beta barium borate crystal. After the interaction, the gate and probe beams are blocked by a second mask, allowing only the DFWM signal beam to pass. The signal is passed through a polarizer set parallel to the probe polarization. A reference pulse, completely characterized using Frequency Resolved Optical Gating is combined with the signal in a spectrometer to obtain the spectral interference measurement necessary for TADPOLE.

*E-mail: niranjan@purdue.edu

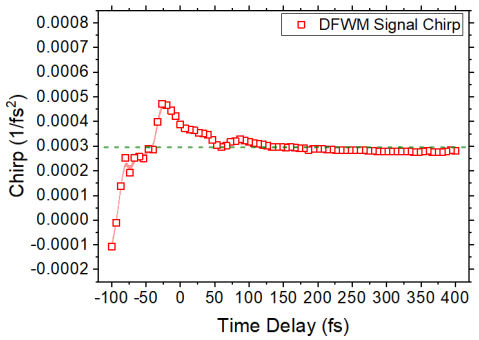


Figure 1. Chirp of the emitted nonlinear signal electric field from carbon dioxide molecules. Dashed line shows input probe chirp.

The amplitude and phase of the weak nonlinear signal electric field is obtained from the TADPOLE measurement as a function of time delay between the gate and probe pulses. Figure 1 shows the measured chirp of the signal electric field as a function of delay, in carbon dioxide molecules. We apply this approach to study materials such as MgO and ZnO as well as strong-field ionized ethylene molecules. Future extension of these measurements to systems excited by extreme-ultraviolet attosecond and femtosecond pulses can yield detailed information on ultrafast dynamics.

References

[1] D N Fittinghoff et.al, Opt. Lett. **21**, 884 (1996).

Laser-driven Bloch electrons in the almost-strong-field regime

A N Pfeiffer[1]*

[1] Institute of Optics and Quantum Electronics, Abbe Center of Photonics, Friedrich Schiller University, Max-Wien-Platz 1, 07743 Jena, Germany

Synopsis In HHG from solids, the electrons typically exceed the edge of the first Brillouin zone. In conventional nonlinear optics, the electron excursion is negligible. Here, the transition from conventional nonlinear optics to the almost-strong-field regime is investigated. The nonlinear optical response changes abruptly and begins to be dominated by the motion of Bloch electrons when the electron trajectories extend over about half of the first Brillouin zone, which is observed by an interference structure in the third-order harmonic generation of few-cycle pulses in a non-collinear geometry.

Two visible-infrared (Vis-IR) pulses A and B are focused into 100-μm-thick crystals. Deep ultraviolet (DUV) light is produced by third-order harmonic generation (THG). The DUV light that is emitted collinearly to A, which is kept at a constant intensity $I_A = 7\,\mathrm{TW/cm^2}$, is detected with a spectrometer. The intensity of B is varied in the range $I_B = [0,\ 8]\,\mathrm{TW/cm^2}$, which varies the peak intensity $I_{peak} = \left(\sqrt{I_A} + \sqrt{I_B}\right)^2$ in the grating. The nonlinear optical response changes abruptly and begins to be dominated by the motion of Bloch electrons when the electron trajectories extend over about half of the first Brillouin zone, which is observed by an interference structure in the THG.

Numerical calculations are performed using semiconductor Bloch equations (SBEs) and the unidirectional pulse propagation equation (UPPE). $P^{(\mathrm{NL})}$ exhibits an interference structure in the relevant intensity range. Although approaching Keldysh parameter $\gamma = 1$, this is not a strong-field effect in the original sense, because the iterative series [1] still converges and reproduces the interference structure. With the Bloch electron motion turned off in a simplified calculation, the interference structure disappears. For lower intensities, the calculations with and without Bloch electron motion agree perfectly. Thus, Bloch electron motion can be neglected at moderate intensities. Moreover, the instantaneous response $P^{(\mathrm{NL})} = \chi^{(3)}E^3$ is a very good approximation for these intensities. In the almost-strong-field regime, the THG intensity deviates from the instantaneous response model for both calculations with and without Bloch electron motion. However, only the full calculation generates the interference structures.

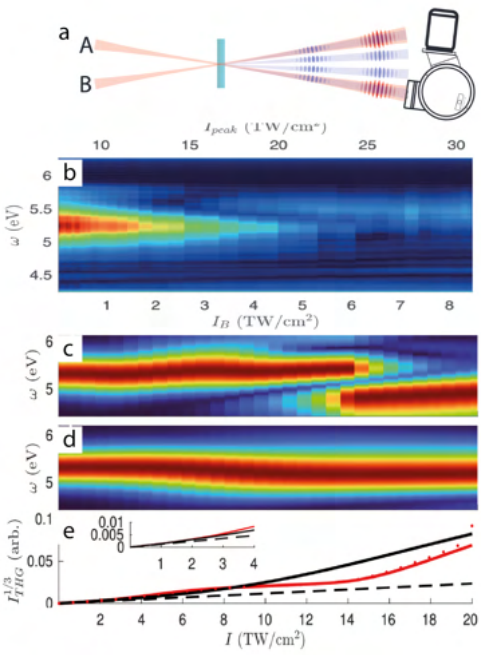


Figure 1. **a**, Setup. **b**, Fourier filtered spectrum of SiO2. $P^{(\mathrm{NL})}$ calculated with (**c**) and without (**d**) Bloch electron motion. **e**, The total THG intensity with (red solid) and without (black solid) Bloch electron motion, iterative calculation (red dotted), instantaneous response (black dashed).

References

[1] A N Pfeiffer, J. Phys. B **53**, 164002 (2020).

*E-mail: a.n.pfeiffer@uni-jena.de

RP

Carrier-Envelope Phase Dependent Harmonics in Solids using a Few-Cycle IR Pulse

H Allegre[1] *, J Turner[1], K Kowalczyk[1], A Pettipher[1], M Matthews[1] and J W G Tisch[1]

[1]Extreme Light Consortium, Imperial College London, SW7 2AZ London

Synopsis We study the carrier envelope phase dependence of high harmonic generation in SiO2 with a few cycle IR pulse. The intensity of the carrier envelope phase stable (CEP) driving field is varied along the value of the CEP and the pulse duration in order to understand the dependence of those parameters. The dependence on the material is also studied.

RP

High Harmonic Generation (HHG) is the phenomenon that enables attosecond metrology and Extreme UV generation More recently it has been studied to understand the ultrafast electon dynamics of solids, band structure and measure valance orbital size [1].

The waveform of the driving field can be controlled through the carrier envelope phase (CEP) setting. Understanding the dependence of the high harmonic spectrum in solids on the CEP is important for understanding the electron dynamics on an ultrafast scale [2].

It has been shown that changing the CEP of the driving field has a direct effect on the generated harmonics, mostly leading to a shift in frequency [3] but we do not fully understand yet the physical origin of the effects. Two pictures are considered for now, the interband and the intraband processes [4]. In one picture, harmonics come from the interband polarization whereas in the other, the intraband currents are responsible for the emission of photons. The variation of the harmonics with the CEP could prove one of the two mechanisms is dominant as it would mean that the harmonics are time-dependent and present an atto-chirp [5].

The goal of this study is to understand better how the shape of the sub-cycle field can affect the harmonics detected and what parameters influence this change.

We investigate solid HHG in wide band gap dielectrics with a CEP stable driving field, generated by a Ti:Sapphire laser.

A few-cycle pulse generated in a differentially pumped hollow core fibre is focused on a SiO2 sample to generate harmonics. The pulse duration is 4fs at 800 nm. Data will be presented showing spectra for different intensities, CEP values, crystal orientation and pulse duration.

The high harmonic vacuum chamber is composed of a 1 m focal lens that focuses the beam on the solid target. The harmonics generated in the solid go through a slit and are directed to a grating and onto an MCP (Figure 1). The intensity scan is done by monitoring an electronic iris before it is focused.

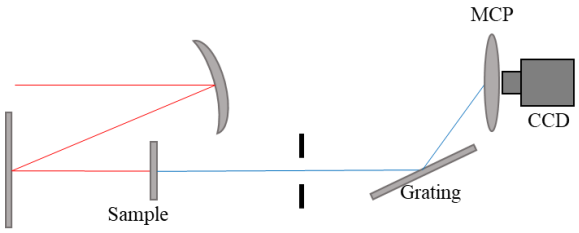


Figure 1. Diagram of the setup generating harmonics in a SiO2 sample.

References

[1] S. Ghimire and D. A. Reis 2019 *Nat. Phys.* doi: 10.1038/s41567-018-0315-5

[2] O. Schubert *et al.* 2014 *Nature photonics* doi: 10.1038/nphoton.2013.349

[3] Y. S. You *et al.* 2017 *Nat. Commun.* doi: 10.1038/s41467-017-00989-4

[4] T. T. Luu *et al.* 2015 *Nature* doi:10.1038/nature14456

[5] Y. S. You *et al.* 2017 *Optics Letters* 1816-1819 285934

* E-mail: hea20@ic.ac.uk

Passively phase-locked 2 mm intense few-cycle optical parametric amplifier at 100 kHz repetition rate

T. Kurihara*, T. Yang, T. Mizuno, T. Kanai, and J Itatani

Institute for Solid State Physics, The University of Tokyo, 5-1-5 Kashiwanoha, Kashiwa, Chiba, 277-8581, Japan

Synopsis Optical parametric amplifier around 1.8 – 2.4 μm spectral region is developed based on Yb:KGW laser system. Intrapulse difference frequency generation from a stable supercontinuum results in carrier-envelope stable mid infrared pulses. Subsequent two-stage parametric amplification by BiB_3O_6 (BiBO) crystals achieves pulse energy of 30 μJ. By transmission through dispersive materials and reflection by chirped mirror pair, the output pulses are compressed down to 22 fs.

High-harmonics generation (HHG) in gasses has been established in the last decades as an ultrafast (sub-fs) source of highly coherent radiation in the region of extreme ultraviolet to the soft X-ray. Its cut-off energy E_c is known to depend strongly on the wavelength of the driving laser as $E_c \propto \lambda^2$. Previously, generation and transient spectroscopy in the water window region of soft X-ray (~400 eV) has been demonstrated using near-infrared (NIR) pulses around 1.5 μm [1]. To achieve even higher photon energies, development of a laser source in the mid-infrared (MIR) is critically important.

In this work, we develop a mid-infrared optical parametric amplifier (OPA) with broadband mid-infrared in the 2 μm region. The system is based on a commercial Yb:KGW system (Carbide, Light Conversion) with central wavelength of 1030 nm, pulse energy of 400 μJ, pulse duration of 290 fs and repetition rate at 100 kHz. Part of the beam is split and focused on a $Y_2Al_5O_{15}$ (YAG) crystal with a thickness of 5 mm to generate supercontinuum spanning from 550 nm to 1400 nm. Spectral components around 650-750nm are temporally overlapped with the fundamental 1030 nm part by a broadband chirped mirror pair. They are injected into a 0.5 mm-thick BiBO crystal, resulting in difference-frequency generation of a passively carrier envelope-phase locked mid-infrared around 1.6-2.5 μm. The Generated MIR seeds the subsequent OPA stages. Both stages consist of 3 mm-thick BiBO that exhibits type-I phase matching (signal (o) + idler (o) = pump (e)). In the first stage, pumping at 1030 nm with 70 μJ pulse energy at a slightly noncollinear geometry, the seed is amplified up to 1 μJ with a high gain (10^4~10^5). The second stage is featured by a lower gain and a high conversion efficiency. Pumping with 270 μJ, the pulse energy is boosted to approximately 30 μJ.

The output spectrum from the second OPA stage is shown in Fig. 1, covering a broadband 1800 nm – 2500 nm range due to the near-degenerate amplification condition. After the amplification, the pulses are temporally compressed by transmission through dispersive media (silicon and CaF_2 plates). The remaining third-irder dispersion is compensated by reflections on a pair of chirped mirror pair. Characterization by second-harmonic frequency-resolved optical gating (SH-FROG) reveals the pulse duration after compression to be approximately 22 fs, corresponding to sub 4-cycle oscillation of electric field.

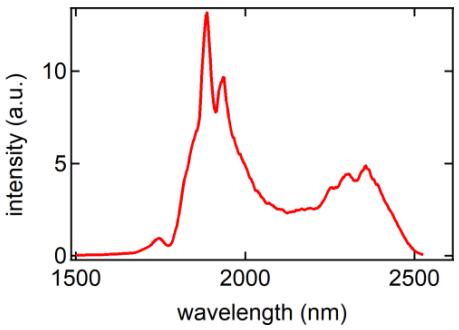


Figure 1. Spectrum of the MIR pulse output from the developed Yb:KGW-based 2-stage BiBO-OPA.

References

[1] N. Ishii, et *al*, Nat. Commun. **5**, 3331 (2014).

* E-mail: takayuki.kurihara@issp.u-tokyo.ac.jp

RP

Generation of annular few-cycle pulses by self-compression and spatial filtering in solid thin plates

X X Zhu[1,2] ,Y T Gao[1,2] , Y B Su[1,4] , S Y Xu[1,4] , K Zhao[1,3] * , S B Fang[1,2] , J F ZHU[4] and Z Y Wei[1,2,3] †

[1]Beijing National Laboratory for Condensed Matter Physics, Institute of Physics, Chinese Academy of Sciences, Beijing 100190, China
[2]Department of Physics, University of Chinese Academy of Sciences, Beijing 100049, China
[3]Songshan Lake Materials Laboratory, Dongguan 523808, China
[4]School of Physics and Optoelectronic Engineering, Xidian University, Xi'an 710071, China

Synopsis Annular-shaped few-cycle pulses are generated by 40fs laser pulses propagating through 6 solid thin plates in experiments as well as in numerical simulations. The generation of such pulses takes advantage of the conical emission caused by plasma effect, which introduces continuously varying off-axis plasma density along the radial direction of the propagating beam. The negative dispersion induced by the plasma causes the pulse at particular radial location to be self-compressed and to form an annular beam of short pulse, which can be extracted simply by spatial filtering. Meanwhile, we obtain a higher compression ratio indicating that the scheme of solid thin plates has the flexibility to regulate the laser intensity so as to plasma density. This method has great potential in high-power few-cycle pulse generation.

RP

Self compression is often reflected in the transmission of femtosecond laser in nonlinear materials [1]. The self compression effect can simplify the pulse compression process and facilitate the generation of high-energy short pulses. However, the formation of self compression effect involves a complex nonlinear process. Therefore, the control of self compression effect is more difficult, especially when the negative dispersion is only introduced by plasma.

In this work, the stable formation of ring femtosecond few period pulses in the group of solid sheets of normal dispersive materials is realized by spatial filtering. The principle is to use the conical radiation caused by the plasma effect. The conical radiation makes the plasma density change continuously along the radial direction of the propagating beam, and the negative dispersion caused by the plasma effect makes the pulse at a specific radial position self compress to form an annular short pulse beam. The spatial filtering operation in the off-axis region avoids the pulse splitting phenomenon caused by the nonlinear dispersion mismatch in the central region of the beam. In addition, using the unique advantages of the solid sheet group structure, we regulate the introduction of plasma density in the propagation process, so as to accurately change the introduction of negative dispersion. In the experiment, a few period pulse as short as 8.8 fs was generated under the pulse injection of 40 fs, and the shortest 5.0 fs pulse was obtained in the simulation. Our work shows a method that can stably generate periodic self compression pulses, and realizes the regulation of ionization in the self compression of solid materials for the first time. It has great potential in the generation of high-power few periodic pulses and subsequent attosecond pulses.

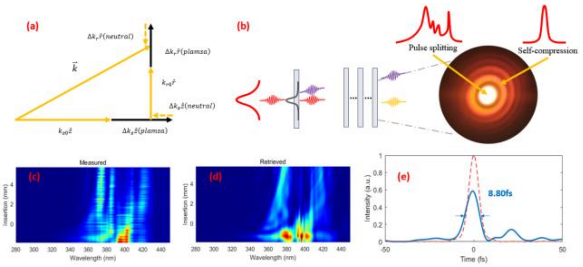


Figure 1. (a) wave vector distribution, (b) schematic diagram, (c) (d) trace diagram of experimental measurement, and (e) time domain of experimental measurement pulse based on self compression of sheet group

References

[1] J. C. Travers, et al., High-energy pulse self-compression and ultraviolet generation through soliton dynamics in hollow capillary fibers, Nat. Photonics. 2019, 13, 547.

* E-mail: zhaokun@iphy.ac.cn
† E-mail: zywei@iphy.ac.cn

Elucidating the Role of Surface States Through High-Harmonic Generation (HHG) Spectroscopy

I. Tigges-Green[1]*, S. Biswas[1], N.M. Fasano[2], M.R. Edwards[3], N. Karpowicz[4], G.D. Scholes[1] and J.M. Mikhailova[2]†

[1]Department of Chemistry, Princeton University, Princeton 08544, USA
[2]Department of Mechanical and Aerospace Engineering, Princeton University, Princeton 08544, USA
[3]Lawrence Livermore National Laboratory, Livermore, 94551, USA
[4]Max Planck Institute of Quantum Optics, Garching, 85748, Germany

Synopsis HHG spectroscopy offers the opportunity to understand material properties at the level of electrons in the solid state. Here, we investigate the HHG from sapphire and Ti:sapphire in both reflection and transmission geometry to understand the relationship between the localized states (i.e. surface state) and HHG processes. This approach promises to reveal insights for the use of sapphire as a table-top extreme ultraviolet source.

RP

Solid-state HHG has emerged in the last few years as a new frontier to probe sub-femtosecond phenomena in condensed matter systems. In the non-perturbative regime, high harmonic generation in solids occurs from inter- and intra-band current [1]. However, the role of bulk states versus surface states contribution to harmonic generation is an open question. Recently, it has been shown that harmonics are predominantly generated from the localized surface states from bulk crystals [2]. However, while 2nd harmonic generation from surface nonlinearities has been observed, it is unclear whether 4th order harmonics can be generated from these surface states [3]. The surface electronic structure is different from the bulk electronic structure, so high harmonics generated from the surface region imprints a unique surface electronic structure. This question will be addressed by studying low-order harmonics (up to 4th order) in both the transmission and reflection geometries of n-doped and undoped sapphire by conducting intensity and polarization dependent scans.

The experiments are carried out with 25-30 fs laser pulses at the central wavelength λ =800nm focused to intensities of about 10^{12} W/cm^2. A schematic of the experimental setup is shown in Fig. 1. The far field beam profiles of light reflected and transmitted through a solid sample are simultaneously imaged by fused silica lenses onto the VUV camera positioned after the fused silica viewport of the experimental vacuum chamber with an appropriate band-pass filter in front of the camera. The polarization state and its angle of incidence on a solid sample are varied in experiments.

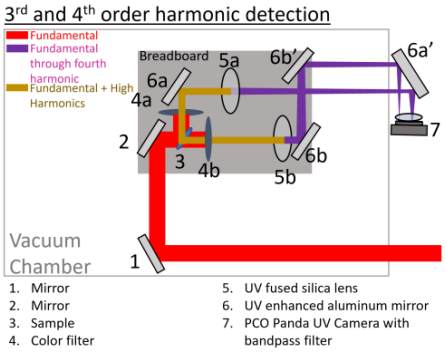


Figure 1. Harmonic detection schematic in reflection (optics labeled with "a") and transmission (optics labeled with "b") geometries.

Conducting these experiments on doped and undoped sapphire may additionally reveal the effect of doping on the harmonic yield and whether doping affects the harmonic generation at the near surface region, therefore bridging the gap between attosecond and surface sciences.

References

[1] Ghimire S *et al. 2018 Nat. Phys.* 10.1038/S41567-018-0315-
[2] Seres J *et al.* 2018 *arXiv preprint arXiv:1805.00388*
[3] Guyot-Sionnest P *et al.* 1988 *Phys. Rev. B.* 10.1103/PhysRevB.38.7985

* E-mail: it6@princeton.edu
† E-mail: j.mikhailova@princeton.edu

Few-cycle short-wave infrared pulse generated via bulk compressions

T C Truong[1], J E Beetar[1], and M Chini[1,2] *

[1]Department of Physics, University of Central Florida, Orlando, FL, 32816, USA
[2] CREOL, the College of Optics and Photonics, University of Central Florida, Orlando, FL, 32816, USA

Synopsis Sources of high-energy, few-cycle pulses in the short-wave infrared (SWIR) are desirable for isolated soft x-ray attosecond pulse generation. Here, we exploit red-shifted supercontinuum generation of laser pulses from a Yb:KGW amplifier in an N_2O-filled hollow-core fiber to generate nearly octave-spanning SWIR supercontinuum spectra which can be compressed using only bulk materials. By separately compressing, and then recombining, the short- and long-wavelength spectral regions, we synthesize sub-two-cycle pulses centered at 1.4 μm wavelength.

RP

Measuring electron dynamics in matter requires attosecond pulses, which can be produced via high harmonic generation (HHG). In HHG, longer driving laser wavelengths are desirable for generating attosecond pulses in the soft x-ray region, due to the cut-off scaling with the square of the wavelength. However, the mainstream long-wavelength sources based on optical parametric amplification followed by nonlinear compression or optical parametric chirped-pulse amplifier, are necessarily more complex than more conventional femtosecond laser amplifiers. Here, we demonstrate a simple, low-cost two-channel field synthesizer capable of generating sub-two-cycle pulses in the SWIR directly from Yb-doped laser amplifiers. The concept relies upon red-shifted supercontinuum generation in a molecular gas-filled fiber [1, 2], and separate compression of the short- and long-wavelength components. The setup uses off-the-shelf optical components for wavelength separation and recombination, and compression is achieved by linear propagation in bulk materials.

Broad bandwidth spectra (~1.05-2.0 μm) were obtained by propagating pulses from a Yb:KGW laser amplifier in an N_2O-filled hollow-core fiber. The red-shifted supercontinuum, caused by the rotational nonlinear response of the molecular gas [1], has a negative chirp on the leading edge of the pulse which can be compressed by the normal dispersion of bulk materials [2]. Due to the lack of materials with suitable dispersion properties, the output spectrum was split into two spectral regions for compression, and then recombined, using dichroic mirrors. The short wavelength region (<1.5 μm) was compressed by positive dispersion of the two dichroic mirrors and CaF2 glass, while the long-wavelength region (>1.5 μm) was compressed by fused silica. The amplitudes of the two arms were adjusted to obtain the shortest pulses. Finally, frequency-resolved optical gating (FROG) was used to characterize the synthesized pulses. Fig. 1 shows the measured and retrieved FROG traces for the synthesized pulses with optimal temporal overlap. The retrieved pulse has 7.5 fs FWHM pulse duration, below two optical cycles at the central wavelength of 1.4 μm.

In conclusion, we demonstrate a simple few-cycle pulse synthesizer in the SWIR, which has the potential for scaling the high harmonic cutoff to higher frequencies. Due to limitations of the spectral broadening caused by thermal excitation of the gas [3], we believe the synthesizer platform is best suited to compressing moderately high-energy pulses with repetition rate below 1kHz.

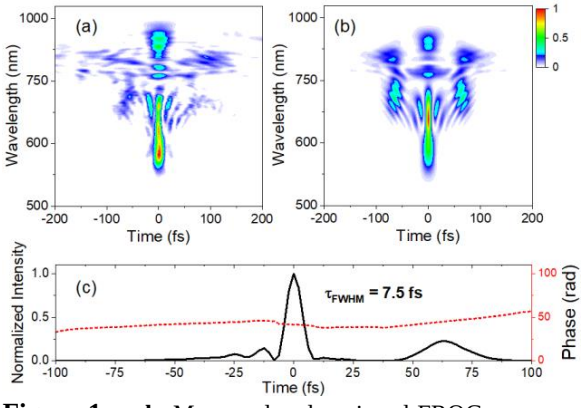


Figure 1. a, b, Measured and retrieved FROG traces; **c,** Calculated temporal intensity and phase.

References

[1] Beetar J E *et al* 2020 *Sci. Adv.* **6** eabb5375
[2] Safaei R *et al* 2020 *Nat. Photonics* **14** 733
[3] Beetar J E *et al* 2021 *Opt Lett* **46** 2437

* E-mail: michael.chini@ucf.edu

Carrier-envelope phase effects in high harmonic generation from thin-film ZnO

Y Liu[1], C Cabello[1], T Journigan[1], S N Berriel[2], T C Truong[1], DS Khatri[1], P Banerjee[2], and M Chini[1,3] *

[1]Department of Physics, University of Central Florida, Orlando FL 32816
[2]Department of Materials Science and Engineering, University of Central Florida, Orlando FL 32816
[3]CREOL, the College of Optics and Photonics, University of Central Florida, Orlando FL 32816

Synopsis We generate high-order harmonics from 30-nm ZnO films using carrier-envelope phase-stable few-cycle mid-infrared laser pulses. When the driving laser pulse duration is close to two optical cycles, even harmonics are observed due to the field asymmetry and the high-order harmonic spectra display a strong dependence on the carrier-envelope phase. By analyzing the carrier-envelope phase-dependent intensity of each harmonic, we find that the modulation phases of odd and even harmonics follow different trends.

High-order harmonic generation (HHG) driven by few-cycle pulses in solids has provided a new platform for studying laser-driven electron dynamics in condensed matter systems [1] and generating isolated attosecond pulses [2]. Here, we use carrier-envelope phase (CEP) stabilized few-cycle mid-infrared (mid-IR) pulses to generate HHG in a thin film c-plane ZnO. When the pulse duration approaches two optical cycles in duration, both odd and even harmonics are generated due to the asymmetry of the driving laser electric field. By varying the CEP of the driving pulses, a clear CEP dependence of both odd and even harmonics is observed.

In the experiments, CEP-stable few-cycle mid-IR pulses are generated by nonlinear compression of multi-cycle mid-IR pulses from an optical parametric amplifier, and characterized using a newly developed single-shot waveform measurement technique [3], as shown in Fig. 1a. After transmitting through a pair of CaF_2 wedges, the pulses are then focused (f = 50 mm) onto a 30-nm thick epitaxial ZnO film, deposited on a c-plane Al_2O_3 substrate using plasma-assisted atomic layer deposition, to generate high-order harmonics. After transmitting through the ZnO, high-order hamonic spectra in the visible and ultraviolet are measured by using a grating spectrometer. While only odd harmonics are observed for multi-cycle drivers, even harmonics appear for compressed pulse durations below ~2.5 optical cycles. By varying the CEP, a clear CEP dependence of the high harmonics spectrum is observed, as shown in Fig. 1b. We find that each harmonic exhibits a periodic intensity modulation with π periodicity. The intensity modulations for odd and even harmonics are plotted separately, as shown in Fig. 1c and d. We observe distinct phase shifts between the neighboring harmonics, with different behavior for odd and even harmonics.

In conclusion, we observe CEP dependence in the high-order harmonics generated by few-cycle mid-IR pulses in epitaxial ZnO films. By varying the CEP, a strong CEP dependence of high harmonic spectra is measured.

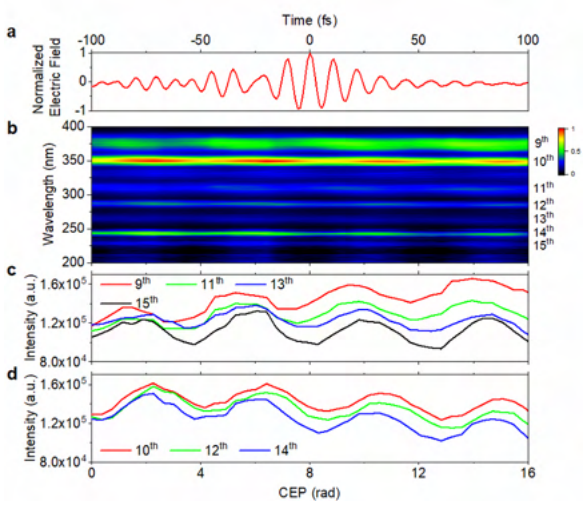


Figure 1. a Driving laser waveform; **b** CEP-dependent high-order harmonic spectra; CEP-dependent intensity modulations of **c** odd and **d** even harmonics.

References

[1] You Y *et al* 2017 *Opt. Lett.* **42** 1816
[2] Garg M *et al* 2016 *Nature* **538** 359
[3] Liu Y *et al* 2022 *Nat. Photonics* **16** 109

* E-mail: michael.chini@ucf.edu

RP

Elliptically Polarized and Structured Harmonics in Reflection from Plasma Mirrors

N M Fasano[1 *], M R Edwards[2], J M Mikhailova[1 †]

[1]Department of Mechanical and Aerospace Engineering, Princeton University, Princeton, 08544, USA
[2]Lawrence Livermore National Laboratory, Livermore, 94551, USA

Synopsis Plasma mirrors have the potential to produce the most powerful harmonic emission from petawatt lasers. Tailoring laser polarization and spatial structure can generate elliptically polarized and vortex harmonics in relativistic laser-solid interactions. Potential applications of these harmonics include probing the spin-resolved features in magnetic materials and molecular chirality on a sub-femtosecond timescale. In this work, we experimentally study the polarization state and spatial properties of harmonics emitted from interactions of elliptically polarized and structured lasers with solids.

RP

Ultrafast extreme ultraviolet sources of radiation with controlled polarization and spatial structure are of great interest for several chirality-sensitive light-matter interactions. One approach for realizing powerful harmonic emission and attosecond light pulses with a tunable polarization and spatial structure is through the process of relativistic high harmonic generation from plasma mirrors [1-3].

In this work, we use a combination of experimental and numerical techniques to characterize harmonics emitted from plasma mirrors driven by elliptically polarized lasers. To model the interaction that we expect under experimental conditions, two-dimensional particle-in-cell simulations were carried out. Figure 1 shows the ellipticity of the first four harmonics as a function of the fraction of energy contained in the s-polarized component of the driving laser, I_S/I_L. Here we can see that there are two regimes where one can produce circularly polarized harmonics. One is when the driving laser is nearly circularly polarized, and the second is when the driving laser is nearly s-polarized. The inset shows more closely the region where the driving laser is circularly polarized, illustrating that not all harmonics are simultaneously circularly polarized for the same ellipticity of the driving laser.

The experimental set-up to realize this polarization-controlled harmonic source uses the 20TW Ti:Sapphire laser system at Princeton University which provides 25fs pulses centered at 800nm with pulse energy that is tunable between 10-400mJ. The laser is focused to intensities above 10^{19} W/cm^2 onto a glass target at 45° angle of incidence. A quarter waveplate located before the focusing optic will be used to tune the ellipticity of the driving laser. The reflected harmonics generated on the surface of the solid target are then analyzed for divergence, spatial structure, and ellipticity.

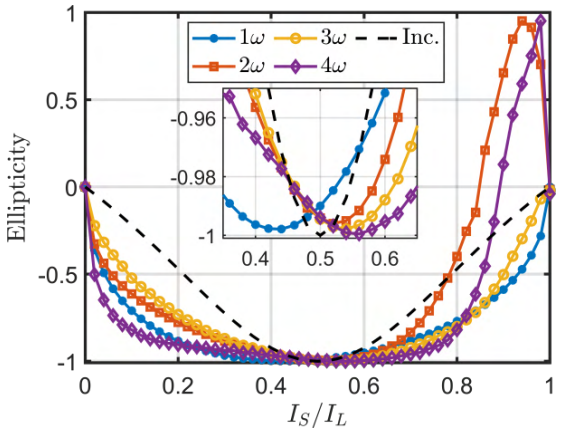


Figure 1. Ellipticity of the first four reflected harmonics as a function of the fraction of energy contained in the s-polarized component of the driving laser. The ellipticity is defined so that a value of ±1 is circularly polarized light. Inset: A zoomed in view of the region where the driving laser is nearly circularly polarized.

References

[1] Edwards M R *et al* 2020 *Sci. Rep.* **10** 5154
[2] Chen Z Y *et al* 2016 *Nat. Commun.* **7** 12515
[3] Denoeud A *et al* 2017 *Phys. Rev. Lett.* **118** 03390

* E-mail: nfasano@princeton.edu
† E-mail: j.mikhailova@princeton.edu

Symmetry Effects in Carrier-Envelope Phase-Dependent Harmonics from ZnO

T Journigan[1], Y Liu[1], C Cabello[1], D S Khatri[1], T C Truong[1], and M Chini[1,2*]

[1]Department of Physics, University of Central Florida, Orlando, Florida, 32816, USA
[2]CREOL, the College of Optics and Photonics, University of Central Florida, Orlando, Florida, 32816, USA

Synopsis We study the carrier-envelope phase (CEP) dependence of high-order harmonics generated in bulk a-plane and c-plane ZnO crystals. The CEP dependences measured for laser polarization oriented parallel to and perpendicular to the c-axis exhibit different periodicities, due to the structural symmetries of the crystal. Furthermore, we observe deviations from the CEP dependences expected from inter- and intra-band currents, which we attribute to nonlinear spectral broadening and self-compression of the driving laser in the bulk ZnO.

High-order harmonic generation (HHG) in solids is an attractive new platform for spectroscopy in condensed matter systems. Previously, we showed that the spectrum and polarization states of harmonics can yield information on symmetry properties of the crystal [1], while electron dynamics have been inferred from delay-dependent measurements in two-color fields [2], intensity-dependent interferometry [3], and carrier-envelope phase (CEP) dependent harmonic spectra [4]. In bulk crystals, however, the microscopic physics can be obscured by nonlinear propagation effects [3, 5]. Here, we study the dependence of the harmonics generated in bulk ZnO crystals on the CEP of the driving laser. While some observations, such as different CEP periodicity for laser polarization along or perpendicular to the ZnO c-axis, align with expectations based on crystal symmetry, we also observe anomalous behavior such as strong CEP dependence for chirped driving pulses and harmonic shifts that contrast with previous measurements.

In the experiments, CEP-stable mid-infrared pulses with central wavelength of 3.4 μm, pulse energy of 10 μJ, and pulse duration of 90 fs are generated by a Yb:KGW-pumped optical parametric amplifier. The pulses are compressed to few-cycle durations using self-compression in a combinaton of thin YAG and Si windows. We focus the few-cycle pulses onto bulk ZnO crystals and detect the harmonic spectra in a transmission geometry. The carrier-envelope phase is controlled using a pair of glass wedges.

In Fig 1, we show the CEP dependence of harmonics generated with laser polarization perpendicular (a) and parallel (b) to the ZnO c-axis. We observe a strong modulation of the harmonics with π periodicity when the laser is polarized perpendicular to the c-axis, and with 2π periodicity for polarization along the c-axis. This behavior is due to the symmetry breaking for electron trajectories driven along the c-axis.

We further observe CEP-dependent shifts in the harmonic frequency. Such shifts have previously been used as evidence for HHG from interband polarization, with the slope of the CEP dependent harmonic energy giving information about the electron trajectories. Prior results in MgO indicate that CEP slope increases with emitted photon energy [4]. In our results, however, the slope of harmonic energy with CEP decreases at short wavelengths. Moreover, the strongest CEP dependence is observed for negatively chirped, multi-cycle driving laser pulses. Preliminary simulations suggest that these effects are likely due to nonlinear propagation effects in the bulk crystal.

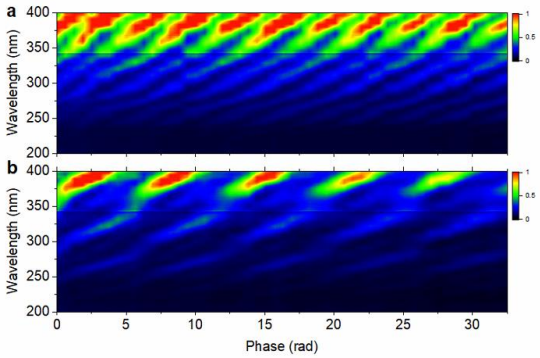


Figure 1. CEP dependence for laser polarization **a** perpendicular to and **b** parallel to the c-axis of ZnO.

References

[1] S. Jiang *et al* 2019 *J. Phys. B* **52** 225601
[2] G Vampa *et al* 2015 *Nature* **522** 462
[3] J Lu *et al* 2019 *Nature Photon.* **13** 96
[4] Y You *et al* 2017 *Opt. Lett.* **42** 1816
[5] P Xia *et al* 2018 *Opt. Express* **26** 29393

* E-mail: Michael.Chini@ucf.edu

RP

Measuring the non-linear susceptibility of a semiconductor by polarization resolved high-order harmonic generation spectroscopy

D Facciala[1*], A Annunziata[1,2], N Tancogne-Dejean[3], A Pusala[1], E Cinquanta[1], G Crippa[1,2], M Devetta[1], G Isella[2], M Bollani[1], U De Giovannini[3], H Huebener[3], A Rubio[3], S Stagira[1,2] and C Vozzi[1]

[1]Istituto di Fotonica e Nanotecnologie, Consiglio Nazionale delle Ricerche, Milano, 20133, Italy
[2]Dipartimento di Fisica, Politecnico di Milano, Milano, 20133, Italy
[3]Max Planck Institute for the Structure and Dynamics of Matter, Center for Free Electron Laser Science, Hamburg, 22761, Germany

Synopsis We studied the non-linear response of a germanium semiconductor under strong-field excitation. We measured the polarization of the high-order harmonic spectrum as a function of the orientation of the crystal, demonstrating the generation of elliptically polarized harmonics using a linearly polarized driving field. Through this angle-resolved and polarization-resolved measurement, we are able to investigate the role of high-order susceptibility in the non-linear process.

RP

High-order harmonic generation (HHG) has been successfully applied to study the band structure [1] and non-linear dynamics [2] of solids, demonstrating the flexibility of this investigation technique as a spectroscopic tool.

We studied the HHG response of n-doped (001) Germanium to an intense linearly polarized (p-pol) 3.2 μm field. The angle of incidence of the driving field was π/4, and harmonics up to the 11th order were observed in reflection. We characterized the polarization state of harmonics H3, H5, and H7 as a function of the crystal axis angle γ. The parameters of the polarization ellipse are shown in Fig. 1 (dots).

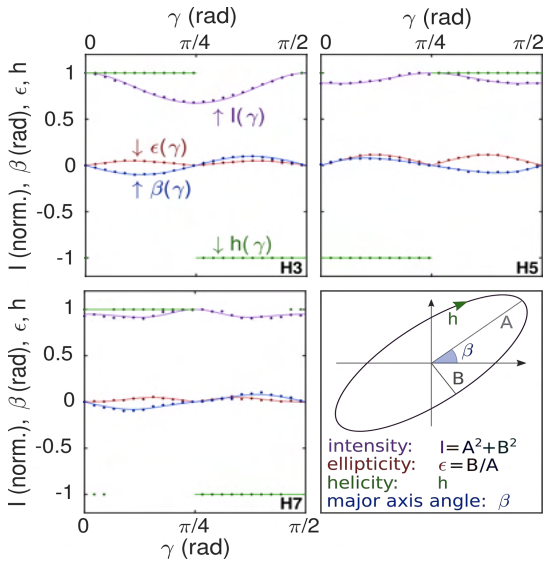


Figure 1. Polarization ellipse parameters (defined in the lower-right panel) for H3, H5, H7 as a function of γ.

We observed elliptically polarized HHG from a linearly polarized driving laser field, where the degree of ellipticity ϵ can be controlled by changing γ. We fitted our results taking into account, for the q[th] harmonic, the contributing non-linear susceptibility $\chi^{(n)}$ terms up to the order n=q+4. The fit is overlaid in Fig.1 (solid lines). For H3, we report the fitted χ terms in Table 1. The presence of high order complex terms indicates that elliptically polarized harmonic generation originates from the non-perturbative excitation.

Table 1. Susceptibility parameters, normalized to $\chi_{0,0}^{(3)}/I_0^{(n-3)}$, with I_0 being the intensity of the fundamental field. For the naming convention, see [3].

$\chi_{2,0}^{(3)}$	$\chi_{0,0}^{(5)}$	$\chi_{2,0}^{(5)}$
0.158	$1.11\cdot10^{-3}$	$2\cdot10^{-3}$
$\chi_{0,0}^{(7)}$	$\chi_{2,0}^{(7)}$	$\chi_{4,0}^{(7)}$
$-1.11\cdot10^{-2}$	$2.2\ i\cdot10^{-3}$	$(5+4i)\cdot10^{-4}$

These results can be exploited for generating harmonics with tunable polarization states, and pave the way towards the full characterization of the high-order non-linear response of the medium. This investigation is currently under way.

References

[1] Vampa G *et al* 2015 *Phis. Rev. Lett.* **115** 193603
[2] Klemke N *et al* 2019 *Nat Commun.* **10** 1319
[3] Zavelishko V I *et al* 2017, *Sov. J. Quantum Electron.* **5** 1392

* E-mail: davide.facciala@cnr.it

Strong-field photoelectron emission of plasmonic nanoparticles

U Thumm[1]*, E Saydanzad[1], J Powell[1,2], and A Rudenko[1]

[1]Department of Physics and J. R.Macdonald Lab., Kansas State University, Manhattan, KS 66506, USA
[2]INRS, Énergie, Matériaux et Télécommunications, 1650 Bld. Lionel Boulet, Varennes, Québec, J3X1S2, Canada

Synopsis Our numerical simulations demonstrate (A) the distinct influence of photoelectron (PE) correlation, residual-charge accumulations, and plasmonic near fields on photoelectron momentum distributions and (B) much larger PE cutoff energies as compared to gaseous atomic targets.

We measured [1] and numerically simulated [2] velocity-map-imaging (VMI) maps resulting from the strong-field PE emission of metal nanoparticles (NPs) by intense infrared laser pulses. Our semi-classical model consists of two distinct steps: (i) PE release by tunneling induced by an intense IR laser pulse and (ii) classical PE propagation to the detector within a trajectory sampling approach [3], distinguishing the effects of PE correlation, PE - residual-charge interactions, PE rescattering and recombination, and transient laser-induced plasmonic fields. By comparing our experimental and numerical results for 5, 30, and 70 nm diameter gold nanospheres and peak laser-pulse intensities of 8×10^{12} and 1.2×10^{13} W/cm^2, we showed how VMI maps are distinctly shaped by PE Coulomb repulsion, residual-charge accumulations, and plasmonic near fields.

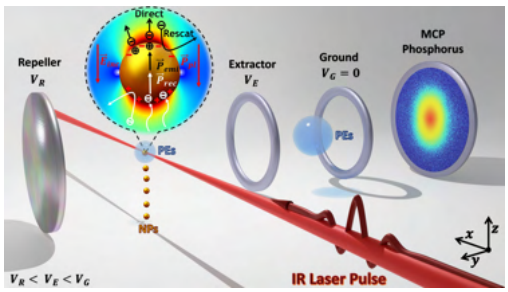


Figure 1. Schematic of the velocity-map-imaging (VMI) assembly.

As seen in Fig. 1, the incident IR laser pulse is linearly polarized in the z-direction, propagates in the x-direction, and intersects a beam of metal NPs. V_R, V_E, and V_G are the respective voltages on the PE repeller, extractor, and ground plates, needed to guide PEs to the multi-channel-plate (MCP) detector. The inset shows processes and fields that occur during the laser-NP interaction, including direct photoemission (Direct), PE rescattering (Rescat) and recombination (rec), the incident laser electric field $\vec{E}_{inc}$, the induced plasmonic polarization $\vec{P}_{pl}$, and the emission ($\vec{P}_{emi}$) and recombination ($\vec{P}_{rec}$) dipoles with their corresponding charge distributions.

Compared to gaseous atomic targets [4], we find much larger PE cutoff energies. These exceed the incident laser-pulse ponderomotive energy by two orders of magnitude, for both directly emitted and rescattered PEs [2].

Supported in part by US AFO award N° FA9550-17-1-0369, NSF grant N° PHY 2110633, and U.S. DOE award N° DE-FG02-86ER13491.

References

[1] J A Powell, Ph.D. thesis, Kansas State University (2017).
[2] E Saydanzad, Ph.D. thesis, Kansas State University (2022); E Saydanzad and U Thumm, Phys. Rev. A (*under review*).
[3] E Saydanzad, J Li, and U Thumm, Phys. Rev. A 95, 053406 (2017); *ibid.* 98, 063422 (2018).
[4] W Becker *et al.*, J. Phys. B **51**, 162002 (2018).

*E-mail: thumm@phys.ksu.edu

RP

Quantification and analysis of spectral broadening of femtosecond pulses in solid medium

Y T Gao[1,2] ,X Z Wang[1] ,X X Zhu[1,2] ,K Zhao[1,3] * ,H Y Liu[1,2] ,Z H Wang[1,3] ,S B Fang[1,2] ,Z Y Wei[1,2,3] †

[1]Beijing National Laboratory for Condensed Matter Physics, Institute of Physics, Chinese Academy of Sciences, Beijing 100190, China
[2]Department of Physics, University of Chinese Academy of Sciences, Beijing 100049, China
[3]Songshan Lake Materials Laboratory, Dongguan 523808, China

Synopsis We propose a concept of ionization integral (P-int) to quantify plasma effect during the spectral broadening process in solid medium by femtosecond pulses. Taking the P-int as a reference, the complex asymmetric broadening of spectrum were investigated. Then, the neural network algorithm is applied in analyzing the theoretical and experimental spectral results, which provides a more accurate understanding of the physics of the entangled nonlinear optics effects and a more convenient tool in the investigation of laser-matter interaction.

RP

Spectral broadening is a necessary process in generating few-cycle pulses as well as isolated attosecond pulse. However, for a higher pulse energy, the nonlinearities behind spectral broadening become more complex and will have a significant effect on the characteristic of laser field. So it is essential to investigate their physical mechanisms and guide the high power few-cycle pulse generation such as through hollow-core fiber[1] and thin plates structure[2].

B-integral[3] has described the strength of the Kerr effect successfully. When the laser intensity step into strong field regime, the plasma effect becomes an non-negligible factor. Here we define the P-integral and apply it in investigating the pulse propagation process by simulating nonlinear envelope equation.

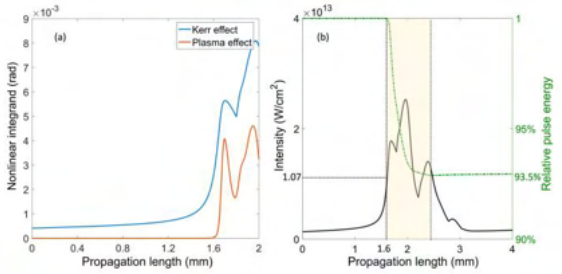


Figure 1. the revolution of integrands in B-int and P-int during the pulse propagation process in solid.

In supercontinuum generation, as the laser intensity rises, the output spectrum changes from a Gaussian form to an irregular shape. We distinguish the supercontinuum generation process in three stages by P-int, and it will deepen the understanding of complex spectrum broadening process .

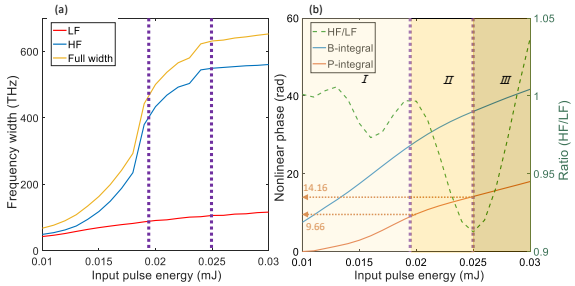


Figure 2. Stages in the complex asymmetric spectral broadening process identified by the ionization integral.

Furthermore, we employ a fully connected MLP[4] to fit the procedure of solving NEE numerically and combining the experimental results. The well-trained MLP helps us predict the initial pulse parameters as well as the B-int and P-int with high efficiency and high precision in experiment.

As we best known, this is the first time that nonlinear effects are quantified in experiments, and its methods, including quantification of nonlinearities and the application of neural network algorithm, will bring great impact to the experimental study of ultrafast nonlinear physics as well as high power few-cycle pulses generation.

References

[1] Seo M, et al 2019 Opt. Lett. **45** 2
[2] Nagy T, et al 2020 Opt. Lett. **45** 3313
[3] Hornik K M *et al* 1989 *Neural Netw. :* **2** 359
[4] Perry M D, et al 1994 Opt. Lett. **19** 2149

* E-mail: zhaokun@iphy.ac.cn
† E-mail: zywei@iphy.ac.cn

On-chip polarization-sensitive time-domain spectroscopy in the near-infrared using plasmonic nanoantenna arrays

M Turchetti[1]*, M R Bionta[1], F Ritzkowsky[2], M Yeung[1], K K Berggren[1] and P D Keathley[1]

[1]Research Laboratory of Electronics, Massachusetts Institute of Technology, Cambridge, MA 02139, USA
[2]Deutsches Elektronen Synchrotron (DESY), 22607 Hamburg, Germany

Synopsis We demonstrate a detector for on-chip polarization-sensitive time-domain spectroscopy of weak (fJ-level) broadband optical fields with sub-femtosecond resolution. This detector enables the measurement of amplitude, phase and polarization of optical field waveforms.

Time-domain spectroscopy, whereby fields of an optical signal waveform are sampled in time with subcycle resolution, provides a direct visualization of light matter interaction dynamics, such as carrier motion or molecular vibrations. Unlike conventional spectroscopy, both amplitude and phase information are provided without the need for post-analysis or retrieval. With the addition of polarization information, a powerfully rich set of information is provided for understanding both dynamics and underlying molecular structure.

Plasmonic nanoantennas have been demonstrated to be able to sample fJ-level fields with sub-fs resolution, allowing for on-chip, broadband, weak field time-domain spectroscopy down to the visible to the near-IR [1]. This is possible thanks to the highly nonlinear nature of the cold-field emission properties of these nanoantennas coupled with the large field enhancement obtained from geometrical and plasmonic effects.

In this work, we demonstrate a nanoantenna array configuration that allows for polarization sensitive optical field sampling. This was achieved by placing nanoantennas with perpendicular orientation on pairs of sinusoidal electrode strips. When a gate pulse illuminates the device with a polarization parallel to one of the two antennas orientations, it enhances signals with the same polarization and suppress signals with perpendicular polarization, as illustrated in Fig. 1. By then scanning the delay between gate and signal the optical field of interest is sampled. An example of this polarization-sensitive sampling measurement is shown in Fig. 1d.

This scheme allows one to selectively measure the polarization of interest and can be used to fully reconstruct an unknown signal in terms of frequency, phase, and polarization.

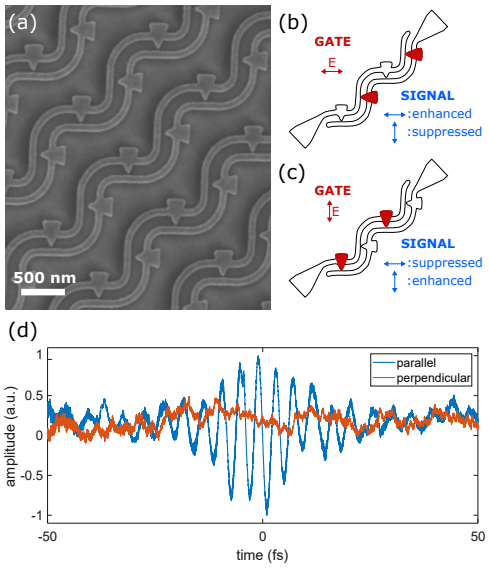


Figure 1. (a) SEM micrograph of the polarization-sensitive detector. (b-c) Schematic of the detection scheme illustrating how a gate signal is used to enhance all the signals polarized parallel to the gate and suppress all the signals perpendicular to it. (d) Cross-correlation measurement with the polarization-sensitive detector showing the sampled signal polarized parallel to the gate (blue), and in the suppressed condition when polarized perpendicular to the gate (red).

References

[1] M R Bionta, Nat. Phot. **15**, 456 (2021).

*E-mail: turchett@mit.edu

RP

Tracking electron dynamics in wide-bandgap semiconductors by transient grating solid-state high harmonic spectroscopy.

Sylvianne D.C. Roscam Abbing[1*], Filippo Campi[1] and Peter M. Kraus[1]

[1]Advanced Research Center for Nanolithography (ARCNL), Science Park 106, 1098 XG Amsterdam, The Netherlands

Synopsis We demonstrate transient grating solid-state high-harmonic spectroscopy in MgO, and perform a background-free measurement of the relaxation dynamics of excited electrons, which have an enhancing effect on solid-state high-harmonic generation.

RP

Solid-state high-harmonic generation (HHG) [1] is revolutionizing the fields of attosecond science and strong-field physics, and allows for compact extreme-ultraviolet light sources for probing the electronic band structure and electron dynamics in condensed matter. The generation originates from two radiation mechanisms: the interband polarization and the intraband current [2]. The strong involvement of both radiation mechanisms with the excited electron population raises the question how a pre-excited electron population will influence the HHG mechanism [3], and also on what time scales any changes take place. Here we demonstrate transient-grating high-harmonic spectroscopy [4] in wide-bandgap semiconductors, and perform a background-free measurement of the relaxation dynamics of excited electrons during HHG.

To obtain an excited electron population, we illuminate the solid sample (MgO) by two crossed interfering 266 nm pulses, see Fig. 1A. Two-photon absorption excites electrons across the 7.8 eV bandgap of MgO. The interference of the two pulses results in regions across the sample with and without excited electron population. We estimate the intensity of the 266 nm pulses at 10^{11}W/cm^2, and approximate the excited electron population to be 0.1% at 0 ps delay. Subsequently a time-delayed infrared pulse generates high-harmonics in the extreme-ultraviolet from both regions. Following [4] we reconstruct the relative amplitude and relative phase between the excited and unexcited region, see Fig. 1B. The relative amplitude confirms that the harmonic amplitude from the excited region is about 40% more efficient than from the unexcited region, for the initial electron excitation of 0.1%. Extrapolating the trend for even higher excited electron fractions, suggests that the harmonic signal of the excited region will be even more enhanced. If the fraction becomes too high, the total signal might decrease again, as shown in [3]. As the excited population decays over time, the relative amplitude approaches the initial value of 1, for which the ground and excited state emission becomes equal. Moreover, we see that the relative phase changes with approximately 1 radian.

Simulating solid-state HHG in an excited MgO sample, will allows us to decouple the interband and intraband contributions, and will let us identify how their contributions will change depending on the excited electron population. In conclusion, we demonstrate transient-grating solid-state HHG spectroscopy in MgO. We observe that a pre-excited electron population leads to more efficient harmonic generation, providing a new strategy towards brighter solid-state high-harmonic sources.

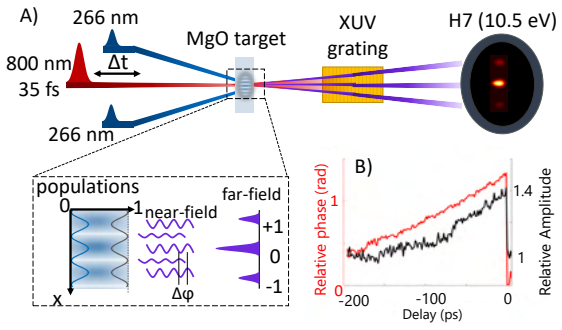


Figure 1. A) Schematic of experimental setup. B) Reconstructed relative amplitude and phase.

References

[1] Ghimire, S.*et al* 2011 *Nature physics* 7(2) 138-141
[2] Golde, D.*et al* 2008 *Phys. Rev. B* 77, 075330.
[3] Wang, Z.*et al* 2017 *Nat. Comm.* 8 1686 1-7.
[4] Wörner, H. J.*et al* 2010 *Nature* 466.7306 604-607.

Author Index

Abanador, Paul, 153
Abbing, Sylvianne Roscam, 320, 388
Abdolghader, Pedram, 170
Abe, Shigeru, 144
Abo-Toame, Salma, 166
AFS (Sponsor), 100
Agostini, Pierre, 82, 111, 291, 334
Ahmadi, Hamed, 145, 160
Alam, Didarul, 316
Alarcon, Miguel, 28
Albrecht, Martin, 338, 353
Alcalà, Jordi, 45
Alexander, Oliver, 42
Alexandridi, Christiana, 116
Allaria, Enrico, 60
Allegre, Hortense, 355, 376
Alqattan, Husain, 21, 105
AlShafey, Abdallah, 26, 103
Alshehri, Nisreen, 235
Amberg, Stefano, 68
Amini, Kasra, 15
Ammitzböll, Mattias, 113, 117
AMPHOS, ii
Anders, Nils, 120, 176, 289, 294
Andriukaitis, Giedrius, 55
Andriyash, Igor, 77
Annunziata, Andrea, 384
Antonov, Vladimir, 324
Anus, M, 369
Arbó, Diego, 321, 322
Ardana-Lams, Fernando, 83
Argenti, Luca, 30, 82, 97, 116, 117, 119, 154, 161, 177, 183, 203, 204, 280
Arnold, Cord, 113, 116, 117, 130, 218, 220, 233, 343, 354
Arthur, Davis, 226
Arusi-Parpar, Talya, 134
Arvind, Shikhar, 245
Atri-Schuller, David, 370
Aufleger, Lennart, 68
Auguste, Thierry, 178
Autuori-Génaud, Alice, 27, 147, 156, 206
Avni, Timur, 42
Ayuso, David, 9, 10, 190, 237, 363
Azoury, Doron, 70

Babbe, Finn, 250
Bachau, Henri, 215
Badano, Laura, 61
Bailey, T P, 35
Baker, Robert, 125, 139
Ballance, Connor, 202
Baltuška, Andrius, 55
Balčiūnas, Tadas, 55, 81, 135, 170, 232
Bandaranayake, Savini, 139
Banerjee, Parag, 381
Banner, Arnold, 164
Barber Belda, Paula, 230
Barbiero, Gaia, 337
Barcons, Xavi, 186
Bargsten, clayton, 245
Barnard, Toby, 42
Barreau, Lou, 89, 95
Bartschat, Klaus, 158, 160, 221, 370
Baruah, Raktim, 104
Bauerhenne, B., 49
Bauers, Sage, 137
Baykusheva, Denitsa, 35
Bañares, Luis, 254, 267
Beauvarlet, Sandra, 8
Becker, Andreas, 208, 210
Beetar, John E, 143, 249, 344, 380
Begusic, Tomislav, 279
Bello, Roger, 159, 265, 272
Belsa, Blanca, 15
Ben Amor, Nadia, 150
Ben Nasr, S, 371
Benda, Jakub, 145, 157
Benedict, Mihály, 318, 319
Bengery, Zsolt, 126, 129, 345, 349
Berggren, K K, 387
Bergues, Boris, 17
Berini, P., 41
Berrah, Nora, 206
Berriel, Sasha, 381
Bertolino, Mattias, 61, 118, 211, 212
Bharti, Amar, 36
Bharti, Divya, 158
Bhattacharya, Utso, 45
Bhogadi, Dileep, 227, 270
Biegert, Jens, 15, 45, 49, 171, 181, 228
Bionta, Mina R, 387
Birk, Michael, 88
Birk, Paul, 230
Biswas, Dipayan, 149
Biswas, Shubhadeep, 37
Biswas, Somnath, 379
Blaga, Cosmin, 291
Blanchet, Valérie, 8, 150
Blinov, S., 95
Bloch, Etienne, 150
Blume, Dörte, 148
Blöchl, Johannes, 17
Bobrova, Nadezhda, 338
Boemer, C., 57
Bollani, Monica, 384
Boltasseva, Alexandra, 44
Bondar, Denys, 103
Borisova, Gergana D, 230
Borne, Kurtis, 227
Borrego-Varillas, Rocio, 110, 213, 222, 267
Borràs, Vicent J., 29, 146
Borsch, Markus, 22
Bosses, Lea, 27, 156
Bourassin-Bouchet, Charles, 89, 205, 307
Boutu, Willem, 169
Bowman, J. M., 12
Boyer, Alexie, 268, 346
Brahms, Christian, 232
Breev, Iakov, 298
Breitkopf, Sven, 126
Brennecke, Simon, 120
Bresteau, David, 27, 38, 53, 147, 156, 178, 219, 341
Brown, Andrew, 202, 365
Brown, Graham G., 4, 179, 180
Brown, Nolan, 227
Bruhnke, Jakob, 273
Bruner, Barry D., 70, 134
Brunner, Eric, 91
Brunner, Fabian, 127
Brédy, Richard, 346
Buchleitner, Andreas, 91, 113
Bucksbaum, Philip, 269
Budriūnas, Rimantas, 348
Burgdörfer, Joachim, 322
Burrows, Spenser, 119, 226
Buss, Jan Heye, 131
Busto, David, 61, 113, 116–118, 145, 160
Bux, Simone, 352
Bučar, Klemen, 60, 323
Böning, Birger, 360
Börzsönyi, Ádám, 126

Cabello, Christian, 381, 383
Cacho, Cephise, 38
Cachon, Javier, 267
Caillat, Jérémie, 27, 147, 156, 206
Calegari, Francesca, 47, 55, 64, 150
Callegari, Carlo, 60, 61
Camacho Garibay, Abraham, 111, 291
Campi, Filippo, 131, 320, 388
Capotondi, Flavio, 53
Cardin, Vincent, 55
Cariker, Coleman, 82, 119, 183
Carlström, Stefanos, 61, 252, 305
Carrascosa, Andrés, 285
Castagna, Jean-Charles, 227, 270
Catoire, Fabrice, 338
Cederbaum, Lorenz, 14
Chacon, Alexis, 35
Chakraborty, Himadri, 216
Chakraborty, Nisnat, 231
Chang, Kristina, 143
Chang, Yi-Ping, 81, 135

Chang, Zenghu, 76, 97, 164, 234, 336, 351
Charalambidis, Dimitris, 123
Chattopadhyay, Siddhartha, 204
Chen, Min, 184
Chen, Ming-Chang, 74
Cheng, Xianchao, 227, 270
Cheng, Zhao, 77
Chevreuil, Pierre-Alexis, 127
Chew, Andrew, 97
Chien, Ying-Hao, 181, 228
Chien, Yu-En, 74
Chini, Michael, 19, 107, 249, 316, 344, 351, 380, 381, 383
Chirvi, Katharina, 15
Cho, Wosik, 293
Chordiya, Kalyani, 368
Chowdhury, Enam, 105
Chu, Shih-I, 299
Chumley, Scott, 356
Ciappina, Marcelo Fabian, 45, 86, 169, 185
Cinquanta, Eugenio, 72, 384
Ciriolo, A. G., 72
Cirmi, Giovanni, 75
Clark, A, 242
Class 5 Photonics (Sponsor), 100
Coffee, Ryan, 227, 270
Cohen, Oren, 88, 358
Colaizzi, Lorenzo, 150
Collaboration, LR25, 65
Collaborations, LCLS Attosecond Campaign, 58, 65
Comby, Antoine, 8
Compagnon, Isabelle, 346
Constant, Eric, 354
Cooper, Jason, 250
Cooper, Rachel, 313
Coreno, Marcello, 60
Corkum, Paul B., 4, 41, 44, 107, 179, 180, 266
Cormier, Eric, 131
Covolo, Antoine, 27, 156
Crippa, Gabriele, 72, 384
Croy, Alexander, 104
Cryan, James, 115, 242, 263, 269, 270
Csizmadia, Tamás, 129, 345, 349
Cubaynes, Denis, 147
Cushing, Scott, 137, 250
Czirják, Attila, 318, 319

Dacasa, Hugo, 354
Dahlström, Jan Marcus, 61, 118, 211, 212, 236, 238, 252, 305
Dakovski, G, 242
Dalui, Malay, 27, 156
Danailov, Miltcho, 61
Dantus, Marcos, 295
Danz, T., 49
David, Christian, 53
Davis, Jody, 356
De Angelis, Dario, 53
De Castro, Catherine, 235
De Giovannini, Umberto, 96, 168, 289, 384
De Marco, Massimo, 129, 345, 349
De Nalda, Rebeca, 254
De Ninno, Giovanni, 53
de Roulet, Bethany R., 106
de Vivie-Riedle, Regina, 69
Decleva, Piero, 10, 190, 263, 275
del Pino, Javier, 98
Dellith, Jan, 104
Demekhin, Philipp, 61
Demjaha, Ron, 113
DePonte, D, 242
Descamps, Dominique, 8
Despré, Victor, 99, 174
Detlefs, B., 57
Devetta, Michele, 72, 384
Dewhurst, K., 49
Di Palo, Nicola, 49, 110, 222
Dienstbier, Philip, 109
Dieny, Bernard, 53
DiFraia, Michele, 60, 61
DiMauro, Louis, 66, 82, 111, 125, 189, 291, 334
Din, N Ud, 316
Ding, Thomas, 68
Ding, Yijue, 264
Dittel, Christoph, 113
Diveki, Zsolt, 343
Dixit, Gopal, 36, 325
Doliveira, Pascal, 38, 219
Dolso, Gian Luca, 110, 222
Donsa, Stefan, 322
Dorney, Kevin, 245
Douguet, Nicolas, 97, 177, 221, 280, 370
Doumy, G, 242
Dowek, Danielle, 219
Dragone, Angelo, 243
Drescher, Lorenz, 90, 106, 124
Driver, Taran, 67, 227, 263, 270
Dröge, Fabian, 310
Du, M, 359
Dube, Zack, 266
Dudovich, Nirit, 8, 40, 70, 134
Duensing, A, 239, 315
Dumergue, Mathieu, 123
Díaz-Tendero, Sergio, 144
Dörner, Reinhard, 120, 148, 176, 289, 294

Eckart, Sebastian, 92, 120, 176, 289, 294
Eckert, Sebastian, 229
Edwards, Matthew, 379, 382
Eidam, Tino, 126
Eikema, K S E, 359
Eitan, Avraham, 166
Ekimova, Maria, 229
El-Youbi, Zakariae, 38
Eldar, Maor, 166
Elliott, P., 49
Elu, Ugaitz, 45
Emma, Claudio, 59
Emmanouilidou, Agapi, 114, 266
Endo, T., 12
Eng-Johnsson, Per, 118, 343, 354
Engel, Volker, 273
Ernotte, Guilmot, 266
Ernstorfer, R., 49
Ertel, Dominik, 145, 160
Esry, Brett, 264
Even Tzur, Matan, 88, 358

Faccialà, Davide, 72, 384
Fan, Daniel, 230
Fan, Guangyu, 55, 340
Fanciulli, Mauro, 38, 53
Fang, Li, 111, 351
Fang, Shaobo, 378, 386
Faria, Carla, 225, 296
Farkas, Balazs, 343
Fasano, Nicholas, 379, 382
FastLite (Sponsor), 100
Fattahi, Hanieh, 350
Fazio, Giuseppe, 81, 232
Federman, Yotam, 70
Fedorov, Alexey, 108
Fehre, Kilian, 92
Feifel, Raimund, 60, 61, 116, 117
Feist, Johannes, 98
Fennel, Thomas, 109
Ferchaud, Clement, 42
Fernández Carbón, Rubén, 161
Fernández-Milán, Pedro, 254
Ferreira da Silva, Rui Emanuel, 98
Fidler, Ashley P, 175, 372
Filus, Zoltán, 129, 345, 349
Finger, Keegan, 370
Finke, Ondřej, 338, 353
Finkelstein-Shapiro, Daniel, 113, 116
FLASH, DESY Collaboration at, 65
Flegel, Alexander, 298
Folorunso, Aderonke, 66, 189
Forembski, Andrew, 217
Forget, Nicolas, 352
Frassetto, Fabio, 72, 145, 345
Fritzsche, Stephan, 360

Frolov, Mikhail, 298
Fross, Patrick, 91
Frusteri, Biagio, 96
Fröhlich, Sven, 169
Fu, Yu-Zhi, 74
Fujise, H., 12
Funke, Lars, 227
Furch, Federico, 146
Fushitani, M., 12

Gaarde, Mette B, 66, 163, 189, 283, 306, 308
Gaida, Christian, 126
Gajapathy, Harshad, 139
Galinis, Gediminas, 42
Gallician, Guillaume, 27, 61, 156
Gallmann, Lukas, 33, 52, 108, 127
Gan, Z, 163, 306
Gao, Yitan, 378, 386
Garcia, M. E., 49
Garcıa-Vidal, Francisco José, 98
Garg, Manish, 51
Garratt, Douglas, 42
Gatti, F., 95
Gatton, Averell, 227, 270
Gauthier, David, 169
Gaynor, James D, 175, 372
Geiger, Chase, 234
George, A, 163, 306
Geyer, Angelina, 92, 176, 289, 294
Ghafur, O, 369
Gharibnejad, Heman, 30, 154, 214
Ghimire, Shambhu, 35, 43
Gholam Mirzaeimoghadar, Shima, 44, 107, 249
Ghomashi, Bejan, 280
Gia, Xuyan, 103
Giannessi, Luca, 61
Gilicze, Barnabás, 126, 129, 345, 349
Giovannetti, Gabriele, 55
Girdauskas, Vytenis, 348
Gisselbrecht, Mathieu, 61, 113, 116–118, 218, 220, 252
Gitzinger, Gregory, 352
Gluszek, Aleksander, 20
Goetz, Esteban, 282
Goldner, Adi, 166, 244
Goldsztejn, Gildas, 147
Golubev, Nikolay, 84, 174, 279, 281
Golz, Torsten, 131
Gong, Shoushu, 103
Gong, Xiaochun, 54
González-Vázquez, Jesús, 29, 146, 254, 263, 267, 275
Gopalakrishna, Harshitha Nandiga, 104
Gorenflot, Julien, 235
Gorfinkiel, Jimena, 157
Gorlach, Alexey, 88
Goto, Soki, 144
Grafstrom, Brock, 367
Granveau, Gabriel, 89, 307
Grass, Tobias, 45
Grebing, Christian, 126
Greene, Chris, 28
Greenman, Loren, 264, 282
Gregory, Andrew, 42
Grell, Gilbert, 263, 275
Grochowski, Piotr T., 45
Grum-Grzhimailo, Alexei N., 160
Gruson, Vincent, 89
Gryzlova, Elena V., 160
Gräfe, Stefanie, 104, 141, 181, 228, 273, 297, 303, 310
Grósz, Tímea, 129, 345, 349
Guan, Qingze, 148
Guillemin, Renaud, 147
Gulley, Jeremy, 313
Gulyás Oldal, Lénárd, 129, 345, 349
Guo, Chen, 113, 117, 130, 218, 220, 233, 354
Guo, Zhaoheng, 263, 314

Hack, Szabolcs, 318, 319
Hadjipittas, Antonios, 114
Haessler, Stefan, 77, 362
Hage, Arvid, 339
Hageman, Stephen, 82
Hamdou, Aimrane, 169
Hamer, Kyle, 66, 189
Hamilton, Kathryn, 158, 160, 370
Han, Meng, 223
Han, Seunghwoi, 97
Harada, Yoshihisa, 165
Haram, Nida, 342
Harkema, Nathan, 183
Hart, Trevor, 226
Harth, Anne, 91, 158
Hartmann, Maximilian, 230
Hartmann, Nadja, 52
Hashmi, Arqum, 167
Hassan, Mohammed, 21, 105
Hatada, Keisuke, 144, 191, 274
Haverkort, Maurits W., 68
He, Feng, 342
Heck, Saijoscha, 54
Heckmann, Olivier, 38
Hehn, Michel, 55
Heide, Christian, 41, 43
Heinz, Tony F, 35, 43
Heinze, Simon, 68
Heitz, Marie-Catherine, 150
Helm, Wolfram, 227, 270
Henrich, Felix, 68
Herbst, Andreas, 350
Hergott, Jean-François, 27, 38, 89, 156, 178, 219, 341
Herrfurth, Oliver, 126
Hervé, Marius, 346
Hessami, Rafi, 59
Hibino, Hiroki, 138
Hill, Wendell, 234
Hirschman, Jack, 227
Hishikawa, A., 12
Hoang, Hung, 278
Hofer, Christina, 20
Hoff, Dominik, 126, 218, 220, 317
Hoflund, Maria, 118, 354
Hofmann, Max, 176, 289, 294
Hogan, Mark, 59
Hogle, Craig, 14
Hollinger, R, 163, 306
Holzmeier, Fabian, 219, 245, 267
Hommelhoff, Peter, 109
Hongliang, Shi, 227
Hort, Ondřej, 338, 353
Houston, P. L., 12
Houver, Jean-Christophe, 219
Hricovini, Karol, 38
Hruska, Emily, 139
Hu, Shuyuan, 230
Huber, Rupert, 22
Huebener, Hannes, 168, 384
Hui, Dandan, 21, 105
Huotari, S., 57
Hutcheson, Lynda, 365
Hwang, Seong In, 290
Hädrich, Steffen, 126
Hünecke, Christian, 104, 141

Ibrahim, Heide, 12, 335, 340
Ilchen, Markus, 227, 270
Im, Jinhyeok, 89, 205
Inhester, Ludger, 81
Inzani, Giacomo, 110, 222
Irani, Elnaz, 141
Isele, Erik, 269
Isella, Giovanni, 384
Ishii, Nobuhisa, 31, 97
Ishikawa, Kenichi L., 246, 284, 287
Isinger, Marcus, 116
Ismail, iyas, 60
Itatani, Jiro, 31, 97, 165, 377
Ito, Kengo, 253
Ivanov, Igor, 115, 301
Ivanov, Maksym, 170, 339, 347
Ivanov, Mikhael Yu, 34, 37, 70, 133, 134, 140, 190, 252, 362, 363

Jahnke, Till, 120, 176, 289, 294
Jain, Swapneal, 119, 226, 356
Jaksic, Jasna, 337

Jal, Emmanuelle, 55
James, Justin, 227, 270
Jančárek, Alexandr, 338
Jaouen, Nicolas, 55
Jaron-Becker, Agnieszka, 210
Jarosch, Sebastian, 42
Jayasinghe, Denawakage, 66, 283
Jelassi, H, 241, 371
Jelivona, Denis, 54
Jeong, Young-Gyun, 347
Ji, Jia-Bao, 223
Jiménez Galán, Álvaro, 37, 133, 134, 140
Jochim, Bethany, 295
Johnson, Amalya Cox, 43
Johnsson, Per, 61
Joly, Y., 49
Jones, Robert, 66, 189
Joseph, Jennifer, 219
Joshi, Chan, 187
Journel, Loïc, 147
Journigan, Troie, 381, 383
Jung, Robert, 337
Jurkovič, Matej, 338, 353
Just, Florian, 126
Jójárt, Péter, 126, 129, 345, 349

Kaassamani, Shatha, 169
Kahaly, Mousumi Upadhyay, 368
Kahaly, Subhendu, 123, 129, 131, 343, 345, 349
Kahvedzic, Resad, 303
Kaksis, Edgar, 55
Kamalov, Andrei, 227, 270
Kaminer, Ido, 88
Kanai, Teruto, 31, 97, 165, 377
Kanno, Manabu, 144
Kapteyn, Henry, 14, 245
Karamatskos, Evangelos, 292
Karl, Florian, 126
Karpowicz, Nicholas, 379
Kartashov, Daniil, 104, 141, 163, 306
Karuthedath, Safakath, 235
Katayama, Ikufumi, 138
Kato, Keiko, 138
Katsoulis, Georgios, 266
Kaur, Jaismeen, 77
Keathley, P D, 387
Keenan, Clare, 175, 372
Keller, Ursula, 33, 52, 108, 127
Kenney, Christopher, 243
Kerker, F., 57
Kern, Klaus, 51
Khairulin, Ilias, 324
Khatri, Dipendra, 19, 107, 381, 383
Kheifets, Anatoli, 115, 207
Kieker, Max, 350
Kienberger, R, 239, 315
Kiesewetter, Dietrich, 334
Kim, Kyung Taec, 290, 293, 301
Kim, Yang Hwan, 290
Kimberg, V., 95
Kira, Mackillo, 22
Kirchmann, Patrick S., 35
Kirrander, Adam, 285
Kiselev, Maxim D., 160
Kishimoto, Naoki, 144
Klein, Isabel, 137, 250
Kleine, Carlo, 229
Klimkin, Nikolai, 140
Kling, Matthias, 17, 37
Klingebiel, Sandro, 337
Kneller, Omer, 8, 70
Ko, Dong Hyuk, 4, 179, 180
Kobayashi, Yuki, 43, 143, 372
Koch, Christiane P., 282
Kocharovskaya, Olga, 324
Koenderink, Femius, 320
Kohrell, F, 373
Kolanz, Lucas, 208
Kolkowski, Radoslaw, 320
Koll, Lisa-Marie, 90
Konrad, Corinna, 128
Kopp, Tristan, 232
Kornilov, Oleg, 124, 254
Korobenko, Aleksey, 41, 44
Korolev, Viacheslav, 104, 141
Kovács, Katalin, 361, 369
Kowalczyk, Katarzyna, 376
Kowalczyk, Maciej, 20
Kranov, P., 95
Kraus, Peter, 320, 388
Krausz, Ferenc, 5, 20, 128
Krebs, D., 57
Kretschmar, Martin, 114
Krishna, Vipin, 141
Krueger, Michael, 70, 166, 244
Kruse, Jan, 148, 294
Krušič, Špela, 60, 323
Krylov, Anna, 242
Krylow, S., 49
Krüger, Michael, 88
Kuleff, Alexander, 84, 174, 188
Kumar, Mayank, 335
Kunihashi, Yoji, 138
Kunitski, Maksim, 92, 120, 148, 176, 289, 294
Kurihara, Takayuki, 31, 165, 377
Kuznetsov, Denis A., 108
Kwon, Ojoon, 340
Kärtner, Franz X., 75
Kübel, Matthias, 224
Kühn, Sergei, 123, 131, 343
Küpper, Jochen, 96, 292
Lablanquie, Pascal, 60, 147
Labranche, Alexis, 339, 347
Lamprou, Theocharis, 86
Landsman, Alexandra S, 26, 103, 239, 367
Langer, Fabian, 130
Laquai, Frédéric, 235
Laramée, Antoine, 335
Larsen, Esben, 42, 245
Larsen, Kirk, 59, 265
Lassonde, Philippe, 12, 335, 340
Laurell, Hugo, 113, 116, 117
Laurent, Guillaume, 119, 226, 356
Layertec (Sponsor), 100
LCLS Attosecond Campaign Collaborations, , 173
Le, Anh-Thu, 300
Le, Cam-Tu, 364
Le, Quynh, 234
Le, Van-Hoang, 357, 364
Leblanc, Adrien, 335
Lee, Min-i, 38
Lein, Manfred, 120, 297
Lejman, Mariusz, 27, 147, 156, 206
Leone, Stephen R, 79, 95, 106, 143, 175, 372
Lepetit, Fabien, 178
Leshchenko, Vyacheslav, 82, 111, 125
Lettau, Thomas, 141
Lewenstein, Maciej, 45, 86, 87, 185, 186, 200
Li, K, 242
Li, Shuai, 242, 295
Li, X, 242
Li, Yang, 287
Li, Zheng, 69
Liang, An-Yuan, 74
Light Conversion (Sponsor), 100
Limpert, Jens, 126
Lin, C-D, 304
Lin, M, 242
Lin, S-C, 247
Lin, Yen-Cheng, 175, 372
Lindroth, Eva, 25, 117–119, 121, 183, 201, 203, 236
Litvinyuk, Igor, 342
Liu, Fang, 43
Liu, Hanzhe, 137, 250
Liu, Heyuan, 386
Liu, Qiaoyi, 334
Liu, Xiaomeng, 359
Liu, Xinyao, 15
Liu, Yangyang, 19, 107, 249, 344, 381, 383
Ljungdahl, Anton, 117, 121, 201, 236

Loh, Z, 242
Londo, Stephen, 139
Longa, Adrien, 335
Lopata, Kenneth, 66, 184, 189, 283, 285
Lopez-Martens, Rodrigo, 77
Loriot, Vincent, 27, 156, 268
Lu, Jian, 35
Lu, Yuan-Ming, 103
Lucchese, Robert, 54, 265, 277
Lucchini, Matteo, 50, 110, 213, 222, 267, 345
Luo, Sizuo, 113, 117
Luo, Yang, 51
Luttmann, Martin, 53, 178, 341
Lytova, Marianna, 362
Lépine, Franck, 27, 47, 156, 268, 346
Légaré, François, 12, 55, 150, 170, 335, 339, 340, 347
Légaré, Katherine, 55, 340
López, Sebastián, 321, 322
Lötgering, Lars, 320
Lüning, Jan, 55
L'Huillier, Anne, 3, 113, 116–118, 130, 218, 220, 233, 252, 343, 354

M Bidhendi, Mahdi, 350
Ma, Boyang, 244
Ma, Lingyu, 285
Mašín, Zdeněk, 145, 157, 276, 288
Machalett, Frank, 224
Maclot, Sylvain, 61, 118, 354
Madjet, Mohamed, 216
Madsen, Lars Bojer, 200
Madugula, Nrisimha Murty, 344
Magrakvelidze, Maia, 216
Magunia, Alexander, 68
Maikowski, Laura, 90
Mainz, Roland E., 75
Mairesse, Yann, 8, 150
Major, Balazs, 114, 129, 345, 349, 366, 369
Majorosi, Szilárd, 318, 319
Mak, Ka Fai, 20
Makos, Ioannis, 145, 160
Maksimenka, Raman, 352
Malinowsky, Gregory, 55
Mallick, Monalisa, 248
Manai, S, 241, 371
Manakov, Nikolai, 298
Manfredda, Michele, 53, 60, 61
Mans, Torsten, 339
Marangos, Jon, 42, 65, 263
Marante, Carlos, 30, 154
Marchenko, Tatiana, 147
Marggi Poullain, Sonia, 143, 254
Marinelli, Agostino, 58, 59, 242, 263
Markovic, Bojan, 243
Marra, Alphonse, 164
Marroux, Hugo J B, 27, 156, 206
Marschner, Heike, 104
Marsh, Kenneth A, 187
Martin, Leigh, 14
Martin, Nazario, 267
Martin-Jimenez, Alberto, 51
Martín, Fernando, 29, 47, 51, 116, 144, 146, 159, 254, 263, 267, 272, 275
Mashiko, Hiroki, 138
Matselyukh, Danylo, 69, 174
Matthews, Mary, 42, 355, 376
Mauger, Francois, 66, 189, 283
Mauritsson, Johan, 252
Maxwell, Andrew S., 86, 186, 200
Mayer, Nicola, 363
Maëder, Lucie, 27, 156, 206
McCaul, Gerard, 103
McCurdy, C. William, 265, 277
McKelvey, Mark, 243
McKeown-Green, Amy Siobhan, 43
Medeghini, Fabio, 222
Medlin, Will, 356
Mehmood, Saad, 119, 203
Meltzer, Thomas, 276
Merdji, Hamed, 169
Metzger, Thomas, 337
Meyer, Michael, 61
Mhatre, Saurabh, 297
Mi, Yonghao, 266
Michelsen, Jonathan, 137, 250
Midorikawa, Katsumi, 73, 271
Mihelič, Andrej, 60, 323
Mikaelsson, Sara, 218, 220
Mikhailova, Julia, 379, 382
Minar, Jan, 38
Minneker, Björn, 360
Miron, Catalin, 61
Miteva, Tsveta, 14
Mitra, Sambit, 37
Mittermair, M, 239, 315
Mizuno, Tomoya, 31, 165, 377
Mocci, Daniele, 213, 267
Modak, P, 304
Moeller, S P, 242
Moio, Bruno, 110, 222
Moioli, Matteo, 145, 160
Molinero, Eduardo B., 311
Mollov, Nikola, 68
Monahan, Nicholas, 83
Mondal, Angana, 136
Monfared, Mohammad, 141
Moon, Taylor, 221
Morales, Felipe, 187, 362
Morandotti, Roberto, 347
Morishita, Toru, 31
Moshammer, Robert, 91, 145, 158, 160
Mrudul, M. S., 36, 325
Mullins, Terry, 96
Murillo-Sánchez, Marta L., 254
Murnane, Margaret, 14
Mustary, M. H., 342
Månsson, Erik P., 150
Müller, Christoph R., 108
Müller, Michael, 126

Nagi, Ladislau, 47
Nagl, Nathalie, 20
Nagy, Tamás, 114
Nagyillés, Balázs, 343
Najafidehaghani, E, 163, 306
Nam, Chang Hee, 290
Nambu, Noa, 187
Nandi, B., 49
Nandi, Saikat, 61, 116, 211, 268
Nandipati, Krishna Reddy, 286
Naumov, Andrei Y., 41, 44, 266
Navarrete, Francisco, 169, 309
Nayak, Arjun, 123
Neb, Sergej, 33, 52, 108
Nebgen, Bailey R, 163, 306, 373
Nefedova, Viktoria, 169
Nejdl, Jaroslav, 338, 353
Neoricic, Lana, 61, 113, 117
Nesper, Jonathan, 249
Neufeld, Ofer, 136, 168, 289
Neuhaus, Marcel, 37
Neumark, Daniel M, 95, 175, 372
Neville, Simon P., 12, 83
Nevrkla, Michal, 338
Ngoko Djiokap, Jean Marcel, 209
Nibbering, Erik T. J., 229
Nie, Zan, 187
Niedermayr, Arthur, 33, 52, 108
Nienhuis, E, 242
Nikolopoulos, Lampros, 215, 217
Nisoli, Mauro, 110, 213, 222, 267, 345
Noblet, T., 95
Nourbakhsh, Zahra, 136
Nuytten, Thomas, 245

O'Neal, Jordan, 173
Obaid, Razib, 227, 270
Oguri, Katsuya, 138
Okamoto, Takuya, 138
Olivieri, Jean-François, 96
Olofsson, Edvin, 61, 211, 305
Olsen, Jeppe, 30, 97, 154
Olsson, Trevor, 119, 226, 356

Onvlee, Jolijn, 96, 292
Oppermann, Florian, 297
Ordóñez, Andrés, 10, 86, 186, 190
Orenstein, Gal, 70, 134
Orfanos, Ioannis, 123
Orimo, Yuki, 284, 287
Orlando, T, 242
Ortmann, Lisa, 26, 367
Osellame, R., 72
Osolodkov, Mikhail, 146
Ota, Fukiko, 144, 191, 274
Otobe, Tomohito, 167
Ott, Christian, 68, 230
Ouillé, Marie, 77

Palacios, Alicia, 263, 267, 272, 275
Palau, Anna, 45
Palaudoux, Jérôme, 60, 147
Pancaldi, Matteo, 53
Pandey, Siddhant, 374
Papoulia, Asimina, 236
Paradis, Clement, 339
Parker, Susan, 42
Paschen, Timo, 109
Patchkovskii, Serguei, 70, 145, 187, 252
Paulus, Gerhard G., 126, 224
Pearce, C, 242
Pedersoli, Emanuele, 53
Pelekanidis, A, 359
Penent, Francis, 60, 147
Penfold, Thomas, 135
Pertot, Yoann, 352
Pervak, Vladimir, 20, 21, 105
Peschel, Jasper, 61, 118, 354
Peschel, Ulf, 104, 141, 310
Petersen, John, 245
Petit, Stéphane, 8
Pettipher, Allan, 355, 376
Pfaff, Yanik, 337
Pfeifer, Thomas, 68, 91, 145, 158, 160, 230
Pfeiffer, Adrian, 375
Phan, Ngoc-Loan, 357, 364
Phong, Pham Nam, 300
Pi, L W, 239
Piccoli, Riccardo, 347
Picón, Antonio, 263
Piecuch, Piotr, 295
Pinoteau, Thomas, 352
Piper, Andrew, 334
Pisanty, Emilio, 86, 185, 360
Pisarra, Michele, 51
Plach, Marius, 118, 354
Platzer, Dominique, 27, 147, 156, 206
Plekan, Oksana, 60, 61
Plunkett, Alexander, 28, 149
Plésiat, Etienne, 263
Poisson, Lionel, 27, 156
Poletto, Luca, 72, 145, 345
Pollanka, M, 239, 315
Pons, Bernard, 8, 150
Popova, Maria M., 160
Powell, Jeffrey, 385
Prejbeanu, Ioan-Lucian, 53
Prince, Kevin, 60, 61
Prior, Adam, 215
Priyadarsini, Swati, 295
Pugžlys, Audrius, 55
Pullerits, Tönu, 113, 116
Pusala, Aditya, 384
Puskar, Nicolette, 175

Qiu, D Y, 163, 306
Qu, C., 12
Quéré, Fabien, 89

Raab, Ann-Kathrin, 130, 218, 220, 233
Raffray, Antoine, 170
Rajak, Debobrata, 8
Ramirez, Alicia, 339, 347
Rampp, Michael, 337
Rana, Navdeep, 325
Randazzo, Juan Martín, 30, 154
Randeria, Mohit, 103
Ranitovic, Predrag, 14, 265
Rashid, S., 41
Raymondson, Daisy, 245
Razzari, Luca, 347
Rebernik, Primoz, 53, 60
Rebholz, Marc, 68
Recio, Pedro, 267
Reduzzi, Maurizio, 49, 181, 228, 267
Rego, Laura, 237
Reichardt, Christian, 104
Reiff, Ran, 210
Reis, David A., 35, 41, 43
Reitsma, Geert, 254
Remacle, Francoise, 13
Renziehausen, Klaus, 310
Rescigno, Thomas, 277
Richter, Christine, 38
Richter, Maria, 362
Richter, Martin, 104
Riedel, Robert, 131
Rist, Jonas, 92, 294
Ritzkowsky, F, 387
Rivas, Daniel, 49
Rivera, Nicholas, 88
Rivera-Dean, Javier, 86
Roantree, Luke, 202
Robinson, Matthew, 292
Robles, River, 59
Rodriguez, Biridiana, 351
Rohringer, Nina, 57
Rolles, Daniel, 264
Ronningen, Theodore, 125
Rook, Thomas, 225
Ropers, C., 49
Ross, A. D., 95
Rossi, Giulio Maria, 75
Rota, Lorenzo, 243
Rott, Florian, 69
Rotundu, Costel R, 35
Rouzee, Arnaud, 229, 292
Rovere, Andrea, 347
Rozen, Shaked, 8
Ruberti, Marco, 155
Rubio, Angel, 33, 52, 96, 108, 136, 168, 169, 289, 384
Ruchon, Thierry, 38, 53, 89, 147, 178, 219, 341
Rudenko, Artem, 264, 385
Rupprecht, Patrick, 68
Ryabchuk, Sergey, 150
Ryabikin, Mikhail, 324
Rösner, Benedikt, 53

Sacchi, Maurizio, 53
Sadeghifaraz, Amin, 141
Saenz, Alejandro, 230
Safaei, Reza, 55, 340
Saha, Soham, 44
Saha, Soumyajit, 121, 201
Sahle, C., 57
Saito, Nariyuki, 97
Sakata, Keisuke, 253
Salhi, D E, 241, 371
Salières, Pascal, 27, 89, 116, 147, 156, 205, 206
Samparisi, Fabio, 345
Sanchez, Aurelien, 15
Sandhu, Arvinder, 28, 80, 149, 183, 231
Sang, Robert T., 342
Sansone, Giuseppe, 145, 160
Santos, Jose, 267
Santra, Robin, 81, 242
Santra, Sayantani, 245
Sapunar, Marin, 288
Saraceno, Clara J., 337
Saraswathula, Krishna, 150
Sasaki, Kakeru, 246
Sato, Shunsuke, 33, 52, 108, 312
Sato, Takeshi, 284, 287
Saydanzad, Erfan, 385
Sayler, A. Max, 224
Scarborough, Timothy, 125
Schade, Daniel, 350
Schafer, Kenneth J, 66, 189, 252, 283, 291, 334

Scheiba, Fabian, 75
Scheidegger, Alan, 281
Schmid, Christoph P, 22
Schmidt, Bruno E., 55, 170, 339, 340, 347
Schmidt, Cedric, 135
Schmidt, Lothar, 92, 120, 176, 289, 294
Schmoll, Marvin, 145, 160
Schnappinger, Thomas, 69
Schneider, Barry, 30, 97, 154, 214
Schneider, Ryan, 214
Scholes, Gregory, 379
Schouder, C, 206
Schröder, C A, 239, 315
Schröter, Claus Dieter, 145, 160
Schubert, Alexander, 310
Schuchter, Maximilian, 175
Schulte, Amelie, 128
Schulz, Claus Peter, 146
Schulz, Michael, 131
Schumacher, Zeno, 33, 52, 108
Schusser, Jakub, 38
Schutlze, Martin, 139
Schuurman, Michael, 12, 83
Schöffler, Markus S., 120, 176, 289, 294
Schötz, Johannes, 17, 128
Schütte, Bernd, 114, 369
Scigalla, P, 239, 315
Seidel, Marcus, 233
Seidu, Issaka, 83
Seiffert, Lennart, 109
Sekikawa, Taro, 253
Sekine, Yoshiaki, 138
Seres, Imre, 126, 129, 345, 349
Severino, Stefano, 49, 181, 228
Shakya, Yashoj, 81
Shalaby, Islam, 231
Shalaev, Vladimir M, 44
Shames, Sergei, 134
Sharma, S., 49
Shestaev, Evgeny, 126
Shi, Hongliang, 227
Shi, Hongyu, 240
Shin, Dongbin, 108
Shin, Jeong-uk, 293
Shinohara, Yasushi, 138, 246
Shivaram, Niranjan, 265, 374
Shobeiry, Farshad, 91, 158
Shrestha, Rajaram, 293
Sidiropoulos, Themistoklis P. H., 45, 49
Silke, Nelson, 227
Silva, Rui, 133, 134, 140, 311
Silva-Toledo, Miguel Angel, 75
Simon, Marc, 147
Simoncig, Alberto, 60
Singh, Dhirendra, 245
Single Cycle Instruments UG, 317
Skantzakis, Emmanouil, 123
Skupin, Stefan, 338
Slaughter, Daniel, 265
Smirnova, Olga, 7, 9, 10, 37, 70, 134, 187, 190, 237, 362, 363
Smith, Bryan, 111
Smith, Gregory, 82
Soavi, Giancarlo, 141
Sobota, Jonathan, 35
Soifer, Hadas, 35
Sollapur, Rudrakant, 248
Son, Sang-Kil, 96
Sotor, Jaroslaw, 20
Sottocorona, Filippo, 60, 61
Sousa, Ricardo, 53
Spanner, Michael, 362
Spezzani, Carlo, 38, 53, 219
Spielmann, Christian, 104, 141, 163, 248, 306
Spies, J A, 373
Squibb, Richard, 60, 61, 116, 117
Srinivas, Hemkumar, 91, 158
Srivastava, Anchit, 350
Stagira, Salvatore, 72, 384
Stamm, Jacob, 295
Stammer, Philipp, 86
Stanislauskas, Tomas, 348
Stanton, J. F., 95
Starosielec, Sebastian, 131
Staudte, Andre, 26, 44, 266
Steinle, Tobias, 15, 45
Steinleitner, Philipp, 20
Stenquist, Axel, 238
Stooss, Veit, 230
Strandsquist, Nathaniel J., 209
Stringer, Patrick, 226
Stutzki, Fabian, 126
Stöhlker, Thomas, 224
Su, Yabei, 378
Summers, Adam, 181, 228
Sun, Hung-Wei, 181, 228
Suñer Rubio, Adrián Jesús, 272
Svirplys, E, 369
Svoboda, Vit, 135, 136
Sytcevich, Ivan, 130, 233
Sébilleau, Didier, 274
Sörngård, Johanna, 121, 201

Tahouri, Rezvan, 236
Takeda, Jun, 138
Takuma, Teramura, 284
Talbert, Kenneth, 291
Tamura, Yoshiaki, 144
Tancogne-Dejean, Nicolas, 136, 169, 384
Tang, Yaguo, 334
Tani, Francesco, 350
Tani, Mizuki, 246
Tao, Zhensheng, 55
Taoutioui, Abdelmalek, 302
Tatum, Morgan, 226
Taïeb, Richard, 27, 147, 206
Tcherbakoff, Olivier, 27, 38, 156, 178, 219, 341
Teisset, Catherine Y., 337
Telnov, Dmitry, 299
Tempea, Gabriel, 339, 347
Texier, A., 95
Therrien, Audrey, 227
Thiré, Nicolas, 352
Thumm, Uwe, 153, 169, 240, 278, 309, 385
Tigges-Green, Isabelle, 379
Tisch, John, 355, 376
Tofful, Alexandra, 42
Tolstikhin, Oleg, 31
Tong, Xiao-Min, 14
Tosa, Valer, 361, 369
Trabattoni, Andrea, 96, 150
Trabert, Daniel, 92, 120, 176, 289, 294
Trallero, Carlos, 339
Travers, John C., 232
Travnikova, Oksana, 147
Trejo, Roger, 227
Trieu, Doan-An, 357
Trippel, Sebastian, 96
TRUMPF, ii
Truong, Tran-Chau, 19, 107, 344, 351, 380, 381, 383
Tsai, Ming-Shian, 74
Tschernajew, Maxim, 126
Tuoc, Vu Ngoc, 300
Turchanin, A, 163, 306
Turchetti, M, 387
Turconi, Margherita, 116
Turkowski, Volodymyr, 251, 316
Turner, James, 355, 376
Tyulnev, Igor, 45, 171
Tzallas, Paraskevas, 86, 123
Tökési, Károly, 302
Tümmler, Johannes, 114

Ueda, Kiyoshi, 14, 144, 191, 274
Uher, C., 35
Ultrafast Innovations (Sponsor), 100
Undisz, Andreas, 104
Unzicker, Brady, 226
Uschmann, Ingo, 104
Utrio Lanfaloni, Valentina, 83

Uzan, Ayelet J., 70, 134
Uzundal, C B, 163, 306

Vacher, Morgane, 268
Vaida, Mihai, 351
Vamos, Lenard, 171
Vampa, Giulio, 41, 44, 133
van der Hart, Hugo, 202, 365
van der Heide, Paul, 245
Vanicek, Jiri, 84, 279, 281
Varjú, Katalin, 123, 129, 131, 343, 345, 349, 366, 369
Varró, Sándor, 318, 319
Vasileiadis, T., 49
Vaughan, John, 119, 226
Vendrell, Oriol, 286
Venzke, Joel, 208
Veyrinas, Kevin, 354
Vila, Laurent, 53
Villanueva, José, 352
Villeneuve, David M., 266
Vimal, Mekha, 53, 178
Vinbladh, Jimmy, 118, 121, 201, 236
Viotti, Anne-Lise, 130, 233
Vismarra, Federico, 213, 267
Vodungbo, Boris, 55
Vogelsang, Jan, 130, 220
Vogwell, Joshua, 9
Volkov, Mikhail, 52
Vozzi, Caterina, 47, 72, 384
Vrakking, Marc J J, 90, 114, 124, 146, 229, 254, 369
Vábek, Jan, 338, 353
Várallyay, Zoltán, 126
Vázquez, R. Martínez, 72

Wahyutama, Imam, 283
Walker, Spencer, 208, 210
Walter, Peter, 227, 243, 263, 270
Walther, Nico, 126
Walz, Francis, 374
Wang, Anna, 115, 269
Wang, Haochuan, 337
Wang, Jun, 151, 269
Wang, Tian, 266
Wang, Xianzhi, 386
Wang, Z. H., 386
Wanie, Vincent, 150
Ward, Rod, 245
Weber, Anne, 360
Weber, Peter, 285
Weber, Thorsten, 265
Wei, Zhiyi, 378, 386
Weidman, Matthew, 128
Weigel, Alexander, 20
Weissenbilder, Robin, 113, 117, 343
Wiese, Joss, 96, 292
Wikmark, Hampus, 118, 354
Will, Ingo, 114
Wilson, Derrek, 170, 339, 347
Winchester, Ethan, 313
Winghart, Marc Oliver, 229
Witte, S, 359
Wittigschlager, Simon, 43
Witting, Tobias, 90, 124, 146
Woldegeorgis, Abel H., 337
Wolf, Jean-Pierre, 55, 81, 135
Wolf, M., 49
Wood, James K., 28, 149
Wragg, Jack, 202
Wu, Wanyang, 342
Wu, Yi, 76, 97, 336
Wu, Yingxuan, 213, 267
Wurmser, Basile, 147
Wustelt, Philipp, 224
Wächtler, Maria, 104
Wörner, Hans Jakob, 54, 69, 81, 83, 94, 135, 136, 170, 174, 223, 232

Xie, Xinhua, 55
XLEAP, , 58
Xu, Han, 342
Xu, Liang, 342
Xu, Siyuan, 378
Xu, Xinlu, 59
Xue, Hao, 144

Yabana, Kazuhiro, 21, 167
Yamada, Atsushi, 167
Yamada, Shunsuke, 21, 167
Yamazaki, Kaoru, 191, 271, 274
Yan, Binghai, 134
Yanez-Pagans, Sergio, 231
Yang, Mengqi, 184, 285
Yang, Tianqi, 31, 165, 377
Yang, Yudong, 75
Ye, Peng, 129, 345, 349
Yeung, M, 387
Yin, Zhong, 81, 135, 136, 232
Ying, Bo, 224
Yong, Haiwang, 285
Yoshioka, Ryo, 138
Young, Linda, 242
Yudin, Sergey N., 160
Yue, Lun, 163, 306, 308
Yuen, C-H, 304
Yuen, Isaac, 282
Yun, Hyeok, 290
Yuwono, Stephen, 295

Zakutayev, Andriy, 137
Zangrando, Marco, 61
Zanotto, Luca, 347
Zapata, Felipe, 61, 118, 236, 238
Zhang, Chunmei, 4, 179, 180
Zhang, F, 359
Zhang, Jin, 168
Zhang, Jinwei, 20
Zhang, Pengju, 69
Zhang, Simin, 105
Zhang, Zhuang-Yan, 229, 320
Zhao, Kun, 378, 386
Zhong, Shiyang, 61, 116
Zhou, Fangjie, 76, 336
Zhu, Jiangfeng, 378
Zhu, Xiaoxian, 378, 386
Ziems, Karl Michael, 181, 228, 273
Zimin, Dmitry, 232
Zinchenko, Kristina S., 83
Zong, A, 247
Zuerch, Michael, 18, 163, 247, 248, 306, 373

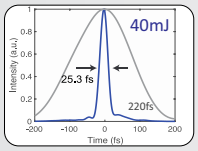
Žitnik, Matjaž, 60, 323

few-cycle™

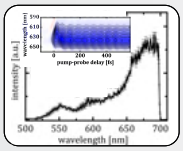
- different solutions

The *few-cycle*™ fiber

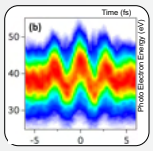
High Energy Pulse Compression
up to 40 mJ output



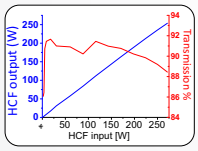
Femtochemistry & 2D Spectroscopy
40 µJ VIS continuum



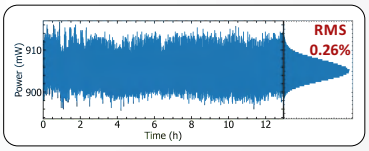
Single Cycle Pulses - Attosecond Science
down to 3 fs @ 800nm



High Transmission 250 W avg. Power
air cooled



Excellent long term stability
13h free running

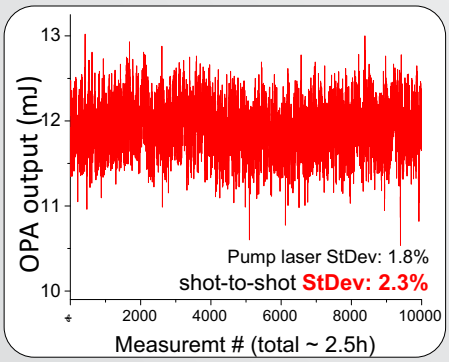


Shortest Pulses - down to 3 fs @ 800 nm
Input Energies - from 20 µJ to 100 mJ
Wavelengths - from UV up to 5 µm
Fiber Length - from 30 cm to 6 m

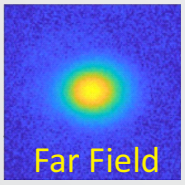
Inner Diameter from 100 µm to 1 mm
Compression Factor up to 20 times
High Transmission > 90%
Average Power > 100 W

High Efficeincy OPA

TiSa Pump: 41 mJ, 45 fs
OPA output: 1.8 µm, 12 mJ, 50 fs



30% Energy conversion pump - idler



All Frequencies - *Orchestra*™ FROG

SHG & TG FROG combined in one device
Total spectral range: 205 nm - 2.1 µm

few-cycle pulses from 400 nm - 1.8 µm

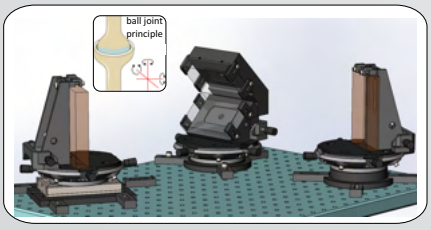
small footprint 16 cm x 16 cm

up to 100 ps scan range

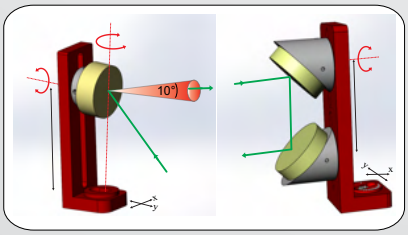
s -or p input pol.



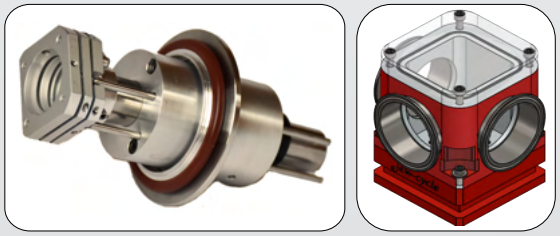
The *screwed*™ Optical Mounts & *vacuum beaming*™ Assemblies



All 3 rotation axes at the grating front surface



Adjustment of horizontal, height, vertical and x/y



Vacube™ - compact beam routing & adjustments under vacuum

[1] "70 mJ nonlinear compression and scaling route for an Yb amplifier using large-core hollow fibers ", G. Fan et al., **OL, 46, 896 (2021)**
[2] "Hollow-core-waveguide compression of multi-millijoule CEP-stable 3.2 µm pulses"G. Fan, et al., **Optica 3, 1308 (2016)**
[3] "Simple fiber-based solution for coherent multi-dimensional spectroscopy in the visible regime", H. Seiler, et al., **OL, 42, 643, (2017)**
[4] "Polarization-assisted amplitude gating as a route to tunable, high-contrast attosecond pulses", H. R. Timmers, et al., **Optica, 3, 707 (2016)**
[5] "Generating high contrast, near single-cycle waveforms with third order dispersion compensation", H. R. Timmers, et al., **OL, 42, 811 (2017)**
[6] "Direct Compression of 170-fs 50-Cycle Pulses down to 1.5 Cycles with 70% Transmission ", Y. Jeong et al., **Scientific Reports, 8 (2018)**

few-cycle.com | info@few-cycle.com | Tel.: (+1) 514-228 6865

ATTO VIII Program at a Glance

	Sun July 10	Mon Jul 11	Tue Jul 12	Wed Jul 13	Thu Jul 14	Fri Jul 15
8:00 AM				7:45 AM Board Buses		
8:15 AM		OPENING		8:00 AM - 9:00 AM transfer to Kennedy Space Center		
8:30 AM		M1 WOLF-PRIZE SESSION: Anne L'Huillier; Paul Corkum; Ferenc Krausz	T1 ATTOSECOND PHOTOIONIZATION DYNAMICS: Eva Lindroth; Alexandra Landsman; Taïeb; Alarcon; Borrás; Randazzo; Mizuno		R1 TIME-RESOLVED CHARGE MIGRATION: Francesca Calegari; Jon Marangos; Folorunso; Driver; Rupprecht; Matselyukh; Kneller	F1 ENTANGLEMENT IN ATTOSECOND PROCESSES: Paraskevas Tzallas; Maciej Lewenstein; Even Tzur; Bourassain-Bouchet; Koll; Shobeiry; Eckart
10:00 AM		COFFEE BREAK			COFFEE BREAK	COFFEE BREAK
10:15 AM		M2 CHIRAL EFFECTS IN ATTOSECOND SCIENCE: Olga Smirnova; Rajak; Vogwell; Ordoñez		9:00 AM - 12:00 PM VISIT KENNEDY SPACE CENTER		
10:45 AM			COFFEE BREAK			
11:00 AM			T2 ATTOSECOND DYNAMICS IN LOW-D MATERIALS: Ursula Keller; Mikhail You Ivanov; Chacon; Bharti; Mitra; Schusser		R2 TABLE-TOP ATTOSECOND SOURCES: Caterina Vozzi; Katsumi Midorikawa; Chen; Mainz; Wu; Haessler	F2 LASER-DRIVEN DYNAMICS IN MOLECULES: Hans Jakob Wörner; Lou Barreau; Trabattoni; Itatani; da Silva; Despré
11:30 AM		COFFEE BREAK				
11:45 AM		M3 IMAGING AND CONTROL OF MOLECULAR STRUCTURE: Heide Ibrahim; Remacle; Ranitovic; Chirvi		12:00 PM - 12:30 PM LUNCH BREAK		
12:30 PM				12:30 PM Board Buses		
1:00 PM		LUNCH	LUNCH; Ist IPC Meeting	12:45 PM - 1:45 PM transfer from KSC back to Conference Hotel	LUNCH; 2nd IPC Meeting	LUNCH
2:00 PM		M4 STRONG-FIELD NONLINEAR OPTICS IN SOLIDS: Matthias Kling; Michael Zuerch; Truong; Nagl; Hassan; Borsch	T3 HIGH-ORDER HARMONIC SPECTROSCOPY AND CONTROL: Nirit Dudovich; Giulio Vampa; Barnard; Heide; Gholam; Tyulnev	LONG COFFEE BREAK (30')	R3 ATTOSECOND TRANSIENT ABSORPTION AND FOUR-WAVE MIXING: Stephen R Leone; Arvinder Sandhu; Yin; Leshcenko; Utrio Lanfaloni; Golubev	TOUR OF PHYSICS AND CREOL ATTO LABS
4:00 PM		Cross road to MIRC	Cross road to MIRC	W1 ATTOSECOND SPECTROSCOPY IN CONDENSED MATTER: Jens Biegert; Matteo Lucchini; Martín; Niedermayr; Ruchon; Heck; Légaré	Cross road to MIRC	END OF CONFERENCE
		POSTER HIGHLIGHTS I	POSTER HIGHLIGHTS II	COFFEE BREAK	POSTER HIGHLIGHTS III	
4:45 PM		POSTER SESSION I	POSTER SESSION II	W2 XFEL FOR ULTRAFAST XUV/X-RAY SCIENCE: Nina Rohringer; Agostino Marinelli; Emma; Penent; Dahlström	POSTER SESSION III	
6:00 PM						
6:30 PM	RECEPTION	DINNER RECESS	DINNER RECESS	DINNER RECESS	CONFERENCE DINNER	
8:00 PM		US FUNDING OPPORTUNITIES IN ATTOSECOND SCIENCE	OVERVIEW OF ATTOCHEM NETWORK	EVENING PANEL: THE FUTURE OF ATTOSECOND SCIENCE		
9:00 PM						